

JOURNAL OF AGRICULTURAL SCIENCES

TARIM BİLİMLERİ DERGİSİ

ANKARA UNIVERSITY FACULTY OF AGRICULTURE

e-ISSN 2148-9297

JIAS



Year 22

Volume 28

Issue 03

Ankara University
Faculty of Agriculture

JOURNAL OF AGRICULTURAL SCIENCES

**TARIM BILIMLERI
DERGISI**

e-ISSN: 2148-9297

Ankara - TURKEY

Year **2022**

Volume **28**

Issue **3**



JOURNAL OF
AGRICULTURAL SCIENCES

TARIM BİLİMLERİ DERGİSİ
ANKARA UNIVERSITY FACULTY OF AGRICULTURE

e-ISSN 2148-9297

Product Information

Publisher	Ankara University, Faculty of Agriculture
Owner (On Behalf of Faculty)	Prof. Dr. Hasan Huseyin ATAR
Editor-in-Chief	Prof. Dr. Halit APAYDIN
In Charge of Publication Unit	Agricultural Engineer Asim GOKKAYA
Journal Administrator	Salih OZAYDIN
Library Coordinator	Dr. Can BESIMOGLU
IT Coordinator	Lecturer Murat KOSECAVUS
Graphic Design	Ismet KARAASLAN
Date of Online Publication	01.9.2022
Frequency	Published four times a year
Type of Publication	Double-blind peer-reviewed, widely distributed periodical
Aims and Scope	JAS publishes high quality original research articles that contain innovation or emerging technology in all fields of agricultural sciences for the development of agriculture.
Indexed and Abstracted in	Clarivate Science Citation Index Expanded (SCIE) Elsevier-Scopus TUBITAK-ULAKBIM-TRDizin CAB International FAO-AGRIS SOBIAD OpenAire
Management Address	Journal of Agricultural Sciences Tarım Bilimleri Dergisi Ankara University Faculty of Agriculture Publication Department 06110 Diskapi/Ankara-TURKEY Telephone : +90 312 596 14 24 Fax : +90 312 317 67 24 E-mail: tbeditor@ankara.edu.tr http://jas.ankara.edu.tr/



JOURNAL OF
AGRICULTURAL SCIENCES

TARIM BİLİMLERİ DERGİSİ
ANKARA UNIVERSITY FACULTY OF AGRICULTURE

e-ISSN 2148-9297

Editor-in-Chief

Halit APAYDIN, Ankara University, Ankara, TURKEY

Managing Editor

Muhittin Onur AKCA, Ankara University, Ankara, TURKEY

Editorial Board

Abdul Shakoor CHAUDHRY, Newcastle University, ENGLAND
Ahmet ULUDAG, Canakkale Onsekiz Mart University, TURKEY
Akasya TOPCU, Ankara University, TURKEY
Ali Adnan HAYALOĞLU, Inonu University, TURKEY
Ali UNLUKARA, Erciyes University, TURKEY
Anna Maria DE GIROLAMO, Italian National Research Council, ITALY
Belgin COSGE ŞENKAL, Yozgat Bozok University, TURKEY
Burhan OZKAN, Akdeniz University, TURKEY
Claudia Di BENE, Research Centre for Agriculture and Environment, ITALY
Donald SUAREZ, USDA ARS Salinity Laboratory, USA
Duygu SEMİZ, Ankara University, TURKEY
Engin YENICE, Ankara University, TURKEY
Erhan MUTLU, Akdeniz University, TURKEY
Farhat JABEEN, Government College University, PAKISTAN
Fazil SEN, Van Yuzuncu Yil University, TURKEY
Filiz ERTUNC, Ankara University, TURKEY
Giuseppe BADAGLIACCA, Mediterranean University of Reggio Calabria, ITALY
Giuseppe GAVAZZI, University of Milan, ITALY
Gniewko NIEDEBALA, Poznań University of Life Sciences, POLAND
Hasan YETİM, Istanbul Sebahattin Zaim University, TURKEY
Huseyin GULER, Ege University, TURKEY
Ismail KARACA, Isparta University of Applied Sciences, TURKEY
Isil CAKCI, Ankara University, TURKEY
Julia MALYSH, All-Russian Institute for Plant Protection, RUSSIA
Karina BATISTA Instituto de Zootecnia, BRAZIL
Kwok-wing CHAU, The Hong Kong Polytechnic University, CHINA
Mahmut ELP, Kastamonu University, TURKEY
Mine TURKTAS, Gazi University, TURKEY
Mehmet Emin CALISKAN, Nigde Omer Halisdemir University, TURKEY
Panagiotis SIMITZIS, Agricultural University of Athens, GREECE
Peter SCHAUSBERGER, University of Vienna, AUSTRIA
Renata BAZOK, University of Zagreb, CROATIA
Sefa TARHAN, Tokat Gaziosmanpaşa University, TURKEY
Selen SAYGIN, Ankara University, TURKEY
Semra DEMİR, Van Yuzuncu Yil University, TURKEY
Serpil SAHİN, Middle East Technical University, TURKEY
Stanislav TRDAN, University of Ljubljana, SLOVENIA
Tuba SANLI, Ankara University, TURKEY
Turkan AKTAS, Namık Kemal University, TURKEY
Umut TOPRAK, Ankara University, TURKEY
Yasemin KAVDIR, Canakkale Onsekiz Mart University, TURKEY
Yildiz AKA KACAR, Cukurova University, TURKEY
Yonca YUCEER, Canakkale Onsekiz Mart University, TURKEY

Advisory Board

Ajit VARMA, Amity University
Erdal OZKAN, The Ohio State University
Ibrahim ORTAS, Çukurova University
Kyeong Uk KIM, Seoul National University
Murad CANAKCI, Akdeniz University



e-ISSN 2148-9297

**JOURNAL OF
AGRICULTURAL SCIENCES**
TARIM BİLİMLERİ DERGİSİ
ANKARA UNIVERSITY FACULTY OF AGRICULTURE

CONTENTS

2022, 28(3)

Review:

- Environmental Abiotic Stress and Secondary Metabolites Production in Medicinal Plants: A Review** 351
Arjita PUNETHA, Dipender KUMAR, Priyanka SURYAVANSHI, Rajendra Chandra PADALIA,
Venkatesha KATANAPALYA THIMMAIAH

Research articles:

- Effect of Parental Genotypes and Their Reciprocal Crosses on Haploid Plant Production by Anther Culture and Confirmation of Double Haploids by Flow Cytometry in Bread Wheat** 363

Hussein Abdullah AHMED AHMED, Güray AKDOĞAN, Sancar Fatih ÖZCAN, Surendra BARPETE

- Characterization of Antimicrobial Peptide Fraction Producing *Lactobacillus* spp. Based on LC/MS-MS and Determination of ACE-inhibitory Activity in Kefir** 372

Merve ATALAY, Didem ŞAHİNGİL

- Effects of Donor x Inducer Interaction on the Success of Haploid Induction and Comparison of Haploid Seed Identification Methods in the In vivo Maternal Haploid Technique in Maize** 385

Fatih KAHRIMAN, Umut SONGUR, Abdullah DİŞBUDAK, Sezgin KIZIK, Berk VURAL

- Effect of Combined or Separate Administration of Beta Carotene-Vitamin E and hCG on Fertility in Sheep Lambs** 396

Mehmet Ferit ÖZMEN, Erkan SAY, Ümüt CİRİT

- Impacts of High and Low-Input Farming Systems on the Quality Change of Safflower Oil While Intercropped with Bitter Vetch** 401

Azin NAJAFABADI, Jalal JALILIAN

- An efficient Regeneration Protocol for *in vitro* Direct Organogenesis in Einkorn (*Triticum monococcum* L.) Wheat** 412

Günce ŞAHİN, Mehmet ÖRGEÇ, Nusret ZENCİRCİ

- Natural Vanillin Production from Isoeugenol by Using *Pseudomonas putida* in Biphasic Bioconversion Medium** 423

Huseyin KARAKAYA, Murat YILMAZTEKİN

- Effect of Supplementation of Urea on the Nutritive Value and Fermentation Characteristics of Apple Pulp Silages** 430

Önder CANBOLAT

- Development of an IoT-Based (LoRaWAN) Tractor Tracking System** 438

Çağdaş CİVELEK

- Possibilities of Use Fertilizer Industry Waste Gypsum Material of Improve Sodic and Boron Soils** 449

Barış BAHÇECİ, Ali Fuat TARI, İdris BAHÇECİ

- Exponential Type Estimators Using Sub-Sampling Method with Applications in Agriculture** 457

Ceren ÜNAL, Cem KADILAR

Biostabilization of Tannery Sludge Compost by Vermicomposting Yiğit Nevzat KAMAN, Nur OKUR, Hüseyin Hüsnü KAYIKÇIOĞLU	473
Effect of Preharvest Calcium Chloride Treatment on Some Quality Characteristics and Bioactive Compounds of Sweet Cherry Cultivars Derya ERBAŞ, Mehmet Ali KOYUNCU	481
Extraction and Physicochemical Characterization of Chitosan from Pink Shrimp (<i>Parapenaeus longirostris</i>) Shell Wastes Özen Yusuf ÖĞRETMEN, Barış KARSLI, Emre ÇAĞLAK	490
Carbon Storage Potential and its Distributions in the Particle Size Fractions in Harran Plain, Turkey İbrahim Halil YANARDAĞ, Asuman BÜYÜKKILIÇ YANARDAĞ, Ahmet R. MERMUT, Ángel FAZ CANO	501
The Effects of Gas Changes in the Shelter in the Summer Period on the Milk yield and Dry Material Consumption of Anatolian Water Buffalo (<i>Bubalus bubalis</i>) Taşkın DEĞİRMENCİOĞLU	511
Genetic Characterization of Some Species of Vetch (<i>VICIA L.</i>) Grown in Turkey with SSR Markers CebraİL YILDIRIM, Onur OKUMUŞ, Satı UZUN, Şeyda Nur TURKAY, Ahmet SAY, Melike BAKIR	518
Determining the Relationship of Evapotranspiration with Precipitation and Temperature Over Turkey Mustafa KUZAY, Mustafa TUNA, Mustafa TOMBUL	525
The Role of Different Planting Types in Mitigating Urban Heat Island Effects: A Case Study of Gaziantep, Turkey Murat YÜCEKAYA, Ahmet Salih GÜNAYDIN	535
Effects of Tillage Method, Drainage Management and Temporal Variability on Some Soil Physical Properties and Organic Matter Mahmoud SHABANPOUR, Salman FEKRI, İraj BAGHERI, Sayed Hossein PAYMAN, Fatemeh RAHIMI-AJDADI	545



Environmental Abiotic Stress and Secondary Metabolites Production in Medicinal Plants: A Review

Arjita PUNETHA^a , Dipender KUMAR^{a*} , Priyanka SURYAVANSHI^b , Rajendra Chandra PADALIA^a ,
Venkatesha KATANAPALYA THIMMAIAH^a 

^aCSIR-Central Institute of Medicinal & Aromatic Plants (CIMAP), Research Centre, Pantnagar, Uttarakhand, INDIA

^bCSIR-Central Institute of Medicinal & Aromatic Plants (CIMAP), Lucknow, Uttar Pradesh, INDIA

ARTICLE INFO

Review Article

Corresponding Author: Dipender KUMAR, E-mail: dipenderkumar@cimap.res.in

Received: 24 September 2021 / Revised: 11 May 2022 / Accepted: 11 May 2022 / Online: 01 September 2022

Cite this article

PUNETHA A, KUMAR D, SURYAVANSHI P, PADALIA R C, VENKATESHA K T (2022). Environmental Abiotic Stress and Secondary Metabolites Production in Medicinal Plants: A Review. *Journal of Agricultural Sciences (Tarim Bilimleri Dergisi)*, 28(3):351-362. DOI: 10.15832/ankutbd.999117

ABSTRACT

Medicinal plants that produce various secondary metabolites are quite useful to us owing to their anti-microbial properties, presence of huge amounts of anti-oxidants, cytotoxic nature, and various other medically significant properties. Medicinal plants, therefore, serve as raw materials for modern pharmaceutical medicines and several herbal medical supplements. Expansion and advancement of growing medicinal plants on large scale has flourished over the last few years. However, prolonged environmental changes have made medicinal plants susceptible to numerous abiotic stresses. On being exposed to abiotic stresses chiefly light (quality and quantity), extreme temperature conditions, water stress (drought or flooding), nutrients available, presence of heavy metals and

salt content in the soil, medicinal plants undergo several changes physiologically and their chemical composition also gets altered. To combat the effects of abiotic stress, several mechanisms at morphological, anatomical, biochemical, and molecular levels are adapted by plants, which also include a change in the production of the secondary metabolites. However, plants cannot cope with extreme events of stress and eventually die. Several strategies stress such as the use of endophytes, chemical treatment, and biotechnological methods have therefore been introduced to help the plants tolerate the period of extreme stress. Moreover, nano bionics is also being developed as new technology to help plants survive stressful conditions.

Keywords: Biochemical, Biotechnological, Nanobionics, Strategies, Technology

1. Introduction

For thousands of years, medicinal plants have served as a source of treatment in local communities across the globe. Medicinal plants function as storehouses of secondary metabolites (SMs) i.e., they have evolved to produce a wide spectrum of SMs that are not implicated straightforwardly in primary processes of plant growth and development, and are produced in response to some kind of stress. SMs comprise of a group of bioactive compounds that are chiefly formed from primary metabolites and are not directly responsible for growth of plant and its development (Kumar et al. 2022). SMs differ from one plant to another and one species to another and generally their levels rise during periods of high stress (Taiz & Zeiger 2006). A number SMs produced by medicinal plants are beneficial to us owing to their anti-microbial properties, presence of huge amounts of anti-oxidants, cytotoxic nature, and other properties that are medically quite significant.

Several modern pharmaceutical medicines and several herbal medical supplements that are obtained from medicinal plants are based on these SMs. Plants that belong to families like Apiaceae, Rutaceae, Asteraceae, Hypericaceae, Papaveraceae, Ginkgoaceae, Lamiaceae, Zingiberaceae, Rhamnaceae, Rubiaceae, and Solanaceae produce rich SMs that provide the majority of pharmaceutical medicines (Gurib-Fakim 2006). Table 1 shows the secondary metabolites produced by a few medicinal plants and their uses. SMs produced by medicinal plants play several roles in plants such as being exclusive sources for pharmaceuticals, like food supplements, flavoring agents, and other industrial materials.

Many phenolic compounds like flavonoids are effective antioxidants and can also serve as free radical scavengers. Some phenolics like quercetin and silybinare known for their anti-inflammatory and anti-hepatotoxic properties respectively, while a few like genistein and daidzein possess phyto-estrogenic activity, and some such as naringenin are insecticidal (Goławska et al. 2014). Alkaloids also exhibit a wide range of pharmacological properties such as stimulator of respiration and relaxation, analgesic, local anesthesia, vasoconstriction, muscle relaxation, hyper and hypotensive. Many alkaloids are severely toxic and can be used as insecticides for instance nicotine and anabasine (Hoffmann 2003). Few saponins also exhibit antitumor,

spermicidal, sedative, and analgesic properties while some saponins show anti-inflammatory properties. Monoterpenes and other volatile terpenes also have several medicinal uses. For instance, camphor and menthol are used as counter-irritants analgesics and anti-itching agents.

Therefore, for drug development, numerous SMs are being taken into account (Sanchita & Sharma 2018). Concomitantly, the introduction, expansion, and advancement of research on herbal substances have flourished over the last few years. To date, millions of people across the globe devour herbal medicines for several medical problems. However, prolonged environmental changes have made medicinal plants susceptible to numerous abiotic stresses. The most significant abiotic stresses are drought, temperature extremes, heavy metal toxicity, salinity, light intensity, UV radiation, nutrient deficiency, etc. On being exposed to environmental stresses, medicinal plants undergo several changes physiologically and their chemical composition also gets altered. Abiotic stresses induce detoxification systems of plants which include enhanced production of the antioxidant enzymes like superoxide dismutase, catalase, ascorbate peroxidase and glutathione peroxidase (Hasanuzzaman et al. 2012). Phenolic compounds like flavonoids and lignin precursors are found to accumulate in plants as a reaction to abiotic stresses and are therefore considered as the basic mechanisms of scavenging Reactive Oxygen Species (ROS). Plants on being exposed to environmental stresses also begin synthesizing SMs, which have significant role in adaptive during conditions of stress. In this review, we have summarized the information on the defense mechanism adopted by medicinal plants at the time of stress, a consequence of abiotic stresses on secondary metabolites made by plants, and approaches to overcome environmental stress in plants.

Table 1- Secondary metabolites produced by few medicinal plants and their uses

S.No	Medicinal plant	Metabolites produced	Medicinal properties	Reference
1	<i>Acanthospermum hispidum</i>	Acanthospermolgalactoside, β -caryophyllene, caffeic acid, cis-cis-germacranolides, flavones, melampolides,	Anti-cancer, anti-microbial, anti-inflammatory, anti-allergic.	Edewor & Olajire (2011)
2	<i>Alpinia officinarum</i>	Diarylheptanoids Alpinoids, officinaruminane, officinin A	Tooth decay, abnormal mensuration, abdominal pain, flatulence, inflammation	Abubakar et al. (2018)
3	<i>Artemisia annua L.</i>	Artemisinin, artemetin, , cirsilineol, casticin, chrysoplenetin	Anti-malarial, anti-inflammatory, anti-cancer	Weathers & Towler (2012)
4	<i>Atropa belladonna L.</i>	Atropine, hyoscyamine, hyoscine	Anti-spasmodic, mydriatic	Okigbo et al. (2008)
5	<i>Cymbopogon flexuosus</i>	Citral, β -myrcene	Anti-inflammatory, anti-fungal, analgesic	Boukhatem et al. (2014)
6	<i>Foeniculum vulgare</i> Mill	Furocoumarins, isopimpinellin, kaempferol, psoralen, quercetin, xanthotoxin	Antioxidants, cardiac stimulant, digestive, vermifuge	Nassaret al. (2010)
7	<i>Matricaria chamomilla</i>	Herniarin, umbelliferone	Anti-inflammatory, spasmolytic, anti-biotic	Eliasova et al. (2004)
8	<i>Mentha piperita</i> Linn.	Hesperidin, menthone, menthol, didymin, buddleoside, diosmin	Anti-tumour, carminative, spasmolytic, anti-diabetic	Zhao et al. (2018)
9	<i>Ocimum sanctum</i>	Eugenol, rosmarinic acid, carvacrol, oleanolic acid	Anti-cancer, anti-oxidants anti-diabetic, cardio protective, analgesic, anti-spasmodic	Prakash & Gupta (2005)
10	<i>Origanum onites</i>	Carvacrol and thymol	Antifungal, antimicrobial, antioxidant, insecticidal, hepatoprotective, and cytotoxic activity	Spyridopoulou et al. (2019)
11	<i>Panax ginseng</i>	Ginsenosides	Anti-tumour, anti-inflammatory and antioxidant properties, and anti-apoptotic	Razgonova et al. (2019)
12	<i>Plantago lanceolata</i>	Alkaloids, fatty acids, flavonoids, glycosides, polyphenols, tannins, terpenoids, iridoid, and polysaccharides	Wound healing, inflammation, cancer, respiratory system disorder, blood circulation, reproductive system, and digestive organs	Abate et al. (2022)
13	<i>Piper nigrum</i> Linn	Piperine	Anti-inflammatory, anti-thyroids, antihypertensive, hepato-protective, anti-allergic, appetizer, anti-histaminic, anti-flatulant	Damanhoury & Ahmad (2014)
14	<i>Scutellaria orientalis</i>	Baicalin, baicalein, wogonin, melatonin, serotonin, viscidulin	Used to treat epilepsy, insomnia, hysteria, anxiety, delirium tremens, bronchitis, hepatitis, jaundice, diarrhea, dysentery, thrombosis, hypertension and cancer	Sherman et al. (2022)
15	<i>Thymus vulgaris</i>	Carvacrol, geraniol, linalool terpineol, thymol,	Respiratory diseases, especially chronic cough, bronchitis, and asthma, vascular problems, diseases of the urinary tract, teeth pain and indigestion	Hossain et al. (2022)
16	<i>Withania somnifera</i>	Withanine, withanolides, withananine, somnine, somniferine,	Anti-oxidant, amnesia, anti-inflammatory, anti-neoplastic, anti-fibrotic, cardiovascular	Brant (2016) ; Bharti et al. (2016)

2. Biochemical mechanisms adopted by plants for abiotic stresses tolerance

Plants react to abiotic stress at morphological, anatomical, biochemical, and molecular levels. Some mechanisms are adopted by plants to overcome the period of stress (Figure 1). Biochemical mechanisms involve the formation of metabolites such as proline, polyamines, terpenes, carbohydrates. As a part of biochemical response, they synthesize several secondary metabolites to survive unfavorable environmental conditions. The most common secondary metabolites produced by medicinal plants as a part of their mechanism to adapt to periods of stress are:

- a) **Terpenes:** Terpenes are one of the many species of SMs that are involved in the different biological processes undergoing in plants. During stress, terpenes reduce the consequences of oxidative stress by two mechanisms: a) reacting directly with oxidants intercellularly and b) altering ROS signaling. Amongst the various kinds of terpenes, the membrane stabilization and direct antioxidant effects of isoprene and monoterpenes minimize abiotic stress in several plant species. In addition to having antioxidant effects, isoprenes and monoterpenes also react quickly with ozone, thereby reducing its toxicity. Being amphipathic, isoprene can improve hydrophobic interactions that occur between membrane proteins and lipids (Sharkey & Yeh 2001) which results in the prevention of membrane and protein disintegration.
- b) **Phenylpropanoids:** Phenylpropanoids are a highly diversified chemical class of metabolites that play a chief role in abiotic stress management in plants. These act as chief constituents in structure formation of the secondary cell wall, protect plants from harmful UV rays, help in ROS scavenging, act as signaling compounds, and are modulators of auxin transportation in plants (Cheynier et al. 2013). Phenolic compounds like flavonoids or coumarins are phenylpropanoids having one or more phenolic rings. Phenolic substances are very crucial for plants since they are major constituents of secondary cell walls, provide antioxidant properties to plants, help in signaling and also act as phytoalexins (Arbona & Gómez-Cadenas 2015). Phenolics have been studied to exhibit activity in response to high intensity of light and UV-B rays. Flavonoids are a type of phenolic compounds that serve as outstanding protectants against UV rays (Schenke et al. 2011).
- c) **Carotenoids:** Carotenoids also serve as vital substances in diverse processes of plants and act as potential antioxidants during the period of stress. They harvest light, quench and scavenge chlorophyll in triplicate state and singlet oxygen species, scatter surplus of harmful energy and stabilize membrane during stress. The production of these metabolites increases excessively at the time of abiotic stress (Espinoza et al. 2013) and might also be related to possessing a protective role and stabilization of the lipids present in thylakoid membranes (Volkova et al. 2009). Additionally, carotenoids also absorb excessive light or UV radiation (Pateraki & Kanellis 2010).

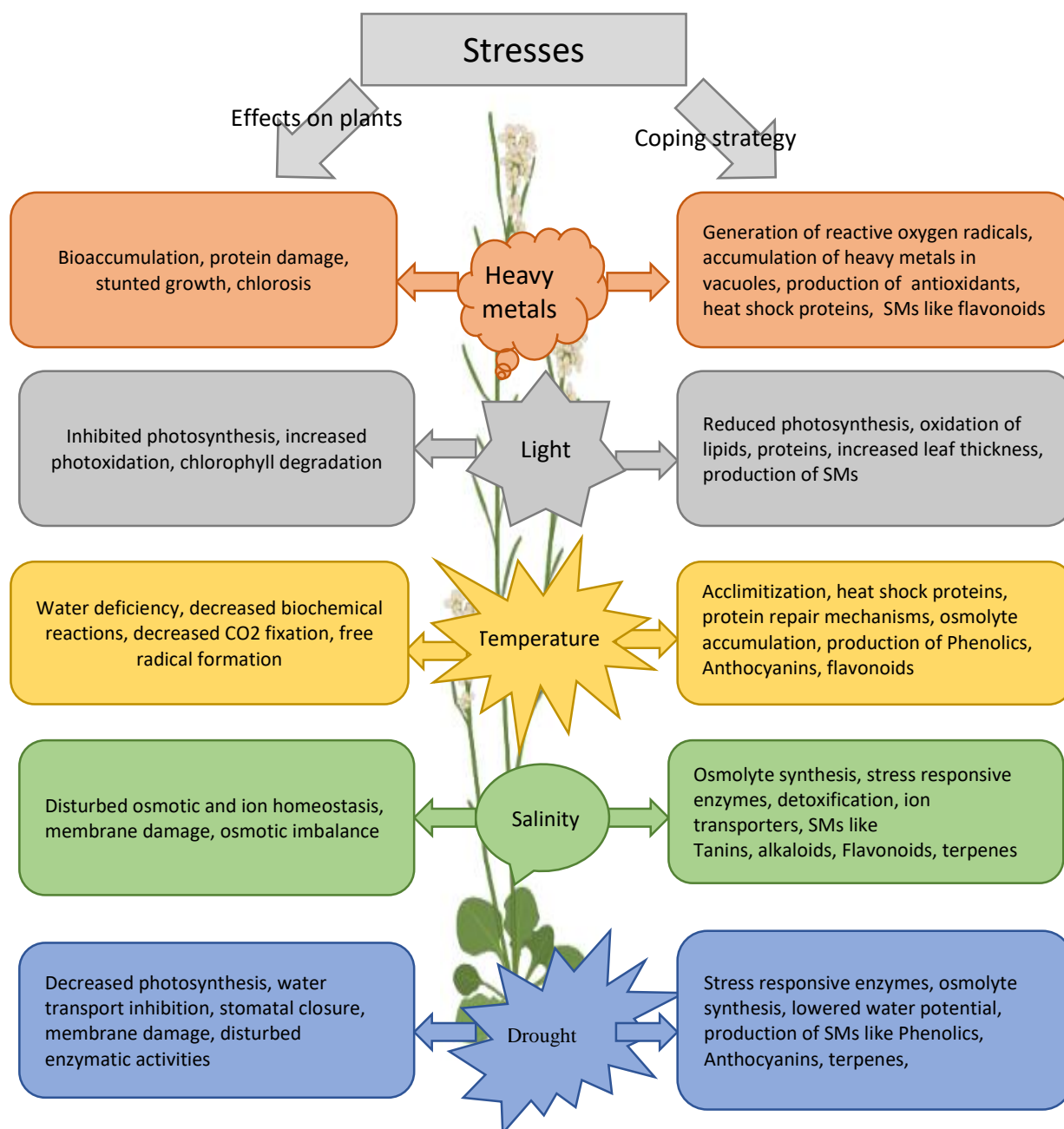


Figure1- Effects of various abiotic stresses on plants and coping strategies adopted by them

3. Influence of abiotic stress on secondary metabolite formation by medicinal plants

The chemical interaction that takes place among plants and their surroundings is primarily conciliated through secondary metabolite formation that helps plants to adapt during adverse environmental conditions (Table 2). Plants being influenced by different kinds of stresses regulate the synthesis of SMs (Verma & Shukla 2015). Abiotic stresses, chiefly light (quality and quantity), extreme temperature conditions, water stress (drought or flooding), nutrients available, presence of heavy metals, and salt content in soil are known to extensively persuade the amount and composition of SMs produced by plants (Khan et al.2016; Sampaio et al. 2016).

- i. **Temperature stress:** Temperature serves as a key physical factor severely affecting the growth and development of plants. Extreme temperature stress that occurs in the form of excessive heat or cold affects basic processes of medicinal plants at biochemical, physiological as well as molecular levels. Temperature stress results in leaf senescence damages the membrane of cells, promotes chlorophyll degradation and results in protein degradation (Pradhan et al. 2017). Medicinal plants can also produce SMs in response to high temperatures (Verma & Shukla 2015). Though some plants have shown an increase in the production of SMs due to high temperatures (Naghiloo et al. 2012), few studies have reported a decrease in the production of SMs (Shibata et al. 1988). It can therefore be said that the production of SMs is dependent on plants and their species. Several studies report the outcome of temperature stress on the content of SMs like phenolics and terpenoids. Loreto &

Schnitzler 2010 reported that terpenes are emitted at a higher amount from plants with an increase in temperature. These terpenes help in the stabilization of thylakoid membranes present in chloroplasts and also possess great antioxidant activity. The ratio of formation of flavonoids namely quercetin: kaempferol has been found to increase with a decrease in temperature in *Arnica Montana* plants. The roots of *Panax quinquefolius* were found to have an increased amount of ginsenoside during elevated temperatures (Jochum et al. 2007). Soufi et al. (2015) demonstrated an increase in the content of chlorophyll and carotenoid in plants of *Stevia rebaudiana* which were exposed to high temperature than control plants that were grown at lower temperatures. Vashisth et al. (2018) demonstrated that exposure of *Artemisia annua* to cold stress improved the accretion of artemisinin as a result of up regulation of genes that are concerned in its biosynthesis. Chan et al. (2010) studied how temperature affects anthocyanin production by *Melastoma malabathricum* and reported that higher amounts got accumulated when the temperature was low (20 ± 2 °C) than in higher temperature conditions (26 ± 2 °C and 29 ± 2 °C).

- ii. **Drought stress:** This is a majorly significant abiotic stress that dramatically affects plant growth and yield. The condition of drought is a result of inadequate rainfall and constant loss of water through transpiration and evaporation as a result of which, the amount of available water in the soil decreases (Jaleel et al. 2007). Several studies report that drought stress affects the production of SMs in medicinal plants. Drastically increased concentration of betulinic acid, flavonoids, and phenolic substances was found in *Hypericum brasiliense* during conditions of drought (Azharet al. 2011). Yang & Li (2011) found raised amounts of anthraquinones, chlorogenic acids, and flavonoids in the leafy area of *Myrica lubra* during a situation of medium water stress condition. Liu et al. (2011) gave an account of the increased content of salvianolic acid B and decreased content of tanshinone IIA in the roots of the plant *Salvia miltiorrhiza*. The production of oleanolic, rosmarinic, as well as ursolic acids increases when *Prunella vulgaris* is exposed to moderately dry conditions (Chen et al. 2011). Disclosure to drought stress in a moderate amount might help the accumulation of baicalin in *Scutellaria baicalensis* (Cheng et al. 2018). Drought stress is also known to enhance the quality of SMs like artemisinin in plants of *Artemisia*. Betulinic acid, quercetin, and rutin are also produced in increased amounts in *Hypericum brasiliense* plants during drought conditions (Verma & Shukla, 2015). Increased production of SMs like phenolics, alkaloids, and terpenoids during stress prevents the production of ROS thereby protecting medicinal plants (Radasci et al. 2010). Thus, drought affected areas can be exploited for growing medicinal plants, which can provide dual benefits a) higher production of secondary metabolites, b) exploitation of drought pretentious land.
- iii. **Salinity stress:** Soil salinity is a chief problem faced worldwide that severely affects plants (Jamil et al. 2006). The use of poor-quality water and excessive amounts of inorganic salts present in water used for irrigation are the major causes of salinity. Medicinal plants produce SMs as defense mechanisms to survive salt stress. *Plantago ovata* plants growing under saline conditions are known to have increased concentrations of alkaloids and tannins (Abd EL-Azim & Ahmed 2009), phenolics (Verma & Shukla 2015), flavonoids, proline, and saponins (Haghighi et al. 2012). The level of ricinine in shoots of *Ricinus communis* is significantly higher under saline conditions (Ali et al. 2008). The concentration of reserpine, solasodine, and vincristine accumulated in *Solanum nigrum*, *Catharanthus roseus*, and *Rauwolfia tetraphylla* respectively, was found to increase on exposure to salt stress (Bhat et al. 2008). Cik et al. (2009) found a considerable rise in the number of phenolics like caffeic, chlorogenic, and protocatechuic acids in *Matricaria chamomilla* during salinity stress. The concentration of phenolics has also been found to increase in plants of *Achillea fragratissima* (Abd El-Azim & Ahmed 2009), *Mentha pulegium* (Queslati et al. 2010), *Nigella sativa* (Bourgou et al. 2010), and *Stevia rebaudiana* (Rathore et al. 2014) on treating with salt. *Nigella sativa* plants grown in saline conditions have been found to have an increased concentration of apigenin, quercetin, and trans-cinnamic acid (Bourgou et al. 2010). Shahverdi et al. (2017) investigated the influence of salt stress on *Stevia rebaudiana* plants and observed an increased percentage of rebaudioside-A and stevioside. Phenolic compounds exhibit antioxidant properties that eradicate ROS produced through the condition of stress (Ksouri et al. 2007). The production of SMs is influenced by several regulatory genes and enzymes that are formed during salinity stress and the level production of SMs changes as per the plants require.
- iv. **Light:** Light is a very crucial abiotic factor responsible for the formation of secondary metabolites by medicinal plants. Light quality (wavelength and color), quantity, and photoperiod severely influence the growth of the plant, its structure, time of flowering, and output (Casal & Yanovsky 2005). Some plants exhibit better growth and more production of SMs on being exposed to the higher irradiance (Zhang et al. 2015). For example, the leaves of *Erigeron breviscapus* developed in sunlight contain a higher amount of scutellarin than those developed in shade (Zhou et al. 2016). Several reports also suggest contradictory situations. For example, in *Flourensia cernua* plants grown at shade, the amount of borneo, b-pinene, bornyl acetate, camphene, sabinene, l, and Z-jasnone were elevated as compared to the ones grown under sunlight (Estell et al. 2016). Barbaloin, homonataloin, and nataloin increase in amounts in *Aloe mutabilis* when developed in shade conditions instead of directly available sunlight. Callus culture of *Zingiber officinale* was found to have more concentration of gingerol and zingiberene when grown in presence of light (Anasori & Asghari 2008). Ultraviolet (UV) radiation can naturally stimulate the synthesis of SMs however, in higher amounts UV-B severely damages the photosynthetic system, DNA or RNA, and proteins and also might cause cell damage (Pell et al. 1997). Flavonoids and phenolic acids were produced in a better amount under influence of UV-B radiation in *Chrysanthemum plants* (Ma et al. 2016). The outcome of UV light exposure on production SMs is helpful in most cases however higher doses negatively affect the rate of photosynthesis, subsequently affecting growth and development in plants (Katerova et al. 2017).

Table 2- Effect of abiotic stress on secondary metabolite production by few plants

<i>Abiotic stress</i>	<i>Plant</i>	<i>Metabolite formed</i>	<i>Effect</i>	<i>Reference</i>
UV-B	<i>Arnica montana</i>	Anthocyanins, lignin, tannins, Phenolic acids	Increase	Spitaler et al. (2006)
	<i>Asparagus officinalis</i>	Flavonol quercetin-4'-O-monoglucoside	Increase	Eichholz et al. (2012)
	<i>Astragalus compactus</i>	Anthocyanins, lignin, tannins, Phenolic acids	Increase	Naghiloo et al. (2012)
	<i>Nasturtium officinale</i>	Glucosinolate	Increase	Reifenrath & Müller (2007)
Light intensity	<i>Aloe vera</i>	Anthocyanin, aloin	Increase	Hazrati et al. (2016)
	<i>Cassia angustifolia</i>	Sennoside	Increase	Raju et al. (2013)
	<i>Erigeron breviscapus</i>	Scutellarin	Increase	Zhou et al. (2016)
	<i>Hypericum perforatum</i>	Naphthodianthrones and phenolic compounds	Increase	Radusiene et al. (2012)
Drought	<i>Mahonia breviflora</i>	Essential oil, Hexadecanoic acid	Increase	Li et al. (2018)
	<i>Artemisia</i>	Artemisinin	Increase	Verma & Shukla (2015)
	<i>H. brasiliense</i>	Rutin, Quercetin, Betulinic acid	Increase	Verma & Shukla (2015)
	<i>Labisia pumila</i>	Total phenolics, anthocyanins	Increase	Jaafar et al. (2012)
	<i>Salvia officinalis</i>	Terpenes	Increase	Nowak et al. (2010)
	<i>Scutellaria baicalensis</i>	Baicalin	Increase	Cheng et al. (2018)
	<i>Thymus vulgaris</i>	Thymol	Decrease	Alavi-Samani et al. (2015)
	<i>T. vulgaris</i>	Thymol, carvacrol, γ -terpinene, and p-cymene	Increase	Mohammadi et al. (2018)
	<i>Trachyspermum ammi</i>	Total phenolics	Increase	Azhar et al. (2011)
	High temperature	<i>A. compactus</i>	Phenolics	Increase
<i>Chrysanthemum</i>		Anthocyanins, α -linolenic, Jasmonic acid	Decrease	Shibata et al. (1988)
<i>Eleutherococcus senticosus</i>		Eleutherosides and chlorogenic acid	Increase	Shohael et al. (2006)
<i>H. perforatum</i>		Naphthodianthrones and phenolics	Increase	Radusiene et al. (2012)
<i>H. perforatum</i>		Hyperforin	Decrease	Radusiene et al. (2012)
<i>Polygonum minus</i>		Flavonols	Increase	Goh et al. (2015)
Low temperature	<i>Artemisia annua</i>	Artemisinin	Increase	Yin et al. (2008)
	<i>Artemisia tilesii</i>	Flavonoids	Decrease	Havryliuk et al. (2017)
	<i>Camellia japonica</i>	Anthocyanins, α -linolenic, Jasmonic acid	Increase	Li et al. (2016)
Salinity	<i>Achillea fragratissima</i>	Tannin, Alkaloid	Increase	Abd EL-Azim & Ahmed (2009)
	<i>Coriandrum sativum</i>	Carvacrol, Octanal; Borneol; (E)-2-Nonenal	Increase	Neffati & Marzouk (2008)
	<i>Coriandrum sativum</i>	γ -trepine, α -Pinene; (Z)-Myroxide	Decrease	Neffati & Marzouk (2008)
	<i>Origanum majorana</i>	cis-Sabinene Hydrate; Linalyl acetate; Terpinene-4-ol	Increase	Baatour et al. (2010)
	<i>Plantago ovata</i>	Flavonoids, Saponins, Proline	Increase	Haghighi et al. (2012)
	<i>Ricinus communis</i>	Recinine alkaloids	Increase	Ali et al. (2008)

1. Strategies enabling plants to tolerate the conditions of extreme stress: Though plants can cope with the conditions of stress on their own using several mechanisms, however, extreme stress conditions severely affect the plants and lead to plant death. Therefore, to ensure plant survival at the time of stress, several strategies are being used to increase plant stress tolerance. Current efforts at increasing stress tolerance in plants include the use of microorganisms, chemical treatment, biotechnological and nano-technological approaches (Figure 2).

i. Biological: This method of ensuring plant survival at the time of severe abiotic stress in plants includes the introduction of plants with endophytes. Endophytes are microbes that live in roots, stems, leaves, and seeds of healthy plants without showing any negative effects on physiological plant functions and also not resulting in any disease. Endophytes help plants in adapting to unfavorable conditions and during stress conditions that limit their growth. During severe conditions, plants develop symbiotic relationships with these microorganisms, which is helpful to both partners. The main functions of these microorganisms which confer resistance to stress in plants are hormone production such as cytokinins, gibberellins, indole-3-acetic acid (IAA), siderophore formation, phosphate solubilization, nutrient uptake, and antagonism to pathogens. Endophytes can stimulate chemical or physical modifications that confer plant protection. Several reports have confirmed that plant growth-promoting fungi (PGPF) can provide aid in escalating tolerance of plants against different environmental stresses such as cold, heat, drought, salinity, and heavy metals (Khan et al. 2012).

ii. Chemical treatment: Chemical treatment mostly involves seed priming. Priming is a technique where plant seeds are chemically treated to provide them protection from unfavorable situations. Chemical substances as priming agents came into use only after they were established to appreciably perk up the ability of plants to bear situations not favorable to them (Irani & Todd 2018). Chemical substances like hydrogen peroxide (H₂O₂), hydrogen sulfide (H₂S) and nitric oxide (NO) are generally used for priming and can provide abiotic stress resistance to plants (Jinet al. 2017; Liang et al. 2018). The seeds are treated with these chemicals before sowing which confers increased tolerance of plants to abiotic stress, without inhibiting plant development (Shi et al. 2014). These compounds might confer priming effects from their signaling functions at the cellular level and or from transcriptional and post-translational regulation (Savvides et al. 2016). Seed priming

increases the percentage of seed germination, decreases the time taken by seeds to germinate and improves the growth of seeds during unfavorable environmental conditions.

iii. Biotechnological: Modifying the regulatory genes like protein kinases and phosphatase that protect plants from abiotic stress or bringing change in transcription factors is an approach that efficiently improves the capacity of plants to resist stress by modulation of stress signals and regulation of several downstream genes. The most suitable approach used to improve abiotic stress tolerance in plants requires strengthening the internal systems by interfering with the sensors and signaling/ regulative elements (i.e. kinases, phosphatases, transcription factors) or genes and effectors (e.g. antioxidant producing enzymes, heat-shock proteins, osmoprotectants synthesizing enzymes) (Reguera et al. 2012). In plants, several protocols have been proposed that develop abiotic stress resistance depending on the enzymes that can produce metabolites having solubility, serve as membrane lipid synthesizers, antioxidant producers, act as protein protectants, and transporters (Yang et al. 2018). For instance, Proline dehydrogenases (ProDH) and $\Delta 1$ -pyrroline-5-carboxylate synthetases (P5CS) are known to confer stress tolerance to plants through regulation of the synthesis of proline. It is an important area of research to identify chief regulators or sensors that acclimatize stress upstream and tolerate abiotic stress.

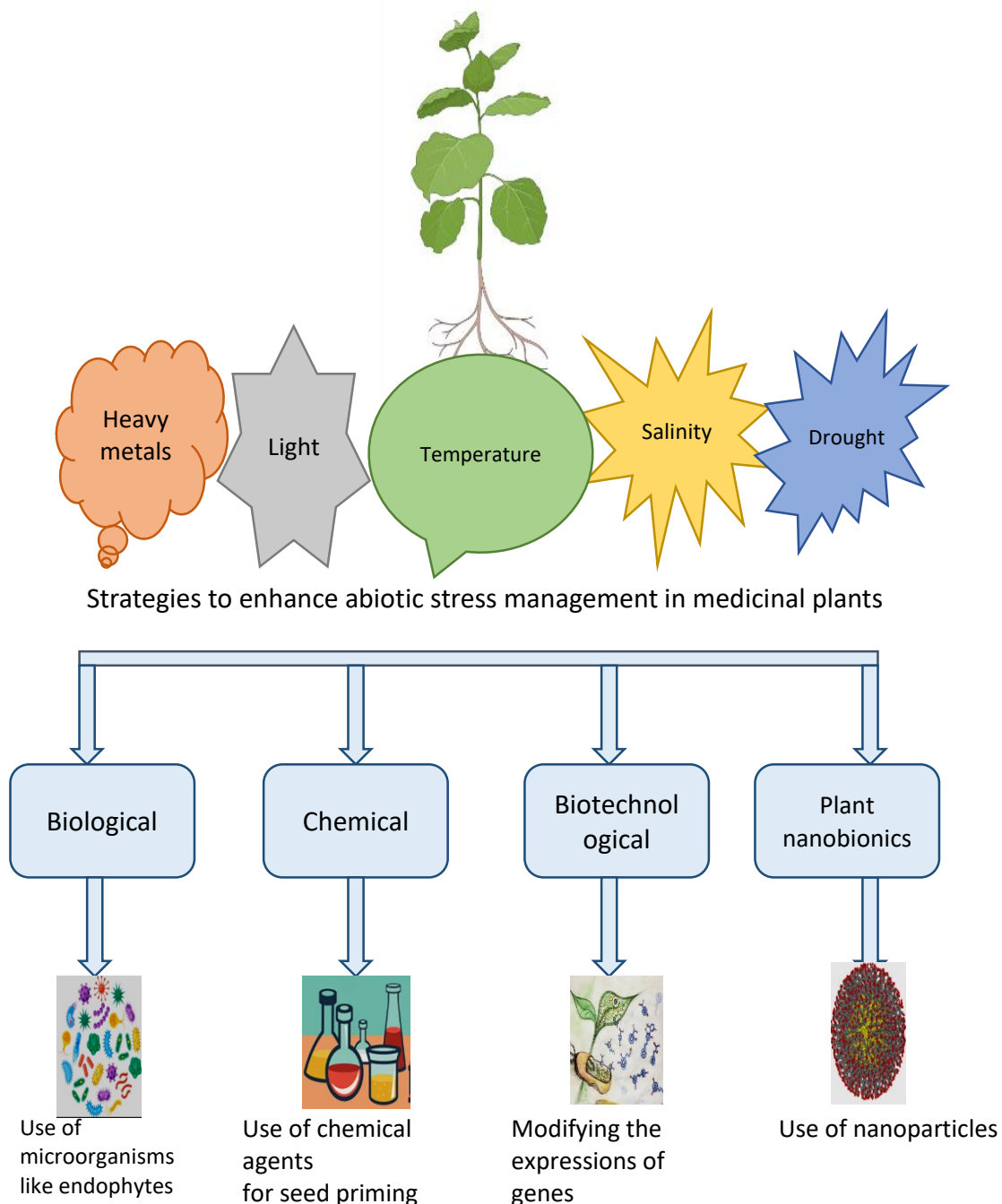


Figure 2- Strategies enhancing the ability of plants to tolerate abiotic stress

- iv. **Plant Nanobionics:** Plant nanobionics is a field of plant science that investigates how nanoparticles (NPs) interact with plant systems to produce novel functions. NPs have sizes ranging from 1 to 100 nanometers and have a high surface energy and surface-to-volume ratio, which increases their reactivity and other biological activity thereby making them quite efficient for a number of purposes. NPs also have the potential to protect plants from a variety of abiotic stresses. Abiotic stresses make photosynthesis particularly sensitive; nevertheless, NMs have been shown to preserve the photosynthetic system and promote photosynthesis by reducing oxidative and osmotic stress (Siddiqui et al. 2014). NPs are also being intensively studied for their ability to help medicinal plants to accumulate valuable secondary metabolites (Paramo et al. 2020). Silver NPs (AgNPs) were observed to augment the ability to bear drought stress in *Thymus daenensis* and *Thymus vulgaris* L. along with enhanced germination and increased length of roots during 200 mM saline conditions (Ghavam 2019). Spraying Iron oxide (Fe_2O_3) NPs in plants of *Dracocephalum moldavica* L. under salt stress (100 mM of NaCl) noticeably improved the canopy, enhanced the rate at which SMs were formed and also improved the antioxidant enzymatic activities (Moradbeygi et al. 2020). Besides, for this plant, Fe_2O_3 NPs can also serve as a basis of Fe supply to this plant. Application of Fe_3O_4 NPs can also assuage toxicity induced by Cd and Pb in the leaves of coriander plants (Fahad et al. 2020). Titanium dioxide (TiO_2) NPs have also been studied for their effects on plants. *Verbascum sinuatum* plants on being treated with TiO_2 were able to alleviate negative effects of exposure to artificial drought and increased the number of pigments assimilated due to stimulation of antioxidant defence systems (Karamian et al. 2020). In contrast to this, the amount of pigments assimilated in the leaves of *Dracocephalum moldavica* plants were reduced significantly when treated with TiO_2 NPs of size 10 ppm (Mohammadi et al. 2016). Additionally, applying 10 ppm TiO_2 NPs on the leaves of *Dracocephalum moldavica* L. plants growing in drought conditions resulted in enhanced dry mass of the shoot and EO content. Plants growing in water deficient conditions in presence of 10 ppm TiO_2 NPs, showed higher concentrations of proline and lower amount of H_2O_2 signifying that TiO_2 NPs are capable of diminishing oxidative damages caused by water deficiency. Under salinity stress, the use of silicon nanoparticles has been demonstrated to have promising impacts on physiological and morphological aspects of basil vegetative properties. Treating basil with silicon nanoparticles and silicon fertilizer, showed a considerable improvement in growth metrics, chlorophyll content, and proline level under salt stress (Kaltech et al. 2014). Reduced Na^+ ion concentration, possibly by lowering Na^+ ion absorption by plant tissues, is a possible approach used by silica nanoparticles to ameliorate salinity stress in plants (Saxena et al. 2016).

4. Conclusions

For thousands of years, secondary metabolites produced by medicinal plants have served as raw materials for the production of pharmaceutical compounds and treatment of several diseases by local communities across the globe. Plants produce SMs as a defence mechanism to combat the conditions of environmental stress. Stresses might lead to change in the quality of the SMs produced by plants along with their quantity. The modification in the quantity and quality of SMs synthesized by plants during stress conditions varies from plant to plant. From the present overview it can be concluded that the production of secondary metabolites can be optimized in plants by exposing them to different kinds of stresses. However, it is extremely necessary to understand that plants can deal with stresses only to a certain extent and extreme stress events lead to the death of plants. Therefore, to protect the plants from the conditions of extreme stress, several biological, chemical and biotechnological methods can be used. In addition to these well known methods, plant nano bionics has also emerged as a new method that helps plants in tolerating or managing stresses. This field is still in its infancy and requires extensive research before being introduced to field conditions.

Acknowledgements

Authors are thankful towards CSIR and Scientist in Charge, CIMAP, Pantnagar

References

- Abate L, Bachheti R K, Tadesse M G & Bachheti A (2022). Ethnobotanical Uses, Chemical Constituents, and Application of *Plantago lanceolata* L. *Journal of Chemistry* 22: 1532031. <https://doi.org/10.1155/2022/1532031>
- Abd El-Azim W M & Ahmed S T H (2009). Effect of salinity and cutting date on growth and chemical constituents of *Achillea fragratissima* Forssk, under RasSudr conditions. *Research Journal of Agriculture and Biological Sciences* 5(6): 1121-1129
- Abubakar I B, Malami I, Yahaya Y & Sule S M (2018). A review on the ethnomedicinal uses, phytochemistry and pharmacology of *Alpinia officinarum* Hance. *Journal of ethnopharmacology* 224: 45-62. DOI: 10.1016/j.jep.2018.05.027
- Alavi-Samani S M, Kachouei M A & Pirbalouti A G (2015). Growth, yield, chemical composition, and antioxidant activity of essential oils from two thyme species under foliar application of jasmonic acid and water deficit conditions. *Horticulture Environment and Biotechnology* 56(4): 411-420. DOI:10.1007/s13580-015-0117-y
- Ali R M, Elfeky S S & Abbas H (2008). Response of salt stressed *Ricinus communis* L. to exogenous application of glycerol and/or aspartic acid. *Journal of Biological Sciences* 8(1): 171-175. DOI: 10.3923/jbs.2008.171.175
- Anasori P & Asghari G (2008). Effects of light and differentiation on gingerol and zingiberene production in callus culture of *Zingiber officinale* Rosc. *Research in Pharmaceutical Sciences* 3: 59-63
- Arbona V & Gómez-Cadenas A (2015). Metabolomics of disease resistance in crops. *Current Issues in Molecular Biology* 19:13-29
- Azhar N, Hussain B, Ashraf Y M & Abbasim K Y (2011). Water stress mediated changes in growth, physiology and secondary metabolites of desi ajwain (*Trachyspermum ammi*). *Pakistan Journal of Botany* 43(9): 15-19

- Baatour O R, Kaddour W, Wannas A, Lachaal M & Marzouk B (2010). Salt effects on the growth, mineral nutrition, essential oil yield and composition of marjoram (*Origanum majorana*). *Acta Physiologiae Plantarum* 32(1): 45-51. DOI: 10.1007/s11738-009-0374-4
- Bharti V K, Malik J K & Gupta R C (2016). Ashwagandha: Multiple health benefits. *Nutraceuticals Efficacy, Safety and Toxicity* pp. 717-733
- Bhat M A, Ahmad S, Aslam J, Mujib A & Mahmooduzzfar (2008). Salinity stress enhances production of solasodine in *Solanum nigrum* L. *Chemical and Pharmaceutical Bulletin* 56(1): 17-21. DOI: 10.1248/cpb.56.17
- Boukhatem M N, Ferhat M A, Kameli A, Saidi F & Kebir H T (2014). Lemon grass (*Cymbopogon citratus*) essential oil as a potent anti-inflammatory and antifungal drugs. *Libyan Journal of Medicine* 9(1):25431. DOI: 10.3402/ljm.v9.25431
- Bourgou S, Kchouk M E, Bellila A & Marzouk B (2010). Effect of salinity on phenolic composition and biological activity of *Nigella sativa*. *Acta Horticulturae* 853: 57-60. DOI: 10.17660/ActaHortic.2010.853.5
- Brant S M G (2016). Nutraceuticals in hepatic diseases. *Nutraceuticals Efficacy, Safety and Toxicity* pp. 87-99
- Casal J J & Yanovsky M J (2005). Regulation of gene expression by light. *The International Journal of Developmental Biology* 49: 501-511. Doi: 10.1387/ijdb.051973jc
- Chan L K, Koay S S, Boey P L & Bhatt A (2010). Effects of abiotic stress on biomass and anthocyanin production in cell cultures of *Melastoma malabathricum*. *Biological Research* 43: 27-135. PMID: 21157639 <http://dx.doi.org/10.4067/S0716-97602010000100014>
- Chen Y, Guo Q, Liu L, Liao L & Zhu Z (2011) Influence of fertilization and drought stress on the growth and production of secondary metabolites in *Prunella vulgaris* L. *Journal of Medicinal Plants Research* 5: 1749-1755
- Cheng L, Han M, Yang L M, Yang L, Sun Z & Zhang T (2018). Changes in the physiological characteristics and baicalin biosynthesis metabolism of *Scutellaria baicalensis* Georgi under drought stress. *Industrial Crops & Products* 122: 473-482. <https://doi.org/10.1016/j.indcrop.2018.06.030>
- Cheyrier V, Comte G, Davies KM, Lattanzio V & Martens S (2013). Plant phenolics: recent advances on their biosynthesis, genetics, and ecophysiology. *Plant Physiology and Biochemistry* 72: 1-20. <https://doi.org/10.1016/j.plaphy.2013.05.009>
- Cik J K, Klejdus, B, Hedbavny J & Backor M (2009). Salicylic acid alleviates NaCl-induced changes in the metabolism of *Matricaria chamomilla* plants. *Ecotoxicology* 18(5): 544-554. DOI: 10.1007/s10646-009-0312-7
- Damanhour Z A & Ahmad A (2014). A review on therapeutic potential of *Piper nigrum* L. (Black pepper): The king of spices. *Medicinal and Aromatic Plants* 3:161. DOI:10.4172/2167-0412.1000161
- Edewor T I & Olajire A A (2011). The flavones from *Acanthospermum hispidum* DC and their antibacterial activity. *International Journal of Organic Chemistry* 1:132-141. DOI: 10.4236/ijoc.2011.13020
- Eichholz I, Rohn S, Gamm A, Beesk N, Herppich W B, Kroh L W, Ulrichs C & Huyskens-Keil S (2012). UV-B-mediated flavonoid synthesis in white asparagus (*Asparagus officinalis* L.). *Food Research International* 48(1):196-201. <https://doi.org/10.1016/j.foodres.2012.03.008>
- Eliasova A, Repcak M & Pastirova A (2004). Quantitative changes of secondary metabolites of *Matricaria chamomilla* by abiotic stress. *Zeitschrift für Naturforschung C* 59(7-8):543-548. DOI: 10.1515/znc-2004-7-817
- Espinoza A, San Martín A, López-Climent M, Ruiz-Lara S, Gómez-Cadenas A & Casaretto J A (2013). Engineered drought-induced biosynthesis of α -tocopherol alleviates stress-induced leaf damage in tobacco. *Journal of Plant Physiology* 170: 1285-1294. DOI: 10.1016/j.jplph.2013.04.004
- Estell R E, Fredrickson E L & James D K (2016). Effect of light intensity and wavelength on concentration of plant secondary metabolites in the leaves of *Flourensia cernua*. *Biochemical Systematics and Ecology* 65: 108-114. <https://doi.org/10.1016/j.bse.2016.02.019>
- Fahad Balouch A, Agheem M H, Memon S A, Baloch A R, Tunio A, Abdullah, Pato A H, Jagirani M S & Panah P (2020). Efficient mitigation of cadmium and lead toxicity in coriander plant utilizing magnetite (Fe₃O₄) nanofertilizer as growth regulator and antimicrobial agent. *International Journal of Environmental Analytical Chemistry* 1-12. <https://doi.org/10.1080/03067319.2020.1776861>
- Ghavam M (2019). Effect of silver nanoparticles on tolerance to drought stress in *Thymus daenensis* Celak and *Thymus vulgaris* L. in germination and early growth stages. *Environmental Stresses in Crop Sciences* 12: 555-566. DOI 10.22077/escs.2018.788.1287
- Goh H H, Khairudin K, Sukiran N A, Normah M N & Baharum S N (2015). Metabolite profiling reveals temperature effects on the VOCs and flavonoids of different plant populations. *Plant Biology* 18:130-139. DOI: 10.1111/plb.12403
- Goławska S, Sprawka I, Łukasik I & Goławski A (2014). Are naringenin and quercetin useful chemicals in pest-management strategies? *Journal of Pest Science* 87(1):173-180 doi: 10.1007/s10340-013-0535-5.
- Gurib-Fakim A (2006). Medicinal plants: traditions of yesterday and drugs of tomorrow. *Molecular Aspects of Medicine* 27(1): 1-93. DOI 10.1016/j.mam.2005.07.008
- Haghighi Z, Modarresi M & Mollayi S (2012). Enhancement of compatible solute and secondary metabolites production in *Plantago ovate* Forsk. by salinity stress. *Journal of Medicinal Plants Research* 6(18): 3495-3500. DOI: 10.5897/JMPR12.159
- Hasanuzzaman M, Hossain M A, da Silva J A T & Fujita M (2012). Plant responses and tolerance to abiotic oxidative stress: antioxidant defenses is a key factor. In: Bandi V, Shanker AK, Shanker C, Mandapaka M (eds) *Crop stress and its management: perspectives and strategies*, Springer, Berlin, pp. 261-316
- Havryliuk O, Matvieieva N, Tashyrev O & Yastremskaya L (2017). Influence of cold stress on growth and flavonoids accumulation in *Artemisia tilesii* "hairy" root culture. *Agrobiodiversity* 163-167. <http://dx.doi.org/10.15414/agrobiodiversity.2017.2585-8246.163-167>
- Hazrati S, Tahmasebi-Sarvestani Z, Modarres-Sanavy SAM, Mokhtassi-Bidgoli A & Nicola S (2016). Effects of water stress and light intensity on chlorophyll fluorescence parameters and pigments of *Aloe vera* L. *Plant Physiology and Biochemistry* 106:141-148. <https://doi.org/10.1016/j.plaphy.2016.04.046>
- Hoffmann D (2003). *Medical Herbalism: The Science and Practice of Herbal Medicine*. Healing Arts Press One Park Street, Rochester, Vermont
- Hossain M A, Alrashdi Y B A & Al Touby S (2022). A review on essential oil analyses and biological activities of the traditionally used medicinal plant *Thymus vulgaris* L. *International Journal of Secondary Metabolite* 9(1):103-111. <https://doi.org/10.21448/ijsm.1029080>
- Irani S & Todd C D (2018). Exogenous allantoin increases *Arabidopsis* seedlings tolerance to NaCl stress and regulates expression of oxidative stress response genes. *Journal of Plant Physiology* 221: 43-50. DOI: 10.1016/j.jplph.2017.11.011
- Jaafar H Z, Ibrahim M H & Mohamad F N F (2012). Impact of soil field water capacity on secondary metabolites, phenylalanine ammonia-lyase (PAL), malondialdehyde (MDA) and photosynthetic responses of Malaysian kacipfatimah (*Labisia pumila* Benth). *Molecules* 17(6): 7305-7322. <https://doi.org/10.3390/molecules17067305>
- Jaleel C A, Manivannan P, Sankar B, Kishorekumar A, Gopi R & Somasundaram R (2007). Induction of drought stress tolerance by ketoconazole in *Catharanthus roseus* is mediated by enhanced antioxidant potentials and secondary metabolite accumulation. *Colloids and Surfaces B: Biointerfaces* 60: 201-206. doi: 10.1016/j.colsurfb.2007.06.010.

- Jamil M, Lee D B, Jung K Y, Lee S C & Rha E S (2006). Effect of salt (NaCl) stress on germination and early seedling growth of four vegetables species. *Journal of Central European Agriculture* 7(2): 273-282
- Jin Z, Wang Z, Ma Q, Sun L, Zhang L, Liu Z, Liu D, Hao X & Pei Y (2017). Hydrogen sulfide mediates ion fluxes inducing stomatal closure in response to drought stress in *Arabidopsis thaliana*. *Plant Soil* 419: 141-152. <https://doi.org/10.1007/s11104-017-3335-5>
- Jochum G M, Mudge K W & Thomas R B (2007). Elevated temperatures increase leaf senescence and root secondary metabolite concentration in the understory herb *Panax quinquefolius* (Araliaceae). *American Journal of Botany* 94: 819-826. doi: 10.3732/ajb.94.5.819
- Karamian R, Ghasemlou F & Amiri H (2020). Physiological evaluation of drought stress tolerance and recovery in *Verbascum sinuatum* plants treated with methyl jasmonate, salicylic acid and titanium dioxide nanoparticles. *Plant Biosystems* 154: 277-287. <https://doi.org/10.1080/11263504.2019.1591535>
- Katerova Z, Todorova D & Sergiev I (2017). Plant Secondary Metabolites and Some Plant Growth Regulators Elicited by UV Irradiation, Light And/or Shade. *Medicinal Plants and Environmental Challenges* pp. 97–121. DOI:10.1007/978-3-319-68717-9_6
- Khan A L, Hamayun M, Hussain J, Kang S M & Lee I J (2012). The newly isolated endophytic fungus *Paraconiothyrium* sp. LK1 produces ascotoxin. *Molecules* 17: 1103–1112. doi: 10.3390/molecules17011103
- Khan M N, Mobin M, Abbas Z K & AL Mutairi K A (2016). Impact of varying elevations on growth and activities of antioxidant enzymes of some medicinal plants of Saudi Arabia. *Acta Ecologica Sinica* 36:141-148. doi:10.1016/j.chnaes.2015.12.009
- Ksouri R, Megdiche W, Debez A, Falleh H, Grignon C & Abdelly C (2007). Salinity effects on polyphenol content and antioxidant activities in leaves of the halophyte *Cakile maritima*. *Plant Physiology and Biochemistry* 45: 244-249. <https://doi.org/10.1016/j.plaphy.2007.02.001>
- Kumar D, Punetha A, Verma P P S & Padalia R C (2022). Micronutrient based approach to increase yield and quality of essential oil in aromatic crops. *Journal of Applied Research on Medicinal and Aromatic Plants* 26: 10036. <https://doi.org/10.1016/j.jarmap.2021.100361>
- Li Q, Lei S, Du K, Li L, Pang X, Wang Z, Wei M, Fu S, Hu L & Xu L (2016). RNAseq based transcriptomic analysis uncovers a-linolenic acid and jasmonic acid biosynthesis pathways respond to cold acclimation in *Camellia japonica*. *Scientific Reports* 6(1): 1-13. <https://doi.org/10.1038/srep36463>
- Li Y Q, Kong D X, Liang H L & Wu H (2018). Alkaloid content and essential oil composition of *Mahonia breviflora* cultivated under different light environments. *Journal of Applied Botany and Food Quality* 91:171-179. DOI: <https://doi.org/10.5073/JABFQ.2018.091.023>
- Liang Y, Zheng P, Li S, Li K Z & Xu H N (2018). Nitrate reductase-dependent NO production is involved in H₂S-induced nitrate stress tolerance in tomato via activation of antioxidant enzymes. *Scientia Horticulturae* 229: 207-214. <https://doi.org/10.1016/j.scienta.2017.10.044>
- Liu H, Wang X, Wang D, Zou Z & Liang Z (2011). Effect of drought stress on growth and accumulation of active constituents in *Salvia miltiorrhiza* Bunge. *Industrial Crops and Products* 33: 84-88. <https://doi.org/10.1016/j.indcrop.2010.09.006>
- Loreto F & Schnitzler J P (2010). Abiotic stress and induced BVOCs. *Trends in Plant Science* 15(3): 154-166. DOI: <https://doi.org/10.1016/j.tplants.2009.12.006>
- Ma C H, Chu J Z, Shi X F, Liu C Q & Yao X Q (2016). Effects of enhanced UV-B radiation on the nutritional and active ingredient contents during the floral development of medicinal chrysanthemum. *Journal of Photochemistry and Photobiology B: Biology* 158: 228-234. <https://doi.org/10.1016/j.jphotobiol.2016.02.019>
- Mohammadi H, Esmailpour M & Gheranpaye A (2016). Effects of TiO₂ nanoparticles and water-deficit stress on morpho-physiological characteristics of dragonhead (*Dracocephalum moldavica* L.) plants. *Acta agriculturae Slovenica* 107:385-396. DOI:10.14720/aas.2016.107.2.11
- Mohammadi H, Ghorbanpour M & Brestic M (2018). Exogenous putrescine changes redox regulations and essential oil constituents in field-grown *Thymus vulgaris* L. under well-watered and drought stress conditions. *Industrial Crops and Products* 122: 119-132. <https://doi.org/10.1016/j.indcrop.2018.05.064>
- Moradbeygi H, Jamei R, Heidari R & Darvishzadeh R (2020). Investigating the enzymatic and non-enzymatic antioxidant defense by applying iron oxide nanoparticles in *Dracocephalum moldavica* L. plant under salinity stress. *Scientia Horticulturae* 272: 109537. <https://doi.org/10.1016/j.scienta.2020.109537>
- Naghiloo S, Movafeghi A, Delazar A, Nazemiyeh H, Asnaashari S & Dadpour M R (2012). Ontogenetic variation of total phenolics and antioxidant activity in roots: leaves and flowers of *Astragalus compactus* Lam. (Fabaceae). *Bioimpacts* 2(2):105–109. DOI: 10.5681/bi.2012.015
- Nassar M I, Aboutabl E S A, Makled Y A, El-Khrisy E D A & Osman A F (2010). Secondary metabolites and pharmacology of *Foeniculum vulgare* Mill. Subsp. Piperitum. *Revistalatio americana de química* 38:2
- Neffati M & Marzouk B (2008). Changes in essential oil and fatty acid composition in coriander (*Coriandrum sativum* L.) leaves under saline conditions. *Industrial Crops and Products* 28:137-142. <https://doi.org/10.1016/j.indcrop.2008.02.005>
- Nowak M, Manderscheid R, Weigel H J, Kleinwachter M & Selmar D (2010). Drought stress increases the accumulation of monoterpenes in sage (*Salvia officinalis*), an effect that is compensated by elevated carbon dioxide concentration. *Journal of Applied Botany and Food Quality* 83:133-136
- Okigbo R N, Eme U E & Ogbogu S (2008). Biodiversity and conservation of medicinal and aromatic plants in Africa. *Biotechnology and Molecular Biology* 3(6):127-134
- Paramo L A, Feregrino-Perez AA, Guevara R, Mendoza S & Esquivel K (2020). Nanoparticles in agroindustry: Applications, toxicity, challenges, and trends. *Nanomaterials* 10: 1654. doi: 10.3390/nano10091654
- Pateraki I & Kanellis A K (2010). Stress and developmental responses of terpenoid biosynthetic genes in *Cistus creticus* subsp. creticus. *Plant Cell Reports* 29:629-41. <https://doi.org/10.1007/s00299-010-0849-1>
- Pell E J, Schlaghauser C D & Artega R N (1997). Ozone induced oxidative stress: mechanism of action and reaction. *Physiologia Plantarum* 100: 264-273. <https://doi.org/10.1111/j.1399-3054.1997.tb04782.x>
- Pradhan J, Sahoo S K, Lalotra S & Sarma R S (2017). Positive impact of abiotic stress on medicinal and aromatic plants. *International Journal of Plant Science* 12(2): 309-313. DOI: 10.15740/HAS/IJPS/12.2/309-313
- Prakash P & Gupta N (2005). Therapeutic uses of *Ocimum sanctum* Linn (Tulsi) with a note on eugenol and its pharmacological actions: a short review. *Indian Journal of Physiology and Pharmacology* 49(2):125-131
- Queslati S, Karray-Bourouai N, Attia H, Rabhi M, Ksouri R & Lachaal M (2010). Physiological and antioxidant responses of *Mentha pulegium* (Pennyroyal) to salt stress. *Acta Physiologica Plantarum* 32(2): 289-296. <https://doi.org/10.1007/s11738-009-0406-0>
- Radasci P, Inotai K, Sarosi S, Czovek P, Bernath J & Nemeth E (2010). Effect of water supply on the physiological characteristics and production of basil (*Ocimum basilicum* L.). *European Journal of Horticultural Science* 75:193-197

- Radusiene J, Karpaviciene B & Stanius Z (2012). Effect of external and internal factors on secondary metabolites accumulation in St. John's Wort. *Botanica Lithuanica* 18(2): 101-108. DOI: 10.2478/v10279-012-0012-8
- Raju S, Shah S & Gajbhiye N (2013). Effect of light intensity on photosynthesis and accumulation of sennosides in plant parts of senna (*Cassia angustifolia* Vahl.). *Indian Journal of Plant Physiology* 18:285-289. DOI: 10.1007/s40502-013-0038-7
- Rathore S, Singh N & Singh S K (2014). Influence of NaCl on biochemical parameters of two cultivars of *Stevia rebaudiana* regenerated in vitro. *Journal of Stress Physiology and Biochemistry* 10(2): 287-296
- Razgonova M P, Veselov V V, Zakharenko A M, Golokhvast K S, Nosyrev A E, Cravotto G & Spandidos DA (2019). *Panax ginseng* components and the pathogenesis of Alzheimer's disease. *Molecular Medicine Reports* 19(4): 2975-2998. <https://doi.org/10.3892/mmr.2019.9972>
- Reguera M, Z Peleg & E Blumwald (2012). Targeting metabolic pathways for genetic engineering abiotic stress-tolerance in crops. *Biochimica et Biophysica Acta* 1819: 186-194. DOI: 10.1016/j.bbagr.2011.08.005
- Reifenrath K & Müller C (2007). Species-specific and leaf-age dependent effects of ultraviolet radiation on two Brassicaceae. *Phytochemistry* 68(6): 875-885. DOI: 10.1016/j.phytochem.2006.12.008
- Sampaio B L, Edrada-ebel R, Batista F & Costa D (2016). Effect of the environment on the secondary metabolic profile of *Tithonia diversifolia*: a model for environmental metabolomics of plants. *Scientific Reports* 6: 1-11. <https://doi.org/10.1038/srep29265>
- Sanchita A & Sharma (2018). Gene Expression Analysis in Medicinal Plants under Abiotic Stress Conditions. *Plant Metabolites and Regulation under Environmental Stress* pp. 407-414. DOI: 10.1016/B978-0-12-812689-9.00023-6
- Savvides A, Ali S, Tester M & Fotopoulos V (2016). Chemical priming of plants against multiple abiotic stresses: Mission possible? *Trends in Plant Science* 21: 329-340. DOI: 10.1016/j.tplants.2015.11.003
- Saxena R, Tomar R S & Kumar M (2016). Exploring nanobiotechnology to mitigate abiotic stress in crop plants. *Journal of Pharmaceutical Sciences and Research* 8(9): 974
- Schenke D, Böttcher C & Scheel D (2011). Crosstalk between abiotic ultraviolet-B stress and biotic (flg22) stress signalling in *Arabidopsis* prevents flavonol accumulation in favor of pathogen defense compound production. *Plant Cell and Environment* 34:1849-1864. DOI: 10.1111/j.1365-3040.2011.02381.x
- Shahverdi M A, Omidi H & Tabatabaei S J (2017). Effect of nutri-priming on germination indices and physiological characteristics of stevia seedling under salinity stress. *Journal of Seed Science* 39: 353-362. <https://doi.org/10.1590/2317-1545v39n4172539>
- Sharkey T D & Yeh S (2001). Isoprene emission from plants. *Annual Review of Plant Biology* 52: 407-436. DOI: 10.1146/annurev.arplant.52.1.407
- Sherman S H & Joshee N (2022). Current status of research on medicinal plant *Scutellaria lateriflora*: A review. *Journal of Medicinally Active Plants* 11(1): 22-38 <https://doi.org/10.7275/shxv-wb39>
- Shi H, Jiang C, Ye T, Tan D-X, Reiter R J, Zhang H, Liu R & Chan Z (2014). Comparative physiological, metabolomic, and transcriptomic analyses reveal mechanisms of improved abiotic stress resistance in bermuda grass [*Cynodon dactylon* (L). Pers.] by exogenous melatonin. *Journal of Experimental Botany* 66: 681-694. DOI: 10.1093/jxb/eru373
- Shibata M, Amano M, Kawata J & Uda M (1988). Breeding process and characteristics of 'Summer Queen', a spray-type chrysanthemum. *Bulletin of the National Research Institute of Vegetables, Ornamental Plants and Tea Series A* 2: 245-255
- Shohael A L M, Ali M B, Yu K, Hahn E & Paek K (2006). Effect of temperature on secondary metabolites production and antioxidant enzyme activities in *Eleutherococcus senticosus* somatic embryos. *Plant Cell Tissue and Organ Culture* 85:219-228. <https://doi.org/10.1007/s11240-005-9075-x>
- Siddiqui M H, Al-Whaibi M & Faisal AAAlsahli (2014). Nano-silicon dioxide mitigates the adverse effects of salt stress on *Cucurbita pepo* L. *Environmental Toxicology and Chemistry* 33: 2429-2437. DOI: 10.1002/etc.2697
- Soufi S, Rezgui S & Bettaieb T (2015). Early effects of chilling stress on the morphological and physiological status of pretreated *Stevia rebaudiana* Bert. seedlings. *Journal of New Sciences, Agriculture and Biotechnology* 14(5): 467-472
- Spitaler R, Schlorhauser P D, Ellmerer E P, Merfort I, Bortenschlager S, Stuppner H & Zidorn C (2006). Altitudinal variation of secondary metabolite profiles in flowering heads of *Arnica montana* cv. ARBO. *Phytochemistry* 67(4): 409-417. DOI: 10.1016/j.phytochem.2005.11.018
- Spyridopoulou K, Fitsiou E, Bouloukosta E, Tiptiri-Kourpeti A, Vamvakias M, Oreopoulou A & Chlichlia K (2019). Extraction, chemical composition, and anticancer potential of *Origanum onites* L. essential oil. *Molecules* 24(14): 2612. <https://doi.org/10.3390/molecules24142612>
- Taiz L & Zeiger E (2006). *Plant physiology*. Sinauer Associates Inc., Sunderland, Massachusetts, USA.
- Vashisth D, Kumar R, Rastogi S, Patel V K, Kalra A, Gupta M M, Gupta AK & Shasany A K (2018). Transcriptome changes induced by abiotic stresses in *Artemisia annua*. *Scientific Reports* 8: 3423. <https://doi.org/10.1038/s41598-018-21598-1>
- Verma N & Shukla S (2015). Impact of various factors responsible for fluctuation in plant secondary metabolites. *Journal of Applied Research on Medicinal and Aromatic Plants* 2:105-113. doi:10.1016/j.jarmap.2015.09.002
- Volkova L, Tausz M, Bennett L T & Dreyer E (2009). Interactive effects of high irradiance and moderate heat on photosynthesis, pigments, and tocopherol in the tree-fern *Dicksonia antarctica*. *Functional Plant Biology* 36:1046. <https://doi.org/10.1071/FP09098>
- Weathers P J & Towler M J (2012). The flavonoids casticin and artemetin are poorly extracted and are unstable in an *Artemisia annua* tea infusion. *Planta Medica* 78(10):1024-1026. DOI: 10.1055/s-0032-1314949
- Yang B & Li J (2011). Responses of the secondary metabolites contents in the leaves of *Myricarubra* cv. Dongkui to light and water stress. *Journal of Henan Agricultural Sciences* 40(7): 118-122
- Yang L, Wu L, Chang W, Li Z, Miao M, Li Y, Yang J, Liu Z & Tan J (2018). Overexpression of the maize E3 ubiquitin ligase gene ZmAIRP4 enhances drought stress tolerance in *Arabidopsis*. *Plant Physiology and Biochemistry* 123: 34-42. <https://doi.org/10.1016/j.plaphy.2017.11.017>
- Yin L, Zhao C, Huang Y, Yang R Y & Zeng Q P (2008). Abiotic stress-induced expression of artemisinin biosynthesis genes in *Artemisia annua* L. Chin. *Journal of Applied Environmental Biology* 14(1): 1-5
- Zhang L X, Guo Q S, Chang Q S, Zhu Z B, Liu L & Chen Y H (2015). Chloroplast ultrastructure, photosynthesis and accumulation of secondary metabolites in *Glechoma longituba* in response to irradiance. *Photosynthetica* 53(1): 144-153. <https://doi.org/10.1007/s11099-015-0092-7>
- Zhao B T, Kim T I, Kim Y H, Kang J S, Min B S, Son J K, et al. (2018). A comparative study of *Mentha arvensis* L. and *Mentha haplocalyx* Briq. by HPLC. *Natural Product Research* 32(2):239-242. <https://doi.org/10.1080/14786419.2017.1343325>

Zhou R, Su W H, Zhang G F, Zhang Y N & Guo X R (2016). Relationship between flavonoids and photoprotection in shade-developed *Erigeron breviscapus* transferred to sunlight. *Photosynthetica* 54(2): 201-209. <https://doi.org/10.1007/s11099-016-0074-4>



© 2022 by the author(s). Published by Ankara University, Faculty of Agriculture, Ankara, Turkey. This is an Open Access article distributed under the terms and conditions of the Creative Commons Attribution (CC BY) license (<http://creativecommons.org/licenses/by/4.0/>), which permits unrestricted use, distribution, and reproduction in any medium, provided the original work is properly cited.



Effect of Parental Genotypes and Their Reciprocal Crosses on Haploid Plant Production by Anther Culture and Confirmation of Double Haploids by Flow Cytometry in Bread Wheat

Hussein Abdullah AHMED AHMED^{a*} , Güray AKDOĞAN^{a*} , Sancar Fatih ÖZCAN^b , Surendra BARPETE^{a,c} 

^aDepartment of Field Crops, Faculty of Agriculture, Ankara University, Ankara, TURKEY

^bCentral Research Institute for Field Crops, Ministry of Food, Agriculture and Livestock, Ankara, TURKEY

^cInternational Center for Agricultural Research in the Dry Areas-Food Legume Research Platform, Amlaha-466113, Sehore, INDIA

ARTICLE INFO

Research Article

Corresponding Authors: Hussein Abdullah AHMED AHMED, Güray AKDOĞAN, E-mail: hahmet@agri.ankara.edu.tr, gakdogan@agri.ankara.edu.tr

Received: 13 November 2020 / Revised: 26 May 2021 / Accepted: 27 May 2021 / Online: 01 September 2022

Cite this article

AHMED AHMED H A, AKDOĞAN G, ÖZCAN S F, BARPETE S (2022). Effect of Parental Genotypes and Their Reciprocal Crosses on Haploid Plant Production by Anther Culture and Confirmation of Double Haploids by Flow Cytometry in Bread Wheat. *Journal of Agricultural Sciences (Tarim Bilimleri Dergisi)*, 28(3):363-371. DOI: 10.15832/ankutbd.825434

ABSTRACT

Double haploids (DHs) production and utilization is an important aspect of wheat breeding programs in worldwide, because, it provides many advantages over the conventional breeding program. Therefore, in vitro and in vivo responses of anther derived two bread wheat cultivars and their F1 crosses were investigated. Results showed significant genetic variation among the tested bread wheat genotypes. The pre-cold treated anther derived embryonic calli and shoot induction (%) were obtained from all genotypes that ranged 44 - 76% and 32 - 58% respectively. The highest shoot induction from embryonic calli was achieved from F1 cross of Zubkov x Atay-85, whereas, lowest induction was obtained from Atay-85 cultivar. The F1 cross (Zubkov x Atay-85) showed a

better response in anther culture in term of shoots per plant and root induction than their respective parental genotypes.

The present results indicated positive and significant heterotic effects of F1 crosses for calli and shoot induction that also showed less albino plant regeneration after colchicine treatments. Total number of 114 anthers driven DHs lines from two genotypes and their F1 crosses were regenerated, confirmed by flow-cytometry and evaluated under field condition. Some DHs lines were found to be significantly superior for agronomical traits including seed yield than the parental genotypes as well as local bread wheat (control) cultivars.

Keywords: Anther culture, Bread wheat, Colchicine, Double haploid, *Triticum aestivum* L.

1. Introduction

Bread wheat (*Triticum aestivum* L.) is one of the most cultivated cereals crop in worldwide including Turkey. The global wheat production is 761.5 million tonnes during 2019 (FAO 2020). Hexaploid (2n=6x=42) bread wheat is an important source of protein, vitamin, and mineral, as well as carbohydrate content for human consumption (Sun et al. 2014). Bread wheat genetic structure is highly affected under adverse agro-ecological conditions in the term of its yield potential. Therefore, there is always a need for wheat varieties that adapt well to regional ecologies, resistant to diseases and pests, tolerant to stress factors such as drought, cold and salinity (Mahmood & Baenziger 2008; Chauhan & Khurana 2011; Başer et al. 2020; Gebremariam et al. 2020; Liu et al. 2020). In conventional wheat breeding programs, many factors affect the development of homozygous lines (variety) after hybridization i.e. improper selection of parents for breeding purposes, genetic dependence of available genetic resources, and success of interspecific and intraspecific crosses for desired agronomical traits. Therefore, there is need to develop efficient double haploid (DH) technology that accelerates the wheat breeding for desirable agronomic traits including yield (Lantos et al. 2013; Asif et al. 2014).

In this aspect, development of haploid plants from hybrids and followed by chromosome doubling by colchicine, paved the way for accelerating the process of pure wheat lines development (Hansen & Andersen 1998; Jarzina et al. 2017). These DHs lines can be utilized as a recombinant wheat genotype with desired gene combinations. Moreover, the double haploid technique can be supplemented with modern technology i.e. gene transformation (Chauhan & Khurana 2011), development of a functional marker CAPS (Yue et al. 2015), identify the molecular markers (Abd El-Fatah et al. 2017) and applied CRISPR system for induction of improve starch quality (Liu et al. 2020) for further improvement and releasing of new bread wheat varieties.

It is well-established fact that anther culture is useful for DHs production in many cultivated crops including wheat. The microspore and anther culture have been widely used to produce haploid followed by DHs plants in wheat program (Gurel et al. 1993; Jauhar et al. 2009; Lantos et al. 2013; Asif et al. 2014; Jarzina et al. 2017). Moreover, chromosome elimination through wide-crosses between genetic incompatible species (wheat and maize or barley) can produce wheat haploids, therefore, well-trained person with controlled conditions required for embryo rescue techniques for fertile and haploid plant regeneration (Jarzina et al. 2017). Doubled haploids developed through colchicine-induced chromosomal doubling leads to the completely homozygous lines production in a single generation and saves at least 5-6 growing season of self-pollinated crop and labour cost for developing completely homozygous lines (Hassawi et al. 2005). On the other hand, anther culture has many difficulties such as, high genotype dependency as well as low frequency of haploid plant regeneration due to complicated in vitro manipulation steps including anther culture condition, growth regulators and media combinations (Gurel et al. 1993; Hansen & Andersen 1998; Redha et al. 2000; Patel et al. 2004; Jauhar et al. 2009; Lantos et al. 2013; Asif et al. 2014; Jarzina et al. 2017).

Almost all the researchers working on the development of haploid plants emphasised that anther culture is a tedious work due to genotype effect, which is the main limiting factor of in vitro androgenesis and makes this technique too expensive for routine purposes (Yermishina et al. 2004). Therefore, it is suggested that tissue culture responsive genotypes should be utilized for anther culture (Andersen et al. 1988). Although, responsiveness of parental genotype to anther culture also affects the response of hybrid combinations, there are evidence that F1 hybrids have a higher androgenetic capacity than the parental genotypes (Zamani et al. 2003). Therefore, this study aimed to screen in vitro anther culture responses of Atay-85 and Zubkov cultivars and their reciprocal crosses.

2. Material and Methods

2.1. Plant materials

In the present study, four hexaploid bread winter wheat genotypes namely Zubkov and Atay-85 cultivars, F1 hybrids of Zubkov × Atay-85 and Atay-85 × Zubkov were used as plant materials. Twenty-five seeds of each genotype were sown in pots filled with sterilized soil under glass-house condition at Department of Field Crops, Faculty of Agriculture, Ankara University, Ankara, Turkey. The bread winter wheat genotypes were obtained from Central Research Institute of Field Crops, Ministry of Food, Agriculture and Livestock, Ankara, Turkey. All the necessary care (irrigation, fertilizer) were taken for the healthy growth of the donor wheat plants. The plants were foliar sprayed with commercial foliar fertilizers NPK (20:20:20) solution.

2.2. Harvesting of spikes

One of the most important factors affecting the rate of double haploid production through anther culture is the microspore development and selection phase at the time when the donor plant spikes were harvested. For cytological examination, a drop of 1.0% acetocarmin was placed on the anthers taken from flowers and viability were examined under a light microscope. On the basis of morphological observation, the spikes were harvested when the distance between the flag leaf and below leaf around 3-5 cm on the donor plants. The spikes were collected at the uninucleate microspores stage (after tetrad stage) and placed in a plastic beaker filled with sterilized double distilled water and subjected to cold treatment (4 °C) for 4 days.

2.3. Anther isolation

After the cold treatment, the spikes were surface-sterilized with 2% commercial bleach (sodium hypochlorite) in a laminar air flow for 20 minutes and rinsed 3×5 minutes with sterilized double distilled water. More than 300 sterilized anthers of each genotypes were aseptically isolated and transferred to disposable petri dish (60 mm x 15 mm) containing 5 mL of CHB3 liquid medium supplemented with 2 mg/L 2,4-D, 2 mg/L kinetin and 90 g/L maltose (Table 1). The cultures were incubated at 25±1 °C under dark condition for 4-5 weeks.

Table 1- Composition of the embryogenic callus induction medium (CHB3), Shoot regeneration medium (SRM4) and Rooting medium (RM2)

<i>Chemical Compounds*</i>	<i>Embryogenic callus-induction media (CHB3) (mg/L)</i>	<i>Regeneration media (SRM4) (mg/L)</i>	<i>Shoot elongation and rooting media (RM2) (mg/L)</i>
Vitamins			
Myo-inositol	300	100	100
Pyridoxine HCl	0.5	5	0.4
Nicotinic acid	0.5	5	0.4
Thiamine HCl	2.5	1	0.4
Pantothenic acid	0.25	-	-
Ascorbic acid	0.25	-	0.4
Biotine	0.25	-	0.4
Macro-elements			
KNO ₃	1415	1000	1900
(NH ₄)SO ₄	232	-	-
KH ₂ PO ₄	200	300	170
MgSO ₄ .7H ₂ O	93	71	370
CaCl ₂ .2H ₂ O	83	-	440
NH ₄ NO ₃	-	1000	164
Ca(NO ₃)4H ₂ O	-	500	-
KCl	-	65	-
Micro-elements			
KI	0.4	0.75	0.83
MnSO ₄ .4H ₂ O	5	4.9	22.3
Na ₂ MoO ₄ .2H ₂ O	0.012	0.2	0.25
ZnSO ₄ .7H ₂ O	5	2.7	8.6
CuSO ₄ .5H ₂ O	0.025	0.076	0.025
CoCl ₂ .6H ₂ O	0.025	0.05	-
H ₃ BO ₃	5	1.6	6.2
Iron source			
FeSO ₄ .7H ₂ O	20	20	20
Na ₂ EDTA	20	20	20
Hormones			
2,4-Dichlorophenoxyacetic acid	2	-	-
Kinetin	2	-	-
IAA	-	1	1
Amino acid			
Glycine	1	2	-
Glutamine	993.5	-	750
Carbon source			
Maltose	90000	-	-
Sucrose	-	20000	20000
Agarose	-	6500	-
Other Material			
Agar	-	-	6000
pH	5.4	5.9	5.8

*: Modified chemical composition of the medium (Picard & De Buyser 1973)

2.4. Embryogenic callus induction and plant regeneration

The anthers were swollen and whitened after one week of culture inoculation. The appearance of embryogenic callus on the anther surface was observed after 4-5 weeks of culture. The embryonic calli were then transferred to agarose solidified regeneration medium (SRM4 medium; Picard & De Buyser 1973) supplemented with 20 g/L sucrose and 1 mg/L IAA in petri dishes and incubated at 25±1 °C with 16/8 h light/dark cycle for 7-8 weeks. The green and healthy plantlets were transferred for shoot elongation and rooting medium (RM2) for 3-4 weeks. The regenerated green plantlets with poor root systems were subcultured on fresh RM2 medium.

2.5. Acclimatization of in vitro plantlets

The plantlets with well established root-shoot system and reach a height of 10-12 cm in the culture vessels were transferred to pots containing peat-moss and perlite mixture (2:1), under 16/12 °C day/night temperature with 80% relative humidity for 2 weeks. The relative humidity was periodically decreased and successfully acclimatized plants were transferred to larger pots containing sterilized field soil.

2.6. Colchicine treatment and production of doubled haploid

The healthy haploid plants were taken from the pots (soil grown) and thoroughly washed with tap water, especially root parts. The root and shoots were trimmed and then immersed in 0.2% colchicine solution for 4 h at room temperature (Pauk et al. 2003; Tadesse et al. 2013). After colchicine treatment, the plants were rinsed with running tap water for 3-4 hours. Thereafter, the plants were transplanted in pots containing peat-moss and perlite mixture (2:1) and covered with transparent polythene bags to create relative humidity. All survived plants were grown until they reach physiological maturity. DH plants were confirmed by Flow Cytometry. The percentage of DHs were calculated by number of regenerated shoots per explant and haploid plant development. The seeds were harvested from mature plants and kept separately.

2.7. Determination of DHs plant through flow cytometry

Determination of ploidy levels in DHs plants were confirmed by flow cytometry (Sysmex UF-100, TOA Medical Electronics/Europe GmbH, Hamburg, Germany) device (Battistelli et al. 2013). The DNA were extracted from the young leaf of the DHs plant and haploid (control) plant. For DNA extraction, leaves were crushed in 0.4 mL of nuclei extraction buffer and incubated for 1 minute at room temperature. The solution was filtered through cellTrics (Sysmex Partec GMBh, Germany) and added 1.6 mL staining buffer (DAPI), and then incubated for 1 min in dark condition. The prepared samples were loaded on the cytometry device and data were recorded.

2.8. Statistical analysis

Each treatment had 15 replicates with 20-30 anthers. Data given in percentage were normalized through arcsine (\sqrt{X}) transformation (Snedecor & Cochran 1967) before statistical analysis, and all data were analyzed with ANOVA and compared via Duncan's multiple range test using SPSS statistical (IBM® SPSS® statistics 24.0 for Windows) analysis at the 5% level of significance.

3. Results and Discussion

The biotechnological techniques especially tissue culture have excellent potential to improve the bread wheat quality through genetic transformation, somaclonal production and DHs production (Tadesse et al. 2013; Jarzina et al. 2017). However, the dedifferentiation (callus induction) and redifferentiation (plant regeneration) is influenced by many factors including extrinsic supply of macro and micronutrients, and growth regulators in culture medium (Barpete et al. 2020). Table-1 depicts that CHB3 medium (Picard & De Buyser 1973) for embryogenic callus induction from sterilized anthers, nutrient media for plant regeneration (SRM4) and shoot elongation and rooting media (RM2). Analysis of variance results showed a significant difference among genotypes ($P \leq 0.05$) on embryonic callus formation (%), shoot induction (%), number of regenerated shoots and roots induction (%) and production of double haploid plants (Table 2).

Table 2- The effect of genotype on callus induction, plant regeneration and doubled haploid plant production

Genotypes and crosses	Embryogenic callus- induction (%)	Shoot-induction (%)	Number of regenerated shoots per embryogenic calli (%)	Root induction (%)	Double Haploid plants production (%)
	CHB3 media*		SRM4 media*	RM2*	
Zubkov	74a	54ab	5.7a	10.6a	4.6
Atay-85	44b	32c	2.4b	5.4b	1.6
F1 (Zubkov x Atay-85)	76a	58a	6.3a	12.4a	5.3
F1 (Atay-85 x Zubkov)	66a	44bc	3.0b	2.8b	1.0

*: Values shown in a columns followed by different letters are statistically different using Duncan's multiple range test at 0.05 level of significance

3.1. Embryogenic callus induction

Anthers of four bread winter wheat genotypes were cultured on modified CHB3 medium supplemented with 2 mg/L 2,4-D and 2 mg/L kinetin for embryogenic callus induction. The results showed a significant difference among cultivars and their F1 hybrid ($P \leq 0.05$) on embryogenic callus induction (Table 2). The embryogenic callus induction was initiated after 3-4 weeks of culture inoculation in CHB3 medium, thereafter, it was observed that the callus size increased significantly. The calli size in the term of anther's genotypes were not significantly differ among wheat genotypes (Figure 1d, e and f). The embryogenic callus induction ranged from 44 to 76% depending on genotypes. The highest callus induction was noted on F1 hybrid of Zubkov x Atay-85, whereas, lowest induction was recorded on Atay-85 cultivar. Moreover, comparing Zubkov and Atay-85 cultivars, Zubkov and their F1 hybrid were superior for embryonic callus development and further culture growth. The present results are in line with the previous studies by Ahmet & Adak (2007), El-Hennawy et al. (2011), Xynias et al. (2014) and Yorgancılar et al. (2016). They also noticed that wheat F1 hybrids were superior to its respective parents.

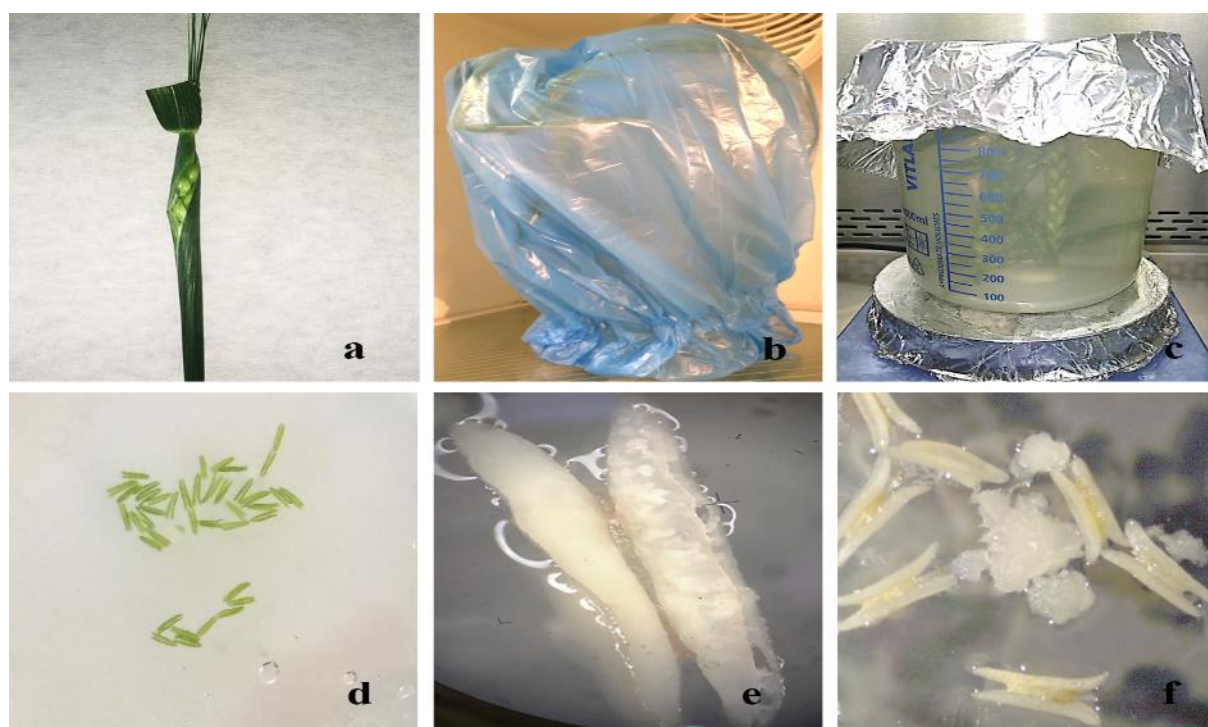


Figure 1- Anther culture technique: a) harvesting of spikes from donor plants, b) cold treatment of spikes, c) surface sterilization of spikes, d) isolation of anthers, e & f) in vitro culture and initiation of embryonic callus

3.2. Shoot induction from anther derived calli

The CHB3 medium was also very responsive for shoot initiation on embryogenic callus and small shoots were observed approximately 5-6 weeks of culture inoculation (Figure 2a, b and c). The callus derived small shoots were further transferred to shoot regeneration (SRM4) media. The analysis of results showed a significant difference among cultivars and F1 hybrids ($P \leq 0.05$) on shoot induction (%) and number of shoots per explant that were ranged from 32–58% and 2.4–6.3, respectively (Figure 2d, e and f). It was well established that generally F1 hybrids always exhibited positive heterosis over their parent when they intraspecific crossed (Ozbay & Özgen 2010). Therefore, F1 hybrid of Zubkov x Atay-85 bread winter wheat showed superior for embryonic callus developments. The highest shoot induction and number of shoots per explant were recorded on F1 hybrid of Zubkov x Atay-85 cultivars. Whereas, the lowest shoot regeneration and number was recorded on Atay-85 cultivar, but, there were no inhibitory effect on growth of regenerated shoots. The all regenerated shoots were healthy and green are in agreement with Ahmet & Adak (2007) and Jarzina et al. (2017). The researchers also recovered green and healthy shoots from anther derived calli of Polish winter and spring wheat varieties and their F1 hybrid. In the present study, rooting was significantly promoted in F1 hybrid (Zubkov x Atay-85) when subcultured on RM2 medium containing 1 mg/L IAA followed by Zubkov cultivar. Root induction were ranged from 2.8 to 12.4% and minimum root induction was noted on F1 hybrid of Atay-85 x Zubkov. Similar results were obtained by Konieczny et al. (2003), Barakat et al. (2012), and Al-Shaker (2013) on bread wheat varieties. They also reported that F1 hybrid always superior for rooting then their respective parental genotypes.

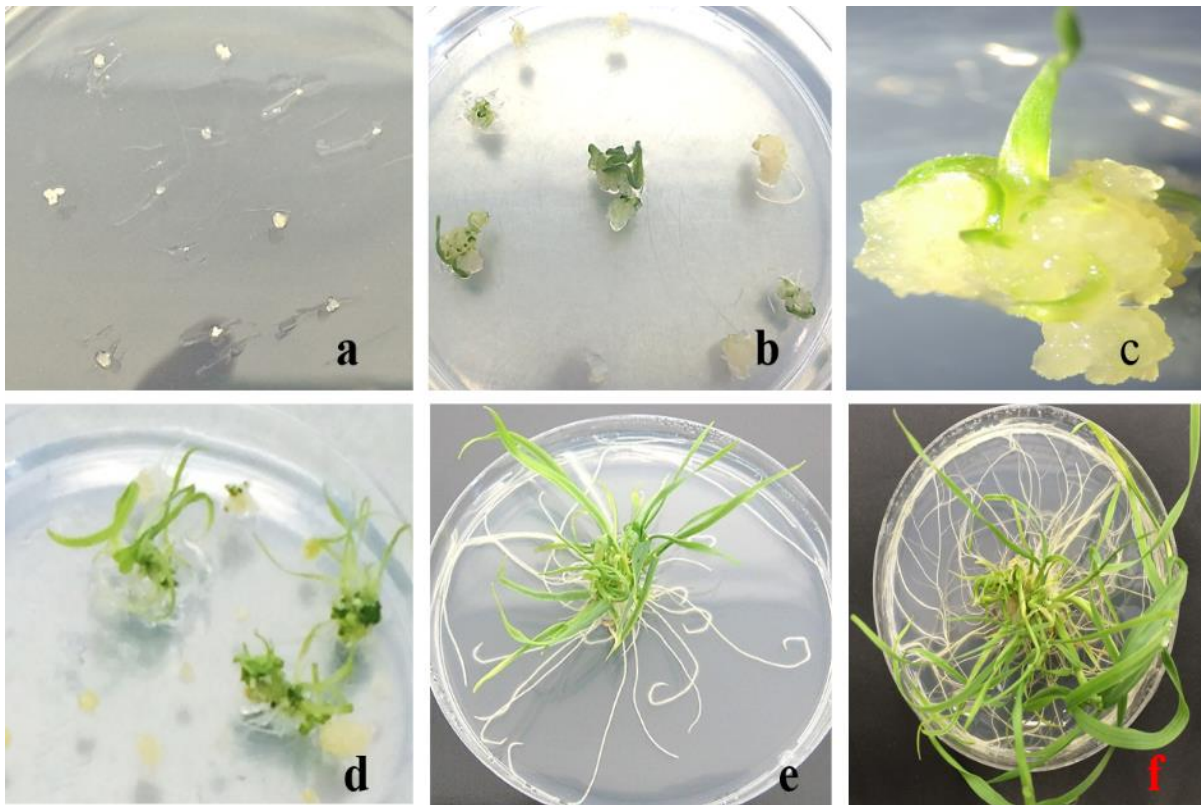


Figure 2- In vitro anther culture of different wheat genotypes and shoot regeneration; a) embryonic callus induction, b, c and d) regeneration of shoots on embryonic callus, e and f) plantlets growing and rotting on SRM4 and RM2 media

3.3. Hardening, colchicine treatment and doubled haploid plant production

The healthy and well rooted in vitro plantlets were transferred to pots for hardening in greenhouse under ambient daylight condition with 80-90% relative humidity (Figure 3a and b). The healthy acclimatized plants with 5-6 leaves were screened and taken from the pots and thoroughly rinsed with running tap water. After washing, root and shoot were trimmed and immersed in 0.2% colchicine solution (Tadesse et al. 2013) and kept at room temperature for 4 hours (Figure 3c). After colchicine treatment, the plants were washed with running tap water for 3-4 hours and then transferred into large pots containing sterilized field soil (Figure 3d, e and f) in a greenhouse and covered with transparent plastic bags for 48 hours. To avoid outcrossing, fertile heads are covered with brown bags before anthesis. Proper care taken for fertilization and irrigation until the plant physiological maturity.

The plant regeneration rate varied significantly depending on genotypes. The genotype Zubkov and F1 of Zubkov x Atay-85 showed higher plant regeneration rates than Atay-85 and F1 of Atay-85 x Zubkov. The rate of regeneration of green plants varied greatly depending on the genotypes. The Zubkov and F1 hybrid of Zubkov x Atay-85 showed higher green plant regeneration rates compared to the genotype Atay-85 and F1 of Atay-85 x Zubkov. Moreover, the rate of albino plant also varied after colchicine treatment. The F1 hybrid of Atay-85 x Zubkov showed higher rate of albino plant than the Zubkov winter wheat cultivar.

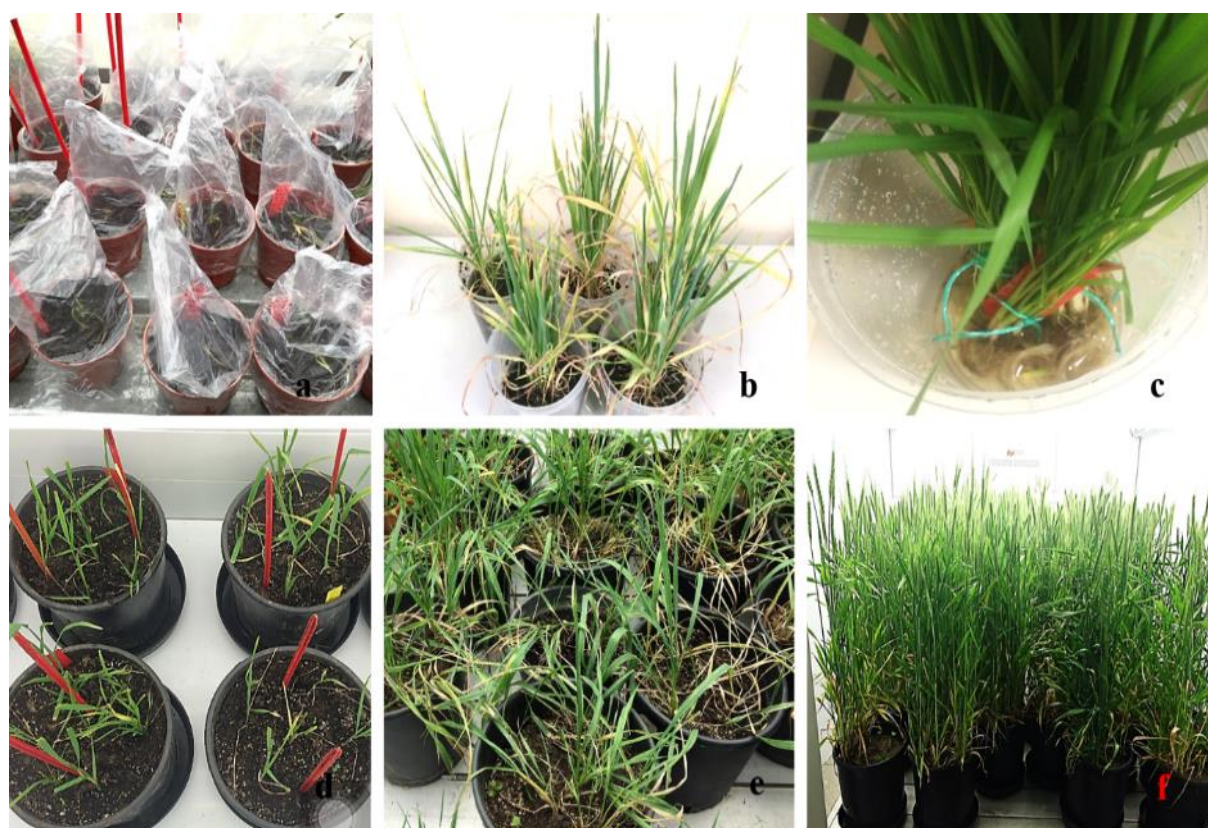


Figure 3- Double haploid plant production from bread wheat anther culture; a and b) haploid plants at acclimatization stage in a greenhouse, c) colchicine treatment of haploid wheat plants, d, e) acclimatization of DHs wheat plants, f) Growing DH wheat lines after confirmation by flow cytometry in controlled condition

A total number of 114 DH lines were obtained as a result of chromosome doubling from Atay-85 and Zubkov cultivars and their reciprocal crosses. The anther derived each DHs lines had 22-87 seeds/plant after physiological maturity. Seeds from individual DHs lines were separately harvested for genetic purity and stability in anther derived DHs lines are in contradictory with Kisana et al. (1993). They found anther-derived DHs wheat lines had cytologically unstable. Whereas, no significant differences found in anther derived and intergeneric crosses made for DHs wheat lines by Bjornstad et al. (1993). On the other hand, El-Hennawy et al. (2011) evaluated and identified highly stable and superior genotypes from anther derived DHs wheat lines. The present study also showed that anther-derived DHs lines are superior over the national control cultivar in agreement with Konieczny et al. (2003), Barakat et al. (2012), and Al-Shaker (2013).

3.4. Confirmation of DH plants by flow cytometry

The winter wheat plants with different ploidy levels including haploids and DHs were identified using flow cytometry analysis. The Figure 4a depicts that the G1 and G2 peak of haploid plant having a DNA concentration of 3.79 and 3.65 pg/2C respectively. Whereas, double haploids plant showed a DNA concentration of 4.63 and 6.02 pg/2C in G1 and G2 peaks respectively. The Figure 4a and 4b histogram displays single high peaks considered the haploid and double haploid plants. Based on the amount of DNA, the duplication (double haploid) was confirmed in regenerated plants. The rate of duplication of F1 hybrids of Zubkov x Atay-85 was also higher compared to the donor genotypes. Whereas, F1 hybrid of Atay-85 x Zubkov shown contradictory results that indicating double haploids production varies between genotypes and its combination. However, several plants (during haploid to DH stage) did not survive till the sample collection as well as physiological maturity. It may be due to toxic effect of colchicine for chromosomal doubling in agreement with Battistelli et al. (2013). A total number of 352 plants were treated with colchicine and 114 plants were survived that taken for flow cytometry analysis. The overall success rate of DH (chromosomal duplication) plant production were ranged from 1.0 to 5.33%. However, the chromosomal duplication phase was most difficult to obtain DHs plant due to higher mortality rates through anther culture in agreement with Grauda et al. (2010), Tadesse et al. (2013) and Jarzina et al. (2017).

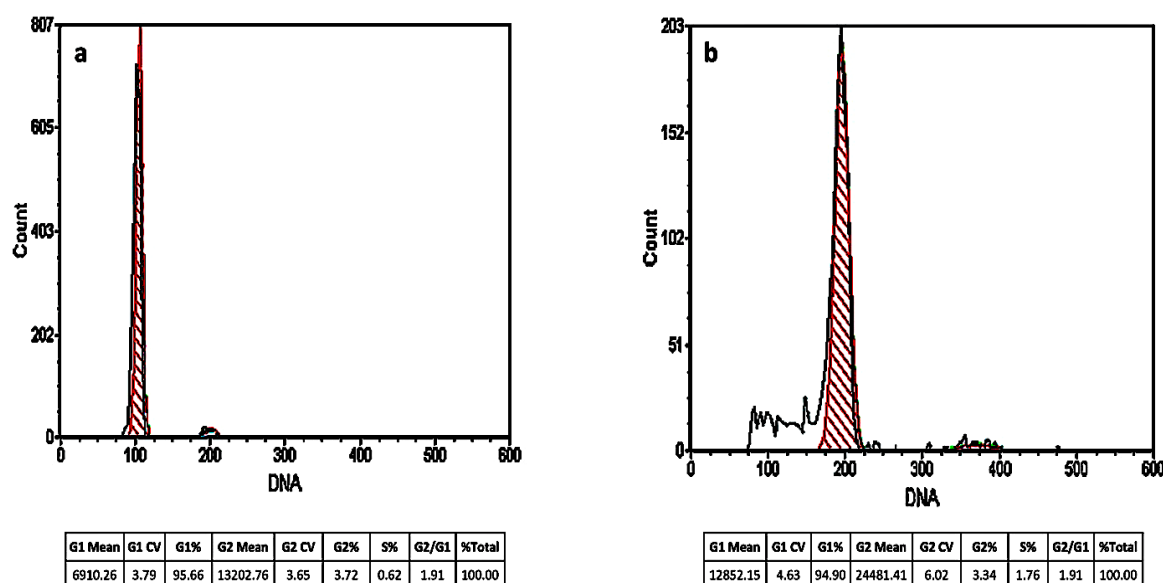


Figure 4- Flow cytometry histograms for quantification of DNA content from bread wheat leaves. a) haploid, and b) doubled haploid plants

4. Conclusions

In conclusion, we found that the donor plant genotype is one of the most important factors affecting the success rate of DHs lines production during in vitro culture and haploid plant development in bread winter wheat. The in vitro culture condition and stage of anther were more suitable for development of full fertile DHs lines. However, F1 hybrids exhibited positive heterosis over their parent when they reciprocal crossed. The outcomes of the study produced a significant number of fertile DHs wheat lines that can be used in bread wheat breeding programmes. Additionally, improved protocol and operational simplicity for production of DHs lines reduced labor requirements and cost effective.

Acknowledgements

The authors are thankful to Faculty of Agriculture, Ankara University, Ankara, Turkey for providing facility and supporting the present research work. We thank to Mikail Çalışkan and Cuma Karaoğlu (Central Research Institute for Field Crops) for ploidy analysis support.

References

- Abd El-Fatah B E S, El-Farash E M M, EL-Aref H M & Mohamed G I A (2017). Genetic analysis and detection molecular markers for response to anther culture in wheat (*Triticum aestivum* L.). *Assiut Journal of Agricultural Sciences* 48(1-1): 120-138
- Ahmet H & Adak M S (2007). Callus induction and plant regeneration in some Iraqi common wheat varieties. *Journal of Agricultural Sciences* 13(3): 285-291 (In Turkish).
- Al-Shaker I M (2013). Anther culture response and salt tolerance in some wheat genotypes. *Annals of Agricultural Science* 58(2): 139-145. <https://doi.org/10.1016/j.aos.2013.07.017>
- Andersen S B, Due I K & Olesen A (1988). Results with anther culture in some important Scandinavian varieties of winter Wheat. *Acta Agriculturae Scandinavica* 38: 289-292. <https://doi.org/10.1080/00015128809437990>
- Asif M, Eudes F, Randhawa H, Amundsen E & Spaner D (2014). Induction medium osmolality improves microspore embryogenesis in wheat and triticale. *In vitro Cellular and Developmental Biology-Plant* 50(1): 121-126. <https://doi.org/10.1007/s11627-013-9545-5>
- Barakat M N, AL-Doss A A, Elshafei A A, Moustafa K A & Ahmed E I (2012). Anther culture response in wheat (*Triticum aestivum* L.) genotypes with HMW alleles. *Cereal Research Communications* 40(4): 583-591. <https://doi.org/10.1556/crc.40.2012.0011>
- Barpete S, Gupta P, Khawar K M, Ozcan S & Kumar S (2020). In vitro approaches for shortening generation cycles and faster breeding of low β -N-oxalyl-L- α , β -diaminopropionic acid content of grass pea (*Lathyrus Sativus* L.). *Fresenius Environmental Bulletin* 29(4): 2698-2706
- Başer İ, Bilgen B B, Balkan A, Korkut Z K, Bilgin O & Gülfidan E (2020). Comparison of bread wheat genotypes for leaf rust resistance genes. *Journal of Agricultural Sciences* 26(1): 22-31. <https://doi.org/10.15832/ankutbd.447752>
- Battistelli G M, Von Pinho R G, Justus A, Couto E G O & Balestre M (2013). Production and identification of doubled haploids in tropical maize. *Genetics and Molecular Research* 12 (4): 4230-4242. <https://doi.org/10.4238/2013.october.7.9>
- Bjornstad A, Skinnis H & Thoresen K (1993). Comparisons between doubled haploid lines produced by anther culture, the Hordeum bulbosum-method and lines produced by single seed descent in barley crosses. *Euphytica* 66: 135-144. <https://doi.org/10.1007/bf00023518>
- Chauhan H & Khurana P (2011). Use of doubled haploid technology for development of stable drought tolerant bread wheat (*Triticum aestivum* L.) transgenics. *Plant Biotechnology Journal* 9: 408-417. <https://doi.org/10.1111/j.1467-7652.2010.00561.x>

- El-Hennawy M A, Abdalla A F, Shafey S A & Al-Ashkar I M (2011). Production of doubled haploid wheat lines (*Triticum aestivum* L.) using anther culture technique. *Annals of Agricultural Science* 56(2): 63-72. <https://doi.org/10.1016/j.aos.2011.05.008>
- FAO (2020). World food situation. Retrieved in July, 16, 2020 from <http://www.fao.org/worldfoodsituation/csdb/en/>
- Gebremariam E S, Karakaya A, Orakçı G E, Dababat A A & Paulitz T C (2020). Assessment of the seedling resistance of spring wheat lines to *Fusarium culmorum*. *Journal of Agricultural Sciences* 26(1): 87-93. <https://doi.org/10.15832/ankutbd.466442>
- Grauda D, Lepse N, Strazdina V, Kokina I, Lapina L, Mikelsons A, Lubinskis L & Rashal I (2010). Obtaining of doubled haploid lines by anther culture method for the Latvian wheat breeding. *Agronomy Research* 8: 545-552
- Gurel A, Tosun M & Demir I (1993). Reactions of some durum and common wheat genotypes to anther culture. *Journal of Aegean Agricultural Research Institute* 3(2): 98-111
- Hansen N J P & Andersen S B (1998). In vitro chromosome doubling with colchicine during microspore culture in wheat (*Triticum aestivum* L.). *Euphytica* 102: 101-108. <https://doi.org/10.1023/A:1018348816205>
- Hassawi D S, Qrunfleh I & Dradkah N (2005). Production of doubled haploids from some Jordanian wheat cultivars via anther culture technique. *Journal of Food, Agriculture and Environment* 3: 161-164
- Jarzina A S, Pudelska H, Woźna J & Pniewski T (2017). Improved production of doubled haploids of winter and spring triticale hybrids via combination of colchicine treatments on anthers and regenerated plants. *Journal of Applied Genetics* 58: 287-295. <https://doi.org/10.1007/s13353-016-0387-9>
- Jauhar P P, Xu S S & Baezinger P S (2009). Haploidy in cultivated wheats: induction and utility in basic and applied research. *Crop Science* 49(3): 737-755. <https://doi.org/10.2135/cropsci2008.08.0462>
- Kisana N S, Nkongolo K K, Quick J S & Johnson D L (1993). Production of doubled haploids by anther culture and wheat x maize method in a wheat breeding programme. *Plant Breeding* 110: 96-102. <https://doi.org/10.1111/j.1439-0523.1993.tb01219.x>
- Konieczny P, Czaplicki A Z, Golczyk H & Przywara L (2003). Two pathways of plant regeneration in wheat anther culture. *Plant Cell, Tissue and Organ Culture* 73: 177-187. <https://doi.org/10.1023/a:1022877807237>
- Lantos C, Weyen J, Orsini JM, Gnad H, Schlieter B, Lein V, Kontowski S, Jacobi A, Mihaly R, Broughton S & Pauk J (2013). Efficient application of in vitro anther culture for different european winter wheat (*Triticum aestivum* L.) breeding programs. *Plant Breeding* 132(1): 149-154. <https://doi.org/10.1111/pbr.12032>
- Liu H, Wang K, Jia Z, Gong Q, Lin Z, Du L, Pei X & Ye X (2020). Efficient induction of haploid plants in wheat by editing of TaMTL using an optimized *Agrobacterium*-mediated CRISPR system. *Journal of Experimental Botany* 71(4): 1337-1349. <https://doi.org/10.1093/jxb/erz529>
- Mahmood A & Baenziger P S (2008). Creation of salt tolerant wheat doubled haploid lines from wheat x maize crosses. *Cereal Research Communications* 36: 361-371. <https://doi.org/10.1556/crc.36.2008.3.1>
- Ozbay A & Özgen M (2010). Is heterosis noticeable in the callus response of winter durum wheat F1 hybrids? *Biologia Plantarum* 54: 769-772. <https://doi.org/10.1007/s10535-010-0139-3>
- Patel M, Darvey N L, Marshall D R & Berry J O (2004). Optimization of culture conditions for improved plant regeneration efficiency from wheat microspore culture. *Euphytica* 140: 197-204. <https://doi.org/10.1007/s10681-004-3036-z>
- Pauk J, Mihály R & Puolimatka M (2003). Protocol for wheat (*Triticum aestivum* L.) anther culture. In: Maluszynski M, Kasha K J, Forster B P & Szarejko I (eds) *Doubled Haploid Production in Crop Plants* pp. 59-64. doi.org/10.1007/978-94-017-1293-4_10
- Picard E & De Buyser J (1973). Obtention de plantules haploïdes de *Triticum aestivum* L. a partir de cultures d'antheres in vitro. *Comptes rendus de l'Académie des Sciences* 277: 1463-1466. [https://doi.org/10.1016/s0764-4469\(97\)89622-9](https://doi.org/10.1016/s0764-4469(97)89622-9)
- Redha A, Islam S M S, Büter B, Stamp P & Schmid J E (2000). The improvement in regenerated doubled haploids from anther culture of wheat by anther transfer. *Plant Cell Tissue and Organ Culture* 63(3): 167-172. <https://doi.org/10.1023/a:1010708529247>
- Snedecor G W & Cochran W G (1967). *Statistical Methods*. The Iowa State University Press, Iowa, USA, 327-329
- Sun F, Guo G, Du J, Guo W, Peng H, Ni Z, Sun Q & Yao Y (2014). Whole-genome discovery of miRNAs and their targets in wheat (*Triticum aestivum* L.). *BMC Plant Biology* 14: 142. <https://doi.org/10.1186/1471-2229-14-142>
- Tadesse W, Tawkaz S, Inagaki M N, Picard E & Baum M (2013). *Methods and applications of doubled haploid technology in wheat breeding*. ICARDA, Aleppo, Syria. 36 pp.
- Xynias I, Koufalis A, Gouli-Vavdinoudi E & Roupakias D (2014). Factors affecting doubled haploid plant production via maize technique in bread wheat. *ACTA Biologica Cracoviensia Series Botanica* 56(2): 1-7. <https://doi.org/10.2478/abcsb-2014-0022>
- Yermishina N M, Kremenevskaja E M & Gukasian O N (2004). Assessment of the combining ability of triticale and secalotriticum with respect to in-vitro androgenesis characteristics. *Russian Journal of Genetics* 40: 282-287. <https://doi.org/10.1023/b:ruge.0000021628.98247.2b>
- Yorgancılar Ö, Yorgancılar A, Dikmen S, Dikmen S, Çarıkçı M, Evcen F, Van F, Uzun P, Yumurtacı A, Kutlu I & Sirel Z (2016). Obtaining the pure line in F2 generation wheat using anther culture technique. *Journal of Field Crops Central Research Institute* 25 (Special issue-1): 237-242. <https://doi.org/10.21566/tarbitderg.280498>
- Yue A, Li A, Mao X, Chang X, Li R & Jing R (2015). Identification and development of a functional marker from 6-SFT-A2 associated with grain weight in wheat. *Molecular Breeding* 35(2): 63. <https://doi.org/10.1007/s11032-015-0266-9>
- Zamani I, Gouli-Vavdinoudi E, Kovacs G, Xynias I, Roupakias D & Barnabas B (2003). Effect of parental genotypes and colchicine treatment on the androgenic response of wheat F1 hybrids. *Plant Breeding* 122: 314-317. <https://doi.org/10.1046/j.1439-0523.2003.00866.x>





Characterization of Antimicrobial Peptide Fraction Producing *Lactobacillus* spp. Based on LC/MS-MS and Determination of ACE-inhibitory Activity in Kefir

Merve ATALAY^a , Didem ŞAHİNGİL^{a*}

^aDepartment of Food Engineering, Engineering Faculty, Inonu University, 44280 Malatya, TURKEY

ARTICLE INFO

Research Article

Corresponding Author: Didem ŞAHİNGİL, E-mail: didem.sahingil@inonu.edu.tr

Received: 15 February 2021 / Revised: 08 June 2021 / Accepted: 09 June 2021 / Online: 01 September 2022

Cite this article

Atalay M, ŞAHİNGİL D (2022). Characterization of Antimicrobial Peptide fraction producing *Lactobacillus* spp. based on LC/MS-MS and Determination of ACE-inhibitory activity in Kefir. *Journal of Agricultural Sciences (Tarim Bilimleri Dergisi)*, 28(3):372-384. DOI: 10.15832/ankutbd.880744

ABSTRACT

In the present study, bioactive properties such as ACE-I activity and antimicrobial activity of kefir using different *Lactobacillus* (*Lactobacillus delbrueckii* ssp. *bulgaricus* ATCC 11842, *Lactobacillus helveticus* ATCC 15009 and *Lactobacillus plantarum* ATCC 14917) on some pathogen and Gram-positive bacteria during 28 day-storage periods was investigated and proteolysis (RP-HPLC peptide profiles, RP-HPLC amino acid profiles) were studied. The antimicrobial activity was investigated in kefir extract and separated peptide fractions (<3 kDa, named F2) which were characterized by LC-MS/MS and precursor and product ions were determined. Antimicrobial activity has been observed

against pathogenic bacteria such as *Escherichia coli* (*E. coli*) in all samples. But the results revealed that the F2 fraction separated from kefir manufactured using *Lactobacillus* had a stronger antibacterial effect than control samples. It was determined that the F2 fraction has antimicrobial activity against *S. aureus*, *S. warneri* 95052 and *S. hominis*. The ACE-I activity of samples A, B, C and K were 76.47%, 84.95%, 87.33% and 85.57%, respectively. In the kefir using *Lactobacillus* has increase of ACE-I activity and was significant (P<0.01). In this study, it was concluded that the using of adjunct *Lactobacillus* contributed to the functional value of kefir.

Keywords: Bioactive peptides, In-Vitro antimicrobial peptides, ACE- I activity, purification, LC-MS/MS

1. Introduction

Kefir is a fermented dairy beverage produced by the actions of the microflora encased in the “kefir grain”, the composition differing according to the source, are a symbiotic association of a variety of bacteria and fungi, such as lactic acid bacteria, acetic acid bacteria, yeasts and molds, etc., originated thousands of years ago in the Caucasus (Pogačić et al. 2013; Purutoglu et al. 2020; Wang et al. 2021). In kefir, the predominant genus was *Lactobacillus*. Low abundant genera, such as *Leuconostoc*, *Lactococcus*, *Streptococcus*, *Acetobacter*, etc were also found from different grains. Yeasts were abundant in fungal microbiota of kefir grains and genera belonging to *Saccharomyces*, *Kazachstania*, *Kluyveromyces*, *Pichia*, etc. (Tas et al. 2012; Prado et al. 2015; Garofalo et al. 2015). The microbiota of kefir grains has been found depending several factors such as the origin of the kefir grain, grain cultivation methods, sanitation conditions, production and storage conditions (Witthuhn et al. 2004; Gul et al. 2018). Accordingly, the differences of microbiota in kefir grains can be responsible for important changes in nutritional and flavor properties of kefir product. It has been determined that milk proteins have the physiological activities by some peptides that are digested with gastric and pancreatic enzymes (Schanbacher et al. 1998). Peptides resulting from proteolysis by microorganisms in kefir grains partially responsible for the biological activity of kefir. Bioactive peptides have been proposed as health-promoting compounds and these peptides comprising 2 to 20 amino acids residues with functional and biological properties such as antihypertensive, antioxidant, antimicrobial, anticancer and opioid (Karami & Akbari-Adergani 2019; Zhu et al. 2019). Many of studies have investigated production and activity of bioactive peptides, i.e. antioxidants, antimicrobial, antithrombotic and immunomodulatory activities (Chandra & Viji 2018; Chandra et al. 2019). Among these peptides, one of the most important and widely studied is ACE-I peptides. ACE is an exopeptidase and it elicits dipeptides from the C-terminal ends of various peptide substrates (Pihlanto-Leppälä 2000). Bioactive compound production may be strikingly increased by controlling the fermentation conditions (Zajsek & Gorsek 2011). Either as starter, as adjunct cultures, or as probiotics, *Lactobacillus* strains are used as food preservatives not only to prevent the development of food spoilage but also to give consumers a health benefit. Some *Lactobacilli* produce bacteriocins, proteins active against other bacteria. According to the literature is examined, it has been found that lactic acid bacteria such as *L. helveticus*, *L. casei* are extensively used in the fermentation of some dairy products (Nielsen et al. 2009; Otte et al. 2011; Sanlı et al. 2018). In a study, it was reported that the antihypertensive peptides can be produced during fermentation of lactic acid bacteria used as adjunct cultures in kefir production contributed in different ways to peptides and also slightly contributed to the formation of ACE-I peptides (Sanlı et al. 2018). However, only a few studies have been published on the ACE-I activity of kefir (Maeda et al. 2004; Quiros et al. 2005) and it needs to be further studied. The types and strains of starter microorganisms used in kefir have affected the bioactivity of the product. The data obtained in a

study showed that the variability in the amino acid content of kefir is a function of the culture type (Ozcan et al. 2019). It was determined that the principal amino acids of buffalo milk kefir produced either by grains or adjunct starter culture were glutamic acid, alanine, serine, tyrosine and the like (Ozcan et al. 2019). Bioactive peptides originating from milk proteins were identified in amino acid sequences of these proteins. It has been shown that these peptides can be expressed by bacterial microbial, coagulant, digestive enzymes, and exogenously added starter lactic acid bacteria (Gobbetti et al. 2002). For this reason, functional foods and bioactive components have begun to attract the attention of food scientists, nutritionists, health professionals and consumers. In a study, it was reported that kefir enriched in terms of probiotic microorganisms was equivalent to traditionally produced kefir, its bioavailability and functionality has been increased, and it was suitable for industrial production and likeable regarding organoleptic properties. (Karacali et al. 2018). Furthermore, kefir represents a good choice as a probiotic food carrier, showing potential advantages for human health over other dairy fermented products. Foodborne diseases, which can cause more than 900 million infectious events, have become a public health problem (He et al. 2018). These diseases are caused by eating foods contaminated with pathogenic microorganisms such as *S. aureus* and *E. coli*. Although the growth of pathogenic bacteria in foods can be effectively controlled with chemical preservatives, consumers are still concerned about some safety issues (Ma et al. 2020). In addition, increased bacterial resistance to common and artificial antibiotics and their side effects have also caused problems in public health leading to the discovery of natural antimicrobial counterparts (Pina-Perez et al. 2015; Sundin & Wang 2018). In addition to its antibacterial, antifungal and antitumor activities, kefir is effective in improving health, strengthening the immune system, balancing blood pressure and lowering serum cholesterol levels. (Ajam & Koohsari 2020). Therefore, there is a need for the development of natural antibacterial agents. Recently, antimicrobial peptides (AMPs) have been gaining widespread attention due to their excellent functional activities. Many natural AMPs such as nisin have been reported today (Miao et al. 2016). However, nisin is the only antimicrobial peptide used in the food field as a natural food preservative (Upendra et al. 2016). Therefore, AMPs are of great importance as a potential food preservative. Several studies are investigating the antibacterial activity of kefir. However, little information is readily available concerning the characterization of antimicrobial peptides from kefir produced using *Lactobacillus*.

This study aimed to the effect of ACE-I activity and the antibacterial activity against selected bacteria in kefir samples produced using *Lactobacillus*. Also, the results can provide information on the amino acid content, to enable a better understanding of the ACE-I activity of kefir. Additionally, characterization of AMP peptide fractions by Liquid chromatography-Mass spectrometry-Mass spectrometry (LC-MS/MS) was provided.

2. Material and Methods

2.1. Materials

Kefir grains were purchased from a local market and groved in skim milk at 22 °C for 24 hours a day. The kefir granules were obtained by continuously growing in skimmed milk. Kefir grains, raw cow's milk used in the production of kefir samples and *Lactobacillus delbrueckii* ssp. *bulgaricus* (*L. delbrueckii* ssp. *bulgaricus*) ATCC 11842, *Lactobacillus helveticus* (*L. helveticus*) ATCC 15009, *Lactobacillus plantarum* (*L. plantarum*) ATCC 14917 used adjunct cultures were provided from the Food Engineering of Inonu University Engineering Faculty (Malatya, Turkey). Raw cow's milk was heated 55-60 °C, then fat value was standardized to 2% with a cream separator. After pasteurization (90 °C for 5 min), the milk was cold at inoculation temperature (23 °C) and is divided into 2 parts. The first part of milk at aseptic conditions, 3% kefir grains are inoculated and incubation is continued for approximately 22-24 hours at 20-25 °C. When the curd acidity reaches pH 4.6, the incubation process was terminated and the kefir grains were separated by filtration (sample K). Second part of milk was inoculated kefir grains at level of 3% (w/v) and the incubation was continued for approximately 22-24 hours at 20-25 °C until pH 4.8, the kefir grains were separated by filtration. The fermented milk divided into 3 parts. Each part was inoculated with the adjunct starter culture (sample A: *L. delbrueckii* ssp. *bulgaricus*, sample B: *L. helveticus*, sample C: *L. plantarum*, 1mL per 100 mL). When the second incubation reaches pH 4.6 at 37 °C, the incubation process was terminated. Kefir samples are stored in 200 mL plastic containers at 4 °C during 28 days.

A 20 g of Kefir sample was mixed 10 mL deionized water and incubated in a shaking water bath for 1 hour at 40±1 °C. Kefir was centrifuged at 3000 × g for 30 min at 4 °C with a cooled centrifuge (model 320R, Hettich, Tutlingen, Germany). Supernatants were filtered through qualitative filter paper (Whatman No: 113) The water-soluble nitrogen (WSN) fractions were freeze-dried used to HPLC peptides analysis and ACE-I activity analysis and antimicrobial activity of the kefir samples.

2.2. Proteolysis

Peptide profile of the freeze-dried WSN fractions of the kefir samples was analyzed by reverse-phase high performance liquid chromatography (RP-HPLC) (Shimadzu LC 20 AD Prominence HPLC) system (Shimadzu Corporation, Kyoto, Japan) according to the method described by Sulejmani & Hayaloglu (2017). The RP-HPLC individual free amino acids contents of water-soluble fractions were determined as previously described by Hayaloglu (2007). The total Free Amino Acids (FAAs) content of the kefir samples was determined by the method described in Sahingil et al. (2019).

2.3. RP-HPLC determination of angiotensin-converting enzyme activity

The ACE-I activity and IC₅₀ value were determined as previously described by Sahingil et al. (2019).

$$IC_{50} = \frac{BSA \times 50}{IR}$$

BSA (Bovine Serum Albumine): mg/L; IR: ACE inhibition rate (%)

2.4. Antimicrobial activity

The antimicrobial activity assay was studied in both kefir and WSN fractions obtained from kefir. The kefir was centrifuged at $3000 \times g$ for 30 min and the supernatant passed through 0.45 μm pore size filter for sterilized. The supernatans were kept at refrigerator temperature until antibacterial activity tests. WSN fractions were freeze-dried used for antimicrobial activity tests. The dried water-soluble fractions were dissolved in ultrapure water to 50 mg/mL. The fractions were separated according to their molecular size using centrifugal filters (Amicon Ultracel-3K, Merck-Millipore Ltd, Cork, Ireland). Then the supernatant was sterilized by filtration using a 0.45- μm pore size syringe filter. *Staphylococcus epidermidis* RSKK 0802 (*S. epidermidis*), *Staphylococcus aureus* 1021/06008 (*S. aureus*), *Staphylococcus warneri* 95052 (*S. warneri*), *Staphylococcus xylosus* (*S. xylosus*), *Shigella flexneri* RSKK 184 (*S. flexneri*), *Bacillus cereus* RS 863 (*B. cereus*), *Escherichia coli* (*E. coli*) (Microbiology laboratory of Inonu University Turgut Özal Medical Center), *Enterococcus faecalis* (*E. faecalis*), *Candida albicans* ATCC 04055 (*C. albicans*), *Streptococcus mutans* (*Str. mutans*), *Enterobacter*, *Salmonella enteritidis* (*S. enteritidis*), *Pseudomonas putida* (*P. putida*) were investigated on antimicrobial effect on 13 different microorganisms. They were procured from Inonu University. Then, the bacteria were recovered in the Brain Heart Infusion medium (Merck) at 37 °C/24 hr in the microbiology laboratory of the Inonu University. Antimicrobial inhibition effects on some pathogenic bacteria and yeast were determined by disc diffusion method (0.6 mm disc diameter). The macrodilution tube method was used based on turbidimetric assay and the highest inhibition zone diameter was selected for the minimum inhibitory concentration (MIC) of kefir. For WSN fractions 5 different concentrations (50-200 mg/mL; 50-75-100-150-200 mg/mL) which prepared in Nutrient Broth (Merck) were studied for determination of minimum inhibitory concentration. The dilution (100 mg/mL) in which microbial turbidity was not observed, as the MIC was reported. A hundred microliters of each WSN extract were by disk diffusion method onto the surface of the agar. For kefir extract 10 different concentrations (100-1000 $\mu\text{L/mL}$; 100-200-300-400-500-600-700-800-900-1000 $\mu\text{L/mL}$) were studied for determination of minimum inhibitory concentration. The dilution (1000 $\mu\text{L/mL}$) in which microbial turbidity was not observed, as the MIC was reported. The plates were incubated for 24 h at 37 °C in anaerobic media. The lyophilized peptide fractions (100 mg/mL) were dissolved in 40 mM sodium phosphate buffer (pH 6.5) and incubated for 24 hours at 37 °C against the test microorganisms. Subsequently, the susceptibility and resistance of each bacteria were determined by measuring the inhibition zone diameter (IZ) (0.6 mm disc diameter) around the wells. The antibiotic standard (Sigma-Oxytetracycline) was used to compare the results (10 mg/mL antibiotic 100 μL enject); 100 mg/mL- dry extract 100 μL , 100 $\mu\text{L/mL}$ - kefir extract 100 μL .

2.5. Isolation of antimicrobial peptides for LC-MS/MS in RP-HPLC

Water-soluble fractions were separated according to their molecular size using centrifugal filters (Amicon Ultracel-3K, Merck-Millipore Ltd, Cork, Ireland). Since peptides showing bioactive properties are generally peptides containing 2-20 amino acids, peptide profile of peptides smaller than 3 kDa was determined by RP-HPLC analysis and they were collected into separate fractions. The total peptide analysis for 80 minutes for fractionation is given in Figure 1b. Antimicrobial activity was examined in the fractions separated from the fraction collector. The peptide fraction named F2 was determined to have antimicrobial ctivity.

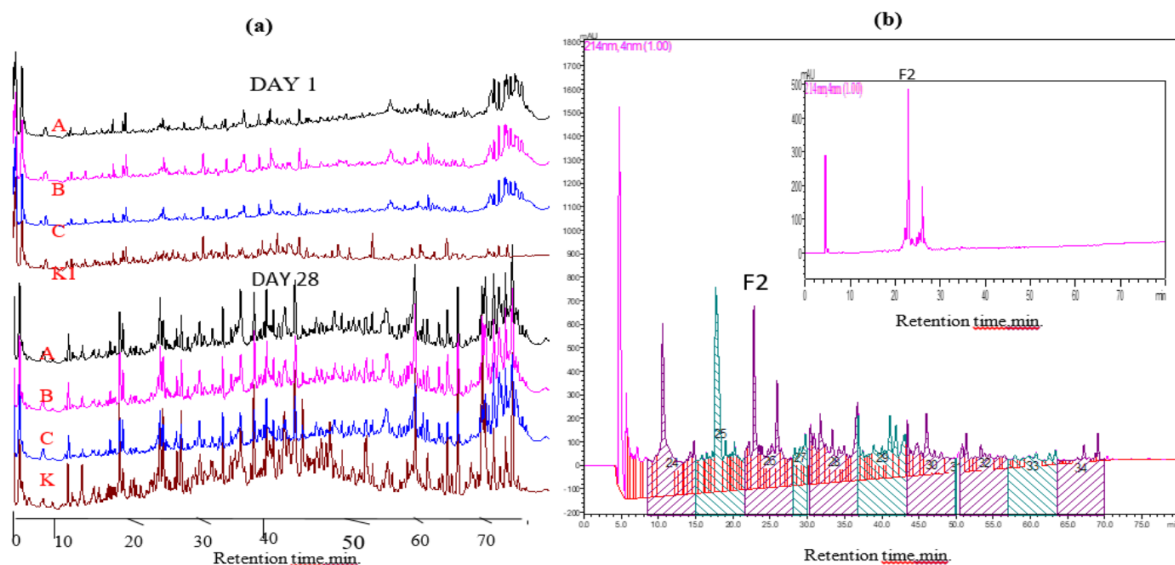


Figure 1- (a) RP-HPLC peptide profile of the kefir samples. Sample K, kefir granule containing; sample A: kefir granule+ *L. bulgaricus*; sample B: kefir granule+ *L. helveticus*; sample C: kefir granule+ *L. plantarum*. (Day 1, 28) (b) Separating peptide fractions of kefir that are less than 3 kDa in HPLC fraction collector. F0, 8.50-15.17 min; F1, 15.20-21.60; F2, 21.70-28.18 min; F3, 28.22-30.00 min; F4, 30.25-36.82 min; F5, 36.83-43.38 min; F6, 43.40-49.88 min; F8-10, 50.45-70.00 min.

2.6. Characterization of antimicrobial peptides in LC-MS/MS

Fractions were separated as shown in Figure 1b and the F2 fraction with antimicrobial activity was analyzed under the conditions specified using liquid chromatography-mass spectrometry (LC-MS/MS) system (Shimadzu LC-MS 8030, Japan) with 0.1% formic acid in 2% acetonitrile as the eluent. Fractions F2 was separated on a C18 reverse-phase capillary column (Agilent Technologies, Zorbax column, 4,6×250mm×5µm). It was column oven 40 °C, 15 µL sample was injected and a flow was set at 1 mL/min, with a linear gradient of eluent B (0.1% formic acid in 95% acetonitrile) in A (0.1% formic acid in water) from 5 to 95% in 70 min. The mass spectrometer was operated in the positive mode with a nebulizer pressure of max 60 MPa. Peptide analysis was performed using data-dependent acquisition of one MS scan (scan range from 100 to 1 900 m/z, depending on the m/z precursor ion) followed by a tandem MS (MS/MS) scan of the 5 most abundant ions in each MS scan.

2.7. Statistical analysis

An ANOVA followed by Duncan test was performed with a 95% confidence, using the SPSS program (SPSS package program, version 13.0, SPSS Inc., USA). Data obtained from two trials were analyzed in duplicate, microbiological analyzes were analyzed in triplicate. Principal component analysis (PCA) was performed using a covariance matrix and varimax rotation between the kefir samples (version 9.0, SPSS Inc., Chicago, IL). The results obtained were directly taken from automatic reporting in LCMS Lab solution Ver 5.72 without any further data manipulation except for the retention time adjustment and peak area integration review. For experimental parameters used the Class-Agent authentication database.

3. Results and Discussion

3.1. The RP-HPLC peptide profiles of the kefir samples

RP-HPLC peptide profiles of days 1 and 28 of the Kefir samples are shown in Figure 1a. The RP-HPLC peptide profiles of the kefir samples were precise and no significant discrepancy between the kefir samples was detected. On the 28th day of storage in sample K, it was found out that almost no new peptides were reproduced with the exception of certain ones. After the 28th day of storage, presence of some peptides was detected in the sample K at the highest concentration point. However, some minor differences were observed depending on the storage period in RP-HPLC chromatograms of kefir samples. During storage, almost identical peptide profiles were observed in all the kefir samples. Peptide profiles of samples A, B and C were similar on all days of storage except for sample K (Figure 1a).

3.2. The RP-HPLC free amino acid profiles of the kefir samples

RP-HPLC free amino acids profile and PCA diagram of RP-HPLC free amino acids of the kefir samples were given (Figure 2a and Table 1) at 1 and 28 days of storage. The level of free amino acids such as Gln, Gly, Thr, Asp, and Ser was higher in the control sample compared to other kefir samples. It was observed that the amount of Arg, Glu and Pro increased at the end of the storage period. The content of Trp, Asn, Ala, Gly increased in samples B and K during storage. Val content decreased during the storage period while Ile content increased in samples B, C and K. Amino acids at the highest concentration in sample K (control) were Ala, Glu, Gly, Asp, Phe respectively while in kefir with adjunct lactobacilli were Ala, Pro, Arg, Leu, Lys. Glu and Lys as an antioxidative component were found (9.39 for K, 8.87 mg/100 g for B) to be present at a high concentration. It has been reported that the intensity of the scavenging activity of peptides could be affected by the hydrophobic amino acid number. In a study, the content of hydrophobic amino acids such as Lys, His and Arg contributed to Fe²⁺ chelating activity, while Met, Pro, Cys, Ala, Gly, Val and Leu have a higher radical scavenging ability (Zhu et al. 2013). The presence of lysine is believed to increase the antioxidant capacity of peptides (Huang et al. 2017). The other study identified the antioxidative peptides included Glu and Lys amino acids in goat milk fermented by *L. plantarum* 60 (Chen et al. 2021). The added adjunct cultures have a pronounced effect on the free amino acid content of kefir samples. The Pro concentration had the highest value in sample C (*L. plantarum*), followed by sample A (*L. delbrueckii* subsp. *bulgaricus*) and sample B (*L. helveticus*). The presence of Pro, Lys and Arg amino acids at the C-terminal ends of ACE-I peptides is generally indicated to increase their bioactivity. Pan et al. (2005) found that antihypertensive peptide was formed in skimmed milk fermented with *Lb. helveticus* JCM1004 and that VPP and IPP peptides including proline had an effect on ACE-I activity. It is suggested that the bioactivity of antihypertensive peptides is due to the hydrophobicity and positively charged amino acids of the peptides in the structure, which are generally found (Prupp et al. 2004). Proline found the highest amount in the free amino acid composition of kefir samples formed of kefir grains applied to conventional milk (Ultra High Temperature) and certificated organic milk, while Ala, Asp, Lys, Arg and Cys is followed by Güler et al. (2016). It was reported that the presence of Try, Val, Lys, Met, Phe, Thr and Ile in kefir (Liutkevičius & Šarkinas, 2004). In a study investigating the chemical properties of Norwegian kefir, it was stated that Glutamic acid has the highest value among free amino acids (Grønnevik et al. 2011). Proline and Glutamic acid had the highest amount of free amino acids; Alanine was the second most abundant amino acid in kefir produced using *L. bulgaricus* HP1 and *L. helveticus* MP12 (Simova et al. 2002). Leucine is classified as an essential amino acid that gives chance to determine the degree of proteolysis. Leu was found at the lowest amount in sample K, the highest values of these amino acids were B added *L. helveticus*. In a study, it was reported that kefir sample supplemented *L. helveticus* MP12 which has high peptidase and aminopeptidase activity compared to *Lactococcus* species, have a unique amino acid profile as respect to control samples, and Leu, Ile, Val, Lys, Phe and Met levels

were found to be 1.5 times higher (Simova et al. 2006). Enzyme systems with different culture types and proteolytic activities cause the degradation of peptides and result in different kinds and amounts of amino acids. Similarity to this study, it was reported that the principal amino acids of kefir produced either by grains or commercial kefir culture including lactobacillus culture were glutamic acid, alanine, proline, valine and the like (Gul et al. 2018; Ozcan et al. 2019). The results of the free amino acid analysis of the kefir were subjected to basic component analysis (PCA) and the graph showing the results of the analysis is shown in Figure 2a). In the PCA graph, which analyzed the results of the storage on days 1, 7, 14, 21 and 28, it was determined that kefir had a distribution depending on the storage period, the addition of *Lactobacillus*, and that kefir exhibited a different amino acid profile. It was found that *L. plantarum* was separated from the other kefir samples (circled in Figure 2a) and contained a higher concentration of amino acids than other kefir samples. Supplementation of *L. helveticus* H9 enhanced fermented milk acidification and proteolysis. These bacteria generally have high extracellular proteinase activities and thus release specific bioactive peptides during milk fermentation (Nielsen et al. 2009; Zhou et al. 2019). *L. helveticus* is known to have high proteolytic activity (Ahtesh et al. 2017). Proteolytic activity of *L. plantarum* and *L. helveticus* strain were evaluated by Beganović et al. (2013). The remarkable proteolytic activity of these strains is possibly due to their ability to release extracellular and intracellular proteases during fermentation (Indarmawan et al. 2016; Fang et al. 2018). The total FAAs levels increased due to storage period (Figure 2b). The use of *Lactobacillus* as an additional culture resulted in a significant increase in total FAAs levels due to proteolytic activity. It was determined that the kefir produced by *Lactobacillus* (*Lb. plantarum* and *L. helveticus*) adjunct starter has a total FAAs value that is higher than the control samples at the end of storage period.

Table 1- HPLC-Free amino acids of kefir samples (mg/100g kefir) storage at 4 °C in 1 and 28 days

Amino acids	DAY 1				DAY 28				Statistics	
	A	B	C	K	A	B	C	K	P_d	P_s
ASP	1.76	1.65	2.7	1.6	7.04	5.46	5.36	8.35	***	***
GLU	2.65	1.38	2.57	9.65	7.53	7.18	9.15	9.39	***	***
ASN	0.07	0.96	0.6	0.5	0.95	4.01	0.79	0.97	**	***
SER	0.4	0.35	2.69	3.08	3.8	0.33	4.45	5.08	***	***
GLN	0.05	0.19	0.48	0.39	0.87	0.24	0.76	0.96	***	***
GLY	0.24	1.99	2.04	1.84	5.67	6.06	7.14	9.09	***	***
HIS	1.34	6.18	5.62	6.48	5.74	5.18	7.85	6.16	***	***
ARG	1.11	2.41	2.39	2.06	8.54	3.14	11.81	1.46	***	***
THR	3.63	1.67	2.61	1.85	4.37	2.08	2.3	1.89	***	***
ALA	11.67	16.18	12.85	11.8	16.13	16.98	16.31	12.66	***	***
PRO	5.51	2.95	4.75	3.93	7.7	5.58	12.35	4.89	***	***
TYR	3.77	2.18	3.33	2.63	3.02	4.45	5.7	2.22	***	***
VAL	6.35	5.92	6.86	5.46	4.32	2.2	0.62	2.39	***	***
MET	0.65	1.69	0.21	1.84	6.1	4.76	2.15	3.72	***	***
CYS	1.1	1.55	5.61	2.67	3.84	5.93	10.84	7.03	***	***
ILE	0.45	0.4	0.6	0.38	0.57	4.97	2.31	3.32	***	***
LEU	4.46	8.54	7.51	7.27	7.66	9.7	8.22	7.21	***	***
PHE	0.33	5.97	2.76	6.79	7.41	6.14	3.22	7.38	***	***
TRP	2.94	1.16	1.12	1.89	6.41	4.13	1.84	5.15	***	***
LYS	2.41	4.53	5.67	4.01	3.21	8.87	7.07	6.41	***	***
TOTAL	50.88	67.83	72.97	76.11	110.88	107.4	120.24	105.73	***	***

P probability; * $P < 0.05$; ** $P < 0.01$; *** $P < 0.001$; P_d : Day; P_s : sample; sample K, kefir granule containing; sample A: kefir granule+ *Lb. bulgaricus*; sample B: kefir granule+ *Lb. helveticus*; sample C: kefir granule+ *Lb. plantarum*.

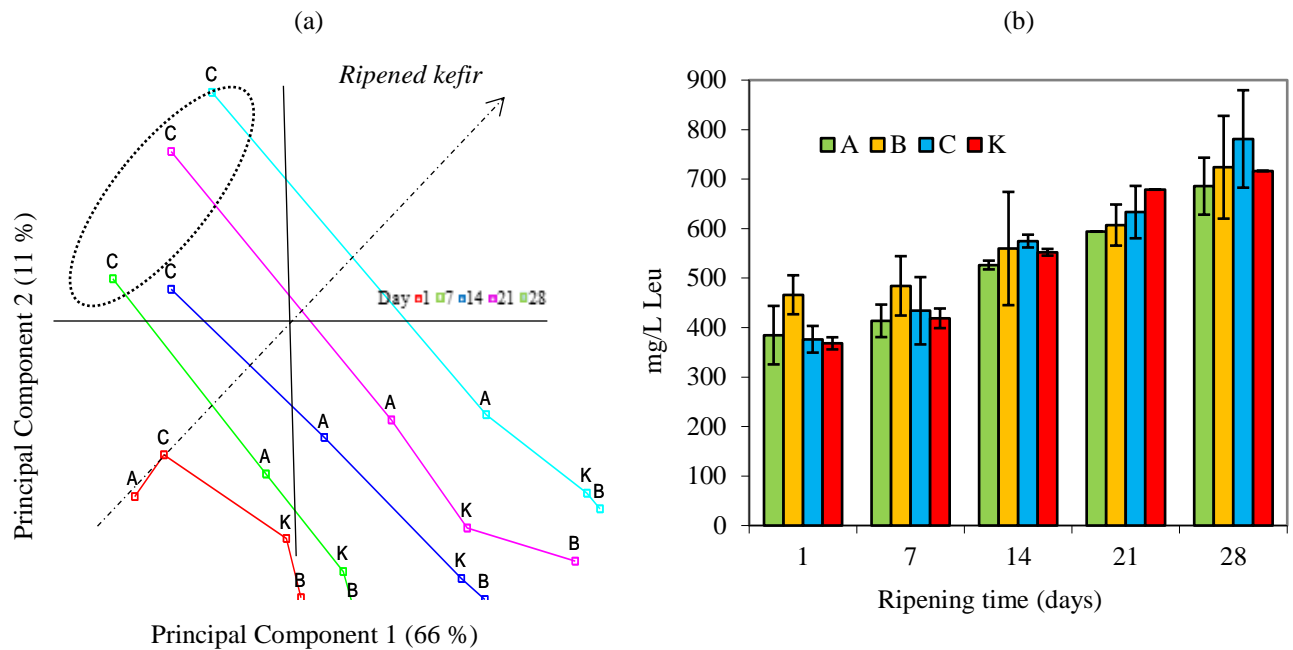


Figure 2- (a) PCA diagram of RP-HPLC Free Amino Acids from samples. Sample K, kefir granule containing; sample A: kefir granule + *L. bulgaricus*; sample B: kefir granule + *L. helveticus*; sample C: kefir granule + *L. plantarum*. (b) Total free amino acids of kefir samples (mg/L, Leu)

3.3. ACE-I activities of kefir samples

Fermented dairy products, such as yogurt, different types of cheese and kefir, contain peptides with ACE-I activity, these inhibitors are used to cure high blood pressure and hypertension (Shu et al. 2017). Proteins are hydrolyzed into plenty of bioactive peptides, antihypertensive activity, by lactic acid bacteria during fermentation especially lactobacilli is one of its important bio-functional properties. It was also found that ACE-I activity as IC_{50} was significantly increased in sample C (14.84 ± 1.2 mg/mL) and sample B (16.73 ± 0.02 mg/mL) (Figure 3a, b). ACE-I activities and IC_{50} values of kefir samples were determined on days 1, 7, 14, 21 and 28 of storage and the results were shown in Figure 3(a, b). The results were expressed as % inhibition and IC_{50} . With the progress of the storage period, it was found that the kefir had an increase in ACE-I activities and this increase was statistically significant ($P < 0.01$). Sample B (including *L. helveticus*) showed strongest inhibition activity ($57.28\% \pm 1.03$) and IC_{50} value of 19.86 ± 0.1 mg/L on the first day. The use of *Lactobacillus* bacteria in kefir production has been associated with a significant increase in ACE-I activity and it has been determined that the bacterium that maximizes ACE-I activity was *L. plantarum*. The highest ACE-I activity revealed that sample C on the 28 day and ACE-I activities of other samples was 76.47%, 84.95%, 87.33% and 85.57% respectively. IC_{50} values between 30.27 ± 1.13 and 19.71 ± 0.73 mg/L. *L. plantarum* showed the strongest ACE-I activity of $87.33 \pm 0.67\%$ ($IC_{50} = 19.71 \pm 0.73$ mg/L) on the last storage day. We may explain that higher ACE-I activity associated with an extensive proteolysis activity which may an increase in the intensity of peptides recognized as potential ACE inhibitors due to the adjunct culture addition especially lactobacilli. This limitation occurs once ACE-I activity depends on antihypertensive peptides' presence, which in turn relies on the balance between the release of bioactive peptides and the cleavage of these fractions in amino acids and inactive peptides (Ahiara et al. 2015; Rutella et al. 2016). Fermentation by lactic acid bacteria could positively contribute to ACE-I activity, as revealed in this study, and as reported by Aihara et al. (2005) who described an increase in activity following fermentation of powdered milk with *L. helveticus*. ACE-I activity showed a significant increase in milk fermented by *L. plantarum* K25 (Zhang et al. 2020). The addition of *Lactobacillus* may technological strategy that can be used in kefir processing to favor the bioactive potential of this product. Almost all the bioactive peptide sequences reported in many studies, including those displaying ACE-I activity, are derived from dairy products, especially fermented milk products, and classified as antihypertensive peptides.

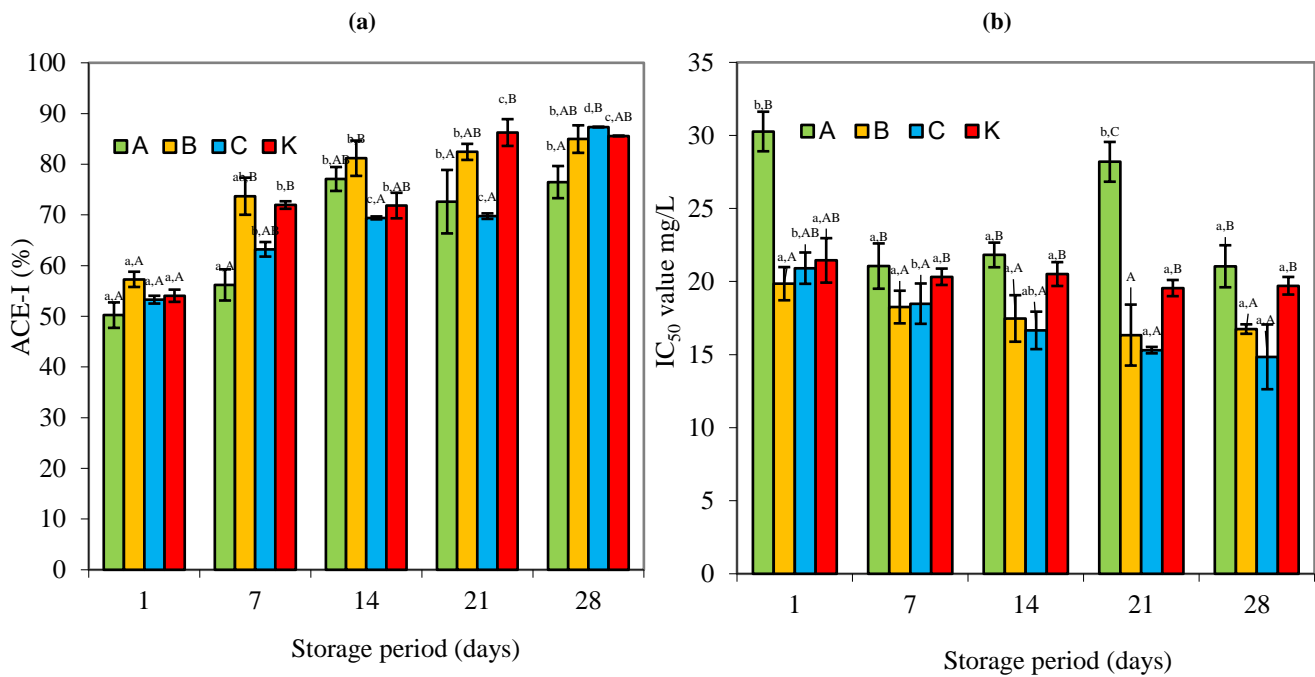


Figure 3- (a) ACE-I activity of Samples. sample K, kefir granule containing; sample A: kefir granule+ *L. bulgaricus*; sample B: kefir granule + *L. helveticus*; sample C: kefir granule + *L. plantarum*. 3 (b) IC₅₀ value (mg/L Bovine Serum Albumin) for ACE-I activity of kefir samples. The capital letters A and B indicate means that significantly differ at P<0.01 between samples kefir. The lower case letters a and b indicate means that significantly differ at P<0.01 between days

3.4. Determination of antimicrobial activity and characterization of antimicrobial peptide by LC/MS-MS

Kefir contains several metabolites and inhibitors such as organic acid, peroxide hydrogen, ethyl alcohol, diacetyl, peptide, and bacteriocins. Antimicrobial activity is derived from lactic acid and other metabolites (Teneva et al. 2017). The metabolites are interacting to improve antimicrobial activity during kefir fermentation. The antimicrobial properties of kefir can be its metabolites produced by kefir microorganisms, such as exclusive peptides and exopolysaccharides (Kim et al. 2016). The indicator and pathogenic microorganisms were selected to determine the antimicrobial activity and disk diffusion test was used to certain the antimicrobial activity of the sample extracts (A, B and C) and lyophilized WSN fractions (<3 kDa). The antimicrobial effect against some microorganisms as inhibition zone diameter (mm) of kefir extract and peptide fraction was given in Table 2. Kefir extract A, B and C showed broader spectrum antimicrobial activity, inhibiting *S. aureus*, *S. warneri*, *S. xylosum*, *B. cereus*, *E. coli*, *E. fecalis*, *Enterobacter*. Sample K (control), on the other hand, showed a narrower spectrum antimicrobial activity by inhibiting *S. aureus*, *E. coli* and *E. fecalis*. However, in the sample K, it set forth the finding that the proteolysis during the kefir fermentation is not high enough to form antimicrobial peptides. Also, the microbial diversity can be different in each fermentation process of kefir. *Lactobacillus* strains that are generally consumed as probiotics and these bacteria may possess antimicrobial activity. This study has shown that the peptide fraction (<3k Dda) from kefir fermented using *Lactobacillus* adjunct culture presented high inhibition of the growth of *S. aureus*, *S. warneri* and *S. hominis* from 28th day of storage. The antimicrobial effect wasn't observed against *C. albicans* for all the kefir extract and peptide fractions in this study. Taşkın & Akköprü (2020) was reported that the antimicrobial activity of kefir may be due to the antimicrobial substances present in the supernatants. It was reported that kefir possessed an antibacterial activity against *E. coli* D157: H7 and *S. aureus* (Kivanc & Yapici 2018). In a study similar to, it was reported that kefir inhibited *B. subtilis*, *S. aureus* and *E. faecalis* and *S. enteritidis* but did not inhibit *C. albicans* (Chifiruc et al. 2011). The higher antibacterial activity of kefir supplemented with lactobacilli may be attributed to the hydrolysis of proteins and its contribution to antimicrobial peptide release by the enzymes of lactobacilli. It was reported that *L. delbrueckii* subsp *bulgaricus* has the antimicrobial activity against some of pathogenic bacteria including *E. coli* and *Shigella*. Presence of lactic acid along with the organic acids, bioactive peptides and bacteriocins may affect the antimicrobial activity of *L. bulgaricus* (Zaeim et al. 2014). Antimicrobial activity of *L. plantarum* against some patogenic bacteria has already been established. Antibacterial property of *L. plantarum* might be due to its ability production of antibacterial compounds, which may inhibit the growth of harmful and pathogenic bacteria (Monteiro et al. 2019). The microbial diversity is responsible for the biological activities depending on the amount and various of *Lactobacillus* in kefir, their microbial diversity is different, and therefore, its antibacterial activity also changes. It means that peptides produced by *Lactobacillus* are more in number than peptides produced by lactic acid bacteria. This result is strongly related to the type and amount of peptidases. To make use of casein in milk, lactic acid bacteria firstly hydrolyze casein into oligopeptides by cell wall proteases and then transport it into cells through a specific oligopeptide transport system, further degrading oligopeptides into smaller peptides and amino acids by intracellular peptidases to provide for the growth and utilization of bacteria. At the same time, intracellular peptides are not only from casein hydrolysis, but also from the *Lactobacillus* itself because of existing bacteria protein degradation (Savijoki et al. 2006). Additionally, to pharmaceutical drugs, without side effects bioactive peptides considered as alternatives daily with a variety of protein-rich foods can be consumed. Bioactive peptides as potent natural ingredients it will contribute to its use in foods. Firstly, separation and detection of antimicrobial peptides should be done in kefir

metabolomics. It is important to investigate this mechanism. Additionally, future studies will focus on sequences of peptides identified in these fractions.

Separation of antimicrobial peptides was analyzed by HPLC. HPLC is a widely used method for the purification of peptides (Ahn et al. 2014; Zheng et al. 2018). The F2 fraction was further separated using HPLC. The chromatographic profile was given in Figure 1b. Total eight fractions were obtained and numbered sequentially F1-8. The antimicrobial activity of the F2 fraction was determined and the results were given (Table 2). F2 fraction had strong antimicrobial activity and no antimicrobial activity was observed in other fractions. Therefore, an attempt was made to determine the peptide characterization of the F2 fraction. In this report, we examined the MS/MS spectra of the protein fractions. The peptide fraction named F2 was determined to have been an antimicrobial inhibitory activity against three bacteria (*S. hominis*, *S. warneri* and *S. aureus*) and was collected from RP-HPLC. The peptide characterization was obtained by direct LC-MS/MS measurement in the m/z range from 100 to 1900 Da. The tuning of peptides was performed through continuous infusion of standards into ESI (positive electrospray ionization) mode source in positive mode at a flow rate of 10 µL/min. We reported the product and precursor ions by determining the m/z value of the peptide fractions that had an antimicrobial effect on *S. aureus*, *S. warneri* and *S. hominis*. Total ion spectra by LC-MS/MS of fraction 2 with three major peaks was given in Figure 4a and 4b for samples A, B and C. Considering the comparison with Figure 4a ve Figure 5, we can see that the peaks of A and C are larger in amount than B and K. The Q3 mass was predominant among the full scan of protonated precursors and the product ions of precursor ions were monitored further. The product ion scan yielded the following predominant fragment ions at m/z values 339.381 and 308 for precursor ions for samples A, B and C (Figure 5).

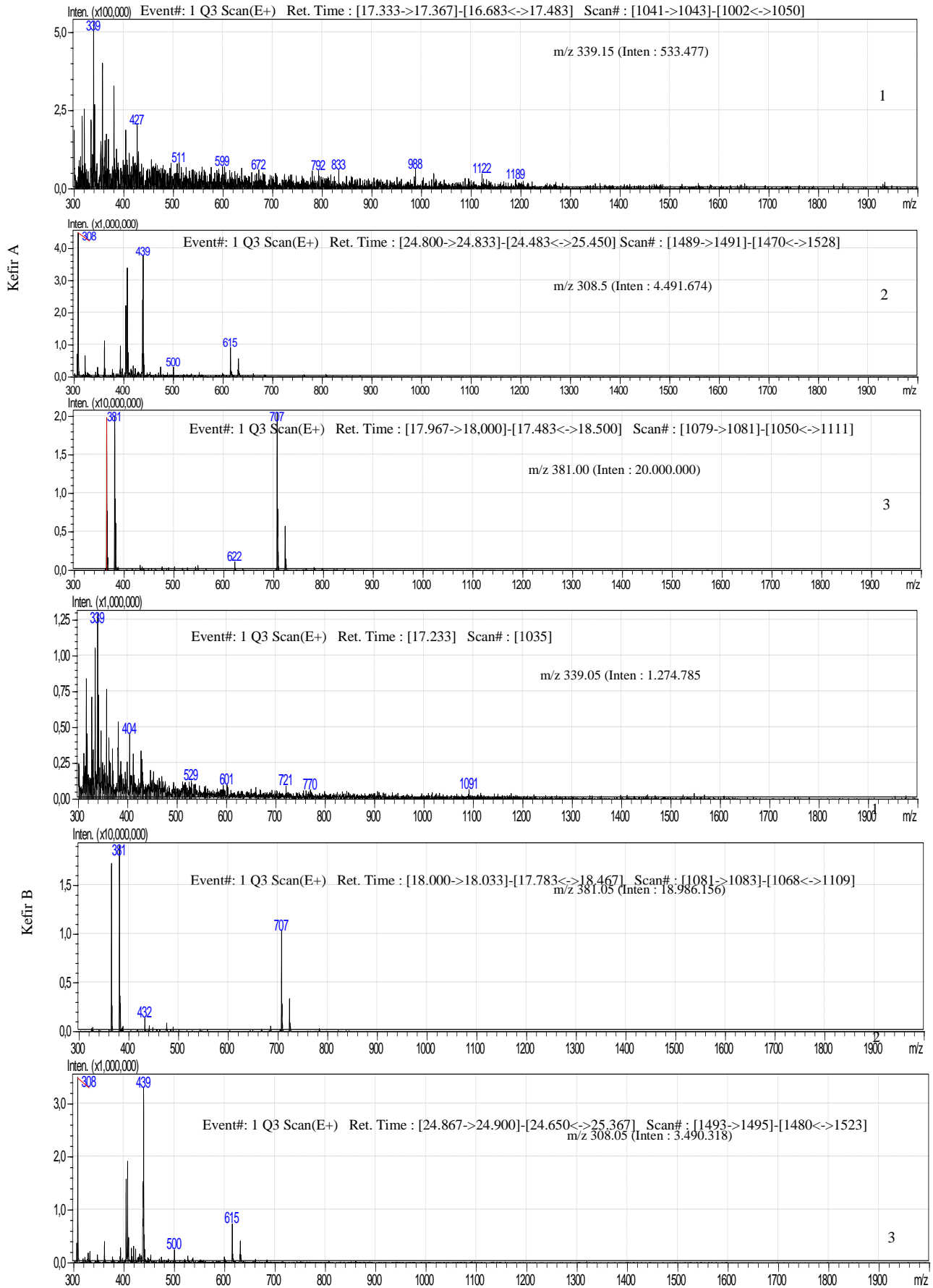
Bioactivity of protein fractions is related to amino acid composition, sequence, size and configuration of peptides (Rutella et al. 2016). Future studies will focus on sequences of peptides identified in this fraction.

Table 2 (a)-Antibacterial activity of peptide fractions (F2) in term of inhibition zone (IZ) in mm (b)Antibacterial activity of sample extract in term of inhibition zone (IZ) in mm

<i>Bacteria</i>	<i>A</i>		<i>B</i>		<i>C</i>		<i>K</i>		<i>Oxytetracycline</i>	
	(a)	(b)	(a)	(b)	(a)	(b)	(a)	(b)	(a)	(b)
<i>S. epidermidis</i>	-	-	-	-	-	-	-	-	+++	+++
<i>S. aureus</i>	+	++	+	++	+	++	-	+	++	++
<i>S. warneri 95052</i>	-	+	+	++	-	+	-	-	+	+
<i>S. xyloso</i>	-	++	-	+++	-	++	-	-	+++	+++
<i>S. flexneri RSKK 184</i>	-	-	-	-	-	-	-	-	+	+
<i>B. cereus RS 863</i>	-	+	-	+	-	-	-	-	+++	+++
<i>E. coli</i>	-	++	-	++	-	++	-	+	++	++
<i>E. faecalis</i>	-	++	-	++	-	++	-	++	++	++
<i>C. albicans ATCC 04055</i>	-	-	-	-	-	-	-	-	ND	ND
<i>Str. mutans</i>	-	-	-	-	-	-	-	-	+++	+++
<i>Enterobacter</i>	-	+	-	+	-	-	-	-	+++	+++
<i>S. enteritidis</i>	-	-	-	+	-	-	-	-	+++	+++
<i>S. hominis</i>	-	-	-	-	++	-	-	-	+++	+++

Sample K, kefir granule containing; sample A: kefir granule + *L. bulgaricus*; sample B: kefir granule + *L. helveticus*; sample C: kefir granule + *L. plantarum*. (+) inhibition positive; (+) inhibition diameter 4-10 mm; (++) inhibition diameter 11-19 mm; (+++) inhibition diameter greater than 20 mm; (-) Inhibition negative.

(4a)



(4b)

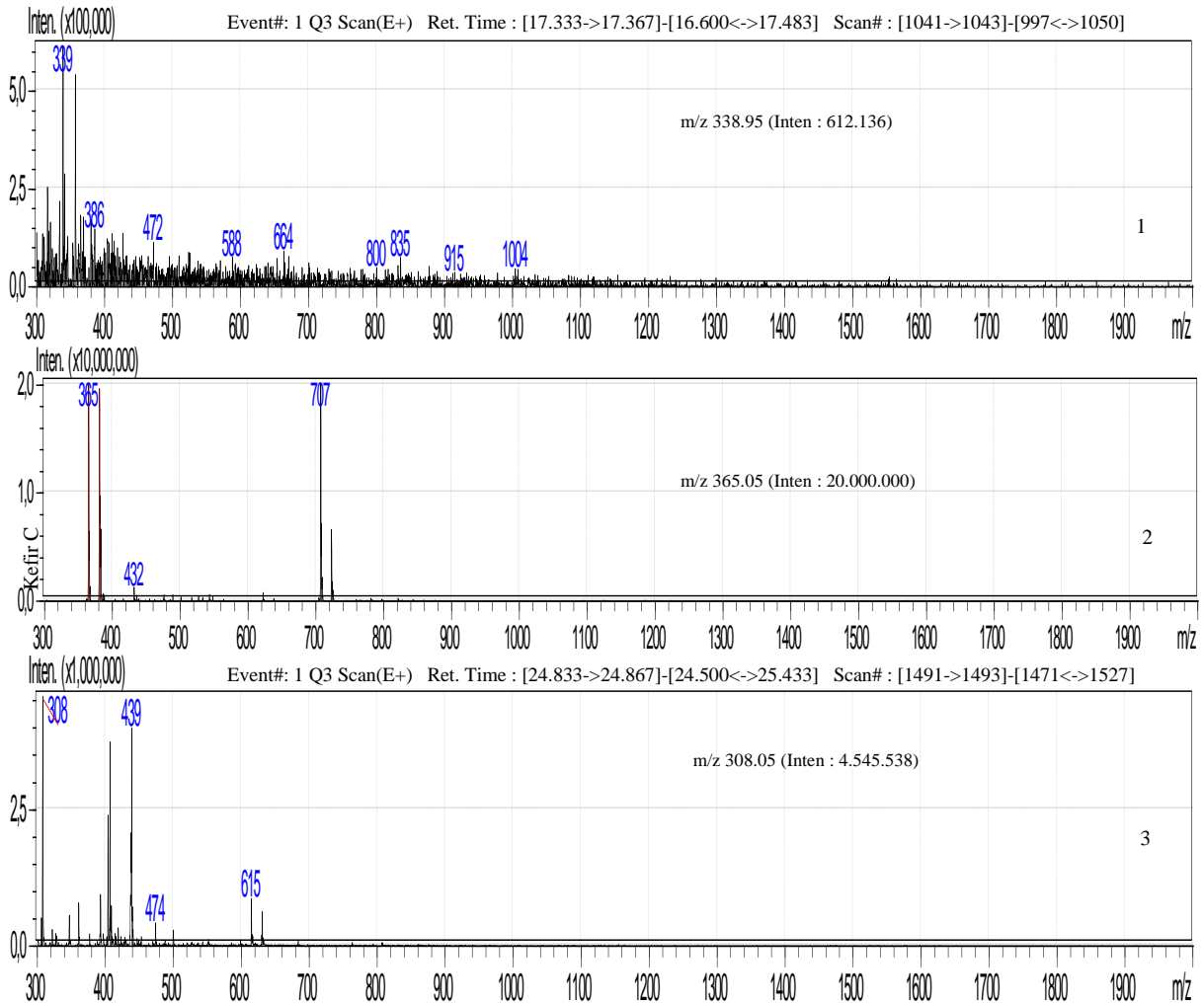


Figure 4- (a) Intensity chromatogram of LCMS/MS spectrum of ions from fraction 2 in sample A; Intensity chromatogram of LCMS/MS spectrum of ions from fraction 2 in sample B. (b) Intensity chromatogram of LCMS/MS spectrum of ions from fraction 2 in sample C.

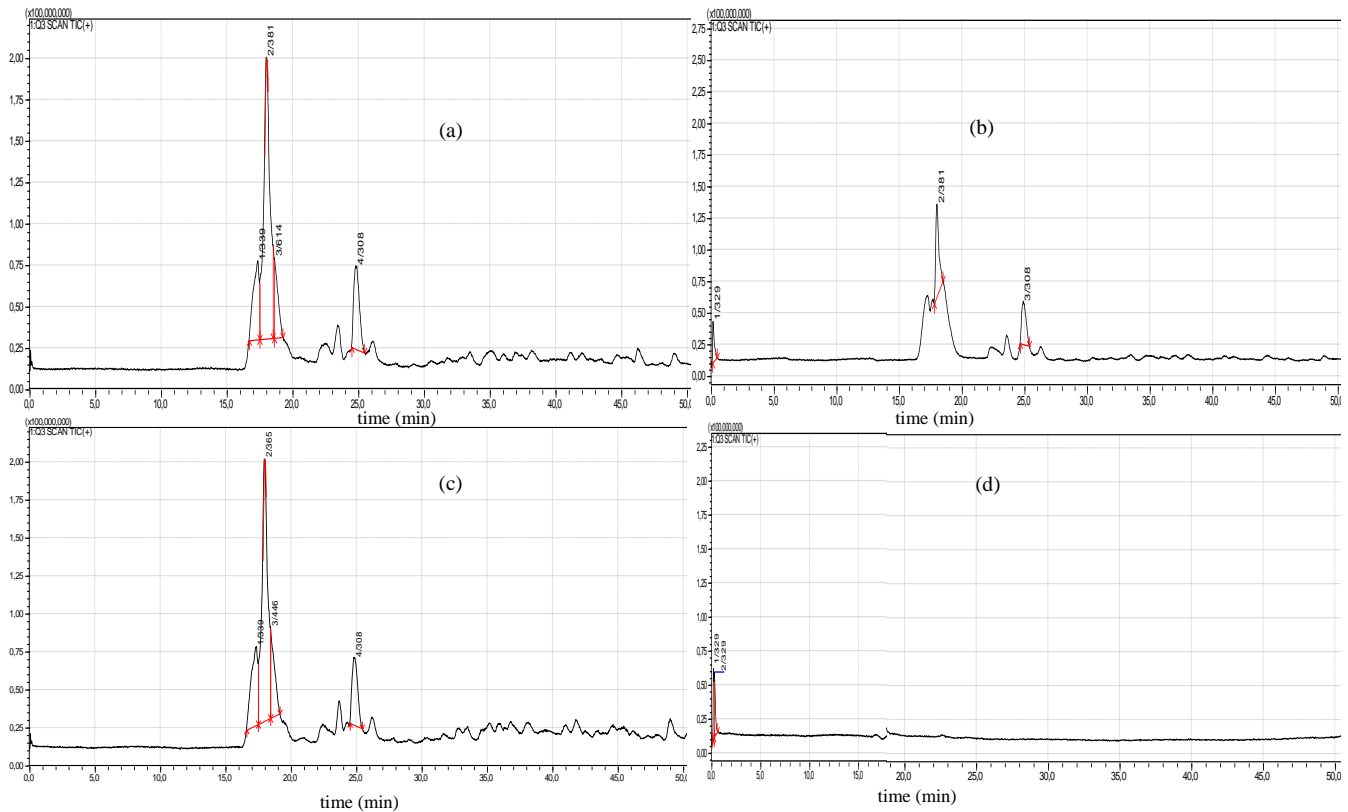


Figure 5- Illustrates total ion chromatogram of fraction 2 with three major peaks. The MS/MS spectrum of peak 1 at 339 m/z, peak 2 at 381 m/z in where the ion of 381 m/z was the most abundant for samples B and A, peak 3 at 308 m/z was shown. The MS/MS spectrum of peak 1 at 339 m/z, peak 2 at 365 m/z in where the ion of 381 m/z was the most abundant for C kefir samples, peak 3 at 308 m/z was shown (a) kefir granule + *L. bulgaricus*; (b) kefir granule + *L. helveticus*; (c) kefir granule + *L. plantarum*, (d) kefir granule containing

4. Conclusions

As a result, the use of adjunct culture in addition to kefir grains obtained better results than the traditional kefir method (produced with kefir grains alone) in terms of proteolysis and bioactive properties. The results show that the ACE-I activity was higher in kefir samples that produced *Lactobacillus* adjunct cultures. It was determined that the peptide fractions (for fraction F2) of the kefir samples produced by the addition of *Lactobacillus* have an antimicrobial effect compared with peptide fractions of sample K. In addition, characterization of the peptide fraction named F2, which has antimicrobial activity against *S. hominis*, *S. warneri* and *S. aureus*, was achieved by LC-MS/MS. These findings supported that the kefir which probiotic fermented product has shown antihypertensive potential as a functional food and indicated application of the peptides as bio-preservative. The shelf life of food products can be extended by using these antimicrobial metabolites produced by selected microorganisms.

Acknowledgments

The authors thank Prof. Dr. Ali Adnan HAYALOGLU for providing the indicator strains used for the antibacterial activity assay and peptides characterization in LC-MS/MS

Financial Support

This study was financially supported by Scientific and Research Project Units of Inonu University, Malatya, Turkey with project number FYL-2017-728.

References

- Ahn C, Kim J & Je J (2014). Purification and antioxidant properties of octapeptide from salmon by product protein hydrolysate by gastrointestinal digestion. *Food Chemistry* 147: 78-83. <https://doi.org/10.1016/j.foodchem.2013.09.136>
- Aihara K, Kajimoto O, Hirata H, Takahashi R & Nakamura Y (2005). Effect of powdered fermented milk with *Lactobacillus helveticus* on subjects with high-normal blood pressure or mild hypertension. *Journal of the American College of Nutrition* 24(4): 257-265. <https://doi.org/10.1080/07315724.2005.10719473>

- Ajam F & Koohsari H (2020). Effect of some fermentation conditions on antibacterial activity of fermented milk by kefir grains. *Journal Food Processing and Preservation* 44(12): 1-14. <https://doi.org/10.1111/jfpp.14913>
- Ahtesh F B, Stojanovska L & Apostolopoulos V (2017). Processing and sensory characteristics of a fermented low-fat skim milk drink containing bioactive antihypertensive peptides, a functional milk product. *International Journal Dairy Technology* 70: 1-10. <https://doi.org/10.1111/1471-0307.12479>
- Beganović J, Kos B, Pavunc A L, Uroić K, Džidara P & Šušković J (2013). Proteolytic activity of probiotic strain *Lactobacillus helveticus* M92. *Anaerobe* 20: 58-64. <https://doi.org/10.1016/j.anaerobe.2013.02.004>
- Chandra P & Vij S (2018). Molecular Characterization and Identification of Bioactive Peptides Producing *Lactobacillus* spp. Based on 16S rRNA Gene Sequencing. *Food Biotechnology* 32(1): 1-14. <https://doi.org/10.1080/08905436.2017.1413657>
- Chandra P, Sharma R K & Singh Arora D (2019). Antioxidant compounds from microbial sources: A review. *Food Research International*, 129: 108849. <https://doi.org/10.1016/j.foodres.2019.108849>
- Chen L, Hui Y, Gao T, Shu G & Chen H (2021). Function and characterization of novel antioxidant peptides by fermentation with a wild *Lactobacillus plantarum* 60. *LWT-Food Science and Technology* 135: 110162. <https://doi.org/10.1016/j.lwt.2020.110162>
- Fang K, Jin X & Hong S H (2018). Probiotic *Escherichia coli* inhibits biofilm formation of pathogenic *E. coli* via extracellular activity of DegP. *Scientific reports* 8(1): 4939. <https://doi.org/10.1038/s41598-018-23180-1>
- Garofalo C, Osimani A, Milanovic V, Aquilanti L, De Filippis F, Stellato G & Clementi F (2015). Bacteria and yeast microbiota in milk kefir grains from different Italian regions. *Food Microbiology*, 49 (7): 123-133. <https://doi.org/10.1016/j.fm.2015.01.017>
- Gobbetti M, Stepaniak L & De Angelis (2002). Latent bioactive peptides in milk proteins: Proteolytic activation and significance in dairy processing. *Critical Reviews in Food Science and Nutrition* 42(3): 223-239. <https://doi.org/10.1080/10408690290825538>
- Grønnevik H, Falstad M & Narvhus J A (2011). Microbiological and chemical properties of Norwegian kefir during storage. *International Dairy Journal* 21(9): 601-606. <https://doi.org/10.1016/j.idairyj.2012.03.005>
- Gul O, Atalar I, Mortas M & Dervisoglu M (2018). Rheological, textural, colour and sensorial properties of kefir produced with buffalo milk using kefir grains and starter culture: A comparison with cows' milk kefir. *International Journal Dairy Technology* 71: 73-80. <https://doi.org/10.1111/1471-0307.12503>
- Güler Z, Tekin A & Park W Y (2016). Comparison of biochemical changes in kefir produced from organic and conventional milk at different inoculation rates of kefir grains. *Journal of Food Science and Nutrition Therapy* 2(1): 8-14. <https://doi.org/10.17352/jfsnt.000003>
- Hayaloglu A A (2007). Comparison of different single-strain starter cultures for their effects on ripening and grading of Beyaz cheese. *Int J Food Science and Technology* 42(8): 930-938. <https://doi.org/10.1111/j.1365-2621.2006.01312.x>
- He B, Ma S, Peng G & He D (2018). TAT-modified self-assembled cationic peptide nanoparticles as an efficient antibacterial agent. *Nanomedicine: Nanotechnol, Bio and Med*, 14(2): 365-372. <https://doi.org/10.1016/j.nano.2017.11.002>
- Huang Y, Ruan G, Qin Z, Li H & Zheng Y (2017). Antioxidant activity measurement and potential antioxidant peptides exploration from hydrolysates of novel continuous microwave-assisted enzymolysis of the *Scomberomorus niphonius* protein. *Food Chemistry* 223: 89-95. <https://doi.org/10.1016/j.foodchem.2016.12.026>
- Indarmawan T, Mustopa A Z, Budiarto B R & Tarman K (2016). Antibacterial activity of extracellular protease isolated from an algicolous fungus *Xylaria psidii* KT30 against gram-positive bacteria. *Hayati Journal of Biosciences* 23(2): 73-78. <https://doi.org/10.1016/j.hjb.2016.06.005>
- Karacalı R, Ozdemir N & Con A H (2018). Aromatic and functional aspects of kefir produced using soya milk and *Bifidobacterium* species. *International Journal Dairy Technology* 71(4): 921-933. <https://doi.org/10.1111/1471-0307.12537>
- Karami Z & Akbari-Adergani B (2019). Bioactive food derived peptides: a review on correlation between structure of bioactive peptides and their functional properties. *Journal Food Science and Technology* 56(2): 535-547. <https://doi.org/10.1007/s13197-018-3549-4>
- Kim D H, Jeong D, Kim H, Kang I B, Chon J W, Song K & Seo K H (2016). Antimicrobial activity of kefir against various food pathogens and spoilage bacteria. *Korean Journal for Food Science of Animal Resources* 36(6): 787-790. <https://doi.org/10.5851/kosfa.2016.36.6.787>
- Kivanc M & Yapici E (2018). Survival of *Escherichia coli* O157: H7 and *Staphylococcus aureus* during the fermentation and storage of kefir. *Food Sci and Technol (Campinas)* 39(1): 225- 230. <https://doi.org/10.1590/ftst.39517>
- Kunji E R S, Mierau I, Hagting A & Poolman W N (1996). Konings The proteolytic systems of lactic acid bacteria. *Antonie Van Leeuwenhoek* 70: 187-221
- Liutkevičius A & Šarkinas (2004). Studies on the growth conditions and composition of Kefir grains-as a food and forage biomass. *Dairy Science Abstracts* 66: 903
- Ma B, Guo Y, Fu X & Jin Y (2020). Identification and antimicrobial mechanisms of a novel peptide derived from egg white ovotransferrin hydrolysates. *LWT - Food Science and Technology* 131: 109720. <https://doi.org/10.1016/j.lwt.2020.109720>
- Maeda H, Zhu X, Suzuki S, Suzuki K & Kitamura S (2004). Structural characterization and biological activities of an exopolysaccharide kefir produced by *Lactobacillus kefir* of strains WT-2B (T). *Journal of Agricultural and Food Chemistry* 52(17): 5533-5538. <https://doi.org/10.1021/jf049617g>
- Miao J, Guo H, Chen F, Zhao L & He L (2016). Antibacterial effects of a cell penetrating peptide isolated from kefir. *Journal of Agricultural and Food Chemistry* 64(16): 3234-3242. <https://doi.org/10.1021/acs.jafc.6b00730>
- Monteiro C, Carmo M do, Melo B, Alves M, dos Santos C, Monteiro S, Bomfim M, Fernandes E & Monteiro-Neto V (2019). In vitro antimicrobial activity and probiotic potential of bifidobacterium and lactobacillus against species of clostridium. *Nutrients* 11(2):448. <https://doi.org/10.3390/nu11020448>
- Nielsen M S, Martinusen T, Flambarb B, Sorensen K I & Otte J (2009). Peptide profiles and angiotensin-I-converting enzyme inhibitory activity of fermented milk products: effect of bacterial strain, fermentation pH and storage time. *International Dairy Journal* 19(3): 155-165. <https://doi.org/10.1016/j.idairyj.2008.10.003>
- Otte J, Lenhard T, Flambarb B & Sorensen (2011). Influence of fermentation temperature and autolysis on ACE-I activity and peptide profiles of milk fermented by selected strains of *Lactobacillus helveticus* and *Lactococcus lactis*. *International Dairy Journal* 21(4): 229-238
- Ozcan T, Sahin S, Akpınar-Bayızıt A & Yılmaz-Ersan L (2019). Assessment of antioxidant capacity by method comparison and amino acid characterisation in buffalo milk kefir. *International Journal of Dairy Technology* 72(1):65-73. <https://doi.org/10.1111/1471-0307.12560>
- Pan D, Luo Y & Tanokura M (2005). Antihypertensive peptides from skimmed milk hydrolysate digested by cell-free extract of *Lactobacillus helveticus* JCM1004. *Food Chemistry* 91: 123-129. <https://doi.org/10.1016/j.foodchem.2004.05.055>
- Pihlanto-Leppälä A (2000). Bioactive peptides derived from bovine whey proteins: Opioid and ACE-I peptides. *Trends in Food Science and Technology* 11(9-10): 347-356. [https://doi.org/10.1016/s0924-2244\(01\)00003-6](https://doi.org/10.1016/s0924-2244(01)00003-6)

- Pina-Perez M C, Rodrigo D & Martinez A (2015). Using natural antimicrobials to enhance the safety and quality of milk. In M. Taylor (Ed.). Handbook of natural antimicrobials for food safety and quality Elsevier Ltd. 327-340.
- Pogačić T, Šinko S, Zamberlin Š & Samaržija D (2013). Microbiota of kefir grains. *Mljekarstvo* 63(1):3-14
- Pripp A H, Isaksson T, Stepniak L, Sorhaug T (2004). Quantitative structure-activity relationship modelling of ACE-inhibitory peptides derived from milk proteins. *European Food Research and Tehcnology* 219(6): 579-583. <https://doi.org/10.1007/s00217-004-1004-4>
- Prado M R, Blandon L M, Vandenbergh L P S, Rodrigues C, Castro G R, Soccolli V T & Soccolli C R (2015). Milk kefir: Composition, microbial cultures, biological activities, and related products. *Frontiers in Microbiology* 6: 1-10. <https://doi.org/10.3389/fmicb.2015.01177>
- Purutoglu K, Ispirli H, Yuzer M O, Serencam H & Dertli E (2020). Diversity and functional characteristics of lactic acid bacteria from traditional kefir grains. *International Journal of Dairy Technology* 73(1): 57-66. <https://doi.org/10.1111/1471-0307.12633>
- Quiros A, Hernandez-Ledesma B, Ramos M, Amigo L & Recio I (2005). Angiotensin-converting enzyme inhibitory activity of peptides derived from caprine Kefir. *Journal Dairy Science* 88(10): 3480-3487. [https://doi.org/10.3168/jds.s0022-0302\(05\)73032-0](https://doi.org/10.3168/jds.s0022-0302(05)73032-0)
- Rutella G S, Tagliacuzzi D & Solieri L (2016). Survival and bioactivities of selected probiotic lactobacilli in yogurt fermentation and cold storage: New insights for developing a bi-functional dairy food. *Food Microbiology* 60: 54-61. <https://doi.org/10.1016/j.fm.2016.06.017>.
- Sahingil D, Gokce Y, Yuceer M & Hayaloglu A A (2019). Optimization of proteolysis and angiotensin converting enzyme inhibition activity in a model cheese using response surface methodology. *LWT-Food Science and Techonology* 99:525-532. <https://doi.org/10.1016/j.lwt.2018.09.076>
- Sanlı T, Akal H C, Yetisemiyen H & Hayaloglu A A (2018). Influence of adjunct cultures on angiotensin-converting enzyme (ACE)-inhibitory activity, organic acid content and peptide profile of kefir. *International Dairy Technology* 71(1):131-139. <https://doi.org/10.1111/1471-0307.12346>
- Savijoki K, Ingmer H & Varmanen P (2006). Proteolytic systems of lactic acid bacteria. *Applied Microbiology Biotechnology* 71: 394-406. <https://doi.org/10.1007/s00253-006-0427-1>
- Schanbacher F L, Talhouk R S, Murray F A, Gherman L I & Willet L B (1998). Milk-born bioactive peptides. *International Dairy Journal* 8(5-6): 393-403
- Shu G, Shi X, Chen H, Ji Z & Meng J (2017). Optimization of goat milk with ACE-Ipeptides fermented by *Lactobacillus bulgaricus* lb6 using response surface methodology. *Molecules* 22(11): 2001. <https://doi.org/10.3390/molecules22112001>
- Simova E, Beshkova D, Angelov A, Hristozova T, Frengova G & Spasov Z (2002). Lactic acid bacteria and yeasts in kefir grains and kefir made from them. *Journal of Industrial Microbiology and Biotec* 28: 1-6
- Simova E, Simov Z, Beshkova D, Frengova G, Dimitrov Z & Spasov Z (2006). Amino acid profiles of lactic acid bacteria, isolated from kefir grains and kefir starter made from them. *International Journal of Food Microbiology* 107(2): 112-123. <https://doi.org/10.1016/j.ijfoodmicro.2005.08.020>
- Sulejmani E & Hayaloglu A A (2017). Characterisation of Macedonian White brined cheese: Effect of raw or heat-treated caprine milk. *International Journal Dairy Technology* 71(2): 408-416. <https://doi.org/10.1111/1471-0307.12486>
- Sundin G W & Wang N (2018). Antibiotic Resistance in Plant-Pathogenic Bacteria. *Annual Review of Phytopathology* 56: 161-180. <https://doi.org/10.1146/annurev-phyto-080417-045946>
- Tas T K, Ekinci F Y & Guzel-Seydim Z B (2012). Identification of microbial flora in kefir grains produced in Turkey using PCR. *International Journal Dairy Technology* 65(1): 126-131. <https://doi.org/10.1111/j.1471-0307.2011.00733.x>
- Taşkın B & Akköprü A (2020). Antibacterial Activity of Different Kefir Types Against Various Plant Pathogenic Bacteria. *Journal of Agricultural Sciences* 26: 316-323. <https://doi.org/10.15832/ankutbd.499790>
- Teneva D, Denkova R, Goranov B, Denkova Z & Kostov G (2017). Antimicrobial activity of *Lactobacillus plantarum* strains against Salmonella pathogens. *Ukrainian Food Journal* 6(1): 125-133. <https://doi.org/10.24263/2304-974x-2017-6-1-14>
- Upendra R S, Khandelwal P, Jana K, Ajay Kumar N, Gayathri Devi M & Stephaney M L (2016). Bacteriocin production from indigenous strains of lactic acid bacteria isolated from selected fermented food sources. *International Journal Pharma Reseource Health Sci* 4(1): 982-990
- Wang H, Sun X M, Song X, Guo & M R (2021) Effects of kefir grains from different origins on proteolysis and volatile profile of goat milk kefir. *Food Chemistry* 339: 128099. <https://doi.org/10.1016/j.foodchem.2020.128099>
- Witthuhn R C, Schoeman T & Britz T J (2004). Isolation and characterization of the microbial population of different South African kefir grains. *International Journal Dairy Technology* 57(1): 33-37. <https://doi.org/10.1111/j.1471-0307.2004.00126.x>
- Zaeim D, Soleimanian-Zad S & Sheikh-Zeinoddin M (2014). Identification and partial characterization of a bacteriocin-like inhibitory substance (BLIS) from *Lb. bulgaricus* K41 isolated from indigenous yogurts. *Journal of Food Science* 79(1):67-73. <https://doi.org/10.1111/1750-3841.12314>
- Zajsek K & Gorsak A (2011). Experimental assessment of the impact of cultivation conditions on kefir production by the mixed microflora imbedded in kefir grains. *Chemical Engineering Transactions* 24: 481-486 2011. <https://doi.org/10.1016/j.foodchem.2012.11.142>
- Zhang M, Jiang Y, Cai M & Yang Z (2020). Characterization and ACE-I activity of fermented milk with probiotic *Lactobacillus plantarum* K25 as analyzed by GC-MS based metabolomics approach. *Journal of Microbiology and Biotechnology* 30(6): 903-911. <https://doi.org/10.4014/jmb.1911.11007>
- Zheng Z, Si D, Ahmad B, Li Z & Zhang R (2018). A novel antioxidative peptide derived from chicken blood corpuscle hydrolysate. *Food Research International* 106: 410-419. <https://doi.org/10.1016/j.foodres.2017.12.078>
- Zhou T, Huo R, Kwok L Y, Li C, Ma Y & Mi Z (2019). Effects of applying *Lactobacillus helveticus* H9 as adjunct starter culture in yogurt fermentation and storage. *Journal of Dairy Science* 102: 223-235. <https://doi.org/10.3168/jds.2019-102-2-1885>
- Zhu B, He H & Hou T (2019). A comprehensive review of corn protein-derived bioactive peptides: production, characterization, bioactivities, and transport pathways. *Comprehensive Reviews Food Sci and Food Safety* 18: 329-345. <https://doi.org/10.1111/1541-4337.12411>
- Zhu C Z, Zhang W G, Zhou G H, Xu X L, Kang Z L & Yin Y (2013). Isolation and identification of antioxidant peptides from Jinhua ham. *Journal of Agricultural and Food Chemistry* 61(6): 1265-1271. <https://doi.org/10.1021/jf3044764>





Effects of Donor x Inducer Interaction on the Success of Haploid Induction and Comparison of Haploid Seed Identification Methods in the In vivo Maternal Haploid Technique in Maize

Fatih KAHRIMAN^{a*} , Umut SONGUR^a , Abdullah DIŞBUDAK^b , Sezgin KIZIK^b , Berk VURAL^b 

^aÇanakkale Onsekiz Mart University, Faculty of Agriculture, Department of Field Crops, Çanakkale, TURKEY

^bAGROMAR Inc., Bandırma Yolu 1. Km., Karacabey, Bursa, TURKEY

ARTICLE INFO

Research Article

Corresponding Author: Fatih KAHRIMAN, E-mail: fkahriman@hotmail.com

Received: 10 November 2020 / Revised: 16 May 2021 / Accepted: 20 June 2021 / Online: 01 September 2022

Cite this article

KAHRIMAN F, SONGUR U, DIŞBUDAK A, KIZIK S, VURAL B (2022). Effects of Donor x Inducer Interaction on the Success of Haploid Induction and Comparison of Haploid Seed Identification Methods in the In vivo Maternal Haploid Technique in Maize. *Journal of Agricultural Sciences (Tarım Bilimleri Dergisi)*, 28(3):385-395. DOI: 10.15832/ankutbd.824114

ABSTRACT

This study was conducted to investigate the effect of donor and inducer lines on the haploid induction rate in the in vivo maternal doubled haploid technique in maize and to compare the methods used in haploid seed separation. In the study, three donor materials were used for induction crossing with two inducer lines. Seedling immersion and stem injection techniques were used as chromosome doubling methods. Eye separation, spectral measurements and image processing were used to identify seed classes. Data were modeled using support vector machine method and created models were evaluated over the complexity matrix. The results of

the research revealed that the haploid induction rate varies depending on the donor genotypes and inducers, and the genotype responses against the applied chromosome doubling method were also different. Differences were observed in the success of the three methods compared for haploid and diploid seed separation. The successful classification rates were 87%, 83%, and 79% in visual, spectral and image processing models, respectively. Results showed that both spectral technique and image processing technique can be used to distinguish haploid/diploid seeds in in vivo maternal haploid technique.

Keywords: Seed classification, Spectral analysis, Ploidy, Chromosome doubling, Support vector machine

1. Introduction

Parental line development is one of the strategic steps in hybrid maize breeding. Traditional methods for developing parental lines require selfing over 6-10 generations (Hallauer et al. 2010). In addition, it is theoretically impossible to reach 100% homozygosity by traditional methods; therefore, there is a need to develop alternative methods. Traditional methods are time consuming and labor-intensive process, which are main disadvantages of them. In vitro (Chidzanga et al. 2017) and in vivo (Chalky 1994) techniques developed as alternatives to classical methods used for pure line development in maize breeding eliminated these disadvantages and proved very convenient to breeders. The in vivo doubled haploid technique is widely preferred compared to in vitro methods due to its ease of application and higher success rate.

The in vivo haploid technique is based on obtaining haploid seeds after hybridization of the donor material with a parent called the “inducer”, and duplication of the chromosome number of haploid seedlings with specific chemical agents. In practice, this technique is applied in two ways, paternal and maternal in vivo haploids. The paternal haploid technique relies on using the donor material as male, while in the maternal haploid technique, the donor material is used as the female parent in the induction cross (Röber et al. 2005; Chidzanga et al. 2017). Almost all maternal haploid inducers currently used are generated from an inducer line called Stock 6 (Choe 1959). While the induction potential of Stock 6 was about 2-3%, the induction potential of materials such as RWS, UH400, PHI and MHI developed from this material was increased to 7% to 16% (Kalinowska et al. 2019). As a result, the use of the in vivo haploid technique in maize breeding studies has recently become popular. Regardless of the induction method or induction line used, increasing the success of this method has strategic importance for maize breeding programs all over the world.

Success with the in vivo haploid technique can be attained by three main factors. The first is the genotypic characteristics of the inducer or donor materials, the second is the chromosome doubling method used, and the third is the identification success of haploid seeds. Obviously, the growing conditions and environmental factors cannot be ignored in the success of the in vivo haploid technique.

The most important genotypic effect in the *in vivo* doubled haploid technique is the induction potential of the inducer line used. Not all inducers provide the same success, and they cannot be used in harmony with every donor (female parent) genotype. In fact, the induction rates achieved in studies using different numbers of donor materials showed a wide variation ranging from 7.1% to 12.8% (Cerit et al. 2016; Zararsız et al. 2019). These results demonstrate that donors and inducers play a key role in the *in vivo* doubled haploid technique.

The second issue affecting the success of the *in vivo* doubled haploid technique is the chromosome doubling method. The main techniques used for chromosome doubling are application of an inducing agent (colchicine) to the stem or seedlings; or alternatively, giving ozone or N₂O gas treatment to seedlings (Chaikam et al. 2019). Among these methods, seedling immersion (Prasanna et al. 2012) and colchicine injection to the stem (Vanous et al. 2017) are among the most widely-used techniques. These techniques show differences in terms of application, and affect both the chromosome doubling rates and the number of DH1 seeds that are finally developed.

The third aspect that influences the success of the *in vivo* haploid technique is the correct identification of haploid seeds. The usual approach used in the selection of haploid seeds is by human eye selection. This selection made anthocyanin production by the effects of marker genes alleles namely as R1-nj and P11 (Uliana Trentin et al. 2020). R1-nj allele causes the seed coloration while P11 allele creates colored roots after induction crossing. Selection by haploids/diploids by eye can be performed based on the color change in the embryo and crown area of the seed or root coloration caused by dominant marker genes carried by the inducer lines (Vanous et al. 2017). Since the labor force required to do this task is high with the visual selection method, and the error rate depends on the person performing the classification, alternative methods are needed. For this purpose, it has been shown that by digitizing images taken of the seeds, visual distinction can be carried out more precisely and faster (Altuntaş et al. 2018; Veeramani et al. 2018; Altuntaş & Kocamaz 2019; Altuntaş et al. 2019).

Studies have also shown that it is possible to separate haploid seeds using near infrared spectroscopy (Jones et al. 2012; Lin et al. 2017). It has also been suggested that haploid seed classification is possible depending on the seed oil content and seed color, and that the oil content can be determined by a nuclear magnetic resonance (NMR) device without damaging the seed (Melchinger et al. 2013; Melchinger et al. 2014). Haploid identification can not only determine the seed level in maize but also be carried out based on plant measurements. Choe et al. (2012) developed a method based on the measurement of stomatal cell width at the 2-leaf stage to differentiate true haploid and diploid plants. They verified the results by coloration in the stalk and flow cytometric measurements and emphasized that this classification was successful in the 7-leaf period.

Studies on the *in vivo* doubled haploid technique in the current literature are constantly increasing. Investigating the interaction of inducer and donor materials, and developing methods for successful haploid/diploid seed classification are among the most studied topics. However, the fact that the techniques used in studies on haploid/diploid seed classification were carried out according to a single method (eye separation, image processing, spectral techniques, etc.) leaves an important gap in the scientific literature. A detailed comparative study is needed to clearly identify the advantages of one method over another. Furthermore, a comparison of haploid induction rates and the success of tropic and temperate inducers are still open to research.

Accordingly, this study was carried out i) to investigate the reactions of donor materials to different inducers and chromosome doubling methods, and ii) to compare the effectiveness of different techniques used in haploid seed classification.

2. Material and Methods

2.1. Plant material

In this study, 3 donors and one inducer (RWK76/RWS) belonging to AGROMAR Inc. Donors are F2 materials from AGROMAR maize genetic stocks. Other inducer line (CIM2GTAIL-P2) was used with permission from The International Maize and Wheat Improvement Center (CIMMYT) for scientific studies in the Field Crops Department of Çanakkale Onsekiz Mart University (Turkey), Faculty of Agriculture (Table 1).

Table 1- Donor and inducer materials used in this study

<i>Code</i>	<i>General Features</i>	<i>Source</i>
DNR1	Donor material	AGROMAR Inc.
DNR4	Donor material	AGROMAR Inc.
DNR5	Donor material	AGROMAR Inc.
CIM2GTAIL-P2	Second generation inducer line	CIMMYT
RWK76/RWS	Inducer hybrids	AGROMAR Inc.

2.2. Induction crossing

Induction hybridization was carried out under greenhouse conditions in this study. Each donor was planted in pots with 60-70 plants. Transplantation was carried out in September 2019. When the plants reached the flowering stage, pollination was carried

out with at least 10 plants belonging to each donor genotype by using each inducer line as the pollen source (male parent). The controlled pollination method suggested by Kahrıman (2016) was used in the pollination process. The harvest was carried out by hand and DH0 seeds obtained from induction crosses were kept at +4 °C for use in the next steps.

2.3. Seed classification methods

Three different classification methods were used in the study, and haploid identification was performed based on observation by eye, spectral data and image data, respectively. At least 200 seeds (100 haploids and 100 diploids) were separated for each donor material and totally 600 seeds were used for performing seed identification methods. Detailed information about the identification methods used is described below.

The first separation of the seed samples (with the eye) was named "Initial Classification" in the study, and classification was made according to the coloration of the embryo and crown area in DH0 seeds. If there was coloration in the crown area and without coloration in embryo of the seed examined, this seed was considered as haploid, and if there was coloration in both the crown area and the embryo region, this seed was evaluated as diploid. A seed-based labeling method was used in order to prevent confusing seed samples classified by eye separation with the stage of the field evaluation. Seed samples were kept at +4 °C in the labeled seed trays until other measurements were carried out.

Image classification at the single seed level was performed by making some revisions to the method suggested by Altuntaş et al. (2018). The images of the seeds, which were separated by the eye, were recorded by the embryo side in the desktop scanner with jpeg extension. The background of the seed images was black and this was removed before the extraction of image features. A total of 6 different features were extracted to be used in modeling studies based on the image data. These were the pixel values of the R, G, B channels of the whole seed image and the pixel values of the R, G, B channels of the embryo region. Segmentation and feature extraction operations were carried out with the R package program (R Core Team 2019). These data were kept as an excel file to be used in model development studies.

Spectral data (1200-2400 nm interval) were taken from each seed that was classified by eye and image processing (Figure 1). Data were collected in terms of the embryo side of the seeds, and for this purpose a special sample cup for single seed measurement was used in the NIR spectroscopy device (Spectrastar 2400D, Unity Scientific, USA). Spectra acquisition was carried out in the stationary measurement mode. The obtained spectral data were recorded with the label given to the individual seed sample and converted into an excel file to create the spectral models.

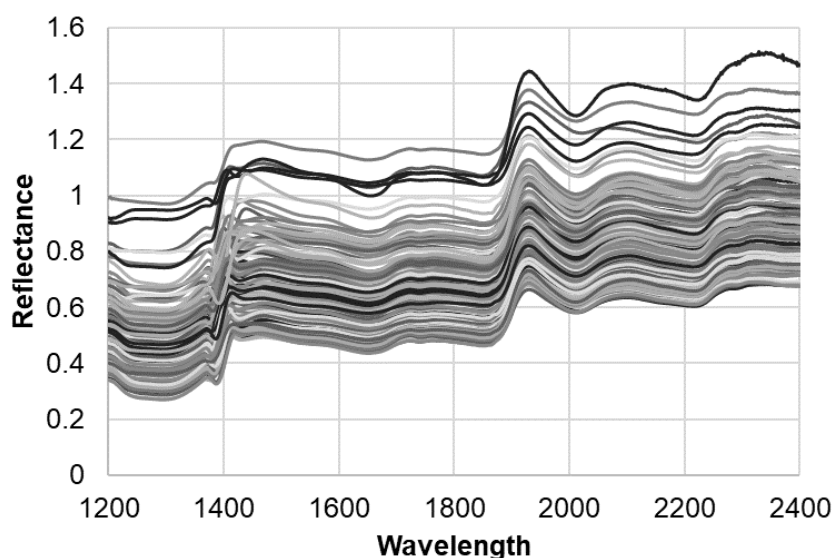


Figure 1- Spectral data obtained from single seed NIR measurements

2.4. Chromosome doubling methods

Two different chromosome doubling methods were used in the study. One of these methods is seedling immersion, which is widely used in the scientific literature (Deimling et al. 1997). The first 50 of the 100 haploid seeds for each donor × inducer cross were germinated in the way that the seed labels were given at the classification stage. After germination, the root tips and coleoptiles (2-3 cm) were cut with a scalpel and kept in a colchicine tank for 12 hours in a solution containing 0.06% colchicine and 0.05% DMSO (Dimethyl sulfoxide). At least 50 seeds per donor remaining from the first method were germinated and the doubling chemical solution was injected into the stem according to the stem injection method proposed by Zabirowa et al. (1996). In the injection, a doubling solution consisting of 100 microliters 0.125% colchicine and 0.5% dimethyl sulfoxide (DMSO) was

injected to stem with a 1 mL sterile syringe at the stage of 2-3 collared leaves (Vanous et al. 2017). After the injection, the plants were kept under greenhouse conditions until they reached the stage to be transplanted in the field. The number of plants that remained alive at the stages of germination, seedling and transplanting to the field was recorded. In both methods, the transplantation process was performed by germinating the diploid seeds without chromosome doubling treatment.

2.5. Growing DH0 plants in the field and determination false classified seeds

At this stage, the colchicine-treated seedlings of haploids and untreated diploid seedlings were transplanted into the field. In the transplanting process, the seedlings obtained from haploid and diploid seeds were transferred to the field in 2-row sub-plots of 5 meters according to the seed labels. One label was used per seedling and the observations made in the field were taken according to these labels, which show the original seed code.

In order to verify the success of the chromosome doubling treatment and the methods used in seed classification, the haploid/diploid plants were subjected to "Final Classification". This classification was made based on the visual state of the plants investigated. Vigorous plants with stem colorization were accepted as diploid, while the plants with erect leaves were classified as haploid. In addition, the success of chromosome doubling process was controlled by checking the fertile plants under field conditions. Records were kept on the labels given to the seeds throughout the whole process, from the beginning of the study to the field stage.

2.6. Statistical analysis

From the calculations made for the first aim of the study, the haploid induction rates and the success of the doubling process according to the state of DH1 plants were determined according to the equations 1, 2, 3, 4, and 5 suggested by Zararsiz et al. (2019).

$$\text{Haploid Induction Rate (HIR)} = \left(\frac{\text{Number of haploid seeds}}{\text{Number of total seeds}} \right) \times 100 \quad (1)$$

$$\text{Haploid Germ. Rate (HGR)} = \left(\frac{\text{No. of haploid seeds} - \text{No. of unger. seeds}}{\text{Num. of total haploid seeds}} \right) \times 100 \quad (2)$$

$$\text{Surviving Seedlings Rate (SSR)} = \left(\frac{\text{Number of transplanted seedlings}}{\text{Number of colchicine-treated seedlings}} \right) \times 100 \quad (3)$$

$$\text{Surviving Plant Ratio (SPR)} = \left(\frac{\text{Number of surviving plants}}{\text{Number of transplanted seedlings}} \right) \times 100 \quad (4)$$

$$\text{Chromosome Duplication Rate (CDR)} = \left(\frac{\text{Number of fertile plants}}{\text{Number of selected plants}} \right) \times 100 \quad (5)$$

For the second aim of the study, the evaluation statistics were calculated over the confusion matrix between the results obtained from the initial classification made by eye and the final classification performed in the field. Initial and final classification data were used as dependent variables in developing classification models based on images and spectral data. In order to develop spectral models, two separate classification models (Spectral Model 1 and Spectral Model 2) were created by using the support vector machines (SVM) method. In these models, spectral data between 1200-2400 nm were used as the predictive variable, and initial classification and final classification data as the predicted variable.

For the purpose of model development based on image data, 6 different features extracted from the images were taken as predictive variables, and two separate classification models (Image Model 1 and Image Model 2) were created using SVM method. Additionally, the Classification and Regression Tree (CRT) method was used in order to determine the features that were effective in haploid/diploid seed classification and the limit values of the features extracted from image data. All analyses were made in the R program (R Core Team 2019). For comparison of the created estimation models, the calculations made over the confusion matrix (Table 2) were used.

Table 2- Confusion matrix template used in calculations for classification of haploid and diploid seeds

Prediction	Actual	
	Haploid	Diploid
Haploid	TP	FP
Diploid	FN	TN

The false discovery rate (FDR) and false negative rate (FNR) were determined using the confusion matrix using Equations 6 and 7 suggested by Melchinger et al. (2013). In addition, the calculations for the classification success of the models were followed by the sensitivity, specificity, prevalence, positive predictive value, negative predictive value, detection rate, detection prevalence, balanced accuracy, and accuracy values over the confusion matrix, calculated according to the equations 8-16.

$$FNR = \frac{FN}{TP+FN} \quad (6)$$

$$FDR = \frac{FP}{TP+FP} \quad (7)$$

$$Sensitivity = \frac{TP}{TP+FN} \quad (8)$$

$$Specificity = \frac{TN}{FP+TN} \quad (9)$$

$$Prevalence = \frac{TP+FN}{TP+FN+FP+TN} \quad (10)$$

$$Pos. Pred. Val. (PPV) = \frac{TP}{TP+FP} \quad (11)$$

$$Neg. Pred. Val (NPV) = \frac{TN}{TN+FN} \quad (12)$$

$$Detection Rate = \frac{TP}{TP+FN+FP+TN} \quad (13)$$

$$Detection Prevalence = \frac{TP+FP}{TP+FN+FP+TN} \quad (14)$$

$$Balanced Accuracy = \frac{Sensitivity+Specificity}{2} \quad (15)$$

$$Accuracy = \frac{TP+TN}{TP+FN+FP+TN} \quad (16)$$

In addition to these calculations, Spearman Rank Correlation was applied in the R program (R Core Team 2019) in order to determine the relationship between model predictions and the actual case. The correlation coefficients obtained are shown in the evaluation table of the model statistics.

3. Results and Discussion

3.1. Donor x inducer interaction on success of haploid induction

The haploid induction rates in this study varied between 9.2% and 16.1% (Table 3). Since HIR calculations were made on all seeds obtained from induction cross, they were not calculated separately according to chromosome doubling methods. It was observed that DNR1 and DNR5 provided higher HIR with RWK76 / RWS inducer line and DNR4 with CIM2GTAIL-P2 inducer line than other induction crosses. After randomly separating two subgroups of haploid seed samples for each chromosome doubling methods, haploid germination rates (HGR) varied between 64% and 100% in seedling immersion method and 72% to 93% in stem injection method. The stem injection method had a higher average for the surviving seedling rate (SSR) than the seedling immersion method. This continued in the plants surviving rate (PSR) in the field and stem injection method was also found to be advantageous compared to seedling immersion method. Chromosome doubling rates of the donors used were found to be higher in seedling immersion method for all donors except for the DNR4xCIM2GTAIL-P2 cross (Table 3).

Table 3- HIR (%), HGR (%), SSR (%), SPR (%) and CDR (%) values for donor materials according to chromosome doubling methods

Chromosome Doubling Method	Induction Cross	HIR [†]	HGR	SSR	SPR	CDR
Seedling Immersion Method	DNR1xCIM2GTAIL-P2	9.20	80.0	56.0	88.0	46.7
	DNR1xRWK76/RWS	10.50	77.0	85.0	100.0	50.0
	DNR4xCIM2GTAIL-P2	13.80	100.0	58.0	60.0	46.2
	DNR4xRWK76/RWS	10.40	98.0	63.0	82.0	39.5
	DNR5xCIM2GTAIL-P2	9.70	64.0	47.0	87.0	42.9
	DNR5xRWK76/RWS	16.10	93.0	68.0	100.0	45.9
	Mean	11.62	85.3	62.8	86.2	45.2
Stem Injection Method	DNR1xCIM2GTAIL-P2	9.2	85.0	100.0	100.0	35.7
	DNR1xRWK76/RWS	10.50	88.0	88.8	100.0	45.7
	DNR4xCIM2GTAIL-P2	13.80	76.0	100.0	100.0	47.2
	DNR4xRWK76/RWS	10.40	93.0	100.0	85.0	32.3
	DNR5xCIM2GTAIL-P2	9.70	88.0	100.0	90.0	39.6
	DNR5xRWK76/RWS	16.10	72.0	100.0	92.0	38.0
	Mean	12.10	83.7	98.1	94.5	39.7

[†]: HIR rate is the same for both chromosome doubling methods due to the HIR calculation based on haploid/diploid seed classification at the beginning of the study

HIR values for the in vivo maternal haploid technique varied between 2.8% and 12.8% in the scientific literature (Eder & Chalyk 2002; Prigge et al. 2012; Cerit et al. 2016; Zararsız et al. 2019). It was emphasized that the HIR varies according to the donors and inducer lines used. The results obtained in the current study are also in agreement with this. The germination rates of haploid seeds are relatively low compared to diploids. In our study, the results obtained during the germination stage are similar to those obtained in previous studies. It was observed that the chromosome doubling treatment had a significant effect on plant viability. Seedling immersion method was found to be disadvantageous in terms of the number of seedlings and plants surviving both in the seedling and field stage compared to stem injection method. In other studies, the number of seedlings and plants surviving with the seedling immersion method were found to be between 57.9% and 72.9%, respectively (Zararsız et al. 2019). These results can be attributed to the adverse effects of root tip cutting on plant growth and survival rate.

Chromosome doubling rates (CDR) are ultimately an important parameter in the in vivo maternal haploid technique. In our study, chromosome doubling rates ranged from 32.3% to 50.0% and these results were similar to the values reported in the current literature (Prasanna et al. 2012; Zararsız et al. 2019). On the other hand, it has been observed that there are significant differences between induction crosses. According to all assessments, the interaction of donor and inducer lines, as well as their reactions to chromosome doubling methods used in the in vivo maternal haploid technique, displayed significant differences.

3.2. Comparison of seed classification techniques

The confusion matrix of the seed classification results is presented in Table 4. In this matrix, haploids are taken as positive groups and diploids as negative groups. The results for initial classification and final classification showed that eye classification had higher rate of misclassification in haploid seeds than diploids (Table 3). Based on initial classification results, 55 of the 245 haploid seeds and 13 out of 300 diploid seeds were misclassified. Considering the numbers in the final classification, 300 diploid and 245 haploid seeds allocated at the initial classification were determined as 342 diploid and 203 haploid seeds. Dang et al. (2012) attributed the increase of misclassification in the eye method to the fact that the donor material did not adequately show the pigmentation resulting from the inducer line or had a genetic structure of donor material that prevented pigment formation. In our study, the emergence of haploid plants from diploids can be attributed to the adequate selection of pigmentation in the endosperm/embryo region or to spontaneous haploid formation. On the other hand, it is understood that the formation of pigmentation in the embryo region of haploid seeds cannot be distinguished by the eye, and as a result, it is possible to classify diploid seeds as haploid. As an alternative method in seed classification, spectral and image processing data are treated as predictive, and the initial and final classification data made by the eye are taken as dependent variables, whereby FP values are higher than visual classification (Table 4). Similarly, FN values are higher than the erroneous seed numbers in classifications made by eye.

Table 4- Confusion matrix values for eye, spectral and image classification

<i>Seed Identification Method</i>	<i>FN</i>	<i>FP</i>	<i>TP</i>	<i>TN</i>
Eye	55	13	190	287
Spectral Model 1	65	23	180	277
Spectral Model 2	69	28	134	314
Image Model 1	81	39	164	261
Image Model 2	79	32	124	310
Mean	70	27	158	270

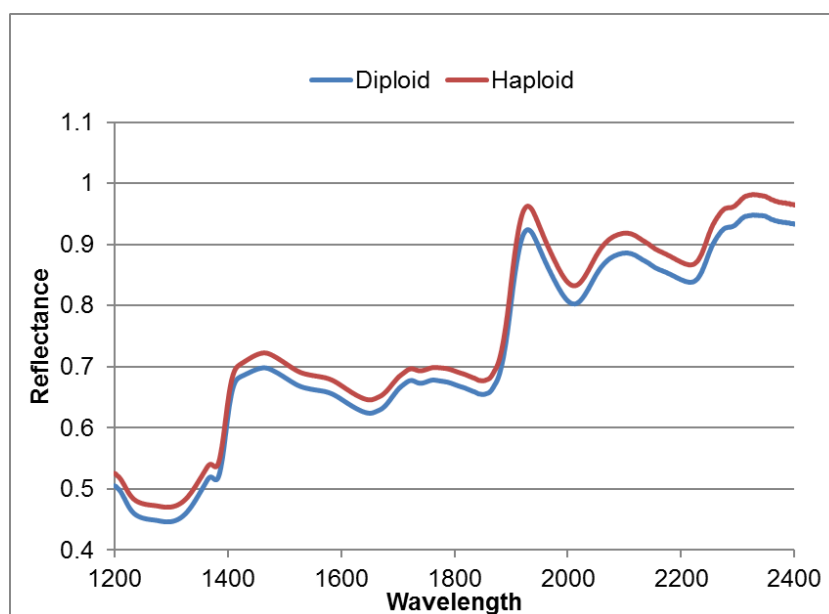
FP: False positive, FN: False negative, TP: True positive, TN: True negative

According to the statistics calculated over the confusion matrix (Table 5), eye classification had a higher accuracy (87.50%) than the accuracy from the spectral models (Spectral Model 1= 0.839, Spectral Model 2= 0.822) and image models (Image Model 1= 0.780, Image Model 2= 0.796). For all models, sensitivity values (Eye= 0.776, Spectral Model 1= 0.735, Spectral Model 2= 0.660, Image Model 1= 0.669, Image Model 2= 0.611), which show the proportion of correctly classified seeds separated as haploid, were lower than specificity values (Eye= 0.957, Spectral Model 1= 0.923, Spectral Model 2= 0.918, Image Model 1= 0.870, Image Model 2 = 0.906), which are related to the proportion of correctly classified diploid seeds (Table 5). This was confirmed by the FNR and FDR figures calculated on the confusion matrix, and the FNR values were found to be higher than the FDR values for all classification models. Considering the rank correlations between the actual and predicted classes, eye classification ($r = 0.753$) was observed to have higher similarity than the classification based on spectral models (r for Spectral Model 1= 0.667, r for Spectral Model 2= 0.612) and image analysis (r for Image Model 1= 0.552, r for Image Model 2= 0.553).

Table 5- Evaluation/statistics based on confusion matrix for eye, spectral and image techniques

Statistics	Eye	Spectral Model 1	Spectral Model 2	Image Model 1	Image Model 2
Sensitivity	0.776	0.735	0.660	0.669	0.611
Specificity	0.957	0.923	0.918	0.870	0.906
Positive Prediction Value	0.936	0.887	0.827	0.808	0.795
Neg. Prediction Value	0.839	0.809	0.820	0.763	0.797
Prevalence	0.450	0.450	0.372	0.450	0.372
Detection Rate	0.349	0.330	0.246	0.301	0.228
Detection Prevalence	0.372	0.372	0.297	0.372	0.286
Balanced Accuracy	0.866	0.829	0.789	0.770	0.759
Accuracy	0.875	0.839	0.822	0.780	0.796
False Discovery Rate	0.064	0.113	0.173	0.192	0.205
False Negative Rate	0.224	0.265	0.340	0.331	0.389
Rank Correlation	0.753	0.667	0.612	0.552	0.553

When the classification methods based on spectral measurement and image analysis (used as alternative methods) were examined, it was observed that the spectral models give more successful results. This result obtained from the spectral models can be attributed to the characteristic features in the spectral data from haploid and diploid seeds. It is seen that the average spectra of haploid seeds are higher than the spectra from diploid seeds throughout the scanned spectral range (1200-2400 nm) (Figure 2). One of the main reasons for this difference is the existence of anthocyanin coloration in the embryo region of the haploid and diploid seeds. In our study, spectral data were collected by the embryo side that is distinctive for haploid/diploid seed classification based on anthocyanin coloration. While coloration is seen in the embryo region in diploid seeds, it does not occur in haploid seeds. Therefore, some of the light energy sent from the spectroscopy device absorbed in the diploid seeds is likely to be higher and lower in haploids. As a result of this, the average reflectance of haploid seeds was higher than that of the diploids.

**Figure 2- Mean spectra obtained from haploid and diploid seed classes**

There are various studies in the literature that support these findings. In a study conducted by Lin et al. (2017), it was reported that haploid seeds have higher reflectance values than diploids in the spectral range of 900-1700 nm. Our results also substantiate these findings. The true classification rates of spectral estimation models were found to be relatively lower than other studies conducted for similar purposes. For example, Liu et al. (2017) found the true classification rate to be 95% based on creating a spectral model using SVM. In a different study, it was reported that over 90% success was achieved in the classification of haploid seeds with NIR spectroscopy (Cui et al. 2019).

The reason for the difference between results can be attributed to several issues. Spectral pre-treatment was applied in the study of Liu et al. (2017). In our study, spectral models were created without any data pre-treatment. On the other hand, there are differences between the measurement specialities of the devices used in these studies. The device used in our study is not suitable for contact measurement and can obtain spectral data in closed measurement mode. Therefore, it is not possible for the light energy sent to the seed surface during measurement to provide regular reflection, as in contact measurements. However, according to the results obtained in our study, the device used achieved an acceptable success (~ 82%) in the haploid/diploid seed classification.

The image analysis method used in the study was the method with the lowest success among the classification techniques compared. One of the main reasons for this may be the use of a standard desktop scanner for collecting the seed images to develop image models. Although this device offers a practical solution in image collection, it is observed that there are unexpected changes in the color channels (R, G, B) of the seed images, except for seed coloration (Figure 3). The low accuracy in models based on these data can be attributed to measurement methodology.

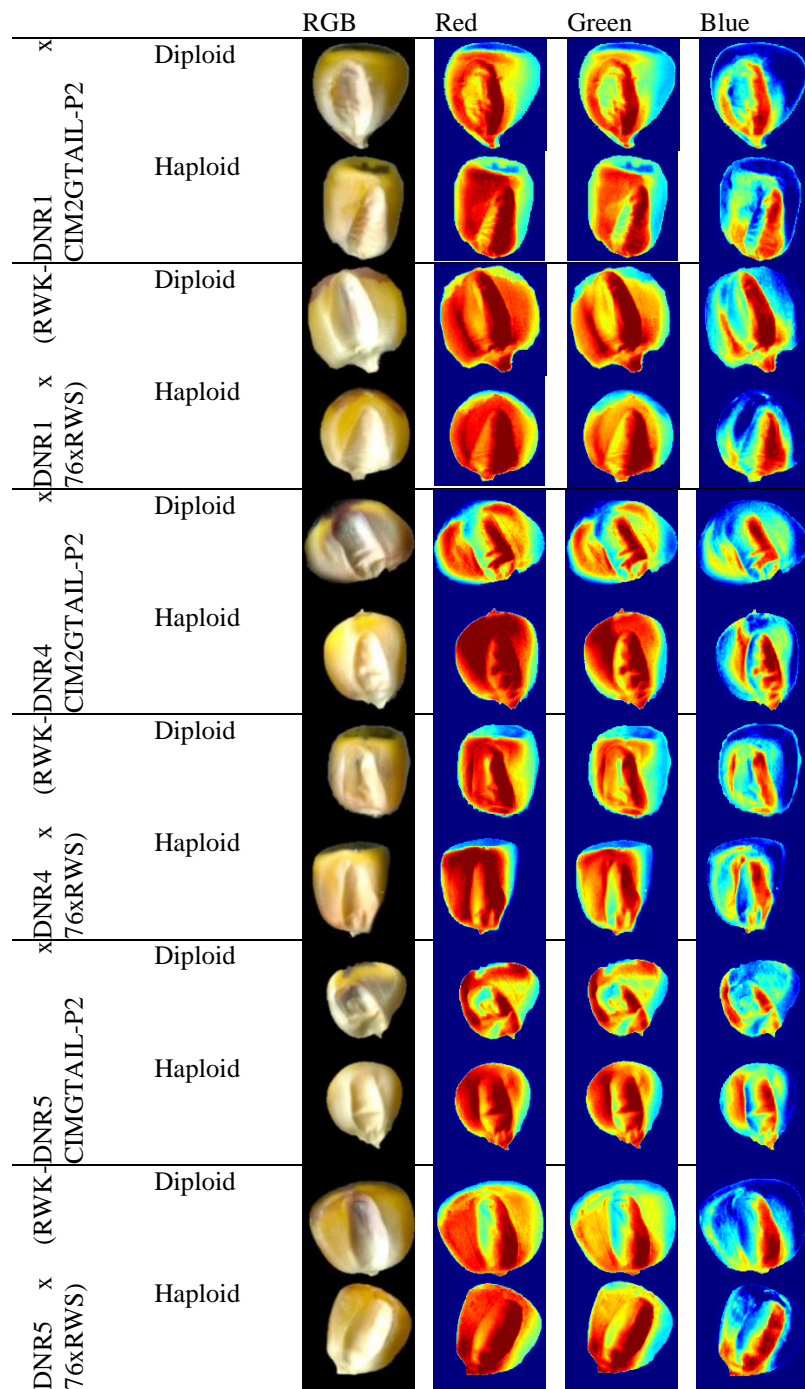


Figure 3- Examples of haploid and diploid seed images of donor materials with RGB, R, G, and B channels

Various studies may be found in the scientific literature on haploid/diploid seed classification with the help of image processing. Veeramani et al. (2018) used SVM, Random Forest (RF) and Logistic Regression (LR) methods to distinguish haploid and diploid seeds by using images taken by the embryo side of seed samples. Researchers achieved 87.6% success in seed classification with the SVM method. In another study in which image data and RGB channels were used in haploid/diploid seed classification, the classification success was 98.04% and 94.4% for haploid and hybrid seeds, respectively (Zhang et al. 2013). It is seen that the correct classification rates of the models created in our study are relatively low when compared with previous studies. This is due to differences in the image acquisition devices used and the method for processing image data. In

our study, data obtained from a desktop scanner was used while high resolution imaging systems were used in other studies. This may have caused a difference in classification success.

On the other hand, it has been reported that automatic classification of haploid/diploid seeds is possible with machine-assisted image processing (Zhang et al. 2013). Integration of models created for image data input into a specific software or machines suitable for automation is possible. To do this, it is important to determine the effect of color channels and the variables that should be included in the models to be created. In our study, the initial classification and final classification data were modeled with CRT analysis to examine the effect of the data of R, G, B color channels taken from the whole seed and embryo region on the classification of haploid/diploid seeds.

CRT output created with the initial classification results, 13 different nodes were formed (Figure 4). Of these, nodes 1, 2, 6, and 12 show the current path to differentiate diploid seeds based on image processing data, while nodes 3, 7 and 13 show the current path to differentiate haploid seeds (Figure 4). According to the CRT graph, it is seen that haploid and diploid seeds can be classified with the help of this model according to the embryo red band value (around 0.9) and the blue band value of the embryo region (0.73). Seed samples were classified under 29 separate nodes in the CRT graph (Figure 5) created based on the final classification data. Of these, nodes 1, 2, 6, 14, and 28 were used for the classification of diploid seeds, and nodes 3, 7, 15 and 29 for the classification of haploid seeds (Figure 5). Considering the effect of the variables of color channels on classification, it is seen that the red band value of the embryo region, the blue band value of the whole seed and the embryo region are effective variables to discriminate haploid/diploid seeds. According to the CRT analysis, it can be said that the red band value and the blue band value of the embryo region are effective features in distinguishing haploid/diploid seeds based on both the initial and final classification. In the “Final Classification”, the red band value of the whole seed is the main feature for distinguishing the seed classes.

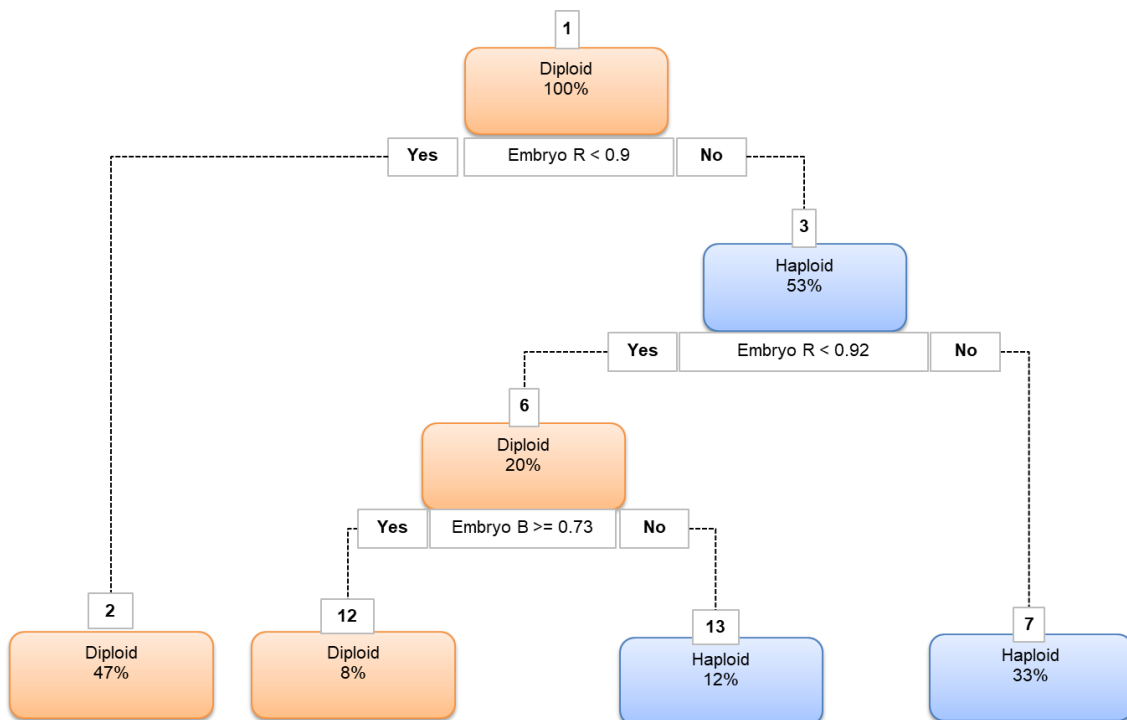


Figure 4- CRT plot generated from seed images based on initial classification of haploid and diploid seed samples obtained from induction crosses

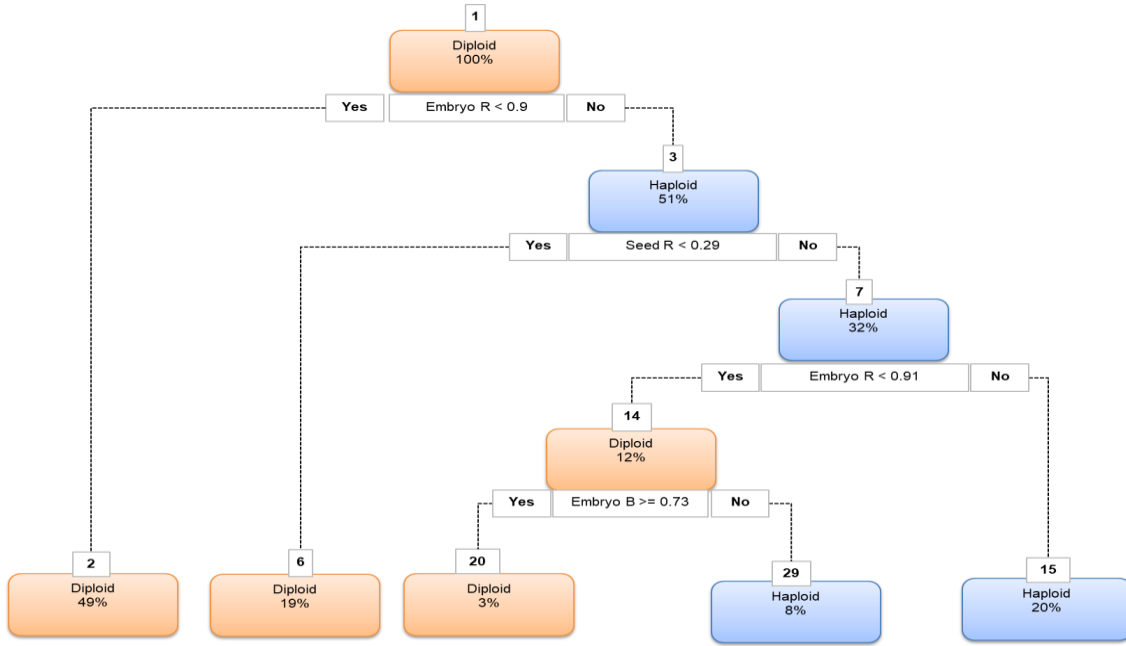


Figure 5- CRT plot generated from seed images based on final classification of haploid and diploid seed samples obtained from induction crosses

4. Conclusions

The results of this study revealed that the donor material, inducer line and chromosome doubling methods have important effects on the success of using the in vivo maternal haploid technique in maize. According to the haploid induction rates and viability levels of the donors used in the study, DNR4 gave more successful results than the others. Among the inducer lines, RWK76xRWS shows good performance compared to CIM2GTAIL-P2. Regarding the chromosome doubling methods compared, the seedling immersion method had a negative effect on the viability of the induction crosses. On the other hand, the number of fertile plants was found to be higher with the seedling immersion method than the stem injection method. The results of the current study are beneficial for researchers who may prefer these methods in further studies. Also, it should be considered that colchicine treatment requires the special setup or controlling areas in both methods. Results indicates that cutting of root and coleoptile parts has a negative effect on the success of seedling immersion method.

Significant differences were observed in the classification success of haploid/diploid seed classification methods compared in the study. The average accuracy of eye separation (87.5%) was higher than the spectral method and image processing methods. Despite this, it was observed that the models created based on spectral and image processing analyses give satisfactory results. It appears possible to develop more successful models by increasing the number of materials/samples used in future studies using powerful spectral and image analysis devices from which the measurements are taken and applying chemometric techniques to the statistical analysis methods used.

Acknowledgements

This work was supported by the Scientific and Technological Research Council of Turkey (TÜBİTAK) (Project number: 119O619) The authors thank TÜBİTAK for their financial support.

Abbreviations and Symbols

CRT	Classification and Regression Tree
DH	Doubled Haploid
SVM	Support Vector Machine
NIR	Near Infrared Reflectance
NMR	Nuclear Magnetic Resonance
RGB	Red, Blue, Green

References

Altuntaş Y & Kocamaz AF (2019). Renk momentleri ve destek vektör makineleri kullanarak haploid mısır tohumlarının tanımlanmasında renk uzaylarının sınıflandırma performansına etkisinin karşılaştırılması. *Fırat Üniversitesi Mühendislik Bilimleri Dergisi* 31(2): 551-560. <https://doi.org/10.35234/fumbd.585312>

- Altuntaş Y, Cömert Z & Kocamaz A F (2019). Identification of haploid and diploid maize seeds using convolutional neural networks and a transfer learning approach. *Computers and Electronics in Agriculture* 163: 1-11. <https://doi.org/10.1016/j.compag.2019.104874>
- Altuntaş Y, Kocamaz A F, Cengiz R & Esmeray M (2018). Classification of haploid and diploid maize seeds by using image processing techniques and support vector machines. In 2018 26th Signal Processing and Communications Applications Conference (SIU) 2-5 May, İzmir, pp. 1-4. <https://doi.org/10.1109/siu.2018.8404800>
- Cerit İ, Cömertpay G, Oyucu R, Çakır B, Hatipoğlu R & Özkan H (2016). Melez mısır ıslahında in-vivo katlanmış haploid tekniğinde kullanılan farklı inducer genotiplerin haploid indirgeme oranların belirlenmesi. *Tarla Bitkileri Merkez Araştırma Enstitüsü Dergisi* 25: 52-57. <https://doi.org/10.21566/tarbitderg.280162>
- Chaikam V, Molenaar W, Melchinger A E & Boddupalli P M (2019). Doubled haploid technology for line development in maize: technical advances and prospects. *Theoretical and Applied Genetics* 132(12): 3227-3243. <https://doi.org/10.1007/s00122-019-03433-x>
- Chalky S T (1994). Properties of maternal haploid maize plants and potential application to maize breeding. *Euphytica* 79: 13-18. <https://doi.org/10.1007/bf00023571>
- Chidzanga C, Muzawazi F, Midzi J & Hove T (2017). Production and use of haploids and doubled haploid in maize breeding: A review. *African Journal of Plant Breeding* 4: 201-213.
- Choe E H (1959). A line of maize with high haploid frequency. *American Naturalist* 93:381-382. <https://doi.org/10.1086/282098>
- Choe E, Carbonero CH, Mulvaney K, Rayburn AL & Muhm RH (2012). Improving in vivo maize doubled haploid production efficiency through early detection of false positives. *Plant Breeding* 131: 399-401. <https://doi.org/10.1111/j.1439-0523.2012.01962.x>
- Cui Y, Ge W, Li J, Zhang J, An D & Wei Y (2019). Screening of maize haploid kernels based on near infrared spectroscopy quantitative analysis. *Computers and Electronics in Agriculture* 158: 358-368. <https://doi.org/10.1016/j.compag.2019.01.038>
- Dang N C, Munsch M, Aulinger I, Renlai W & Stamp P (2012). Inducer line generated double haploid seeds for combined waxy and opaque 2 grain quality in subtropical maize (*Zea mays*. L.). *Euphytica* 183(2): 153-160. <https://doi.org/10.1007/s10681-011-0423-0>
- Deimling S, Röber F K & Geiger H H (1997). Methodology and genetics of in vivo haploid induction in maize. *Vortr Pflanzenzuchtg* 38: 203-224.
- Eder J & Chalys S (2002). In vivo haploid induction in maize. *Theoretical and Applied Genetics* 104(4): 703-708. <https://doi.org/10.1007/s00122-001-0773-4>
- Hallauer A R, Carena M J & Miranda F J B (2010). *Quantitative Genetics in Maize Breeding*. Springer New York. <https://doi.org/10.1007/978-1-4419-0766-0>
- Jones R W, Reniot T, Frei U K, Tseng Y, Lubberstedt T & McClelland J F (2012). Selection of haploid maize kernels from hybrid kernels for plant breeding using near infrared spectroscopy and SIMCA analysis. *Applied Spectroscopy* 66: 447-450. <https://doi.org/10.1366/11-06426>
- Kahrman F (2016). Mısırdaki Polen Etkisi ve Bu Etkinin Kontrolünde Uygulanan Yöntemler. Lambert Academic Publishing Saarbrücken, Almanya.
- Kalinowska K, Chamas S, Unkel K, Demidov D, Lermontova I, Dresselhaus T, Kumlehn J, Dunemann F, Houben A (2019). State-of-the-art and novel developments of in vivo haploid technologies. *Theoretical and Applied Genetics* 132(3):593-605. <https://doi.org/10.1007/s00122-018-3261-9>
- Lin J, Yu L, Li W & Qin H (2017). Method for identifying maize haploid seeds by applying diffuse transmission near-infrared spectroscopy. *Applied Spectroscopy* 72(4): 611-617. <https://doi.org/10.1177/0003702817742790>
- Liu W J, Li W J, Li H G, Qin H & Ning X (2017). Research on the method of identifying maize haploid based on KPCA and near infrared spectrum. *Spectroscopy and Spectral Analysis* 37(7): 2024-2027. [https://doi.org/10.3964/j.issn.1000-0593\(2017\)07-2024-04](https://doi.org/10.3964/j.issn.1000-0593(2017)07-2024-04)
- Melchinger A E, Schipprack W, Würschum T, Chen S & Technow F (2013). Rapid and accurate identification of in vivo-induced haploid seeds based on oil content in maize. *Scientific Reports* 3: 2129. <https://doi.org/10.1038/srep02129>
- Melchinger A E, Schipprack W, Utz H F & Mirdita V (2014). In vivo haploid induction in maize: identification of haploid seeds by their oil content. *Crop Science* 54: 1-8. <https://doi.org/10.2135/cropsci2013.12.0851>
- Prasanna BM, Chaikam V & Mahuku G (2012). Doubled haploid technology in maize breeding: theory and practice. *CIMMYT*.
- Prigge V, Schipprack W, Mahuku G, Atlin G N & Melchinger A E (2012). Development of in vivo haploid inducers for tropical maize breeding programs. *Euphytica* 185(3): 481-490. <https://doi.org/10.1007/s10681-012-0657-5>
- R Core Team (2019). R: A language and environment for statistical computing. R Foundation for Statistical Computing. <https://www.R-project.org/>.
- Röber F K, Gordillo G A & Geiger H H (2005). In vivo haploid induction in maize-performance of new inducers and significance of doubled haploid lines in hybrid breeding. *Maydica* 50: 275-283
- Uliana Trentin H, Frei U K & Lübberstedt T (2020) Breeding maize maternal haploid inducers. *Plants (Basel)* 9(5):614. <https://doi.org/10.3390/plants9050614>
- Vanous K, Vanous A, Frei UK & Lübberstedt T (2017). Generation of maize (*Zea mays*) doubled haploids via traditional methods. *Current Protocols in Plant Biology* 2(2): 147-157. <https://doi.org/10.1002/cppb.20050>
- Veeramani B, Raymond J W & Chanda P (2018). DeepSort: deep convolutional networks for sorting haploid maize seeds. *BMC Bioinformatics* 19(9): 289. <https://doi.org/10.1186/s12859-018-2267-2>
- Zabirova E R, Chumak M V, Shatskaia O A & Scherbak V S (1996). Technology of the mass accelerated production of homozygous lines (in Russian). *Kukuruza Sorgo* 4: 17-19
- Zararsız D, Öztürk L, Yanıkoğlu S, Turgut I, Kizik S & Bilgin B (2019). Production of double haploid plants using in vivo haploid techniques in corn. *Journal of Agricultural Sciences* 25(1): 62-69. <https://doi.org/10.15832/ankutbd.539000>
- Zhang J, Wu Z, Song P, Li W, Chen S & Liu J (2013). Embryo feature extraction and dynamic recognition method for maize haploid seeds. *Transactions of the Chinese Society of Agricultural Engineering* 29(4): 199-203. <https://doi.org/10.3969/j.issn.1002-6819.2013.04.025>





Effect of Combined or Separate Administration of Beta Carotene-Vitamin E and hCG on Fertility in Sheep Lambs

Mehmet Ferit ÖZMEN^{a*} , Erkan SAY^b , Ümüt CİRİT^c 

^aDepartment of Reproduction and Artificial Insemination, Faculty of Veterinary Medicine, Dicle University, 21280, Diyarbakir, TURKEY

^bEastern Mediterranean Agricultural Research Institute, Dogankent, Yüreğir, Adana, TURKEY

^cDepartment of Reproduction and Artificial Insemination, Faculty of Ceyhan Veterinary Medicine, Çukurova University, 01920, Adana, TURKEY

ARTICLE INFO

Research Article

Corresponding Author: Mehmet Ferit ÖZMEN, E-mail: ferit-ozmen@hotmail.com

Received: 04 May 2021 / Revised: 21 June 2021 / Accepted: 22 June 2021 / Online: 01 September 2022

Cite this article

ÖZMEN F M, SAY E, CİRİT Ü (2022). Effect of Combined or Separate Administration of Beta Carotene-Vitamin E and hCG on Fertility in Sheep Lambs. *Journal of Agricultural Sciences (Tarim Bilimleri Dergisi)*, 28(3):396-400. DOI: 10.15832/ankutbd.932413

ABSTRACT

This study was performed to investigate the effect of beta carotene-vitamin E and hCG treatments alone or a combination of both on fertility in estrus synchronized Awassi ewe lambs. A total of 103 Awassi ewe lambs were divided into four groups before the study. Lambs were treated with a progesterone sponge for 12 days, PGF_{2α} two days before sponge removal, 600 IU PMSG on sponge removal day, and 150 IU hCG on the day of mating. The control group (n: 25) did not receive any additional treatment. The Vitamin group (β carotene + vitamin E) (n: 26) was treated twice with vitamin combination. The first treatment was on the 7th day before the sponge insertion and the second treatment was on the day of mating. The hCG group (n: 24) was treated with 150 IU hCG on day 12

after mating. The HCG + vitamin group (n: 28) was treated with both β carotene-vitamin E and hCG. Ewe lambs standing to be mounted were considered in estrus and mated. Pregnancy was determined by ultrasound the 30th day after the mating. There were no significant differences between the control and hCG, vitamin and hCG + vitamin groups concerning estrus, conception, lambing, abortion, twinning, fecundity rate, and litter size (P>0.05). It was concluded that the treatments with β-carotene-vitamin E and hCG or both, in addition to estrus synchronization out of the breeding season in Awassi ewe lambs did not improve the investigated fertility indices.

Keywords: *Beta carotene; Estrus synchronization; Ewe lambs; hCG; Progesterone*

1. Introduction

One of the important aspects for a profitable livestock is reproductive performance (Ataç & Kaymakçı 2021). Ewe lambs reach the reproductive ability at an average age of 8 months. However, if they are not in the breeding season, mating is delayed which results in losses for sheep farms. This negative situation can only be overcome by using estrus synchronization methods. The use of this method is limited due to the high embryonic mortality rate in pregnancies after estrus synchronization in ewe lambs out of the breeding season. In the first 3 weeks of gestation, the embryonic mortality rate varies between 30 and 40% in adult ewes, but this rate reaches 50% in ewe lambs (Bolet 1986; Nancarrow 1994; Michels et al. 1998). It was reported that this rate is raised to 63% in ewe lambs that mated in estrus induced by Progestagen-eCG application (Gordon 1997). 70-80% of embryonic deaths occur between 8th -16th days after insemination (Sreenan et al. 1996). Luteal dysfunction is considered as the major cause of embryonic death (Wilmot et al. 1986; Ashworth & Bazer 1989; Nancarrow 1994). In the early stages of pregnancy, hCG or GnRH applications are considered as alternatives to reduce embryonic death rates by causing an increase in the amount of progesterone (Sreenan et al. 1996). The majority of this increase in progesterone level is mainly attributed to the formation of new corpus luteums (CL) (Mann & Picton 1995; Beck et al. 1996). Increases in progesterone production on the 12th day of mating or the following days may increase interferon-tau (IFN-τ) production. (Thatcher et al. 1995). In the natural oestrus cycle, the IFN-τ increase in this period when the corpus luteum starts to regress can prevent luteolysis by preventing PGF_{2α} secretion (Bazer et al. 1998). It has been reported that administration of hCG or GnRH on the 12th day after mating improves the reproductive performance of sheep and hCG administration also increases fetal growth (Cam & Kuran 2004; Khan et al. 2007).

Another strategy applied to reduce the embryonic mortality rate in ewes is to use some vitamins and minerals. The body levels of some vitamins and minerals [beta (β) carotene, vitamin E, selenium, etc.] that are contained in pasture affect fertility rates. In case of deficiencies of these substances, they should be supplemented (Yokuş et al. 2006; Panousis et al. 2007). Previous studies have shown that the addition of β-carotene to animals such as cows, sheep, rabbits, and pigs improves their performance and reproductive functions (Ahlsweide & Lotthammer 1978; Brief & Chew 1985; Kormann et al. 1989). It has been reported that

the CL is rich in β -carotene and therefore β -carotene along with vitamin A has an important effect on the functions of luteal cells (Graves-Hoagland et al. 1989; Ceylan et al. 2007). Rapaport et al. (1998) determined that the progesterone secretion capacity of the corpus luteum is associated with the high β -carotene content in the ovaries. Because β -carotene is the only source of vitamin A in granulosa cells, it plays a role in the synthesis of steroid hormones and ovulation. In addition, there is a positive relationship between the plasma β -carotene level and the follicular fluid and luteal tissues as well as the weight of the corpus luteum (Ayaşan & Karakozak 2010).

Vitamin E (α -tocopherol) protects cell membranes from oxidation by reacting with lipid radicals produced in lipid peroxidation reactions (Traber & Atkinson 2007). This removes free radical intermediates and prevents oxidation reactions (Mohebbi-Fani et al. 2012). Oxidative damage to the ovarian epithelium due to stimulation of ovulation in sheep can be prevented by vitamin E supplementation (Murdoch & Martinchic 2004). Various results have been reported in previous studies investigating the effects of vitamin E on fertility. Although Koyuncu & Yerlikaya (2007) reported that vitamin E supplementation increased the incidence of estrus and fertility in sheep, some other researchers did not find the same effect (Kott et al. 1983; Kumagai & White 1995; Gabryszuk & Klewicz 2002; Yaprak et al. 2004).

Some studies have evaluated the effects of supplementation with various vitamins or hCG on reproduction in sheep. (Kaya et al. 2013; Köse et al. 2013; Catalano et al. 2015). However, to the best of the authors' knowledge, there is no study investigating the effects of co-administration of hCG and β -carotene + vitamin E on reproduction in ewe lambs. Therefore, this research was aimed to evaluate the effects of hCG treatment on the 12th day after mating and β -carotene + vitamin E treatment, which was applied twice, or co-administration of these two treatment strategies in estrus synchronized ewe lambs out of the breeding season.

2. Material and Methods

This study was approved by Dicle University, Animal Local Ethics Committee (DÜ-HADYEK; 25249). The experiment was conducted on a commercial sheep farm in the period from the second half of April to the first week of May in the southeastern part of Turkey out of the breeding season. The study was carried out on a livestock farm in Diyarbakır province. This region is situated at 37°55'01" N latitude, and 40°16'46" E longitude, and at an altitude of 660 meters.

2.1. Animals and experimental design

A total of 103, eight months old Awassi ewe lambs were allocated into four groups. Ewe lambs were selected randomly. They grazed on natural pasture all day and water were offered *ad libitum*. All ewe lambs were synchronized for estrus using progesterone-containing vaginal sponges (20 mg flugeston acetate, Chronogest CR, Intervet) for 12 days. Two days before sponge removal, prostaglandin F2 alpha (PGF2 α , 250 mcg, Estrumate, Intervet) was injected via the i.m. route. On the day of sponge removal, 600 IU equine chorionic gonadotropin (eCG, i.m., Chronogest, Intervet) and then on the mating day 150 IU human chorionic gonadotropin (hCG, i.m., Chorulon, Intervet) were applied via i.m. route. No additional treatment was applied to the lambs in the control group (n= 25). The lambs in the vitamin group (n= 26) received Beta (β) carotene + vitamin E (0.5 ml / 10 kg, i.m. Ovostim, Provet) twice, one week before sponge application and on the day of mating. The hCG group of lambs (n= 24) was injected hCG (150 IU, i.m.) on day 12 after mating. The lambs in the hCG + vitamin group (n: 28) were treated with both hCG and β -carotene + vitamin E.

Estrus was determined by fertile rams (3-5 old) for 4 hours in the morning and evening for 4 days from the day of sponge removal. The lambs in oestrus were mated with fertile rams (lambs to ram ratio 10:1). Pregnancy was determined with the help of an ultrasound on the 30th day after the mating.

2.2. Statistical analysis

The data were analyzed using the SPSS (Statistical Package for the Social Sciences) /PC program (Version 10.0; SPSS, Chicago, IL, USA). Results were expressed as percentages and comparisons among groups were evaluated using the Chi-Square test. The significance level was accepted as P<0.05.

3. Results

The fertility results of the ewe lambs in the control and treatment groups are given in Table 1. Pregnancy, lambing and fecundity rates of hCG and hCG + vitamin groups were numerically (but not statistically) higher than the control group. Unexpectedly, the multiple births rate of the control group was numerically higher than all of the other groups. However, estrus, pregnancy, lambing, abortion, twinning, multiple births and fecundity rates, and litter size were found to be similar statistically in all groups (P>0.05).

Table 1- Comparison of fertility results among groups

Groups	Control n: 25	hCG n:24	Vitamin (β -Carotene + Vitamin E) n: 26	hCG + Vitamin n: 28
Estrus rate (%)	96.0 (24/25)	100.0 (24/24)	100.0 (26/26)	96.4 (27/28)
Pregnancy rate ¹ (%)	62.5 (15/24)	79.2 (19/24)	69.2 (18/26)	77.8 (21/27)
Lambing rate ² (%)	58.3 (14/24)	75.0 (18/24)	65.4 (17/26)	74.1 (20/27)
Abortion rate ³ (%)	6.7 (1/15)	5.3 (1/19)	5.6 (1/18)	4.8 (1/21)
Multiple births rate ⁴ (%)	35.7 (5/14)	27.8 (5/18)	29.4 (5/17)	25.0 (5/20)
Fecundity rate ⁵ (%)	79.2 (19/24)	95.8 (23/24)	84.6 (22/26)	92.6 (25/27)
Litter size ⁶ (%)	135.7 (19/14)	127.8 (23/18)	129.4 (22/17)	125.0 (25/20)

¹: Number of pregnant ewe lambs /all ewe lambs mated; ²: Number of ewe lambs lambing/all ewe lambs mated; ³: Number of ewe lambs aborted / number of ewe lambs pregnant; ⁴: Number of ewe lambs giving twin births/number of ewe lambs lambing; ⁵: Number of lambs born/ number of ewe lambs mated; ⁶: At the birth number of lambs born/ number of ewes lambed

4. Discussion

It has been suggested that GnRH or hCG administration on day 10, 11, 12 or 13 post-mating improves plasma progesterone (P4) concentrations (Cam et al. 2002), early embryonic survival (Beck et al. 1994), pregnancy rate (McMillan et al. 1986), and litter size (Cam et al. 2002) in sheep. On the other hand, in several studies, it is noted that GnRH-treated sheep have consistently lower plasma P4 concentrations when compared to hCG-treated sheep (Ishida et al. 1999; Khan et al. 2007; Fernandez et al. 2018). Fernandez et al. (2018) have reported that hCG has a double effect on P4 concentrations, as it both stimulates the development of the original CL, which directly affects the LH receptors in the ovary and induces the formation of accessory CL. The hCG has a longer half-life than GnRH (Cole 2012; Fernandez et al. 2018) and it has a 3-30 fold higher binding affinity compared to LH induced by GnRH treatment (Hunter et al. 1986, 1988).

It has been reported that hCG injections administered in the early embryonic period positively affect interferon tau (Nephew et al. 1994) and/or progesterone synthesis (Khan et al. 2007; Fernandez et al. 2018; Mehri et al. 2018). The hCG stimulates blastocyst expansion and larger blastocysts release more interferon tau (Nephew et al. 1994), which results in a reduction in the number of estradiol and oxytocin receptors and inhibits or delays the luteolytic mechanism by suppressing PGF_{2 α} secretion (Khan et al. 2007). Several researchers applied different doses of hCG in various ways to the synchronized ewe lambs and they reported different effects on fertility. Khan et al. (2007), who investigated the effects of hCG and GnRH applied to the ewes and ewe lambs on day 12 postmating, found that hCG or GnRH treatments can increase ovarian function, conceptus growth, and placental attachment in ewes but these improvements were less intense in ewe lambs. In another study, Khan et al. (2009) injected 200 IU hCG to estrus synchronized ewe lambs on day 12 after the mating. These authors reported that hCG treatment did not affect improving the reproductive performance of cyclic ewe lambs and ewes induced for reproduction in late anoestrus. Catalano et al. (2015) applied 300 IU hCG on the 12th day after mating to 8-month-old Corridella ewe lambs synchronized with P4 containing sponges and PMSG applications out of the season. They reported no improvement in pregnancy rate or fetal weight, but hCG treatment increased plasma progesterone concentration and multiple ovulation. These authors also reported that the percentage of ewe lambs showing multiple ovulation was higher in the hCG-300 group than the control group (77.8% vs 20.0%; P <0.05). In the present study, although pregnancy, lambing and fecundity rates in hCG group of ewe lambs were numerically higher than the control group, these differences were not statistically significant.

It has been reported that β -carotene deficiency in feed adversely affects, either directly or indirectly, reproductive parameters such as estrus, conception, and pregnancy by changing ovary functions and intrauterine environment (Arıkan & Muğlalı 1999; Kaçar et al. 2008). Özpınar et al. (1994) reported that β -carotene injection at 20-day intervals increased the pregnancy rate, offspring yield and twinning rate at the first insemination in ewes. Salem et al. (2015) reported that injection of β -carotene to Farafra ewe lambs every 15 days for 4 months before puberty increased the concentration of estradiol-17 β and vitamin A, and lambs in this group showed more oestrus (P<0.05). In the present study, pregnancy, lambing and fecundity rates of β -carotene and vitamin E treated ewe lambs were found to be numerically higher than those of the control group, but these differences were not statistically significant. The reason for the lack of difference in the present study may be due to the period in which the study was conducted. Ewe lambs probably consumed plenty of green grass for 2-3 months before the study, and therefore may receive a sufficient amount of vitamins and minerals from pasture. This assumption was supported by the results of the study conducted by Beytut et al. (2005), who determined the levels of vitamins A and E as well as β -carotene levels of meadow-pasture grasses and feed substances in Kars province and its surroundings and reported the highest blood plasma β -carotene levels in spring and

summer seasons. Moreover, Afshari et al. (2008) also reported that vitamin A and β -carotene levels were significantly lower in Gezel sheep in Iran during the winter compared to the summer season. Further detailed studies are needed to determine the effects of β -carotene-vitamin E on reproduction in ewe lambs in periods when green grass is absent or scarce.

In this study, the multiple births rate of the control group was numerically higher than those of all the other groups. This was not an expected result, although the differences were not found to be statistically significant. The results of our study did not support the hypothesis that co-administration of beta carotene + vitamin E and hCG can affect fertility positively in ewe lambs.

5. Conclusions

As it was concluded from the present study, administration of either β -carotene-vitamin E, hCG, or both, in addition to the estrus synchronization protocol out of the breeding season, did not significantly affect the reproductive performance in Awassi ewe lambs. For all that, in the field conditions, treating ewe lambs with hCG 12 days after estrus-synchronized matings may provide an economic contribution by increasing the pregnancy, lambing and fecundity rates numerically.

References

- Afshari G, Hasanpoor A, Hagpanah H & Amoughll-Tabrizi A (2008). Seasonal variation of vitamin A and β -carotene levels in Ghezel Sheep. *Turkish Journal of Veterinary and Animal Sciences* 32(2): 127-129
- Ahlsvede L & Lotthammer K H (1978). Untersuchungen über eine spezifische, Vitamin A- unabhängige Wirkung des β -Carotins auf die Fertilität des Rindes: 5. Mitteilung: Organuntersuchungen (Ovarien, Corpora lutea, Leber, Fettgewebe, Uterussekret, Nebennieren) Gewichts und Gehaltsbestimmungen. *Deutsche Tierärztliche Wochenschr* 85: 7-12 (in German language)
- Arikan S & Muğlalı Ö H (1999). Effect of β -carotene on reproductive functions of some farm animals (In Turkish). *Livestock Studies* 39(2): 87-94
- Ashworth C J & Bazer F W (1989). Changes in ovine conceptus and endometrial function following asynchronous embryo transfer or administration of progesterone. *Biology of Reproduction* 40(2): 425-433. DOI: 10.1095/biolreprod40.2.425
- Ataç F E & Kaymakçı M (2021). Reproductive characteristics of chios ram lambs during the first year of life in rural farm conditions. *Journal of Agricultural Sciences* 27(1): 98-105. DOI: 10.15832/ankutbd.544225
- Ayaşan T & Karakozak E (2010). Use of β -carotene in animal nutrition and its effects (In Turkish). *Kafkas Üniversitesi Veteriner Fakültesi Dergisi* 16.4: 697-705
- Bazer F W, Ott T L & Spencer T E (1998). Maternal recognition of pregnancy: comparative aspects a review. *Trophoblast Research* 12: 375-386. DOI: 10.1016/S0143-4004(98)80055-6
- Beck N F G, Peters A R & Williams S P (1994). The effect of GnRH agonist (buserelin) treatment on day 12 post mating on the reproductive performance of ewes. *Animal Science* 58(2): 243-247. DOI: 10.1017/S1357729800042557
- Beck N F, Jones M, Davies B, Mann G E & Peters A R (1996). The effect of GnRH analogue (buserelin) treatment on day 12 post mating on ovarian structure and plasma progesterone and oestradiol concentration in ewes. *Animal Science* 63(3): 407-412. DOI: 10.1017/S1357729800015290
- Beytut E, Kamiloğlu N N, Gökçe G & Beytut E (2005). Season variation of vitamin A, E and beta carotene levels in plasma of sheep and meadow hay in the region of Kars and its surrounds (In Turkish). *Kafkas Üniversitesi Veteriner Fakültesi Dergisi* 11(1): 17-24
- Bolet G (1986). Timing and extent of embryonic mortality in pigs, sheep and goats: genetic variability. In: Sreenan, J.M., Diskin, M.G. (Eds.), *Embryonic Mortality in Farm Animals*. Martinus Nijhoff, Hague
- Brief S & Chew B P (1985). Effects of vitamin A and β -carotene on reproductive performance in gilts. *Journal of Animal Science* 60(4): 998-1004. DOI: 10.2527/jas1985.604998x
- Cam M A & Kuran M (2004). Effects of a single injection of hCG or GnRH agonist on day 12 post mating on fetal growth and reproductive performance of sheep. *Animal Reproduction Science* 80(1-2): 81-90. DOI: 10.1016/S0378-4320(03)00158-1
- Cam M A, Kuran M, Yildiz S & Selcuk E (2002). Fetal growth and reproductive performance in ewes administered GnRH agonist on day 12 post-mating. *Animal Reproduction Science* 72(1-2): 73-82. DOI: 10.1016/S0378-4320(02)00071-4
- Catalano M T, González C, Williams S, Videla D I & Callejas S (2015). Reproductive performance of ewe lambs in non-breeding season exposed to hCG at day 12 post mating. *Small Ruminant Research* 124: 63-67. DOI: 10.1016/j.smallrumres.2014.12.014
- Ceylan A, Serin İ, Akşit H, Seyrek K & Gökbulu T C (2007). Investigation of vitamins A, E, beta-carotene, cholesterol and triglyceride concentrations in dairy cows with repeat breeder and anestrus (In Turkish). *Kafkas Üniversitesi Veteriner Fakültesi Dergisi* 13(2): 143-147. DOI: 10.9775/kvdf.2007.23-A
- Cole L A (2012). hCG, the wonder of today's science. *Reproductive Biology and Endocrinology* 10(1): 1-18
- Fernandez J, Bruno-Galarraga M M, Soto A T, de la Sota R L, Cueto M I, Lacau I M & Gibbons A E (2018). Hormonal therapeutic strategy on the induction of accessory corpora lutea in relation to follicle size and on the increase of progesterone in sheep. *Theriogenology* 105: 184-188. DOI: 10.1016/j.theriogenology.2017.09.020
- Gabryszuk M & Klewicz J (2002). Effect of injecting 2- and 3-year-old ewes with selenium-vitamin-E on reproduction and rearing of lambs. *Small Ruminant Research* 43(2): 127-132. DOI: 10.1016/S0921-4488(02)00005-6
- Gordon I R (1997). Controlled reproduction in sheep and goats. Cab. International. (2) Ireland, 450
- Graves-Hoagland R L, Hoagland T A & Woody C O (1989). Relationship of plasma β -carotene and vitamin A to postpartum cattle. *Journal of Dairy Science* 72(7): 1854-1858. DOI: 10.3168/jds.S0022-0302(89)79303-6
- Hunter M G, Southee J A & Lamming G E (1988). Function of abnormal corpora lutea in vitro after GnRH induced ovulation in the anoestrous ewe. *Journal of Reproduction and Fertility* 84: 139-148. DOI: 10.1530/jrf.0.0840139
- Hunter M G, Southee J A, McLeod B J & Haresign W (1986). Progesterone treatment has a direct effect on GnRH induced preovulatory follicles to determine their ability to develop into normal corpora lutea in anoestrous ewes. *Journal of Reproduction and Fertility* 76: 349-363. DOI: 10.1530/jrf.0.0760349

- Ishida N, Okada M, Sebata K, Minato M & Fukui Y (1999). Effects of GnRH and hCG treatment for enhancing corpus luteum function to increase lambing rate of ewes artificially inseminated during the non-breeding season. *Journal of Reproduction and Development* 45: 73-79. DOI: 10.1262/jrd.45.73
- Kaçar C, Kamiloğlu N N, Gürbulak K, Pancarci Ş M, Güngör Ö, Guevenc K & Saban E (2008). The Effect of administration of testosterone antibody, β -carotene and vitamin E on multiple pregnancy and MDA (Malondialdehyde) in Tuj breed sheep in non-breeding season (In Turkish). *Kafkas Üniversitesi Veteriner Fakültesi Dergisi* 14(1): 51-56. DOI: 10.9775/kvfd.2008.03-A
- Kaya S, Kaçar C, Kaya D & Aslan S (2013). The effectiveness of supplemental administration of progesterone with GnRH, hCG and PGF_{2a} on the fertility of Tuj sheep during the non-breeding season. *Small Ruminant Research* 113(2-3): 365-370. DOI: 10.1016/j.smallrumres.2013.03.018
- Khan T H, Beck N F & Khalid M (2007). The effects of GnRH analogue (buserelin) or hCG (Chorulon) on Day 12 of pregnancy on ovarian function, plasma hormone concentrations, conceptus growth and placentation in ewes and ewe lambs. *Animal Reproduction Science* 102(3-4): 247-257. DOI: 10.1016/j.anireprosci.2006.11.007
- Khan T H, Beck N F G & Khalid M (2009). The effect of hCG treatment on Day 12 post-mating on ovarian function and reproductive performance of ewes and ewe lambs. *Animal Reproduction Science* 116(1-2): 162-168. DOI: 10.1016/j.anireprosci.2009.01.010
- Kormann A W, Riss G & Weiser H (1989). Improved reproductive performance of rabbit does supplemented with dietary beta-carotene. *The Journal of Applied Rabbit Research* 12: 15-21
- Kott R W, Ruttler J L & Southward G M (1983). Effects of vitamin E and selenium injections on reproduction and preweaning lamb survival in ewes consuming diets marginally deficient in selenium. *Journal of Animal Science* 57(3): 331-337. DOI: 10.2527/jas1983.573553x
- Koyuncu M & Yerlikaya H (2007). Effect of selenium-vitamin E injections of ewes on reproduction and growth of their lambs. *South African Journal of Animal Science* 37(4): 233-236. DOI: 10.4314/sajas.v37i4.4095
- Köse M, Kırbaş M, Dursun Ş & Bayrıl T (2013). The effect of injections of β -carotene or vitamin E + selenium on fertility in ewes in anestrus season (In Turkish). *Van Veterinary Journal* 24(2): 83-86
- Kumagai H & White C L (1995). The effect of supplementary minerals, retinol and α -tocopherol on the vitamin status and productivity of pregnant merino ewes. *Australian Journal of Agricultural Research* 46(6): 1159-1174. DOI: 10.1071/AR9951159
- Mann G E & Picton H M (1995). Ovarian and uterine effects of a single buserelin injection on day 12 of the oestrous cycle in the cow. *Journal of Reproduction and Fertility Abstr. Ser.* 15:23
- McMillan W H, Knight T W & Macmillan K L (1986). Effects of gonadotrophin releasing hormone (buserelin) on sheep fertility. *Proceedings of the New Zealand Society of Animal Production* 46: 161-163
- Mehri R, Rostami B, Masoumi R & Shahir M H (2018). Effect of injection of GnRH and hCG on day 5 post mating on maternal P4 concentration and reproductive performance in Afshari ewes. *Journal of Comparative Pathobiology* 14: 2363-2370
- Michels H, Vanmontfort D & Dewil E (1998). Decuypere E. genetic variation of prenatal survival in relation to ovulation rate in sheep: a review. *Small Ruminant Research* 29(2): 129-142. DOI: 10.1016/S0921-4488(97)00126-0
- Mohebbi-Fani M, Mirzaei A, Nazifi S & Shabbooe Z (2012). Changes of vitamins A, E, and C and lipid peroxidation status of breeding and pregnant sheep during dry seasons on medium-to-low quality forages. *Tropical Animal Health and Production* 44: 259-265
- Murdoch W J & Martinchick J F (2004). Oxidative damage to DNA of ovarian surface epithelial cells affected by ovulation: carcinogenic implication and chemoprevention. *Experimental Biology and Medicine* 229(6): 546-552. DOI: 10.1177/153537020422900613
- Nancarrow C D (1994). Embryonic mortality in the ewe and doe. In: Zavy, M.T., Geisart RD (Eds.), *Embryonic Mortality in Domestic Species*, London, pp. 79-97
- Nephew K P, Cardenas H, McClure K E, Ott T L & Bazer F (1994). Effects of administration of human chorionic gonadotropin or progesterone before maternal recognition of pregnancy on blastocyst development and pregnancy in sheep. *Journal of Animal Science* 72: 453-458. DOI: 10.2527/1994.722453x
- Özpinar H, Şenel H S, Özpinar A & Çekgöl E (1994). Pharmacokinetics of intramuscular administered β -carotene and its effects on reproduction in sheep. *Wiener Tierärztliche Monatsschrift* 82: 229-231
- Panousis N, Giadinis N, Roubies N, Fytianou A, Kalaitzakis E, Pourliotis K, Polizopoulou Z & Karatzias H (2007). Selenium, vitamin E and vitamin A status in dairy sheep reared under different feeding systems in Greece. *Journal of Veterinary Medicine Series A* 54(3): 123-127. DOI: 10.1111/j.1439-0442.2007.00907.x
- Rapaport R, Sklan D, Wolfenson D, Shaham-Albalancy A & Hanukoglu I (1998). Antioxidant capacity is correlated with steroidogenic status of the corpus luteum during the bovine estrous cycle. *Biochimica et Biophysica Acta* 1380(1): 133-140. DOI: 10.1016/S0304-4165(97)00136-0
- Salem A A, El-Shahawy N A & Soliman I A (2015). "Effect of beta-carotene injection on estrus, vitamin A and estradiol-17- β concentrations in pubertal farafra ewe lambs. *Egypt Journal Animal Production* 52: 123-128
- Sreenan J, Diskin M & Dunne L (1996). Embryonic mortality the major cause of reproductive wastage in cattle. In: *Proceedings of the 47th Annual Meeting of the European Association of Animal Production*, Lillhammer, August. Páginas
- Thatcher W W, Meyer M D & Danet-Desnoyers G (1995). Maternal recognition of pregnancy. *Journal of Reproduction and Fertility* 49(Suppl.): 15-28
- Traber M G & Atkinson J (2007). Vitamin E, antioxidant and nothing more. *Free Radical Biology and Medicine* 43(1): 4-15. DOI: 10.1016/j.freeradbiomed.2007.03.024
- Wilmut I, Sales D I & Ashworth C J (1986). Maternal and embryonic factors associated with prenatal loss in mammals. *Journal of Reproduction and Fertility* 76(2): 851-864. DOI: 10.1530/jrf.0.0760851
- Yaprak M, Emsen E, Emsen B & Macit M (2004). The influence of vitamin E supplementation during late pregnancy on lamb mortality and ewe productivity in Awassi ewes. *Journal of Animal and Veterinary Advances* 3: 190-193
- Yokuş B, Cakır D U, Kanay Z, Gulden T & Uysal E (2006). Effects of seasonal and physiological variations on the serum chemistry, vitamins and thyroid hormone concentrations in sheep. *Journal of Veterinary Medicine* 53(6): 271-276. DOI: 10.1111/j.1439-0442.2006.00831.x





Impacts of High and Low-Input Farming Systems on the Quality Change of Safflower Oil While Intercropped with Bitter Vetch

Azin NAJAFABADI^a , Jalal JALILIAN^{a*}

^aDepartment of Plant Production and Genetics, Faculty of Agriculture, Urmia University, Urmia, IRAN

ARTICLE INFO

Research Article

Corresponding Author: Jalal JALILIAN, E-mail: j.jalilian@urmia.ac.ir

Received: 09 January 2021; Revised: 13 July 2021 / Accepted: 14 July 2021 / Online: 01 September 2022

Cite this article

NAJAFABADI A, JALILIAN J (2022). Impacts of High and Low-input Farming Systems on the Quality Change of Safflower oil While Intercropped with Bitter Vetch. *Journal of Agricultural Sciences (Tarim Bilimleri Dergisi)*, 28(3):401-411. DOI: 10.15832/ankutbd.857026

ABSTRACT

The purpose of this factorial field experiment was to investigate the influence of farming systems and intercropping patterns (IPs) on the physiological aspects of safflower and bitter vetch. Treatments included high and low-input farming systems and various IPs that exchanged safflower and bitter vetch with row ratios of 2:2, 2:3, 2:4, 2:5, while sole cropping safflower and bitter vetch were used as control. The highest grain yield of both plants was obtained from the high input farming system (HIFS). The most safflower oil yield and protein yield of bitter vetch were achieved from sole cropping in the HIFS. Safflower sole

cropping in the Low-input farming system (LIFS) had the highest oil content, but in other traits, HIFS had superior to LIFS. Intercropping resulted in high P and N content and low stearic acid in safflower compared with sole cropping. These novel findings demonstrate that HIFS was beneficial than LIFS in all traits of both plants except safflower oil content and some fatty acids content like palmitic acid. Also, in the 2:2 IP monetary advantage index (MAI) and the land equivalent ratio (LER=1.13) were highest that indicating that 13% additional area needed by the sole cropping system to provide an equivalent yield in HIFS.

Keywords: Fatty acid composition; Grain yield; Land equivalent ratio; Monetary advantage index; Oil and protein yield

1. Introduction

Conventional farming referred to as a high input system has a crucial result in enhancing food production but had a tremendous troublesome environmental impact (Lichtfouse et al. 2009). This cropping system depends on extensive inputs like pesticides and fertilizers, which produce wastes that damage the environment. Attentions have been given to finding ways to decrease restore the harmful effects of various agricultural systems. Low input farming systems help farms that utilize less out-farm inputs, integrate plant production and animal, and keep a better biotic diversity (Chaplin-Kramer et al. 2015). This farming system utilizes lower amounts of pesticides and chemical elements than the high-input farming system (Berbeć et al. 2020). So low input farming systems include exploitation techniques to obtain maximum yields without harming the health of the inhabitants and the environment (Sarkar et al. 2020).

In terms of ecology and environment, mono-cropping has a significant problem that leads to reducing soil nutrients and crop yield (Bennett et al. 2012). Compared with mono-cropping, better use of agricultural resources was observed in intercropping studies (Khan et al. 2014; Jalilian et al. 2017). Franco et al. (2015) reported that a combination of intercropping species might prepare sustainable producers and allows farmers to diminish inputs while increasing total yields. Saeidi et al. (2018) indicated that integrated use of chemical and biofertilizers in safflower/faba bean intercropping system caused to improved growth and quality of safflower.

Legumes in intercropping systems are a critical purposeful plant and are extraordinarily valuable for the agro-ecological system (Duchene et al. 2017). Bitter vetch (*Vicia ervilia* L.) is a grain legume, and old legume of the Mediterranean region belongs to the Fabaceae family that has been used for forage and grain production. It has a variety of positive aspect, like high yield, drought also pest's resistance, and has a protein that creates it an economically helpful supply for animal diets (González-Verdejo et al. 2020). Earlier researches have explored the possibility of intercropping of legumes and non-legumes with oilseed crops to improve land productivity, economic returns, and produce quality (Cadoux et al. 2015; Zafaranih 2015).

Safflower (*Carthamus tinctorius* L.) belongs to Asteraceae family is a broadleaf annual oilseed plant and acclimate to irrigated farming systems or dry land (Kohnward et al. 2012). It was reported that safflower/fenugreek intercropping improve

safflower oil and protein content (Abdelkader & Hamad 2015). Zafarani (2015) indicated that various combinations of intercropping significantly influenced yield, yield components, and LER of safflower/chickpea in an intercropped system.

There is minor information on the impacts of various farming systems and intercropping patterns on physiological characteristics of bitter vetch and safflower. Therefore, the objective of this study was the evaluation of crop yield, protein, N and P content changes in safflower and bitter vetch and oil and fatty acid composition of safflower under low and high input intercropping farming systems.

2. Material and Methods

2.1. Experimental site and meteorological data

This field study was done at the Urmia University research farm, West Azerbaijan Province, Urmia-Iran (44° 58' E, 37° 39' N; 1365 m above sea level) in 2013-2014 growing seasons. Because the weather conditions have a direct impact on the growth characteristics of the plants, therefore the mean air temperature and monthly precipitation as an experimental site weather conditions are compared with long-term averages (1985-2014) in Figure 1. The farm was deeply plowed in the past fall and early spring; disk and cultivator were done for land preparation.

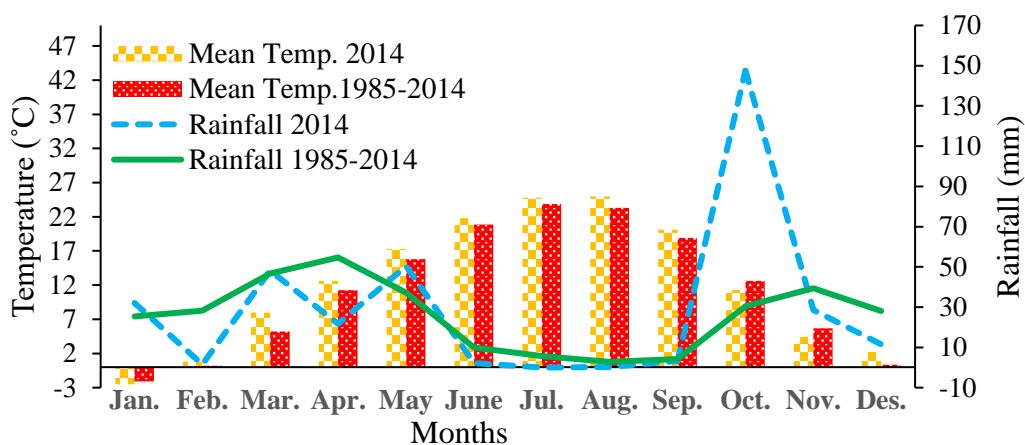


Figure 1- The mean monthly rainfall and temperature in 2014 are compared with long-term (1985-2014)

2.2. Experimental design and crop husbandry

Two farming systems (high and low input) and six intercropping patterns (IP) were replicated three times using a factorial experiment arranged as randomized complete block design. Intercropping patterns consist of two rows of safflower (100 cm wide) and various bitter vetch row ratios (two, three, four, and five rows with 50, 75, 100, and 125 cm wide, respectively; safflower and bitter vetch sole cropping as the control). For bitter vetch and safflower, the space between rows was 25 and 50 cm, respectively (Figure 2).

A 30 cm inter-row space was allowed between bitter vetch and safflower strips, with a one-meter buffer between plots. In four respective patterns, the intercropping space ratios occupied by safflower and bitter vetch were 67%:33%, 57%:43%, 50%:50% and 45%:55%, respectively. The area of intercropping plots was 15.75, 17.5, 19.25 and 21 m² for the four respective patterns, 10 m² for sole bitter vetch and 15 m² for sole safflower. At the end of April and middle of May, bitter vetch and safflower were sown by hand, respectively, in loamy clay soil (32% clay, 37% silt, 31% sand) with PH 7.21 (High Input Farming System - HIFS) and 7.06 (Low Input Farming System - LIFS).

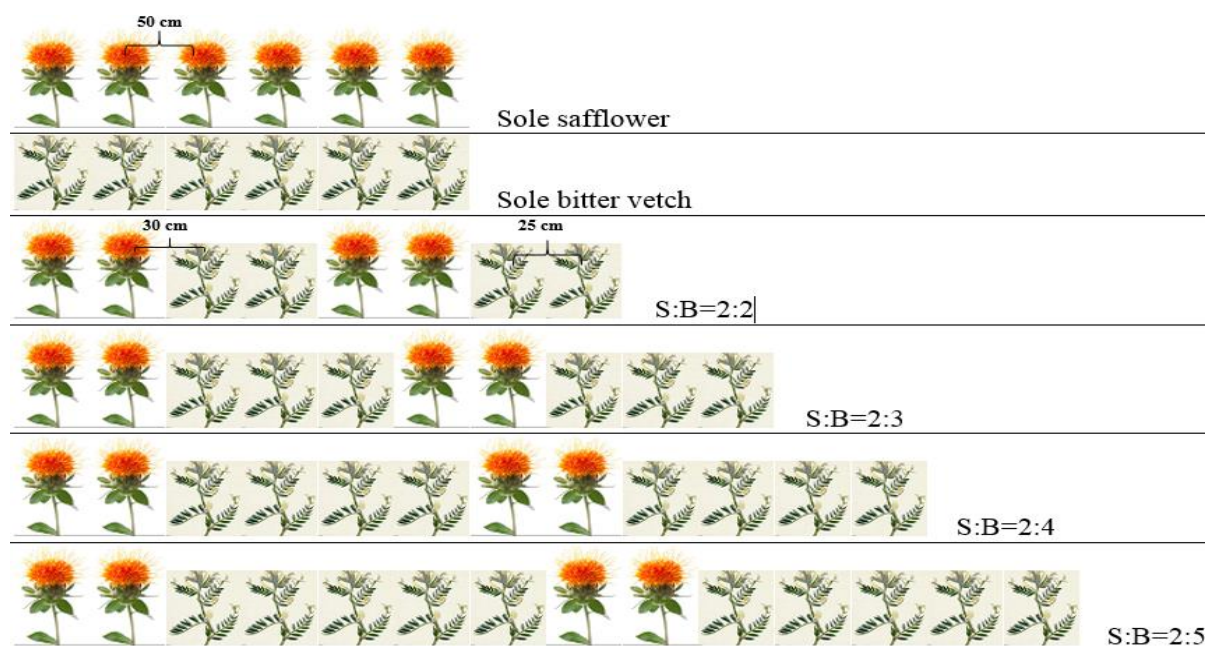


Figure 2- Graphic description of sole safflower, sole bitter vetch, and intercropping pattern between safflower (S) and Bitter vetch (B)

In HIFS, agronomic practices included tillage operations, shovel and rake, 120 kg ha⁻¹ urea and 90 kg ha⁻¹ triple superphosphate and the *Acanthiophilus helianthi* Rossi and weeds chemical control, with the application of Metasystox and Gallant, respectively were done. In LIFS, weed removal was done by hand, just rake was used and 40 t ha⁻¹ cow manure before planting was mixed with soil. Also, in LIFS treatment, seeds before planting inoculated with Nitroxin (*Azospirillum lipoferum* and *Azotobacter chroococcum*) and Biophosphate (*Bacillus lentus*, *Pseudomonas putida*) suspensions bacteria at 10⁹ CFU mL⁻¹ for 30 min (Ozturk et al. 2003). All plants were irrigated uniformly between 7 to 9 days depending on weather temperature.

2.3. Measurements

Safflower grain oil content was determined using a soxhlet fat extraction method by AOAC methods (AOAC 2000). By multiplying the oil content in grain yield, oil yield was obtained and expressed in kilograms per hectare (kg ha⁻¹). Determination of fatty acids composition in safflower seeds was done according to the method of Metcalfe et al. (1966) using an Agilent gas chromatograph (a capillary column, BPX 70, 50 m by 0.25 mm with an FID detector and the carrier gas was nitrogen and hydrogen). Grain nitrogen content was measured using the Kjeldahl method. By multiplying the protein percentage in the grain yield, protein yield was obtained and expressed in kilograms per hectare (kg ha⁻¹). The vanadate-molybdate yellow color method was used to measure grain phosphorus percentage (Chapman et al. 1961). To determine the grain yield for each plot, two lateral rows and half a meter from the beginning and the ends were ignored, and the grain yield was determined from one square meter. The index for measure the intercropping advantage, the land equivalent ratio (LER) calculated from grain yield as follows (Fetene 2003):

$$\text{LER} = Y_{is}/Y_{ss} + Y_{ib}/Y_{sb} \quad (1)$$

Where; Y_{is} , Y_{ss} , Y_{ib} and Y_{sb} are the yield of intercropping and sole cropping of safflower and bitter vetch, respectively.

To compute the economic advantage, Banik et al. (2000) introduced the monetary advantage index (MAI). MAI was calculated as follows:

$$\text{MAI} = [(Y_{is} \times P_s) + (Y_{ib} \times P_b)] \times \left(\frac{\text{LER}-1}{\text{LER}} \right) \quad (2)$$

Where: Y_{is} and Y_{ib} are the yield of intercropping of safflower and bitter vetch; P_s and P_b are the price of safflower and bitter vetch, respectively. LER is land equivalent ratio. Guaranteed purchase price in Iran for safflower and bitter vetch seeds in 2020 were 100000 IRR (=0.5 \$) and 150000 IRR (=0.75 \$) per kilogram, respectively.

2.4. Statistical analysis

The statistical analysis system (SAS Institute 2003) was used for the analysis of variance. Duncan's multiple-compare range test used for means comparison at 1% level.

3. Results and Discussion

A significant effect of treatment interaction was shown for safflower oil content and oil yield (Table 1).

Table 1- Analysis of variance (mean square) for some physiological characteristics and grain yield of safflower/bitter vetch intercropping affected by different farming systems

<i>Safflower</i>		<i>Oil content</i>	<i>Oil yield</i>	<i>N content</i>	<i>Protein content</i>	<i>Protein yield</i>	<i>P content</i>	<i>Grain yield</i>
Source of variation	df							
Replication	2	0.37 ^{ns}	4030.6 ^{**}	0.00056 ^{ns}	0.021 ^{ns}	1241.8 ^{**}	0.000 ^{ns}	396.55 ^{**}
FS	1	93.35 ^{**}	247335.5 ^{**}	0.056 ^{**}	2.19 ^{**}	473461 ^{**}	0.007 ^{**}	69153.3 ^{**}
IP	4	32.76 ^{**}	373285.3 ^{**}	0.36 ^{**}	14.09 ^{**}	234110 ^{**}	0.000008 ^{ns}	39358.6 ^{**}
FS×IP	4	2.07 ^{**}	3329 ^{**}	0.00049 ^{ns}	0.019 ^{ns}	12483 ^{**}	0.000005 ^{ns}	1309.01 ^{**}
Error	18	0.22	536.5	0.0043	0.016	142.5	0.0007	33.31
Coefficient of variation (%)		1.77	3.13	0.61	0.61	1.97	1.06	2.09
<i>Bitter vetch</i>								
Replication	2	-	-	0.005 ^{ns}	4.81 ^{ns}	373.8 ^{ns}	0.000006 ^{ns}	6.13 ^{ns}
FS	1	-	-	1.44 ^{**}	87.34 ^{**}	83029 ^{**}	0.0017 ^{**}	6912.6 ^{**}
IP	4	-	-	0.09 ^{**}	9.51 [*]	170584 ^{**}	0.00002 ^{ns}	29306 ^{**}
FS×IP	4	-	-	0.004 ^{ns}	3.24 ^{ns}	5399.1 ^{**}	0.000001 ^{ns}	517.78 ^{**}
Error	18	-	-	0.004	3.03	442.7	0.0000015	10.12
Coefficient of variation (%)		-	-	1.92	8.02	8.15	0.66	2.73

ns, * and **: not significant, significant at 0.05 and 0.01 probability level, respectively. FS= Farming system, IP=Intercropping patterns.

3.1. Oil content and oil yield of safflower

The most oil content of safflower with a significant difference with other treatments was observed in sole cropping located in LIFS. This value was 9.19% higher than sole cropping in HIFS (Table 2). Mean comparison showed that the highest oil yield of safflower was achieved from sole cropping in HIFS. Also, in LIFS, sole cropping was the most effective in oil yield than other IPs (Table 2). Oil yield in sole cropping of HIFS was 18.95% more than the same pattern in LIFS (Table 2).

Table 2-Mean compares some physiological characteristics and grain yield of safflower and bitter vetch affected by farming systems and different intercropping patterns

FS	IP	<i>Safflower</i>				<i>Bitter vetch</i>	
		<i>Oil content (%)</i>	<i>Oil yield (Kg ha⁻¹)</i>	<i>Protein yield (Kg ha⁻¹)</i>	<i>Grain yield (Kg ha⁻¹)</i>	<i>Protein yield (Kg ha⁻¹)</i>	<i>Grain yield (Kg ha⁻¹)</i>
High-input (HIFS)	SS	28.16±0.65c	1188.39±44.4a	834.96±17.9b	4220.14±93.7a	-	-
	2:2	22±0.10f	833.8±4.9b	1025.78±5.1a	3790.02±8.9b	139.1±22.5f	590.75±64.2f
	2:3	23.66±0.38e	811.72±14c	775.62±23c	3430.8±110c	196.6±4.5e	840.22±21.8e
	2:4	22.58±0.48f	634.58±18.8d	625.51±19e	2810.4±102f	256.81.95d	1110.1±22.5d
	2:5	27.3±0.36c	524.26±22.8f	386.73±10.7h	1920.4±62.4h	317.9±10.5c	1390.2±39.2c
	SB	-	-	-	-	642.9±12.9a	2620.6±39.1a
Low-input (LIFS)	SS	31.01±0.79a	961.52±57.3b	592.92±19.3f	3100.7±106d	-	-
	2:2	27.31±0.36c	734.69±9.7c	666.95±7.1d	2690.2±40.3e	90.8±7.7g	440.67±25.5g
	2:3	27.33±0.037c	587.62±34.9e	437.94±21.3g	2150.1±105g	129.7±1.27f	630.67±6.1f
	2:4	26.23±0.58d	461.8±20.8g	385.34±8.9h	1760.6±42.6i	177.08±1.23e	880.08±11.1e
	2:5	29.46±0.41b	412.49±27.4h	273.19±13.9i	1400.2±75.5j	182.06±6.4e	1080.1±24d
	SB	-	-	-	-	447.6±58.6b	2000.6±12b

Values are Mean ± Standard deviation; SD: The same letters in each column show non-significant difference at P≤0.05 by Duncan test; SS and SB: means safflower and bitter vetch sole cropping, respectively; FS: Farming system; IP: Intercropping patterns.

Safflower sole cropping in LIFS and HIFS had the highest oil content and oil yield, respectively. High oil yield in sole cropping was due to high grain yield in this intercropping pattern (Table 2). Since the oil content is negatively correlated with N fertilizer rate, in LIFS, due to less nitrogen availability than HIFS, the amount of oil was higher than HIFS. It is possible that in HIFS, more nitrogen resources were available for plants than organic fertilizers (Nitroxin, Biophosphate and cow manure). This reverse relationship is often attributed to the competition between oil and protein concentrations in grain for carbon skeletons throughout carbohydrate metabolism (Rathke et al. 2005). Similar results in increasing the oil content of sesame in the application

of organic fertilizers compared to chemical fertilizers have been reported (Ratna et al. 2015). It has been reported that excessive use of nitrogen fertilizers caused a decrease in the availability of carbohydrates for oil synthesis (Rathke et al. 2005).

In sole cropping, due to the absence of bitter vetch that is a weaker competitor than safflower in nitrogen absorption, the amount of available nitrogen was less than mixed patterns; hence, the oil content in this pattern was more than IPs. Considering the beneficial properties of safflower oil and its application in traditional medicine, production of organic oil that is free of chemicals is essential. The production of good oil content is one of the main goals of oilseeds cultivation in low-input agriculture, a goal that has been achieved in this experiment (Table 2). Abdelkader & Hamad (2015) also concluded that intercropping of safflower with fenugreek reduced amount of grain oil than sole cropping. Nasim et al. (2012) reported that nitrogen is the essential element to improve grain oil content, however, additional nitrogen rates reduced seed oil percentage and improved sunflower seed yield.

3.2. Fatty acids composition of safflower seeds

Variance analysis showed that the main effect of farming systems and intercropping patterns was significant on palmitic and linolenic acid content. Safflower stearic, oleic and linoleic acid were affected by the interaction of treatments (Table 3).

Table 3-Analysis of variance (mean square) for fatty acids composition of safflower intercropped with bitter vetch affected by different farming systems

Source of variation	df	Palmitic acid	Stearic acid	Oleic acid	Linoleic acid	Linolenic acid
Replication	2	0.069 ^{ns}	0.036 ^{ns}	0.007 ^{ns}	0.53 ^{ns}	0.59 ^{ns}
FS	1	2.8*	0.5 ^{ns}	0.031 ^{ns}	113.33**	2.43*
IP	4	1.76**	0.01*	5.45**	35.96**	3.38**
FS×IP	4	0.39 ^{ns}	0.86**	1.05*	16.45**	0.3 ^{ns}
Error	18	0.34	0.23	0.26	1.55	0.31
Coefficient of variation (%)		11.18	10.3	5.53	1.94	14.2

ns, * and **: not significant, Significant at 0.05 and 0.01 probability level, respectively; FS: Farming system; IP: Intercropping patterns

Results in Table 4 show that sole cropping had the most palmitic acid content but it's a difference with 2:2, 2:3, and 2:5 IPs were not significant. The 2:4 IP with the lowest palmitic acid content, contributed to improving the quality of produced oil in comparison with sole cropping and other IPs (Table 4). Results of mean comparison indicated that plants in HIFS had more palmitic acid than plants located in LIFS (Table 4). According to the mean comparison, HIFS had the most linolenic acid content than LIFS (Table 4).

Table 4-Palmitic and Linolenic acid percentage of safflower seeds affected by farming systems and intercropping patterns

Farming systems	Palmitic acid (%)	Linolenic acid (%)
High- input (HIFS)	5.56 ± 0.81a	4.25 ± 1.02a
Low- input (LIFS)	4.95 ± 0.61b	3.68 ± 0.78b
Intercropping patterns (IP)		
SS	5.62 ± 0.96a	3.02 ± 0.38d
2:2	5.41 ± 0.80a	3.57 ± 0.46cd
2:3	5.48 ± 0.37a	3.91 ± 0.93 bc
2:4	4.29 ± 0.36b	5.01 ± 0.48a
2:5	5.48 ± 0.54a	4.31 ± 0.86b

Values are Mean ± Standard deviation; SD: The same letters in each column show the non-significant difference at P≤0.05 by the Duncan test; SS and SB: mean safflower and bitter vetch sole cropping, respectively.

Also, the results showed that 4:2 IP with a significant difference with other IPs had the highest amount of linolenic acid (Table 4). Our results showed that the 2:4 IP and LIFS had significantly reduced palmitic acid than other treatments (Table 4). The results showed that LIFS with the application of organic and biological fertilizer had 10.97% lower palmitic acid content than HIFS (Table 4). Therefore, LIFS reduced the harmful saturation fatty acid content in safflower oil. It has been reported that organic fertilizers reduce palmitic and stearic acid in safflower compared with chemical fertilizers (Onemli 2014). In another experiment, the reduction of palmitic fatty acids due to the application of organic fertilizers than chemicals were reported (Akbari et al. 2011). Results indicated that linolenic acid had the highest content in HIFS and 2:4 IP (Table 3). Although Linolenic acid content in HIFS was 13% higher than LIFS, nevertheless non-chemical use increased the quality of products and health of consumers and this advantage compensates for the high percentage of this fatty acid in HIFS (Table 4).

The results of the mean comparison showed that sole cropping in HIFS had the highest amount of stearic acid and its difference with the 2:2 intercropping pattern in the HIFS and 2:2, 3:2, 4:2 and 5:2 IPs in LIFS was not significant (Table 5).

Table 5-Fatty acid percentage of safflower affected by farming systems and intercropped with bitter vetch

Farming systems	Intercropping patterns	Stearic acid (%)	Oleic acid (%)	Linoleic acid (%)
High- input (HIFS)	SS	5.68±0.31a	11.35±0.43a	62.31±0.57de
	2:2	5.03±0.59 abc	9.44±0.49cde	65.28±1.9bc
	2:3	4.59±0.58bcd	8.51±0.68ef	66.5±2.1bc
	2:4	4.51±0.36bcd	8.56±0.11def	69.25±1.07a
	2:5	4.36±0.08cde	9.01±0.73cdef	66.8±0.6b
Low- input (LIFS)	SS	3.88±0.59de	10.43±0.23b	62.05±0.13e
	2:2	5.2±0.75abc	9.83±0.84bc	60.13±1.7e
	2:3	4.97±0.41abc	9.55±0.36bcd	64.35±0.49cd
	2:4	4.97±0.32abc	8.68±0.11def	64.35±1.08cd
	2:5	5.31±0.09ab	8.14±0.24f	57.88±0.41f

Values are Mean ± Standard deviation; SD: The same letters in each column show non-significant difference at $P \leq 0.05$ by Duncan test; SS: means safflower sole cropping

The mean comparison showed that sole cropping of safflower in HIFS had the highest amount of oleic acid, with a significant difference from other treatments (Table 5). Generally, in both farming systems, sole cropping had the highest percentage of oleic acid (Table 5). The mean comparison results showed that the maximum amount of linoleic acid was achieved from 2:4 IP in HIFS, which statistically had a significant difference with other treatments in this experiment (Table 5). The lowest amount of stearic acid belonged to the sole cropping located in LIFS which was 31.69% lower than sole cropping in HIFS but it's the difference with 2:3, 2:4 and 2:5 IPs in HIFS was not significant (Table 5). Our results have shown that the amount of oleic acid in the sole cropping of HIFS was 8.1% more than the similar pattern in LIFS (Table 5). There is a significant negative relationship between linoleic and oleic acid content so that when the value of one decrease, the value of the other increases, as evident in this experiment (Table 5).

3.3. Grain nitrogen, protein content and protein yield

Means comparison showed that safflower and bitter vetch grains had the most nitrogen and protein content in HIFS (Figure 3). The most nitrogen and protein content of safflower and bitter vetch grains were obtained in a high input farming system (Figure 3).

In HIFS, more availability of N and P caused improvement in some physiological traits (Figures 3, 4, 5 and Tables 2, 4 and 5).

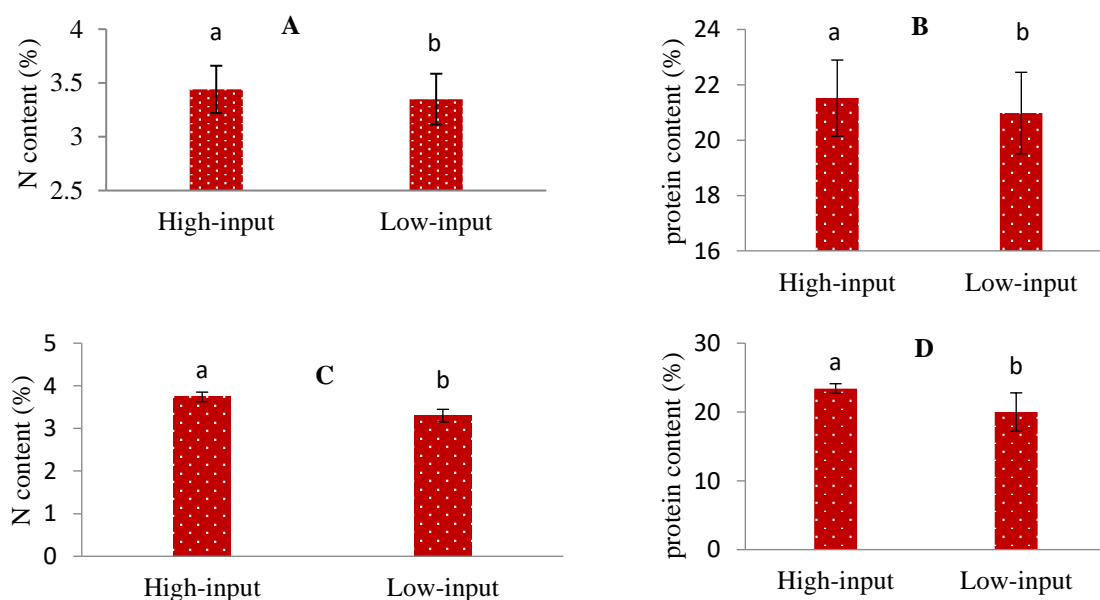


Figure 3- Mean (± Standard deviation, SD) comparison for safflower nitrogen (A), protein content (B) and bitter vetch nitrogen (C), protein content (D) influenced by farming systems. Error bars show standard errors of the mean. The same letters show the non-significant difference at $P \leq 0.05$ by the Duncan test

Since nitrogen is the main component of proteins, Nitrogen fertilizer can increase the nitrogen and subsequently protein content of grains. It has been reported that a sufficient amount of phosphorus also affects RNA synthesis, which increases protein synthesis (Raven 2013). A large part of plant nitrogen participates in rubisco structure after performing its photosynthesis role during plant growth, in the leaf's senescence with chlorophyll degradation, nitrogen is removed from the structure of rubisco

and transferred to the growing grains and is eventually used during the synthesis of protein in seeds (Li et al. 2020). Figure 3B shows that all IPs, especially 2:2 IP, have superiority to sole cropping of safflower and this shows advantages of intercropping in protein content improvement. The availability of suitable nitrogen concentration and less competitive ability of bitter vetch in 2:2 IP caused the more generous amount of nitrogen and protein.

The most protein and nitrogen content of safflower grains were obtained from 2:2 IP, and the lowest were observed in sole cropping (Figure 4A and B). In bitter vetch, sole cropping had the highest seed protein and nitrogen (Figure 4C and D).

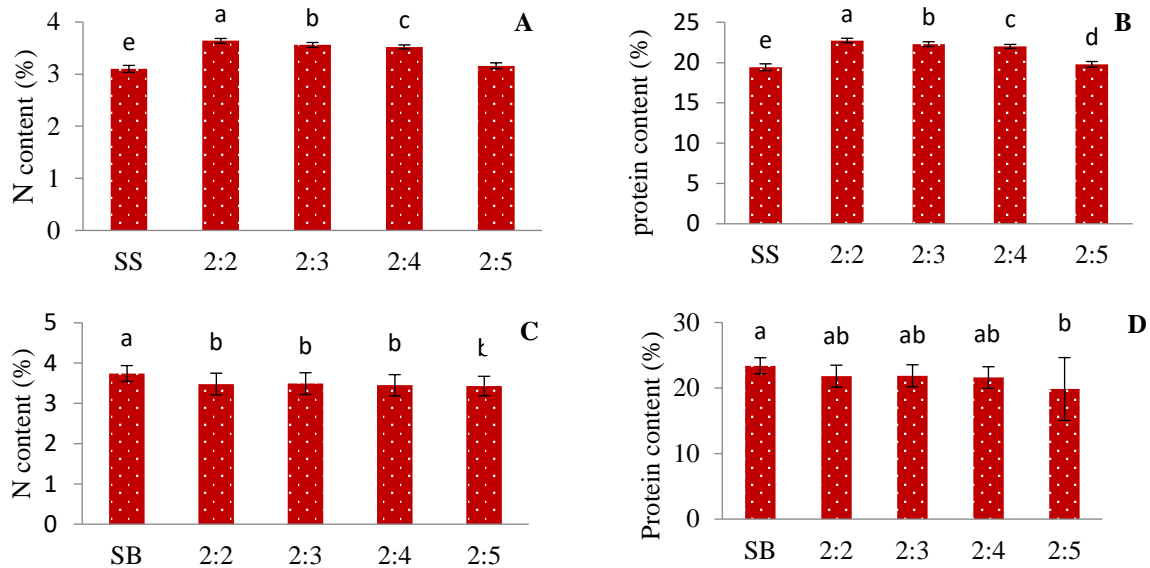


Figure 4- Mean (\pm Standard deviation, SD) comparison for safflower nitrogen (A), protein content (B) and bitter vetch nitrogen (C), protein content (D) influenced by different intercropping patterns. Error bars show standard errors of the mean. The same letters show non-significant difference at $P \leq 0.05$ by the Duncan test. SS and SB mean safflower and bitter vetch sole cropping, respectively

The high nitrogen and protein content of bitter vetch in sole cropping may be associated with a lack of safflower in this pattern. Since safflower is a more competitive plant than bitter vetch, in sole cropping of bitter vetch, more nitrogen and phosphorus are available for this plant with less competition. Because safflower has higher competitive abilities like more extensive shoot and root compared with bitter vetch, it was dominant in competition. According to the results mentioned, bitter vetch had the most protein content (Figure 4D) and seed yield in sole cropping under HIFS (Table 2). Therefore, this treatment was effective in increasing protein yield.

The mean comparison showed that 2:2 IP in HIFS had the highest protein yield in safflower, which its difference with other IPs was significant. In both HIFS and LIFS, safflower had the highest protein yield in the 2:2 IP (Table 2).

High protein content in 2:2 IP (Figure 4B) caused high protein yield in this pattern (Table 2). In bitter vetch, the most protein yield was observed in sole cropping in HIFS, which had a significant difference with other treatments (Table 2).

3.4. Grain yield and phosphorus content

The mean comparison showed that, sole cropping of safflower and bitter vetch in HIFS had the highest grain yield, with a significant difference with other IPs (Table 2). Comparison between intercropping patterns showed that in both farming systems, safflower had the most grain yield at 2:2 IP (Table 2), but the maximum grain yield for bitter vetch was obtained from 2:5 intercropping pattern (Table 2). The absence of competition for resources, also the use of pest management and fertilizers, led to the highest grain yield in HIFS for sole cropping of bitter vetch (Table 2). Yield reduction at IPs may be arising from competition for water, nutrients and solar radiation compared with sole cropping (Belel et al. 2014). Because of more input usage, the total yield of both plants increased in HIFS compared to LIFS (Table 2). The sole cropping of safflower for each system yielded more than the entire bitter vetch: safflower intercropping. High grain yield in sole cropping pattern of safflower and the superiority of the IPs can be justified by land equivalent ratio (LER) Index. The grain yield of safflower was higher than bitter vetch. The facilitative influence of bitter vetch can offer nitrogen through symbiotic nitrogen fixation that successively reduces the overburden pressure on soil nitrogen sources. In sole cropping of bitter vetch, access to inputs may increase yield. Decreasing grain yield in the LIFS compare with HIFS may be due to low access to nutrients by plants, especially nitrogen and phosphorus, when plants require elements. It has been reported that nitrate and ammonium released by organic residues cannot provide optimum nutritional requirements for plants. Thus, low input farming productivity is limited by the availability of nitrogen

(Zarabi & Jalali 2012). Rouphael et al. (2015) have also reported reduced Perilla grain yield by 27% in low-input farming systems than the high-input farming system.

Mean comparison indicated that in both safflower and bitter vetch, grains in both plants located in HIFS had the most phosphorus content and its difference with LIFS was significant (Figure 5A and B). High input farming system in comparison with a low input farming system increase phosphorus content in safflower and bitter vetch seeds by 14.81 and 5.26% respectively (Figure 5A and B). Gaj & Gorski (2014) in their research, demonstrated that the application of phosphorus increased nitrogen, phosphorus, potassium, calcium and magnesium uptake in winter wheat. The type of tillage in HIFS is such that the elements in the surface layer are mixed with deep layers, but in the LIFS, the tillage was superficial, so nutrients cannot penetrate in depths and are not available for deeper roots (Cai et al. 2014).

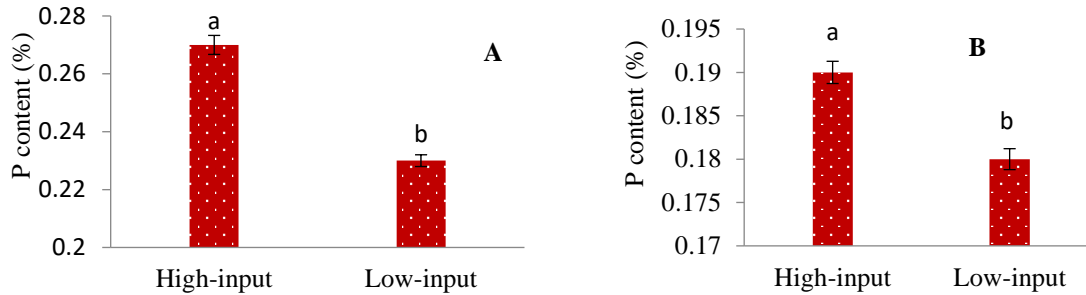


Figure 5- Mean (\pm Standard deviation, SD) comparison for grain phosphorus (P) content of safflower (A) and bitter vetch (B) affected by farming systems. Error bars show standard errors of the mean. The same letters show non-significant difference at $P \leq 0.05$ by the Duncan test

3.5. Land equivalent ratio (LER)

In Figure 6 LER data of various intercropping patterns are given. The amounts of LER for all intercropping patterns were more than one except for 2:5 IP. In both systems, the 2:2 IP had yield advantages that suggest the preference of intercropping relative to sole cropping. Results indicated that by increasing bitter vetch density, the value of LER decreased. As shown in Figure 6 only the LER of 2:5 intercropping pattern was less than one. All intercropping patterns except 5:2 in HIFS had the most amount of LER value compared with LIFS (Figure 6).

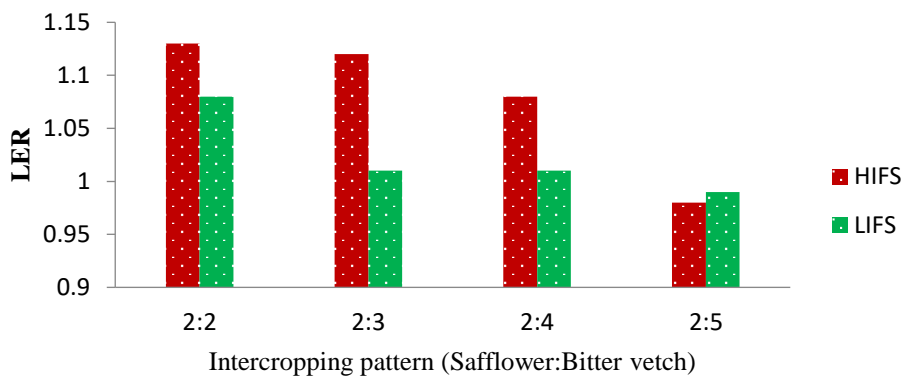


Figure 6- LER values of various intercropping patterns of safflower and bitter vetch influenced by the farming system. HIFS: High input farming system, LIFS: Low input farming system

The land equivalent ratio is mixed cropping benefits index, which indicates the degree of inter-species competition or facilitating of mixed cropping system (Fetene 2003). Land equivalent ratio more than one in mixed cropping is because of the efficient use of environmental resources, element's exchange, increasing of competitive ability of plants with weeds, nitrogen fixation by legumes, as well as differences in root system and different physiological and morphological requirements of components of mix cropping and the higher absorption of radiation (Vandermeer 1989). The productivity of intercropping than sole cropping, introduced by LER value, has been reported by many researchers (Hamdani & Suradinata 2015; Metwally et al. 2015; Nyoki & Ndakidemi 2017).

3.6. Monetary advantage index (MAI)

This index is the result of the value of intercropped crops and land equivalent ratio. The higher MAI value shows the more profitable (Dhima et al. 2007). In Fact, the positiveness of this index indicates the usefulness and economic advantage of

intercropped cultivation and better use of available resources by plants compared to sole cropping of them. The results of MAI calculation (Figure 7) showed that HIFS was superior than LIFS in 2:2, 2:3 and 2:4 intercropping patterns, but in 2:5 intercropping patterns, LIFS was better than HIFS. 2:2 intercropping pattern in both HIFS and LIFS had the most MAI index than other IP (Figure 7).

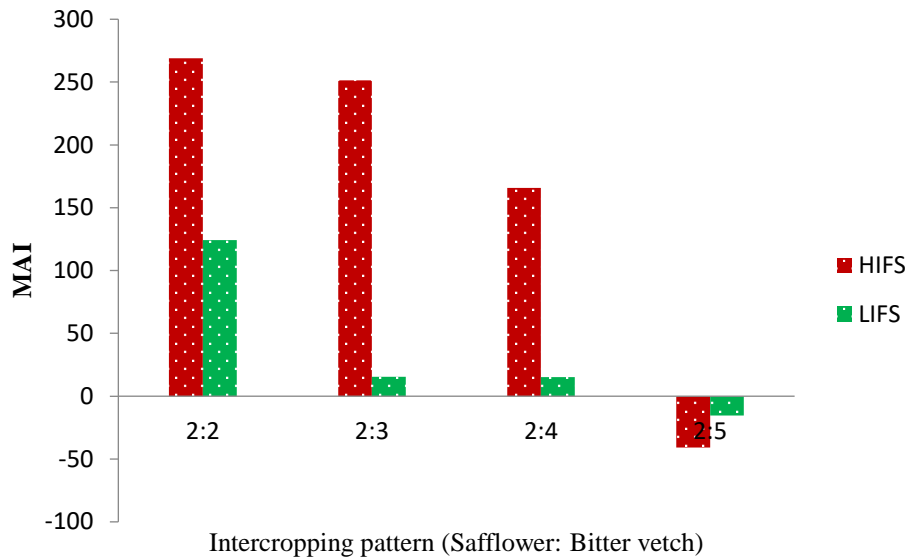


Figure 7- MAI values of various intercropping patterns of safflower and bitter vetch influenced by the farming system. HIFS: High input farming system, LIFS: Low input farming system

Khippal et al. (2016) reported that the maximum monetary advantage index in the intercropping of sugarcane with peas and recommended the implementation of this planting system in order to obtain more income for farmers. It is also reported a decrease in barley yield by using different barley and alfalfa intercropping systems, but in the treatment of 2 rows of barley + 2 rows of alfalfa and 6 rows of barley + 2 rows of alfalfa, due to increased alfalfa seed yield that it had a higher economic value, eventually the monetary advantage index increased (Esmaeili et al. 2011).

4. Conclusions

The study shows that in all traits of both safflower and bitter vetch except safflower oil content and some fatty acids content like palmitic acid, HIFS was beneficial and had a significant difference with LIFS. The characteristics of safflower were affected by intercropping patterns. In most studied traits, sole cropping was the most advantageous pattern, but in some characteristics, IPs was beneficial, especially 2:2 IP, which was superior to sole cropping. However, in all traits of bitter vetch, sole cropping was useful and this was probably due to the dominance of safflower compared to the bitter vetch. Depending on our purpose of the intercropping of these two plants, different patterns and systems are recommended. To harvest high levels of safflower protein, 2:2 IP has a better result than other mixed patterns but to achieve high oil content, sole cropping must be used. Concerning oil quality, 2:4 IP had the highest linoleic acid content which increased oil quality. Results showed that LIFS had the highest percentage of oil production. Although HIFS had higher grain yield and compensated for the low amount of oil, but the healthy product in the LIFS made it superior to HIFS. According to the results of the land equivalent ratio (LER) and monetary advantage index (MDI), the highest values of these indices were observed in 2:2 IP in HIFS and this can be the advantageous IP than other intercropping patterns.

Acknowledgments

Urmia University of Iran (Ph.D. Thesis of the first author) supported this research and we dedicate it to our late colleague Dr. Mohammad Reza Zardashti.

Abbreviations and Symbols

FS	Farming systems
HIFS	High input farming system
IPs	Intercropping patterns
LER	Land equivalent ratio
LIFS	Low input farming system
SB	Sole cropping bitter vetch
SS	Sole cropping safflower
MAI	Monetary advantage index

References

- Abdelkader M A I & Hamad E H A (2015). Evaluation of productivity and competition indices of safflower and fenugreek as affected by intercropping pattern and foliar fertilization rate. *Middle East Journal of Agricultural Research* 4(4): 956-966
- Akbari P, Ghalavand A, Sanavy A M & Alikhani M A (2011). The effect of biofertilizers, nitrogen fertilizer and farmyard manure on grain yield and seed quality of sunflower (*Helianthus annuus* L.). *Journal of Agricultural Science and Technology* 7(1): 173-184
- AOAC (2000). *Fatty acids in oils and fats*. Official methods of analysis of the AOAC, 17th Ed. AOAC, Arlington, Virginia USA.
- Banik P, Sasmal T, Ghosal P K & Bagchi D K (2000). Evaluation of mustard (*Brassica campestris* Var. Toria) and legume intercropping under 1:1 and 2:1 row-replacement series systems. *Journal of Agronomy and Crop Science* 185: 9-14. DOI: 10.1046/j.1439-037X.2000.00388.x
- Belel M D, Halim R A, Raffii M Y & Saud H M (2014). Intercropping of corn with some selected legumes for improved forage production: a review. *Journal of Agricultural Science* 6(3):48-62. DOI: 10.5539/jas.v6n3p48
- Bennett A, Bending G, Chandler D, Hilton S & Mills P (2012). Meeting the demand for crop production: the challenge of yield decline in crops grown in short rotations. *Biological Reviews* 87: 52-71. DOI: 10.1111/j.1469-185X.2011.00184.x.
- Berbec A K, Staniak M, Feledyn-Szewczyk B, Kocira A & Stalenga J (2020). Organic but also low-input conventional farming systems support high biodiversity of weed species in winter cereals. *Agriculture* 10(9):413. DOI: 10.3390/agriculture10090413
- Cadoux S, Sauzet G, Valantin-Morison M, Pontet C, Champolivier L, Céline R, Lieven J, Flénet F, Mangenot O, Fauvin P & Landé N (2015). Intercropping frost-sensitive legume crops with winter oilseed rape reduces weed competition, insect damage, and improves nitrogen use efficiency. *Oilseeds and Fats, Crops and Lipids* 22(3): 1-11. DOI: 10.1051/ocf/2015014
- Cai H, Ma W, Zhangm, Ping J, Yan X, Liu J, Yuan J, Wang L & Ren J (2014). Effect of subsoil tillage depth on nutrient accumulation, root distribution, and grain yield in spring maize. *Crop Journal* 2: 297-307. DOI: 10.1016/j.cj.2014.04.006
- Chaplin-Kramer R, Sharp R P, Mandle L, Sin S, Johnson J, Butnar I, Mila I Canals L, Eichelberger BA, Ramler I, Mueller C, Mclacclan N, Yousefi A, King H & Kareiva P M (2015). Spatial patterns of agricultural expansion determine impacts on biodiversity and carbon storage. *Proceedings of the National Academy of Sciences of the USA* 112: 7402-7407. DOI: 10.1073/pnas.1406485112
- Chapman H D & Pratt P F (1961). *Method of analysis for soil, plants, and waters*. University of California. Division of agricultural science. Berkeley, California, 309 p.
- Dhima K V, Lithourgidis A S, Vasilakoglou I B & Dordas C A (2007). Competition indices of common vetch and cereal intercrops in two seeding ratios. *Field Crops Research* 100: 249-256. DOI: 10.1016/j.fcr.2006.07.008
- Duchene O, Vian J F & Celette F (2017). Intercropping with legume for agroecological cropping systems: Complementarity and facilitation processes and the importance of soil microorganisms: a review. *Agriculture, Ecosystem and Environment* 240:148-161. DOI: 10.1016/j.agee.2017.02.019
- Esmaeili A, Sadeghpour A, Hosseini S M B, Jahanzad E, Chaichi M R & Hashemi M (2011). Evaluation of seed yield and competition indices for intercropped barley (*Hordeum vulgare*) and annual medic (*Medicago scutellata*). *International Journal of Plant Production* 5(4): 395-404. DOI: 10.22069/IJPP.2012.749
- Fetene M (2003). Intra- and inter-specific competition between seedlings of *Acacia etbaica* and a perennial grass (*Hypparrenia hirta*). *Journal of Arid Environments* 55(3): 441-451. DOI: 10.1016/S0140-1963(03)00052-1
- Franco J G, King R S, Masabni G J & Volder A (2015). Plant functional diversity improves short-term yields in a low-input intercropping system. *Agriculture, Ecosystem and Environment* 203: 1-10. DOI: 10.1016/j.agee.2015.01.018
- Gaj R & Gorski D (2014). Effects of different phosphorus and potassium fertilization on contents and uptake of macronutrients (N, P, K, Ca, Mg) in winter wheat I. Content of macronutrients. *Journal of Central European Agriculture* 15(4): 169-187. DOI: 10.5513/jcea.v15i4.2877
- González-Verdejo C I, Fernández-Aparicio M, Córdoba E M & Nadal S (2020). Identification of *Vicia ervilia* germplasm resistant to *orobanche crenata*. *Plants* 9(11): 1568. DOI: 10.3390/plants9111568
- Hamdani J S & Suradinata Y R (2015). Effects of row intercropping system of corn and potato and row spacing of corn on the growth and yields of Atlantic potato cultivar planted in medium altitude. *Asian Journal of Agricultural Research* 9(3): 104-112. DOI: 10.3923/ajar.2015.104.112
- Jalilian J, Najafabadi A & Zardashti M R (2017). Intercropping patterns and different farming systems affect the yield and yield components of safflower and bitter vetch. *Journal of Plant Interactions* 12: 92-99. DOI: 10.1080/17429145.2017.1294712
- Khan S, Khan M A, Akmal M, Ahmad M, Zafar M & Jabeen A (2014). Efficiency of wheat brassica mixtures with different seed rates in rainfed areas of Potohar-Pakistan. *Pakistan Journal of Botany* 46(2): 759-766
- Khippal A, Singh S, Chand M, Sheokand R, Singh J, Verma R & Kumar R (2016). Mechanized and profitable intercropping of legumes in autumn planted sugarcane. *Legume Research* 39(3): 411-418. DOI: 10.18805/lr.v0i0F.10283
- Kohnaward P, Jalilian J & Pirzad A (2012). Effect of foliar application of micro-nutrients on yield and yield components of safflower under conventional and ecological cropping systems. *International Research Journal of Applied and Basic Sciences* 3(7): 1460-1469
- Li Y T, Li Y, Li Y N, Liang Y, Sun Q, Li G, Liu P, Zhang Z S & Gao H Y (2020). Dynamic light caused less photosynthetic suppression, rather than more, under nitrogen deficient conditions than under sufficient nitrogen supply conditions in soybean. *BMC plant biology* 20(1):1-13. DOI: 10.1186/s12870-020-02516-y
- Lichtfouse E, Navarrete M, Debaeke P, Souchère V, Alberola C & Ménassieu J (2009). Agronomy for sustainable agriculture: a review. *Agronomy for Sustainable Development* 29:1-6. DOI: 10.1051/agro:2008054

- Metcalfe L D, Schmitz A A & Pelka J R (1966). Rapid preparation of fatty acid esters from lipid for gas chromatography analysis. *Analytical Chemistry* 38: 514-515. DOI: 10.1021/ac60235a044
- Metwally A A, Safina S A & Noaman A H (2015). Yield and land equivalent ratio of intercropping maize with Egyptian cotton. *Journal of Agri-Food and Applied Sciences* 3(4): 85-93
- Nasim W, Ahmad A, Hammad H M, Chaudhary H J & Munis M F H (2012). Effect of nitrogen on growth and yield of sunflower under semi-arid conditions of Pakistan. *Pakistan Journal of Botany* 44(2): 639-648
- Nyoki D & Ndakidemi P A (2017). Assessing the land equivalent ratio (LER) of maize (*Zea mays* L.) intercropped with Rhizobium inoculated soybean (*Glycine max* [L.] Merr.) at various P and K levels. *International Journal of Biosciences* 10(3): 275-282. DOI: 10.12692/ijb/10.3.275-282
- Onemli F (2014). Fatty acid content of seed at different development stages in canola on different soil types with low organic matter. *Plant Production Science* 17(3): 253-259. DOI: 10.1626/pp.s.17.253
- Ozturk A, Caglar O & Sahin F (2003). Yield response of wheat and barley to inoculation of plant growth promoting rhizobacteria at various levels of nitrogen fertilization. *Journal of Plant Nutrition and Soil Science* 166: 262-266. DOI: 10.1002/jpln.200390038
- Rathke G W, Christen O & Diepenbrock W (2005). Effects of nitrogen source and rate on productivity and quality of winter oilseed rape (*Brassica napus* L.) grown in different crop rotations. *Field Crops Research* 94: 103-113. DOI: 10.1016/j.fcr.2004.11.010
- Ratna N D, Sarwono A E & Hariyono B (2015). *The Effect of organic and inorganic fertilizer on production, sesame seed oil content, and feasibility in sandy coastal land*. In: Hongladarom, S. (ed.) Food security and food safety for the twenty-first century. Springer, Singapore, pp. 119-129
- Raven J A (2013). RNA function and phosphorus use by photosynthetic organisms. *Frontiers in Plant Science* 4: 1-13. DOI: 10.3389/fpls.2013.00536
- Rouphael Y, Raimondi G, Paduano A, Sacchi R, Barbieri G & De Pascale S (2015). Influence of organic and conventional farming on seed yield, fatty acid composition and tocopherols of Perilla. *Australian Journal of Crop Science* 9(4): 303-308
- Saeidi M, Yaghoub R A E I, Amini R, Taghizadeh A, & Pasban-Eslam B (2018). Changes in fatty acid and protein of safflower as response to biofertilizers and cropping system. *Turkish Journal of Field Crops* 23(2): 117-126. DOI: 10.17557/tjfc.471666
- Sarkar D, Kar S K, Chattopadhyay A, Rakshit A, Tripathi V K, Dubey P K & Abhilash P C (2020). Low input sustainable agriculture: A viable climate-smart option for boosting food production in a warming world. *Ecological Indicators* 115: 106412. 10.1016/j.ecolind.2020.106412
- SAS Institute (2003). *The SAS system for windows*. Release 9.1. SAS Inst., Cary, NC.
- Vandermeer J H (1989). *The ecology of intercropping*. Cambridge University Press, Cambridge 237 p. DOI: 10.1017/CBO9780511623523.
- Zafarani M (2015). Effect of various combinations of safflower and chickpea intercropping on yield and yield components of safflower. *Agriculture Science Developments* 4: 31-34
- Zarabi M & Jalai M (2012). Rate of nitrate and ammonium release from organic residues. *Compost Science and Utilization* 20: 222-229. DOI: 10.65657X.2012.10737052



© 2022 by the author(s). Published by Ankara University, Faculty of Agriculture, Ankara, Turkey. This is an Open Access article distributed under the terms and conditions of the Creative Commons Attribution (CC BY) license (<http://creativecommons.org/licenses/by/4.0/>), which permits unrestricted use, distribution, and reproduction in any medium, provided the original work is properly cited.



An efficient Regeneration Protocol for *in vitro* Direct Organogenesis in Einkorn (*Triticum monococcum* L.) Wheat

Günce ŞAHİN^{a*} , Mehmet ÖRGEÇ^a , Nusret ZENCİRÇİ^a 

^aBolu Abant İzzet Baysal University, Faculty of Arts and Science, Department of Biology, Bolu, TURKEY

ARTICLE INFO

Research Article

Corresponding Author: Günce ŞAHİN, E-mail: guncesahin@gmail.com

Received: 5 March 2021 / Revised: 17 July 2021 / Accepted: 14 July 2021 / Online: 01 September 2022

Cite this article

ŞAHİN G, ÖRGEÇ M, ZENCİRÇİ N (2022). An efficient Regeneration Protocol for *in vitro* Direct Organogenesis in Einkorn (*Triticum monococcum* L.) Wheat. *Journal of Agricultural Sciences (Tarim Bilimleri Dergisi)*, 28(3):412-422. DOI: 10.15832/ankutbd.891812

ABSTRACT

Coleoptile, leaf, and root explants of the einkorn (*Triticum monococcum* ssp. *monococcum*) were cultured *in vitro* to obtain an efficient plant regeneration protocol through direct shoot formation by using different combinations and concentrations of various plant growth regulators. A total of 180 different auxin and cytokinin combinations were tested for regeneration. Shoot formation was not observed with the root and leaf explants. Shoot formation was obtained only from the coleoptile explants, with a mean of 1.20±0.24 shoots/explant and 86.60% of shoot formation frequency and with a 1.20±0.53 shoots/explant and 80.00% shoot formation frequency on medium supplemented with 0.5 mg L⁻¹ TDZ and 1 mg L⁻¹ TDZ plus 1 mg L⁻¹ NAA, respectively. The shoots were

subcultured on the MS medium containing the most effective hormonal combination concurrently continued to shoot and root formation for 45 days. It is noteworthy that 3.66±0.66 shoots per explant were induced by MS, which contained 1 mg L⁻¹ TDZ plus 1 mg L⁻¹ NAA and 2.0 mg L⁻¹ KIN plus 0.5 mg L⁻¹ NAA for 45 days. Of the different auxin concentrations tested for rooting, 2.0 mg L⁻¹ IAA was predominant, with the greatest number of roots (12.33±0.88) produced per regenerated shoot. Finally, these well-developed plantlets were acclimatized with a 100% success rate and were transferred to the *ex vitro* conditions. A highly efficient regeneration protocol for einkorn wheat was developed using somatic tissue as an explant source for the first time.

Keywords: Coleoptile, Direct regeneration protocol, Tissue culture, Einkorn wheat (*Triticum monococcum* ssp. *monococcum*)

1. Introduction

Micropropagation is used commercially worldwide, but the capacity of plant regeneration and somatic organogenesis varies greatly among species (Bidabadi & Jain 2020). Wheat includes more than 20 cultivated species (Goncharov 2011), however, *in vitro* plant regeneration ability of many wheat species has not been studied until recently. *Triticum monococcum* ssp. *monococcum* (einkorn) wheat, diploid ancestral wheat, intervened in the spread and rise of agriculture for several thousand years until more productive polyploid wheat was replaced with it (Nesbitt & Samuel 1996). But nowadays, the renewed interest in studies related to this cereal is on the rise because of its putative low allergenicity, disease resistance properties, and lower gluten but higher lutein and protein content (Hidalgo et al. 2006; Özgen et al. 2017). Moreover, it has been recently included in modern wheat breeding programs, as donors of stress resistance genes (Nevo 2011; Login & Reif 2014; Alikina et al. 2016).

Improving crops to create genetic variability and increase the number of desirable germplasms is dependent on the establishment of a highly regenerative tissue culture system for many plant species, particularly cereals. Many factors can affect this system, such as culture medium, growth conditions, genotypes, and explant types. Currently, in tissue culture studies on wheat and other cereal crops, immature-mature embryos and inflorescences have been traditionally used as the most suitable explant source and the regeneration capacity of plants has been reported with varying degrees of success (Benlioğlu & Birsin 2017).

In comparison to other wheat tissues, immature zygotic embryos are the most commonly and efficiently used explants for plant regeneration in hexaploid bread wheat, tetraploid durum wheat, and only a few numbers of studies that have been conducted on diploid wheats (Miroshnichenko et al. 2017). The standard technique entails the cultivation of immature tissues on 2,4-D-containing media in the dark, followed by plant differentiation in the light on media devoid of phytohormones (Fennell et al. 1996; Tama's et al. 2004; Chauhan et al. 2007; Miroshnichenko et al. 2016). However, this conventional protocol is often ineffective for many wheat genotypes due to the inability to regenerate entire plants on a regular basis. Moreover, the cultivation of donor plants to obtain embryos involves the expenditure of much time and money.

Although using somatic tissues as an explant source makes it possible to obtain a great amount of material regardless of these short-comings, ventures to determine a reliable plant regeneration protocol using somatic cell cultures for diploid wheat species did not produce positive results (Alikina et al. 2016). Similarly, no shoot differentiation was observed in somatic cell cultures of tetraploid and hexaploid wheat genotypes (Lazar et al. 1983; Bi & Wang 2008; Özgen et al. 2017). Therefore, even after many years of research, especially in the genotypes of wheat, screening of germplasms *in vitro* response is very important for biotechnological applications.

The objective of this study was to investigate a highly effective *in vitro* regeneration protocol for the einkorn wheat via adventitious shoot formation from the root, coleoptile, and leaf explants cultured on the MS medium containing different combinations and concentrations of plant growth regulators for the first time. Direct shoot formation from somatic tissue is a remarkable feature of this regeneration protocol.

2. Material and Methods

2.1. Plant materials and growth condition

Seeds of the einkorn (*Triticum monococcum* ssp. *monococcum*) wheat were collected from İhsangazi / Kastamonu, Turkey in 2014-2015. Seeds were disinfected with 100 ml distilled water containing 5 drops of Tween20 (Merck, Darmstadt, Germany) for 1 min, then sterilized with 40% commercial bleach (4.6% NaClO; Domestos, Istanbul, Turkey) for 15 min, and finally washed three times with sterile dH₂O (Örgeç et al. 2018). Seeds (20 seeds / 100 mm×15 mm Petri dish) were cultured on the MS (Duchefa-Haarlem, Netherlands) medium (pH: 5.8), (Murashige & Skoog 1962) containing 2.5% (w/v) sucrose (Merck Darmstadt, Germany) and 0.75% (w/v) agar (Duchefa-Haarlem, Netherlands). The seeds were grown for germination under a 16/8 h photoperiod at 24±2 °C (climate room conditions) for 10 days.

2.2. Shoot regeneration

Five to eight mm segments of the leaf, coleoptile, and root sliced from ten-days old germinated seedlings were cultured on the MS medium containing different concentrations (from 0.5 to 3 mg L⁻¹) of IAA (indole acetic acid) (Duchefa-Haarlem), NAA (α -naphthalene acetic acid) or 2,4-D (2,4-dichloro phenoxy acetic acid) (Sigma-Aldrich, Steinheim, Germany) and combined with TDZ (thidiazuron) (Duchefa-Haarlem), KIN (kinetin) or BAP (6-benzyl amino purine) ranging from 0.5 to 3 mg L⁻¹. The mean number of shoots/explant and the percentage (%) of developing shoots were enrolled 15 days after the culture grown under climate room conditions (16 h light:8 h dark photoperiod at 23±2 °C), respectively. After a period of 15 days, plantlets were transferred to MS which contained the best response hormone combination to obtain more shoots and observed for up to 45 days. The data were recorded continuously.

2.3. Rooting of the shoots, hardening, and acclimatization

Forty-five days old shoots were transferred to MS medium supplemented with IAA (ranging from 0.5 to 5 mg L⁻¹) to observe root formation for 30 days. After 30 days, the mean numbers of roots/explant were recorded. Then, well-developed plantlets were transferred to Magenta vessels (77 mm × 77 mm × 97 mm) containing a mixture of vermiculite and soil (1:2) for acclimatization. The plantlets were kept in the climate room for 1 week. After 1 week, the plantlets were transferred to room conditions.

2.4. Statistical analysis

The data were statistically analyzed using SPSS 16.0 (SPSS Inc., Chicago, IL, USA). Differences in means ± SD (standard deviation) were analyzed using Duncan's multiple range test at P<0.05.

3. Results and Discussion

This study provided an efficient protocol for the direct formation of shoots from different explants, the first as such report for einkorn wheat. The traditional method for wheat propagation is using an immature and mature embryo as an explant source. Several studies have been conducted to determine the indirect regeneration protocol from immature and mature embryo cultures in the einkorn wheat (Yang et al. 2015; Alikina et al. 2016; Miroshnichenko et al. 2016). However, there are no reports on einkorn cultures in which improvement in direct shoot production using somatic tissues has been achieved. For this reason, two sets of experiments were carried out. In the first set, the regeneration capacity of three different explant sources (leaf, coleoptile, and root) cultured on the MS medium containing various concentrations of BAP, KIN, or TDZ, in combination with NAA, 2,4-D, or IAA ranging from 0.5 to 3 mg L⁻¹ were obtained. In the second set, the most effective hormone combinations were selected to increase the number of shoots.

A total of 180 different hormone combinations were tested for regeneration and variable growth rates were recorded. Control treatments without PGRs produced no shoots. In all tested hormone combinations, shoot formation was not observed with leaf

and root explants. It was observed that coleoptile was the best as an explant source referring to both the percentages of explants forming shoots and the mean number of shoots/explant with TDZ (Table 1 and Figure 1). The TDZ/NAA combination was more effective than the TDZ/IAA or TDZ/2,4-D combination for shoot propagation in this study. When explants were cultured on MS containing KIN or BA in combination with NAA or 2,4-D, the frequency of formation and the number of shoots were found at approximately the same levels. Optimum shoot formation was detected from coleoptile explants, with a mean of 1.20 ± 0.24 shoots/explant and 86.60% shoot formation percentage and with a 1.20 ± 0.53 shoots/explant and 80% shoot formation percentage on medium supplemented with 0.5 mg L^{-1} TDZ and 1 mg L^{-1} TDZ+ 1 mg L^{-1} NAA, respectively (Table 1).

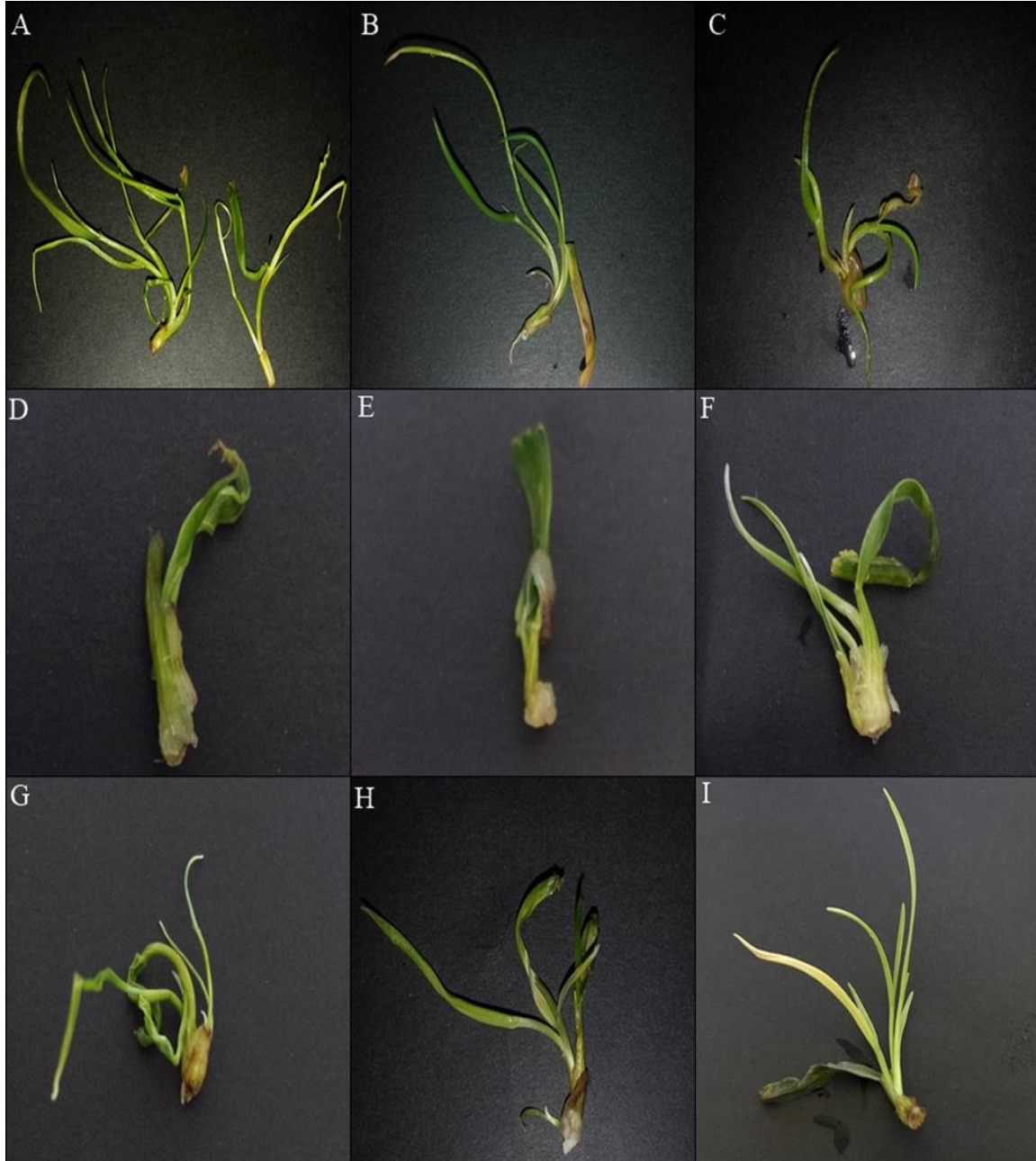


Figure 1- The effects of various concentrations of BA, KIN or TDZ, in combination with NAA, 2,4-D or IAA ranging from 0.5 to 3 mg L^{-1} on shoot formation (A) 0.5 mg L^{-1} TDZ. (B) 1 mg L^{-1} KIN. (C) 2 mg L^{-1} BA+ 0.5 mg L^{-1} IAA. (D) 2 mg L^{-1} TDZ+ 1 mg L^{-1} 2,4-D. (E) 0.5 mg L^{-1} KIN+ 1 mg L^{-1} 2,4-D (F) 3 mg L^{-1} BA+ 2 mg L^{-1} 2,4-D. (G) 1 mg/l TDZ+ 1 mg/l NAA (H) 2.0 mg/l KIN+ 0.5 mg/l NAA. (I) 0.5 mg/l BA+ 2.0 mg NAA

Table 1- Shoot regeneration from coleoptile explants cultured on MS medium containing different combinations of KIN, TDZ or BA with NAA, 2,4 D or IAA. Mean-values with the same letters within vertical columns are not significantly different (P>0.05). Control means are with no PGR treatment

<i>PGRs (mg L⁻¹)</i>	<i>Mean number of shoots/explant</i>	<i>Shoot formation percentage (%)</i>	<i>PGRs (mg L⁻¹)</i>	<i>Mean number of shoots/explant</i>	<i>Shoot formation percentage (%)</i>	<i>PGRs (mg L⁻¹)</i>	<i>Mean number of shoots/explant</i>	<i>Shoot formation percentage (%)</i>
<i>Control</i>	-	-	-	-	-	-	-	-
<i>TDZ – IAA</i>			<i>KIN – IAA</i>			<i>BA – IAA</i>		
0.5 – 0	1.20±0.24^a	86.60	0.5 – 0	0.89±0.38 ^{abcde}	86.60	0.5 – 0	0.64±0.24 ^{bcdefghi}	46.60
1.0 – 0	0.78±0.23 ^{abcdefg}	60.00	1.0 – 0	0.93±0.34 ^{abcd}	73.30	1.0 – 0	0.64±0.29 ^{bcdefghi}	40.00
2.0 – 0	0.93±0.38 ^{abcd}	66.60	2.0 – 0	0.87±0.30 ^{abcde}	73.30	2.0 – 0	0.78±0.21 ^{abcdefg}	53.30
3.0 – 0	0.82±0.27 ^{abcdef}	73.30	3.0 – 0	0.71±0.22 ^{bcdefgh}	66.60	3.0 – 0	0.62±0.25 ^{bcdefghi}	46.60
0.5 – 0.5	0.73±0.23 ^{abcdefg}	60.00	0.5 – 0.5	0.40±0.22 ^{efghi}	40.00	0.5 – 0.5	0.73±0.11 ^{abcdefg}	66.60
1.0 – 0.5	0.80±0.20 ^{abcdef}	66.60	1.0 – 0.5	0.87±0.30 ^{abcde}	60.00	1.0 – 0.5	0.67±0.50 ^{bcdefgh}	53.30
2.0 – 0.5	0.73±0.61 ^{abcdefg}	53.30	2.0 – 0.5	0.33±0.11 ^{fghi}	33.30	2.0 – 0.5	0.87±0.30 ^{abcde}	60.00
3.0 – 0.5	0.73±0.12 ^{bcdefg}	60.00	3.0 – 0.5	0.40±0.22 ^{efghi}	33.30	3.0 – 0.5	1.00±0.40 ^{abc}	60.00
0.5 – 1.0	0.60±0.20 ^{bcdefghi}	60.00	0.5 – 1.0	0.53±0.11 ^{cdefghi}	46.60	0.5 – 1.0	0.53±0.11 ^{cdefghi}	53.30
1.0 – 1.0	0.73±0.12 ^{abcdefg}	60.00	1.0 – 1.0	0.47±0.46 ^{defghi}	20.00	1.0 – 1.0	0.47±0.11 ^{defghi}	46.60
2.0 – 1.0	0.60±0.20 ^{bcdefghi}	60.00	2.0 – 1.0	0.73±0.11 ^{abcdefg}	33.30	2.0 – 1.0	0.33±0.11 ^{fghi}	33.30
3.0 – 1.0	0.60±0.20 ^{bcdefghi}	60.00	3.0 – 1.0	0.20±0.11 ^{hi}	20.00	3.0 – 1.0	0.47±0.30 ^{defghi}	40.00
0.5 – 2.0	0.73±0.12 ^{abcdefg}	60.00	0.5 – 2.0	0.33±0.23 ^{fghi}	26.60	0.5 – 2.0	0.67±0.23 ^{bcdefgh}	60.00
1.0 – 2.0	0.87±0.50 ^{abcde}	53.30	1.0 – 2.0	0.33±0.30 ^{fghi}	33.30	1.0 – 2.0	0.20±0.11 ^{hi}	20.00
2.0 – 2.0	0.73±0.23 ^{abcdefg}	73.30	2.0 – 2.0	0.40±0.20 ^{efghi}	26.60	2.0 – 2.0	0.53±0.11 ^{cdefghi}	46.60
3.0 – 2.0	0.67±0.12 ^{bcdefgh}	73.30	3.0 – 2.0	0.27±0.23 ^{ghi}	26.60	3.0 – 2.0	0.73±0.22 ^{abcdefg}	53.30
0.5 – 3.0	0.67±0.46 ^{bcdefgh}	53.30	0.5 – 3.0	0.40±0.20 ^{efghi}	40.00	0.5 – 3.0	0.53±0.11 ^{cdefghi}	53.30
1.0 – 3.0	0.80±0.34 ^{abcdef}	66.60	1.0 – 3.0	0.47±0.23 ^{defghi}	40.00	1.0 – 3.0	0.20±0.11 ^{hi}	20.00
2.0 – 3.0	0.73±0.41 ^{abcdefg}	53.30	2.0 – 3.0	0.53±0.11 ^{cdefghi}	40.00	2.0 – 3.0	0.40±0.20 ^{efghi}	46.60
3.0 – 3.0	0.80±0.20 ^{abcdef}	53.30	3.0 – 3.0	0.73±0.30 ^{abcdefg}	46.60	3.0 – 3.0	0.40±0.20 ^{efghi}	40.00

Table 1 (Continue)- Shoot regeneration from coleoptile explants cultured on MS medium containing different combinations of KIN, TDZ or BA with NAA, 2,4 D or IAA. Mean-values with the same letters within vertical columns are not significantly different (P>0.05). Control means are with no PGR treatment

<i>PGRs (mg L⁻¹)</i>	<i>Mean number of shoots/explant</i>	<i>Shoot formation percentage (%)</i>	<i>PGRs (mg L⁻¹)</i>	<i>Mean number of shoots/explant</i>	<i>Shoot formation f percentage (%)</i>	<i>PGRs (mg L⁻¹)</i>	<i>Mean number of shoots/explant</i>	<i>Shoot formation percentage (%)</i>
<i>Control</i>	-	-	-	-	-	-	-	-
TDZ – 2,4-D			KIN – 2,4-D			BA – 2,4-D		
0.5 – 0.5	0.80±0.20 ^{abcdef}	73.30	0.5 – 0.5	0.67±0.31 ^{bcdefgh}	53.30	0.5 – 0.5	0.33±0.12 ^{fghi}	33.30
1.0 – 0.5	0.53±0.23 ^{cdefghi}	46.60	1.0 – 0.5	0.60±0.20 ^{bcdefghi}	60.00	1.0 – 0.5	0.67±0.61 ^{bcdefgh}	53.30
2.0 – 0.5	0.67±0.31 ^{bcdefgh}	60.00	2.0 – 0.5	0.60±0.20 ^{bcdefghi}	60.00	2.0 – 0.5	0.47±0.42 ^{defghi}	46.60
3.0 – 0.5	0.60±0.20 ^{bcdefghi}	60.00	3.0 – 0.5	0.53±0.31 ^{cdefghi}	53.30	3.0 – 0.5	0.40±0.20 ^{efghi}	40.00
0.5 – 1.0	0.67±0.42 ^{bcdefgh}	60.00	0.5 – 1.0	0.73±0.12 ^{abcdefg}	73.30	0.5 – 1.0	0.40±0.20 ^{efghi}	40.00
1.0 – 1.0	0.87±0.12 ^{abcde}	86.60	1.0 – 1.0	0.67±0.12 ^{bcdefgh}	66.60	1.0 – 1.0	0.67±0.31 ^{bcdefgh}	60.00
2.0 – 1.0	0.93±0.12 ^{abcd}	86.60	2.0 – 1.0	0.53±0.12 ^{cdefghi}	53.30	2.0 – 1.0	0.47±0.12 ^{defghi}	40.00
3.0 – 1.0	0.73±0.23 ^{bcdefg}	66.60	3.0 – 1.0	0.60±0.40 ^{bcdefghi}	53.30	3.0 – 1.0	0.33±0.23 ^{fghi}	33.30
0.5 – 2.0	0.73±0.12 ^{bcdefg}	66.60	0.5 – 2.0	0.40±0.40 ^{efghi}	40.00	0.5 – 2.0	0.20±0.00 ^{hi}	20.00
1.0 – 2.0	0.67±0.23 ^{bcdefgh}	66.60	1.0 – 2.0	0.33±0.31 ^{fghi}	33.30	1.0 – 2.0	0.60±0.20 ^{bcdefghi}	60.00
2.0 – 2.0	0.67±0.31 ^{bcdefgh}	66.60	2.0 – 2.0	0.60±0.00 ^{bcdefghi}	60.00	2.0 – 2.0	0.53±0.12 ^{cdefghi}	53.30
3.0 – 2.0	0.53±0.12 ^{cdefghi}	53.30	3.0 – 2.0	0.47±0.31 ^{defghi}	46.60	3.0 – 2.0	0.93±0.12 ^{abcd}	80.00
0.5 – 3.0	0.67±0.23 ^{bcdefgh}	66.60	0.5 – 3.0	0.60±0.20 ^{bcdefghi}	60.00	0.5 – 3.0	0.60±0.00 ^{bcdefghi}	60.00
1.0 – 3.0	0.73±0.12 ^{bcdefg}	73.30	1.0 – 3.0	0.33±0.12 ^{fghi}	33.30	1.0 – 3.0	0.27±0.31 ^{ghi}	20.00
2.0 – 3.0	0.47±0.12 ^{defghi}	46.60	2.0 – 3.0	0.40±0.00 ^{efghi}	40.00	2.0 – 3.0	0.67±0.12 ^{bcdefgh}	53.30
3.0 – 3.0	0.13±0.12 ⁱ	20.00	3.0 – 3.0	0.47±0.12 ^{defghi}	46.60	3.0 – 3.0	0.60±0.00 ^{bcdefghi}	60.00
TDZ – NAA			KIN – NAA			BA – NAA		
0.5 – 0.5	0.33±0.12 ^{fghi}	33.30	0.5 – 0.5	0.67±0.12 ^{bcdefgh}	66.60	0.5 – 0.5	0.67±0.12 ^{bcdefgh}	66.60
1.0 – 0.5	1.00±0.20 ^{abc}	66.60	1.0 – 0.5	0.73±0.31 ^{abcdefg}	73.30	1.0 – 0.5	0.87±0.23 ^{abcde}	73.30
2.0 – 0.5	0.73±0.12 ^{bcdefg}	66.60	2.0 – 0.5	0.93±0.12 ^{abcd}	93.30	2.0 – 0.5	0.67±0.12 ^{bcdefgh}	66.60
3.0 – 0.5	0.47±0.12 ^{defghi}	46.60	3.0 – 0.5	0.27±0.46 ^{ghi}	26.60	3.0 – 0.5	0.80±0.20 ^{abcdef}	66.60
0.5 – 1.0	1.07±0.12 ^{ab}	86.60	0.5 – 1.0	0.47±0.12 ^{defghi}	46.60	0.5 – 1.0	0.67±0.23 ^{bcdefgh}	66.60
1.0 – 1.0	1.20±0.53^a	80.00	1.0 – 1.0	0.47±0.12 ^{defghi}	46.60	1.0 – 1.0	0.60±0.20 ^{cdefghi}	60.00
2.0 – 1.0	0.67±0.12 ^{bcdefgh}	66.60	2.0 – 1.0	0.53±0.31 ^{cdefghi}	60.00	2.0 – 1.0	0.87±0.12 ^{abcde}	73.30
3.0 – 1.0	0.67±0.12 ^{bcdefgh}	66.60	3.0 – 1.0	0.80±0.20 ^{abcdef}	60.00	3.0 – 1.0	0.33±0.31 ^{fghi}	33.30
0.5 – 2.0	0.67±0.12 ^{bcdefgh}	80.00	0.5 – 2.0	0.33±0.12 ^{fghi}	26.60	0.5 – 2.0	1.00±0.53 ^{abc}	66.60
1.0 – 2.0	0.80±0.40 ^{abcdef}	60.00	1.0 – 2.0	0.67±0.31 ^{bcdefgh}	60.00	1.0 – 2.0	0.53±0.12 ^{cdefghi}	53.30
2.0 – 2.0	0.67±0.12 ^{bcdefgh}	60.00	2.0 – 2.0	0.53±0.12 ^{cdefghi}	53.30	2.0 – 2.0	0.60±0.20 ^{cdefghi}	60.00
3.0 – 2.0	0.87±0.12 ^{abcde}	80.00	3.0 – 2.0	0.27±0.23 ^{ghi}	26.60	3.0 – 2.0	0.93±0.12 ^{abcd}	73.30
0.5 – 3.0	0.73±0.12 ^{bcdefg}	73.30	0.5 – 3.0	0.60±0.20 ^{bcdefghi}	53.30	0.5 – 3.0	0.53±0.31 ^{cdefghi}	53.30
1.0 – 3.0	0.67±0.12 ^{bcdefgh}	66.60	1.0 – 3.0	0.53±0.12 ^{cdefghi}	53.30	1.0 – 3.0	0.67±0.12 ^{bcdefgh}	66.60
2.0 – 3.0	0.73±0.12 ^{bcdefg}	73.30	2.0 – 3.0	0.47±0.31 ^{defghi}	46.60	2.0 – 3.0	0.53±0.12 ^{cdefghi}	66.60
3.0 – 3.0	0.67±0.12 ^{bcdefgh}	66.60	3.0 – 3.0	0.27±0.12 ^{ghi}	26.60	3.0 – 3.0	0.80±0.00 ^{abcdef}	80.00

Recent research found that immature and mature zygotic embryos of einkorn could induce embryogenic callus to a satisfactory level, however, the number of regenerated shoots was less than 0.5 per explant (Özgen et al. 2017) or there was no information regarding the number of regenerated shoots (Yang et al. 2015). Öргеç et al. (2021) found that coleoptile explants

showed the greatest performance for callus induction and indirect plant regeneration compared with root and leaf explants. Furthermore, it was also reported that callus cultures derived from coleoptile explants were capable of plant regeneration whereas callus cultures derived from leaf and root explants were not. A similar result by Sarker & Biswas (2002), stating that root explants of *Triticum aestivum* L. wheat cultivars developed callus that could not regenerate plants, whereas the leaf explants did not produce callus. Benkirane et al. (2000) also showed that the coleoptile explants of *Triticum turgidum* ssp. *durum*. had a higher callus percentage and plant regeneration potential. All these investigations show that the type of explant has a major impact on the regeneration capability. Our findings corroborate previous findings that coleoptile explants were suitable for shoot regeneration and outperformed all other explant types evaluated.

The supporting effect of TDZ on the plant regeneration process has been recently reported for many species (Phippen & Simon 2000; Yucesan et al. 2007; Wang & Bao 2007; Ekmekci & Aasim 2014). Improved regeneration protocols using varied concentrations of thidiazuron (TDZ) applied alone or in conjunction with other plant growth regulators were also developed for a variety of polyploid wheat cultivars (Shan et al. 2000; Ganeshan et al. 2006; She et al. 2013). Miroshnichenko et al. (2016) reported that TDZ enhanced the regeneration capacity of embryonic callus in cultures of *T. kiharae*. Benlioğlu & Birsin (2017) reported that TDZ had a positive effect on plant regeneration from immature embryo-derived *T. aestivum* L. callus. Different concentrations of TDZ promoted plant regeneration from einkorn callus derived from immature embryo explants (Miroshnichenko et al. 2017). Callus derived from coleoptile explants of *T. monococcum* L. was stimulated by TDZ to regenerate plants (Örgeç et al. 2021). Similarly, in our study, TDZ was a more influential hormone than BA or KIN on the shoot regeneration process (Table 1).

In the second stage of our study, shoots were subcultured on media containing all effective hormonal combinations for 45 days (Table 2). It was noteworthy that 3.66 shoots per explant were induced by the MS medium containing 1 mg L⁻¹ TDZ plus 1 mg L⁻¹ NAA and 2 mg L⁻¹ KIN plus 0.5 mg L⁻¹ NAA for 45 days (Figure 2). Induction media comprising 2 mg L⁻¹ 2,4-D plus 3 mg L⁻¹ BA was found inappropriate for continuous shoot formation. However, the callus formation was observed. This observation is in line with several studies (Dale & Deambrogio 1979; Benkirane et al. 2000; Sarker & Biswas 2002; Alikina et al. 2016). It was found that an increased concentration of 2,4-D induced callusing in *Triticum aestivum* L. (Mahmood et al. 2012) and *T. monococcum* L. (Örgeç et al. 2021). 2,4-D is an auxin-like plant growth regulator that is commonly used in cereals for callus production however it displays low effect for improving somatic embryogenesis and plant regeneration (Miroshnichenko et al. 2017). Similarly, in our study, interaction with 2,4-D increased the callusing potential while decreasing shoot formation capacity. The variability in callus formation frequency in return for various levels of 2,4-D may be due to differences in genes controlling callusing or genes may not express themselves fully in some cultivars contrary to others supplemented with an optimum concentration of 2,4-D. Our findings are in concurrence with other researchers who also suggested genotypic differences of wheat for callus formation and regeneration abilities (Kilinc 2004; Nasircilar et al. 2006; Hassan et al. 2009; Örgeç et al. 2021). Although various researchers had standardized the concentration of 2,4-D at the optimum level for diverse genotypes of wheat (Satyavathi et al. 2004; Sarker & Biswas 2002) the induction media should be standardized for maximum callusing in einkorn wheat.

Table 2- Shoot regeneration obtained from *in vitro*-grown regenerants subcultured on MS medium containing the most effective hormone combination. Mean values (± SD) with the different letters in the same columns are significantly different (P < 0.05)

<i>Combinations of PGRs</i>	<i>Mean number of shoots/explant</i>	<i>Shoot formation percentage (%)</i>
Control	0.66 ^{ab} ± 0.20	26.66
0.5 mg L ⁻¹ TDZ	2.33 ^a ± 0.88	73.33
1 mg L ⁻¹ TDZ+1 mg L ⁻¹ NAA	3.66 ^a ± 0.66	73.33
2 mg L ⁻¹ TDZ	3.00 ^a ± 0.33	46.66
0.5 mg L ⁻¹ BA+2 mg L ⁻¹ NAA	2.66 ^a ± 0.57	60.00
3 mg L ⁻¹ BA+0.5 mg L ⁻¹ IAA	3.33 ^a ± 0.88	66.60
3 mg L ⁻¹ BA+2 mg L ⁻¹ 2,4-D	0.46 ^{ab} ± 0.33	60.00
0.5 mg L ⁻¹ KIN+1 mg L ⁻¹ 2,4-D	3.00 ^a ± 0.57	33.33
1 mg L ⁻¹ KIN	3.00 ^a ± 1.00	60.00
2 mg L ⁻¹ KIN+0.5 mg L ⁻¹ NAA	3.66 ^a ± 0.33	60.00

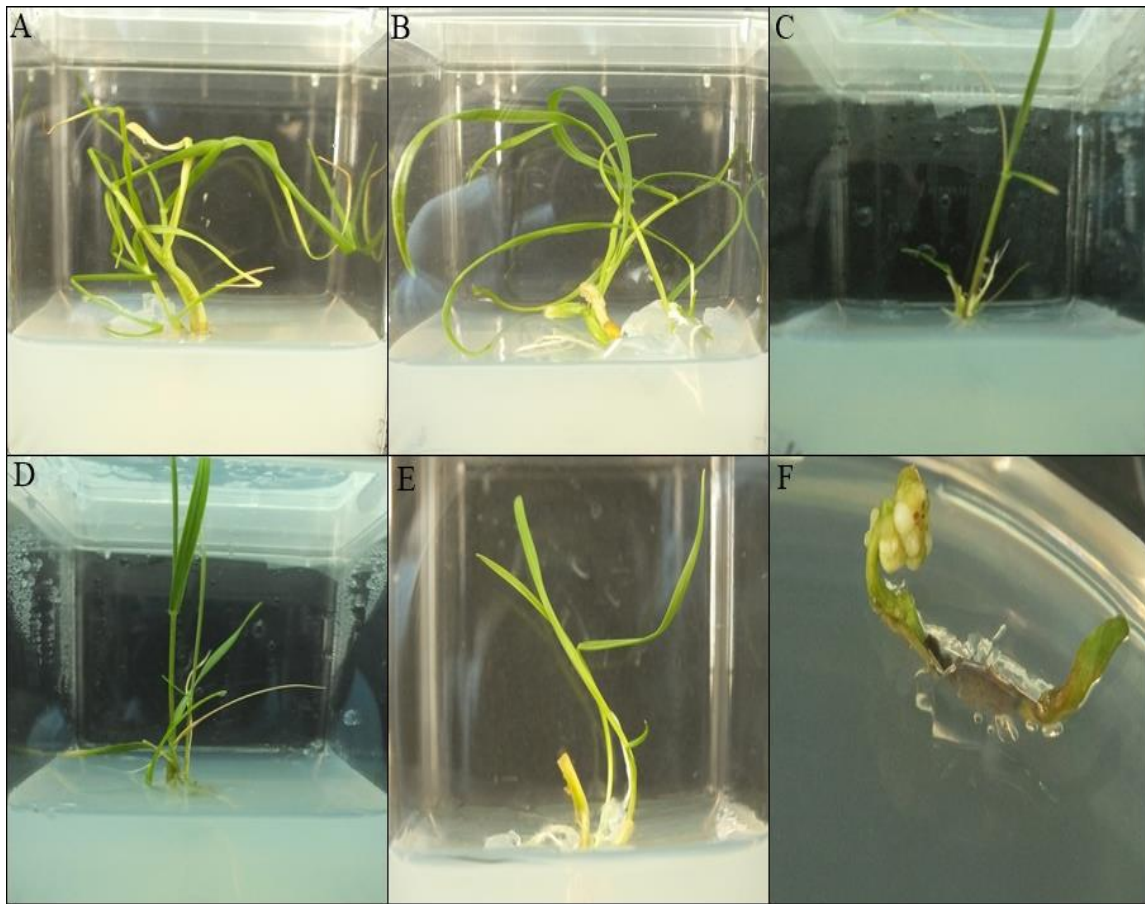


Figure 2- The shoots were subcultured on the MS medium containing the most effective hormone combinations. (A) 2.0 mg L⁻¹ KIN + 0.5 mg L⁻¹ NAA (B) 1.0 mg L⁻¹ TDZ + 1.0 mg L⁻¹ NAA. (C) 0.5 mg L⁻¹ TDZ. (D) 0.5 mg L⁻¹ TDZ + 2.0 mg L⁻¹ NAA. (E) 1.0 mg L⁻¹ KIN. (F) 3.0 mg L⁻¹ BA + 2.0 mg L⁻¹ 2,4-D

Early in the 1930s, indole-3-acetic acid (IAA) was identified to be the most effective auxin in promoting the development of adventitious root (Thimann & Koepfli 1935), and since then IAA has been widely used to induce adventitious root formation in the clonal propagation of various species (Shu et al. 2019). Although only a few studies have focused on the root formation for *in vitro* study of wheat, IAA has been one of the most widely used auxin-hormone to induce root induction (Kopertekh & Stribnaya 2003; Öргеç et al. 2021).

In our study, to induce root formation, regenerated shoots (45 days of culture) were cultured on MS medium with different concentrations of IAA ranging from 0.5 to 5 mg L⁻¹ (Table 2). They formed roots in one week. Among the different IAA concentrations tested, 2 mg L⁻¹ IAA was the most effective hormone concentration for rooting (Figure 3). 12.33±0.88 roots produced per regenerated shoot. When IAA concentration was increased from 0.5 to 2 mg L⁻¹, more root formation was observed. However, when IAA concentration was increased from 2 to 5 mg L⁻¹, the mean number of roots began to decline (Table 3). To get the acquisition of the meristematic competence of the cells, auxin is accepted as the most effective hormone in tissue culture experiments. However, it was known that after this competence was established, excessive auxin concentration inhibited further adventitious or embryonic root development (Gurel & Wren 1995; Charriere et al. 1999).

Table 3- Effects of the tested auxins on rooting. Mean values (± SD) with the different letters in the same columns are significantly different (P < 0.05)

<i>Auxin concentration</i>	<i>Mean number of roots/shoot</i>	<i>Root formation percentage (%)</i>
0.5 mg L ⁻¹ IAA	9.00 ^b ± 1.00	100
1 mg L ⁻¹ IAA	11.67 ^a ± 0.66	100
2 mg L ⁻¹ IAA	12.33 ^a ± 0.88	100
3 mg L ⁻¹ IAA	7.33 ^{bc} ± 0.33	100
5 mg L ⁻¹ IAA	5.33 ^c ± 0.88	100

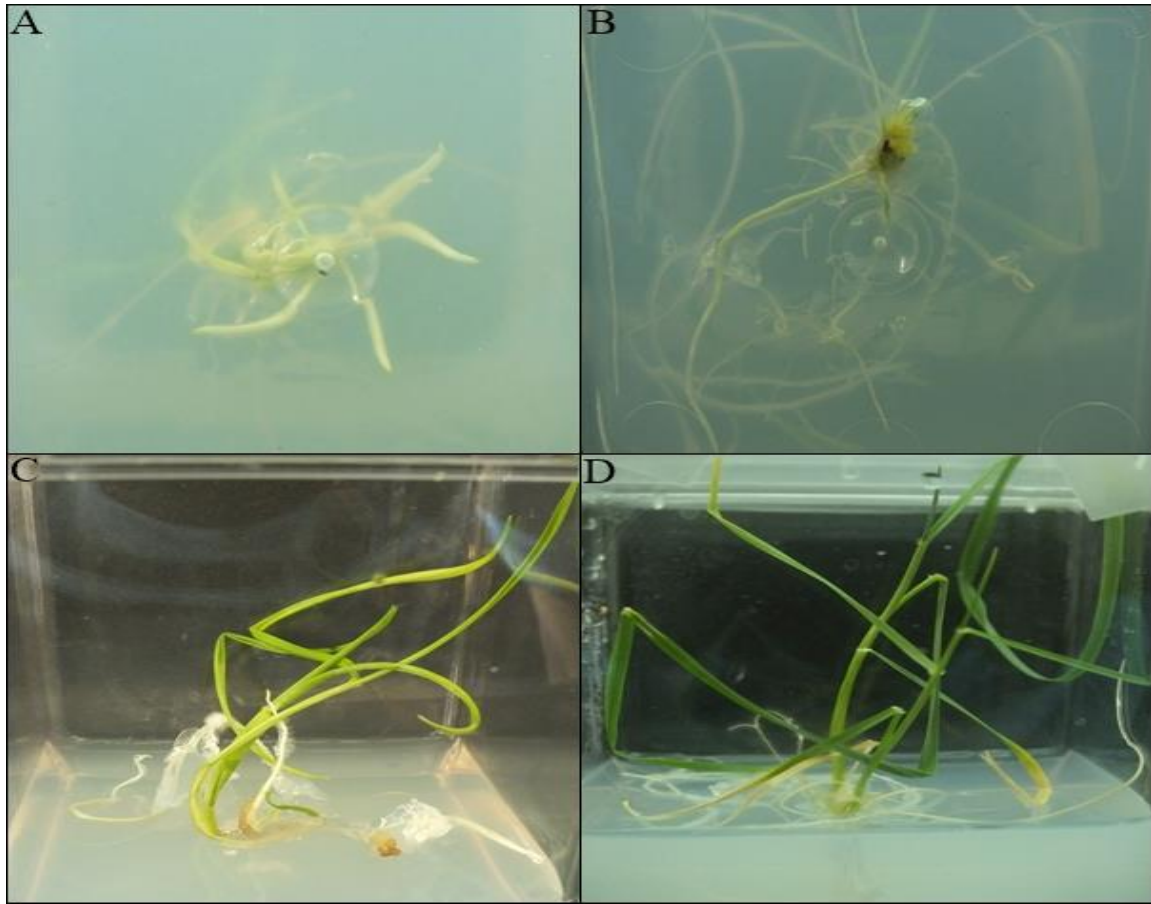


Figure 3- Effect of 2 mg L⁻¹ IAA on root formation from regenerated shoots

Finally, these well-developed plantlets were transferred to plastic pots containing a mixture of vermiculite and soil (1:2). For acclimatization, they were kept in the climate room for one week. After one week, the plantlets were transferred to pots containing commercial soil, kept under room conditions (Figure 4. a–f). Eventually, all the plantlets were established in the field, with 100% survival.

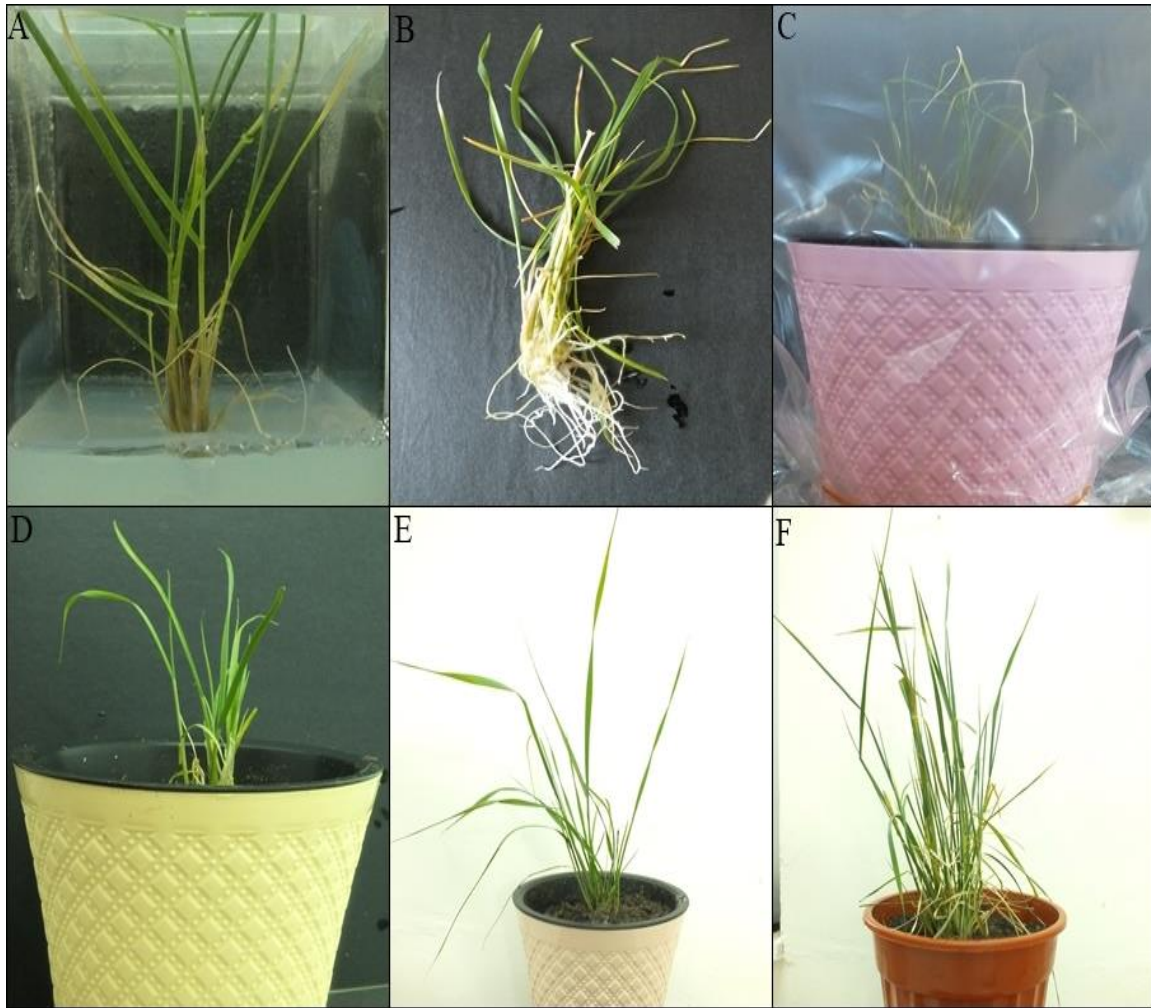


Figure 4- Direct shoot and plant regeneration from coleoptile explants of *Triticum monococcum* L. (A) Rooting of the regenerated shoots on medium containing 2.0 mg l^{-1} IAA after three weeks in culture. (B-C) Regenerated plants transferred to pots containing a mixture of vermiculite and soil (1:2) under climate room conditions. (D-F) Regenerated plants transferred to pots containing sterile soil under room conditions.

4. Conclusions

This article describes an efficient protocol for direct plant regeneration using somatic tissues in einkorn by testing different concentrations of TDZ, KIN, and BAP in combination with NAA, IAA, and 2.4-D. The present investigation elucidates that the coleoptile part of wheat can serve as a potential source for direct shoot regeneration under suitable conditions. This method is an efficient one for the *ex vitro* conservation of kinds of ancient wheat genetic resources and clonal propagation.

Acknowledgments

This study was supported by the Bolu Abant İzzet Baysal University Research Foundation (Project No: BAP – 2017.03.01.1130). The authors thank to the Bolu Municipality (2018/2019) for a research grant.

References

- Alikina O, Chernobrovkina M, Dolgov S & Miroshnichenko D (2016). Tissue culture efficiency of wheat species with different genomic formulas. *Crop Breeding and Applied Biotechnology* 16: 307-314. <https://doi.org/10.1590/1984-70332016v16n4a46>
- Benkirane H, Sabounji K, Chlyah A & Chlyah H (2000). Somatic embryogenesis and plant regeneration from fragments of immature inflorescences and coleoptiles of durum wheat. *Plant Cell Tissue Organ Culture* 61: 107-113. <https://doi.org/10.1023/a:1006464208686>
- Benlioğlu B & Birsin M A (2017). A thidiazuron (TDZ) – based efficient plant regeneration system from callus cultures, obtained through various embryo sources, in common winter wheat (*Triticum aestivum* L.). *Ciência e Técnica Vitivinícola* 32: 108-119
- Bi R & Wang H (2008). Primary studies on tissue culture of mature embryo from diploid and tetraploid wheat. *Frontiers of Agriculture in China* 2: 262-265. <https://doi.org/10.1007/s11703-008-0038-y>
- Bidabadi S S & Jain S M (2020). Cellular, molecular, and physiological aspects of *in vitro* plant regeneration. *Plants* 9:702-722. <https://doi.org/10.3390/plants9060702>

- Charriere F, Sotta B, Emile M & Günther H (1999). Induction of adventitious shoots or somatic embryos on *in vitro* cultured zygotic embryos of *Helianthus annuus*: variation of endogenous hormone levels. *Plant Physiology Biochemistry* 37: 751–757. [https://doi.org/10.1016/s0981-9428\(00\)86688-7](https://doi.org/10.1016/s0981-9428(00)86688-7)
- Chauhan H, Desai S A & Khurana P (2007). Comparative analysis of the differential regeneration response of various genotypes of *Triticum aestivum*, *Triticum durum* and *Triticum dicoccum*. *Plant Cell Tissue and Organ Culture* 91: 191-199. <https://doi.org/10.1007/s11240-007-9285-5>
- Dale P J & Deambrogio E (1979). A Comparison of callus induction and plant regeneration from different explants of *Hordeum vulgare*. *Zeitschrift für Pflanzenphysiologie* 94: 65-77. [https://doi.org/10.1016/s0044-328x\(79\)80249-4](https://doi.org/10.1016/s0044-328x(79)80249-4)
- Ekmekci H & Aasim M (2014). *In vitro* plant regeneration of Turkish sweet basil (*Ocimum basilicum*). *The Journal of Animal & Plant Sciences* 24(6): 1758-1765
- Fennell S, Bohorova N, Ginkel M V, Crossa J & Hoisington D (1996). Plant regeneration from immature embryos of 48 elite CIMMYT bread wheats. *Theoretical and Applied Genetics* 92: 163-169. <https://doi.org/10.1007/bf00223371>
- Goncharov N P (2011). Genus *Triticum* L. taxonomy: the present and the future. *Plant Systematics and Evolution* 295: 1-11
- Gurel E & Wren M J (1995). *In vitro* development from leaf explants of sugar beet (*Beta vulgaris* L.) Rhizogenesis and the effect of sequential exposure to auxin and cytokinin. *Annual Botany* 75:31–38. [https://doi.org/10.1016/s0305-7364\(05\)80006-x](https://doi.org/10.1016/s0305-7364(05)80006-x)
- Hassan M U, Ahmed Z, Munir M, Malik S I & Shahzad K (2009). Effect of sorbitol in callus induction and plant regeneration in wheat. *African Journal of Biotechnology* 8(23): 6529-6535
- Hidalgo A, Andrea B A, Pompeia C & Piscozzia R (2006). Carotenoids and tocopherols of einkorn wheat (*Triticum monococcum* ssp. *monococcum* L.). *Journal of Cereal Science* 44: 182–193. <https://doi.org/10.1016/j.jcs.2006.06.002>
- Kilinc M (2004). Effects of dicamba concentration on the embryo cultures of some bread wheat (*Triticum aestivum* L.) genotypes. *Biotechnology & Biotechnology Equipment* 58-61. <https://doi.org/10.1080/13102818.2004.10817087>
- Kopertekh L G & Stribnaya A (2003). Regeneration from wheat leaf explants. *Russian Journal of Plant Physiology* 50(3): 365-369
- Lazar M D, Collins G B & Vian W E (1983). Genetic and environmental effects on the growth and differentiation of wheat somatic cell cultures. *Journal of Heredity* 74: 353-357. <https://doi.org/10.1093/oxfordjournals.jhered.a109809>
- Mahmood I A, Razaq Z, Khan I, Hafiz A & Kaleem S (2012). Evaluation of tissue culture responses of promising wheat (*Triticum aestivum* L.) cultivars and development of an efficient regeneration system. *Pakistan Journal of Botany* 44: 277-284
- Miroshnichenko D, Chernobrovkina M & Dolgov S (2016). Somatic embryogenesis and plant regeneration from immature embryos of *Triticum timopheevii* and *Triticum kiharae* Dorof. et Migusch, wheat species with G genome. *Plant Cell Tissue and Organ Culture* 125: 495-508. <https://doi.org/10.1007/s11240-016-0965-x>
- Miroshnichenko D, Chaban I, Chernobrovkina M & Dolgov S (2017). Protocol for efficient regulation of *in vitro* morphogenesis in einkorn (*Triticum monococcum* L.), a recalcitrant diploid wheat species. *Plos One* 12(3): e0173533 <https://doi.org/10.1371/journal.pone.0173533>
- Murashige T & Skoog F (1962). A revised medium for rapid growth and bioassays with tobacco tissue cultures. *Physiology and Plantarum* 15: 473-497. <https://doi.org/10.1111/j.1399-3054.1962.tb08052.x>
- Nasircilar A G, Turgu K & Fiskin K (2006). Callus induction and plant regeneration from mature embryos of different wheat genotypes. *Pakistan Journal of Botany* 2006; 38(2): 637-645
- Nesbitt M & Samuel D (1996). From staple crop to extinction? The archaeology and history of the hulled wheat. In: Padulosi S, Hammer K, Heller J (eds) *Hulled wheats, promoting the conservation and use of underutilized and neglected crops*. IPGRI, Rome 1996; p. 40-99
- Nevo E (2011). *Triticum*. In Kole C (ed) *Wild crop relatives: genomic and breeding resources, cereals*. Springer Verlag, Berlin, 2011; p. 407-456. https://doi.org/10.1007/978-3-642-14228-4_10
- Örgeç M, Karakaş F P, Şahin G, Ağıl F & Zencirci N (2018). Einkorn (*Triticum monococcum* spp. *monococcum*) *In Vitro* propagation sterilization protocol. *International Journal of Secondary Metabolite* 5(2): 67-74. <https://doi.org/10.21448/ijsm.399094>
- Örgeç M, Verma S K, Şahin G, Zencirci N & Gürel E (2021) *In vitro* tissue culture protocol of ancient einkorn (*Triticum monococcum* ssp. *monococum*) wheat via indirect shoot regeneration. *In Vitro Cellular & Developmental Biology – Plant* 57: 143-151. <https://doi.org/10.1007/s11627-020-10122-8>
- Özgen M, Birsin M A & Benlioglu B (2017). Biotechnological characterization of a diverse set of wheat progenitors (*Aegilops* sp. and *Triticum* sp.) using callus culture parameters. *Plant Genetic Resources* 15(01):45-50. <https://doi.org/10.1017/s1479262115000350>
- Phippen W B & Simon J E (2000). Shoot regeneration of young leaf explants from basil (*Ocimum basilicum* L.). *In Vitro Cellular & Developmental Biology - Plant* 36: 250–254. <https://doi.org/10.1007/s11627-000-0046-y>
- Sarker R H & Biswas A (2002). *In vitro* plantlet regeneration and *Agrobacterium*-mediated genetic transformation of wheat (*Triticum aestivum* L.). *Plant Tissue Culture* 12: 155- 165.
- Satyavathi V V, Jauhar P P, Elias E M & Rao M B (2004). Effects of growth regulators on *in vitro* plant regeneration in durum wheat. *Crop Science* 44: 1839-1846. <https://doi.org/10.2135/cropsci2004.1839>
- Shan X Y, Li D S & Qu R D (2000). Thidiazuron promotes *in vitro* regeneration of wheat and barley. *In Vitro Cellular & Development Biology - Plant* 36: 207-210. <https://doi.org/10.1007/s11627-000-0038-y>
- She M Y, Yin G X, Li J R, Li X, Du L P & Ma W J (2013). Efficient regeneration potential is closely related to auxin exposure time and catalase metabolism during the somatic embryogenesis of immature embryos in *Triticum aestivum* L. *Molecular Biotechnology* 54: 451-460. <https://doi.org/10.1007/s12033-012-9583-y>
- Shu W, Zhou H, Jiang C, Zhao S, Wang L, Li Q, Yang Z & Groover A (2019). The auxin receptor TIR1 homolog (PagFBL1) regulates adventitious rooting through interactions with Aux/IAA28 in *Populus*. *Plant Biotechnology Journal* 17: 338-349. <https://doi.org/10.1111/pbi.12980>
- Tama's C, Szucs P, Rakszegi M, Tama's L & Bedò Z (2004). Effect of combined changes in culture medium and incubation conditions on the regeneration from immature embryos of elite varieties of winter wheat. *Plant Cell Tissue and Organ Culture* 79: 39-44. <https://doi.org/10.1023/b:ticu.0000049447.81409.ed>
- Thimann K V & Koepfli J B (1935). Identity of the growth promoting and root-forming substances of plants. *Nature* 135: 101–102. <https://doi.org/10.1038/135101a0>
- Wang J & Bao M (2007). Plant regeneration of pansy (*Viola wittrockiana*) 'Caidie' via petiole-derived callus. *Scientia Horticulturae* 111: 266–270. <https://doi.org/10.1016/j.scienta.2006.10.011>
- Yang S, Xu K, Wang Y, Bu B, Huang W, Sun F, Liu S & Xi Y (2015). Analysis of biochemical and physiological changes in wheat tissue culture using different germplasms and explant types. *Acta Physiologiae Plantarum* 37: 1-10. <https://doi.org/10.1007/s11738-015-1861-4>

Yucesan B, Turker A U & Gurel E (2007). TDZ-induced high frequency plant regeneration through multiple shoot formation in witloof chicory (*Cichorium intybus* L.). Plant Cell Tissue and Organ Culture 91: 243–250. <https://doi.org/10.1007/s11240-007-9290-8>



© 2022 by the author(s). Published by Ankara University, Faculty of Agriculture, Ankara, Turkey. This is an Open Access article distributed under the terms and conditions of the Creative Commons Attribution (CC BY) license (<http://creativecommons.org/licenses/by/4.0/>), which permits unrestricted use, distribution, and reproduction in any medium, provided the original work is properly cited.



Natural Vanillin Production from Isoeugenol by Using *Pseudomonas putida* in Biphasic Bioconversion Medium

Huseyin KARAKAYA^a , Murat YILMAZTEKIN^{a*}

^aInonu University, Faculty of Engineering, Department of Food Engineering, 44280, Malatya, TURKEY

ARTICLE INFO

Research Article

Corresponding Author: Murat YILMAZTEKIN, E-mail: murat.yilmaztekin@inonu.edu.tr

Received: 22 January 2021 / Revised: 8 May 2021 / Accepted: 14 July 2021 / Online: 01 September 2022

Cite this article

KARAKAYA H, YILMAZTEKIN M (2022). Natural Vanillin Production from Isoeugenol by Using *Pseudomonas putida* in Biphasic Bioconversion Medium. Journal of Agricultural Sciences (Tarim Bilimleri Dergisi), 28(3):423-429. DOI: 10.15832/ankutbd.866426

ABSTRACT

Vanillin, is one of the most demanded flavoring agents in the world. Because of insufficient supply of natural vanillin, market demand is usually supplied by synthetic ones. In this study, it was investigated possibility of usage biphasic system in bioconversion of isoeugenol to vanillin by *Pseudomonas putida* (HUT 8100). Organic phase was composed of isoeugenol while biocatalyst, *P. putida* culture, was dispersed in aqueous phosphate solution. Isoeugenol was used as sole carbon source in concentrations ranging between 50-600 g L⁻¹. Incubation was performed at 28 °C, at pH 6.3 and 180 rpm shaking. Effect of initial

substrate concentration and bioconversion time were investigated. Isoeugenol and vanillin amounts in medium were simultaneously analyzed in HPLC system. After 120 h incubation, vanillin reached the its highest level when 400 g L⁻¹ isoeugenol was applied in medium. In specified conditions, it was achieved to produce 11.95 g L⁻¹ vanillin with 6.2% molar yield within 15 days of bioconversion. It is thought that, obtained result by using biphasic system is very important for the industrial applications in production of natural vanillin via bioconversion.

Keywords: Bioconversion, Biphasic system, Isoeugenol, Natural flavor, Vanillin

1. Introduction

Vanillin (4-hydroxy-3-methoxybenzaldehyde) which naturally occurs in vanilla orchid pods, is one of the most important flavoring compounds (Singh et al. 2015). It is widely used in food, beverages, perfume and pharmaceutical industries (Zhao et al. 2018). However, vanillin derived from the pods serves less than 1% of global market volume (Singh et al. 2015). 85% of annual vanillin production is came from a petro-based compound, guaiacol, and the rest is synthesized from lignin (Zhu et al. 2018). Market value of synthetic vanillin is only about 10-20 USD kg⁻¹ while vanillin derived from *Vanilla* spp. is 1500 USD kg⁻¹ (van Leeuwen et al. 2018). Although there is a distinct price advantage of the synthetic counterparts, consumer interests to natural compounds, that considered as healthy, has forced many companies to discover new strategies to produce natural flavors such as vanillin (Luziatelli et al. 2019).

Biotechnological approaches have been known for many years and they include more environment-friendly processes compared to chemical synthesis (Franco et al. 2017). Compounds produced by biotechnological routes are labeled as "natural" according to Europe (EC 1334/2008, EC 1223/2009, EC 872/2012) and US (US CFR 1990) regulations (Castro et al. 2021). Isoeugenol has been raised concern of researchers being convertible to vanillin in one-step besides to be cheap and commercially available (Wang et al. 2021). Unfortunately, majority of aromatic compounds has cytotoxic activity on biocatalyst cells (Priebe & Daugulis 2018). In recent years, biphasic system (organic/inorganic) has been preferred in bio-flavor studies to overcome this problem. In this method, a non-aqueous phase is used to sequester the substrate from aqueous solution that includes the cells. Low amount of substrate is continuously transferred between the phases from non-aqueous to aqueous (Priebe et al. 2018). It also provides a protection to the cells against product toxicity (Bicas et al. 2010). Using biphasic medium offers numerous advantages for biotransformation studies apart from prevention of toxicity. Dissolution of product in one of the phases ensures *in situ* removal and makes recovering process easier (Chreptowicz & Mierzejewska 2018). Losses depend on volatility can be decreased in biphasic system, especially working with monoterpenic constituents. Bioconversion yield may be raised by manipulating oxygen transfer rate in medium according to organic phase features (Bicas et al. 2010). It was investigated usage of biphasic system in various flavor production studies such as cinnamyl alcohol (Zhang et al. 2020), 2-phenylethanol (Chreptowicz & Mierzejewska 2018), R-(+)- α -terpineol (Bicas et al. 2010) and concluded that the method was very effective on raising catalytic performance of the cells. Unlike the other vanillin studies, Zhao et al. (2005) used a biphasic medium containing 60% (v/v) isoeugenol and achieved to produce 32.5 g L⁻¹ vanillin which is the highest in literature, according to our knowledge.

A strong growth is expected in natural vanillin market with a compound annual growth rate (CAGR) of 7.4% from 2017 to 2025. In natural vanillin production, biotechnological approaches give an opportunity for producers (Luziatelli et al. 2019). Unfortunately, the production amounts remain very low due to substrate toxicity and hence, basic dispersion method is not applicable for industrial production. Thus, it is put emphasis on developing of current processes or constructing new alternative routes (Franco et al. 2017). Biphasic system has been come to the fore with high production rates as mentioned above. There is limited number of works for vanillin production in organic/inorganic bioconversion medium. Effects of temperature, pH and aeration in aqueous bioconversion medium were reported in our previous study (Karakaya & Yilmaztekin 2020). However, it was not possible to give results of biphasic (organic/inorganic) system within the same article due to limited scope. In this study, it was aimed to investigate biphasic medium usage for increasing vanillin production.

2. Material and Methods

2.1. Microorganism culture and chemicals

P. putida (HUT 8100) strain was supplied from HUT Culture Collection (Hiroshima, Japan). Culture was stored in IFO 802 (Institute of Fermentation, Osaka, Japan) medium slants at +4 °C until use. IFO 802 medium was prepared according to instructions of culture collection as followings: 10 g L⁻¹ peptone, 2 g L⁻¹ yeast extract, 1 g L⁻¹ MgSO₄ and 15 g L⁻¹ agar (HUT 2015).

Ethanol (96%, food grade) was purchased from Tekkim (Bursa, Turkey). Acetic acid (chromatographic grade) was supplied from Carlo-Erba (Milano, Italy). Medium ingredients, methanol, vanillin, isoeugenol and all other chemicals were purchased from Sigma-Aldrich (St. Louis, MO) unless otherwise specified.

2.2. Preparation of resting cells and bioconversion medium

Microorganism culture was grown in Glucose-Yeast Extract-Peptone (GYE) broth before inoculating to bioconversion medium. GYE was prepared in 1 L distilled water as followings: 5 g glucose, 5 g yeast extract, 5 g peptone, 14 g K₂HPO₄·3H₂O, 5.2 g KH₂PO₄ and 1 g MgSO₄·7H₂O (Zhao et al. 2005). 250 mL-sterile flasks containing 50 mL of GYE broth were inoculated with a loopful bacterial culture. They were incubated at 28 °C and 180 rpm orbital shaking (Sartorius Certomat IS, Germany) for 48 h. Medium contents were divided to two equal portions of 25 mL and transferred into sterile 50 mL-polypropylene tubes at the end of incubation. The tubes were centrifugated with 3600 xg at 4 °C for 15 min (Thermo Scientific SL 16R, MA). Clarified liquid sections were discarded and biomass in each tube was reconstituted with appropriate amount of phosphate buffer solution (4.84 g L⁻¹ K₂HPO₄ and 16.65 g L⁻¹ KH₂PO₄, pH: 6.3). Suspensions were homogenized and combined in a 250 mL-flask to obtain resting cells (Karakaya & Yilmaztekin 2020).

A total of 20 mL bioconversion medium was used in biphasic system trials. The aqueous part was formed by phosphate solution with resting cells while the organic phase was solely consisted of isoeugenol. The amount of substrate must be sufficient to form two distinctly separated surfaces. For the purpose, initial isoeugenol concentration was used in range of 50-600 g L⁻¹. Higher concentrations were not applied, since the aqueous phase was not capable of covering organic surface, completely. Bioconversion medium was left to incubation at 28 °C and 180 rpm orbital shaking for 120 h. Initial substrate ratio which provides maximal vanillin production was applied in bioconversion time trials. A separate flask was prepared with same content for each sampling time. At the end of target sampling time, whole flask content was extracted according to the procedures given in Section 2.4. Unused isoeugenol and produced vanillin amounts were determined by HPLC system. Time trials were continued until no significant change was observed in vanillin accumulation between successive samplings.

2.3. Viability test

Cell viability was checked with *p*-iodo nitrotriazolium (INT) indicator. Samples (2 mL) were collected from bioconversion medium into sterile test tubes and 0.4 mL INT solution (0.2 mg mL⁻¹, in distilled water) was dropped into each tube. Procedure was applied the sample tubes which contains uninoculated bioconversion medium, too. Tubes were incubated for additional 30 min at 28 °C without shaking. Viability was determined according to red color formation in the tubes (Eloff 1998).

2.4. Extraction

Extraction was performed following after incubation in concentration (120 h) and time (1-17 days) trials. The bioconversion medium (20 mL) was transferred to 50-mL polypropylene tubes in given sampling time. 96% ethanol was added over in ratio of 1:1 (v:v) and the tubes were homogenized for 1 min. Suspension was centrifugated with 3600 xg at 4 °C for 15 min. Supernatant was taken to a new tube and 7.5 mL of 96% ethanol was added over biomass. The tube content was homogenized and centrifugated again in same conditions. The procedure was applied two times and supernatants were combined in a new tube. Extracts were filtered through 0.45 µm nylon membrane filters and taken to amber colored HPLC vials (2 mL) for analysis (Karakaya & Yilmaztekin 2020).

2.5. HPLC analysis

Isoeugenol and vanillin amounts in bioconversion medium were determined by HPLC (Shimadzu LC-20A, Japan). Degasser (DGPU-20A5), pump (LC-20AD), autosampler (SIL-20A) units and UV-visible detector (SPD-M20A) which are directly integrated to HPLC system were used for the purpose. Compound separation was achieved by Licrospher RP18 (25 cm x 4.60 mm, 5.5 µm particle size) column. A binary solvent system was used as follows: ultrapure water containing 0.01% acetic acid (A) and methanol (99.9%) (B). Gradient elution was applied according to procedures stated by Li et al. (2004), with minor modifications. Briefly, phase B was flowed as following ratios: 60% between 0-3 min, decrease to 50% between 3-5 min, raise to 100% between 5-9 min and left to flow 100% B for 4 min. It was decreased to 60% again between 13-15 min and flowed 60% mobile phase B for 3 min to prepare the column to next injection. Total analysis time was estimated 18 min. Elution was simultaneously screened with UV detector at 270 nm. Isoeugenol and vanillin were identified by using authentic standards. Quantification was performed using a calibration curve prepared by five-point serial dilutions of corresponding standards. Bioconversion efficiency was determined with molar yield equation (1) (Karakaya & Yilmaztekin 2020):

$$\text{Molar yield (\%)} = \frac{\text{Produced vanillin (g)} \times \text{Molar weight of isoeugenol (g/mol)}}{\text{Consumed isoeugenol (g)} \times \text{Molar weight of vanillin (g/mol)}} \times 100 \quad (1)$$

2.6. Statistical analysis

Isoeugenol consumption and vanillin production in biphasic medium were analyzed by analysis of variance (ANOVA). Statistical analysis was carried out in SPSS package program version 16.0 (SPSS Inc., Chicago, IL). Tukey's multiple comparison test was used to compare means at a significance level of $P < 0.05$. All trials were performed in triplicate and results were expressed as mean ± standard deviation.

3. Results and Discussion

3.1. Cell viability

Growing cells need energy to multiply their biomass and this causes a fall in bioconversion yield. Unlike growing cells, resting forms that non-growing but metabolically active, use their metabolism more efficiently due to high substrate specificity (Julsing et al. 2012). It can be prepared by transferring of growing cells to phosphate buffer solutions (Hua et al. 2007; Yamada et al. 2007). In this study, culture was dispersed in K_2HPO_4 and KH_2PO_4 solution to obtain resting cells.

Biocatalyst were obliged to use limited isoeugenol dissolved in aqueous phase to survive. Cell death may occur in bioconversion medium depend on nutritional deficiency, substrate, product or by-product toxicity. If there is bacterial viability, color in test tubes turns to red in presence of INT indicator. There is no color change on the contrary (Eloff 1998). In both of initial concentration and bioconversion time trials, red color formation was observed in all test tubes which was accepted as evidence of bacterial viability. Bioconversion medium was found suitable to keep cells alive although it contained less ingredient compared to a simple growing medium. In addition, there was not encountered vanillin formation in the absence of either isoeugenol or cell culture in medium. Biphasic system results on viability were in accordance with previous findings (Karakaya & Yilmaztekin 2020).

3.2. Effect of initial substrate concentration

It is known that many substrates and products in bioconversion studies have low solubility in water (Carreno et al. 2014). Isoeugenol may be thought unfavorable substrate for bioconversion because its solubility is only 6 mM which is quite low (Yamada et al. 2007; Ashengroph et al. 2011). Actually, it presents an opportunity to use it in high concentration to form a biphasic system. Bioconversion media was prepared by using 50-600 g L⁻¹ isoeugenol and left to incubation for 120 h. The media containing 300 and 400 g L⁻¹ isoeugenol were differed from the others with regard to significantly higher ($P < 0.05$) vanillin content (Figure 1). It was produced 9.14 ± 0.62 g L⁻¹ vanillin in the medium containing 400 g L⁻¹ isoeugenol.

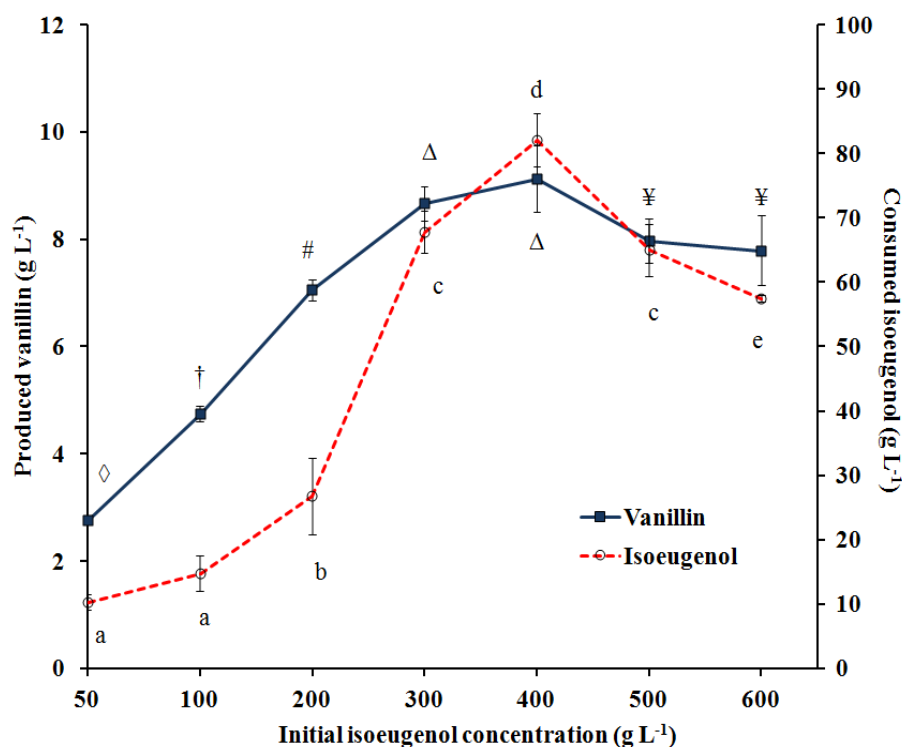


Figure 1- Changes in vanillin and isoegenol amounts depending on different initial substrate concentrations (Error bars indicate standard deviation. Significant differences are marked with symbols for vanillin and letters for isoegenol, $P < 0.05$)

Various biocatalysts were used in conversion of isoegenol to vanillin, especially *Arthrobacter* (Shimoni et al. 2003), *Bacillus* (Hua et al. 2007), *Trichosporon asahii* (Ashengroph & Amini 2017) and *Pseudomonas* (Yamada et al. 2007; Karakaya & Yilmaztekin 2020) species. Nevertheless, produced vanillin was less than 5 g L^{-1} in many of these studies. It was due to low solubility of isoegenol, substrate or product toxicity on culture in aqueous dispersions (Ashengroph & Amini 2017). In previous study, vanillin production in isoegenol-phosphate dispersion was only about 877.9 mg L^{-1} , although some conditions (pH, temperature and aeration) were optimized (Karakaya & Yilmaztekin 2020). In dispersion systems, access to substrate by cells may have been limited due to insufficient surface area depend on low isoegenol concentration. Isoegenol in high quantities acts as a substrate and solvent which cause an increase on vanillin production (Zhao et al. 2005). It is thought that biphasic system made easier to reach sole carbon source, isoegenol, by *P. putida* cells. It allowed to use high substrate amounts up to 400 g L^{-1} without showing any toxic effect on biocatalyst. However, a decline in vanillin production was observed when higher substrate concentrations were applied. Biocatalytic activity is inhibited when substrate or product concentration exceeds the critical level (Carreno et al. 2014). Cell viability is an essential factor in whole cell biotransformation processes (Sendovski et al. 2010). It has been thought that dispersed isoegenol ratio was increased enough to have toxic effect on the cells by using 500 g L^{-1} isoegenol or more.

P. putida cells performed an effective vanillin production yield although the medium was solely consisted of isoegenol as carbon source. Bacterial contamination risk can be reduced due to nutrient deficient medium (Wang et al. 2006). Moreover, using minimal ingredients in medium makes the purification step easier in bioprocesses. Distinct differences between organic/inorganic phase features provide an efficient extraction of biomolecules (Nouri et al. 2019). On the other hand, separated layers in the medium effect oxygen transfer rate. Bicas et al. (2010) used sunflower oil as organic phase on top layer and decreased oxygen transfer rate to inorganic phase. Anaerobic condition was promoted R-(+)- α -terpineol production in given study. However, lowering the oxygenation of medium adversely affects *P. putida* cells in vanillin bioconversion (Karakaya & Yilmaztekin 2020). In contrast to many essential oil constituents, density of isoegenol is higher than water in constant temperature (Nielsen et al. 2017). Therefore, it showed tendency to precipitate in aqueous solutions and inorganic phase took part in upper side of biphasic system. It must have been facilitated the access to oxygen by cells.

3.3. Bioconversion time

Various parameters such as high production rates, yield and process duration have importance for industrial operations. Bioconversion was followed for 17 days in 400 g L^{-1} isoegenol containing medium (Figure 2). It was determined a significant difference ($P < 0.05$) on vanillin accumulation between beginning and ending days of bioconversion. Although there was a slight decrease in vanillin amount on 17th day, change was no meaningful. Aldehyde structured compounds have high chemical reactivity and in general, they rarely accumulate in biological systems (Muheim & Lerch 1999). As an aldehyde, vanillin was expressed as an obligate intermediate for some *Pseudomonas* sp. (Overhage et al. 1999). It can be oxidized to vanillic acid or

reduced to vanillyl alcohol depend on enzyme diversity of biocatalyst (Luziatelli et al. 2019). This fall may be due to further degradation of vanillin by biocatalyst to avoid product toxicity in harsh conditions. It was achieved to produce 11.95 g L⁻¹ vanillin with 6.2% molar yield after 15 days of bioconversion. 48.3% (w/w) of isoeugenol remained unused at the moment. In past studies, it was stated that residual isoeugenol could be recovered and utilized once again in a new bioconversion cycle (Zhao et al. 2006).

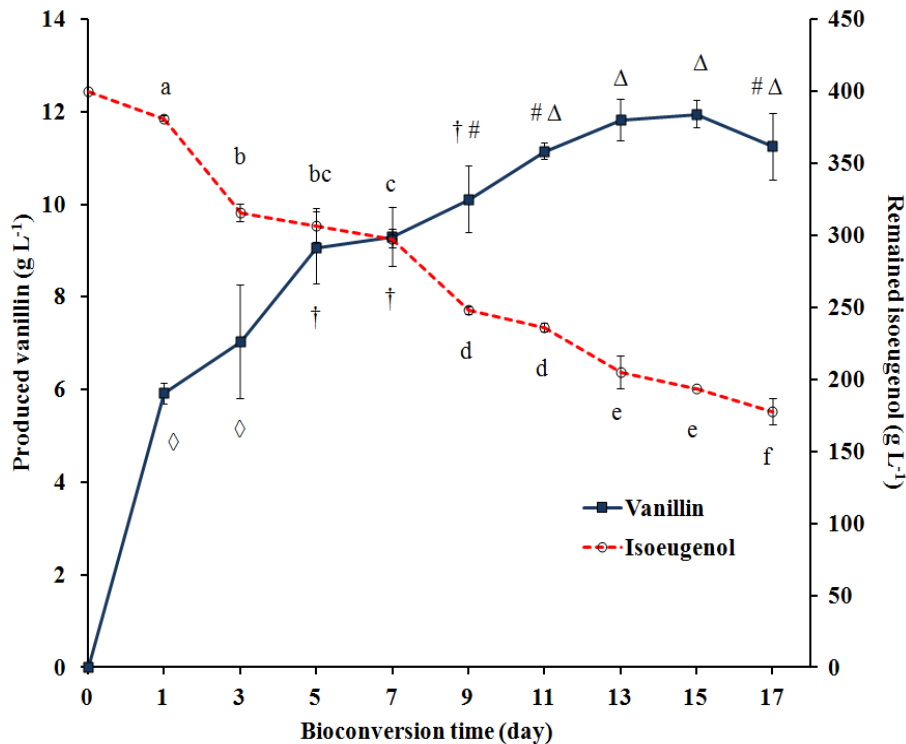


Figure 2- Changes in vanillin and isoeugenol amounts depending on time in medium containing 400 g L⁻¹ substrate (Error bars indicate standard deviation. Significant differences are marked with symbols for vanillin and letters for isoeugenol, P<0.05)

It has been shown that multiple-feeding at different times promotes the vanillin production compared to single feeding strategy (Valerio et al. 2021). However, processes must be interrupted to replace the current medium with fresh one. Considering industrial mass production, it may lead to loss of time and contamination risk. As opposed to aqueous dispersions, feeding occurs spontaneously in biphasic system by transfer of limited amount of isoeugenol from organic to aqueous layer. Zhao et al. (2005) stated that 0.2-0.9 g L⁻¹ isoeugenol was dispersed in aqueous phase when 60% isoeugenol and 180 rpm shaking were applied in biphasic medium. There are limited number of works came up with high vanillin yield but the techniques used in these studies had some disadvantageous properties. For instance, Yamada et al. (2007) achieved to produce 16.1 g L⁻¹ vanillin with the help of 10% (v/v) DMSO in bioconversion medium. Despite the fact that an effective vanillin production was carried out, method is unfeasible for industrial operations. DMSO presents high polarity and high boiling points and these make the product isolation impossible for further process steps. (Ashengroph & Amini 2017). Since it was not desired to obtain uniform solution in this study, emulsifier agent was not used in medium. In another study, it was managed to produce 28.3 g L⁻¹ vanillin by using recombinant *E. coli* cells (Yamada et al. 2008). However, genetic modified organisms have a negative effect on consumer perception and moreover they are perceived as risky, avoidable and fearful (Boccia et al. 2018). Biphasic system is taken attention because of its high production rates in various bioconversion process (Zhao et al. 2005; Chreptowicz & Mierzejewska 2018; Zhang et al. 2020). It was aimed to enhance vanillin production by using biphasic medium in the study and findings are compatible with those of mentioned references.

4. Conclusions

In this study, natural vanillin was produced from isoeugenol as an alternative to botanical extracts. This work has been differed from past studies that was possible to apply high substrate concentrations in biphasic system avoiding substrate toxicity. Biocatalyst, *P. putida* (HUT 8100) culture, was dispersed in inorganic buffer solution and isoeugenol was used with the aim of both, substrate and organic phase. Distinct specifications of the phases (such as density and polarity) made easier to form a biphasic medium. Biocatalyst cells were in contact with substrate at the phase interface and not directly exposed to high amount of isoeugenol which provided a protection against to substrate toxicity. A limited amount of isoeugenol was continuously dispersed in aqueous phase by shaking. Thus, there was no need to substrate addition during bioconversion and spontaneous feeding was provided by organic layer. Using 400 g L⁻¹ isoeugenol, it was achieved to produce 11.95 g L⁻¹ vanillin with 6.2%

molar yield in 15 days. Biphasic system has brought out higher vanillin production rate compared to many other reports on literature. It did not require to use of any emulsifier agent or additional nutrient. Therefore, it is expected to reduce operational costs and make the purification step easier due to minimal content. However, being free from toxic solvents makes the process eco-friendly and removes the risk of residual solvent in final product. It has been thought that findings have an importance for industrial scale production of bio-vanillin. It is suggested to work on residual isoeugenol utilization and vanillin purification for further studies. Using appropriate macroporous resin can provide an effective separation for both, isoeugenol and vanillin.

Acknowledgements

This study was supported by Inonu University Scientific Research Projects Coordination Unit (Project number: 2015/17). Authors owe to thanks to HUT Culture Collection in supply of bacteria culture.

References

- Ashengroph M & Amini J (2017). Bioconversion of isoeugenol to vanillin and vanillic acid using the resting cells of *Trichosporon asahii*. *3 Biotech* 7: 358
- Ashengroph M, Nahvi I, Zarkesh-Esfahani H & Momenbeik F (2011). Use of growing cells of *Pseudomonas aeruginosa* for synthesis of the natural vanillin via conversion of isoeugenol. *Iranian Journal of Pharmaceutical Research* 10(4): 749-757
- Bicas J L, Fontanille P, Pastore G M & Larroche C (2010). A bioprocess for the production of high concentrations of R-(+)- α -terpineol from R-(+)-limonene. *Process Biochemistry* 45: 481-486
- Boccia F, Covino D & Sarnacchiaro P (2018). Genetically modified foods versus knowledge and fear: A numeric approach for consumer behavior. *Food Research International* 111: 682-688
- Carreno D M P, Quinones O M R, Calvo J R V & Ochoa S H (2014). Bioconversion of (+)-nootkatone by *Botryodiplodia theobromae* using a membrane aerated biofilm reactor. *Revista Mexicana de Ingenieria Quimica* 13(3): 757-764
- Castro P S, Soares F & Santos P M (2021). Current advances in the bacterial toolbox for the biotechnological production of monoterpene-based aroma compounds. *Molecules* 26(91): 1-31
- Chreptowicz K & Mierzejewska J (2018). Enhanced bioproduction of 2-phenylethanol in a biphasic system with rapeseed oil. *New Biotechnology* 42: 56-61
- Eloff J N (1998). A sensitive and quick microplate method to determine the minimal inhibitory concentration of plant extracts for bacteria. *Planta Medica* 64: 711-713
- Franco A, De S, Balu A M, Romero A A & Luque R (2017). Selective oxidation of isoeugenol to vanillin over mechanochemically synthesized aluminosilicate supported transition metal catalysts. *ChemistrySelect* 2: 9546-9551
- Hua D, Ma C, Lin S, Song L, Deng Z, Maomy Z, Zhang Z, Yu B & Xu P (2007). Biotransformation of isoeugenol to vanillin by a newly isolated *Bacillus pumilus* strain: identification of major metabolites. *Journal of Biotechnology* 130: 463-470
- HUT (2015). Medeam. Retrieved in June, 11, 2015 from <https://home.hiroshima-u.ac.jp/hut/mideum.html>
- Julsing M K, Kuhn D, Schmid A & Bühler B (2012). Resting cells of recombinant *E. coli* show high epoxidation yields on energy source and high sensitivity to product inhibition. *Biotechnology and Bioengineering* 109(5): 1109-1119
- Karakaya H & Yilmaztekin M (2020). *Pseudomonas putida* ile izoöjenolden doğal vanilin üretiminde bazı ortam koşullarının molar verim üzerine etkisi. *Gıda* 45(1): 9-19
- Li Y H, Sun Z H & Zheng P (2004). Determination of vanillin, eugenol and isoeugenol by RP-HPLC. *Chromatographia* 60: 709-713
- Luziatelli F, Brunetti L, Ficca A G & Ruzzi M (2019). Maximizing the efficiency of vanillin production by biocatalyst enhancement and process optimization. *Frontiers in Bioengineering and Biotechnology* 7: 279
- Muheim A & Lerch K (1999). Towards a high-yield bioconversion of ferulic acid to vanillin. *Applied Microbiology and Biotechnology* 51: 456-461
- Nielsen C K, Kjems J, Mygind T, Snabe T, Schwarz K, Serfert Y & Meyer R L (2017). Antimicrobial effect of emulsion-encapsulated isoeugenol against biofilms of food pathogens and spoiled bacteria. *International Journal of Food Microbiology* 242: 7-12
- Nouri M, Shahriari S & Pazuki G (2019). Increase of vanillin partitioning using aqueous two phase system with promising nanoparticles. *Scientific Reports* 9: 19665
- Overhage J, Priefert H, Rabenhorst J & Steinbüchel A (1999). Biotransformation of eugenol to vanillin by a mutant of *Pseudomonas* sp. strain HR199 constructed by disruption of the vanillin dehydrogenase (vdh) gene. *Applied Microbiology and Biotechnology* 52: 820-828
- Priebe X & Daugulis A J (2018). Thermodynamic affinity-based considerations for the rational selection of biphasic systems for microbial flavor and fragrance production. *Journal of Chemical Technology & Biotechnology* 93: 656-666
- Priebe X, Daschner M, Schwab W & Weuster-Botz D (2018). Rational selection of biphasic reaction systems for geranyl glucoside production by *Escherichia coli* whole-cell biocatalysts. *Enzyme and Microbial Technology* 112: 79-87
- Sendovski M, Nir N & Fishman A (2010). Bioproduction of 2-phenylethanol in a biphasic ionic liquid aqueous system. *Journal of Agricultural and Food Chemistry* 58: 2260-2265
- Shimoni E, Baasov T, Ravid U & Shoham Y (2003). Biotransformations of propenylbenzenes by an *Arthrobacter* sp. and its *t*-anethole blocked mutants. *Journal of Biotechnology* 105: 61-70

- Singh B, Khan S, Pandey S S, Singh M, Banerjee S, Kitamura Y & ur Rahman L (2015). Vanillin production in metabolically engineered *Beta vulgaris* hairy roots through heterologous expression of *Pseudomonas fluorescens* HCHL gene. *Industrial Crops and Products* 74: 839-848
- Valerio R, Bernardino A R S, Torres C A V, Brazinha C, Tavares M L, Crespo J G & Reis M A M (2021). Feeding strategies to optimize vanillin production by *Amycolatopsis* sp. ATCC 39116. *Bioprocess and Biosystems Engineering* 44: 737-747
- van Leeuwen K A, Prenzler P D, Ryan D, Paolini M & Camin F (2018). Differentiation of wood-derived vanillin from synthetic vanillin in distillates using gas chromatography/combustion/isotope ratio mass spectrometry for $\delta^{13}\text{C}$ analysis. *Rapid Communication in Mass Spectrometry* 32: 311-318
- Wang Z, Zhao F, Chen D & Li D (2006). Biotransformation of phytosterol to produce androsta-diene-dione by resting cells of *Mycobacterium* in cloud point system. *Process Biochemistry* 41: 557-561
- Wang Q, Wu X, Lu X, He Y, Ma B & Xu Y (2021). Efficient biosynthesis of vanillin from isoeugenol by recombinant isoeugenol monooxygenase from *Pseudomonas nitroreducens* Jin1. *Applied Biochemistry and Biotechnology*, Published online: 07.01.2021
- Yamada M, Okada Y, Yoshida T & Nagasawa T (2007). Biotransformation of isoeugenol to vanillin by *Pseudomonas putida* IE27 cells. *Applied Microbiology and Biotechnology* 73: 1025-1030
- Yamada M, Okada Y, Yoshida T & Nagasawa T (2008). Vanillin production using *Escherichia coli* cells over-expressing isoeugenol monooxygenase of *Pseudomonas putida*. *Biotechnology Letters* 30: 665-670
- Zhang C, Xu Q, Hou H, Wu J, Zheng Z & Ouyang J (2020). Efficient biosynthesis of cinnamyl alcohol by engineered *Escherichia coli* overexpressing carboxylic acid reductase in a biphasic system. *Microbial Cell Factories* 19: 163
- Zhao L Q, Sun Z H, Zheng P & Zhu L L (2005). Biotransformation of isoeugenol to vanillin by a novel strain of *Bacillus fusiformis*. *Biotechnology Letters* 27: 1505-1509
- Zhao L Q, Sun Z H, Zheng P & He J Y (2006). Biotransformation of isoeugenol to vanillin by *Bacillus fusiformis* CGMCC1347 with the addition of resin HD-8. *Process Biochemistry* 41: 1673-1676
- Zhao L, Xie Y, Chen L, Xuefeng X, Zhao C X & Cheng F (2018). Efficient biotransformation of isoeugenol to vanillin in recombinant strains of *Escherichia coli* by using engineered isoeugenol monooxygenase and sol-gel chitosan membrane. *Process Biochemistry* 71: 76-81
- Zhu Y, Liu J, Liao Y, Lv W, Ma L & Wang C (2018). Degradation of vanillin during lignin valorization under alkaline oxidation. *Topics in Current Chemistry* 376: 29



© 2022 by the author(s). Published by Ankara University, Faculty of Agriculture, Ankara, Turkey. This is an Open Access article distributed under the terms and conditions of the Creative Commons Attribution (CC BY) license (<http://creativecommons.org/licenses/by/4.0/>), which permits unrestricted use, distribution, and reproduction in any medium, provided the original work is properly cited.



Effect of Supplementation of Urea on the Nutritive Value and Fermentation Characteristics of Apple Pulp Silages

Önder CANBOLAT^a 

^aBursa Uludağ University, Faculty of Agriculture, Department of Animal Science, Bursa, TÜRKİYE

ARTICLE INFO

Research Article

Corresponding Author: Önder CANBOLAT, E-mail: canbolat@uludag.edu.tr

Received: 16 April 2021 / Revised: 27 July 2021 / Accepted: 28 July 2021 / Online: 01 September 2022

Cite this article

CANBOLAT Ö (2022). Effect of Supplementation of Urea on the Nutritive Value and Fermentation Characteristics of Apple Pulp Silages. *Journal of Agricultural Sciences (Tarim Bilimleri Dergisi)*, 28(3):430-437. DOI: 10.15832/ankutbd.917540

ABSTRACT

The aim of current experiment was to determine the effect of supplementation of urea on the nutritive value and fermentation characteristics of apple pulp silage. Apple pulp obtained from apple with Granny Smith (*Malus domestica*) varieties was used in the research. Apple pulp were ensiled in special glass jars with 1.5 L capacity. Urea (0, 0.5, 1.0, 1.5, 2.0 and 2.5% on DM basis) was added homogeneously to apple pulp in triplicate. The experimental silos were placed in a room until opening after 45 day of preservation to determine chemical composition and silage fermentation parameters. The addition of urea to apple pulp reduced the water soluble carbohydrate (WSC), content of neutral detergent fiber (NDF), acid detergent fiber (ADF) and acid detergent lignin (ADL) whereas the supplementation of urea significantly ($P<0.01$)

increased crude protein (CP) contents of resultant silages. The addition of urea to apple pulp significantly ($P<0.01$) increased pH, lactic acid (LA), propionic acid (PA), butyric acid (BA) and ammonia nitrogen ($\text{NH}_3\text{-N}$) contents of the resultant silages whereas the supplementation of urea significantly ($P<0.01$) reduced the acetic acid (AA) contents. Addition of urea to apple pulp increased in vitro gas production, digestible organic matter (DOM), metabolic energy (ME) and lactic acid bacteria (LAB), and significantly reduced yeast and mold count ($P<0.01$). The urea supplementation also increased the aerobic stability of the resultant silages. It can be concluded that supplementation of urea to apple pulp at 2.0 and 2.5% can be recommended to improve the nutritive value and fermentation parameters of the resultant silages.

Keywords: Apple Pomace, Silage, Urea, In Vitro Gas Production, Silage Fermentation

1. Introduction

Recently apple production increased from 2.6 million tons in 2010 to 4.3 million tons in 2021 due to an increased demand for apple consumption in Turkey (Anonymous 2022). Apple is consumed not only fresh but used to produce apple juice in Turkey. Therefore, considerable amount of apple pulp is produced during apple juice production. The pulp constitutes 25-30 % of total processed apple and consists of a crust, flesh and seeds (Ajila et al. 2015; Skinner et al. 2018). Although the moisture content of the apple pulp is very high at the time of production, pulp contains considerable amount of cellulose, pectin, minerals, vitamin C, anti-oxidant, water soluble carbohydrate (WSC) and some organic acids (Alibes et al. 1984; Vrhovsek et al. 2004; Varzakas et al. 2016; Islam et al. 2018a). In dry matter (DM), the crude protein (CP), neutral detergent fiber (NDF) and acid detergent fiber (ADF) contents of apple pulp ranges from 19-65 g/kg Carson et al. 1994), 300-482 g/kg and 250-420 g/kg, respectively (Wolter et al. 1980; Singhal et al. 1991). The metabolisable energy (ME) value of apple pulp may vary from 7.7 to 9.1 MJ/kg DM (MAFF 1984). The mean protein degradability of apple pulp reported by NRC (2001) was 68.4%.

Generally, apple pulp is used in the feeding of ruminant animals in the form of fresh, dry and silage (Fontenot et al. 1977; Alibes et al. 1984; Gasa et al. 1992; Kennedy et al. 1999; Taasoli & Kafilzadeh 2008; Ajila et al. 2015; Islam et al. 2018a). It is very difficult to store the apple pulp due to high moisture content (Alibes et al. 1984; Fang et al. 2016; Islam et al. 2018b). Therefore, the apple pulp can be preserved by ensiling (McDonald et al. 1991; Fang et al. 2016; Islam et al. 2018a), since that contains water soluble carbohydrates which is required by lactic acid bacteria to produce lactic acid which is responsible for the decrease in pH of silage (Afzal et al. 2015; Skinner et al. 2018). Previous investigations clearly showed that apple pulp silage is an ideal feed for ruminant animals (Rumsey 1978; Pirmohammadi et al. 2006; Ajila et al. 2015; Islam et al. 2018a; Islam et al. 2018b; García-Rodríguez et al. 2019). Although apple pulp has high energy value, its protein content is low (Gasa et al. 1992; Taasoli and Kafilzadeh 2008). The fact that apple pulp contains low digestible protein is an important factor that limits the nutritive value (Rumsey 1978; Ajila et al. 2015). Therefore, urea can be used as silage additive to increase the crude protein content of the resultant silage (Alibes et al. 1984; McDonald et al. 1991; Filya et al. 2004; Canbolat et al. 2014). It was recommended that urea can be added to silage material with a low protein content at level of 40-50 kg/ton DM to increase the

crude protein content of silage (Kaiser 2004). Supplementation of urea not only improve the crude protein content but also improve the aerobic stability of the resultant silage (McDonald et al. 1991; Filya et al. 2004; Canbolat et al. 2014). Therefore, the aim of current experiment was to determine the effect of supplementation of urea on the nutritive value and fermentation properties of apple pulp silage.

2. Material and Methods

2.1. Feed and silo material

The feed material of the research was composed of apple pulp (*Malus domestica*: Granny Smith) left from apple juice production in Bursa Uludag University Agricultural Research and Application Center. Urea was obtained from a commercial firm. 1.5 L special glass silos (Weck®, Germany) were used for ensiling the apple pulp.

2.2. Animal material

In order to apply the *in vitro* gas production technique, rumen fluid was taken from 3 Merino rams after slaughtering.

2.3. Preparation of silages

Apple pulp were ensiled in special glass jars with 1.5 L capacity. Urea (0, 0.5, 1.0, 1.5, 2.0 and 2.5% on DM basis) was added homogeneously to apple pulp in triplicate. The experimental silos were placed in a room until opening after 45 day of preservation.

2.4. Chemical analyses

The experimental silos of apple pulp silages were opened on the 45th day of silo. Apple pulp silage was dried in the oven at 65 °C for 48 hours. Dried silages were grinded to a 1 mm sieve diameter and used in chemical analyses. Dry matter, crude ash, ether extract and crude protein contents of silages were determined using the methods described by AOAC (2000). Neutral detergent fiber, acid detergent fiber and acid detergent lignin contents of silages were determined using the method suggested by Van Soest et al. (1990).

The pH of the silages was determined using the digital pH meter (Sartorius PB-20, Goettingen, Germany) and ammonia nitrogen (NH₃-N) contents of silages were determined using the method described by AOAC (2000). Lactic acid, acetic, propionic and butyric acid contents of silages were determined with gas chromatography device (Agilent Technologies 6890N, column properties: Stabilwax-DA, 30 m, 0.25 mm ID, 0.25 µm df. Max. Temp: 260 °C. Cat. 11023) using the spectrophotometric method (Barker & Summerson 1941). Water soluble carbohydrate (WSC) contents were determined according to the phenol sulphuric acid method (Dubois et al. 1956).

Lactic acid bacteria (LAB), yeast and mold counts of silages were determined according to the method reported by Seale et al. (1990). De Man, Rogosa and Sharpe (MRS) agar for LAB, Malt Extract agar for yeast and molds were used as a cultivation medium. Lactic acid bacteria, yeast and mold counts of the silages were incubated for 3 days at 30 °C. The LAB, yeast and mold numbers were explained as coliform unit (cfu/g). Aerobic stability of silages was performed according to the method developed by Ashbell et al. (1991).

2.5. Determination of *in vitro* gas production of apple pulp silages

In vitro gas production of apple pulp silages were determined using the *in vitro* gas production technique reported by Menke et al. (1979). Approximately 200 mg silage samples were incubated in special 100 mL glass syringes (Model Fortuna, Häberle Labortechnik, Lonsee-Ettlenschie, Germany) in triplicate. 30 mL of buffered rumen fluid was transferred into glass syringes containing silage samples. Glass syringes were incubated in a water bath at 39 °C and *in vitro* gas production was measured at 24 hours after incubation.

Organic matter digestibility and metabolisable energy contents of apple pulp silages were calculated using the following equations (Menke & Steingass 1988).

$$\text{OMD, \%} = 15.38 + 0.8453 \times \text{GP} + 0.0595 \times \text{CP} + 0.0675 \times \text{CA}$$

$$\text{ME, MJ/kg DM} = 2.20 + 0.1357 \times \text{GP} + 0.0057 \times \text{CP} + 0.0002859 \times \text{CF}^2$$

(GP: Net gas amount produced by 200 mg feed sample for 24 hours. CP: crude protein, EE: ether extract and CA: crude ash, g/kg DM).

2.6. Statistical analysis

Data obtained in the current experiment were subjected to variance analysis (ANOVA) using the General Linear Model (Minitab 2013). The significance between the treatment groups were determined by Duncan multiple comparison test (Snedecor & Cochran 1976).

3. Results

Effect of urea supplementation on chemical composition of apple pulp silages was given in Table 1. Urea supplementation had a significant ($P<0.01$) effect on chemical composition of the resultant apple pulp silages.

Table 1- Effect of urea supplementation on chemical composition of apple pulp silages, %

Urea Treatment (%)	DM	CP	EE	CA	NDF	ADF	ADL	WSC
0.0	26.74 ^f	7.64 ^f	4.40 ^a	2.43 ^f	47.68 ^a	38.96 ^a	7.24 ^a	7.37 ^a
0.5	27.09 ^e	8.57 ^e	4.40 ^a	2.53 ^e	46.42 ^b	38.77 ^a	7.20 ^a	6.59 ^b
1.0	27.72 ^d	9.18 ^d	4.37 ^{ab}	2.62 ^d	45.73 ^{bc}	37.92 ^{ab}	7.15 ^a	6.41 ^c
1.5	27.93 ^c	10.14 ^c	4.35 ^{abc}	2.69 ^c	44.88 ^{cd}	37.22 ^{bc}	7.06 ^b	6.30 ^c
2.0	28.22 ^b	10.75 ^b	4.30 ^{bc}	2.79 ^b	43.93 ^d	36.47 ^c	7.04 ^b	5.11 ^d
2.5	28.79 ^a	11.29 ^a	4.29 ^c	2.90 ^a	42.63 ^e	34.32 ^d	6.95 ^c	4.83 ^e
*SD	0.081	0.090	0.042	0.029	0.638	0.590	0.263	0.091

a,b,c,d,e,f: The differences between the means indicated by different letters in the same column are significant ($P<0.01$); *SD: Standard deviation; DM: Dry matter; CP: Crude protein; CA: Crude ash; EE: Ether extract; NDF: Neutral detergent fiber; ADF: Acid detergent fiber; ADL: Acid detergent lignin; WSC: Water soluble carbohydrate

The DM, CP and CA contents of the resultant silage increased ($P<0.01$) in a dose dependent manner of urea whereas NDF, ADF, ADL and WSC contents decreased ($P<0.01$).

Effect of urea supplementation on apple pulp silage fermentation characteristics are given in Table 2.

Table 2- Effect of urea supplementation on apple pulp silages fermentation characteristics

Urea Treatment (%)	pH	g/kg DM					
		Lactic acid	Acetic acid	Propionic acid	Butyric acid	Ethanol	NH ₃ -N
0.0	3.72 ^f	42.25 ^e	26.07 ^a	3.13 ^e	1.35 ^a	2.85 ^a	13.14 ^f
0.5	3.85 ^e	44.44 ^d	25.36 ^{ab}	3.23 ^d	1.17 ^b	2.12 ^b	14.37 ^e
1.0	3.90 ^d	48.85 ^c	24.15 ^{bc}	3.30 ^c	1.16 ^b	1.70 ^c	15.61 ^d
1.5	3.94 ^c	51.51 ^b	23.56 ^c	3.40 ^b	1.01 ^c	1.61 ^{cb}	16.46 ^c
2.0	4.13 ^b	53.69 ^a	20.95 ^d	3.45 ^b	0.78 ^d	1.51 ^d	17.89 ^b
2.5	4.21 ^a	54.62 ^a	18.61 ^e	3.59 ^a	0.64 ^e	1.30 ^e	19.07 ^a
*SD	0.058	1.184	0.771	0.032	0.065	0.073	0.365

a,b,c,d,f: The differences between the means indicated by different letters in the same column are significant ($P<0.01$); *SD: Standard deviation; NH₃-N: Ammonia nitrogen (NH₃-N is given as % of total N)

Urea supplementation had a significant ($P<0.01$) effect on fermentation characteristics of the resultant apple pulp silages. The pH, lactic acid and NH₃-N, propionic acid, also contents of the resultant silage increased ($P<0.01$) in a dose dependent manner of urea whereas acetic, butyric acid and ethanol contents decreased ($P<0.01$). Accordingly, the most effective urea dose on silage parameters was 2.5%.

Effect of urea supplementation on silage microbiology of apple pulp silages was given in Table 3.

Table 3- Effect of urea supplementation on silage microbiology of apple pulp silages

Urea Treatment (%)	LAB (cfu/g FM)	Yeast (cfu/g FM)	Mold (cfu/g FM)
0.0	10.47 ^d	3.73 ^a	1.67 ^a
0.5	12.15 ^c	3.62 ^{ab}	1.33 ^a
1.0	13.89 ^b	3.56 ^{abc}	1.00 ^{ab}
1.5	14.63 ^b	3.19 ^{bc}	1.00 ^{ab}
2.0	15.55 ^a	3.07 ^{cd}	0.33 ^b
2.5	16.30 ^a	2.65 ^d	0.33 ^b
*SD	0.507	0.287	0.471

a,b,c,d: The differences between the means indicated by different letters in the same column are significant ($P<0.01$); *SD: Standard deviation; LAB: Lactic acid bacteria; FM: Fresh material

Urea addition affected the LAB production of apple pulp silages. Depending on the dose of urea addition to apple pulp, the number of LAB increased significantly ($P<0.01$). In addition, adding urea to apple pulp silage decreased the number of yeast and mold ($P<0.01$). In addition, depending on the dose of urea addition to apple pulp, the number of yeast and mold significantly decreased ($P<0.01$). The most effective urea dose was 2.0% and above.

Effect of urea supplementation on aerobic stability of silage is given Table 4.

Table 4- Effect of urea supplementation on aerobic stability of silages

Urea Treatment (%)	pH	CO ₂ (g/kg DM)	Mold (cfu/g FM)
0.0	3.92 ^c	29.74 ^a	3.99 ^a
0.5	4.12 ^b	27.51 ^b	3.53 ^b
1.0	4.26 ^a	26.18 ^c	3.17 ^c
1.5	4.32 ^a	22.53 ^d	3.09 ^c
2.0	4.33 ^a	21.19 ^e	3.01 ^c
2.5	4.35 ^a	18.85 ^f	2.59 ^d
*SD	0.064	0.728	0.095

a,b,c,d,f: The differences between the means indicated by different letters in the same column are significant ($P<0.01$); *SD: Standard deviation; CO₂: Carbon dioxide; FM: Fresh material

Urea supplementation decreased ($P<0.01$) the CO₂ (g/kg DM) and mold number. The most effective urea dose on carbon dioxide (CO₂) and mold production was 2.5% and reduced these parameters.

Effect of urea supplementation on *in vitro* gas production, digestible organic matter and metabolic energy contents of apple pulp silages are given Table 5.

Table 5- Effect of urea supplementation on *in vitro* gas production, organic matter digestibility and metabolic energy contents of apple pulp silages

Urea treatment (%)	Gas production	OMD	ME
0.0	43.86 ^e	65.43 ^f	9.14 ^f
0.5	45.69 ^d	67.96 ^e	9.45 ^e
1.0	46.00 ^d	69.09 ^d	9.56 ^d
1.5	48.15 ^c	71.98 ^c	9.91 ^c
2.0	50.43 ^b	74.70 ^b	10.24 ^b
2.5	51.31 ^a	76.21 ^a	10.41 ^a
*SD	0.427	0.404	0.059

a,b,c,d,e,f: The differences between the means indicated by different letters in the same column are significant ($P<0.01$). *SD: Standard deviation; Gas production (mL/200 mg DM); OMD: Organic matter digestibility (%); ME: Metabolisable energy (ME/kg DM)

The gas production, OMD and ME contents of the resultant silage increased ($P<0.01$) in a dose dependent manner of urea. Depending on the urea dose added to the silage, *in vitro* gas production, ME and OMS increased, and the most effective urea dose was 2.5%.

4. Discussion

4.1. Chemical composition of feed and silages

Urea supplementation to apple pulp significantly increased CP content of silage ($P<0.01$). These results are consistent with those reported by Filya et al. (2004), Pirmohammadi et al. (2006), Celik et al. (2009) and Canbolat et al. (2014). Crude protein content of apple pulp silages obtained in the current study was lower than that reported by Islam et al. (2014) whereas it was higher than that reported by Kara et al. (2018). The differences among the studies might be associated with variety of apple used for pulp.

The addition of urea to apple pulp silage reduced the NDF, ADF and ADL contents of the silages ($P<0.01$). The decrease in the NDF, ADF and ADL content of the silages in the addition of urea to apple pulp can probably be attributed to an increase in the number of lactic acid bacteria (LAB) that use urea as a nitrogen source. It can be said that the amount of LAB in silage increases due to the breakdown of cell wall components.

Indeed, Filya et al. (2004), Canbolat et al. (2014) and Kang et al. (2018) explained that the decrease in the amount of NDF and ADF of the silage by increasing the number of lactic acid bacteria and some anaerobic bacteria in the silages of the nitrogen source urea, increasing the degradability of NDF, ADF and crude cellulose. Similar results Celik et al. (2009), Demirel and Yildiz. (2001) and Islam et al. (2014) were also reported by. Although the NDF and ADF content detected in apple pulp silage was lower than those determined by Fang et al. (2016), it was found higher than the data determined by Kara et al. (2018). The amount of NDF (45.3%) and ADF (38.0%) found in this study were similar to the data reported by Abdollahzadeh et al. (2010).

The addition of urea to the silage also significantly reduced the WSC content of the silages ($P < 0.01$). Increasing the amount of WSC in the feed structure improves the ensilability of the feeds (McDonald et al. 1991; Kaiser 2004; Canbolat et al. 2014). For lactic acid fermentation and development of LAB, the WSC content in the feed should be higher than 2.5% (Kaiser 2004). The high content of WSC (39.58%) in apple pulp increases the ensilability of apple pulp. Due to this feature, apple pulp is feed quite suitable for ensiling. The WSC content of apple pulp used in this study was lower than the values reported by Skinner et al. (2018) and similar to the research results reported by Islam et al. (2018a) ($40.4 \pm 0.4\%$). The water soluble carbohydrate content (39.58%) of apple pulp decreased significantly by fermentation in the silo. The addition of urea to apple pulp significantly reduced the WSC content of silages and regardless of that improved silage fermentation (Table 2). Findings in this research with apple pulp silage were similar to the results of Canbolat et al. (2014) working with pomegranate pulp silage.

4.2. Fermentation properties of silages

It was found that increasing doses of urea in apple pulp significantly affected the VFA contents of the silage ($P < 0.01$). With the greater content of urea in apple pulp silage, the amount of acetic acid, butyric acid and ethanol decreased, and the amount of lactic acid and propionic acid increased significantly ($P < 0.01$). In other words, the larger amounts of urea positively affected the fermentation of apple pulp silage.

One of the most important parameters that determine the quality of ensiled feeds is the lactic acid level. As the amount of lactic acid increases in ensiled silo feed, silage quality also increases (McDonald et al. 1991; Kaiser 2004). The addition of urea to ensiled apple pulp increased the amount of lactic acid by 2.5%, compared with ensiled material that was not supplemented with urea. The addition of urea to apple pulp silages increased the amount of lactic acid in by silage by about 29.28%. Increasing the urea dose decreased the amount of acetic acid (28.62%) and butyric acid (52.59%) of apple silage.

The high content of WSC (Table 1) of apple pulp increased lactic and propionic acid production and reduced butyric acid production in apple pulp silage (McDonald et al. 1991; Filya et al. 2004; Kaiser 2004; Yalcinkaya et al. 2012; Canbolat et al. 2014). It can be said that the addition of urea to apple pulp can provide high quality silages with high lactic and propionic acid content, as well as with low acetic and butyric acid content. It is reported that the addition of straw and urea to apple pulp increases the amount of lactic acid and decreases the amount of acetic acid and butyric acid (Yalcinkaya et al. 2012). These findings are similar to those of Canbolat et al. (2014), which added urea to pomegranate pulp silage and Filya et al. (2004)24, which added urea to corn silage.

The addition of urea to apple pulp significantly increased silage pH and ammonia nitrogen (NH_3N) ($P < 0.01$). Supplementation of urea to apple pulp increased the $\text{NH}_3\text{-N}$ content of silages by increasing proteolysis (Filya et al. 2004; Canbolat et al. 2014). In this way, it can be said that it causes nitrogen loss in ensiled feeds. The highest NH_3N was detected in apple pulp silage with 2.5% added urea. The amount of NH_3N detected in apple pulp silage was found similar to pomegranate pulp silage supplemented with urea (Canbolat et al. 2014).

The addition of urea has increased ammonia nitrogen, which is alkaline (Table 2). This situation increased the silage pH of apple pulp silages. However, the apple pulp silage pH remained at the recommended level for ensiled feeds (McDonald et al. 1991; Kaiser 2004). The highest pH was found in the apple pulp silage group, in which 2.5% urea was added. It has been demonstrated by many studies that urea increases pH in silo feeds (Filya et al. 2004; Celik et al. 2009; Canbolat et al. 2014, Kang et al. 2018).

4.3. Microbiological properties of silages

Adding urea to apple pulp has been found to affect and increase LAB values of apple pulp silage ($P < 0.01$). The highest LAB value was found in apple pulp silage with 2.5% urea added. Due to the increase in the urea dose added to apple pulp, the CP level of silages increased and the level of NDF and ADF decreased (Table 1). This provided more nutrients for LAB, and therefore LAB values in the silage increased. The LAB levels determined in this study were found to be higher than the values obtained from the studies of Filya et al. (2004) and Canbolat et al. (2014).

The use of urea in ensiled apple pulp caused a decrease in the number of yeast and mold of the silage ($P < 0.01$). The decrease in the number of yeast and mold effected the development of fermentation in the desired direction. It is also the result of the antifungal effect of urea by turning into ammonia in silage (Table 3) (McDonald et al. 1991; Filya et al. 2004; Canbolat et al.

2103). The numbers of yeasts and molds found in actual research were similar to the results reported by Filya et al. (2004) and Canbolat et al. (2014).

4.4. Aerobic stability characteristics of silages

The pH values were determined after the aerobic stability test of apple pulp silages. The pH in the control group was significantly higher than the other silage groups with urea supplemented ($P < 0.01$). Adding urea to ensiled material increased the pH value of silage. This increase can be explained by hydrolysis of urea to ammonia that increased the buffer capacity of silages (McDonald et al. 1991).

The addition of urea to apple pulp significantly reduced the CO_2 production of silages ($P < 0.01$). There was found the lowest value of CO_2 (18.85 g/kg DM) in the silage with the greater added amount of urea (2.5%). Due to the addition of urea, the CO_2 level decreased by about 36.62%. In this study, it can be said that 2.5% urea improves the aerobic stability of apple pulp silage. These research findings were similar to studies with urea added to the corn silage (Filya et al. 2004) and pomegranate pulp silage (Canbolat et al. 2014).

The addition of urea to apple pulp silages also significantly reduced the number of molds ($P < 0.01$). This indicates that the addition of urea to apple pulp will protect silage during feed (McDonald et al. 1991; Kaiser 2004).

4.5. *In vitro* gas production features of silages

Adding urea to apple pulp silage increased *in vitro* gas production ($P < 0.01$). The highest *in vitro* gas production was determined in the silage added with 2.5% urea and the lowest in the control group ($P < 0.01$). The addition of urea to apple pulp increased the CP content of silage and decreased the NDF and ADF content (Table 1), which likely could increase *in vitro* gas production. The effect of added urea to ensiled material has been demonstrated by studies in which *in vitro* gas production also was increased (Canbolat et al. 2014; Kang et al. 2018). *In vitro* gas production of apple pulp silages was lower than the results reported by Mirzaei-Aghsaghali et al. (2011). It was found to be higher than *in vitro* gas production reported by García-Rodríguez et al. (2019) in apple pulp. Determined values were higher than *in vitro* gas production detected in pomegranate pulp silage (Canbolat et al. 2014).

Supplementing urea to apple pulp increased the silage DOM and ME contents. This situation increased *in vitro* gas production (24 hours). As a result of increased *in vitro* gas production, there were increased the DOM and ME levels in apple pulp silages. This situation was found similar to the findings of Canbolat et al. (2014) adding urea to pomegranate pulp silage. In addition, Kang et al. (2018) reported that the supplementation of urea to cassava silage increased the DOM content of silages. Apple pulp ME contents were found similar to those reported by Pirmohammadi et al. (2006), Mirzaei-Aghsaghali et al. (2011) and García-Rodríguez et al. (2019).

The digestible organic matter content of apple pulp has been consistent with the research findings reported by Mirzaei-Aghsaghali et al. (2011), while the content of apple pulp silage DOM was higher than the results reported by Abdollahzadeh et al. (2010) and Kara et al. (2018).

5. Conclusions

As a result, it can be said that apple pulp is a quality silage material due to the high WSC content. It has been revealed that urea can be used as a nitrogen source in increasing the crude protein content of apple pulp. In addition, the supplementation of urea to ensiled apple pulp has been found to improve silage nutrient composition, fermentation properties, aerobic stability, *in vitro* gas production, DOM and ME levels. According to the findings obtained from the research, it was concluded that 2.5% urea can be used in apple pulp silage.

References

- Abdollahzadeh F, Pirmohammadi R, Farhoomand P, Fatehi F & Pazhoh F F (2010). The effect of ensiled mixed tomato and apple pomace on holstein dairy cow. *Italian Journal of Animal Science* 9(2): 212-216. <https://doi.org/10.4081/ijas.2010.e41>
- Afzal B Y, Ganai A M & Ahmad H A (2015). Utilisation of apple pomace as livestock feed: A review. *Indian Journal of Small Ruminants* 21(2): 165-179. <https://doi.org/10.5958/0973-9718.2015.00054.9>
- Ajila C M, Saurabh S J, Brar S K, Godbout S, Cote M, Guay F, Verma M & Valéro J R (2015). Fermented apple pomace as a feed additive to enhance growth performance of growing pigs and its effects on emissions. *Agriculture* 5(2): 313-329. <https://doi.org/10.3390/agriculture5020313>
- Alibes X, Munoz F & Rodríguez J (1984). Feeding value of apple pomace silage for sheep. *Animal Feed Science and Technology* 11(3): 189-197. [https://doi.org/10.1016/0377-8401\(84\)90062-2](https://doi.org/10.1016/0377-8401(84)90062-2)
- Anonymous (2022). Statistical tables. Fruits, nuts and beverage crops balance sheets. <https://data.tuik.gov.tr/Kategori/GetKategori?p=tarim-111&dil=1>
- AOAC (2000). Official Methods of Analysis, 17th Edition, Association of Official Analytical Chemist International, Washington DC.
- Ashbell G, Weinberg Z G, Azrieli A, Hen Y & Horev B (1991). A simple system to study the aerobic deterioration of silages. *Canadian Agricultural Engineering* 33: 391-393

- Barker S B & Summerson W H (1941). The colorimetric determination of lactic acid in biological material. *Journal of Biological Chemistry* 138(2): 535-554. [https://doi.org/10.1016/s0021-9258\(18\)51379-x](https://doi.org/10.1016/s0021-9258(18)51379-x)
- Canbolat Ö, Kamalak A & Kara H (2014). The effects of urea supplementation on pomegranate pulp (*Punica granatum L.*) silage fermentation, aerobic stability and in vitro gas production. *Ankara Üniversitesi Veteriner Fakültesi Dergisi* 61 (3): 217-223
- Carson K J, Collins J L & Penfield M P (1994). Unrefined, dried apple pomace as a potential food ingredient. *Journal of Food Science* 59(6): 1213-1215. <https://doi.org/10.1111/j.1365-2621.1994.tb14679.x>
- Celik S, Budag C, Demirel M, Bakici Y & Celik S (2009). The Effects of adding urea and molasses to corn harvested at dough stage on silage fermentation quality, in vitro organic matter digestibility and metabolic energy contents. *Journal of Animal and Veterinary Advances* 8(10): 1921-1924
- Demirel M. & Yildiz S (2001). The effect of whole-crop barley harvested at milk stage by adding urea and molasses on silage quality and nutrient degradability in the rumen. *Yuzuncu Yil University Journal of Agricultural Sciences* 11(1): 55-62
- Dubois M, Giles K A, Hamilton J K, Rebes P A & Smith F (1956). Colorimetric method for determination of sugars and related substances. *Analytical Chemistry* 28(3): 350-356. <https://doi.org/10.1021/ac60111a017>
- Fang J, Cao Y, Matsuzaki M, Suzuki H & Kimura H (2016). Effects of apple pomace-mixed silage on growth performance and meat quality in finishing pigs. *Animal Science Journal* 87(12): 1516-1521. <https://doi.org/10.1111/asj.12601>
- Filya I, Sucu E & Hanoğlu H (2004). Effects of urea application on the silage fermentation, aerobic stability ruminal degradability and fattening performance of lambs. *Journal of Agricultural Sciences* 10 (3): 258-262
- Fontenot J P, Bovard K P, Oltjen R R, Rumsey T S & Priode B M (1977). Supplementation of apple pomace with non-protein nitrogen for gestating beef cows. Feed intake and performance. *Journal of Animal Science* 45(3): 513-522. <https://doi.org/10.2527/jas1977.453513x>
- García-Rodríguez J, Ranilla M J, France J, Alaiz-Moretón H, Carro M D & López S (2019). Chemical composition, in vitro digestibility and rumen fermentation kinetics of agro-industrial by-products. *Animals* 9(11): 1-13. <https://doi.org/10.3390/ani9110861>
- Gasa J, Castrillo C, Guada J A & Balcells J (1992). Rumen digestion of ensiled apple pomace in sheep: effect of proportion in diet and source of nitrogen supplementation. *Animal Feed Science and Technology* 39(3-4): 193-207. [https://doi.org/10.1016/0377-8401\(92\)90041-4](https://doi.org/10.1016/0377-8401(92)90041-4)
- Islam S, Islam M & Matsuzaki M (2014). Apple pomace silage ethanol intake and its effect on sheep. *Bangladesh Journal of Animal Science* 43(3): 224-231. <https://doi.org/10.3329/bjas.v43i3.21655>
- Islam S, Islam M N & Matsuzaki M (2018a). Nutritive value of fermented apple pomace silage and its effect in Suffolk ewes. *Journal of Agricultural Science and Food Technology* 4(4): 80-91
- Islam S, Islam M N & Matsuzaki M (2018b). Effect of apple pomace silage on blood parameters in Suffolk ewe. *Bangladesh Journal of Animal Science* 47(2): 51-60. <https://doi.org/10.3329/bjas.v47i2.40234>
- Kaiser A G (2004). Silage additives. Chapter 7 in *Successful Silage*. Kaiser AG, Piltz JW, Burns HM, Griffiths NW. (eds). Dairy Australia and New South Wales Department of Primary Industries. New South Wales, Australia.
- Kang S, Wanapat M & Nunoi A (2018). Effect of urea and molasses supplementation on quality of cassava top silage. *Journal of Agricultural Science and Food Technology* 27(1): 74-80. <https://doi.org/10.22358/jafs/85544/2018>
- Kara K, Kocaoğlu Guclu B, Baytok E, Aktug E, Karakas Oguz F, Kamalak A & Atalay A I (2018). Investigation in terms of digestive values, silages quality and nutrient content of the using pomegranate pomace in the ensiling of apple pomace with high moisture contents. *Journal of Applied Animal Research* 46(1): 1233-1241. <https://doi.org/10.1080/09712119.2018.1490300>
- Kennedy M, List D, Lu Y, Newman R H, Sims I M & Bain P J S (1999). Apple pomace and products derived from apple pomace: uses, composition and analysis. In: *Analysis of Plant Waste Materials*, vol. 20. Springer-Verlag, Berlin, pp. 75-119
- MAFF (Ministry of Agriculture, Fisheries and Food) (1984). *Energy allowances and feeding systems for ruminants*, ADAS Reference Book 433, HMSO, London
- McDonald P, Henderson A R & Heron S J E (1991). *The Biochemistry of Silage* (2nd ed.). Chalcombe Publ., Church Lane, Kingston, Canterbury, Kent, UK.
- Menke K H & Steingass H (1988). Estimation of the energetic feed value obtained from chemical analysis and in vitro gas production using rumen fluid. *Animal Research and Development* (28): 7-55
- Menke K H, Raab L, Salewski A, Steingass H, Fritz D & Schneider W (1979). The estimation of the digestibility and metabolizable energy content of ruminant feedingstuffs from the gas production when they are incubated with rumen liquor in vitro. *Journal of Agricultural Science* 93(1): 217-222. <https://doi.org/10.1017/s0021859600086305>
- Minitab (2013). Minitab® 17 Statistical Software.
- Mirzaei-Aghsaghali A, Maheri-Sis N, Mansouri H, Razeghi ME, Shayegh J & Aghajanzadeh-Golshani A. (2011). Evaluating nutritional value of apple pomace for ruminants using in vitro gas production technique. *Annals of Biological Research* 2(1):100-106
- NRC (National Research Council). (2001). *Nutrient Requirements of Dairy Cattle*. 7th revised edn. National Research Council, National Academy of Sciences, Washington, D.C., U.S.A.
- Pirmohammadi R, Rouzbahan Y, Rezayazdi K & Zahedifar M (2006). Chemical composition, digestibility and in situ degradability of dried and ensiled apple pomace and maize silage. *Small Ruminant Research* 66(1-3): 150-155. <https://doi.org/10.1016/j.smallrumres.2005.07.054>
- Rumsey T (1978). Ruminant fermentation products and plasma ammonia of fistulated steers fed apple pomace-urea diets. *Journal of Animal Science* 47(4): 967-976. <https://doi.org/10.2527/jas1978.474967x>
- Seale D R, Pahlow G, Spoelstra S F, Lindgren S, Dellaglio F & Lowe J F (1990). Methods for the microbiological analysis of silage. *Proceeding of The Eurobac Conference*, 147, Uppsala.
- Singhal K K, Thakur S S & Sharma D D (1991). Nutritive value of dried and stored apple pomace and its further processing for improved utilization. *Indian Journal of Animal Nutrition* 8(3): 213-216
- Skinner R C, Gigliotti J C, Ku K M & Tou J C (2018). A comprehensive analysis of the composition, health benefits, and safety of apple pomace. *Nutrition Reviews* 76(12): 893-909. <https://doi.org/10.1093/nutrit/nuy033>
- Snedecor G W & Cochran W (1976). *Statistical methods*. The Iowa State Univ. Pres Amer IA.
- Taasoli G & Kafilzadeh F (2008). Effects of Dried and Ensiled Apple Pomace from Puree Making on Performance of Finishing Lambs. *Pakistan Journal of Biological Sciences* 11(2): 294-297. <https://doi.org/10.3923/pjbs.2008.294.297>
- Van Soest P J, Robertson J B & Lewis B.A. (1991). Methods for dietary fiber, neutral detergent fiber, and non-starch polysaccharides in relation to animal nutrition. *Journal of Dairy Science* 74(10): 3583-3597. [https://doi.org/10.3168/jds.s0022-0302\(91\)78551-2](https://doi.org/10.3168/jds.s0022-0302(91)78551-2)
- Varzakas T, Zakyntinos G & Verpoort F (2016). Plant Food Residues as a Source of Nutraceuticals and Functional Foods. *Foods* 5(4): 1-32. <https://doi.org/10.3390/foods5040088>
- Vrhovsek U, Rigo A, Tonon D & Mattivi F (2004). Quantitation of polyphenols in different apple varieties. *Journal of Agricultural and Food Chemistry* 52(21): 6532-6538. <https://doi.org/10.1021/jf049317z>

- Wolter R, Durix A, Letourneau J C, Carcelen M & Veis T (1980). Estimation of total digestibility of soybean hulls, apple pomace, carob husk, grape seed oil meal. *Annales de zootechnie* 29(4): 377-385
- Yalcinkaya M Y, Baytok E & Yörük. (2012). Some Physical and Chemical Properties of Different Fruit Pulp Silages. *Journal of The Faculty of Veterinary Medicine Erciyes University* 9(2): 95-106



© 2022 by the author(s). Published by Ankara University, Faculty of Agriculture, Ankara, Turkey. This is an Open Access article distributed under the terms and conditions of the Creative Commons Attribution (CC BY) license (<http://creativecommons.org/licenses/by/4.0/>), which permits unrestricted use, distribution, and reproduction in any medium, provided the original work is properly cited.



Development of an IoT-Based (LoRaWAN) Tractor Tracking System

Çağdaş CİVELEK ^{a*}

^aÇukurova University, Faculty of Agriculture, Agricultural Machinery and Technologies Engineering Department, Sarıcam, Adana, TURKEY

ARTICLE INFO

Research Article

Corresponding Author: Çağdaş CİVELEK, E-mail: ccivelek@cu.edu.tr

Received: 14 July 2020/ Revised: 05 August 2021/ Accepted: 05 August 2021/ Online: 01 September 2022

Cite this article

CİVELEK Ç (2022). Development of an IoT-Based (LoRaWAN) Tractor Tracking System. *Journal of Agricultural Sciences (Tarim Bilimleri Dergisi)*, 28(3):438-448. DOI: 10.15832/ankutbd.769200

ABSTRACT

The use of new technologies and precision agriculture (PA) in farms has become more important due to the need for enough agricultural production for increasing world population opposed to decreasing farm areas. PA covers wide range of technologies like sensors, microcontroller-based devices, machine to machine communication technologies, global positioning systems but, the investment costs of these devices are literally expensive which become a constraint for farmers especially in developing countries. Internet of things (IoT) technology is a new era that agricultural production will be the one area

mostly affected by. LoRaWAN is one of the new communication technologies for IoT which enables almost everything on the planet to be connected to internet and deliver high amount of data with no expense. In this research by using the advantages of LoRaWAN, a new IoT-based tractor tracking system including a LoRaWAN module and a web-based software was developed, and the test results were evaluated. As a result, it was found that the developed system was capable of measuring and sending tractor sensor data along with geospatial position of the tractor and serving the data on the web-based user interface.

Keywords: Tractor tracking, Asset tracking, Precision farming, LPWAN, IoT technology

1. Introduction

The world population is expected to reach 9 billion people in 2050, and today's 3.75 tons per hectare of wheat production should be as high as 6.25 tons per hectare (Meola 2017). This projection necessitates a 70% wheat production yield increase to feed that much population by 2050 however, it becomes more difficult to achieve this projection in countries where average farm areas are very small, the yield is low and PA technology use in farms is weak.

Pierce & Novak (1999) have defined the PA as doing the right thing, in the right place and on the right time. Without enabling precision agriculture in the farms, yield and quality losses are inevitable. So, new technologies should be integrated into agricultural machines to implement PA to the farms to produce higher quantity and quality of product despite of the fact that the farm areas are consistently decreasing.

Tractors are the main power source in the farms so, new technologies should be integrated on them at first to make the farm practices more efficient. However, developing countries have huge barriers to implement new technologies on their tractors. In these countries, farmers' income is very low which forces farmers to use very old tractors that are incompatible to use with new high-tech PA devices (Onwunde et al. 2018). On the contrary, in developed countries farms are so big that farmers can use new high-technology tractors with several sensors and GPS (global positioning system) implemented.

In USA it is known that GNSS (global navigation satellite systems) technologies are used by more than 80% of farmers, and the use of GPS-based automatic steering systems has moved from 6% to 78% from 2005 to 2017 which requires the use of newer tractors (Erickson et al. 2017). Moreover, the use of precision farming technologies has reached 35% in Europe (Das et al 2019). In Turkey more than 45% of 1.8 million tractors (Turkish Statistical Institute 2019a) are more than 25 years old, and 21.4% of all are more than 10 years old (Turkish Statistical Institute 2019b) which makes the integration of PA technology on tractors very difficult. The farms in Adana region could be a good example of the need for implementation of new technologies on tractors however, farmers are having difficulty to invest in these devices. According to the survey that was done in Adana region with seven big farms, each one having more than 50 hectares of arable land and 3 tractors, it was revealed that in none of them PA technology was used on tractors (Civelek 2020). In a recent study to determine farmers' aim to use auto guidance systems in Adana region, it was found out that 96.4% of the farmers did not use PA technologies, since they did not know about it (Keskin et al. 2018). In another research had been conducted in the same region, however 35.9% of the farmers did not know about PA,

92.3% of them reported that they had followed new trends in agriculture, yet 61.5% of them were interested in satellite positioning systems on the contrary not being interested in automatic steering or variable rate application systems by 38.5% and 28.2%, respectively (Keskin & Sekerli 2016). The results of the last survey in the same region showed that besides most of the participated farmers were using computer and smart phones, none of them had unmanned vehicles, whereas 3 out of 422 farmers were using sensor equipped machinery (Saygılı et al. 2020).

Today's information technology covers digitalization, big data, IoT and blockchain, and IoT is expected to have the biggest effect on agriculture. European Commission declares that the development of digitalization in agriculture depends on connecting tractors to the internet using IoT technology either using 2G or LPWAN (low-power wide area network) which have advantages like wide coverage area and low-investment costs (European Commission 2017). In the literature several studies were found based on the integration of IoT into agriculture. Some of these studies were solar-powered automated IoT-based drip irrigation system (Barman et al. 2020), IoT-based soil health monitoring and recommendation system (Bhatnagar & Chandra 2020), IoT-based technology for low-cost precision apiculture (Dasig Jr. & Mendez 2020), IoT-based smart tree management (Shabandri & Madara 2020) and frost prediction in highland crops management using IoT (Mendez & Dasig 2020) in which the importance of integration IoT in agriculture was emphasized. However, from the literature research no evidence could be found related to the use of IoT technology on tractors. LoRaWAN communication technology was used on the hardware because of having several advantages over other IoT-based communication technologies, like transmitting data up to 5 km urban and 15 km in suburban areas and no registration requirement which makes it free to use (Davcev et al. 2018; Sahana et al. 2020). The main objective of this manuscript was to explain the adoption easiness, performance, production and purchasing costs, and advantages of the developed IoT-based tractor tracking system consists of a hardware and a software.

2. Material and Methods

2.1. Materials

Proposed IoT-based tractor tracking system was designed to provide farmers to track and analyze tractor performance data along with geospatial data. Overall design of the system consisted of two parts which were hardware and software.

The hardware was designed to connect several sensors such as fuel flow meter and PTO (power take off) torque meter sensors to measure fuel consumption and PTO power use. The hardware also had a GPS module to get geospatial position of the tractor on the farm using GPS satellites. All these tractor performance data were combined and sent to a server on the cloud using LoRaWAN protocol (Figure 1). One of the reasons for using LoRaWAN was that in several places of rural areas GSM (global system for mobile communication) base station coverage area is not enough which results in no internet connection.

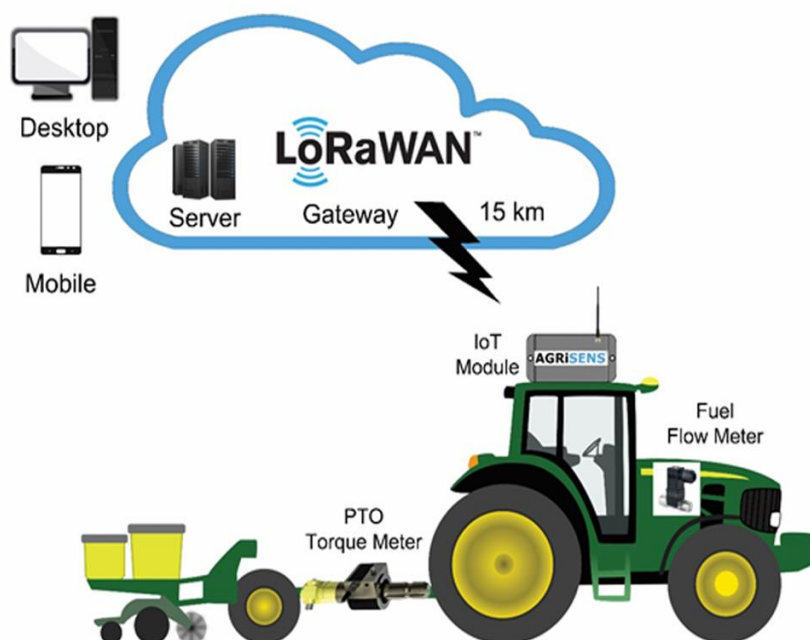


Figure 1- General view of the designed system

Hardware's circuit diagram and the design of the motherboard were developed using Proteus software. The design of the PCB (printed circuit board) required to select proper electronic components like resistance, capacitance, crystal, regulator and microprocessors. Selected components were placed and connected to each other based on the requirements of the hardware and short-circuit tests were also conducted on the Proteus, and then PCB was produced based on the overall design (Figure 2 and 3).

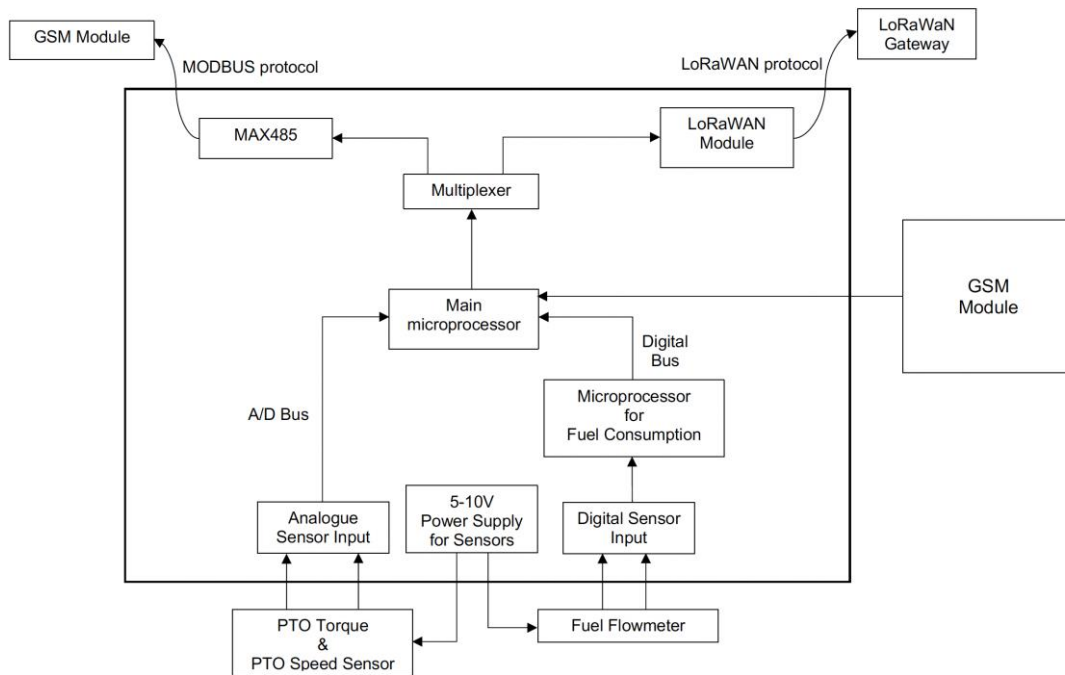


Figure 2- Design scheme of the developed hardware



Figure 3- Developed hardware (Patent pending, under Turkish Patent Institute, patent no. 2020/04858)

Microchip's PIC18F46K22 microprocessor was used as the main microprocessor of the developed hardware. Used microprocessor was capable of gathering and processing data using ADC (analogue digital converter) on which several sensors were connected.

Microchip's RN2483 LoRaWAN modulation module was used as the data transmission module to send data to the developed database on the cloud. This module was capable of sending data using either using 868 MHz frequency for Europe or 936 MHz frequency for USA.

A MODBUS communication port was also added onto the PCB for connecting a GSM module to maintain connection of the hardware to the internet where LoRaWAN communication is unavailable. For using MODBUS protocol, a MAX487 transceiver was embedded onto the motherboard. This transceiver was capable of transmitting gathered and processed data to the main microprocessor using MODBUS protocol via RS-485 port.

TELIT's SE868K7-A GPS module was chosen to get the real position data of the tractor (Figure 4). Small one-sided PCB was developed using Proteus software to integrate GPS module and to connect it to the motherboard over connection pins using 4-pin cable. The GPS module was controlled by the main microprocessor. GPS data was received in different modes by the module. After the module had fixed to the required GPS satellites, the data flowed in a row, delivered to the main microprocessor, and the data was parsed by the developed embedded software running in the main microprocessor. Using the parsed data, latitude, longitude and speed values were gathered with the sensor data.



Figure 4- GPS module for tracking global position of the tractor

Example: \$GPRMC,084722.000,A,3702.5115,N,03521.6524,E,0.17,206.91,270219,,A*66

2 analogue and 2 digital I/O (input output) ports were added onto the developed PCB to connect different sensors to the developed hardware. Analogue ports were added to connect PTO torque meter to measure the torque and the speed of the PTO for calculation of the required power by the machine attached to the tractor, whereas digital input ports were added to connect two fuel flow meters, one for consumed fuel and the other one for returning fuel to tank from injectors, so that the fuel consumption could be calculated. The module was designed to run with a 3.3V battery to send the geospatial position of the tractor even when the engine was not running. Since most of the sensors needed higher voltage than the motherboard's supply voltage, tractor's battery was also used to supply energy for the sensors. To achieve this, a power connection port was added onto the developed hardware to energize the sensors. With the used 7805CV regulator on the developed PCB, 5V or 12V DC power could be supplied to the hardware based on the voltage required by the sensors.

A PIC16F1826 microprocessor was also embedded onto the motherboard to record and send fuel flow meters' data in case of an unexpected cut down on the energy supplied from the tractor's accumulator due to a sudden stop of the engine. At the time of an energy loss, energy was supplied to the hardware for several milliseconds by a capacitor that was soldered onto the motherboard so that the PIC16F1826 microprocessor had enough time to calculate the last measured fuel flow and send it to the main microprocessor.

The main microprocessor's embedded software was written using CCS C compiler and then it was programmed using Microchip Pickit3 circuit debugger. After the microprocessor was programmed, it was put under debugging test circle to find out and correct software errors using MPLAB software using the circuit debugger.

To deliver the data from the developed hardware to the database on the cloud, Kerlink's Wirnet Station gateway was used in the trials (Figure 5). Used gateway was capable to use whether 868 or 925 MHz frequencies for connection, more than 15 km coverage range, easy installation, and low-power consumption.



Figure 5- LoRaWAN gateway for data transmission

The developed web-based software was consisted of front-end interface, back-end interface, and a database. A database was developed using MySQL to store the data that was sent by the developed hardware to the cloud. The database was capable of storing user information along with farm area, tractor and machine make and models, and also several tractor performance data tables were included, such as Nebraska tractor performance test results to be used as a guidance for farmers to select their tractors.

The front-end interface of the software was developed on the web basis to provide flexibility for the user to get access from any type of device, such as mobile phone, tablet or PC. So, it was developed using HTML (hypertext markup language) and PHP (hypertext pre-processor) programming languages. To record data sent by the hardware to the database, an algorithm was developed using JSON (java script object notation) format using PHP (Algorithm 1). When a data packet was sent by the developed hardware over the gateway, the developed PHP file was triggered, and the data was recorded into the database. Data packet was sent in a combined format including developed module's data such as used identifier, battery status, used frequency, date, RSSI (received signal strength), SNR (signal to noise ratio) values and transmitted tractor performance and GPS data. When the developed PHP file was triggered, combined data was parsed into the blocks and recorded corresponding header of the table in the database.

Algorithm 1- Developed data recording algorithm

```
<?php
include 'databaseconnect.php';
$request=file_get_contents('php://input');
$input=json_decode($request,TRUE);
$cmd=$input['cmd'];
$EUI=$input['EUI'];
$ts=$input['ts'];
$ack=$input['ack'];
$seqno=$input['seqno'];
$fcnt=$input['fcnt'];
$port=$input['port'];
$bat=$input['bat'];
$data=$input['data'];
$freq=$input['freq'];
$dr=$input['dr'];
$rssi=$input['rssi'];
$toa=$input['toa'];
$snr=$input['snr'];
$date=time();
$query=mysqli_query($db,'INSERT INTO test2
(cmd,time,EUI,ts,ack,seqno,fcnt,port,bat,data,freq,dr,rssi,toa,snr)
VALUES
('".$cmd."','".$date."','".$EUI."','".$ts."','".$ack."','".$seqno."','".$fcnt."','".$port."','".$bat.'
','".$data."','".$freq."','".$dr."','".$rssi."','".$toa."','".$snr.'"));
?>
```

The developed software enabled users to create user accounts and add related tractors in their farms. After user had added the tractors, an EUI (extended unique identifier) was assigned to that tractor in related with the module attached onto the tractor. With this unique identifier, user could reach each tractor's performance data like tractor usage time, fuel consumption, power use and geospatial position of the tractor on the map. Also, the developed software was designed so as to enable user to enter data based on farm area size, tractor and machine make and models. Since the LoRaWAN protocol allowed to send maximum 18-byte data in each 2.5 minutes, whole tractor performance and geospatial position data was recorded into the database in hexadecimal format. When the end-user requested to see the related data, a developed PHP file was triggered to convert recorded data from hexadecimal to decimal format and shown on the web page (Algorithm 2).

Algorithm 2- Data conversion algorithm for front-end user

```

<?php
echo '<table align="center" border="0" class="dashboard"><tr>';
echo '<th>Show postion</th>';
echo '<th>Date</th>';
echo '<th>EUI</th>';
echo '<th>LAT</th>';
echo '<th>LON</th>';
echo '<th>Speed<br>(km/h)</th>';
echo '<th>Torque<br>(Nm)</th>';
echo '<th>PTO Speed<br>(1/min)</th>';
echo '<th>Power<br>(kW)</th>';
echo '<th>Fuel Consumption<br>(L/h)</th></tr>';
$coef = 1;
$query = mysqli_query($db, 'SELECT * FROM table WHERE EUI="'.$_GET['tractoreui'].'"
ORDER BY id DESC LIMIT 50');
mysqli_set_charset($db, "utf8");
while ($row = mysqli_fetch_array($query)) {
    echo '<tr>';
    echo '<td><form action="map.php" method="post"><input type="hidden" name="id"
value="'.$row['id'].'"><button name="map">Position</button></form></td>';
    $date = date('d-m-Y H:i:s', $row['time']);
    echo '<td>' . $date . '</td>';
    echo '<td>' . $row['EUI'] . '</td>';
    $data = $row['data'];
    $dataarray = array(substr($data, 0, 4),substr($data, 4, 4),substr($data, 8, 4),substr($data, 12,
4),substr($data, 16, 4),substr($data, 20, 4),substr($data, 24, 4),substr($data, 28,
4),substr($data, 32, 2),substr($data, 34, 2),);
    $val0 = (hexdec($dataarray[0])) * $coef;
    $val1 = (hexdec($dataarray[1])) * $coef;
    $val2 = (hexdec($dataarray[2])) * $coef;
    $val3 = (hexdec($dataarray[3])) * $coef;
    $val4 = (hexdec($dataarray[4])) * $coef;
    $val5 = (hexdec($dataarray[5])) * $coef;
    $val6 = (hexdec($dataarray[6])) * $coef;
    $val7 = (hexdec($dataarray[7])) * $coef;
    $val8 = (hexdec($dataarray[8])) * $coef;
    $val9 = (hexdec($dataarray[9])) * $coef;
    echo '<td>' . round($val0, 2) . '</td>';
    echo '<td>' . round($val1, 2) . '</td>';
    $lat=($val0*1000+$val1)/100000;
    $lon=($val2*1000+$val3)/100000;
    echo '<td>' . $lat.chr($val4). '</td>';
    echo '<td>' . $lon.chr($val5). '</td>';
    echo '<td>' . round($val6, 2) . '</td>';
    echo '<td>' . round($val7, 2) . '</td>';
    $power=$val6*$val7/9550;
    echo '<td>' . $power. '</td>';
    echo '<td>' . (($val8*65535)+$val9). '</td>';
    echo '</tr>';
}
echo '</table>';
?>

```

2.2. Methods

As the developed hardware had 2 analogue ports for measurement of the tractor PTO torque and speed and 2 digital ports for connecting two fuel flowmeters, the measurement reliability tests of the hardware should have been done in laboratory tests. The hardware was put under calibration tests using these connection ports. For analogue port tests, voltages between 1 to 10V by 0.02V step increments were applied each port using AA Tech ADC-3303 voltage generator, measurements were read using a Fluke 17B+ multimeter, recorded in an Excel sheet, and evaluated statistically.

For the calibration of the digital ports, pulses for different frequencies were applied to digital ports using UNI-T make UTG9005C model pulse generator. 10 measurements were taken in each 30 seconds for 6 different frequencies which were 4, 10, 50, 1000, 16000 and 32000 Hz, respectively.

For continuous data transmission and battery drain tests, the developed hardware was left in the laboratory sending data packages in every 2.5 minutes until the battery fully drained. The data packages were analyzed at the end of the battery life, and by using the time data recorded into the database battery life was calculated.

For data transmission and GPS tests, Kerlink's Winet Station gateway was set up outside of the laboratory. For GPS data gathering and transmission tests, the developed hardware was taken several places in Cukurova University Campus. Data packages sent and recorded into the database by the developed hardware were analyzed. Developed web-based software was used to confirm the data package and reliability of the front-end user interface as shown in Figure 6. Tractor's geospatial data was also checked in the front-end user interface according to the related data point (Figure 7). Lastly, SNR (signal to noise ratio) values were gathered and analyzed in the data transmission tests.

The developed hardware's bill of materials (BOM) was also calculated to compare the affordability of the developed hardware with other devices available in the market.

Date	EUI	LON	LAT	Speed (km/h)	Torque (Nm)	PTO Speed (1/min)	Power (kW)	Fuel Consumption (L/h)
2019-10-17 10:32:10	01-AC-1A-6A	35.3802143033490700	37.0339733622635800	0.7300	26.7760	452.5030	1.2700	0.0000
2019-10-17 10:32:10	01-AC-1A-6A	35.3802936355921300	37.0340480878807700	3.6900	135.2200	451.7810	6.4000	0.0000
2019-10-17 10:32:10	01-AC-1A-6A	35.3803464217200300	37.0340978126449700	-0.1500	-5.3490	444.3950	-0.2500	0.0000
2019-10-17 10:32:10	01-AC-1A-6A	35.3803991278397500	37.0341474612389900	2.9500	108.0480	454.5770	5.1400	0.0000
2019-10-17 10:32:10	01-AC-1A-6A	35.3804254543910700	37.0341722643516200	0.1600	5.8950	449.3630	0.2800	0.0000
2019-10-17 10:32:10	01-AC-1A-6A	35.3805043415130000	37.0342466236715800	1.8800	68.6890	451.4420	3.2500	0.0000
2019-10-17 10:32:10	01-AC-1A-6A	35.3806093734203900	37.0343457822708300	-0.0400	-1.5050	446.4390	-0.0700	0.0000
2019-10-17 10:32:10	01-AC-1A-6A	35.3807053412623300	37.0344363830520800	2.5000	91.4050	451.4480	4.3200	0.0000
2019-10-17 10:32:10	01-AC-1A-6A	35.3808369037815400	37.0345442918182400	1.3100	47.8670	452.6280	2.2700	0.0000
2019-10-17 10:32:10	01-AC-1A-6A	35.3808974956543500	37.0346013718246200	0.7400	27.2240	450.3900	1.2800	0.0000
2019-10-17 10:32:10	01-AC-1A-6A	35.3809838659392400	37.0346827488100000	0.8600	31.3790	448.7540	1.4700	0.0000

Figure 6- Front-end presentation of the developed web-based software (Power equals to PTO power)

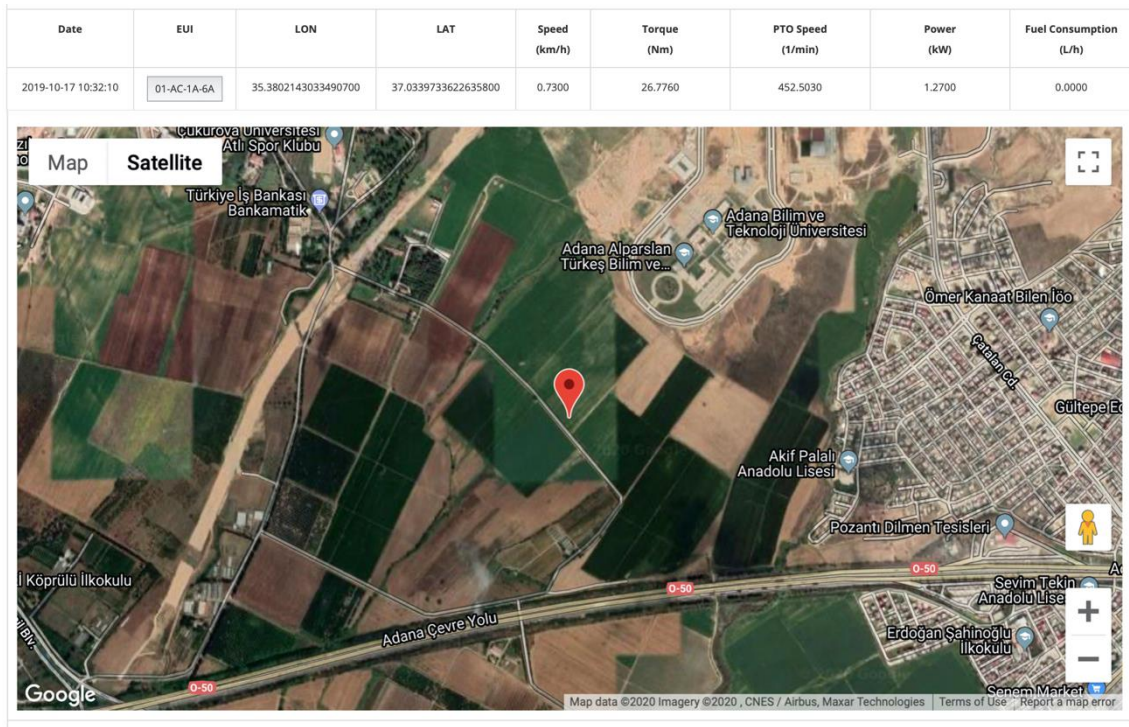


Figure 7- Presentation of tractor position and basic data on the map

3. Results and Discussion

For analogue port calibration tests 451 data points were gathered between 1-10V. The results of the regression analyze according to the analogue sensor test were given in Table 1. The ANOVA results showed that the measured voltage had a linear increment with R^2 value of 0.99. Using gathered test data, a calibration formula was developed (Equation 1), and the main microprocessor was programmed using this formula to measure correct values for analogue ports. In the Equation 1, y is defined as applied voltage and x is the voltage measured by the developed hardware.

$$y = 0.01737357 + 0.000189173 \times x \quad (\text{Eq.1})$$

Table 1- Regression analyze results of the analogue ports

Result	Degrees of freedom	Multiple R	R square	Standard Error	Observations
Linear	1	0.999997514	0.999995029	0.005818474	451

For digital port calibration tests, the difference of the last recorded two pulses was calculated so that the exact pulse number could be found for 30 seconds. It was found that the difference of the pulses for each measurement points in each frequency range had a linear differentiation (Figure 8). Regression analyses showed that the changes in each 30 seconds of measurement points were linear with R^2 value of 0.99 for each frequency (Table 2).

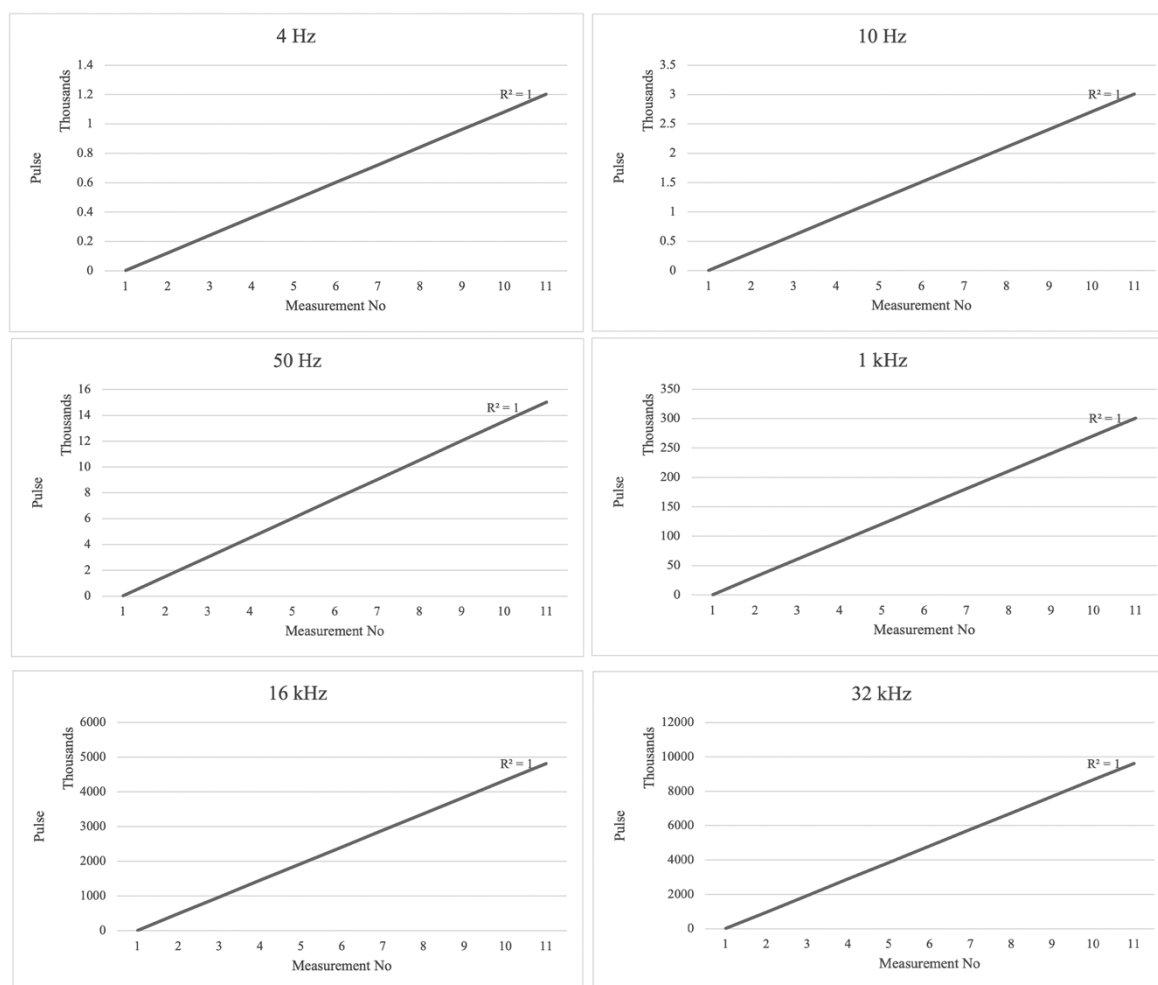


Figure 8- Digital channel calibration trial results of the developed hardware

Table 2- Regression analysis results of digital channels

Frequency (Hz)	R Square	Significance F
4	0.994	$1.6 \cdot 10^{-11}$
10	0.994	$1.61 \cdot 10^{-11}$
50	0.993	$1.64 \cdot 10^{-11}$
1000	0.994	$1.52 \cdot 10^{-11}$
16000	0.994	$1.62 \cdot 10^{-11}$
32000	0.994	$1.59 \cdot 10^{-11}$

Data transmission and battery drain tests were also conducted to measure reliability of the developed hardware. To achieve this, the hardware was left to send dummy data to be saved in the developed database. Two trials were ended in total 6 months, the hardware created 49121 and 52766 data points, and the batteries were drained in 95 and 98 days which confirms the assumptions that were given in by Aqeel-Ur-Rehman et al. (2014).

From the GPS tests that were conducted outside of the laboratory it was revealed that the position of the developed hardware was sensed with a maximum 3 meters of error which was declared by the producer of the GPS module. At the time of these tests, SNR values of the data sent by the hardware was also measured and analyzed. Average SNR value was found to be -11.13 ± 1.21 dB (0.95 confidence interval) with 2.47 standard deviation which showed similar results with the LoRaWAN-based IoT device developed for personal mobility vehicles by Santa et al. (2019).

From the BOM costs calculations, it was found out that the hardware could be produced for \$55 including PCB manufacturing costs and taxes, excluding software development for the hardware according to prices in May 2020. When one of the tractor manufacturer's 4G LTE (long-term evolution) based unused device price was considered, which was \$795 in the same date including taxes and excluding subscription to the service, it was evaluated that the IoT-based devices could be produced cheaper than commercially available ones. This situation concludes that IoT-based tractor tracking devices could be competitive to the

4G LTE-based ones. However, according to the information gathered from dealers, when commercially available devices were compared with the developed hardware, it was found that some of these devices cannot meet the communication frequency regulations declared by the government in every country, so that the farmers cannot use these devices on their tractors even if they could have afforded.

4. Conclusions

With the study it was revealed that an IoT-based tractor-tracking system for tracking of the performance and geospatial position of the tractor could be produced with a low production cost. The test results for the measurement reliability of the developed hardware showed that the data gathered from the sensors attached to the tractor could be measured with high sensitivity. The gathered data could be transferred to the database on the cloud and showed on the web-based interface. The LoRaWAN communication technology used in the developed hardware had an advantage over GSM communication technologies not only by providing data transmission with no expense but also using a free communication frequency which has no restriction or need any license to use.

The developed system in this research was not only low cost but also scalable. The developed database and web-based user interface are compatible with different sensors using LoRaWAN technology and communication protocol so, different sensors, such as soil moisture and temperature, could be set up in the farm and the data could be tracked using the developed software. When the necessity to achieve high yield and quality of agricultural products to feed increasing world population, it is clear that using newer technologies on tractors and agricultural machines is inevitable so, the developed system has an advantage for enabling farmers to purchase and adopt their tractors to use precision agriculture techniques in their farms, especially for developing countries.

As a future study, the developed hardware has been being tested on a farm, and the gathered data is being analyzed for further development of the web-based interface by using mathematical models and embedding artificial intelligence for providing farmers to make detailed analyzes.

Acknowledgments

This study was financially supported by The Scientific and Technological Research Council of Turkey (TÜBİTAK) under the Project number 2170351.

Abbreviations and Symbols

ADC	Analogue digital channels
AI	Artificial intelligence
BOM	Bill of materials
EUI	Extended unique identifier
GNSS	Global navigation satellite system
GPS	Global positioning system
GSM	Global system for mobile communication
HTML	Hypertext markup language
I/O	Input output
IoT	Internet of things
ISM	Industrial scientific and medical
JSON	Java script object notation
LPWAN	Low-power wide area network
LTE	Long term evolution
MHz	Megahertz
PA	Precision agriculture
PCB	Printed circuit board
PHP	Hypertext preprocessor
PTO	Power take off
RSSI	Received signal strength indicator
SNR	Signal to noise ratio

References

- Aqeel-Ur-Rehman Abbasi A Z, Islam N & Shaikh Z A (2014). A review of wireless sensors and networks' applications in agriculture. *Computer Standards and Interfaces* 36(2): 263-270. <https://doi.org/10.1016/j.csi.2011.03.004>
- Barman A, Neogi B & Pal S (2020). Solar-powered automated IoT-based drip irrigation system. *IoT and Analytics for Agriculture, Studies in Big Data* 63: 27-49. https://doi.org/10.1007/978-981-13-9177-4_2

- Bhatnagar V & Chandra R (2020). IoT-based soil health monitoring and recommendation system. *IoT and Analytics for Agriculture*, Vol. 2, *Studies in Big Data* 67: 1-21. https://doi.org/10.1007/978-981-15-0663-5_1https://doi.org/10.1007/978-981-15-0663-5_1
- Civelek Ç (2020). Evaluation of internet of things (IoT) technology to be used as a precision agriculture solution for Turkey's agriculture. *Fresenius Environmental Bulletin* 29(07-A): 5689-5695
- Das V J, Sharma S & Kaushik A (2019). Views of Irish farmers on smart farming technologies: an observational study. *AgriEngineering* 1(2): 164-187. <https://doi.org/10.3390/agriengineering1020013>
- Dasig Jr D D & Mendez J M (2020). An IoT and wireless sensor network-based technology for a low-cost precision apiculture. *IoT and Analytics for Agriculture*, Vol. 2, *Studies in Big Data* 67: 23-44. https://doi.org/10.1007/978-981-15-0663-5_4
- Davcev D, Mitreski K, Trajkovic S, Nikolovski V & Koteli N (2018). IoT agriculture system based on LoRaWAN. 2018 14th IEEE International Workshop on Factory Communication Systems (WFCS), Imperia, Italy, 13-15 June 2018
- Erickson B, Lowenberg-De Boer J & Bradford J (2017). 2017 Precision agriculture dealership survey. *Departments of Agricultural Economics and Agronomy, Purdue University*
- European Commission (2017). Industry 4.0 in agriculture: Focus on IoT aspects. https://ec.europa.eu/growth/tools-databases/dem/monitor/sites/default/files/DTM_Agriculture%204.0%20IoT%20v1.pdf. (accessed 4 February 2020)
- Keskin M & Sekerli Y E (2016). Awareness and adoption of precision agriculture in the Cukurova region of Turkey. *Agronomy Research* 14(4): 1307-1320
- Keskin M, Say S M & Görücü Keskin S (2018). Farmers' experiences with GNSS-based tractor auto guidance in Adana province of Turkey. *Journal of Agricultural Faculty of Gaziosmanpaşa University* 35(2): 172-181
- Mendez J M & Dasig D D (2020). Frost prediction in highland crops management using IoT-enabled system and multiple regression. *IoT and Analytics for Agriculture*, Vol. 2, *Studies in Big Data* 67: 261-288. https://doi.org/10.1007/978-981-15-0663-5_13
- Meola A (2017). Why IoT, big data & smart farming are the future of agriculture. *Business Insider*. Available online: <http://www.businessinsider.com/internet-of-things-smart-agriculture-2016-10> (Last accessed 10 December 2017)
- Onwunde D I, Chen G, Hashim N, Esdale J R, Gomes C, Khaled A Y, Alonge A F & Ikrang E (2018). Mechanization of agricultural Production in developing countries. *Advances in Agricultural Machinery and Technologies*. Taylor and Francis Group, Boca Raton, Florida, USA. 472 pp. ISBN: 978-1-4987-5412-5
- Pierce F J & Nowak P (1999). Aspects of precision agriculture. *Advances in Agronomy* 67: 1-85. [https://doi.org/10.1016/S0065-2113\(08\)60513-1](https://doi.org/10.1016/S0065-2113(08)60513-1)
- Sahana S, Singh D, Pal S, Sarddar D A (2020). Design of IoT-based agricultural system for optimal management. *IoT and Analytics for Agriculture*, *Studies in Big Data* 63: 211-227. https://doi.org/10.1007/978-981-13-9177-4_10
- Santa J, Bernal-Escobedo L, Sanchez-Iborra R (2019). On-board unit to connect personal mobility vehicles to the IoT. *Procedia Computer Science* 175: 173-180
- Saygılı F, Kaya A, Çalışkan E T & Kozal E (2020). Global integration of Turkish agriculture and agriculture 4.0. *İzmir Commodity Exchange* No: 98: 100 pp. <https://itb.org.tr/img/userfiles/files/ITB%20TARIM.pdf?v=1550751511711>. (In Turkish) (Last accessed 19 May 2020)
- Shabandri B & Madara S R (2020). IoT-based smart tree management solution for green cities. *IoT and Analytics for Agriculture*, Vol. 2, *Studies in Big Data*, 67, 181-199. https://doi.org/10.1007/978-981-15-0663-5_9
- Turkish Statistical Institute (TÜİK) (2019a). Number of road motor vehicles by model years. http://www.tuik.gov.tr/PreIstatistikTablo.do?istab_id=355. (Last accessed 2 August 2019)
- Turkish Statistical Institute (TÜİK) (2019b). Number of road motor vehicles by model years. Number of Main Agricultural Machinery and Equipment by Size of Holdings and Forms of Ownership. http://www.tuik.gov.tr/PreIstatistikTablo.do?istab_id=298. (Last accessed 2 August 2019)



© 2022 by the author(s). Published by Ankara University, Faculty of Agriculture, Ankara, Turkey. This is an Open Access article distributed under the terms and conditions of the Creative Commons Attribution (CC BY) license (<http://creativecommons.org/licenses/by/4.0/>), which permits unrestricted use, distribution, and reproduction in any medium, provided the original work is properly cited.



Possibilities of Use Fertilizer Industry Waste Gypsum Material of Improve Sodic and Boron Soils

Barış BAHÇECİ^{a*} , Ali Fuat TARI^b , İdris BAHÇECİ^b 

^aÇukurova University, Faculty of Agriculture, Department of Agricultural Structures and Irrigation, Adana, TURKEY

^bHarran University, Faculty of Agriculture, Department of Agricultural Structures and Irrigation, Şanlıurfa, TURKEY

^bHarran University, Faculty of Agriculture, Department of Agricultural Structures and Irrigation (Retired), Şanlıurfa, TURKEY

ARTICLE INFO

Research Article

Corresponding Author: Barış BAHÇECİ, E-mail: baris_bahceci@hotmail.com

Received: 16 February 2020 / Revised: 08 August 2021 / Accepted: 11 August 2021 / Online: 01 September 2022

Cite this article

BAHÇECİ B, TARI F A, BAHÇECİ İ (2022). Possibilities of Use Fertilizer Industry Waste Gypsum Material of Improve Sodic and Boron Soils. *Journal of Agricultural Sciences (Tarim Bilimleri Dergisi)*, 28(3):449-456. DOI: 10.15832/ankutbd.856762

ABSTRACT

The effect of the Fertilizer Industry Waste Gypsum Material (FIWGM) on the rehabilitation of barren soils has been investigated with this research. The soil improvement tests were carried out in randomized blocks with three replications and 0, 20, 40 and 60 tons ha⁻¹ of FIWGM have been applied. By the intermittent ponding method, a total of 360 cm of water has been given, including 30 cm at each time. At the end of the trial, the application of FIWGM has showed positive effect on the physical and chemical properties of the soil. As the dose of FIWGM

increased, soil infiltration rates increased, and soil sodium and boron concentrations decreased significantly. 360 cm of leaching water provided the removal of exchangeable sodium equivalent to 33.7 and 42.9 tons of gypsum for 100 cm of soil depth, with 20 and 40 tons per hectare of FIWGM applied to the test plots. The statistically significant correlation coefficient ($R^2=0.921^{**}$) has been determined between the leaching water depth (Dlw)/soil depth (Ds) and the boron/initial boron remaining (B/Bo) in the soil ($B/Bo = 0.622-0.168Ln Dlw/Ds$).

Keywords: Sodic soils, Industrial gypsum, Waste material, Leaching water, Boron leaching, FIWGM

1. Introduction

Salt-affected soils are considered to be one of the main problems affecting agriculture, as well as a global environmental problem (Martinez-Beltran & Manzur 2005). According to the FAO/UNESCO soil map (1970-1980), the global total area of saline soils was 397 million hectares, while the total area of sodic soils 434 million hectares (FAO 2019).

A number of studies have been conducted for a long time on the use of different industrial wastes containing gypsum in the improvement and use of sodic soils (Hussain et al. 2001). For example, the addition of organic bio-ameliorants into sodic-soils has significantly increased root growth and yield of wheat (Gill et al. 2009). The application of gypsum, as well as organic fertilizer which reduces the sodicity of the soil, improves physicochemical properties by reducing pH, exchangeable sodium percentage (ESP) and bulk density and, as a result, improves the availability of nutrients in the soil (Singh et al. 2013). Matured municipal solid waste compost effectively recovered degraded soils with high soluble salt content and exchangeable sodium content (Hanay et al. 2013). In recent years, researchers have used different substances to properly treat barren lands. It was quite effective; mixtures of fly ash and sewage sludge were applied to saline-sodic soils for the purpose of soil recovery and environmentally friendly waste recycling (Örs et al. 2014). Recycled sewage sludge and fly ash allowed for cheap saline-sodic soil reclamation. The use of gypsum with biological modifications provided is more beneficial for the recovery of sodic and saline-sodic soils than for gypsum alone (Sisoday & Vaghani 2016), the combination of farmyard manure (FYM) and gypsum has increased physiological growth (Haque et al. 2015). Gypsum and calcium chloride provided direct source of Ca²⁺ to replace Na⁺, while sulphuric acid increases the calcite dissolution (Gupta & Abrol 1990; Mace et al. 1999; Qadir et al. 2001). Gharaibeh et al. (2010) have demonstrated that phosphoric acid can be used to reclaim saline-sodic soils, and the use of organic modification by Diacono & Montemurro (2015) must be considered an effective measure to restore soil quality in salt-affected soils. On the other hand, with the application of domestic solid waste and farm waste, soil pH was lowered and the bulk density and seepage properties of the soil (Singh et al. 2017).

Global studies have demonstrated that the most reliable method to determine the reclamation criteria for saline-sodic soils with high boron content improvement is to carry out experimental trials in the problematic areas. Therefore, this study presents a paper on soil and land reclamation in the Ereğli Plain, which is located in the Center Anatolia in Turkey. The objective of the

study was to determine reclamation criteria like required Fertilizer Industry Waste Gypsum Material (FIWGM), amount of leaching water, reclamation time, and the effect of the difference FIWGM dosages on the exchangeable sodium removal and infiltration rate of the soil for the sodic and boron soils in the area.

2. Material and Methods

1.1. Trial site

The test area is located in the Ereğli Plain, 1044 m above sea level, and it is a closed basin, with no outlet to discharge its waters into the sea, therefore its water is discharged to Lake Akgöl. The plain, which is the research area, has an agricultural land area of approximately 95 000 ha (Figure 1).

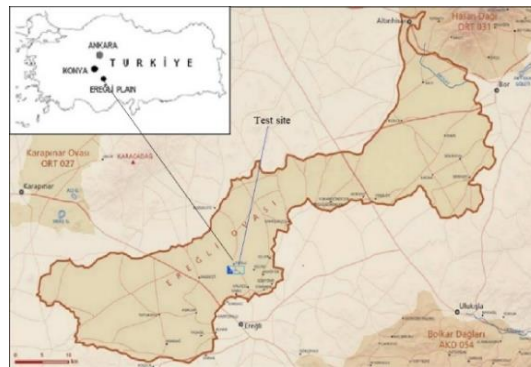


Figure 1- Geographic location of the trial

2.2. Climate characteristics

The region wherein the research is conducted has a semi-arid, continental climate conditions. The average annual precipitation is 320 mm, 10% of which falls in the summer, while the rest falls approximately equally in the other season. Summer is hot and dry, and it is cold in winter.

2.3. Soil characteristics

Research site soils have clay textures and a high amount of lime content (30–40%) and cation exchange capacity (CEC) is low, sodium exchangeable and soil salinity is high and the dominant salt type is sulphate, while soil pH varies from 8.0 to 8.4 (Table 1).

Table 1- Soil chemical and physical properties of experimental plots before treatment

Depth cm	pH	Saturation %	EC _e dS m ⁻¹	CEC cmol ⁺ kg ⁻¹	Exc. Na cmol ⁺ kg ⁻¹	ESP %	SAR	Lime %	BD g cm ⁻³
0-20	8.0	92.2	16.12	20.10	14.3	73.4	77	35.3	1.26
20-40	8.3	87.0	5.45	14.10	6.4	45.6	30	35.3	1.39
40-60	8.3	79.2	2.98	11.45	3.8	33.5	17	37.0	1.40
60-80	8.4	71.8	1.88	8.63	1.9	22.5	14	41.6	1.56
80-100	8.3	69.0	1.33	10.28	1.6	15.3	7	41.1	1.58

EC_e: electrical conductivity of the saturation extract; CEC: Exchangeable Sodium Percentage; SAR: Sodium Adsorption Ratio; Exc. Na: Exchangeable Sodium; BD: Bulk Density

2.4. Leaching water

The electrical conductivity of the leaching water used in this experiment is 0.520 dS m⁻¹ and the SAR value is approximately 0.45. The groundwater salinity is 1.72 dS m⁻¹ and the SAR value is 8.2. (Table 2).

Table 2- Chemical properties of the leaching water and groundwater

Water resource	pH	EC dS m ⁻¹	Cations, meq L ⁻¹				Anions, meq L ⁻¹			Total	SAR
			Na	K	Ca	Mg	HCO ₃	Cl	SO ₄		
Leaching water	8.2	0.52	0.83	0.1	1.52	5.30	3.80	0.30	3.60	7.74	0.45
Groundwater	8.2	1.72	11.3	0.2	2.39	11.86	8.20	1.40	16.19	25.79	8.2

FIWGM is the waste generated during the phosphorus fertilizer production in Mersin fertilizer factory. It is in powder form and its purity level is between 85% and 90%. FIWGM has been applied by hand spread to the soil surface and mechanically mixed with shovels approximately within the 30-40 cm of soil depth.

2.5. Experimental set-up

The research has been designed for remediation trials; data on infiltration have also been provided for these trials. The research was developed with the design of a randomized block of four FIWGM dosage treatments and three replications. The dimensions of the plot are arranged as 3 m x 5 m= 15 m².

The soil has been plowed deep with the plow to increase the water permeability at the research site and to ensure that the breeding agent blends well into the soil. In order to prevent leakage to the sides, the edges of the parcel have been covered by a plastic cover, approximately 40-50 cm deep.

2.6. Procedures

Leaching water has been given in 30 cm portions. When the water was infiltrated, the plots were expected to dry for about three days. After soil samples have been taken from the middle of the plots, the holes were filled with soil and the sampling points were marked with a wooden stake.

Soil and water samples analyzed using the methods described by Richards (1954) and the hydrometer texture (Bouyoucos 1951). Carbonates analyzed by calcimeter, salinity (EC_e) analyzed by conductivity meter, CEC and exchangeable sodium (NaX) were determined using a flame photometer (Tüzüner 1990).

2.7. Assessment of data

The time of application of water and infiltration has been recorded for each 30 cm of water depth and for each plot. The infiltration capacity of each treatment has been determined separately. Consequently, the average of these values for each FIWGM treatment has been calculated. Cumulative infiltrated (Z) has been determined using the mean values and infiltration equation (Kostiakov 1932) as follows:

$$Z = KT^n \quad (1)$$

Where: K, constant; T; time (h) and n, exponent.

2.8. Exchangeable Na removal

The theoretical gypsum requirement for each soil depth was calculated using the following equations, taking into account the ESP value below 10:

$$GR = EW \times 10^{-5} \times A \times BD \times D_s \times ((ESP_i - ESP_f) / 100) \times CEC \quad (2)$$

$$ESP = (NaX / CEC) \times 100 \quad (3)$$

The following abbreviations have been used in equation; GR; gypsum requirement (cmol⁺kg⁻¹ dry weight), EW, the equivalent weight of gypsum (cmol⁺kg⁻¹ dry weight), ESP; exchangeable sodium percentage (%), ESP_i and ESP_f; initial and final ESP value (%), CEC; cation exchange capacity (cmol⁺kg⁻¹), BD; bulk density of the soil (g cm⁻³), A; area m² and D_s; soil depth m, NaX; exchangeable sodium, cmol⁺kg⁻¹ dry weight.

First, a certain amount of leaching water for each FIWGM, and for each soil layer using the GR equation, and how much gypsum equivalent of the exchangeable sodium removed from the soil profile has been calculated.

2.9. Boron leaching

The arithmetic average of three plots was used in all assessments. The remaining boron (B) after leaching was divided by the initial boron value (B₀) and therefore the values of B/B₀ were obtained by each leaching water depth. For each FIWGM dose, the ratio of leaching water (D_{lw}) to soil depth (D_s) has been calculated. Thus, the depth of the leaching water and the boron has been removed independently of the soil depth, and the boron leaching curve and function were obtained as reported by Boumans et al. (1963).

3. Results and Discussion

3.1. Change of hydraulic properties of soil

The infiltration rate is a rather sensitive indicator of soil physical conditions. Sodium disrupts the soil structure, disperses soil particles, blocks pores, and slows down the flow of water. When a calcium source is used for soil rehabilitation, the process is reversed and the soil coagulation is regenerated, leading to a noticeable increase in soil porosity.

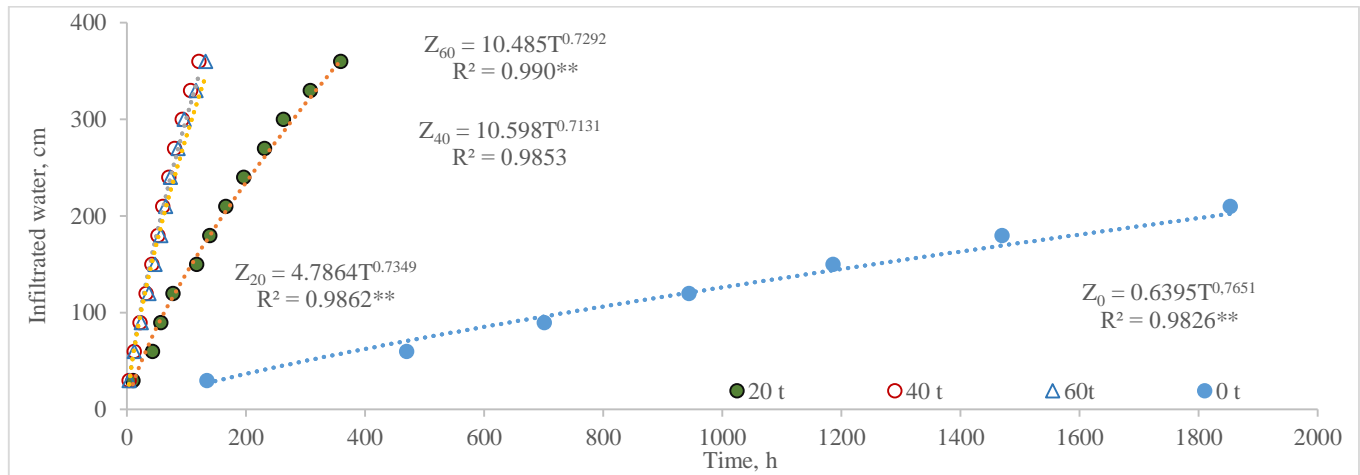


Figure 2- Effect of different doses of FIWGM on infiltration capacity of soil

The passage of water through the soil profile is, therefore, easier and the hydraulic conductivity increases significantly (Qadir & Scuhbert 2002). These research findings are consistent with the above-mentioned hypothesis. The soil infiltration rate increased as the dose of FIWGM applied increased (Figure 2).

Initially, while the infiltration rate (I) in the plot without FIGWM has been 0.22 cm h^{-1} , when 20, 40 and 60 tons of FIWGM have been applied per hectare, the infiltration rates increased to 3.0 , 8.57 , and 8.57 cm h^{-1} , respectively (Table 3, Figure 2).

Table 3- Effect of different doses of industrial gypsum on infiltration capacity

Applied water depth, cm	FIWGM, $t \text{ ha}^{-1}$											
	0			20			40			60		
	Time, h			I, cm h^{-1}			Average I, cm h^{-1}					
0	134	10	3.5	3.5	0.22	3.00	8.57	8.57	0.22	3.00	8.57	8.57
210	1853	166	65	60	0.08	1.11	3.75	3.75	0.11	0.18	3.23	3.50
330	-	308	116	107	-	0.67	1.50	2.14	-	0.10	2.84	3.08
360	-	359	132	121	-	0.59	1.88	2.14	-	0.08	2.73	2.98

As can be seen, the FIWGM application has enabled significant increases in infiltration rates. In plots where FIWGM was applied, 360 cm of leaching water has been infiltrated, while in plots without FIWGM, only 210 cm of leaching water could be infiltrated. In plots where 20, 40 and 60 tons of treatment material have been used, the infiltration rates at the end of the test have been 1.11 , 3.75 and 3.75 cm h^{-1} , respectively. Exponential relationships with high correlation coefficients have been identified between cumulative infiltration and time for different FIWGM doses (Figure 2).

The use of gypsum on the soil surface has been commonly used for a long time in California to reclamation sodic soils and improve infiltration rates (Oster et al. 1996). The application of gypsum spread to soil has increased the rate of infiltration by 152% (Raza et al. 2001). The use of gypsum in sodium-affected soils is commonly used to increase aggregate stability and infiltration rates (Agassi et al. 1981; Keren & Shainberg 1981). Soluble salts promote flocculation in the soil (Keren & Shainberg 1984) as well as a decrease in the relative sodium content and an increase in the salt content of the water influence the rate of infiltration (Ayers & Westcott 1985). In this trial, the applying FIWGM developed the physical properties of the soil and provided a significant level of an increase in the rate of infiltration. It was understood that test area soils could not be recovered without the use of any reclamation material due to very low infiltration capacity. Considering the gypsum content of FIWGM, it has been concluded that the expected results of this study had been achieved.

3.2. Leaching of exchangeable sodium

In this research, the fertilizer industry waste gypsum material (FIWGM) containing approximately 85-90% gypsum has been used as a reclamation material.

While 360 cm of water has been infiltrated which passes through the profile in the plots where FIWGM is applied, in the plots without FIWGM application, only 210 cm of water could be infiltrated during the whole phase. Without FIWGM, NaX decreased significantly only in the upper soil. Infiltration capacity was very low in these plots, and the amount of NaX removed was very small and, finally, the soil could not be rehabilitated.

In the FIWGM applied plots, the soil analysis revealed that the exchangeable sodium was removed from the topsoil layers and accumulated in the lower soil layers following the completion of the leaching (Table 4, Figure 3a).

At the end of 20 tons per hectare, FIWGM and 240, 300 and 360 cm of leaching water applications, the ESP values in the upper layer (20 cm) decreased to 6, 8 and 2, respectively (Figure 3b). No more NaX has been leached from the lower layers after 240 and 300 cm of leaching water. Whereas, at the end of 360 cm of leaching water, the ESP values decreased below 15 in 100 cm of the soil profile and ranged between 2-12 % across the entire profile (Table 4).

Table 4- Average exchangeable sodium (NaX) and exchangeable sodium percentage (ESP) of soils prior to and after leaching with 240, 300 and 360 cm water

FIWGM applied $t\ ha^{-1}$	Soil depth cm	Bulk density $g\ cm^{-3}$	Leaching water, $\frac{0\ 240\ 300\ 360}{NaX, cmol^+kg^{-1}}$				CEC $cmol^+kg^{-1}$	Leaching water $\frac{0\ 240\ 300\ 360}{ESP}$			
			0	240	300	360		0	240	300	360
0	0-20	1.26	11.51	9.47	-	-	18.41	62	51	-	-
	20-40	1.39	5.57	9.56	-	-	12.65	44	52	-	-
	40-60	1.40	2.20	4.50	-	-	10.00	22	45	-	-
20	0-20	1.26	11.07	1.04	1.35	0.36	17.37	64	6	8	2
	20-40	1.39	3.69	2.59	4.55	1.2	12.72	29	21	38	9
	40-60	1.40	2.01	2.60	3.6	0.67	10.48	19	25	34	12
40	0-20	1.26	11.79	1.45	1.13	0.67	17.96	65	8	6	4
	20-40	1.39	5.36	1.63	1.5	1.61	12.94	41	13	12	12
	40-60	1.40	3.37	2.65	1.62	1.55	10.56	32	25	15	15
60	0-20	1.26	10.23	1.17	0.98	0.68	17.51	58	7	6	4
	20-40	1.39	5.19	1.43	1.99	2.24	12.18	43	12	16	18
	40-60	1.40	2.34	2.06	1.86	2.67	10.73	22	19	17	25

However, even when 40 tons per hectare of industrial gypsum and 240 cm of leaching water have been used, the ESP values in the 40 cm soil profile dropped to safe values. When the water depth of the leaching is 300 cm, the ESP values in the 100 cm profile have dropped below 15%, except for the soil depth of 60-80 cm. When 360 cm of leaching water has been applied, the ESP values have been lower than 15% in the entire profile (Figure 3c).

However, the application of 60 $t\ ha^{-1}$ of FIWGM could not provide for further sodium removal in all leaching waters (Figure 3d). From this point on, it has been concluded that the applied irrigation water was not sufficient to dissolve more FIWGM.

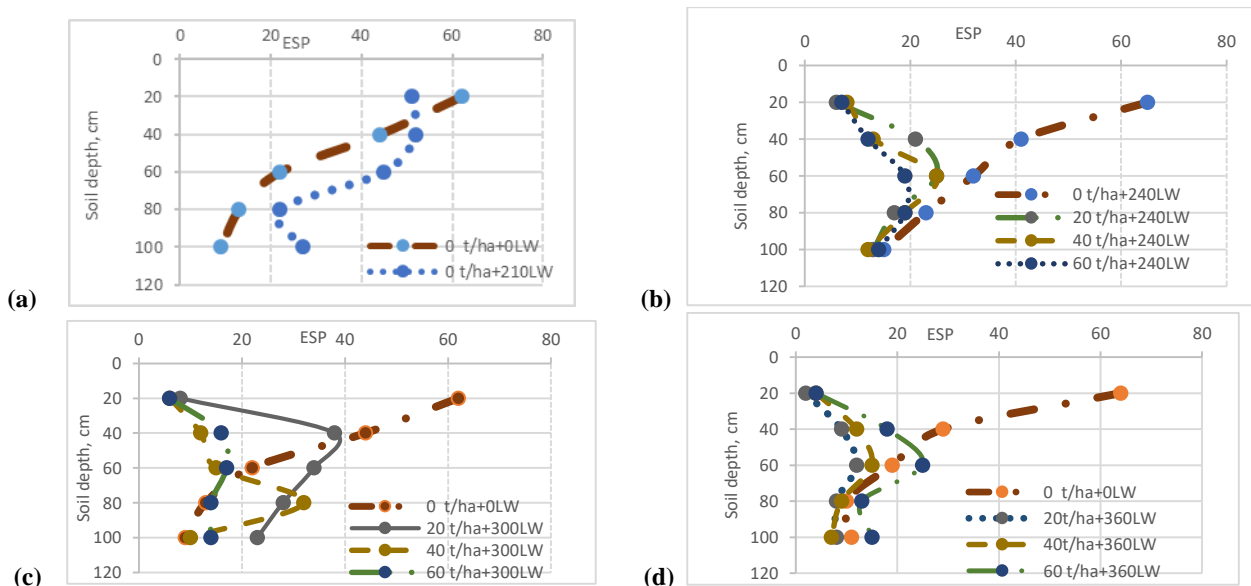


Figure 3- Effect of different leaching water (LW) at different FIWGM dosages on change ESP at the soil profile

A similar situation has also been observed in some studies, and it has been observed that the administered FIWGM dose increases and the sodium removed for each mined gypsum unit decreases (Beyce 1977, Bahçeci 2008).

Overall, the results have shown that favorable leaching of interchangeable sodium at the site of the test site is not possible without some kind of reclaimed chemical material. Therefore, in recent years, lower doses have been recommended instead of the theoretically calculated amount of gypsum.

3.3 Gypsum calibration curves for sodic soils reclamation

Table 5 shows the quantities of theoretical gypsum calculated for the removal of the exchangeable Na at different soil depths and at two leaching water levels. As can be seen, in plots where FIWGM has not been applied, sodium leached is approximately 4.420 tons per hectare equivalent to gypsum.

Table 5- Theoretical amounts of gypsum calculated for the replaced exchangeable Na with amendments in different doses on the sodic soils

FIWGM applied $t\ ha^{-1}$	Soil Depth, (cm)	Leaching water, (cm)		Soil Depth, (cm)	Leaching water, (cm)	
		300	360		300	360
		Theoretical gypsum calculated for removed NaX, ($t\ ha^{-1}$)		Cumulative removed, NaX ($t\ ha^{-1}$)		
0	0-20	4.420	4.420	20	4.420	4.420
20	0-20	21.07	23.21	20	21.07	23.21
	20-40		5.95	40	21.06	29.16
40	0-20	23.10	24.10	20	23.10	24.10
	20-40	9.23	8.97	40	32.33	33.06
	40-60	4.21	4.38	60	36.54	37.45
	60-80		3.43	80	36.54	40.88
	80-100	1.30	1.96	100	37.85	42.84
60	0-20	20.05	20.70	20	20.05	20.70
	20-40	7.65	7.05	40	27.70	27.75
	40-60	1.16	.	60	28.85	27.75

Whereas 20 tons per hectare of FIWGM and 300 and 360 cm of leaching water have been used, 24 and 29 tons of gypsum sodium equivalent have been removed, respectively. In a previous study conducted at this research site, the application of 20 and 40 tons per hectare of mined gypsum, along with 360 cm of gypsum leaching water, removed an exchangeable sodium equivalent of 38 and 56 tons of gypsum per hectare (Bahçeci 2008).

As can be seen in Figure 4, when 40 tons of FIWGM were applied per hectare, the quantity of sodium leachable removed from the soil profile is approximately 43 tons per hectare. However, as the doses of FIWGM increase, the amount of exchangeable sodium leached did not increase at the same rate. The effect of the treatment material at lower doses was higher and the effect of the treatment agent at high doses applied to the removal of interchangeable sodium was found to be lower.

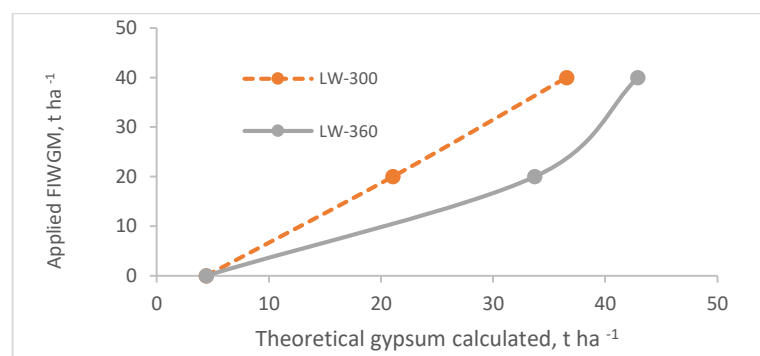


Figure 4- Gypsum calibration curves at two leaching waters levels for 100 cm soil profile

The amount of FIWGM required can be estimated to reclaim sodic-soil using these calibration curves in Figure 4. For example, if the required FIWGM was theoretically calculated at 20 tons per hectare, in this case 10 tons per hectare of FIWGM and 360 cm of leaching water used, the quantity of exchangeable sodium removed would be 20 tons per hectare of gypsum equivalent for 100 cm of soil depth.

The time required to infiltrate the applied water is estimated to be approximately 380 hours or 16 days using the cumulative infiltration curve in Figure 2. The time required for improvement is calculated by adding weighting intervals to the infiltration time.

3.4 Boron leaching

High boron concentrations were formed in the experimental area by the evaporation of shallow groundwater. Consequently, while the upper layer of the soil has a high boron excess in the research area, the boron concentration in the lower layers has been low.

To improve is very difficult boron soils. The amount of water required for boron leaching in soils with a high boron content by nature is approximately twice the amount required for salt leaching (USSL 1981; Hoffman 1986). Rehabilitation of boron soils is costly and time-consuming and labour-intensive. However, it is still a common view that more accurate and consistent results are obtained with on-site field trials.

In this research, along with leaching water applications, the boron content also decreased and, at the end of 360 cm of leaching water, the boron concentration decreased to 2 ppm in the upper soil and lower levels in the lower layers (Table 6, Figure 5).

As explained in the method, using the average data obtained, a regression analysis has been conducted to determine the relationship between the boron left after leaching and the ratio of the water depth applied to the soil depth based on the initial boron concentration in the soil.

Table 6- Average boron status (ppm) in test plots before and after leaching

Soil depth, cm	Leaching water, cm							
	0	30	60	120	180	240	300	360
0-20	13.30	9.17	10.23	5.72	3.87	2.27	3.03	2.08
20-40	3.74	3.45	5.90	4.82	3.62	1.32	1.41	1.88
40-60	2.73	0.97	2.78	2.04	1.83	1.52	1.80	0.50
60-80	1.19	0.18	2.30	1.04	1.38	0.10	1.61	0.15
80-100	1.89	0.56	0.90	0.81	1.26	0.20	1.15	0.10

A statistically significant logarithmic relationship between leaching water depth (D_{lw})/soil depth (D_s) and remaining boron/initial boron values (B/B_0) has been identified. As a result of the regression analysis, the equation obtained is as follows: $B/B_0 = 0.622 - 0.168 \ln D_{lw}/D_s$, ($R^2 = 0.921^{**}$).

As can be seen, the resulting equation has a high correlation coefficient, which is statistically significant at $p = 0.01$.

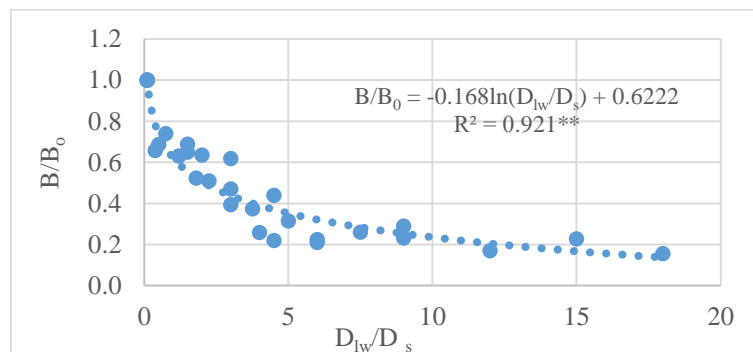


Figure 5- Boron leaching curve

4. Conclusions

The field experiments have demonstrated that an increase in FIWGM application rate up to 40 tons per hectare has resulted in significant increase in the removal of exchangeable sodium. Results also indicated that the application of 20 tons FIWGM per hectare, along with 300 and 360 cm water could remove the exchangeable sodium equivalent to 23.21 and 29.16 tons per hectare gypsum, respectively.

When 40 tons of FIWGM have been used per hectare, sodium equivalent to 42.89 tons of gypsum has been removed from the soil profile. Whereas, if 60 tons of FIWGM was applied to a hectare with 300 and 360 mm of leaching water, the amount of sodium leached has been only 28.85 and 27.75 tons of equivalent gypsum, respectively. This suggests that the quantity of water applied has not been sufficient to dissolve the FIWGM applied at high doses.

Since soil infiltration capacity has been very low, it is highly recommended to start with the application of 10 tons per hectare of FIWGM and to increase the amount of application needed to gradually remove salts and sodium exchangeable from the soil profile.

References

- Agassi M, Shainberg I & Morin I (1981). Effect of electrolyte concentration and soil sodicity on the infiltration rate and crust formation. *Soil Sci.Soc. A. J.* 45: 848-851
- Ayers R S & Westcott D W (1985). *Water Quality for Irrigation*. FAO Irrigation and Drainage Paper 29. FAO: Rome.
- Bahçeci İ (2008). Determination of salt leaching and gypsum requirements with field tests of saline-sodic soils in Central Turkey, *Irr. and Drainage* 58(3):332-345. <https://doi.org/10.1002/ird.406>
- Beyce Ö (1977). A Study on the Determination of the Amount of Leaching Water and Improvement Agents in Salty and Sodium Soils in Some Irrigation Development Areas of Turkey, Merkez TOPRAKSU Research Institute. Gn.Spring. no. 44, Serial No: T-25. 143 s. (in Turkish with an abstract in English)
- Boumans J H, Hulsbes W C, Lindenberg H L J & Sluis, P M van der (1963). Reclamation of salt affected soil in Iraq. *Int. Inst. Ld Reclam. Improv. Pub.* no. 11.
- Bouyoucos G S (1951). A recalibration of the hydrometer method for making mechanical analysis of soils. *Agronomy Journal* 43: 434-448
- Diacono M & Montemurro F (2015). Effectiveness of Organic Wastes as Fertilizers and Amendments in Salt-Affected Soils *Agric.* 2015, 5, 221-230. doi:10.3390/agriculture 5020221
- FAO (2019). FAO Soil Portal, Food and Agricultural Organization of the United Nation <http://www.fao.org/home/en/>
- Gharaibeh M A, Eltaif N I & Shra'ah S H (2010). Reclamation of a calcareous saline-sodic soil using phosphoric acid and by-product gypsum. *Soil Use Management* 26(2):141-148. <https://doi.org/10.1111/j.1475-2743.2010.00260.x>
- Gill J S, Sale P W G, Peries R R & Tang C (2009). Changes in physical properties and crop root growth in dense sodic subsoil following incorporation of organic amendments, *Field Crops Res.* 114:137-146. <https://doi.org/10.1016/j.fcr.2009.07.018>
- Gupta R K & Abrol I P (1990). Salt-affected soils: their reclamation and management for crop production. *Adv Soil Sci* 11:223-288
- Haque N A, Haque M E, Hossain M E, Khan M K & Razzaque A H M (2015). Effect of Farm Yard Manure, Gypsum and Nitrogen on Growth and Yield of Rice in Saline Soil of Satkhira District, Bangladesh, *Journal of Bioscience and Agric. Research*, vol. 3(2), 2015, p. 65-72. <https://doi.org/10.18801/jbar.030215.32>
- Hanay A, Büyüksönmez F, Kızıloğlu F M & Canbolat M Y (2013). Reclamation of Saline-Sodic Soils with Gypsum and MSW Compost, *Compost Science & Utilization*. <https://doi.org/10.1080/1065657x.2004.10702177>
- Hoffman G J (1986). Guidelines for reclamation of salt-affected soils. *Applied Agricultural Research* 1(2):65-72
- Hussain N S, Mehdi M, Khan G D & Iqbal Z (2001). Industrial wastes as reclaimant for sodic soils. *Pakistan J. Bio. Sci.* 4(3): 193-195
- Keren R & Shainberg I (1981). Effect of dissolution rate on the efficiency of industrial and mined gypsum in improving infiltration of a sodic soil. *Soil Sci. Soc.Am.J.* 45: 103-107
- Keren R & Shainberg I (1984). Colloid properties of clay minerals in saline and sodic solutions. In *Soil Salinity under Irrigation*, Shainberg I, Shalhevet J, (eds). Springer-Verlag: Berlin.
- Kostiakov A N (1932). On the dynamics of the coefficient of water percolation in soils and on the necessity for studying it from a dynamic point of view for purposes of amelioration. In: *Trans. 6th Comm. Int. Sot. Soil Sci. Russian Part A*: 17-21
- Mace J E, Amrhein C & Oster J D (1999). Comparison of gypsum and sulfuric acid for sodic soil reclamation. *Arid Soil Res Rehabilitation* 13: 171-188
- Martinez-Beltran J & Manzur C L (2005). Overview of salinity problems in the world and FAO strategies to address the problem. *Proc. Int. Salinity Forum*. Riverside, California, April 2005, pp. 311-313
- Oster J D, Shainberg I & Abrol J P (1996). Reclamation of salt-affected soil. In *Soil Erosion, Conservation and Rehabilitation*, Agassi M (ed.). Marcel Dekker: New York; 315-351
- Örs S, Sahin Ü & Khadra R (2014). Reclamation of Saline Sodic Soils with the Use of Mixed Fly Ash and Sewage Sludge, *Arid Land Res. and Management Vol. 29*, 2014-Issue 1
- Qadir M, Schubert S, Ghafoor A & Murtaza G (2001). Amelioration strategies for sodic soils: a review. *Land Degradation Development Vol.12*: 357-386
- Qadir M & Schubert S (2002). Degradation process and nutrient constraints in sodic soils. *Land Degradation Development Vol. 13*:275-294
- Raza Z I, Rafiq M S & Abdur R (2001). Gypsum application in slots for reclamation of saline sodic soils. *Int. J. of Agric. and Biology* 3(3): 281-285
- Richards L A (1954). *Diagnosis and Improvement of Saline and Alkaline Soils*, United States Salinity Staff, Agricultural Handbook 60, US Department of Agriculture, Washington DC.
- Singh Y P, Dubey U C, Singh S & Dubey S K (2013) Interventions of Sodic Soil Reclamation Technologies and Constraints in their Adoption”, *Indian Research Journal of Extent and Education*, vol. 13(2), 2013, p. 36-40
- Singh Y P, Arora S, Mishra V K, Dixit H & Gupta R K (2017). Composting of municipal solid waste and farm wastes for its use as amendment in sodic soil. *Journal of Soil and Water Conservation* 16(2): 172-177. <https://doi.org/10.5958/2455-7145.2017.00025.x>
- Sisoday V & Vaghani M (2016). Reclamation of Saline and Sodic Soil: The State of GRD Journals *Global Research and Development Journal for Engineering | Recent Advances in Civil Engineering for Global Sustainability | March 2016*
- Tüzüner A (1990). *Handbook of Soil and Water Analysis Laboratories*. General Directorate of Rural Services. (in Turkish)
- USSL (1981). *Salinity management in agriculture*. (US Salinity Laboratory Staff) Given in *Irrigation Challenges of the 80s* as in preparation in 1981



© 2022 by the author(s). Published by Ankara University, Faculty of Agriculture, Ankara, Turkey. This is an Open Access article distributed under the terms and conditions of the Creative Commons Attribution (CC BY) license (<http://creativecommons.org/licenses/by/4.0/>), which permits unrestricted use, distribution, and reproduction in any medium, provided the original work is properly cited.



Exponential Type Estimators Using Sub-Sampling Method with Applications in Agriculture

Ceren ÜNAL^{a*} , Cem KADILAR^b 

^aHacettepe University, Institute of Science, Beytepe, Ankara, TURKEY

^bDepartment of Statistics, Hacettepe University, 06800 Beytepe, Ankara, TURKEY

ARTICLE INFO

Research Article

Corresponding Author: Ceren ÜNAL, E-mail: cerenunal@hacettepe.edu.tr

Received: 14 April 2020 / Revised: 29 August 2021 / Accepted: 01 September 2021 / Online: 01 September 2022

[Cite this article](#)

ÜNAL C, KADILAR C (2022). Exponential Type Estimators Using SUB-Sampling Method with Applications in Agriculture. *Journal of Agricultural Sciences (Tarim Bilimleri Dergisi)*, 28(3):457-472. DOI: 10.15832/ankutbd.915999

ABSTRACT

In this article, the family of exponential type estimators with the auxiliary variable is proposed in the case of non-response scheme for the purpose of obtaining the unknown population mean of the study variable. The non-response scheme is examined under two main cases as Case I and Case II. The bias, mean square error (MSE) and minimum MSE of the proposed family of estimators are obtained in detail for both cases. After theoretical inferences, empirical studies are carried out to show the appropriateness

of the proposed family of estimators in the field of agriculture. The MSE and PRE (Percentage Relative Efficiency) values are obtained. According to the results, the proposed estimators provide more efficient results than existing estimators in the literature under the obtained conditions for both cases. We conclude that the proposed family of estimators can be applied to the agriculture data successfully.

Keywords: Agriculture, Efficiency, Non-response, Population mean estimator, Simple random sampling

1. Introduction

Instead of population, working on a sample plays an important role in terms of time, money, and labor force. The parameters of the population, such as total, mean, proportions and variance can be obtained via estimators in sample surveys. Here, the main aim is to propose more efficient estimator than other estimators in literature. For this reason, the information of the auxiliary variable is used extensively in order to obtain the efficient results. In literature, we may see various types of estimators, such as ratio, regression, product, exponential and so on in the presence of the auxiliary variable. In these types of estimators, if the relation between study (y) and auxiliary variable (x) is a straight line passing through the origin, the usual regression, ratio and product types of estimators have equal efficiencies. However, when the line does not pass through the origin, the regression, ratio and product types of estimators do not have equal efficiencies (Solanki et al. 2012). For this reason, exponential type of estimators becomes prominent among others.

In general, the estimators are proposed when all information on variables is present. However, some units on several variables cannot be obtained all the time. This situation is the most important problem in the sample survey that is named as non-response (Dansawad 2019). In order to deal with this situation, Hansen and Hurwitz (1946) introduced a new technique of sub-sampling. Here, the main aim is to reduce the effect of non-response using both response and non-response units in the estimator.

In this technique, from a population size of N units, as $S = (S_1, S_2, \dots, S_N)$, a sample of size n units is drawn. However, the population size N ($N_1 + N_2 = N$) is divided into two groups, N_1 and N_2 , as respondent and non-respondent units, respectively. Similarly, the response units are available only on n_1 while n_2 ($n_2 = n - n_1$) units are obtained as non-response. Due to the extra effort, a sub-sample size of $r = \frac{n_2}{z}$ ($z > 1$) is drawn from n_2 . Thus, the population mean can be estimated by using $(n_1 + r)$ units, instead of n units, in this sub-sampling technique. Note that z is the inverse of the sampling rate whose different values are used for the MSE and PRE values.

The unbiased estimator is defined by Hansen and Hurwitz (1946) to estimate the population mean for the first time in the sub-sampling technique as follows:

$$t_H = w_1 \bar{y}_1 + w_2 \bar{y}_{2(r)}, \tag{1}$$

whose variance is given by

$$V(t_H) = \bar{Y}^2 \left(\lambda C_y^2 + \frac{W_2(z-1)}{n} C_{y(2)}^2 \right). \tag{2}$$

In Equation (1), $w_1 = \frac{n_1}{n}$ and $w_2 = \frac{n_2}{n}$ refer the weights of response and non-response units for the sample, respectively.

Besides, \bar{y}_1 and $\bar{y}_{2(r)}$ denote the sample means of y based on n_1 and r ($r = n_2/z$) units. In Equation (2),

$f = \frac{n}{N}$, $\lambda = \frac{1-f}{n}$, $C_y^2 = \frac{S_y^2}{\bar{Y}^2}$ and $C_{y(2)}^2 = \frac{S_{y(2)}^2}{\bar{Y}^2}$. In addition, $W_2 = \frac{N_2}{N}$ is the weight of N_2 units in the population.

The non-response situation is examined under Case I and Case II, separately. In Case I, units of non-response exist only on y . In Case II, units of non-response exist on both y and x . In addition to this, the population mean of x is known for both cases.

After the sub-sampling method and pioneer study of Hansen and Hurwitz (1946), many estimators have been proposed in the literature considering the non-response scheme. Some of the estimators for the population mean are given in Tables 1 and 2, according to the Cases I and II, respectively.

Using the sub-sampling method, Rao (1986) proposed the classical ratio (t_{R1}) and regression (t_{reg1}) estimators under the Case I. Singh et al. (2009) first defined the exponential type estimator (t_{exp1}) by adapting the estimator proposed by Bahl and Tuteja (1991) to the Case I. Following these estimators, Olufadi and Kumar (2014), Yadav et al. (2016), Kumar and Kumar (2017), Pal and Singh (2016, 2017, 2018), Dansawad (2019), Singh and Usman (2019a, 2019b), Unal and Kadilar (2021) proposed various estimators taking the advantage of the exponential function.

In these estimators, \bar{y}^* is the sample mean of y under the non-response scheme. Also, \bar{x} and \bar{X} are the sample and the population means of x , respectively, while \bar{Y} is the population mean of y .

Under the Case II, Cochran (1977) defined the ratio (t_{R2}) and regression (t_{reg2}) estimators while Singh et al. (2009) proposed the exponential type estimator for the population mean. Following these estimators, Kumar and Bhougul (2011), Kumar (2013), Yadav et al (2016), Kumar and Kumar (2017), Pal and Singh (2016, 2017, 2018), Singh and Usman (2019a, 2019b), Unal and Kadilar (2020, 2021) and Riaz et al. (2020) proposed estimators using the exponential function for the population mean for the Case II.

Note that in Tables 1 and 2, \bar{x}^* refers the sample mean of x in the case of non-response and the coefficient of the population correlation between x and y for the non-response group is referred as $\rho_{yx(2)}$.

Table 1- Existing estimators in literature for the Case I

<i>Authors</i>	<i>Estimators</i>
Rao (1986)	$t_{R1} = \bar{y}^* \frac{\bar{X}}{\bar{x}}$
Rao (1986)	$t_{reg1} = \bar{y}^* + b^* (\bar{X} - \bar{x}), b^* = \frac{S_{xy}^*}{S_x^{*2}}$
Singh et al. (2009)	$t_{exp1} = \bar{y}^* \exp\left(\frac{\bar{X} - \bar{x}}{\bar{X} + \bar{x}}\right)$
Olufadi and Kumar (2014)	$t_{YK1} = \bar{y}^* \left\{ \alpha \exp\left(\frac{\bar{X} - \bar{x}}{\bar{X} + \bar{x}}\right) + (1 - \alpha) \exp\left(\frac{\bar{x} - \bar{X}}{\bar{x} + \bar{X}}\right) \right\}$
Yadav et al. (2016)	$t_{Y1} = \bar{y}^* \exp\left(\frac{\bar{X} - \bar{x}}{\bar{X} + (\alpha - 1)\bar{x}}\right)$
Pal and Singh (2016)	$t_{(\alpha,\delta),1} = \bar{y}^* \left(\frac{\bar{X}}{\bar{x}}\right)^\alpha \exp\left\{\left[\frac{\delta(\bar{X} - \bar{x})}{\bar{x} + \bar{X}}\right]\right\}$
Pal and Singh (2017)	$t_{PS1} = \alpha \bar{y}^* \left(\frac{\bar{X}}{\bar{x}}\right) + (1 - \alpha) \bar{y}^* \exp\left(\frac{\bar{X} - \bar{x}}{\bar{X} + \bar{x}}\right)$
Kumar and Kumar (2017)	$t_{KK1} = d_1^* \bar{y}^* \exp\left(\frac{\bar{X} - \bar{x}}{\bar{X} + \bar{x}}\right)$
Pal and Singh (2018)	$t_{SP1} = \bar{y}^* \left[\eta \left\{ \frac{(1 - \delta)\bar{x} + \delta\bar{X}}{\delta\bar{x} + (1 - \delta)\bar{X}} \right\} + (1 - \eta) \left\{ \frac{\delta\bar{x} + (1 - \delta)\bar{X}}{(1 - \delta)\bar{x} + \delta\bar{X}} \right\} \right]$
Dansawad (2019)	$t_D = \bar{y}^* \exp\left(\frac{(a\bar{X} + b) - (a\bar{x} + b)}{(a\bar{X} + b) + (a\bar{x} + b)}\right)$
Singh and Usman (2019a)	$t_{US1} = \bar{y}^* \left(\frac{\bar{X}}{\bar{x}}\right)^\alpha \exp\left\{\left[c \frac{\bar{X} - \bar{x}}{\bar{X} + \bar{x}}\right]\right\}$
Singh and Usman (2019b)	$t_{SU1} = [d_1^* \bar{y}^* + d_2^* (\bar{X} - \bar{x})] \exp\left(\frac{\bar{X} - \bar{x}}{\bar{X} + \bar{x}}\right)$
Unal and Kadilar (2021)	$t_{1,i} = k\bar{y}^* \left(\frac{a\bar{X} + b}{a\bar{x} + b}\right)^c \exp\left(\frac{a(\bar{X} - \bar{x})}{a(\bar{X} + \bar{x}) + 2b}\right)$

Table 2- Existing estimators in literature for the Case II

<i>Authors</i>	<i>Estimators</i>
Cochran (1977)	$t_{R2} = \bar{y}^* \frac{\bar{X}}{\bar{x}^*}$
Cochran (1977)	$t_{reg2} = \bar{y}^* + b^* (\bar{X} - \bar{x}^*)$
Singh et al. (2009)	$t_{exp2} = \bar{y}^* \exp\left(\frac{\bar{X} - \bar{x}^*}{\bar{X} + \bar{x}^*}\right)$
Kumar and Bhougat (2011)	$t_{KB} = \bar{y}^* \left\{ \alpha \exp\left(\frac{\bar{X} - \bar{x}^*}{\bar{X} + \bar{x}^*}\right) + (1 - \alpha) \exp\left(\frac{\bar{x}^* - \bar{X}}{\bar{x}^* + \bar{X}}\right) \right\}$
Kumar (2013)	$t_K = \bar{y}^* \exp\left(\frac{(a\bar{X} + b) - (a\bar{x}^* + b)}{(a\bar{X} + b) + (a\bar{x}^* + b)}\right)$
Yadav et al. (2016)	$t_{Y2} = \bar{y}^* \exp\left(\frac{\bar{X} - \bar{x}^*}{\bar{X} + (\alpha - 1)\bar{x}^*}\right)$
Pal and Singh (2016)	$t_{(\alpha,\delta),2} = \bar{y}^* \left(\frac{\bar{X}}{\bar{x}^*}\right)^\alpha \exp\left\{\left[\frac{\delta(\bar{X} - \bar{x}^*)}{\bar{X} + \bar{x}^*}\right]\right\}$
Pal and Singh (2017)	$t_{PS2} = \alpha \bar{y}^* \left(\frac{\bar{X}}{\bar{x}^*}\right) + (1 - \alpha) \bar{y}^* \exp\left(\frac{\bar{X} - \bar{x}^*}{\bar{X} + \bar{x}^*}\right)$
Kumar and Kumar (2017)	$t_{KK2} = d_1^* \bar{y}^* \exp\left(\frac{\bar{X} - \bar{x}^*}{\bar{X} + \bar{x}^*}\right)$
Pal and Singh (2018)	$t_{SP2} = \bar{y}^* \left[\eta \left\{ \frac{(1 - \delta)\bar{x}^* + \delta\bar{X}}{\delta\bar{x}^* + (1 - \delta)\bar{X}} \right\} + (1 - \eta) \left\{ \frac{\delta\bar{x}^* + (1 - \delta)\bar{X}}{(1 - \delta)\bar{x}^* + \delta\bar{X}} \right\} \right]$
Singh and Usman (2019a)	$t_{US2} = \bar{y}^* \left(\frac{\bar{X}}{\bar{x}^*}\right)^\alpha \exp\left\{c \frac{\bar{X} - \bar{x}^*}{\bar{X} + \bar{x}^*}\right\}$
Singh and Usman (2019b)	$t_{SU2} = [d_1^* \bar{y}^* + d_2^* (\bar{X} - \bar{x}^*)] \exp\left(\frac{\bar{X} - \bar{x}^*}{\bar{X} + \bar{x}^*}\right)$
Unal and Kadilar (2020)	$t_{UK} = \bar{y}^* \left(\frac{\bar{x}^*}{\bar{X}}\right)^\alpha \exp\left(\frac{\bar{X} - \bar{x}^*}{\bar{X} + \bar{x}^*}\right)$
Riaz et al. (2020)	$t_{RNAQ} = \bar{y}^* [d_1^* + d_2^* (a\bar{X} - a\bar{x}^*)] \exp\left(\frac{c(a\bar{X} - a\bar{x}^*)}{(a\bar{X} - a\bar{x}^*) + 2b}\right)$
Unal and Kadilar (2021)	$t_{2,i} = k\bar{y}^* \left(\frac{a\bar{X} + b}{a\bar{x}^* + b}\right)^c \exp\left(\frac{a(\bar{X} - \bar{x}^*)}{a(\bar{X} + \bar{x}^*) + 2b}\right)$

In Tables 1 – 2, $\alpha, d_1^*, d_2^*, k, \eta$ and δ are chosen constants that make MSE minimum and c takes the (0, -1, 1) values. Besides, a and b are either function of the known parameters of x or real numbers.

For this study, our main motivation is proposing more efficient estimator than existing estimators in literature in the presence of both non-response schemes as Case I and Case II. In this article, we introduce the proposed family of estimators for both cases. The appropriateness of the proposed family of estimators is examined theoretically and numerically on agriculture in Sections 4 and 5, respectively. Finally, the article is concluded with the obtained results.

2. Proposed Family of Estimators

Singh et al. (2020) proposed a new estimator using the exponential function. Based on this estimator, a new family of estimators for the population mean is proposed under the non-response scheme, Case I and Case II, respectively, as follows:

3.1. CASE I:

The first family of estimators is defined as

$$t_{C1,j} = \bar{y}^* \left(v_1 + v_2 \frac{\bar{X}}{\bar{x}} \right) \exp \left(\frac{\phi(\bar{X} - \bar{x})}{\phi(\bar{X} + \bar{x}) + 2\varphi} \right), j=1, 2, \dots, 10, \tag{3}$$

Where; v_1 and v_2 are constants that make the $MSE(t_{C1,j}), j = 1, 2, \dots, 10$ minimum. Besides, ϕ and φ are either functions of the known parameters of x or real numbers.

In order to obtain the bias and MSE of the $t_{C1,j}, j = 1, 2, \dots, 10$, we use the following notations as

$$\bar{y}^* = (\bar{Y}e_y^* + \bar{Y}), \bar{x} = (\bar{X}e_x + \bar{X}), \quad E(e_x) = 0, E(e_x^2) = \lambda C_x^2, E(e_y^*) = 0, E(e_y^{*2}) = \left(\lambda C_y^2 + \frac{W_2(z-1)}{n} C_{y(2)}^2 \right)$$

$$E(e_y^* e_x) = \lambda C_{yx},$$

Where; $C_x^2 = \frac{S_x^2}{\bar{X}^2}, C_{xy} = \rho_{xy} C_x C_y, C_{x(2)}^2 = \frac{S_{x(2)}^2}{\bar{X}^2}, C_{yx(2)} = \rho_{yx(2)} C_{x(2)} C_{y(2)}$ and ρ_{xy} is the coefficient of the population correlation between y and x .

We re-write the Equation (3) using these notations as follows:

$$t_{C1,j} = \bar{Y} (1 + e_y^*) \left(v_1 + v_2 \frac{\bar{X}}{\bar{X}(1 + e_x)} \right) \left(1 - \vartheta e_x + \frac{3\vartheta^2}{2} e_x^2 \right)$$

$$= \bar{Y} (1 + e_y^*) \left(v_1 - v_1 \vartheta e_x + \frac{3v_1 \vartheta^2}{2} e_x^2 + v_2 - v_2 \vartheta e_x + \frac{3v_2 \vartheta^2}{2} e_x^2 - v_2 e_x + v_2 \vartheta e_x^2 + v_2 e_x^2 \right), \tag{4}$$

Where; $\vartheta = \frac{\phi \bar{X}}{2(\phi \bar{X} + \varphi)}$.

Using different ϕ and φ values, we can propose various estimators and some members of the proposed estimators are given in Table 3.

Table 3- Some members of the $t_{CI,j}$, $j = 1, 2, \dots, 10$

Values			Estimators
\mathcal{G}_i	ϕ	φ	
$\mathcal{G}_1 = \frac{\bar{X}}{2(\bar{X}+1)}$	1	1	$t_{CI,1} = \bar{y}^* \left(\nu_1 + \nu_2 \frac{\bar{X}}{\bar{x}} \right) \exp \left(\frac{(\bar{X} - \bar{x})}{(\bar{X} + \bar{x}) + 2} \right)$
$\mathcal{G}_2 = \frac{\bar{X}}{2(\bar{X} + \beta_2(x))}$	1	$\beta_2(x)$	$t_{CI,2} = \bar{y}^* \left(\nu_1 + \nu_2 \frac{\bar{X}}{\bar{x}} \right) \exp \left(\frac{(\bar{X} - \bar{x})}{(\bar{X} + \bar{x}) + 2\beta_2(x)} \right)$
$\mathcal{G}_3 = \frac{\bar{X}}{2(\bar{X} + C_x)}$	1	C_x	$t_{CI,3} = \bar{y}^* \left(\nu_1 + \nu_2 \frac{\bar{X}}{\bar{x}} \right) \exp \left(\frac{(\bar{X} - \bar{x})}{(\bar{X} + \bar{x}) + 2\varphi} \right)$
$\mathcal{G}_4 = \frac{\bar{X}}{2(\bar{X} + \rho)}$	1	ρ	$t_{CI,4} = \bar{y}^* \left(\nu_1 + \nu_2 \frac{\bar{X}}{\bar{x}} \right) \exp \left(\frac{(\bar{X} - \bar{x})}{(\bar{X} + \bar{x}) + 2\rho} \right)$
$\mathcal{G}_5 = \frac{\beta_2(x)\bar{X}}{2(\beta_2(x)\bar{X} + C_x)}$	$\beta_2(x)$	C_x	$t_{CI,5} = \bar{y}^* \left(\nu_1 + \nu_2 \frac{\bar{X}}{\bar{x}} \right) \exp \left(\frac{\beta_2(x)(\bar{X} - \bar{x})}{\beta_2(x)(\bar{X} + \bar{x}) + 2C_x} \right)$
$\mathcal{G}_6 = \frac{C_x\bar{X}}{2(C_x\bar{X} + \beta_2(x))}$	C_x	$\beta_2(x)$	$t_{CI,6} = \bar{y}^* \left(\nu_1 + \nu_2 \frac{\bar{X}}{\bar{x}} \right) \exp \left(\frac{C_x(\bar{X} - \bar{x})}{C_x(\bar{X} + \bar{x}) + 2\beta_2(x)} \right)$
$\mathcal{G}_7 = \frac{C_x\bar{X}}{2(C_x\bar{X} + \rho)}$	C_x	ρ	$t_{CI,7} = \bar{y}^* \left(\nu_1 + \nu_2 \frac{\bar{X}}{\bar{x}} \right) \exp \left(\frac{C_x(\bar{X} - \bar{x})}{C_x(\bar{X} + \bar{x}) + 2\rho} \right)$
$\mathcal{G}_8 = \frac{\rho\bar{X}}{2(\rho\bar{X} + C_x)}$	ρ	C_x	$t_{CI,8} = \bar{y}^* \left(\nu_1 + \nu_2 \frac{\bar{X}}{\bar{x}} \right) \exp \left(\frac{\rho(\bar{X} - \bar{x})}{\rho(\bar{X} + \bar{x}) + 2C_x} \right)$
$\mathcal{G}_9 = \frac{\beta_2(x)\bar{X}}{2(\beta_2(x)\bar{X} + \rho)}$	$\beta_2(x)$	ρ	$t_{CI,9} = \bar{y}^* \left(\nu_1 + \nu_2 \frac{\bar{X}}{\bar{x}} \right) \exp \left(\frac{\beta_2(x)(\bar{X} - \bar{x})}{\beta_2(x)(\bar{X} + \bar{x}) + 2\rho} \right)$
$\mathcal{G}_{10} = \frac{\rho\bar{X}}{2(\rho\bar{X} + \beta_2(x))}$	ρ	$\beta_2(x)$	$t_{CI,10} = \bar{y}^* \left(\nu_1 + \nu_2 \frac{\bar{X}}{\bar{x}} \right) \exp \left(\frac{\rho(\bar{X} - \bar{x})}{\rho(\bar{X} + \bar{x}) + 2\beta_2(x)} \right)$

We expand the right hand side of Equation (4) and after the terms, having powers of e_y^* and e_x two and higher, are neglected, we have

$$\begin{aligned}
 (t_{CI,j} - \bar{Y}) = \bar{Y} & \left(\nu_1 - \nu_1 \mathcal{G} e_x + \frac{3\nu_1 \mathcal{G}^2}{2} e_x^2 + \nu_2 - \nu_2 \mathcal{G} e_x + \frac{3\nu_2 \mathcal{G}^2}{2} e_x^2 - \nu_2 e_x + \nu_2 \mathcal{G} e_x^2 \right. \\
 & \left. + \nu_2 e_x^2 + \nu_1 e_y^* - \nu_1 \mathcal{G} e_y^* e_x + \nu_2 e_y^* - \nu_2 \mathcal{G} e_y^* e_x - \nu_2 e_y^* e_x - 1 \right)
 \end{aligned}
 \tag{5}$$

We take the expectation on both sides of Equation (5) to derive $B(t_{CI})$ as

$$\begin{aligned}
 E(t_{CI,j} - \bar{Y}) & = \bar{Y} \left((\nu_1 + \nu_2 - 1) + E(e_x^2) \left(\frac{3\mathcal{G}^2}{2} (\nu_1 + \nu_2) + \nu_2 (\mathcal{G} + 1) \right) - E(e_y^* e_x) (\nu_1 \mathcal{G} + \nu_2 (\mathcal{G} + 1)) \right) \\
 B(t_{CI,j}) & = \bar{Y} \left((\nu_1 + \nu_2 - 1) + \lambda C_x^2 \left(\frac{3\mathcal{G}^2}{2} (\nu_1 + \nu_2) + \nu_2 (\mathcal{G} + 1) \right) - \lambda C_{yx} (\nu_1 \mathcal{G} + \nu_2 (\mathcal{G} + 1)) \right).
 \end{aligned}$$

Expressions of the MSE are computed as follows:

$$\begin{aligned} (t_{Cl,j} - \bar{Y})^2 = & \bar{Y}^2 \left(1 + v_1^2 \left(1 + e_y^{*2} + 4g^2 e_x^2 - 4ge_y^* e_x \right) \right. \\ & + v_2^2 \left(1 + e_y^{*2} + 3e_x^2 + 4ge_x^2 + 4g^2 e_x^2 - 4ge_y^* e_x - 4e_y^* e_x \right) \\ & + v_1 v_2 \left(2 + 2e_y^{*2} + 2e_x^2 + 4ge_x^2 + 8g^2 e_x^2 - 8ge_y^* e_x - 4e_y^* e_x \right) \\ & - v_1 \left(2 + 3g^2 e_x^2 - 2ge_y^* e_x \right) \\ & \left. - v_2 \left(2 + 3g^2 e_x^2 + 2ge_x^2 + 2e_x^2 - 2ge_y^* e_x - 2e_y^* e_x \right) \right), \end{aligned}$$

$$\begin{aligned} E(t_{Cl,j} - \bar{Y})^2 = & \bar{Y}^2 \left(1 + v_1^2 \left(1 + E(e_y^{*2}) + 4g^2 E(e_x^2) - 4gE(e_y^* e_x) \right) \right. \\ & + v_2^2 \left(1 + E(e_y^{*2}) + 3E(e_x^2) + 4gE(e_x^2) + 4g^2 E(e_x^2) - 4gE(e_y^* e_x) - 4E(e_y^* e_x) \right) \\ & + v_1 v_2 \left(2 + 2E(e_y^{*2}) + 2E(e_x^2) + 4gE(e_x^2) + 8g^2 E(e_x^2) - 8gE(e_y^* e_x) - 4E(e_y^* e_x) \right) \\ & - v_1 \left(2 + 3g^2 E(e_x^2) - 2gE(e_y^* e_x) \right) \\ & \left. - v_2 \left(2 + 3g^2 E(e_x^2) + 2gE(e_x^2) + 2E(e_x^2) - 2gE(e_y^* e_x) - 2E(e_y^* e_x) \right) \right), \end{aligned}$$

Where;

$$\begin{aligned} A_1 &= \left(1 + E(e_y^{*2}) + 4g^2 E(e_x^2) - 4gE(e_y^* e_x) \right) \\ A_2 &= \left(1 + E(e_y^{*2}) + 3E(e_x^2) + 4gE(e_x^2) + 4g^2 E(e_x^2) - 4gE(e_y^* e_x) - 4E(e_y^* e_x) \right) \\ A_3 &= \left(1 + \frac{3}{2} g^2 E(e_x^2) - gE(e_y^* e_x) \right) \\ A_4 &= \left(1 + \frac{3}{2} g^2 E(e_x^2) + gE(e_x^2) + E(e_x^2) - gE(e_y^* e_x) - E(e_y^* e_x) \right) \\ A_5 &= \left(1 + E(e_y^{*2}) + E(e_x^2) + 2gE(e_x^2) + 4g^2 E(e_x^2) - 4gE(e_y^* e_x) - 2E(e_y^* e_x) \right) \end{aligned}$$

and then we obtain $MSE(t_{Cl,j}), j = 1, 2, \dots, 10$ as

$$MSE(t_{Cl,j}) = \bar{Y}^2 \left(1 + A_1 v_1^2 + A_2 v_2^2 + 2A_5 v_1 v_2 - 2A_3 v_1 - 2A_4 v_2 \right), j = 1, 2, \dots, 10. \tag{6}$$

To obtain the minimum MSE of the $t_{Cl,j}, j = 1, 2, \dots, 10$, we get the optimal values of v_1 and v_2 , respectively, as follows:

$$v_1^* = \frac{A_2 A_3 - A_5 A_4}{A_1 A_2 - A_5^2}, v_2^* = \frac{A_1 A_4 - A_3 A_5}{A_1 A_2 - A_5^2}.$$

Using the optimal values, v_1^* and v_2^* , and substituting them in Equation (6), we obtain

$$MSE_{\min}(t_{Cl,j}) = \bar{Y}^2 \left(1 + A_1 v_1^{*2} + A_2 v_2^{*2} + 2A_5 v_1^* v_2^* - 2A_3 v_1^* - 2A_4 v_2^* \right) \tag{7}$$

$$= \bar{Y}^2 \left(1 - \frac{A_2 A_3^2 + A_1 A_4^2 - 2A_3 A_4 A_5}{A_1 A_2 - A_5^2} \right), j = 1, 2, \dots, 10. \tag{8}$$

3.2. CASE II:

The second family of estimators is proposed as

$$t_{C2,j} = \bar{y}^* \left(v_1 + v_2 \frac{\bar{X}}{\bar{x}^*} \right) \exp \left(\frac{\phi(\bar{X} - \bar{x}^*)}{\phi(\bar{X} + \bar{x}^*) + 2\phi} \right), j=1, 2, \dots, 10. \quad (9)$$

Similarly, in the Case I, we re-write Equation (9) as

$$\begin{aligned} t_{C2,j} &= \bar{Y} (1 + e_y^*) \left(v_1 + v_2 \frac{\bar{X}}{\bar{X}(1 + e_x^*)} \right) \left(1 - \mathcal{G}e_x^* + \frac{3\mathcal{G}^2}{2} e_x^{*2} \right), \\ &= \bar{Y} (1 + e_y^*) \left(v_1 - v_1 \mathcal{G}e_x^* + \frac{3v_1 \mathcal{G}^2}{2} e_x^{*2} + v_2 - v_2 \mathcal{G}e_x^* + \frac{3v_2 \mathcal{G}^2}{2} e_x^{*2} - v_2 e_x^* + v_2 \mathcal{G}e_x^{*2} + v_2 e_x^{*2} \right). \end{aligned} \quad (10)$$

We can write some members of the family of estimators for the Case II as in Table 4.

Expanding the right hand side of Equation (10) and then neglecting the terms having powers of e_y^* and e_x^* two and higher, we have

$$\begin{aligned} (t_{C2,j} - \bar{Y}) &= \bar{Y} \left(v_1 - v_1 \mathcal{G}e_x^* + \frac{3v_1 \mathcal{G}^2}{2} e_x^{*2} + v_2 - v_2 \mathcal{G}e_x^* + \frac{3v_2 \mathcal{G}^2}{2} e_x^{*2} - v_2 e_x^* + v_2 \mathcal{G}e_x^{*2} \right. \\ &\quad \left. + v_2 e_x^{*2} + v_1 e_y^* - v_1 \mathcal{G}e_y^* e_x^* + v_2 e_y^* - v_2 \mathcal{G}e_y^* e_x^* - v_2 e_y^* e_x^* - 1 \right), j=1, 2, \dots, 10. \end{aligned} \quad (11)$$

We take the expectation on both sides of Equation (11) as

$$E(t_{C2,j} - \bar{Y}) = \bar{Y} \left((v_1 + v_2 - 1) + E(e_x^{*2}) \left(\frac{3\mathcal{G}^2}{2} (v_1 + v_2) + v_2 (\mathcal{G} + 1) \right) - E(e_y^* e_x^*) (v_1 \mathcal{G} + v_2 (\mathcal{G} + 1)) \right).$$

Using $E(e_x^*) = 0$, $E(e_y^*) = 0$, $E(e_x^{*2}) = \lambda C_x^2 + \frac{W_2(z-1)}{n} C_{x(2)}^2$, $E(e_y^* e_x^*) = \lambda \rho_{xy} C_x C_y + \frac{W_2(z-1)}{n} C_{xy(2)}$

$E(e_y^{*2}) = \lambda C_y^2 + \frac{W_2(z-1)}{n} C_{y(2)}^2$ notations, we obtain the bias of the $t_{C2,j}$, $j=1, 2, \dots, 10$ as follows:

Table 4- Some members of the $t_{C2,j}$, $j = 1, 2, \dots, 10$

Values			Estimators
\mathcal{G}_i	ϕ	φ	
$\mathcal{G}_1 = \frac{\bar{X}}{2(\bar{X}+1)}$	1	1	$t_{C2,1} = \bar{y}^* \left(v_1 + v_2 \frac{\bar{X}}{\bar{x}^*} \right) \exp \left(\frac{(\bar{X} - \bar{x}^*)}{(\bar{X} + \bar{x}^*) + 2} \right)$
$\mathcal{G}_2 = \frac{\bar{X}}{2(\bar{X} + \beta_2(x))}$	1	$\beta_2(x)$	$t_{C2,2} = \bar{y}^* \left(v_1 + v_2 \frac{\bar{X}}{\bar{x}^*} \right) \exp \left(\frac{(\bar{X} - \bar{x}^*)}{(\bar{X} + \bar{x}^*) + 2\beta_2(x)} \right)$
$\mathcal{G}_3 = \frac{\bar{X}}{2(\bar{X} + C_x)}$	1	C_x	$t_{C2,3} = \bar{y}^* \left(v_1 + v_2 \frac{\bar{X}}{\bar{x}^*} \right) \exp \left(\frac{(\bar{X} - \bar{x}^*)}{(\bar{X} + \bar{x}^*) + 2\varphi} \right)$
$\mathcal{G}_4 = \frac{\bar{X}}{2(\bar{X} + \rho)}$	1	ρ	$t_{C2,4} = \bar{y}^* \left(v_1 + v_2 \frac{\bar{X}}{\bar{x}^*} \right) \exp \left(\frac{(\bar{X} - \bar{x}^*)}{(\bar{X} + \bar{x}^*) + 2\rho} \right)$
$\mathcal{G}_5 = \frac{\beta_2(x)\bar{X}}{2(\beta_2(x)\bar{X} + C_x)}$	$\beta_2(x)$	C_x	$t_{C2,5} = \bar{y}^* \left(v_1 + v_2 \frac{\bar{X}}{\bar{x}^*} \right) \exp \left(\frac{\beta_2(x)(\bar{X} - \bar{x}^*)}{\beta_2(x)(\bar{X} + \bar{x}^*) + 2C_x} \right)$
$\mathcal{G}_6 = \frac{C_x\bar{X}}{2(C_x\bar{X} + \beta_2(x))}$	C_x	$\beta_2(x)$	$t_{C2,6} = \bar{y}^* \left(v_1 + v_2 \frac{\bar{X}}{\bar{x}^*} \right) \exp \left(\frac{C_x(\bar{X} - \bar{x}^*)}{C_x(\bar{X} + \bar{x}^*) + 2\beta_2(x)} \right)$
$\mathcal{G}_7 = \frac{C_x\bar{X}}{2(C_x\bar{X} + \rho)}$	C_x	ρ	$t_{C2,7} = \bar{y}^* \left(v_1 + v_2 \frac{\bar{X}}{\bar{x}^*} \right) \exp \left(\frac{C_x(\bar{X} - \bar{x}^*)}{C_x(\bar{X} + \bar{x}^*) + 2\rho} \right)$
$\mathcal{G}_8 = \frac{\rho\bar{X}}{2(\rho\bar{X} + C_x)}$	ρ	C_x	$t_{C2,8} = \bar{y}^* \left(v_1 + v_2 \frac{\bar{X}}{\bar{x}^*} \right) \exp \left(\frac{\rho(\bar{X} - \bar{x}^*)}{\rho(\bar{X} + \bar{x}^*) + 2C_x} \right)$
$\mathcal{G}_9 = \frac{\beta_2(x)\bar{X}}{2(\beta_2(x)\bar{X} + \rho)}$	$\beta_2(x)$	ρ	$t_{C2,9} = \bar{y}^* \left(v_1 + v_2 \frac{\bar{X}}{\bar{x}^*} \right) \exp \left(\frac{\beta_2(x)(\bar{X} - \bar{x}^*)}{\beta_2(x)(\bar{X} + \bar{x}^*) + 2\rho} \right)$
$\mathcal{G}_{10} = \frac{\rho\bar{X}}{2(\rho\bar{X} + \beta_2(x))}$	ρ	$\beta_2(x)$	$t_{C2,10} = \bar{y}^* \left(v_1 + v_2 \frac{\bar{X}}{\bar{x}^*} \right) \exp \left(\frac{\rho(\bar{X} - \bar{x}^*)}{\rho(\bar{X} + \bar{x}^*) + 2\beta_2(x)} \right)$

$$B(t_{C2,j}) = \bar{Y} \left((v_1 + v_2 - 1) + \left(\lambda C_x^2 + \frac{W_2(z-1)}{n} C_{x(2)}^2 \right) \left(\frac{3\mathcal{G}^2}{2} (v_1 + v_2) + v_2 (\mathcal{G} + 1) \right) - \left(\lambda C_{yx} + \frac{W_2(z-1)}{n} C_{yx(2)} \right) (v_1 \mathcal{G} + v_2 (\mathcal{G} + 1)) \right), j = 1, 2, \dots, 10.$$

Similarly, expressions of the $MSE(t_{C2,j})$, $j = 1, 2, \dots, 10$ are computed, respectively, as follows:

$$\begin{aligned} (t_{C2,j} - \bar{Y})^2 = & \bar{Y}^2 \left(1 + v_1^2 (1 + e_y^{*2} + 4\mathcal{G}^2 e_x^{*2} - 4\mathcal{G} e_y^* e_x^*) \right. \\ & + v_2^2 (1 + e_y^{*2} + 3e_x^{*2} + 4\mathcal{G} e_x^{*2} + 4\mathcal{G}^2 e_x^{*2} - 4\mathcal{G} e_y^* e_x^* - 4e_y^* e_x^*) \\ & + v_1 v_2 (2 + 2e_y^{*2} + 2e_x^{*2} + 4\mathcal{G} e_x^{*2} + 8\mathcal{G}^2 e_x^{*2} - 8\mathcal{G} e_y^* e_x^* - 4e_y^* e_x^*) \\ & - v_1 (2 + 3\mathcal{G}^2 e_x^{*2} - 2\mathcal{G} e_y^* e_x^*) \\ & \left. - v_2 (2 + 3\mathcal{G}^2 e_x^{*2} + 2\mathcal{G} e_x^{*2} + 2e_x^{*2} - 2\mathcal{G} e_y^* e_x^* - 2e_y^* e_x^*) \right) \end{aligned}$$

$$\begin{aligned}
E(t_{C2,j} - \bar{Y})^2 &= \bar{Y}^2 \left(1 + v_1^2 \left(1 + E(e_y^{*2}) + 4g^2 E(e_x^{*2}) - 4gE(e_y^* e_x^*) \right) \right. \\
&\quad + v_2^2 \left(1 + E(e_y^{*2}) + 3E(e_x^{*2}) + 4gE(e_x^{*2}) + 4g^2 E(e_x^{*2}) - 4gE(e_y^* e_x^*) - 4E(e_y^* e_x^*) \right) \\
&\quad + v_1 v_2 \left(2 + 2E(e_y^{*2}) + 2E(e_x^{*2}) + 4gE(e_x^{*2}) + 8g^2 E(e_x^{*2}) - 8gE(e_y^* e_x^*) - 4E(e_y^* e_x^*) \right) \\
&\quad - v_1 \left(2 + 3g^2 E(e_x^{*2}) - 2gE(e_y^* e_x^*) \right) \\
&\quad \left. - v_2 \left(2 + 3g^2 E(e_x^{*2}) + 2gE(e_x^{*2}) + 2E(e_x^{*2}) - 2gE(e_y^* e_x^*) - 2E(e_y^* e_x^*) \right) \right)
\end{aligned}$$

Where;

$$\begin{aligned}
B_1 &= \left(1 + E(e_y^{*2}) + 4g^2 E(e_x^{*2}) - 4gE(e_y^* e_x^*) \right) \\
B_2 &= \left(1 + E(e_y^{*2}) + 3E(e_x^{*2}) + 4gE(e_x^{*2}) + 4g^2 E(e_x^{*2}) - 4gE(e_y^* e_x^*) - 4E(e_y^* e_x^*) \right) \\
B_3 &= \left(1 + \frac{3}{2} g^2 E(e_x^{*2}) - gE(e_y^* e_x^*) \right) \\
B_4 &= \left(1 + \frac{3}{2} g^2 E(e_x^{*2}) + gE(e_x^{*2}) + E(e_x^{*2}) - gE(e_y^* e_x^*) - E(e_y^* e_x^*) \right) \\
B_5 &= \left(1 + E(e_y^{*2}) + E(e_x^{*2}) + 2gE(e_x^{*2}) + 4g^2 E(e_x^{*2}) - 4gE(e_y^* e_x^*) - 2E(e_y^* e_x^*) \right)
\end{aligned}$$

and then we obtain $MSE(t_{C2,j})$, $j = 1, 2, \dots, 10$ as

$$MSE(t_{C2,j}) = \bar{Y}^2 (1 + B_1 v_1^2 + B_2 v_2^2 + 2B_5 v_1 v_2 - 2B_3 v_1 - 2B_4 v_2), \quad j = 1, 2, \dots, 10. \quad (12)$$

The optimal values of v_1 and v_2 are obtained as

$$v_1^{**} = \frac{B_2 B_3 - B_3 B_4}{B_1 B_2 - B_5^2}, \quad v_2^{**} = \frac{B_1 B_4 - B_3 B_5}{B_1 B_2 - B_5^2}.$$

Using v_1^{**} and v_2^{**} and substituting them in Equation (22), we get

$$\begin{aligned}
MSE_{\min}(t_{C2,j}) &= \bar{Y}^2 \left(1 + B_1 v_1^{**2} + B_2 v_2^{**2} + 2B_5 v_1^{**} v_2^{**} - 2B_3 v_1^{**} - 2B_4 v_2^{**} \right) \\
&= \bar{Y}^2 \left(1 - \frac{B_2 B_3^2 + B_1 B_4^2 - 2B_3 B_4 B_5}{B_1 B_2 - B_5^2} \right), \quad j = 1, 2, \dots, 10. \quad (13)
\end{aligned}$$

3. Efficiency Comparisons

One of the important features of an estimator is efficiency. After the theoretical inferences of the $t_{C1,j}$ and $t_{C2,j}$, $j=1, 2, \dots, 10$ estimators, we obtain the efficiency comparisons for each case, separately. The conditions are given for the Case I and Case II in the next sub-sections.

a. Efficiency comparisons for the first case

We use the variance of the t_H and the MSE Equation of the t_{R1} , t_{expl} , t_{reg1} , $t_{C1,j}$, $j=1, 2, \dots, 10$, respectively, as follows:

$$MSE(t_{R1}) = \bar{Y}^2 \left(\lambda(C_x^2 - 2C_{yx} + C_y^2) + \frac{W_2(z-1)}{n} C_{y(2)}^2 \right), \tag{14}$$

$$MSE(t_{exp1}) = \bar{Y}^2 \left(\lambda \left(C_y^2 + \frac{C_x^2}{4} - C_{yx} \right) + \frac{W_2(z-1)}{n} C_{y(2)}^2 \right), \tag{15}$$

$$MSE(t_{reg1}) = \bar{Y}^2 \left(\lambda C_y^2 (1 - \rho_{xy}^2) + \frac{W_2(z-1)}{n} C_{y(2)}^2 \right) \tag{16}$$

and using Equations (2), (14), (15), and (16), we obtain that

- $[V(t_H) - MSE_{\min}(t_{C1,j})] > 0, j = 1, 2, \dots, 10$
 $\left(\lambda C_y^2 + \frac{W_2(z-1)}{n} C_{y(2)}^2 \right) - \left(1 - \frac{A_2 A_3^2 + A_1 A_4^2 - 2A_3 A_4 A_5}{A_1 A_2 - A_5^2} \right) > 0$ \tag{17}

- $[MSE(t_{R1}) - MSE_{\min}(t_{C1,j})] > 0, j = 1, 2, \dots, 10$
 $\left(\lambda(C_x^2 - 2C_{yx} + C_y^2) + \frac{W_2(z-1)}{n} C_{y(2)}^2 \right) - \left(1 - \frac{A_2 A_3^2 + A_1 A_4^2 - 2A_3 A_4 A_5}{A_1 A_2 - A_5^2} \right) > 0$ \tag{18}

- $[MSE(t_{exp1}) - MSE_{\min}(t_{C1,j})] > 0, j = 1, 2, \dots, 10$
 $\left(\lambda \left(C_y^2 + \frac{C_x^2}{4} - C_{yx} \right) + \frac{W_2(z-1)}{n} C_{y(2)}^2 \right) - \left(1 - \frac{A_2 A_3^2 + A_1 A_4^2 - 2A_3 A_4 A_5}{A_1 A_2 - A_5^2} \right) > 0$ \tag{19}

- $[MSE(t_{reg1}) - MSE_{\min}(t_{C1,j})] > 0, j = 1, 2, \dots, 10$
 $\left(\lambda C_y^2 (1 - \rho_{xy}^2) + \frac{W_2(z-1)}{n} C_{y(2)}^2 \right) - \left(1 - \frac{A_2 A_3^2 + A_1 A_4^2 - 2A_3 A_4 A_5}{A_1 A_2 - A_5^2} \right) > 0$ \tag{20}

b. Efficiency comparisons for the second case

We use the variance of the t_H and the MSE Equation of the $t_{R2}, t_{exp2}, t_{reg2}, t_{C2,j}, j=1, 2, \dots, 10$, respectively, as follows:

$$MSE(t_{R2}) = \bar{Y}^2 \left(\lambda(C_x^2 - 2C_{yx} + C_y^2) + \frac{W_2(z-1)}{n} (C_{y(2)}^2 + C_{x(2)}^2 - 2C_{yx(2)}) \right), \tag{21}$$

$$MSE(t_{exp2}) = \bar{Y}^2 \left(\lambda C_y^2 + \lambda \frac{C_x^2}{4} - \lambda C_{yx} + \frac{W_2(z-1)}{n} \left(C_{y(2)}^2 + \frac{C_{x(2)}^2}{4} - C_{yx(2)} \right) \right), \tag{22}$$

$$MSE(t_{reg2}) = \bar{Y}^2 \left(\lambda C_y^2 (1 - \rho_{xy}^2) + \frac{W_2(z-1)}{n} \left(C_{y(2)}^2 + \rho_{xy}^2 \frac{C_y^2}{C_x^2} C_{x(2)}^2 - 2\rho_{xy} \frac{C_y}{C_x} C_{yx(2)} \right) \right), \tag{23}$$

and using Equations (2), (21), (22) and (23), we obtain that

- $[V(t_H) - MSE_{\min}(t_{C2,j})] > 0, j = 1, 2, \dots, 10$
 $\left(\lambda C_y^2 + \frac{W_2(z-1)}{n} C_{y(2)}^2 \right) - \left(1 - \frac{B_2 B_3^2 + B_1 B_4^2 - 2B_3 B_4 B_5}{B_1 B_2 - B_5^2} \right) > 0$ \tag{24}

- $[MSE(t_{R2}) - MSE_{\min}(t_{C2,j})] > 0, j = 1, 2, \dots, 10$
 $\left(\lambda(C_x^2 - 2C_{yx} + C_y^2) + \frac{W_2(z-1)}{n} (C_{y(2)}^2 + C_{x(2)}^2 - 2C_{yx(2)}) \right) - \left(1 - \frac{B_2 B_3^2 + B_1 B_4^2 - 2B_3 B_4 B_5}{B_1 B_2 - B_5^2} \right) > 0$ \tag{25}

$$\begin{aligned}
 & \bullet \left[MSE(t_{\text{exp}2}) - MSE_{\min}(t_{C2,j}) \right] > 0, j = 1, 2, \dots, 10 \\
 & \left(\lambda C_y^2 + \lambda \frac{C_x^2}{4} - \lambda C_{yx} + \frac{W_2(z-1)}{n} \left(C_{y(2)}^2 + \frac{C_{x(2)}^2}{4} - C_{yx(2)} \right) \right) - \left(1 - \frac{B_2 B_3^2 + B_1 B_4^2 - 2 B_3 B_4 B_5}{B_1 B_2 - B_5^2} \right) > 0 \tag{26}
 \end{aligned}$$

$$\begin{aligned}
 & \bullet \left[MSE(t_{\text{reg}2}) - MSE_{\min}(t_{C2,j}) \right] > 0, j = 1, 2, \dots, 10 \\
 & \left(\lambda C_y^2 (1 - \rho_{xy}^2) + \frac{W_2(z-1)}{n} \left(C_{y(2)}^2 + \rho_{xy}^2 \frac{C_y^2}{C_x^2} C_{x(2)}^2 - 2 \rho_{xy} \frac{C_y}{C_x} C_{yx(2)} \right) \right) - \left(1 - \frac{B_2 B_3^2 + B_1 B_4^2 - 2 B_3 B_4 B_5}{B_1 B_2 - B_5^2} \right) > 0 \tag{27}
 \end{aligned}$$

The family of estimators, $t_{C1,j}$ and $t_{C2,j}$ $j=1,2,\dots,10$ are more efficient than others if the conditions for the efficiency, given in Equation (17) – Equation (20) and Equation (24) – Equation (27), are satisfied for both cases, respectively.

4. Empirical Studies

After theoretical inferences and comparisons, numerical illustrations are conducted in this section. The two real data sets are used to deal with the situation in which $t_{C1,j}$ and $t_{C2,j}$, $j = 1, 2, \dots, 10$ estimators are more efficient than others. These data sets are also related with the agriculture for the purpose of showing the appropriateness of the proposed estimators, $t_{C1,j}$ and $t_{C2,j}$, $j = 1, 2, \dots, 10$, in the agricultural field.

The parameter values for the Population 1 and Population 2 are given as follows:

Population 1. [Khare and Sinha (2009)]

In this population, the number of agriculture labors and the area of the village (in hectares) are considered as y and x , respectively. In this population, 25% of villages is greater than 160 ha and they symbolize the non-response group.

$N = 96$	$n = 40$	$\rho_{yx(2)} = 0.72$	$C_{yx} = 0.8232$	$C_{yx(2)} = 1.4077$
$\bar{X} = 144.87$	$W_2 = 0.25$	$\rho_{yx} = 0.77$	$C_x = 0.81$	$C_{x(2)} = 0.94$
$\bar{Y} = 137.92$	$\lambda = 0.01458, f = 0.42$	$\beta_2(x) = 1.19$	$C_y = 1.32$	$C_{y(2)} = 2.08$

Population 2. [Khare and Srivastava (1993)]

In population 2, the cultivated area (in acres) and the population of the village are considered as y and x , respectively. In this population, 14 villages (i.e. 20% villages) are considered as non-response units.

$N = 70$	$n = 35$	$\rho_{yx(2)} = 0.445$	$C_{yx} = 0.3896$	$C_{yx(2)} = 0.104$
$\bar{X} = 1755.53$	$W_2 = 0.2$	$\rho_{yx} = 0.778$	$C_x = 0.801$	$C_{x(2)} = 0.574$
$\bar{Y} = 981.29$	$\lambda = 0.0143, f = 0.50$	$\beta_2(x) = 0.34$	$C_y = 0.6254$	$C_{y(2)} = 0.4087$

In Tables 5 and 6, we present the MSE values of the $t_{C1,j}$, $j = 1, 2, \dots, 10$ and some main estimators for the Populations 1 and 2, respectively. According to the results, we conclude that the $t_{C1,j}$, $j = 1, 2, \dots, 10$ estimator has the minimum MSE value among other compared estimators using the different values of z for both populations.

Similarly, we present the MSE values of the $t_{C2,j}$, $j = 1, 2, \dots, 10$ and other same estimators for the Populations 1 and 2, respectively, in Tables 7 and 8. According to the various values of z , we conclude that the $t_{C2,j}$, $j = 1, 2, \dots, 10$ estimator has the minimum MSE value among others for both populations under the Case II as in the Case I.

Table 5- MSE values of the $t_{C1,j}, j = 1, 2, \dots, 10$ and existing estimators for the Population I

Estimators	$z=2$	$z=3$	$z=4$	$z=5$	$z=6$
$t_{C1,1}$	686.3603	1152.707	1595.907	2017.642	2419.43350
$t_{C1,2}$	686.3668	1152.718	1595.922	2017.660	2419.45502
$t_{C1,3}$	686.3542	1152.697	1595.893	2017.624	2419.41298
$t_{C1,4}$	686.3529	1152.695	1595.890	2017.621	2419.40865
$t_{C1,5}$	686.3498	1152.690	1595.883	2017.612	2419.39836
$t_{C1,6}$	686.3758	1152.733	1595.942	2017.685	2419.48517
$t_{C1,7}$	686.3587	1152.704	1595.903	2017.637	2419.42817
$t_{C1,8}$	686.3620	1152.710	1595.911	2017.646	2419.43910
$t_{C1,9}$	686.3487	1152.688	1595.881	2017.609	2419.39474
$t_{C1,10}$	686.3782	1152.737	1595.948	2017.692	2419.49339
t_H	997.7000	1512.053	2026.406	2540.759	3055.11160
t_{R1}	722.9411	1237.294	1751.647	2265.999	2780.35271
t_{reg1}	711.1235	1225.476	1739.829	2254.182	2768.53507
t_{exp1}	814.8195	1329.172	1843.525	2357.878	2872.23111

Table 6- MSE values of the $t_{C1,j}, j = 1, 2, \dots, 10$ and existing estimators for the Population II

Estimators	$z=2$	$z=3$	$z=4$	$z=5$	$z=6$
$t_{C1,1}$	3021.606751	3931.230876	4839.120003	5745.279089	6649.71308
$t_{C1,2}$	3021.605021	3931.228783	4839.117541	5745.276256	6649.70987
$t_{C1,3}$	3021.60623	3931.230246	4839.119261	5745.278236	6649.71211
$t_{C1,4}$	3021.60617	3931.230173	4839.119176	5745.278138	6649.71200
$t_{C1,5}$	3021.61030	3931.235167	4839.125048	5745.284896	6649.71965
$t_{C1,6}$	3021.60524	3931.229051	4839.117856	5745.276618	6649.71028
$t_{C1,7}$	3021.60668	3931.230786	4839.119896	5745.278967	6649.71294
$t_{C1,8}$	3021.60683	3931.230969	4839.120112	5745.279215	6649.71322
$t_{C1,9}$	3021.61012	3931.234955	4839.124798	5745.284609	6649.71933
$t_{C1,10}$	3021.60528	3931.229090	4839.117903	5745.276672	6649.71034
t_H	6299.48072	7218.587508	8137.694294	9056.801081	9975.90787
t_{R1}	4402.05564	5321.162427	6240.269214	7159.3760	8078.48279
t_{reg1}	3042.82647	3961.933251	4881.040038	5800.146825	6719.25361
t_{exp1}	3144.83018	4063.936966	4983.043753	5902.15054	6821.25733

Table 7- MSE values of the $t_{C2,j}, j = 1, 2, \dots, 10$ and existing estimators for the Population I

Estimators	$z=2$	$z=3$	$z=4$	$z=5$	$z=6$
$t_{C2,1}$	444.1827	685.4467	921.5507	1153.376	1381.321333
$t_{C2,2}$	444.1895	685.4614	921.5759	1153.414	1381.37485
$t_{C2,3}$	444.1762	685.4328	921.5268	1153.339	1381.270296
$t_{C2,4}$	444.1748	685.4298	921.5217	1153.332	1381.259528
$t_{C2,5}$	444.1716	685.4228	921.5097	1153.314	1381.233925
$t_{C2,6}$	444.199	685.4819	921.6111	1153.467	1381.449836
$t_{C2,7}$	444.181	685.4431	921.5445	1153.366	1381.308086
$t_{C2,8}$	444.1844	685.4505	921.5573	1153.386	1381.335255
$t_{C2,9}$	444.1704	685.4204	921.5054	1153.307	1381.224929
$t_{C2,10}$	444.2016	685.4875	921.6207	1153.482	1381.470268
t_H	997.7000	1512.053	2026.4058	2540.7587	3055.111599
t_{R2}	493.2647	777.9412	1062.6176	1347.2940	1631.970482
t_{reg2}	456.5109	716.2512	975.9915	1235.732	1495.472056
t_{exp2}	673.7192	1046.972	1420.2242	1793.4767	2166.729263

Table 8- MSE values of the $t_{C2,j}, j = 1, 2, \dots, 10$ and existing estimators for the Population II

Estimators	$z=2$	$z=3$	$z=4$	$z=5$	$z=6$
$t_{C2,1}$	2965.84881	3783.26051	4576.61636	5353.6645	6119.0051
$t_{C3,2}$	2965.84763	3783.25975	4576.61625	5353.6652	6119.0068
$t_{C2,3}$	2965.84846	3783.26028	4576.61633	5353.6647	6119.0055
$t_{C2,4}$	2965.84842	3783.26026	4576.61633	5353.6647	6119.0056
$t_{C3,5}$	2965.85124	3783.26205	4576.61658	5353.6630	6119.0014
$t_{C2,6}$	2965.84778	3783.25985	4576.61626	5353.6651	6119.0065
$t_{C2,7}$	2965.84876	3783.26048	4576.61636	5353.6645	6119.0051
$t_{C2,8}$	2965.84887	3783.26055	4576.61637	5353.6644	6119.0049
$t_{C2,9}$	2965.85112	3783.26198	4576.61657	5353.6630	6119.0016
$t_{C2,10}$	2965.84780	3783.25987	4576.61627	5353.6651	6119.0065
t_H	6299.48072	7218.58751	8137.69429	9056.8011	9975.9079
t_{R2}	5065.70210	6648.45535	8231.20860	9813.9618	11396.7150
t_{reg2}	3013.88002	3904.04037	4794.20072	5684.3611	6574.52141
t_{exp2}	3023.57939	3821.43539	4619.29140	5417.1474	6215.0034

The Percentage Relative Efficiency (PRE) values of $t_{C1,j}, j = 1, 2, \dots, 10$ and $t_{C2,j}, j = 1, 2, \dots, 10$ and existing estimators in literature for various values of z with respect to the Hansen and Hurwitz estimator (t_H) are presented in Tables 9 – 12 based on Populations 1 – 2, respectively, using the formulae as follows:

$$PRE(t) = \frac{MSE(t_H)}{MSE(t)} \times 100.$$

Table 9- PRE values of the $t_{C1,j}, j = 1, 2, \dots, 10$ and existing estimators for the Population I

Estimators	$z=2$	$z=3$	$z=4$	$z=5$	$z=6$
$t_{C1,1}$	145.3609723	131.1740864	126.9751881	125.9271596	126.2738405
$t_{C1,2}$	145.3596104	131.1728691	126.9740256	125.9260232	126.2727173
$t_{C1,3}$	145.3622712	131.1752472	126.9762967	125.9282433	126.2749115
$t_{C1,4}$	145.3625452	131.1754922	126.9765306	125.928472	126.2751375
$t_{C1,5}$	145.3631968	131.1760745	126.9770867	125.9290156	126.2756748
$t_{C1,6}$	145.3577021	131.1711634	126.9723966	125.9244308	126.2711436
$t_{C1,7}$	145.3613094	131.1743877	126.9754758	125.9274409	126.2741185
$t_{C1,8}$	145.360618	131.1737697	126.9748857	125.926864	126.2735483
$t_{C1,9}$	145.3634257	131.1762791	126.9772821	125.9292066	126.2758636
$t_{C1,10}$	145.3571821	131.1706986	126.9719528	125.9239969	126.2707148
t_H	100	100	100	100	100
t_{R1}	138.0057057	122.2064342	115.6857459	112.1252828	109.8821594
t_{reg1}	140.2991209	123.3849076	116.4715312	112.713104	110.3511972
t_{exp1}	122.4442927	113.7589736	109.9201504	107.7561464	106.3671926

Table 10- PRE values of the $t_{C1,j}, j = 1, 2, \dots, 10$ and existing estimators for the Population II

Estimators	$z=2$	$z=3$	$z=4$	$z=5$	$z=6$
$t_{C1,1}$	208.4811572	183.6215612	168.164755	157.6390101	150.020125
$t_{C1,2}$	208.4812766	183.6216589	168.1648405	157.6390878	150.0201974
$t_{C1,3}$	208.4811932	183.6215906	168.1647807	157.6390335	150.0201468
$t_{C1,4}$	208.4811973	183.621594	168.1647837	157.6390362	150.0201493
$t_{C1,5}$	208.4809126	183.6213607	168.1645796	157.6388507	150.0199766
$t_{C1,6}$	208.4812613	183.6216464	168.1648295	157.6390778	150.0201881
$t_{C1,7}$	208.4811624	183.6215654	168.1647587	157.6390134	150.0201281
$t_{C1,8}$	208.4811519	183.6215568	168.1647511	157.6390066	150.0201218
$t_{C1,9}$	208.4809247	183.6213707	168.1645883	157.6388586	150.0199839
$t_{C1,10}$	208.481259	183.6216446	168.1648279	157.6390764	150.0201867
t_H	100	100	100	100	100
t_{R1}	143.1031599	135.6580936	130.4061414	126.50266	123.487394
t_{reg1}	207.0272753	182.1986149	166.7204987	156.14779	148.4675002
t_{exp1}	200.31227	177.6254791	163.307703	153.4491711	146.2473469

According to the PRE values, the proposed family of estimators, $t_{C1,j}$, $j = 1, 2, \dots, 10$, perform better than compared estimators, t_{R1} , t_{reg1} and t_{exp1} , under the Case I for both populations.

Table 11- PRE values of the $t_{C2,j}$, $j = 1, 2, \dots, 10$ and existing estimators for the Population I

Estimators	$z=2$	$z=3$	$z=4$	$z=5$	$z=6$
$t_{C2,1}$	224.6148091	220.5937908	219.8908604	220.2888855	221.1731279
$t_{C3,2}$	224.6113763	220.5890807	219.8848622	220.2816	221.1645593
$t_{C2,3}$	224.6180833	220.5982832	219.8965812	220.2958339	221.1813001
$t_{C2,4}$	224.6187742	220.5992311	219.8977883	220.2973	221.1830244
$t_{C3,5}$	224.6204171	220.6014849	219.9006584	220.300786	221.1871243
$t_{C2,6}$	224.6065675	220.582482	219.8764587	220.2713929	221.1525544
$t_{C2,7}$	224.6156589	220.5949568	219.8923452	220.290689	221.175249
$t_{C2,8}$	224.613916	220.5925654	219.8892999	220.2869901	221.1708987
$t_{C2,9}$	224.6209943	220.6022769	219.9016669	220.3020109	221.188565
$t_{C2,10}$	224.6052573	220.5806842	219.8741691	220.2686119	221.1492835
t_H	100	100	100	100	100
t_{R2}	202.2646312	194.3659785	190.6994416	188.5823463	187.2038515
t_{reg2}	218.5490019	211.1065133	207.6253587	205.6076222	204.2907847
t_{exp2}	148.0884119	144.421566	142.6821051	141.6666661	141.0010771

Table 12- PRE values of the $t_{C2,j}$, $j = 1, 2, \dots, 10$ and existing estimators for the Population II

Estimators	$z=2$	$z=3$	$z=4$	$z=5$	$z=6$
$t_{C2,1}$	212.4006015	190.8033424	177.8102783	169.1701289	163.0315363
$t_{C3,2}$	212.4006865	190.8033807	177.8102828	169.170106	163.0314897
$t_{C2,3}$	212.4006271	190.8033539	177.8102797	169.170122	163.0315222
$t_{C2,4}$	212.40063	190.8033552	177.8102798	169.1701212	163.0315206
$t_{C3,5}$	212.4004277	190.8032646	177.8102699	169.1701767	163.0316328
$t_{C2,6}$	212.4006756	190.8033758	177.8102822	169.1701089	163.0314957
$t_{C2,7}$	212.4006052	190.8033441	177.8102785	169.1701279	163.0315342
$t_{C2,8}$	212.4005977	190.8033407	177.8102781	169.1701299	163.0315383
$t_{C2,9}$	212.4004363	190.8032685	177.8102703	169.1701743	163.031628
$t_{C2,10}$	212.400674	190.803375	177.8102822	169.1701094	163.0314965
t_H	100	100	100	100	100
t_{R2}	124.3555305	108.5754078	98.86390559	92.28486137	87.53318644
t_{reg2}	209.0156433	184.9004319	169.7403754	159.3283921	151.7358793
t_{exp2}	208.34514	188.8972797	176.1675893	167.1876435	160.5133131

Similarly in $t_{C1,j}$, $j = 1, 2, \dots, 10$, it is shown that the proposed family of estimators, $t_{C2,j}$, $j = 1, 2, \dots, 10$, perform better than compared estimators, t_{R2} , t_{reg2} and t_{exp2} , under the Case II for both populations.

These results show that the proposed families of estimators $t_{C1,j}$ and $t_{C2,j}$, $j = 1, 2, \dots, 10$ can be applied for estimating the population mean in the agriculture field for both cases.

5. Conclusions

This article proposes a family of estimators using the exponential function on estimation of the population mean in the presence of non-response. Firstly, we obtain the theoretical inferences and comparisons for the estimators under the Case I and Case II and then we found that the $t_{C1,j}$ and $t_{C2,j}$, $j = 1, 2, \dots, 10$ estimators are more efficient than others in literature under the obtained conditions for both cases. In empirical studies, we use real data sets with the aim of showing the appropriateness of estimators in agriculture. According to the obtained results, the proposed family of estimators can appropriately be used in the agriculture on the estimation of the population mean.

Acknowledgements

This publication is a part of PhD thesis of the first author.

References

- Bahl S, Tuteja R K (1991). Ratio and product type exponential estimators. *Journal of Information and Optimization Sciences* 12(1): 159-164. <https://doi.org/10.1080/02522667.1991.10699058>
- Cochran W G (1977). *Sampling Techniques*, John Wiley and Sons, New York.
- Dansawad N (2019). A Class of Exponential Estimator to Estimate the Population Mean in the Presence of Non-Response. *Naresuan University Journal: Science and Technology (NUJST)* 27(4): 20-26. <https://doi.org/10.14456/nujst.2019.33>
- Hansen M H & Hurwitz W N (1946). The problem of non-response in sample surveys. *Journal of the American Statistical Association* 41(236): 517-529. <https://doi.org/10.1080/01621459.1946.10501894>
- Khare B B & Sinha R R (2009). On class of estimators for population mean using multi-auxiliary characters in the presence of non-response. *Statistics in Transition* 10(1): 3-14
- Khare B B & Srivastava S (1993). Estimation of population mean using auxiliary character in presence of non-response. *National Academy Science Letters, India* 16: 111-114
- Kumar S (2013). Improved exponential estimator for estimating the population mean in the presence of non-response. *Communications for Statistical Applications and Methods* 20(5): 357-366. <https://doi.org/10.5351/csam.2013.20.5.357>
- Kumar S & Bhougal S (2011). Estimation of the population mean in presence of non-response. *Communications for Statistical Applications and Methods* 18(4): 537-548. <https://doi.org/10.5351/ckss.2011.18.4.537>
- Kumar K & Kumar M (2017). Improved exponential ratio and product type estimators for population mean in the presence of nonresponse. *Bulletin of Mathematics and Statistics Research* 5(2): 68-76
- Pal S K & Singh H P (2016). Finite population mean estimation through a two-parameter ratio estimator using auxiliary information in presence of non-response. *Journal of Applied Mathematics, Statistics and Informatics* 12(2): 5-39. <https://doi.org/10.1515/jamsi-2016-0006>
- Pal S K & Singh H P (2017). A class of ratio-cum-ratio-type exponential estimators for population mean with sub sampling the non-respondents. *Jordan Journal of Mathematics and Statistics* 10(1): 73-94
- Pal S K & Singh H P (2018). Estimation of finite population mean using auxiliary information in presence of non-response. *Communications in Statistics-Simulation and Computation* 47(1): 143-165. <https://doi.org/10.1080/03610918.2017.1280161>
- Rao P S R S (1986). Ratio estimation with sub sampling the non-respondents. *Survey Methodology* 12: 217-230
- Riaz S, Nazeer A, Abbasi J & Qamar S (2020). On the generalized class of estimators for estimation of finite population mean in the presence of non-response problem. *Journal of Prime Research in Mathematics* 16(1): 52-63
- Solanki R S, Singh H P & Rathour A (2012). An alternative estimator for estimating the finite population mean using auxiliary information in sample surveys. *International Scholarly Research Notices* 1-14. <https://doi.org/10.5402/2012/657682>
- Singh R, Kumar M, Chaudhary M K & Smarandache F (2009). Estimation of mean in presence of non-response using exponential estimator. Unpublished manuscript. arXiv preprint arXiv:0906.2462.
- Singh R, Mishra P, Auduudu A & Khare S (2020). Exponential type estimator for estimating finite population mean. *International Journal of Computational and Theoretical Statistics* 7(1): 37-41
- Singh G N & Usman M (2019a). Ratio-to-product exponential-type estimators under non-response. *Jordan Journal of Mathematics and Statistics* 12(4): 593-616
- Singh G N & Usman M (2019b). Efficient combination of various estimators in the presence of non-response. *Communications in Statistics-Simulation and Computation* 1-35. <https://doi.org/10.1080/03610918.2019.1614618>
- Unal C & Kadilar C (2020). Exponential type estimator for the population mean in the presence of non-response. *Journal of Statistics and Management Systems* 23(3): 603-615. <https://doi.org/10.1080/09720510.2019.1668158>
- Unal C & Kadilar C (2021). Improved family of estimators using exponential function for the population mean in the presence of non-response. *Communications in Statistics - Theory and Methods* 50(1): 237-248. <https://doi.org/10.1080/03610926.2019.1634818>
- Yadav S K, Subramani J, Misra S, Singh L & Mishra S S (2016). Improved estimation of population mean in presence of non-response using exponential estimator. *International Journal of Agricultural and Statistical Sciences* 12(1): 271-276
- Olufadi Y & Kumar S (2014). Ratio-cum-product estimator using exponential estimator in the presence of non-response. *Journal of Advanced Computing* 3(1): 1-11. <https://doi.org/10.7726/jac.2014.1001>



© 2022 by the author(s). Published by Ankara University, Faculty of Agriculture, Ankara, Turkey. This is an Open Access article distributed under the terms and conditions of the Creative Commons Attribution (CC BY) license (<http://creativecommons.org/licenses/by/4.0/>), which permits unrestricted use, distribution, and reproduction in any medium, provided the original work is properly cited.



Biostabilization of Tannery Sludge Compost by Vermicomposting

Yiğit Nevzat KAMAN^a , Nur OKUR^{b*} , Hüseyin Hüsnü KAYIKÇIOĞLU^b

^aLeather Working Group, Kings Park Road, Moulton Park, Northampton, UNITED KINGDOM

^bEge University, Agricultural Faculty, Soil Science and Plant Nutrition Department, Bornova, Izmir, TURKEY

ARTICLE INFO

Research Article

Corresponding Author: Nur OKUR, E-mail: nur.okur@ege.edu.tr

Received: 10 April 2021 / Revised: 29 August 2021 / Accepted: 08 September 2021 / Online: 01 September 2022

Cite this article

KAMAN N Y, OKUR N, KAYIKÇIOĞLU H H (2022). Biostabilization of Tannery Sludge Compost by Vermicomposting. *Journal of Agricultural Sciences (Tarim Bilimleri Dergisi)*, 28(3):473-480. DOI: 10.15832/ankutbd.912938

ABSTRACT

The aim of this study is to investigate the stabilization of tannery sludge compost mixed with cattle manure at the different ratios by employing an epigeic earthworm *Eisenia foetida* and bioaccumulation of Cr in tannery sludge by earthworms. Organic cattle manure (M) and sludge compost (S) were mixed in certain proportions, moistened and *Eisenia foetida* worms were added. Mixing ratios were as follows: 100% M (M_{100S0}), 70% M + 30% S (M_{70S30}), 50% M + 50% S (M_{50S50}) and 30% M + 70% S (M_{30S70}). The experiment was carried out at a constant temperature of 24 °C and in a dark environment according to a randomized plot design with three replicates. The experiment ended after 120 days and the following parameters were evaluated in vermicomposts: pH, electrical conductivity (EC), total nitrogen (TN), total organic carbon (TOC), C:N ratio, and total macro and micro elements. In addition, it was determined total Cr, Cr (VI) in vermicomposts and total Cr in *E. foetida* body. The results for TOC,

C:N ratio and total Cr showed decreases in their values at the end of the vermicomposting process, whereas values for pH, EC, TON, Ca, and Mg increase, indicating that the vermicomposting reached the maturity level. All values of Cr (VI) of vermicomposts were below the detectable level. During the vermicomposting process, the reduction rates of the total Cr amounts were 96% (M_{70S30}), 96% (M_{50S50}) and 30% (M_{30S70}), respectively. While the highest total Cr amount in the earthworm body was determined in M_{30S70} treatment, the amount of this element in the earthworm body decreased due to the decreasing doses of tannery sludge compost. These results show that *E. foetida* can bioaccumulate the chromium in tannery sludge compost. As a result, it was determined that vermicomposting can be an alternate technology for the recycling and environmentally safe disposal/management of tannery sludge compost using an epigeic earthworm *E. foetida*.

Keywords: Chemical properties, *Eisenia foetida*, Tannery sludge compost, Total chromium, Vermicomposting

1. Introduction

Turkey is one of the biggest producers of high quality leather products in the world. One billion 181 million USD leather and related products were exported in 2020 (TÜİK 2021). However, the leather production increased the amount of industrial waste which known as tannery sludge, generated during the processes. Tannery sludge can include heavy metals (mainly Cr), leather fragments, soluble proteins, hairs, lime, sodium sulphate, sodium hydroxide and phenolic substances depending on the treatment process (Gupta and Sinha 2007; Küçükpelvan et al. 2017). The characteristics and pollution load of the wastes vary according to the quality and quantity of the chemicals used in the treatment. About 90 % of hides/skins in the world and Turkey are still tanned with Cr³⁺, because of giving a high hydrothermal stability and other use properties to leather compared to the other tanning materials (IPPC, 2003). In soils with pH values above 5.0, Cr is in the trivalent form (Cr³⁺), which is more stable, and has a low solubility and mobility (Alcântara & Camargo 2001). But Cr³⁺ can be oxidized to the hexavalent form (Cr⁶⁺) which is very toxic, mutagenic, and carcinogenic for humans (Kolomaznik et al. 2008). Therefore, safe disposal of tannery waste requires special attention and is one of the major environmental troubles worldwide.

Currently, tannery sludge is disposed by land filling or land application techniques (Singh & Agrawal, 2010). However, land filling is not a suitable method because a large volume of soil is needed to fill the waste. Since land filling is an expensive method, the industries consequently want to choose for cheaper alternatives to dispose their wastes. Therefore, there is a need the research on cheap and usable new techniques for recycling of organic waste (Ahlberg et al. 2006). Composting is one of the cheapest and effective alternative method for organic waste recycling (Singh & Agrawal 2010). There are some studies that the amounts of hazardous chemicals in tannery wastes can be reduced by composting. Onyuka et al. (2012) were found 73% degree of humification and C/N ratio of 29/1 in composted tannery hair waste. Shukla et al. (2009) determined that the tannery effluent treated with aquatic macrophyte *Vallisneria spiralis* L. provided significant improvement in physico-chemical properties and reduction in Cr content. During the composting process, Cr⁶⁺ was transformed to Cr³⁺ by the microbial activity. Haroun et al.

(2007) studied the heavy metal concentrations in tannery sludge during a 50-day composting process and determined an increase in the removal of Cr, Cd, Pb, Zn and Cu in the final product.

Besides of conventional composting, vermicomposting is also suggested as an alternative method for recycling tannery wastes. Organic solid wastes can be efficiently managed by converting into organic manure/soil conditioners by vermicomposting (Garg et al. 2005). Earthworms can be used for solid waste management, organic matter stabilization, soil detoxification, and vermicompost production (Gupta & Garg 2008). Cardoso - Vigueros & Ramirez - Camperos (2006) determined that electrical conductivity (EC) value in tannery sludge decreased from 13.88 to 12.50 dS m⁻¹ and Cr concentration from 3240 to 562 mg kg⁻¹ after vermicomposting for 8 months. It is suggested that the organic matter in sludge must be stabilized with a biological process as composting and vermicomposting for landfill disposal. The tannery sludge was vermicomposted after mixed with sawdust, cardboard and straw and a decline in water extracted chromium was noted in result of vermicomposting. In addition, chromium concentration in *E. foetida* body tissues was significantly positively correlated with its content in sludge (Gondek 2008). The mixtures of tannery solid waste (TSW), cow dung and agricultural residues were vermicomposted for 50 days and a notable increase in earthworm biomass was determined. The tannery solid waste was converted into nutrient-enriched products by the earthworm *E. foetida* (Ravindran et al. 2008). In another study, fermented animal fleshing mixed with cow dung and leaf litter was vermicomposted with the earthworm *E. eugeniae* and the FT-IR analyses showed the complete mineralisation of polypeptides, polysaccharides, aliphatic methyl groups and lignin in vermicompost compared to without earthworm treatment realized (Ravindran et al. 2013). Additionally, they recorded a decrease of 58.5% in Cu, 55.8% in Cr, 35.7% in Zn, 23.4% in Mn and 19% in Fe in SSF (+worms) treatment (Ravindran et al. 2014). Nunes et al. (2016) determined that Cr⁶⁺ concentration in vermicompost obtained from tannery residues was below the detectable level and the Cr⁶⁺ content had probably been biologically converted into Cr³⁺. The authors suggested that vermicomposting could be used as an effective technology for recycling of industrial tannery waste.

There are also some difficulties in the management of industrial tannery waste and sludge in Turkey and are needed the studies on the stabilization of such wastes. The aim of this study was to study the stabilization of tannery sludge compost mixed with cattle manure at the different ratios by employing an epigeic earthworm *Eisenia foetida*. Moreover, bioaccumulation of Cr in earthworm and the management of the end product as a soil conditioner or a waste that can be safely disposed to the land were investigated.

2. Material and Methods

2.1. Tannery sludge, cattle manure and *Eisenia foetida*

The tannery sludge (S) collected from Sepiciler Caybaşı Leather Inc. in Torbalı, İzmir, Turkey is dehydrated treatment sludge formed by the treatment of wastewater generated during production. It contains vegetable tanned leather shavings and protein phase of skinning waste. Before the experiment, sludge was composted aerobically, and the thermophilic stage has been completed. Cattle manure (M) was mixed with the tannery sludge compost to constitute an organic nutrient source and to support for earthworms and microorganisms inside the vermicomposters. Organic cattle manure (Eco-Fert) has been stabilized under aerobic conditions for 40 - 60 days and then passed through a separator. Non-clitellated earthworm *Eisenia foetida*, weighing 500–600 mg live weight, were randomly picked from a stock culture maintained in a vermicomposting farm. Chemical properties of tannery sludge compost (S) and cattle manure (M) are given in Table 1.

2.2. Experimental design

Styrofoam boxes (30 cm x 40 cm) were filled with the mixtures including different ratios of organic cattle manure (M) and tannery sludge compost (S). Mixing ratios were as follows: 100% M (M₁₀₀S₀), 70% M + 30% S (M₇₀S₃₀), 50% M + 50% S (M₅₀S₅₀) and 30% M + 70% S (M₃₀S₇₀). The total amounts of mixing were calculated as 4 kg dry weight basis. A cheesecloth was used to prevent the earthworms escaping from the boxes. The feed materials were mixed manually every day for 14 days to vapour the toxic gases. After 14 days, 200 non-clitellated *E. foetida* were left in each box. The moisture content of feeds was maintained to 70–80% during the vermicomposting process by adding of adequate quantity of water. The experiment was carried out under laboratory conditions in a dark environment with a constant temperature of 24 °C according to the randomized plot design with 3 replicates. Before the earthworms were removed, samples were taken from the mixtures for chemical analysis. The vermicompost was air dried and sieved for chemical analysis. The vermicomposting process was performed for 120 days. At the end of the experiment, earthworms were removed and counted.

Table 1- Initial chemical properties of tannery sludge compost (S) and cattle manure (M)

<i>Parameters</i>	<i>S</i>	<i>M</i>
pH	7.75	8.25
EC (dS m ⁻¹)	6.16	3.18
Total C, %	18.00	44.00
Total N, %	1.85	1.00
C/N	10	44
Total P, %	0.20	0.55
Total K, %	0.10	1.78
Total Ca, %	1.88	2.58
Total Mg, %	1.91	0.96
Total Fe, mg kg ⁻¹	1920.7	204.1
Total Zn, mg kg ⁻¹	194.4	344.8
Total Cu, mg kg ⁻¹	12.5	178.7
Total Mn, mg kg ⁻¹	400.5	184.7
Total Cr, mg kg ⁻¹	1862.10	<0.05
Cr ⁶⁺ , mg kg ⁻¹	6.20	<0.05

2.3. Chemical analysis

The pH and electrical conductivity (EC) of samples were measured using a pH-meter (WTW 526) and conductivity meter (WTW 720). Total organic carbon (TOC) was measured using the method of Nelson and Sommers (1982). Total N (TN) was determined by the Kjeldahl method (Bremner & Mulvaney, 1982). Total P was analysed using the colorimetric method with molybdenum in sulphuric acid. Total K and Ca were determined flame-photometrically, while Mg, Fe, Cu, Zn, Mn, and Cr were determined by atomic absorption spectrometry after wet digestion with HNO₃-HClO₄ (4:1) mixing solution (Kacar & Inal 2010). Cr (VI) was analysed using UV/VIS spectrometer (US EPA 1992).

2.4. Statistical analyses

The results given in the study are the means of three replicates (n=3). All data were subjected to ANOVA analysis using SPSS 16.0 (SPSS Inc., Chicago, IL, USA) to find significant differences between treatments at different sampling times with Duncan's multiple range test (P<0.05).

3. Results and Discussion

3.1. Changes of some chemical parameters by vermicomposting

Some chemical properties of initial mixtures and vermicomposts were given in Table 2. The treatments of M₁₀₀S₀ and M₇₀S₃₀ had higher pH values compared to the other two treatments (M₅₀S₅₀ and M₃₀S₇₀) in both sampling times due to the higher pH of cattle manure. During the vermicomposting, pH increased significantly in the treatments of M₁₀₀S₀, M₇₀S₃₀ and M₅₀S₅₀, probably due to excess of ammonia not required by microbes (Rynk 1992; Vig et al. 2011). The reason for a slight decrease in pH in the application of M₃₀S₇₀, where the wastewater sludge is more and both bacteria and earthworm activity are less, can be resulted from the formation of organic acids during the biotransformation of organic material (Ndegwa et al. 2000). While M₁₀₀S₀ treatment had higher EC value compared to the other treatments at the beginning of the experiment, the EC difference among the treatments was disappeared at the end of the experiment and EC values of all the treatments varied between 1.85 to 2.47 dS m⁻¹. Although the EC values of the treatments containing tannery sludge compost increased during the vermicomposting, the EC values of the final products remained below the limit value (<10 dS m⁻¹) (Official Newspaper No: 30341). The loss of organic matter and release of different mineral salts during vermicomposting process probably increased EC in the vermicomposts (Kaviraj & Sharma 2003). Gunadi & Edwards (2003) have suggested that EC and pH of feed could be the limiting factor for the survival and growth of *E. foetida*. *E. foetida* could not survive in the cattle manure with pH of 9.5 and EC of 5.0 dS m⁻¹ (Mitchell 1997). pH and EC values of vermicomposts obtained in our study were suitable for the survival and growth of *E. foetida*. Total organic carbon (TOC) of the final vermicompost significantly decreased as compared to the initial feed materials (Table 2). TOC loss occurred between 1.70% and 38.8%. The decrease in TOC during vermicomposting indicates organic matter stabilization in the feed materials due to combined action of *E. foetida* and microbiota (Gupta and Garg, 2008). Other co-workers (Elvira et al. 1998; Kaushik & Garg 2003; Garg & Kaushik 2005) who have reported 20-45% loss of TOC during vermicomposting of different industrial sludges support our data. In our study, the highest TOC loss was determined in M₁₀₀S₀ treatment and TOC loss decreased due to increasing doses of tannery sludge compost (38.8% in M₁₀₀S₀, 18.5% in M₇₀S₃₀, 16.2% in M₅₀S₅₀ and 1.7% in M₃₀S₇₀). In the treatment of M₃₀S₇₀ where the lowest TOC loss was found, probably negatively affected the population of heterotrophic microorganisms and earthworms due to the high rate of tannery sludge. Total nitrogen (TN) content in the vermicomposts was higher than initial feed materials. The initial TN content of the initial feed materials was in the range of 1.0% – 1.35%. Whereas TN content of vermicomposts was in the range of 1.85% - 2.10% after vermicomposting. TN increased 1.4-

2.1 fold at the end of vermicomposting process. Earthworms accelerate the nitrogen mineralization in organic material. In addition, they produced the substances including nitrogen such as mucus and excretory substances during the digestion of organic matter (Hobson et al. 2005; Suthar 2006). These substances, which are not found in raw materials, later contribute as an additional nitrogen source because of vermicomposting. The initial C/N ratio of raw materials was in the range of 23.0 to 43.9, but after 120 days C/N ratio significantly decreased in all the treatments. Final C/N ratio was between 12.8 and 16.5%. The reduction in C/N ratio was determined 1.4 – 3.4 fold in final vermicomposts. The C/N ratio indicates the level of stabilization of a waste, as carbon is lost as CO₂ during vermicomposting whereas nitrogen content is enhanced during this process and these factors contribute to the lowering of C/N ratio (Yadav & Garg 2011). The C/N ratio below 20 is indicator of acceptable maturity (Morais & Queda 2003). The vermicomposts obtained in our study had the C/N ratio within the acceptable limit for composts.

3.2. Changes of total element amounts by vermicomposting

The change of total P, K, Ca, and Mg amounts during vermicomposting process were given in Table 3. Since cattle manure contains higher total P and K than tannery sludge compost (Table 1), the highest total P and total K amounts were obtained in M₁₀₀S₀ treatment, while the lowest amount of these elements was determined in M₃₀S₇₀ treatment. Although it was not statistically significant, a slight increase in the total P amounts was determined at the end of the vermicomposting. This increase was probably due to the mineralization of P depending on the bacterial and faecal phosphatase activity of the earthworms (Edwards and Lofty, 1972). Satchell & Martin (1984) suggested that an increase in the total P amount of vermicomposts is directly related to gut enzymes of earthworms and indirectly with the stimulation of microorganisms. Otherwise, the total K content of vermicomposts did not significantly change or slightly decreased during vermicomposting. There are different results regarding the total K content in the vermicomposts obtained from different wastes. Delgado et al. (1995) have reported a higher content of total K in the sewage sludge vermicomposts. Whereas Orozco et al. (1996) determined a decrease in total K in coffee pulp waste vermicomposts. These differences in the results may have resulted from the different chemical properties of the feed materials. The total Ca and Mg amounts were slightly higher in the vermicomposts than their raw materials for all treatments except total Mg amount under M₁₀₀S₀ treatment. These increases may have resulted from the decrease in compost volume during the vermicomposting process as reported by Malafaia et al. (2015). Veras & Povinelli (2004), who detect increases in Ca and Mg amounts in vermicomposts but could not detect in composts without *E. foetida*, also confirmed this hypothesis.

The change of total Fe, Zn, Cu, and Mn amounts during vermicomposting process were given in Table 4. Total Fe and Mn amounts significantly increased depending on increasing the dose of tannery sludge compost and the highest Fe and Mn amounts were found in M₃₀S₇₀ treatment as 2110.1 mg kg⁻¹ and 468.4 mg kg⁻¹, respectively. The opposite results were obtained for Zn and Cu and the highest amounts of these elements were determined in M₁₀₀S₀ treatment as 362.1 mg kg⁻¹ and 224.5 mg kg⁻¹, respectively, because the cattle manure contains higher Zn and Cu elements compared to tannery sludge compost (Table 1). The amount of microelements did not change significantly during the vermicomposting process.

3.3. Changes of total Cr and Cr (VI) amounts by vermicomposting and total Cr amount in earthworm body

Table 5 shows the amounts of total Cr and Cr (VI) during vermicomposting process and total Cr amount in earthworm body. The results for total Cr were 6.20-9.19, 554.60-23.29, 920.30-35.28 and 1311.60-920.59 mg kg⁻¹ for M₁₀₀S₀, M₇₀S₃₀, M₅₀S₅₀ and M₃₀S₇₀ treatments, respectively. All treatments that included tannery sludge compost showed significant decreases in their Cr content. During vermicomposting, the reduction rates of the total Cr amounts were 96% (M₇₀S₃₀), 96% (M₅₀S₅₀) and 30% (M₃₀S₇₀), respectively. While the highest total Cr amount in the earthworm body was found in M₃₀S₇₀ treatment, the amount of this element in the earthworm body decreased due to the decreasing doses of tannery sludge compost. The lowest total Cr content was determined in M₁₀₀S₀ treatment. These results show that *E. foetida* can bioaccumulate Cr in tannery sludge compost. Similar results have been reported by Cardoso - Vigueros & Ramirez - Camperos (2006) during the vermicomposting of tannery wastes and sewage sludge by *E. foetida* and Cr concentration decreased from 3240 mg kg⁻¹ to 562 mg kg⁻¹ after vermicomposting for 8 months. In addition, Gondek (2008) found that the amount of water extractable chromium in the final product decreased because of vermicomposting of the mixture of tannery sludge and sawdust, straw and cardboard by *E. foetida* for 12 months. It was also found that Cr accumulated 13-20 times more in earthworm tissue compared to control and there was a positive relationship between the amount of Cr in earthworms and the amount of Cr in vermicompost. Malecki et al. (1982) suggested that *Eisenia foetida* can tolerate relatively great contents of heavy metals in the substrates and Hartenstein et al. (1980) explained that Cr in sewage sludge is not harmful for redworm growth, even in high concentrations. Earthworms change the physico-chemical structure of ingested organic materials and convert it more available forms to organisms. So, the metal content reduces in digested organic material due to bioaccumulations of more soluble fractions of metals (Suthar 2006). The concentration of Cr (VI) was lower from detectable level in all treatments (Table 5), probably due to the high pH levels of raw materials and vermicomposts (Table 2). Bartlett and James (1977) found lower pH increased the formation of Cr⁶⁺, and at pH 3.2 all Cr³⁺ was oxidized to Cr⁶⁺.

Table 2 - pH, electrical conductivity (EC), the amounts of total organic C (TOC) and total N (TN) and C/N ratio of initial feed mixtures and vermicomposts

	pH		EC (dS m ⁻¹)		TOC, %		TON, %		C/N ratio	
	Initial	End	Initial	End	Initial	End	Initial	End	Initial	End
M ₁₀₀ S ₀	8.25 a B	8.41 a A	3.18 a A	2.47 a B	43.88 a A	26.83 a B	1.00 b B	2.10 a A	43.9 a A	12.8 a B
M ₇₀ S ₃₀	8.27 a B	8.55 a A	1.74 b B	1.85 a A	33.99 ab A	27.69 a B	1.27 a B	1.86 a A	26.8 b A	14.9 a B
M ₅₀ S ₅₀	7.85 b B	7.94 b A	1.68 b B	2.05 a A	31.12 b A	26.06 a B	1.34 a B	1.88 a A	23.2 b A	13.9 a B
M ₃₀ S ₇₀	7.77 b A	7.73 b A	1.62 b B	2.44 a A	31.10 b A	30.58 a B	1.35 a B	1.85 a A	23.0 b A	16.5 a b

Lowercase letters in each sampling period represent the statistical difference between treatments; uppercase letters in each treatment represent the statistical difference between sampling periods (P= 0.05, Duncan's test).

Table 3- The amounts of total P, K, Ca and Mg of initial feed mixtures and vermicomposts

	Total P, %		Total K, %		Total Ca, %		Total Mg, %	
	Initial	End	Initial	End	Initial	End	Initial	End
M ₁₀₀ S ₀	0.55 a A	0.58 a A	1.88 a A	1.78 a A	2.58 a B*	3.23 a A	0.96 c A	1.07 b A
M ₇₀ S ₃₀	0.37 b A	0.48 b A	1.06 b A	1.06 b A	2.65 a B	3.33 a A	1.23 b B	2.29 a A
M ₅₀ S ₅₀	0.40 b A	0.49 b A	0.90 c A	0.80 b A	2.57 a B	2.89 a A	1.56 ab B	2.14 a A
M ₃₀ S ₇₀	0.25 c A	0.37 c A	0.64 d A	0.59 c A	2.66 a B	3.28 a A	2.20 a B	2.89 a A

Lowercase letters in each sampling period represent the statistical difference between treatments; uppercase letters in each treatment represent the statistical difference between sampling periods (P= 0.05, Duncan's test).

Table 4- The amounts of total Fe, Zn, Cu and Mn of initial feed mixtures and vermicomposts

	Total Fe, mg kg ⁻¹		Total Zn, mg kg ⁻¹		Total Cu, mg kg ⁻¹		Total Mn, mg kg ⁻¹	
	Initial	End	Initial	End	Initial	End	Initial	End
M ₁₀₀ S ₀	204.1 b A	282.6 b A	344.8 a A*	362.1 a A	178.7 a A	224.5 a A	184.6 b A	212.9 c A
M ₇₀ S ₃₀	1597.6 ab A	1600.5 ab A	318.9 ab A	282.3 b A	100.8 b A	105.4 b A	387.6 ab A	439.2 b A
M ₅₀ S ₅₀	1644.4 ab A	1708.4 ab A	297.1 ab A	248.2 b A	66.6 c A	79.5 c A	418.7 ab A	456.2 ab A
M ₃₀ S ₇₀	1984.7 a A	2110.1 a A	263.4 b A	266.7 b A	50.5 c A	59.9 d A	456.6 a A	468.4 a A

Lowercase letters in each sampling period represent the statistical difference between treatments; uppercase letters in each treatment represent the statistical difference between sampling periods (P= 0.05, Duncan's test).

Table 5- The amounts of total Cr and Cr (VI) of initial feed mixtures and vermicomposts and the amount of total Cr of *E.foetida* body

	Total Cr, mg kg ⁻¹		Cr (VI), mg kg ⁻¹		Total Cr in earthworm body, mg kg ⁻¹ fresh matter
	Initial	End	Initial	End	
M ₁₀₀ S ₀	6.20 d A	9.19 b A	< 0.05	< 0.05	2.68 d
M ₇₀ S ₃₀	554.60 c A	23.29 b B	< 0.05	< 0.05	31.46 c
M ₅₀ S ₅₀	920.30 b A	35.28 b B	< 0.05	< 0.05	163.39 b
M ₃₀ S ₇₀	1311.60 a A	920.59 a B	< 0.05	< 0.05	523.26 a

Lowercase letters in each sampling period represent the statistical difference between treatments; uppercase letters in each treatment represent the statistical difference between sampling periods (P= 0.05, Duncan's test).

3.4. The growth of *Eisenia foetida* by vermicomposting

At the beginning of the experiment, the number of 200 earthworms were left in each box. After 4 months, they were counted and higher number of earthworms were found in M₁₀₀S₀, M₇₀S₃₀ and M₅₀S₅₀ treatments (Figure 1). The numbers for earthworms were 186, 204, 205 and 139 for M₁₀₀S₀, M₇₀S₃₀, M₅₀S₅₀ and M₃₀S₇₀ treatments, respectively. The lowest earthworm number was found in M₃₀S₇₀. It was observed that sufficient cocoon formation occurred in M₁₀₀S₀, M₇₀S₃₀, M₅₀S₅₀ treatments and these cocoons later hatched (Figure 2 and 3). In the last treatment where the highest treatment sludge dose was applied (M₃₀S₇₀), very few cocoons were observed. These results show that there is no problem in the development and reproduction of *Eisenia foetida* in tannery sludge composts mixed in the rates of 30% and 50% of cattle manure. However, when the ratio of tannery sludge compost increased to 70%, the earthworms had trouble staying alive. Vig et al. (2011) have reported similar observations during vermicomposting of tannery sludge and cow dung that the number of earthworms decreased from 15th day of experiment in the treatments including high concentrations of tannery sludge. The maximum mortality of earthworms was determined as 60% in 75% tannery sludge+25% cow dung feed mixture. The kind and quality of feed materials directly affected the survival, growth, and reproduction of earthworms (Gajalakshmi et al. 2005). Therefore, vermicomposting and cattle manure acting as a

complementary waste improved its quality of tannery sludge compost and converted it into a compost that can be used as a soil conditioner and being dispose into the land more safely.

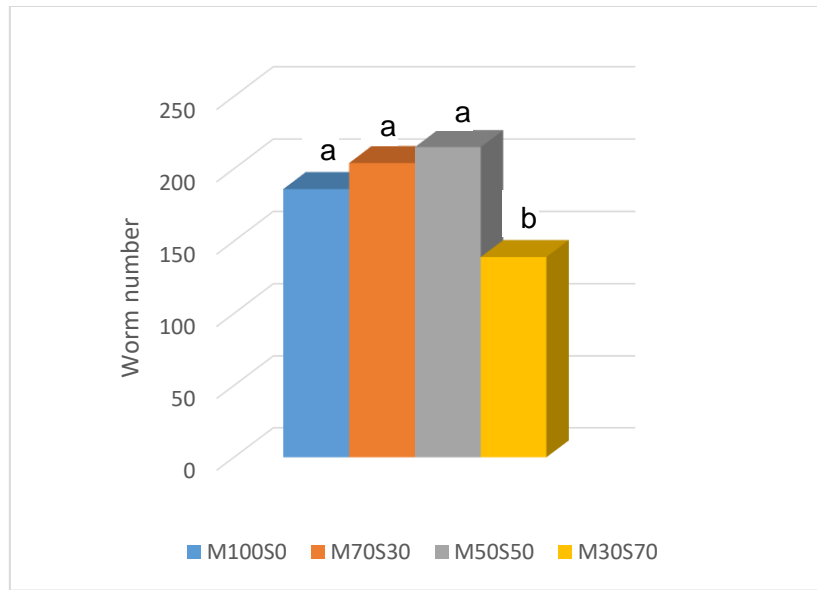


Figure 1- The numbers of *E. foetida* at the end of the vermicomposting process. The difference in mean values between the treatments followed by the same letter are not statistically different at $P < 0.05$ from each other, according to Duncan's test.



Figure 2- The view of cocoons in M₇₀S₃₀ treatment.



Figure 3- The hatchlings emerging from the cocoons

3. Conclusions

This study was carried out to investigate the usage possibilities of vermicomposting technology for waste management of tannery sludge. Different combinations of tannery sludge compost with cattle manure were vermicomposted using an epigeic earthworm (*E. fetida*) and some chemical properties and growth of earthworms were determined in vermicomposts. pH and EC values of vermicomposts increased slightly but they remained within accepted limit values. The vermicomposts had higher amounts of nutrients such as N, Ca, Mg and lower C:N ratio than 20 which indicate their stabilization. The amounts of P, K, Fe, Zn, Cu and Mn did not change during vermicomposting. Total Cr content of mixing combinations significantly decreased and toxic Cr⁶⁺ content was lower than the detectable level for all treatments. The decreasing of total Cr content in vermicompost but the increasing in earthworm body indicated that the Cr element can bioaccumulate in earthworms. As a result of this study, it was determined that vermicomposting can be an alternative technique for the recycling and safe disposal/management of tannery sludge compost by using *E. foetida*.

Acknowledgments

This work was supported by Ege University Scientific Research Projects Coordination Unit (Project Number:17 ZRF 032).

References

- Ahlberg O, Gustafsson P & Wedel P (2006). Leaching of metals from sewage sludge during one year and their relation to particle size. *Environmental Pollution* 144:545-553. <https://doi.org/10.1016/j.envpol.2006.01.022>
- Alcântara MAK & Camargo OA (2001). Retarding factor and dispersion-diffusion coefficient for chromium (III) in highly weathered soils, influenced by pH, texture and organic matter. *Revista Brasileira de Ciência do Solo* 25 (1):209-216
- Bartlett R & James B (1979). Behavior of chromium in soils: III. Oxidation I. *Journal of Environmental Quality* 8 (1):31-35. <https://doi.org/10.2134/jeq1979.00472425000800010008x>
- Bremner J M & Mulvaney C S (1982). Nitrogen-total. In: Page AL, Miller RH, Keeney DR (editors). *Methods of Soil Analysis: Part II. Chemical and Microbiological Properties*. Madison, WI, USA: American Society of Agronomy, pp. 595-641
- Cardossa-Vigueros L & Ramirez-Camperos E (2006). Tannery wastes and sewage sludge biodegradation by composting and vermicomposting process. *Ingenieria Hidraulica En Mexico*. 21(2):93-103
- Delgado M, Bigeriego M, Walter I & Calbo R (1995). Use of California redworm in sewage sludge transformation. *Turrialba*. 45: 33-41
- Edwards C A & Lofty J R (1972). *Biology of Earthworms*. Chapman and Hall, London. https://doi.org/10.1007/978-1-4899-6912-5_7
- Elvira C A, Sampedro L, Benitez E & Nogales R (1998). Vermicomposting of sludges from paper mill and dairy industries with *Eisenia andrei*: a pilot scale study. *Bioresource Technology* 63:205-211. [https://doi.org/10.1016/s0960-8524\(97\)00145-4](https://doi.org/10.1016/s0960-8524(97)00145-4)
- Gajalakshmi S, Ramasamy E V & Abbasi S A (2005). Composting-vermicomposting of leaf litter ensuing from the trees of mango (*Mangifera indica*). *Bioresource Technology* 96 (9): 1057-1061. <https://doi.org/10.1016/j.biortech.2004.09.002>
- Garg P, Gupta A & Satya S (2005). Vermicomposting of different types of waste using *Eisenia foetida*: A comparative study. *Bioresource Technology* 97: 391-395. <https://doi.org/10.1016/j.biortech.2005.03.009>
- Garg V K & Kaushik P (2005). Vermistabilization of textile mill sludge spiked with poultry droppings by an epigeic earthworm *Eisenia foetida*. *Bioresource Technology* 96:1063-1071. <https://doi.org/10.1016/j.biortech.2004.09.003>
- Gondek K (2008). Chromium bioaccumulation from composts and vermicomposts based on tannery sludges. *J. Central European Agriculture* 9(1): 129-140
- Gunadi B & Edwards C A (2003). The effects of multiple applications of different organic wastes on the growth, fecundity, and survival of *Eisenia fetida* (Savigny) (Lumbricidae). *Pedobiologia* 47(4):321-329
- Gupta A K & Sinha S (2007). Phytoextraction capacity of the plants growing on tannery sludge dumping sites. *Bioresource Technology* 98:1788-1794. <https://doi.org/10.1016/j.biortech.2006.06.028>
- Gupta R & Garg V K (2008). Stabilization of primary sewage sludge during vermicomposting. *J. Hazard. Mater.* 162:430-439. <https://doi.org/10.1016/j.jhazmat.2007.09.055>
- Haroun M, Idris A & Omar S R S (2007). A study of heavy metals and their fate in the composting of tannery sludge. *Waste Management*, 27: 1541-1550. <https://doi.org/10.1016/j.wasman.2006.09.006>
- Hartenstein R, Neuhauser E F & Collier J (1980). Accumulation of heavy metals in the earthworm *Eisenia fetida*. *J. Environ. Qual.*, 9: 23-26. <https://doi.org/10.2134/jeq1980.00472425000900010007x>
- Hobson A M, Frederickson J & Dise N B (2005). CH₄ and N₂O from mechanically turned windrow and vermicomposting systems following in-vessel pre-treatment. *Waste Management*, 25(4): 345-352. <https://doi.org/10.1016/j.wasman.2005.02.015>
- IPPC (2003). Reference Document on Best Available Techniques for the Tanning of Hides and Skins. European Commission: Integrated Pollution Prevention and Control (IPPC). 246 p.
- Kacar B, İnal A (2010). *Plant Analysis* (in Turkish). 2nd ed., Nobel Publishing, Ankara, Turkey.
- Kaushik P & Garg V K (2003). Vermicomposting of mixed solid textile mill sludge and cow dung with the epigeic earthworm *Eisenia foetida*. *Bioresource Technology* 90(3):311-316. [https://doi.org/10.1016/s0960-8524\(03\)00146-9](https://doi.org/10.1016/s0960-8524(03)00146-9)
- Kaviraj S S & Sharma S (2003). Municipal solid waste management through vermicomposting employing exotic and local species of earthworms. *Bioresource Technology* 90:169-173. [https://doi.org/10.1016/s0960-8524\(03\)00123-8](https://doi.org/10.1016/s0960-8524(03)00123-8)
- Kolomaznik K, Adamek M, Andel I & Uhlířova M (2008). Leather waste - potential threat to human health and new technology of its treatment. *Journal of Hazardous Materials* 160:514-520. <https://doi.org/10.1016/j.jhazmat.2008.03.070>
- Küçükpelvan H, Yarımtepe C C & Öz N A (2017). Treatment Methods for Tannery Wastewater. (in Turkish) Çanakkale Onsekiz Mart University Journal of Science Institute, 3(1):59-96. <https://dergipark.org.tr/tr/download/article-file/308096>
- Malafaia G, Jordão C R, de Araújo FG, Leandro W M & de Lima Rodrigues A S (2015). Vermicomposting of tannery sludge mixed with cattle dung using *Eisenia fetida*. *Eng. Sanit. Ambient.* 20(4):709-716. <https://doi.org/10.1590/s1413-41522015020040134645>

- Malecki M R, Neuhauser E F & Loehr R C (1982). The effect of metals on the growth and reproduction of *Eisenia fetida* (*Oligochaeta, Lumbricidae*). *Pedobiologia* 24: 129-137
- Mitchell A (1997). Production of *Eisenia fetida* and vermicompost from feed-lot cattle manure. *Soil Biol. Biochem.* 29(3-4): 763-766
- Morais F M C & Queda C A C (2003). Study of storage influence on evolution of stability and maturity properties of MSW composts. In: Pro-ceedings of the fourth International Conference of ORBIT Association on Biological Processing of Organics: Advances for a Sustainable Society Part II, Perth, Australia
- Ndegwa P M, Thompson S A & Das K C (2000). Effects of stocking density and feeding rate on vermicomposting of biosolids. *Bioresource Technology* 71(1):5-12. [https://doi.org/10.1016/S0960-8524\(99\)00055-3](https://doi.org/10.1016/S0960-8524(99)00055-3)
- Nelson D W & Sommers L E (1982). Total carbon, organic carbon and organic matter: In: Page AL, Miller RH, Keeney DR (editors). *Methods of Soil Analysis: Part II. Chemical and Microbiological Properties*. Madison, WI, USA: American Society of Agronomy, pp. 539-579
- Nunes R R, Bontempi R M, Mendonça G, Galetti G & Rezende M O O (2016). Vermicomposting as an advanced biological treatment for industrial waste from the leather industry, *Journal of Environmental Science and Health, Part B* 51(5):271-277. <https://doi.org/10.1080/03601234.2015.1128737>
- Official Newspaper No: 30341. Regulation on Organic, Mineral and Microbial Fertilizers used in agriculture. Ministry of Food, Agriculture and Livestock, 23 February 2018.
- Onyuka A S, Bates M, Attenburrow G, Covington A D & Antunes A P M (2012). Parameters for composting tannery hair waste. *J. of the American Leather Chemists Association* 107: 159-166
- Orozco F H, Cegarra J, Trujillo L M & Roig A (1996). Vermicomposting of coffee pulp using the earthworm *Eisenia fetida*: effects on C and N contents and the availability of nutrients. *Biol. Fert. Soils* 22: 162-166. <https://doi.org/10.1007/bf00384449>
- Ravindran B, Contreras-Ramos S M, Wong J W C, Selvam A & Sekeran G (2014). Nutrient and enzymatic changes of hydrolysed tannery solid waste treated with epigeic earthworm *Eudrilus eugeniae* and phytotoxicity assessment on selected commercial crops. *Environ Sci Pollut Res.*, 21:641-651. <https://doi.org/10.1007/s11356-013-1897-1>
- Ravindran B, Dinesh S L, John Kennedy L & Sekeran G (2008). Vermicomposting of solid biodegradation by composting and vermicomposting process. *Ingeneria Hidraulica En Mexico*, 21(2): 93-103
- Ravindran B, Sravani R, Mandal A B, Contreras-Ramos S M & Sekeran G (2013). Instrumental evidence for biodegradation of tannery waste during vermicomposting process using *Eudrilus eugeniae*. *J Therm Anal Calorim.*, 111:1675-1684. <https://doi.org/10.1007/s10973-011-2081-9>
- Rynk R (1992). On farm composting handbook. Northeast Regional Agricultural Engineering Service (NRAES-54), New York, USA, pp.54.
- Satchell J E & Martin K (1984). Phosphatase activity in earthworm faeces. *Soil Biol Biochem* 16:191-194. [https://doi.org/10.1016/0038-0717\(84\)90111-1](https://doi.org/10.1016/0038-0717(84)90111-1)
- Shukla O P, Rai U N & Dubey S (2009). Involvement and interaction of microbial communities in the transformation and stabilization of chromium during the composting of tannery effluent treated biomass of *Valisneria spiralis* L. *Bioresource Technology*, 100:2198-2203. <https://doi.org/10.1016/j.biortech.2008.10.036>
- Singh R P & Agrawal M (2010). Variations in heavy metal accumulation, growth and yield of rice plants grown at different sewage sludge amendment rates. *Ecotoxicology and Environmental Safety* 73:632-641. <https://doi.org/10.1016/j.ecoenv.2010.01.020>
- SPSS Inc. Released 2007. SPSS for Windows, Version 16.0. Chicago, SPSS Inc.
- Suthar S (2006). Potential utilization of guargum industrial waste in vermicompost production. *Bioresource Technology* 97:2474-2477. <https://doi.org/10.1016/j.biortech.2005.10.018>
- TÜİK (2021). Turkish Statistical Institute. (in Turkish) Number: 37414. Publication date: 31 March 2021
- US EPA (1992). United States Environmental Protection Agency, Method 7196A. Chromium, Hexavalent (colorimetric). <https://www.epa.gov/sites/default/files/2015-12/documents/7196a.pdf>
- Veras L R V & Povinelli J (2004). A Vermicompostagem do Lodo de Lagoas de Tratamento de Efluentes Industriais Consorciada com Composto de Lixo Urbano. *Revista Engenharia Sanitária e Ambiental* 9(3):218-224. <https://doi.org/10.1590/S1413-41522004000300008>
- Vig A P, Singh J, Wani S H & Dhaliwal S S (2011). Vermicomposting of tannery sludge mixed with cattle dung into valuable manure using earthworm *Eisenia fetida* (Savigny). *Bioresource Technology* 102: 7941-7945. <https://doi.org/10.1016/j.biortech.2011.05.056>
- Yadav A & Garg V K (2011). Recycling of organic wastes by employing *Eisenia fetida*. *Bioresource Technology* 102:2874-2888. <https://doi.org/10.1016/j.biortech.2010.10.083>



© 2022 by the author(s). Published by Ankara University, Faculty of Agriculture, Ankara, Turkey. This is an Open Access article distributed under the terms and conditions of the Creative Commons Attribution (CC BY) license (<http://creativecommons.org/licenses/by/4.0/>), which permits unrestricted use, distribution, and reproduction in any medium, provided the original work is properly cited.



Effect of Preharvest Calcium Chloride Treatment on Some Quality Characteristics and Bioactive Compounds of Sweet Cherry Cultivars

Derya ERBAŞ^{a*} , Mehmet Ali KOYUNCU^a 

^aIsparta University of Applied Sciences, Faculty of Agriculture, Department of Horticulture, Isparta, TURKEY

ARTICLE INFO

Research Article

Corresponding Author: Derya ERBAŞ, E-mail: deryabyndr@gmail.com

Received: 04 February 2021 / Revised: 05 October 2021 / Accepted: 5 October 2021 / Online: 01 September 2022

Cite this article

ERBAŞ D, KOYUNCU M A (2022). Effect of Preharvest Calcium Chloride Treatment on Some Quality Characteristics and Bioactive Compounds of Sweet Cherry Cultivars. *Journal of Agricultural Sciences (Tarim Bilimleri Dergisi)*, 28(3):481-489. DOI: 10.15832/ankutbd.874567

ABSTRACT

The effects of preharvest calcium chloride (CaCl₂) treatment on some quality characteristics and bioactive compounds of sweet cherry fruit (*Prunus avium* L. cvs. 0900 Ziraat, Sweetheart and Merton Late) were investigated. The CaCl₂ (1%) solution was sprayed to the cherry trees at 21 and 35 days after full bloom stage. The trees served as control were treated with distilled water at the same days. CaCl₂ treatment remarkably suppressed the respiration rate and increased titratable acidity and fruit firmness of cherries. Treated fruit had more attractive skin colour with higher h^o and L* values compared to control. The

individual soluble sugars and total sugar contents of CaCl₂ treated cherries were lower than those of control fruit. The accumulation of ascorbic acid, stem chlorophyll, total phenolics and anthocyanin contents of fruit were delayed by CaCl₂ treatment in all varieties. The antioxidant activities of all treated varieties were lower than those of control fruit. Based on these results, it can be set forth that preharvest CaCl₂ treatment suppressed ripening processes including respiration rate and maintained firmness and titratable acidity of cherries by maintaining cell integrity in all varieties during the fruit development period.

Keywords: Antioxidant activity, Ascorbic acid, Firmness, Fruit sugars, Total phenolic content, *Prunus avium* L

1. Introduction

In recent years, sweet cherry (*Prunus avium* L.) has become one of the most attractive fruit for producers in the world because of its increasing economic value (Winkler & Knoche 2019). It has also gained popularity for consumers due to its organoleptic and nutritional characteristics. Cherries are rich in nutrients such as vitamin C, A and K, magnesium, potassium and some other minerals. In addition, sweet cherry contains bioactive compounds with antioxidant characteristics (Ozturk et al. 2019), which have positive effects on human health (Ballistreri et al. 2013). Sweet cherry is generally consumed as fresh; therefore, the improved quality characteristics that affect consumer acceptability are mostly important. The outstanding quality characteristics of sweet cherry are fruit firmness, fruit skin and stem color, acidity and sugar content, which influence consumer acceptance. Especially the fruit firmness, affected by preharvest calcium (Ca) treatments, is indispensable for quality evaluation and reaching overseas markets (Romano et al. 2006; Göksel 2011). Additionally, preharvest Ca treatments can reduce cracking rate which causes significant economic loss and reduces fruit quality at harvest time (Erogul 2014). The harvested sweet cherry fruit are susceptible to handling, transportation and storage due to perishability and high respiration rate (Mozetič et al. 2006; Romano et al. 2006). The main causes of quality losses during marketing chain are water losses, softening, color deterioration and stem browning (Martínez-Romero et al. 2006). Therefore, all preharvest treatments, which increase flesh firmness and suppress ripening and senescence processes including respiration, to improve postharvest quality of sweet cherries are very crucial. Dong et al. (2019) reported that strategies to increase fruit firmness are essential to obtain high quality sweet cherries for high-value export markets.

Ca affects the cell wall structure via cross-linking of pectins, regulates the membrane permeability of tissues and plays an important role in cellular signalling responses in fruit (Kirkby & Pilbeam 1984; Tsantili et al. 2007). Sweet cherries that contain insufficient Ca are susceptible to some quality losses related to fruit firmness (Dong et al. 2019). It is known that, preharvest Ca treatments directly improve fruit quality, especially flesh firmness, of sweet cherries (Tsantili et al. 2007). Furthermore, it was reported that Ca applications extended postharvest life and delayed quality losses of sweet cherries by suppressing respiration rate and increasing tissue strength of fruit (Vangdal et al. 2008; Wang et al. 2014). However, these studies revealed different results depending on the source of Ca, sweet cherry cultivars, treatment time and dose (Correia et al. 2019). Similarly, Tsantili et al. (2007) and Winkler & Knoche (2019) have reported that, interestingly, little is known about the detailed effect of preharvest Ca treatments on sweet cherry quality at harvest. These authors also indicated that Ca treatments

gave beneficial and clear results in some studies, while there was no significant effect in others. On the other hand, although Ca treatments have positive effects on fruit quality, it has been stated that inorganic salts sometimes cause bitter and salty taste, especially in high dose (Monsalve-Gonzalez et al. 1993). Likewise, Wang et al. (2014) found an increased stem browning in sweet cherries treated with higher dose than 1%. These findings reveal that detailed information about the effects of preharvest Ca treatments on the quality of sweet cherries is urgently needed. Therefore, this study aimed to determine the effects of preharvest CaCl_2 treatment on some quality characteristics and bioactive compounds of sweet cherry at harvest time.

2. Material and Methods

2.1. Plant material

0900 Ziraat, Sweetheart and Merton Late sweet cherry (*Prunus avium*) varieties, 16 years old and grafted on *Prunus avium* L. rootstocks, were used for preharvest CaCl_2 treatment in 2019. The CaCl_2 [(1%), Merck, Germany] solution containing Tween 20 [(0.1%), Merck, Germany] was applied to the trees two times (three replicates- one tree for each) by using hand sprayer (Pomilsan, Turkey) at 21 and 35 days after full bloom (DAFB) stage. The application dose (1%) was determined based on previous studies (Tsantili et al. 2007; Vangdal et al. 2008; Wang et al. 2014). Control trees were sprayed with distilled water (0.1% Tween 20) at the same days (21 and 35 DAFB). Fruit were hand-harvested at optimum stage based on fruit skin color and maturity index (SSC/TA) from the research orchard of the Isparta, Turkey. The sweet cherry trees were planted at 4×3 m spacing and trained by Goble pruning system. Cultural practices (fertilization, disease control and irrigation) of orchard were regularly applied. Immediately after harvest, sweet cherry fruit were transported (within half-hour) to the laboratory, and foreign parts and injured fruit were removed. The following analyses were performed as three replicates using randomly selected fruit samples.

2.2. Fruit firmness (FF)

Fifteen sweet cherry fruit from each replicate were used for firmness evaluation. The firmness of sweet cherries was measured by a texture analyzer machine (LF Plus-Lloyd Instruments) with a 50 N load cell (5 mm cylindrical probe). The results were expressed as Newton (N).

2.3. Soluble solids content (SSC) and titratable acidity (TA)

The SSC of sweet cherries was determined using a digital refractometer (Atago-Pal 1). For TA, fruit juice (10 mL) was titrated using sodium hydroxide (0.1 N) up to pH 8.1. The results were expressed as the equivalent percentage (%) of malic acid (Erbaş et al. 2018)

2.4. Fruit skin color

Skin color of sweet cherries (20 fruit for each replicate) was determined using colorimeter (Minolta CR-300). The L^* , a^* and b^* values, used to determine a three-dimensional color space, were measured, and then the chroma [$C^* = (a^{*2} + b^{*2})^{1/2}$] and hue angle ($h^\circ = \tan^{-1}b^*/a^*$) were calculated using a^* and b^* values.

2.5. Respiration rate (RR)

Respiration rate of cherry fruit was measured by a gas chromatography. Fruit (140-150 g) were placed in a hermetically sealed glass jar (1 L) and kept at room condition. After 1 h, gas sample was taken from glass jar using a gas-tight syringe, and injected into a gas chromatography (Agilent, 6890N). The thermal conductivity detector was used for the analysis of CO_2 . The RR was calculated based on CO_2 released by fruit, and results were expressed as $\text{mL CO}_2 \text{ kg}^{-1}\text{h}^{-1}$ (Erbaş et al. 2018).

2.6. Stem chlorophyll content (SCC)

Chlorophyll extraction and stem chlorophyll analysis were performed according to procedure described by Göksel (2011). The stem samples (3 g) were placed in test tubes and added 50 mL acetone (90%). The samples with acetone (Sigma, Aldrich) were kept at dark for overnight. After extraction, the absorbance of the samples was read at 663 and 645 nm using a spectrophotometer (Varian Cary Bio 100, Australia). The values were calculated as $[8.02 \times (A_{663}) + 20.2 \times (A_{645})]$, and results were expressed as $\text{mg } 100\text{g}^{-1}$.

2.7. Ascorbic acid (AsA)

Ascorbic acid analysis of sweet cherry fruit was performed by HPLC method recommended by Watada (1982). The 5 mL sweet cherry juice was placed in a test tube, and 5 mL metaphosphoric acid (HPO_3) solution (6%) was added. The mixture was centrifuged at 4 °C for 10 min, and then 0.5 mL of the clear portion of the centrifuge tube was added to 10 mL of HPO_3 solution (6%). This mixture was injected into the HPLC device after filtration with a PVDF (polyvinylidene fluoride) filter

(Millipore, Bedford, Mass., USA) with a pore diameter of 0.45 μm . Ascorbic acid was identified by comparison with the arrival time of the peak in the chromatogram of the samples and the arrival time of the peak in the chromatogram of the ascorbic acid standard. [Column: ODS-3 C-18 column (5 μm , 250 \times 4.6 i.d.); Column temperature: 25 $^{\circ}\text{C}$; Mobile phase: Potassium dihydrogen phosphate (KH_2PO_4); Flow rate: 0.5 mL min^{-1} ; Injection amount: 10 μL ; Wavelength: 210 nm]. The AsA content was expressed as mg in 100 g (FW).

2.8. Extraction for total phenolic content (TPC) and antioxidant activity (AA)

The sweet cherry sample (5 g) was placed in a tube (50 mL), and 5 mL 80% methanol (Sigma, Aldrich) was added. After homogenization with a homogenizer (IKA, Germany) samples were kept at dark condition (4 $^{\circ}\text{C}$) for 14-16 h. The supernatants were stored in a deep freezer at -20 $^{\circ}\text{C}$ until the day of analysis (up to a week) (Thaipong et al. 2006).

2.9. TPC and AA

Total phenolic content of sweet cherries was determined using the Folin-Ciocalteu method as described by Thaipong et al. (2006). The standard curve was developed using gallic acid standard (Merck). The absorbance was read by a spectrophotometer (Varian Cary Bio 100, Australia) at 725 nm. Results were calculated as mg of gallic acid equivalent (GAE) per 100 g^{-1} FW. The ferric reducing antioxidant power (FRAP) assay were used for evaluation of antioxidant capacity in sweet cherry fruit (Thaipong et al. 2006). The calibration curve was developed using Trolox standard (Sigma, Aldrich). The absorbance was read by a spectrophotometer (Varian Cary Bio 100, Australia) at 593 nm. Results were calculated as Trolox equivalents (TE) in mg g^{-1} FW.

3. Total anthocyanin content (TAC)

The pH differential method proposed by Ağlar et al. (2017) was used to determine the TAC. The extracted samples were combined with potassium chloride and sodium acetate buffers (pH 1.0 and 4.5, respectively) in a 1:20 ratio (v:v). After kept for 15 min (for equilibration period) the absorbances of solutions were measured using a spectrophotometer (Varian Cary Bio 100, Australia) at 533 and 700 nm. A corrected absorbance value was calculated as $[(A_{520}-A_{700})_{\text{pH } 1.0}-(A_{520}-A_{700})_{\text{pH } 4.5}]$. The results were expressed as mg in kg cyanidin 3-glucoside (cy-3-glu) on FW basis (mg cy-3-glu kg FW).

3.1. Sugars

Sugar profile analysis of sweet cherries was performed by HPLC according to Melgarejo et al. (2000). Cherry samples were centrifuged at 20 $^{\circ}\text{C}$ for 30 min. After centrifugation, the clarified portion was filtered with PVDF filter (0.45 μm , Millipore, Bedford, Mass., USA) and injected to the HPLC. Glucose, fructose and sucrose solutions were analyzed in the same conditions, and the equations defining the curves were calculated by linear regression analysis. Using this equation, the amount of sugar in sweet cherry fruit was determined as g kg^{-1} . Each sugar is defined by comparison with the arrival time of the peak in the chromatogram of the samples and the arrival time of the peak in the standard chromatogram. The Shimadzu RID-10A model refractive index detector was used. Acetonitrile/water (70/30) was used as the mobile phase for separation of sugar components. The separation was performed isocratically with an Inertsil NH_2 (5 μm , 250 \times 4.6 i.d.) column at a flow rate of 0.9 mL min^{-1} . The volume of injection and the column temperature were 10 μL and 25 $^{\circ}\text{C}$, respectively.

3.2. Statistical analysis

The study was conducted using completely randomized factorial design with 3 replicates (each tree was considered as a replicate). The data were analyzed using Minitab 18 statistics software. The differences among means were compared with Tukey's range test (5%).

4. Results and Discussion

4.1. Fruit firmness

Fruit firmness is, probably, one of the most important quality characteristics in sweet cherry for consumer acceptance. Preharvest CaCl_2 treatment significantly increased fruit firmness in all varieties compared to control samples. At harvest, the firmness values of Ca treated cherries were 6.1 N (0900 Ziraat), 4.9 N (Sweetheart) and 3.9 N (Merton Late) whereas, control fruit had 5.8 N, 4.7 N and 3.3 N fruit firmness, respectively (Figure 1). Similarly, Winkler & Knoche (2019) stated an improvement in the fruit firmness of sweet cherries by pre- and postharvest Ca applications. Moreover, Lidster et al. (1978) determined a highly-significant relationship ($r^2=0.88$) between the fruit firmness of sweet cherries and Ca content in fruit. This strong relationship can be explained by that Ca maintains the mechanical properties and integrity of the cell wall, and thus retards fruit softening (Saba & Sogvar 2016). The membrane stabilization in fruit tissues is achieved by Ca ion, which bridges phosphate and carboxylate groups of phospholipids and proteins at membrane (Winkler et al. 2020). The findings of the

present study are in agreement with the previous works on sweet cherries (Tsantili et al. 2007; Dong et al. 2019) in which preharvest Ca treatments remarkably increased fruit firmness.

4.2. Soluble solids content and titratable acidity

The SSC, which represents soluble sugars, was decreased by Ca treatment compared to control regardless of variety, varying between 11.8% (0900 Ziraat) and 16.3% (Sweetheart) at harvest. Control fruit had 24.6% (0900 Ziraat), 17.9% (Sweetheart) and 1.7% (Merton Late) higher SSC than those of Ca treated cherries. These results can be attributed to the suppressed ripening processes, which result in decreased respiration rate (Figure 1), in Ca-treated cherry fruit depending on cell integrity and suppressed metabolic processes. Diaz-Mula et al. (2017) reported that Ca treatment retarded the increase of SSC in sweet cherries by slowing down the metabolic activities via stabilization of the cell wall and inhibiting the activity of cell wall degradation enzymes. In sweet cherry, TA is very important quality parameter for consumer preference, because the flavor loss of cherries is mainly associated with organic acid degradation. Although, there was no statistically difference between treated and control samples, Ca treated fruit exhibited relatively higher TA content in all varieties in relation to slowed ripening processes. Ca treated cherries had 2.7% (0900 Ziraat), 5.1% (Sweetheart) and 8.7% (Merton Late) higher TA than those of control samples (Figure 1). In accordance with the present study, Tsantili et al. (2007) reported that preharvest Ca treatments maintained TA content of sweet cherries compared to control at harvest. The delay in acidity loss during fruit growing period can be explained by the suppressing effect of Ca on fruit metabolic activity, including ripening processes and respiration rate (Figure 1). It is well known that organic acids are a major component of respiration processes, and the use of organic acids as substrates in these reactions reduces acid content in fruit.

4.3. Respiration rate (RR)

The effect of Ca treatment on the RR of sweet cherries was statistically significant. The RR, an indicator of metabolic activity and ripening processes, was remarkably decreased by Ca treatment in all varieties at harvest. The lowest RR was obtained from the Ca treated fruit of 0900 Ziraat ($3.2 \text{ mLCO}_2 \text{ kg}^{-1}\text{h}^{-1}$) followed by Merton Late ($4.4 \text{ mLCO}_2 \text{ kg}^{-1}\text{h}^{-1}$) and Sweetheart ($7.6 \text{ mLCO}_2 \text{ kg}^{-1}\text{h}^{-1}$), and these values were $4.7 \text{ mLCO}_2 \text{ kg}^{-1}\text{h}^{-1}$, $5.2 \text{ mLCO}_2 \text{ kg}^{-1}\text{h}^{-1}$ and $8.0 \text{ mLCO}_2 \text{ kg}^{-1}\text{h}^{-1}$, respectively in control samples (Figure 1). These findings revealed that preharvest Ca treatment suppressed the RR of cherries by delaying senescence processes compared to control fruit. Likewise, the decrease in SSC and total sugars, and the increase in TA and fruit firmness by Ca treatment during fruit maturation (Figure 1 and Figure 3) are also indicators of delayed senescence. Kirkby & Pilbeam (1984) have reported that senescence is related to some processes such as the breakdown in the compartmentation of the cell and the increase in respiration rate after the leakage of respiratory substrates from the vacuole to the cytoplasm containing respiratory enzymes. The monosaccharides produced by dissolving of cell wall pectin and hemicellulose are used as respiratory substrates (Ranjbar et al. 2018). These metabolic processes are closely related to cell wall integrity and tissue strength, which might be achieved by Ca treatments in fruit. Similarly, it has been speculated that the typical signs of senescence in fruit during maturation are similar to those of Ca deficiency and can be delayed by Ca treatment (Kirkby & Pilbeam 1984).

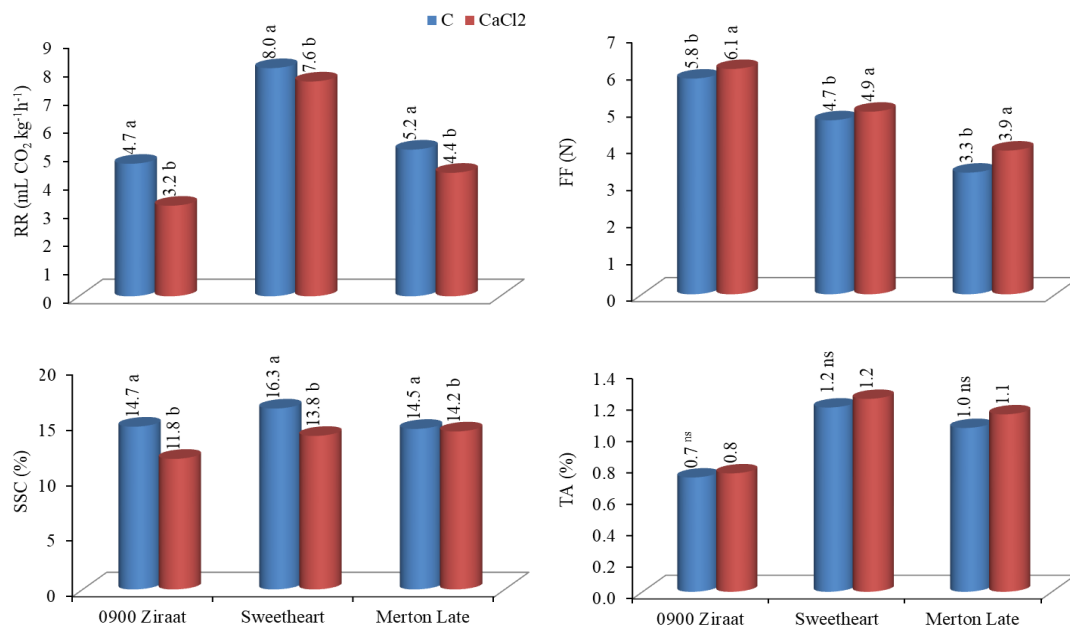


Figure 1- The effect of preharvest CaCl₂ treatment on RR, FF, SSC and TA of different sweet cherry varieties. RR: Respiration rate, FF: Fruit firmness, SSC: Soluble solids content, TA: Titratable acidity, C: Control, CaCl₂: Calcium chloride, ns: represents non-significance P<0.05. Statistical comparisons were made within each cultivar. Means followed by different letters are statistically significant at P<0.05

4.4. Fruit skin color

The effect of treatment on L^* and h° values was significant except for Sweetheart variety but C^* value was not affected by preharvest CaCl_2 treatment (Figure 2). Crisosto et al. (2003) reported that the consumer acceptance of sweet cherries was associated with mainly skin color, which changes depending on pre- and postharvest applications. The chromatic functions of L^* , C^* and h° correlate closely with the change of color and anthocyanin accumulation in sweet cherries during maturation (Mozetic et al. 2004; Gonçalves et al. 2007). In the present study, control fruit had less attractive skin color, which are correlated with the reduction of h° and L^* values. The Ca treated cherries showed higher L^* and h° values compared to control fruit in all varieties at harvest. The highest L^* (47.2) and h° (37.8) values were obtained from the Ca treated fruit of 0900 Ziraat variety. Mozetic et al. (2004) indicated that the accumulation of anthocyanins in sweet cherries during ripening resulted in a decrease in color intensity and redness as described by L^* , C^* and h° values. Moreover, a negative correlation was found between anthocyanin content and L^* and h° values of sweet cherries during maturation (Gonçalves et al. 2007). Based on these findings, it can be speculated that suppressed ripening and respiration processes by CaCl_2 , in the present study, resulted in higher color values such as L^* and h° . In accordance with this thought, Gonçalves et al. (2007) reported that the L^* and h° values of the ripe sweet cherries were always lower than those of partially ripe fruit.

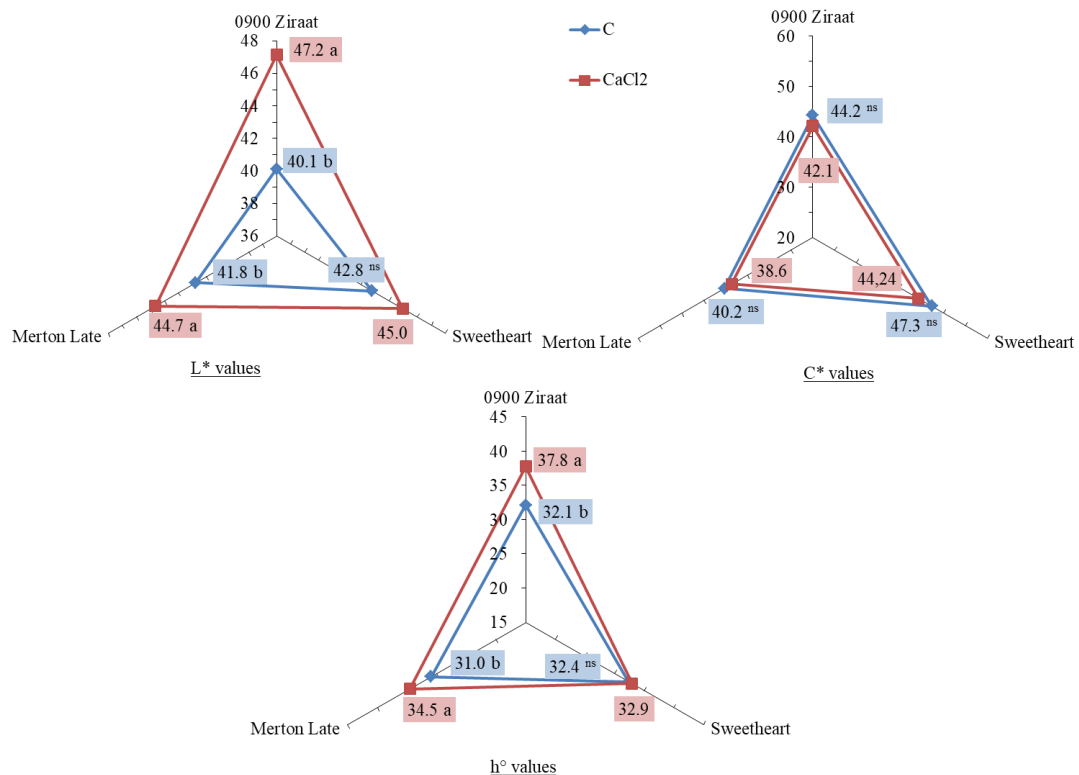


Figure 2- The effect of preharvest CaCl_2 treatment on fruit skin color (L^* , C^* and h°) of different sweet cherry varieties. C: Control, CaCl_2 : Calcium chloride, C^* : Chroma, h° : Hue angle, ns: represents non-significance $P < 0.05$. Statistical comparisons were made within each cultivar. Means followed by different letters are statistically significant at $P < 0.05$.

4.5. Sugars

The CaCl_2 treatment significantly influenced the glucose and sucrose contents of all varieties but the fructose was affected only in Merton Late variety. The glucose and fructose were the major soluble sugars followed by sucrose at harvest (Figure 3) as reported in previous studies carried out on sweet cherry (Serrano et al. 2005; Mahmood et al. 2012; Michailidis et al. 2017). Both individual soluble sugar (glucose, fructose, sucrose) and total sugar contents of CaCl_2 treated cherries were lower than those of control fruit. However, the effect of CaCl_2 treatments varied depending on varieties. For example, the control fruit of Merton Late had remarkable higher glucose (11.8%) and fructose (11.4%) content than those of Ca treated cherries, while these differentiations between treated and untreated samples were 0.5% and 1.0% in Sweetheart variety, respectively (Figure 3). It is known that different sweet cherry varieties exhibit various sugar profiles during maturation (Mahmood et al. 2012). The total sugar contents of control fruit were also higher 5.8% (0900 Ziraat), 1.2% (Sweetheart) and 1.6% (Merton Late) than those treated with CaCl_2 (Figure 3). The lower sugar content of Ca treated fruit in all varieties at harvest might be attributed to the suppressing effect of CaCl_2 on fruit metabolic processes including ripening due to increased cell integrity and tissue strength. It is well known from previous studies that the soluble sugar (glucose, fructose and sucrose) concentration of cherry fruit increases as the fruit ripens (Romano et al. 2006; Mahmood et al. 2012). Moreover, Serrano et al. (2005) found a linear relationship ($R^2 = 0.99$) between the soluble sugar accumulation and ripening in sweet cherry fruit during fruit development

period. On the other hand, Michailidis et al. (2017) reported that the strengthened cell wall in sweet cherries might reduce polygalacturonase activity by limiting the contact of enzyme with substrates. These results are consistent with the findings of our study that showed a higher fruit firmness and lower respiration rate in Ca treated fruit (Figure 1).

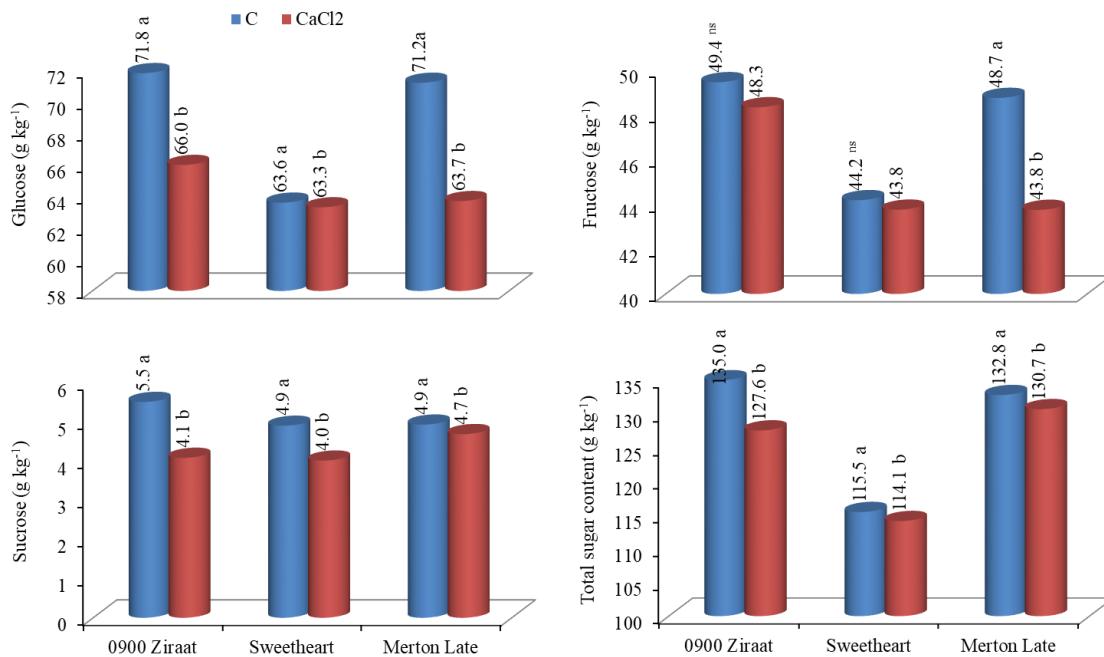


Figure 3- The effect of preharvest CaCl₂ treatment on glucose, fructose, sucrose and total sugar content of different sweet cherry varieties. C: Control, CaCl₂: Calcium chloride, ns: represents non-significance P<0.05. Statistical comparisons were made within each cultivar. Means followed by different letters are statistically significant at P<0.05.

4.6. Stem chlorophyll content

Consumers prefer green stem color, which is an indicator of the freshness in sweet cherry fruit (Schick & Toivonen 2002). Stem color of sweet cherry fruit turns from green to brown because of the breakdown of chlorophyll during ripening processes. In the present study, the chlorophyll contents of CaCl₂ treated cherry stems were 4.7% (0900 Ziraat), 11.3% (Sweetheart) and 17.3% (Merton Late) higher than those of control fruit (Table 1). These results revealed that Ca treatments delayed chlorophyll degradation of stems, in agreement with of Wang et al. (2014) who reported that Ca treatments maintained the green color of cheery stems during senescence. The stem browning of cherries is a result of the reduced membrane integrity caused by damaged cells, which allows to mix polyphenol oxidase and polyphenol substance in cell (Wang et al. 2014). Similar to our findings, Göksel (2011) also noted a rapid decline in total chlorophyll content of cherry stems throughout ripening. The highest chlorophyll content was obtained from Sweetheart (3.6 mg 100 g⁻¹) followed by 0900 Ziraat (2.9 mg 100 g⁻¹) and Merton Late (2.7 mg 100 g⁻¹) varieties at harvest (Table 1). These different results can be attributed to the variation in the response of each variety to CaCl₂. This positive effect of Ca on chlorophyll degradation can also be explained by its reducing effect on the oxidation and senescence processes of fruit stems. Similarly, the delaying in stem browning (oxidation) of sweet cherries was attributed to the suppressed ripening and senescence processes by CaCl₂ treatment (Tsantili et al. 2007).

4.7. Ascorbic acid

Ascorbic acid is considered a crucial nutritional component in fresh horticultural crops (Koyuncu et al. 2019). Preharvest CaCl₂ treatment significantly decreased the AsA content of sweet cherries except for 0900 Ziraat variety. The AsA contents of fruit were determined as 10.1, 12.6 and 9.0 mg 100 g⁻¹ in 0900 Ziraat, Sweetheart and Merton Late varieties at harvest, respectively. These values changed between 10.2 mg 100 g⁻¹ (Merton Late) and 14.5 mg 100 g⁻¹ (Sweetheart) in control fruit (Table 1). The decreasing of AsA content by preharvest Ca treatment can be attributed to the reduced ripening processes. It is known that preharvest Ca treatments retard fruit ripening (Tsantili et al. 2007), and thus the accumulation of AsA, during fruit development period (from full bloom to harvest) in sweet cherries. On the other hand, postharvest Ca treatments increased AsA content of Carnelion sweet cherry (Aghdam et al. 2013). These various results can be due to different variety, maturity stage and application doses and time.

Table 1- The effect of preharvest CaCl₂ treatment on TPC, AsA, TAC, AA and SSC of different sweet cherry varieties

Cultivars	T	TPC	AsA	TAC	AA	SSC
0900 Ziraat	C	35.3 a	10.3	22.1 a	3.5	2.8
	CaCl ₂	34.5 b	10.1	19.7 b	3.4	2.9
	P	*	ns	**	ns	ns
Sweetheart	C	49.9 a	14.5 a	27.5 a	3.3 a	3.2
	CaCl ₂	47.9 b	12.6 b	25.6 b	3.2 b	3.6
	P	*	*	*	*	ns
Merton Late	C	64.9 a	10.2 a	26.9 a	3.8 a	2.3
	CaCl ₂	60.1 b	9.0 b	25.1 b	3.7 b	2.7
	P	*	*	*	*	ns

T: Treatments; C: Control; CaCl₂: Calcium chloride; TPC: Total phenolics content (mg GAE 100g⁻¹ FW); AsA: Ascorbic acid (mg 100 g⁻¹ FW); TAC: Total anthocyanin content (mg cy-3-glu kg⁻¹ FW); AA: Antioxidant activity (mg TE g⁻¹ FW); SSC: Stem chlorophyll content (mg 100g⁻¹); ns: represents non-significance at P<0.05; **: Represents significance at the 0.01 level; *: Represents significance at the 0.05 level. Statistical comparisons were made within each cultivar. Means followed by different letters are significantly different (P<0.05)

4.8. Total phenolics, total anthocyanin and antioxidant activity

Sweet cherry is an important source of phenolic compounds, which exhibit high antioxidant activity and are essential for human diet (Correia et al. 2017). Phenolic compounds also have important role on some quality characteristics of fruit such as color, taste and aroma (Göksel 2011). In the present study, the TPC and TAC were significantly affected by CaCl₂ treatment in all varieties. The preharvest Ca treatment delayed the accumulation of both TPC and TAC of cherries compared to control during fruit growth period. The TPC of Ca treated fruit were 2.6% (0900 Ziraat), 4.05% (Sweetheart) and 8.0% (Merton Late) lower than those of control samples. Similar trend was also observed for TAC, and the control fruit had 12.4% (0900 Ziraat), 7.8% (Sweetheart) and 7.2% (Merton Late) higher TAC (Table 1). The slowed accumulation of TPC and TAC in treated fruit can be explained by the suppressing effect of CaCl₂ on the ripening processes of cherries. This thought is in agreement with of Correia et al. (2017) who reported that phenolic compounds in sweet cherries, concentrated in the skin, increased with ripening together with total anthocyanin. As can be seen in Figure 1, CaCl₂ significantly reduced the respiration rate, an indicator of ripening processes, of sweet cherries. Metabolic processes, including respiration rate, are closely associated with cell wall integrity and enzyme activity, which can be affected by Ca treatments in fruit. Likewise, Sairam et al. (2011) reported that calcium delays ripening and senescence by strengthening the cell wall structure and affecting enzyme activity, and thus reducing the lipid peroxidation in fruit. On the other hand, the suppressing effect of Ca on the accumulation of TPC and TAC was also recorded after harvest. For example, Diaz-Mula et al. (2017) reported a slow accumulation in total phenolic and anthocyanin of Ca treated cherries during the first two weeks of cold storage. Similarly, Vangdal et al. (2008) speculated that a reduction in phenolic compounds could be expected in calcium treated sweet cherries compared to control during cold storage.

In accordance to TPC and TAC, the antioxidant activity of all treated varieties was lower compared to control fruit as expected (Table 1). There is a highly correlated relationship between total antioxidant activity and total phenolics and anthocyanin in fruit (Saracoglu et al. 2017; Koyuncu et al. 2019). The effect of Ca treatment on AA of sweet cherries was significant except for 0900 Ziraat variety. The AA of treated cherries were determined as 3.4, 3.2 and 3.7 mg TE g⁻¹ FW in 0900 Ziraat, Sweetheart and Merton Late, respectively, which 3-4 % lower than those of control fruit (Table 1). As mentioned above, this can be due to the slowing down of ripening and senescence processes by CaCl₂ treatment. Supporting this thought, Serradilla et al. (2012) determined a significant increase in total phenols and antioxidant activity of sweet cherries during ripening.

5. Conclusions

Preharvest CaCl₂ treatment remarkable reduced respiration rate and SSC and maintained titratable acidity and fruit firmness of sweet cherries compared to control at ripening stage. In all varieties, CaCl₂ delayed the accumulation of AsA, SCC, TPC and TAC in comparison to control fruit. Similar to TPC and TAC, the antioxidant activity of fruit was reduced by CaCl₂ treatment at harvest. The skin color of treated fruit was more attractive, with higher h^o and L* values, compared to control. The glucose and fructose, the major soluble sugars, and total sugar contents of treated cherries were lower than those of control fruit at harvest. The response level of each variety to preharvest CaCl₂ treatment varied; however, the direction of changes was similar for each quality characteristic in all varieties.

References

- Aghdam M S, Dokhanieh A Y, Hassanpour H & Fard J R (2013). Enhancement of antioxidant capacity of cornelian cherry (*Cornus mas*) fruit by postharvest calcium treatment. *Scientia Horticulturae* 161: 160-164. <https://doi.org/10.1016/j.scienta.2013.07.006>
- Ağlar E, Öztürk B, Güler S K, Karakaya O, Uzun S & Saraçoğlu O (2017). Effect of modified atmosphere packaging and 'Parka' treatments on fruit quality characteristics of sweet cherry fruits (*Prunus avium* L. 0900 Ziraat) during cold storage and shelf life. *Scientia Horticulture* 222: 162-168. <https://doi.org/10.1016/j.scienta.2017.05.024>

- Ballistreri G, Continella A, Gentile A, Amenta M, Fabroni S & Rapisarda P (2013). Fruit quality and bioactive compounds relevant to human health of sweet cherry (*Prunus avium* L.) cultivars grown in Italy. *Food Chemistry* 140(4): 630-638. <https://doi.org/10.1016/j.foodchem.2012.11.024>
- Correia S, Schouten R, Silva A P & Gonçalves B (2017). Factors affecting quality and health promoting compounds during growth and postharvest life of sweet cherry (*Prunus avium* L.). *Frontiers in Plant Science* 8: 2166. <https://doi.org/10.3389/fpls.2017.02166>
- Correia S, Queirós F, Ribeiro C, Vilela A, Aires A, Barros A I, Schouten R, Silva A P & Gonçalves B (2019). Effects of calcium and growth regulators on sweet cherry (*Prunus avium* L.) quality and sensory attributes at harvest. *Scientia Horticulturae* 248: 231-240. <https://doi.org/10.1016/j.scienta.2019.01.024>
- Crisosto CH, Crisosto GM & Metheny P (2003). Consumer acceptance of 'Brooks' and 'Bing' cherries is mainly dependent on fruit SSC and visual skin color. *Postharvest Biology and Technology* 28: 159-167. [https://doi.org/10.1016/S0925-5214\(02\)00173-4](https://doi.org/10.1016/S0925-5214(02)00173-4)
- Díaz-Mula H M, Valero D, Guillén F, Valverde J M, Zapata P J & Serrano M (2017). Postharvest treatment with calcium delayed ripening and enhanced bioactive compounds and antioxidant activity of 'Cristalina' sweet cherry. *Acta Horticulturae* 1161: 511-514. <https://doi.org/10.17660/ActaHortic.2017.1161.81>
- Dong Y, Zhi H & Wang Y (2019). Cooperative effects of pre-harvest calcium and gibberellic acid on tissue calcium content, quality attributes, and in relation to postharvest disorders of late-maturing sweet cherry. *Scientia Horticulturae* 246: 123-128. <https://doi.org/10.1016/j.scienta.2018.10.067>
- Erbaş D, Koyuncu M A, Özüsoy F & Onursal C E (2018). Effects of pre-harvest putrescine treatment on fruit quality of sweet cherry cv. 0900 Ziraat. *Academic Journal of Agriculture* 7(2): 151-156. <http://dx.doi.org/10.29278/azd.476202> (In Turkish)
- Erogul D (2014). Effect of preharvest calcium treatments on sweet cherry fruit quality. *Notulae Botanicae Horti Agrobotanici Cluj-Napoca* 42(1): 150-153. <https://doi.org/10.15835/nbha4219369>
- Göksel Z (2011). Effects of some pre-treatments on storability of sweet cherries. PhD Thesis, Ege University, Turkey (Pressed).
- Gonçalves B, Silva A P, Moutinho-Pereira J, Bacelar E, Rosa E & Meyer A S (2007). Effect of ripeness and postharvest storage on the evolution of colour and anthocyanins in cherries (*Prunus avium* L.). *Food Chemistry* 103: 976-984. <https://doi.org/10.1016/j.foodchem.2006.08.039>
- Kirkby E A & Pilbeam D J (1984). Calcium as a plant nutrient. *Plant, Cell and Environment* 7: 397-405. <https://doi.org/10.1111/j.1365-3040.1984.tb01429.x>
- Koyuncu M A, Erbaş D, Onursal C E, Seçmen T, Güneçli A & Üzümcü S S (2019). Postharvest treatments of salicylic acid, oxalic acid and putrescine influences bioactive compounds and quality of pomegranate during controlled atmosphere storage. *Journal of Food Science and Technology* 56(1): 350-359. <https://doi.org/10.1007/s13197-018-3495-1>
- Lidster P D, Porritt S W & Tung M A (1978). Texture modification of 'Van' sweet cherries by postharvest calcium treatments. *Journal of the American Society for Horticultural Science* 103: 527-530
- Mahmood M, Anwar F, Abbas M, Boyce M C & Saari N (2012). Compositional variation in sugars and organic acids at different maturity stages in selected small fruits from Pakistan. *International Journal of Molecular Sciences* 13: 1380-1392. <https://doi.org/10.3390/ijms13021380>
- Martínez-Romero D, Alburquerque N, Valverde J M, Guillén F, Castillo S, Valero D & Serrano M (2006). Postharvest sweet cherry quality and safety maintenance by aloe vera treatment: A new edible coating. *Postharvest Biology and Technology* 39(1): 93-100. <https://doi.org/10.1016/j.postharvbio.2005.09.006>
- Melgarejo P, Salazar D M & Artes F (2000). Organic acid and sugar composition of harvested pomegranate fruits. *European Food Research and Technology* 211: 185-190. <https://doi.org/10.1007/s002170050021>
- Michailidis M, Karagiannis E, Tanou G, Karamanolis K, Lazaridou A, Matsi T & Molassiotis A (2017). Metabolomic and physico-chemical approach unravel dynamic regulation of calcium in sweet cherry fruit physiology. *Plant Physiology and Biochemistry* 116: 68-79. <https://doi.org/10.1016/j.plaphy.2017.05.005>
- Monsalve-Gonzalez A, Barbosa-Cánovas G V & Cavalieri R P (1993). Mass transfer and textural changes during processing of apples by combined methods. *Journal of Food Science* 58(5): 1118-1124. <https://doi.org/10.1111/j.1365-2621.1993.tb06128.x>
- Mozetič B, Trebše P, Simičič M & Hribar J (2004). Changes of anthocyanins and hydroxycinnamic acids affecting the skin colour during maturation of sweet cherry (*Prunus avium* L.). *Lebensmittel-Wissenschaft und -Technologie* 37: 123-128. [https://doi.org/10.1016/S0023-6438\(03\)00143-9](https://doi.org/10.1016/S0023-6438(03)00143-9)
- Mozetič B, Simičič M & Trebše P (2006). Anthocyanins and hydroxycinnamic acids of Lambert Compact cherries (*Prunus avium* L.) after cold storage and 1-methylcyclopropene treatment. *Food Chemistry* 97(2): 302-309. <https://doi.org/10.1016/j.foodchem.2005.04.018>
- Ozturk B, Aglar E, Karakaya O, Saracoglu O & Gun S (2019). Effects of preharvest GA₃, CaCl₂ and modified atmosphere packaging treatments on specific phenolic compounds of sweet cherry. *Turkish Journal of Food and Agriculture Sciences* 1(2): 44-56. <https://doi.org/10.14744/turkjfas.2019.009>
- Ranjbar S, Rahemi M & Ramezani A (2018). Comparison of nano-calcium and calcium chloride spray on postharvest quality and cell wall enzymes activity in apple cv. Red Delicious. *Scientia Horticulturae* 240: 57-64. <https://doi.org/10.1016/j.scienta.2018.05.035>
- Romano G S, Cittadini E D, Pugh B & Schouten R (2006). Sweet cherry quality in the horticultural production chain. *Stewart Postharvest Review* 6(2): 1-9. <https://doi.org/10.2212/spr.2006.6.2>
- Saba M K & Sogvar O B (2016). Combination of carboxymethyl cellulose-based coatings with calcium and ascorbic acid impacts in browning and quality of fresh-cut apples. *LWT - Food Science and Technology* 66: 165-171. <https://doi.org/10.1016/j.lwt.2015.10.022>
- Saracoglu O, Ozturk B, Yildiz K & Kucuker E (2017). Pre-harvest methyl jasmonate treatments delayed ripening and improved quality of sweet cherry fruits. *Scientia Horticulturae* 226: 19-23. <https://doi.org/10.1016/j.scienta.2017.08.024>
- Sairam R K, Vasanthan B & Arora A (2011). Calcium regulates *Gladiolus* flower senescence by influencing antioxidative enzymes activity. *Acta Physiologiae Plantarum* 33: 1897-1904. <https://doi.org/10.1007/s11738-011-0734-8>
- Schick J L & Toivonen P M (2002). Reflective tarps at harvest reduce stem browning and improve fruit quality of cherries during subsequent storage. *Postharvest Biology and Technology* 25(1): 117-121. [https://doi.org/10.1016/S0925-5214\(01\)00145-4](https://doi.org/10.1016/S0925-5214(01)00145-4)
- Serradilla M J, Martín A, Ruiz-Moyano S, Hernández A M, López-Corrales M & Córdoba M G (2012). Physicochemical and sensorial characterisation of four sweet cherry cultivars grown in Jerte Valley (Spain). *Food Chemistry* 133: 1551-1559. <https://doi.org/10.1016/j.foodchem.2012.02.048>
- Serrano M, Guillén F, Martínez-Romero D, Castillo S & Valero D (2005). Chemical constituents and antioxidant activity of sweet cherry at different ripening stages. *Journal of Agricultural and Food Chemistry* 53: 2741-2745. <https://doi.org/10.1021/jf0479160>

- Thaipong K, Boonprakob U, Crosby K, Cisneros-Zevallos L & Byrne D H (2006). Comparison of ABTS, DPPH, FRAP, and ORAC assays for estimating antioxidant activity from guava fruit extracts. *Journal of Food Composition and Analysis* 19: 669–675. <https://doi.org/10.1016/j.jfca.2006.01.003>
- Tsantili E, Rouskas D, Christopoulos M V, Stanidis V, Akrivos J & Papanikolaou D (2007). Effects of two pre-harvest calcium treatments on physiological and quality parameters in ‘Vogue’ cherries during storage. *The Journal of Horticultural Science and Biotechnology* 82(4): 657-663. <https://doi.org/10.1080/14620316.2007.11512287>
- Vangdal E, Hovland K L, Børve J, Sekse L & Slimestad R (2008). Foliar application of calcium reduces postharvest decay in sweet cherry fruit by various mechanisms. *Acta Horticulturae* 768: 143-148. <https://doi.org/10.17660/ActaHortic.2008.768.16>
- Wang Y, Xie X & Long L E (2014). The effect of postharvest calcium application in hydro-cooling water on tissue calcium content, biochemical changes, and quality attributes of sweet cherry fruit. *Food Chemistry* 160: 22-30. <https://doi.org/10.1016/j.foodchem.2014.03.073>
- Watada A E (1982). A high-performance liquid chromatography method for determining ascorbic acid content of fresh fruits and vegetables. *HortScience* 17(3): 334-335
- Winkler A & Knoche M (2019). Calcium and the physiology of sweet cherries: A review. *Scientia Horticulturae* 245: 107-115. <https://doi.org/10.1016/j.scienta.2018.10.012>
- Winkler A, Fiedler B & Knoche M 2020. Calcium physiology of sweet cherry fruits. *Trees-Structure and Function* 34 (2020): 1157-1167. <https://doi.org/10.1007/s00468-020-01986-9>



© 2022 by the author(s). Published by Ankara University, Faculty of Agriculture, Ankara, Turkey. This is an Open Access article distributed under the terms and conditions of the Creative Commons Attribution (CC BY) license (<http://creativecommons.org/licenses/by/4.0/>), which permits unrestricted use, distribution, and reproduction in any medium, provided the original work is properly cited.



Extraction and Physicochemical Characterization of Chitosan from Pink Shrimp (*Parapenaeus longirostris*) Shell Wastes

Özen Yusuf ÖĞRETMEN^{a*}, Barış KARSLI^a, Emre ÇAĞLAK^a

^aDepartment of Processing Technology, Faculty of Fisheries, Recep Tayyip Erdogan University, Rize, TURKEY

ARTICLE INFO

Research Article

Corresponding Author: Özen Yusuf ÖĞRETMEN, E-mail: ozenyusuf.ogretmen@erdogan.edu.tr

Received: 15 January 2020 / Revised: 29 September 2021 / Accepted: 07 October 2021 / Online: 01 September 2022

Cite this article

ÖĞRETMEN Ö Y, KARSLI B, ÇAĞLAK E (2022). Extraction and Physicochemical Characterization of Chitosan from Pink Shrimp (*Parapenaeus longirostris*) Shell Wastes. *Journal of Agricultural Sciences (Tarım Bilimleri Dergisi)*, 28(3):490-500. DOI: 10.15832/ankutbd.861909

ABSTRACT

This study aimed to evaluate the extract of chitosan obtained from pink shrimp (*Parapenaeus longirostris*) shell wastes in Balıkesir, the Marmara Sea in Turkey, and to characterize its quality. The physicochemical properties of biopolymer chitosan such as moisture content, solubility, degree of deacetylation (DD), molecular weight (MW), particle size, bulk density, pH, water-binding capacity (WBC), fat-binding capacity (FBC), and color attributes were examined. The obtained chitosan was characterized by Fourier transform infrared spektrofotometer (FT-IR), Dynamic light scattering (DLS), and Thermogravimetric measurements (TG/DTA/DTG). Results indicated that the yield and moisture content of

chitosan was 18.82% and 3.62%, respectively. DD was 81.50% while solubility was 86.79%. MW of chitosan was found to be 310 kDa. The presence of the amino group was confirmed from the FT-IR spectra of the synthesized chitosan. Thermogravimetric measurements showed that chitosan had low thermal stability. SEM analysis revealed that the surface morphologies of chitosan consisted of relatively smooth surface and nanofiber structures. Based on the physicochemical characteristics obtained in the present study, pink shrimp could be a potential source to produce high-quality chitosan for industrial applications.

Keywords: Natural polymer, Autoclave extraction, Waste recycling, Degree of deacetylation, Molecular weight

1. Introduction

Chitin is the second most common organic polymer on earth after cellulose (Kucukgulmez et al. 2011) and can be abundantly found in marine invertebrates, crab, shrimp, insects, yeast, and fungi (Samar et al. 2013). In general, dry shrimp waste contains 30-40% protein, 30-50% calcium carbonate, and 20-30% chitin (Ben Seghir & Benhamza 2017). Chitosan is obtained by the deacetylation of chitin in the solid-state and under alkaline circumstances or by hydrolysis of chitin by chitin deacetylase (Daraghmeh et al. 2011). Chitosan consists of randomly distributed N-acetyl-D-glucosamine and D-glucosamine units (El Knidri et al. 2017) and is widely used in chemical industries, food processing, production of cosmetics, and biomedical and pharmaceutical industries (No et al. 2002). Chitosan and its oligomers have attracted considerable attention because of their antimicrobial, antitumor, and hypocholesterolemic properties (No et al. 2002; Rinaudo 2006). It is generally soluble in aqueous acid solutions such as citric acid, formic acid, acetic acid, lactic acid, etc. but insoluble in water (Karsli et al. 2019). Further, it is non-toxic, biodegradable, and biocompatible (Mourya & Inamdar 2008). Deacetylation degree (DD) and molecular weight (MW) are critical parameters that strongly affect most of its physicochemical properties and biological activities (El Knidri et al. 2017).

There are many studies showing that chitin and chitosan are prepared by biological and chemical methods. The chemical extraction processes of chitosan have been developed by many researchers by trying different methods (Amoo et al. 2019; Abirami et al. 2021; Hao et al. 2021; Mittal et al. 2021; Vallejo-Dominguez et al. 2021). Traditional isolation of chitin from crustacean shell waste consists of three basic steps: demineralization to remove calcium carbonate and calcium phosphate separation and deproteinization to separate protein and decolorization to removal of pigments. For the production of chitosan, the deacetylation process is applied in addition to these standard process steps used in the production of chitin (Vallejo-Dominguez et al. 2021). Finally, chitin is converted into chitosan that achieved by treatment with concentrated sodium hydroxide solution (between 40-50%) at 100 °C or higher temperature to remove some or all of the acetyl group from the chitin (Galed et al. 2008). There are many studies about chitosan production from shrimp waste in literature (Varun et al. 2017; Ait et al. 2018; del Carmen Borja-Urzola et al. 2020; Dominguez et al. 2021; Mittal et al. 2021). In Turkey, there are some studies relating to the evaluation of these waste. Kucukgulmez et al. (2011) determined the physicochemical properties, yield, moisture and ash contents, degree of deacetylation, molecular weight, water and oil binding capacities, apparent viscosity and color properties of

chitosan extracted from *Metapenaeus stebbingi* shells. Tokatlı & Demirdöven (2018) conducted a study on the optimization and characterization of chitin and chitosan production from shrimp waste. However, the studies on the characterization of chitosan from pink shrimp in Turkey are limited. Only Kucukgulmez et al. (2017) investigated the physicochemical properties of chitosan extracted from the pink shrimp shell and reported that according to the research findings, chitosan production would be beneficial for the economic use of shrimp waste in Turkey.

Total world shrimp production, which reached 5.03 million tons in 2020, is expected to increase to 7.28 million tons by 2025. However, the amount of pink shrimp caught in Turkey has reported as 1413 tons in 2010 and it has increased to 3851.9 tons in 2019 (TUIK 2020). Approximately 50-60% of solid wastes generated during shrimp processing are by-products such as head, viscera, and shell (Nirmal et al. 2020). For this reason, recovering these wastes generated during processing will be beneficial for the shrimp processors and the economy of the country. Based on the above explanation, the aim of the present study was to obtain chitosan from pink shrimp (*Parapenaeus longirostris*) shell wastes and to investigate its physicochemical characteristics properties such as the MW, DD, color, water- and fat-binding capacities, solubility and moisture content.

2. Material and Methods

2.1. Chemicals

Chemicals used in the chitosan extraction process are hydrochloric acid (ACS reagent, 37%) and sodium hydroxide (reagent grade, $\geq 98\%$) and they were purchased from Merck, Darmstadt, Germany.

2.2. Raw material

Shell wastes from pink shrimp (*Parapenaeus longirostris*) were collected from a local factory from Balıkesir, Marmara Sea, Turkey, then the samples were packed in plastic bags and stored at $-20\text{ }^{\circ}\text{C}$ until further use. The shell wastes were separated from other waste materials in a laboratory and stored in a refrigerator at $4\text{ }^{\circ}\text{C}$. Then, cleaned shrimp shell wastes were washed with distilled water and dried for 24 h at $60\text{ }^{\circ}\text{C}$. Approximately 500 g of dry shrimp shells were used for this study.

2.3. Extraction of chitosan

Dried shrimp shell wastes were ground for chitosan extraction and subjected to demineralization, deproteinization, and deacetylation processes.

2.3.1. Demineralization

The demineralization process was carried out by modifying the extraction time of the procedure performed by Boudouaia et al. (2019). According to demineralization protocol, shrimp shell powder was treated with 1.35 N (5% v/v) HCl solution (10:1 v/w) at ambient temperature on a magnetic stirrer (Weightlab Instruments, WF-MID1 model) at a speed of 250 rpm for 24 h. The extract was then filtered through Whatman No. 541 filter paper and filtered samples were washed with distilled water until its pH was neutral.

2.3.2. Deproteinization

The deproteinization process was performed by modifying the concentration of NaOH in the procedure followed by Boudouaia et al. (2019). Deproteinization was performed using 1.75 N (7% w/v) NaOH solution (10:1 v/w) at ambient temperature on a magnetic stirrer at a speed of 250 rpm for 24 h. After deproteinization, the samples were filtered through Whatman No. 541 filter paper and then washed until its pH reached neutral. After these processes, chitin yield was calculated as 24.44%.

2.3.3. Deacetylation

Deacetylation was performed using concentrated NaOH solution. After deproteinization, the dried samples were heated in an autoclave (Dathan Scientific, WAC-47 model, Seoul-Korea) at 1 atm pressure (Byun et al. 2013), i.e. $121.1\text{ }^{\circ}\text{C}$ for 40 min with 50% NaOH solution (Sedaghat et al. 2017) and a solid/solvent ratio of 1:20 w/v. After deacetylation, the samples were filtered and washed with distilled water until the pH was neutral, and then dried in an oven at $60\text{ }^{\circ}\text{C}$ for 20 h. Figure 1 shows the various steps involved in the chitosan preparation from pink shrimp shell wastes, where major steps such as demineralization, deproteinization, and deacetylation were followed.

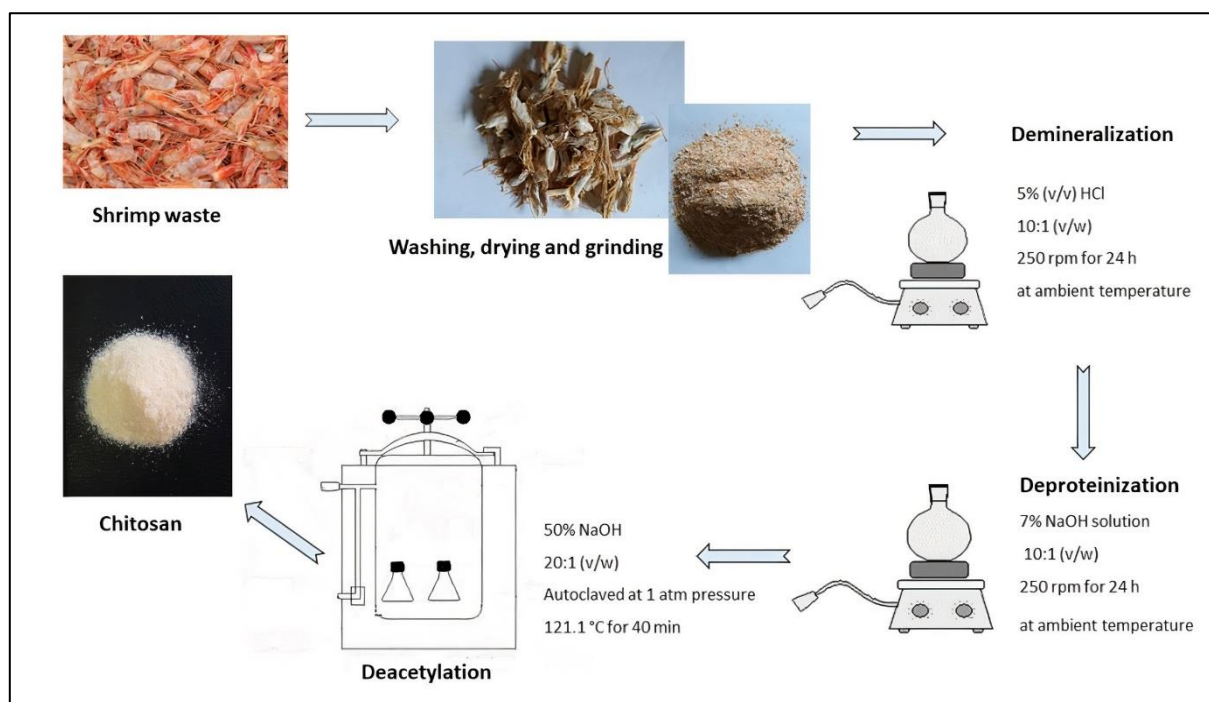


Figure 1- Extraction process of chitosan from pink shrimp shell wastes

2.4. Characterization of chitosan

2.4.1. Determination of yield and moisture content

Chitosan yield (%) was determined as the percentage of dried shrimp shells. The moisture contents of the extracted chitosan were analysed by using the standard AOAC method (AOAC 1995).

$$\text{Chitosan yield (\%)} = [\text{dry wt. of obtained chitosan/dry wt. of shrimp shell waste}] \times 100$$

2.4.2. Determination of deacetylation degree

DD (%) was determined by FT-IR spectroscopy and calculated using the Domszya & Roberts (1985) equation:

$$\text{DD (\%)} = 100 - (A_{1655}/A_{3450} \times 100/1.33)$$

A_{1655} : absorbance of the amide-I band at 1655 cm^{-1} , A_{3450} : absorbance of the hydroxyl band at 3450 cm^{-1} . The factor 1.33 denotes the value of the ratio of A_{1655}/A_{3455} for N-acetylated chitosan.

2.4.3. Molecular weight

The MW of chitosan was determined by the dynamic light scattering (DLS) method. Zetasizer Nano ZSP light scattering system (Malvern Instruments) was used to investigate the chitosan particles (Amiri et al. 2019). DLS was performed at $25 \text{ }^\circ\text{C}$ with a laser wavelength of 633 nm and a scattering detection of $173 \text{ }^\circ\text{C}$. Acetic acid solution with a concentration of 0.1 mg/mL was used for the analysis.

2.4.4. Water- and fat-binding capacities

The water-binding capacity (WBC) and fat-binding capacity (FBC) of the chitosan samples were determined according to the method proposed by Knorr (1982). FBC of chitosan extracted from pink shrimp shells was measured using sunflower oil.

2.4.5. Colorimetric measurement

Chitosan samples were spread on a petri dish. The colorimetric parameters of the samples were measured using a Konica Minolta colorimeter (model CR-14, Osaka, Japan). The results were denoted as L^* , a^* , b^* , and whiteness index. The whiteness index of the extracted chitosan was calculated based on the following equation (Seo et al. 2007).

$$\text{Whiteness index} = 100 - [(100 - L^*)^2 + (a^*)^2 + (b^*)^2]^{1/2}$$

2.4.6. Scanning electron microscopic (SEM) analysis

Morphology and physical state of the surface of chitosan was detected by scanning electron microscopy (Metin et al. 2019). SEM analysis was performed using a JEOL JSM-6610 scanning electron microscope operated at an accelerating voltage of 15kV.

2.4.7. FT-IR analysis

The FT-IR spectra of chitosan were analysed using an FT-IR spectrophotometer (PerkinElmer Spectrum 100 Universal ATR Sampling Accessory) at a wave range of 400 to 4000 cm^{-1} and a resolution of 4 cm^{-1} using the ATR mode of operation.

2.4.8. Thermogravimetric analysis

Thermogravimetric analysis of the chitosan samples (TG/DTA/DTG) was performed using an SII TG/DTG analyzer equipped with A6 6300 under a constant flow of static air atmosphere (heating rate: 10 $^{\circ}\text{C}/\text{min}$, platinum crucibles, mass: 9.705 mg and temperature range: 25–1000 $^{\circ}\text{C}$) (Hong et al. 2007).

2.4.9. Solubility, bulk density, particle sizes, and pH value of chitosan

For measuring the solubility of chitosan, 0.1 g of chitosan was dissolved in 10 mL of 1% acetic acid for 30 min and then centrifuged at 10,000 x g for 10 min at room temperature (Nessa et al. 2011). The bulk density of chitosan was measured according to the procedure described by Cho et al. (1998) and calculated into a 25-mL measuring cylinder as g/mL of the sample. The particle size of chitosan was determined using a laser scattering size analyzer (Malvern, model 'Mastersizer Hydro 2000 MU). The pH measurement of chitosan solutions (chitosan/distilled water ratio of 1:10 w/v) was carried out using a pH meter (Hanna, HI 3220, Germany).

2.5. Statistical analysis

All analytical determinations were performed in triplicate. The descriptive statistical parameters (mean and standard error) were determined using MS Excel, MS Office 2016 (Microsoft Corporation, Redmond, Washington, USA).

3. Results and Discussion

Results of yield, moisture content, DD, WW, WBC, FBC, solubility, and colorimetric parameters of the chitosan samples are provided in Table 1.

Table 1- Physicochemical analysis of the extracted chitosan from shrimp shell waste

Analysis	Extracted chitosan	
Yield (%)	18.82	
Moisture (%)	3.65±0.36	
Deacetylation degree (%)	81.50	
Molecular weight (kDa)	310	
Water binding capacity (%)	685.46±23.25	
Fat binding capacity (%)	523.76±15.65	
Solubility (%)	86.79±0.03	
Color measurement	L*	75.81±1.26
	a*	8.53±0.98
	b*	21.95±0.55
	Whiteness	66.25
Bulk density (g/mL)	0.19±0.002	
Particle size (nm)	1606	
pH	6.99±0.11	

Chitosan yield of 18.82% as determined in this study was higher than that reported by Varun et al. (2017) who obtained a yield of 12.03%. On the other hand, the yield obtained in the present study was higher than that reported by Ait et al. (2018) who obtained a yield between 2.1% and 4.4%. Kucukgulmez et al. (2011) extracted chitosan from *Metapenaeus stebbingi* shell waste

and reported a yield of 17.48%. Nessa et al. (2011) found that yield for chitosan extracted from prawn shell waste ranged from 16.4-19.6%. The chitosan yield of pink shrimp shell used in the present study was higher than those obtained from some species by Varun et al. (2017) and Ait et al. (2018); however, it was comparable with those reported by Kucukgulmez et al. (2011) and Nessa et al. (2011). This high chitosan yield determined in this study may be due to the use of autoclave method in the deacetylation step. Sedaghat et al. (2017) compared three different (traditional, microwave, and autoclave) methods to obtain chitosan from shrimp shells and reported that the highest chitosan yield was obtained with the autoclave method. Hossain & Iqbal (2014) reported that the low concentration of HCl used in demineralization steps could not remove minerals from shrimp shells. They also added that lower chitosan yield might be due to depolymerization of the chitosan polymer, loss of sample mass/weight from excessive removal of acetyl groups from the polymer during deacetylation, and loss of chitosan particles during washing. In addition, Samar et al. (2013) reported that yields of chitosan increased significantly by increasing the concentration of NaOH solution used in the deacetylation process. Similarly, Fatima (2020) reported that the yields of chitosan increased with decreasing the chitin particle size and increasing the concentration of NaOH solution used in deacetylation step. This variation in chitosan yield may be due to different shrimp species and different extraction methods (such as different sodium hydroxide ratio and deacetylation temperature etc.) used in deproteinization, demineralization, and deacetylation process. At the same time, these differences in chitosan yield may be associated with effectiveness in removing process of minerals and proteins attached to them.

Khan et al. (2002) explained that chitosan is hygroscopic in nature so it can be affected by moisture absorption during storage. Li et al. (1992) reported that commercial chitosan may contain <10% moisture content. The moisture content of the shrimp shell chitosan samples was $3.65 \pm 0.36\%$. Kucukgulmez et al. (2017) reported that the moisture content of chitosan extracted from pink shrimp was between 1.52% and 1.80%. Hossain & Iqbal (2014) determined moisture content ranging from 7.69% to 8.25% for chitosan obtained from shrimp shell waste. Nessa et al. (2011) investigated that the moisture content of shrimp chitosan is ranging from 0.34% to 0.45%. There are differences in the amount of moisture between the present study and the several studies. These differences are thought to be due to different processing protocols such as extraction temperatures, time, and drying conditions (Hossain & Iqbal 2014).

The DD has a vital feature for chitosan as it affects the physical, chemical and biological properties, acid-base and electrostatic properties, biodegradability properties of chitosan (Li et al. 1992). DD is an important parameter that determines the industrial quality of chitosan (Samar et al. 2013). Considering the importance of this parameter, Li et al. (1992) reported that the term chitosan should be used when the degree of deacetylation is above 70%. Kumari et al. (2017) found the degree of deacetylation at 75%, 78%, and 70% for chitosan obtained from fish, shrimp, and crab, respectively. Hossain & Iqbal (2014) extracted chitosan-based on different concentrations of NaOH treatment and found the degree of deacetylation between 45.50-81.24%. In the present study, the DD of the extracted chitosan was found to be 81.50%. Kucukgulmez et al. (2017) reported that the DD of chitosan extracted from pink shrimp was 72.86% in the low degree group and 93.70% in the high degree group. Sudatta et al. (2020) found that the deacetylation degree of chitosan from *Pinna bicolor* was 59.76%. Mittal et al. (2021) found that the deacetylation degree of chitosan produced under various temperatures for different times ranged from 71.93% to 79.14%. del Carmen Borja-Urzola et al. (2020) reported that deacetylation degrees of chitosan extracted based on with and without ultrasound-stir were 48.98% and 65.16%, respectively.

Molecular weight is one of the most important factors that affect the physicochemical and functional properties of chitosan (Yen et al. 2009; Fernández-Martin et al. 2014). Biological and biomedical applications of chitosan are highly dependent on both the DD and the MW of the polymer (Abdou et al. 2008). In the present study, the MW was determined to be 310 kDa. This data was agreement with the Mw (161-451 kDa) of chitosan prepared from chitin with different treated conditions (Trung et al. 2020). A similar study performed by Kucukgulmez et al. (2011) reported the MW of 2.20 kDa for chitosan obtained from *Metapenaeus stebbingi* shells while Samar et al. (2013) found the MW in the range from 866.03 to 4467.05 kDa for chitosan obtained from shrimp shell wastes. Boudouaia et al. (2019) obtained two different types of chitosan from shrimp shells and found their MW as 354 kDa and 412 kDa. Kumari et al. (2017) detected low MW (6.273 kDa) in chitosan from shrimp shells and reported that this may be due to low degree of deacetylation. The MW of chitosan extracted from shrimp shell wastes in the present study is not comparable to that reported in previous studies and the difference could be ascribed to several factors involved in the preparation of chitosan samples such as temperature, concentration of alkali and acid solutions, sources of chitosan, and treatments before chitosan.

WBC and FBC of chitosan extracted from shrimp shells wastes in the present study were found to be $685.46 \pm 23.25\%$ and $523.76 \pm 15.65\%$, respectively. And these results are consistent with the WBC (712.99%) and FBC (531.15%) data reported by Kucukgulmez et al. (2011). Similarly, Abirami et al. (2021) reported that the WBC and FBC for shrimp shells were 601.11% and 441.07%, respectively. Hossain & Iqbal (2014) reported that WBC and FBC for shrimp chitosan were 537.29% and 427.98%, respectively. On the other hand, No et al. (2000) determined that the WBCs and FBCs values of six commercial chitosan samples ranged from 355% to 611% and 217% to 477%, respectively. Cho et al. (1998) reported that the WBC and FBC for different commercial chitosan ranged from 458% to 805% and 314% to 535%, respectively. In another study, Kumari et al. (2017) found lower WBC (358%) and FBC (246%) for shrimp chitosan, respectively. However, Mohanasrinivasan et al. (2014) determined higher WBC (1136%) and FBC (772%) for chitosan compared to the result of the present study. WBC and FBC basically depend

on the demineralization and deproteinization procedure, but different chitosan sources are also important factors affecting this situation (Kumari et al. 2017).

Solubility is an important parameter for determining the quality of chitosan and factors such as deacetylation time, temperature, the concentration of NaOH solution, and particle size play a critical role in determining solubility (Hossain & Iqbal 2014). Samar et al. (2013) obtained excellent solubility ranging from 83.28% to 99.05% by modulating particle size and concentration of NaOH solution. Hossain & Iqbal (2014) determined the solubility of chitosan ranging from 48.3% to 97.65% at different NaOH concentrations. The solubility of chitosan extracted from shrimp shell wastes in this study was found to be $86.79 \pm 0.03\%$, which is comparable with the values reported by Hossain & Iqbal (2014) and Samar et al. (2013).

The colorimetric parameters L^* , a^* , b^* , and whiteness index of the chitosan samples are given in Table 1. In the present study, the values of L^* , a^* , b^* , and whiteness index were determined to be 75.81, 8.53, 21.95, and 66.25, respectively. Based on visual observations, the color of chitosan samples ranged from white to light yellow. The L^* value of the chitosan samples in this study is similar to that reported in previous studies (Alishahi et al. 2011; Kucukgulmez et al. 2011). The redness value (denoted by a^*) of the extracted chitosan was of the highest intensity, which may have been due to contamination caused by the pigments present in chitin during the deacetylation process. While the b^* value of chitosan obtained in this study was found to be comparable with the values of Kucukgulmez et al. (2011), it was found to be higher than that reported (10.1-13.65) by Alishahi et al. (2011). The whiteness index (66.25) determined in this study was found to be higher than those (35.78-43.30) of chitosan obtained from shrimp shell by Vallejo-Domínguez et al. (2021). They reported that this lower whiteness index may be due to the oxidization of samples during the sonication process.

In the present study, the bulk density of chitosan was found as 19 g/mL. Trung et al. (2006) determined that the bulk density of 75%, 87%, and 96% deacetylation grade chitosan from shrimp shells were 0.59, 0.54, and 0.531 g/mL, respectively. No et al. (2000) found the bulk density of chitosan from six different sources as 0.18-0.33 g/mL. Rout (2001) reported that the bulk density decreased with increasing deacetylation degree. The results of the present study showed similarity with the data reported by No et al. (2000), but they were different from the data determined by Trung et al. (2006). This may be due to the porosity of the material before treatment.

In this study, the particle size of chitosan was found to be 1606 nm. Similarly, Dananjaya et al. (2017) reported that particle size of chitosan was 1658 nm. Kong et al. (2010) reviewed that decreasing particle size improved antibacterial activity. Also, Liu et al. (2018) reported that small particle size is preferred in drug delivery systems. Bough et al. (1978) reported that smaller particle size (1 mm) exhibited higher MW and viscosity than those with either 2 or 6.4 mm particle size.

The pH value of chitosan produced from pink shrimp shells was found to be 6.99 ± 0.11 . Similarly, Paul et al. (2014) determined the pH value of chitosan from sea prawn (*Fenneropenaeus indicus*) as 6.7. The researchers reported that the pH value of chitosan from *Panaeus monodon* shell was 8.5 (Puvvada et al. 2012) and 8.0 (Divya et al. 2014). This is probably due to differences in experimental methods and chitosan characteristics.

The FT-IR spectra of the extracted chitosan samples are presented in Figure 2. The spectra showed peaks around 3256 to 3422 cm^{-1} , indicating that the stretching vibration of O-H and N-H bands. The 1661 cm^{-1} peak in the spectra denotes the vibrations of the carbonyl group (amide band I). The peak at 1619 cm^{-1} shows N-H bending (amide II). Amide I and amide II are known as the characteristic bands for chitosan and were observed at around 1661 and 1619 cm^{-1} . This characteristic band is commonly assigned to the stretching of the CO group hydrogen bonded to amide group of the neighboring intra-sheet chain (Al Sagheer et al. 2009). The band at 1153 cm^{-1} was assigned to amide III. For the $-\text{CH}_2$ groups in CH_2OH , peaks spiked at 3103 and 1554 cm^{-1} for the extracted chitosan samples. Oxygen stretching of glycosidic linkage was found to be 1062 cm^{-1} . The C-O stretching of the structure was observed at 1008 and 950 cm^{-1} . The $-\text{CH}_3$ group of NHCOCH_3 (amide bond) can be seen at 1376 cm^{-1} . The pyranose ring was found at 895 cm^{-1} . The FT-IR spectrophotometry results of the extracted chitosan samples used in the present study were confirmed with those of the previous studies (Kucukgulmez et al. 2011; Varun et al. 2017; Ibitoye et al. 2018).

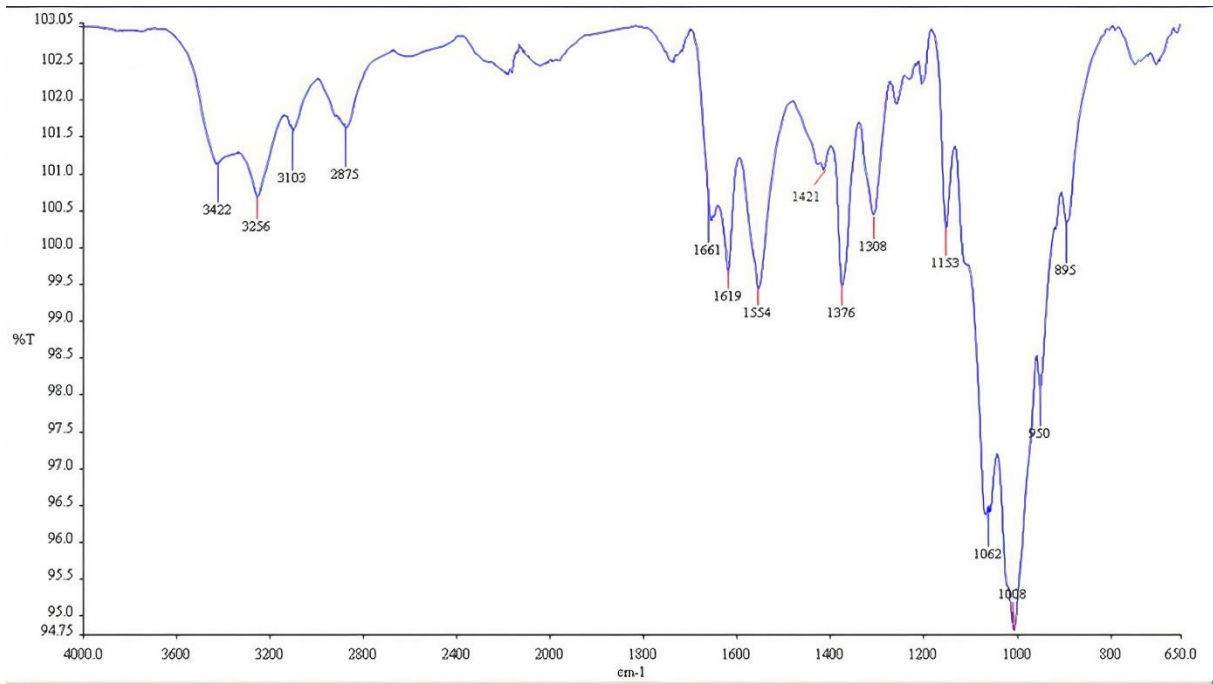


Figure 2- The FT-IR spectrum of extracted chitosan.

SEM analysis was performed to determine the molecular structure of the extracted chitosan (Fig. 3). A layer of flakes is obvious in Figures 3A and 3B, which is similar to that reported by Kucukgulmez et al. (2011). A fibrous structure with a rough surface including pores of chitosan derivatives can be distinguished in Figures 3C and 3D, which is similar to that reported by Hassan et al. (2018). Micropores of extracted chitosan derivatives can be seen clearly in Figures 3E and 3F.

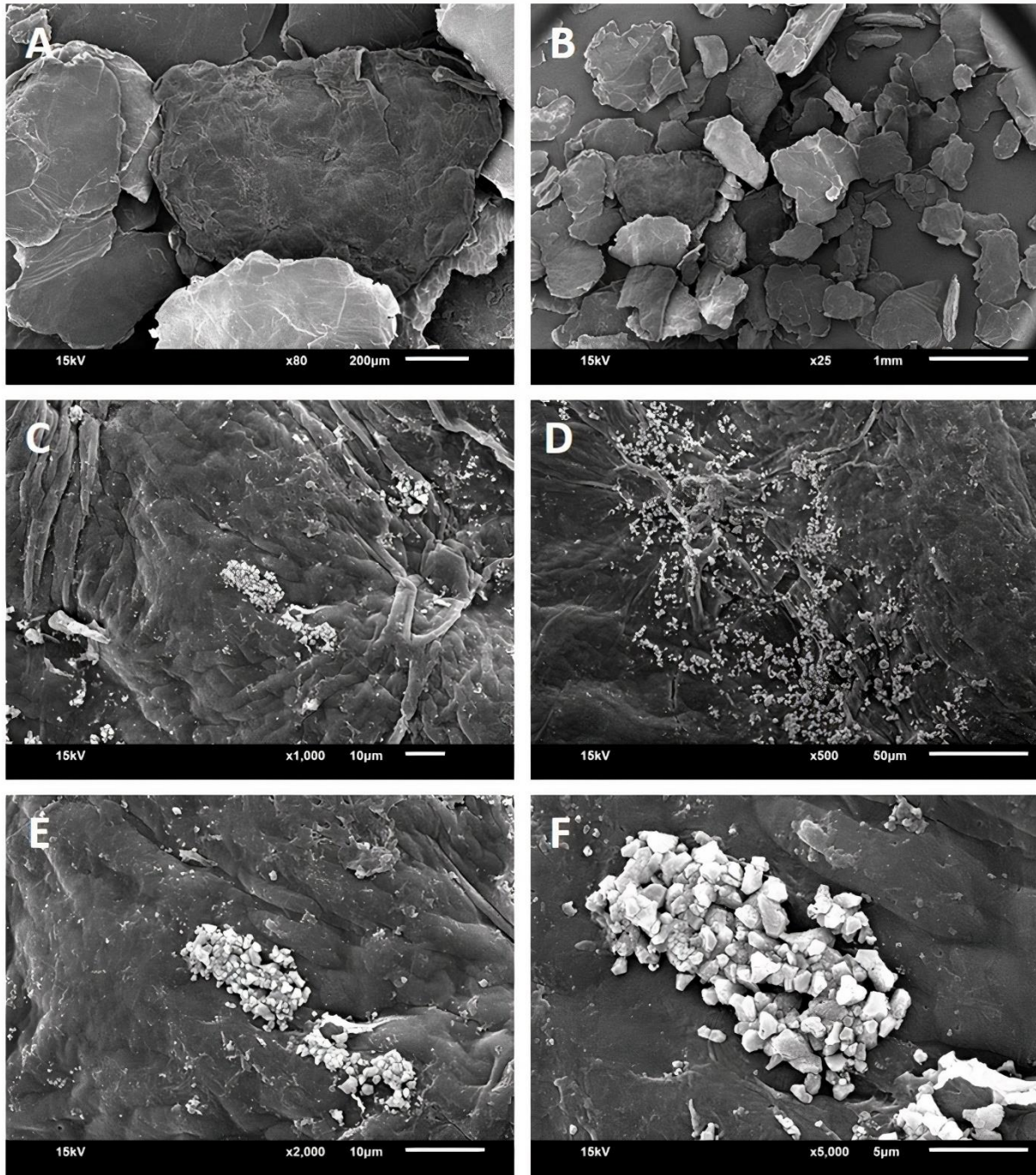


Figure 3- SEM micrographs of the extracted chitosan at (A) 80x (B) 25x (C) 1000x (D) 500x (E) 2000x (F) 5000x magnifications.

The TG, DTG, and DTA curves obtained by the thermal degradation of the extracted chitosan at a heating rate of $10\text{ }^{\circ}\text{C min}^{-1}$ are shown in Figure 4. The blue curve indicates TGA, the red one indicates DTA, and the green one indicates DTG. The initial temperature of weight loss (T_0) is $250\text{ }^{\circ}\text{C}$ (weight loss 8%), the final temperature of weight loss (T_f) is $355\text{ }^{\circ}\text{C}$ (weight loss 60%) and the temperature (T_p) at maximum weight loss rate is $340\text{ }^{\circ}\text{C}$ (weight loss 43%). The residual product is 40%. Chitosan film lost almost all of its weight at $560\text{ }^{\circ}\text{C}$ (92%).

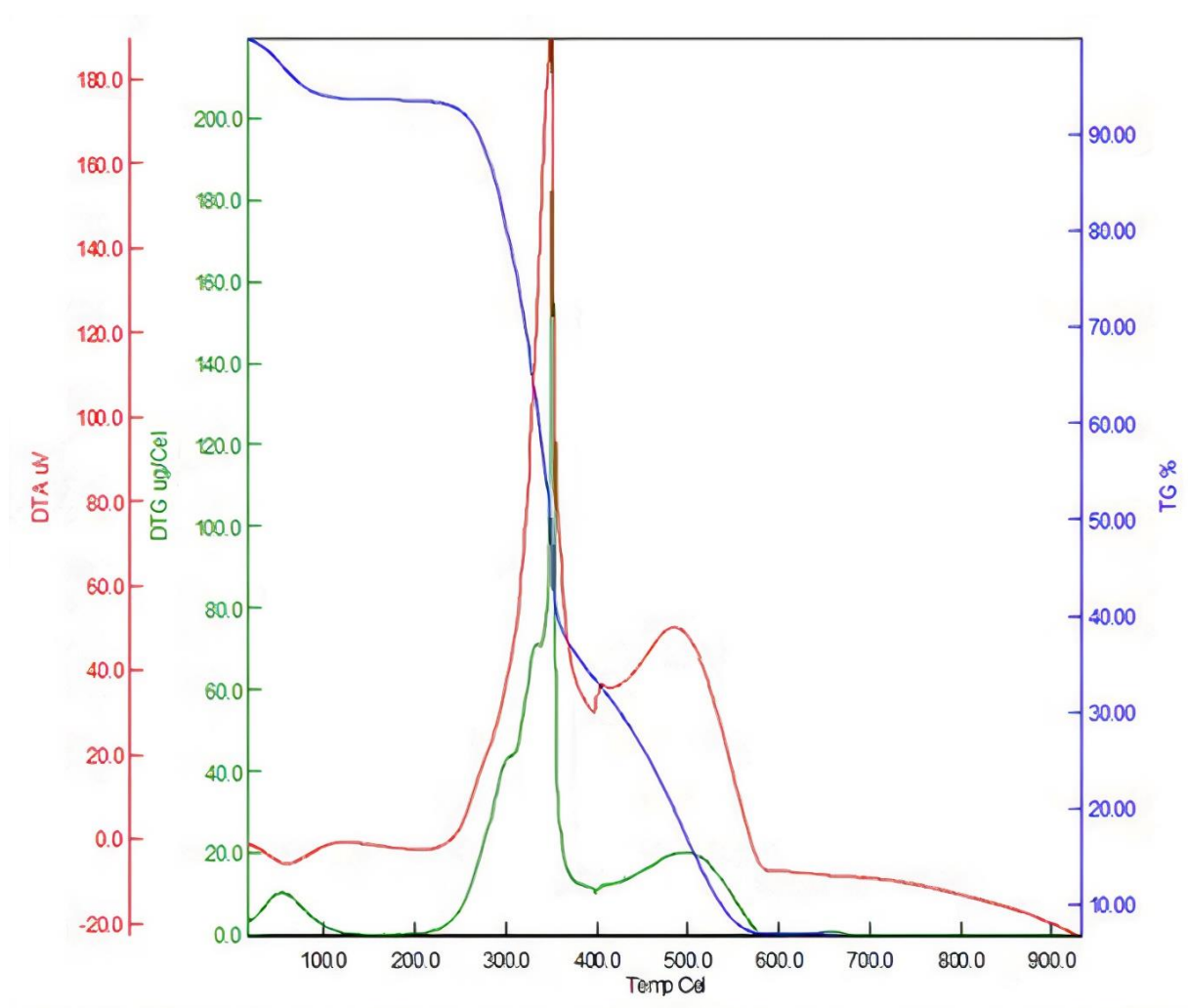


Figure 4- TGA, DTA, and DTG analyses of extracted chitosan

4. Conclusions

Waste recycling is a global concern and we believe that biowaste generated from the seafood industry such as shrimp shell wastes can be put to better use by extracting chitosan from such waste products and utilizing the same in a wide variety of applications such as in chemical, food processing, cosmetic, and biomedical and pharmaceutical industries. The physicochemical characteristics such as MW, DD, solubility, moisture, WBC, and FBC determined in the present study indicate that the quality of chitosan obtained from pink shrimp shell waste has the potential of being a high-quality source of chitosan for such applications. Therefore, further studies are recommended to understand the antimicrobial and antioxidant effect of the chitosan produced from pink shrimp shells.

Acknowledgments

The authors would like to thank Recep Tayyip Erdogan University the Faculty of Arts and Sciences (Department of Chemistry) for their contribution during analyses (FT-IR, SEM, TG, DTA, DTG).

References

- Abdou E S, Nagy K S A & Elsabee M Z (2008). Extraction and characterization of chitin and chitosan from local sources, *Bioresources Technology* 99: 1359-1367. <https://doi.org/10.1016/j.biortech.2007.01.051>
- Abirami S, Nagarajan D, Antony V S, Mini Varsini A, Sugasini A & Anand D A (2021) Extraction, characterization, and utilization of shrimp waste chitin derived chitosan in antimicrobial activity, seed germination, preservative, and microparticle formulation. *Biointerface Research in Applied Chemistry* 11(2): 8725-8739. <https://doi.org/10.33263/BRIAC112.87258739>
- Ait B M, Chairi H, Laglaoui A, Arakrak A, Zantar S, Bakkali M & Hassani M (2018). Optimization and characterization of gelatin and chitosan extracted from fish and shrimp waste. *E3S Web of Conferences*, 37, 02006. <https://doi.org/10.1051/e3sconf/20183702006>
- Alishahi A, Mirvaghefi A, Tehrani M R, Farahmand H, Shojaosadati S A, Dorkoosh F A & Elsabee M Z (2011). Enhancement and characterization of chitosan extraction from the wastes of shrimp packaging plants. *Journal of Polymers and the Environment* 19: 776-783. <https://doi.org/10.1007/s10924-011-0321-5>

- Al Sagheer F A, Al-Sughayer M A, Muslim S & Elsabee M Z (2009). Extraction and characterization of chitin and chitosan from marine sources in Arabian Gulf. *Carbohydrate Polymers* 77(2): 410-419. <https://doi.org/10.1016/j.carbpol.2009.01.032>
- Amiri E, Rahmaninia M & Khosravani A (2019). Effect of chitosan molecular weight on the performance of chitosan-silica nanoparticle system in recycled pulp. *BioResources* 14(4): 7687-7701.
- Amoo K O, Olafadehan O A & Ajayi T O (2019). Optimization studies of chitin and chitosan production from *Penaeus notialis* shell waste. *African Journal of Biotechnology* 18(27): 670-688. <https://doi.org/10.5897/AJB2019.16861>
- AOAC (1995). Official methods of analysis of AOAC International, 16th edition. Volume 2. 1995. AOAC (Association of Official Analytical Chemists) International; Arlington; USA.
- Ben Seghir B & Benhamza MH (2017). Preparation, optimization and characterization of chitosan polymer from shrimp shells. *Journal of Food Measurement & Characterization* 11: 1137-1147. <https://doi.org/10.1007/s11694-017-9490-9>
- Boudouaia N, Bengharez Z & Jellali S (2019). Preparation and characterization of chitosan extracted from shrimp shells waste and chitosan film: application for Eriochrome black T removal from aqueous solutions. *Applied Water Science*, 9, 91. <https://doi.org/10.1007/s13201-019-0967-z>
- Bough W A, Salter W L, Wu A C M & Perkins B E (1978). Influence of manufacturing variables on the characteristics and effectiveness of chitosan products. I. Chemical composition, viscosity, and molecular-weight distribution of chitosan products. *Biotechnology and Bioengineering* 20: 1931-1943. <https://doi.org/10.1002/bit.260201208>
- Byun S M, No H K, Hong J H, Lee S I & Prinyawiwatkul W (2013). Comparison of physicochemical, binding, antioxidant and antibacterial properties of chitosans prepared from ground and entire crab leg shells. *International Journal of Food Science & Technology* 48(1): 136-142. <https://doi.org/10.1111/j.1365-2621.2012.03169.x>
- Cho Y I, No H K & Meyers S P (1998). Physicochemical characteristics and functional properties of various commercial chitin and chitosan products. *Journal of Agricultural and Food Chemistry* 46: 3839-3843. <https://doi.org/10.1021/jf971047f>
- Dananjaya S H S, Erandani W K C U, Kim C H, Nikapitiya C, Lee J & De Zoysa M (2017). Comparative study on antifungal activities of chitosan nanoparticles and chitosan silver nano composites against *Fusarium oxysporum* species complex. *International journal of biological macromolecules* 105: 478-488. <https://doi.org/10.1016/j.ijbiomac.2017.07.056>
- Daraghme N H, Chowdhry B Z, Leharne S A, Al Omari M M & Badwan AA (2011). Chitin. Profiles of Drug Substances, Excipients and Related Methodology 36: 35-102. <https://doi.org/10.1016/B978-0-12-387667-6.00002-6>
- del Carmen Borja-Urzola A, García-Gómez R S, Flores R & del Carmen Durán-Domínguez-de M (2020). Chitosan from shrimp residues with a saturated solution of calcium chloride in metanol and water. *Carbohydrate Research*, 497, 108116. <https://doi.org/10.1016/j.carres.2020.108116>
- Divya K, Rebello S & Jisha M S (2014). A simple and effective method for extraction of high purity chitosan from shrimp shell waste. In: Proceedings of the International Conference on Advances in Applied Science & Environmental Engineering pp. 141-145. ASEE. <https://doi.org/10.15224/978-1-63248-004-0-93>
- Domszya J G & Roberts G A F (1985). Evaluation of infrared spectroscopic techniques for analyzing chitosan. *Die Makromolekulare Chemie* 186: 1671-1677. <https://doi.org/10.1002/macp.1985.021860815>
- El Knidri H, Belaabed R, El Khalifaouy R, Laajeb A, Addaou A & Lahsini A (2017). Physicochemical characterization of chitin and chitosan produced from *Parapenaeus longirostris* shrimp shell wastes. *Journal of Materials and Environmental Sciences* 8: 3648-3653
- Fatima B (2020). Quantitative Analysis by IR: Determination of Chitin/Chitosan DD. *Modern Spectroscopic Techniques and Applications* 107 p. <https://doi.org/10.5772/intechopen.89708>
- Fernández-Martín F, Arancibia M, López-Caballero E, Gómez-Guillén C, Montero P & Fernández-García M (2014). Preparation and molecular characterization of chitosans obtained from shrimp (*Litopenaeus vannamei*) shells. *Journal of Food Science* 79: E1722-E1731. <https://doi.org/10.1111/1750-3841.12572>
- Galed G, Diaz E, Goycoolea F M & Heras A (2008). Influence of N-deacetylation conditions on chitosan production from α -chitin. *Natural Product Communications* 3: 543-550. <https://doi.org/10.1177/1934578x0800300414>
- Hao G, Hu Y, Shi L, Chen J, Cui A, Weng W & Osako K (2021). Physicochemical characteristics of chitosan from swimming crab (*Portunus trituberculatus*) shells prepared by subcritical water pretreatment. *Scientific Reports* 11(1): 1-9. <https://doi.org/10.1038/s41598-021-81318-0>
- Hassan M A, Omer A M, Abbas E, Baset W M A & Tamer M T (2018). Preparation, physicochemical characterization and antimicrobial activities of novel two phenolic chitosan Schiff base derivatives. *Scientific Reports* 8: 11416. <https://doi.org/10.1038/s41598-018-29650-w>
- Hong P Z, Li S D, Ou C Y, Li C P, Yang L & Zhang C H (2007). Thermogravimetric analysis of chitosan. *Journal of applied polymer science* 105(2): 547-551
- Hossain M & Iqbal A (2014). Production and characterization of chitosan from shrimp waste. *Journal of the Bangladesh Agricultural University* 12: 153-160. <https://doi.org/10.3329/jbau.v12i1.21405>
- Ibitoye E B, Lokman I H, Hezme M N M, Goh Y M, Zuki A B Z & Jimoh A A (2018). Extraction and physicochemical characterization of chitin and chitosan isolated from house cricket. *Biomedical Materials (Bristol)* 13(2018): 025009. <https://doi.org/10.1088/1748-605X/aa9dde>
- Karsli B, Caglak E, Li D, Rubio N K, Janes M & Prinyawiwatkul W (2019). Inhibition of selected pathogens inoculated on the surface of catfish fillets by high molecular weight chitosan coating. *International Journal of Food Science and Technology* 54: 25-33. <https://doi.org/10.1111/ijfs.13897>
- Khan T A, Peh K K & Ch'ng H S (2002). Reporting degree of deacetylation values of chitosan: The influence of analytical methods. *Journal of Pharmacy and Pharmaceutical Sciences* 5: 205-212
- Knorr D (1982). Functional properties of chitin and chitosan. *Journal of Food Science* 47: 593-595. <https://doi.org/10.1111/j.1365-2621.1982.tb10131.x>
- Kong M, Chen X G, Xing K & Park H J (2010). Antimicrobial properties of chitosan and mode of action: A state of the art review. *International Journal of Food Microbiology* 144: 51-63. <https://doi.org/10.1016/j.ijfoodmicro.2010.09.012>
- Kucukgulmez A, Celik M, Yanar Y, Sen D, Polat H & Kadak A E (2011). Physicochemical characterization of chitosan extracted from *Metapenaeus stebbingi* shells. *Food Chemistry* 126: 1144-1148. <https://doi.org/10.1016/j.foodchem.2010.11.148>
- Kucukgulmez A, Kadak A E, Celik L, Farivar A & Celik M (2017). Comparison of the physicochemical properties of chitosan extracted from shrimp shell waste with different deacetylation degrees. *Feb-Fresenius Environmental Bulletin* 26: 7750-7755

- Kumari S, Annamareddy S H K, Abanti S & Rath P K (2017). Physicochemical properties and characterization of chitosan synthesized from fish scales, crab and shrimp shells. *International Journal of Biological Macromolecules* 104(B): 1697-1705. <https://doi.org/10.1016/j.ijbiomac.2017.04.119>
- Li Q, Dunn E T, Grandmaison E W & Goosen M F A (1992). Applications and properties of chitosan. *Journal of Bioactive and Compatible Polymers* 7: 370-397. <https://doi.org/10.1177/088391159200700406>
- Metin C, Alparslan Y, Baygar T & Baygar T (2019). Physicochemical, microstructural and thermal characterization of chitosan from blue crab shell waste and its bioactivity characteristics. *Journal of Polymers and the Environment* 27(11): 2552-2561. <https://doi.org/10.1007/s10924-019-01539-3>
- Mittal A, Singh A, Aluko R E & Benjakul S (2021). Pacific white shrimp (*Litopenaeus vannamei*) shell chitosan and the conjugate with epigallocatechin gallate: Antioxidative and antimicrobial activities. *Journal of Food Biochemistry* 45(1): e13569. <https://doi.org/10.1111/jfbc.13569>
- Mohanasrinivasan V, Mishra M, Paliwal J S, Singh S K, Selvarajan E, Suganthi V & Devi C S (2014). Studies on heavy metal removal efficiency and antibacterial activity of chitosan prepared from shrimp shell waste. *3 Biotech* 4(2): 167-175. <https://doi.org/10.1007/s13205-013-0140-6>
- Mourya V K & Inamdar N N (2008). Chitosan-modifications and applications: Opportunities galore. *Reactive and Functional Polymers* 68: 1013-1051. <https://doi.org/10.1016/j.reactfunctpolym.2008.03.002>
- Nessa F, Masum S M, Asaduzzaman M, Roy S, Hossain M & Jahan M (2011). A process for the preparation of chitin and chitosan from prawn shell waste. *Bangladesh Journal of Scientific and Industrial Research* 45: 323-330. <https://doi.org/10.3329/bjsir.v45i4.7330>
- Nirmal N P, Santivarangkna C, Rajput M S & Benjakul S (2020). Trends in shrimp processing waste utilization: An industrial prospective. *Trends in Food Science & Technology* 103: 20-35. <https://doi.org/10.1016/j.tifs.2020.07.001>
- No H K, Lee K S & Meyers S P (2000). Correlation between physicochemical characteristics and binding capacities of chitosan products. *Journal of Food Science* 65: 1134-1137. <https://doi.org/10.1111/j.1365-2621.2000.tb10252.x>
- No H K, Park N Y, Lee S H & Meyers S P (2002). Antibacterial activity of chitosans and chitosan oligomers with different molecular weights. *International Journal of Food Microbiology* 74: 65-72. [https://doi.org/10.1016/S0168-1605\(01\)00717-6](https://doi.org/10.1016/S0168-1605(01)00717-6)
- Paul S, Jayan A, Sasikumar C S & Cherian S M (2014). Extraction and purification of chitosan from chitin isolated from sea prawn (*Fenneropenaeus indicus*). *Asian Journal of Pharmaceutical and Clinical Research* 7: 201-204
- Puvvada Y, Vankayalapati S & Sukhavasi S (2012). Extraction of chitin from chitosan from exoskeleton of shrimp for application in the pharmaceutical industry. *International Current Pharmaceutical Journal* 1: 258-263. <https://doi.org/10.3329/icpj.v1i9.11616>
- Rinaudo M (2006). Chitin and chitosan: Properties and applications. *Progress in Polymer Science* 31: 603-632. <https://doi.org/10.1016/j.progpolymsci.2006.06.001>
- Rout S K (2001). Physicochemical, functional and spectroscopic analysis of crawfish chitin and chitosan as affected by process modification. LSU Historical Dissertations and Theses. Louisiana State University, Baton Rouge, LA, USA. https://digitalcommons.lsu.edu/gradschool_disstheses/432
- Samar M M, El-Kalyoubi M H, Khalaf M M & Abd El-Razik M M (2013). Physicochemical, functional, antioxidant and antibacterial properties of chitosan extracted from shrimp wastes by microwave technique. *Annals of Agricultural Sciences* 58: 33-41. <https://doi.org/10.1016/j.aas.2013.01.006>
- Sedaghat F, Yousefzadi M, Toiserkani H & Najafipour S (2017). Bioconversion of shrimp waste *Penaeus merguensis* using lactic acid fermentation: An alternative procedure for chemical extraction of chitin and chitosan. *International Journal of Biological Macromolecules* 104: 883-888. <https://doi.org/10.1016/j.ijbiomac.2017.06.099>
- Seo S, King J M & Prinyawiwatkul W (2007). Simultaneous depolymerization and decolorization of chitosan by ozone treatment. *Journal of Food Science* 72: 522-526. <https://doi.org/10.1111/j.1750-3841.2007.00563.x>
- Sudatta B P, Sugumar V, Varma R & Nigariga P (2020). Extraction, characterization and antimicrobial activity of chitosan from pen shell, *Pinna bicolor*. *International Journal of Biological Macromolecules* 163: 423-430. <https://doi.org/10.1016/j.ijbiomac.2020.06.291>
- Tokatlı K & Demirdöven A (2018). Optimization of chitin and chitosan production from shrimp wastes and characterization. *Journal of Food Processing and Preservation* 42(2): e13494.
- Trung T S, Thein-Han W W, Qui N T, Ng C H & Stevens W F (2006). Functional characteristics of shrimp chitosan and its membranes as affected by the degree of deacetylation. *Bioresource Technology* 97: 659-663. <https://doi.org/10.1016/j.biortech.2005.03.023>
- Trung T S, Tram L H, Van N V, Hoa N V, Minh N C, Loc P T & Stevens W F (2020). Improved method for production of chitin and chitosan from shrimp shells. *Carbohydrate Research* 489, 107913. <https://doi.org/10.1016/j.carres.2020.107913>
- TUIK (2020). Turkish Statistical Institute, Quantity of caught other sea fish (crustaceans, molluscs) in Turkey. <http://www.tuik.gov.tr/Start.do>, 2020 (accessed 28 July 2020) (In Turkish)
- Vallejo-Domínguez D, Rubio-Rosas E, Aguila-Almanza E, Hernández-Cocoletzi H, Ramos-Cassellis M E, Luna-Guevara M L & Show P L (2021). Ultrasound in the deproteinization process for chitin and chitosan production. *Ultrasonics Sonochemistry*, 72, 105417. <https://doi.org/10.1016/j.ultsonch.2020.105417>
- Varun T K, Senani S, Jayapal N, Chikkerur J, Roy S, Tekulapally V B & Kumar N (2017). Extraction of chitosan and its oligomers from shrimp shell waste, their characterization and antimicrobial effect. *Veterinary World* 10: 170-175. <https://doi.org/10.14202/vetworld.2017.170-175>
- Yen M T, Yang J H & Mau J L (2009). Physicochemical characterization of chitin and chitosan from crab shells. *Carbohydrate Polymers* 75: 15-21. <https://doi.org/10.1016/j.carbpol.2008.06.006>





Carbon Storage Potential and its Distributions in the Particle Size Fractions in Harran Plain, Turkey

İbrahim Halil YANARDAĞ^{a*} , Asuman BÜYÜKKILIÇ YANARDAĞ^a , Ahmet R. MERMUT^{b,c} ,
Ángel FAZ CANO^d 

^aSoil Science and Plant Nutrition Department, Agriculture Faculty, Malatya Turgut Özal University, Battalgazi, Malatya, TURKEY

^bSoil Science Department, Agriculture Faculty, Harran University, Şanlıurfa, TURKEY

^cDepartment of Soil Science, University of Saskatchewan, Saskatoon, Saskatchewan, CANADA

^dSustainable Use, Management, and Reclamation of Soil and Water Research Group, Agrarian Science and Technology Department, Technical University of Cartagena, Cartagena, Murcia, SPAIN

ARTICLE INFO

Research Article

Corresponding Author: İbrahim Halil YANARDAĞ, E-mail: ibrahim.yanardag@ozal.edu.tr

Received: 1 April 2021 / Revised: 8 October 2021 / Accepted: 9 October 2021 / Online: 01 September 2022

Cite this article

YANARDAĞ İ H, BÜYÜKKILIÇ YANARDAĞ A, MERMUT A R, FAZ CANO A (2022). Carbon Storage Potential and its Distributions in the Particle Size Fractions in Harran Plain, Turkey. *Journal of Agricultural Sciences (Tarim Bilimleri Dergisi)*, 28(3):501-510. DOI: 10.15832/ankutbd.907173

ABSTRACT

In recent years, there has been increasing international interest in increasing and sustainably managing soil C stocks to contribute to combating climate change and support food security. In this context, determining the C storage capacity of soils and examining the distribution of soil C based on fractions is of great importance for a better understanding of C dynamics. The present study investigated the storage potential of soil organic carbon (SOC), inorganic carbon (SIC) and total carbon (TC) in 16 selected profiles, and SOC and SIC distribution in five different particle size fractions (2000-425µm, 425-150 µm, 150-106 µm, 106-75 µm, <75 µm) of the Harran plain in Turkey. The results revealed

that the particle size distribution in the surface layer varied in the following order depending on soil weight: 850-250 > 2000-850 > 250-150 > 150-75 > 75 µm. The organic C content of the soils is low due to the semi-arid climate conditions. Fraction-based soil SOC distribution was in the following order: 11% at 2000-850 µm, 15% at 850-250 µm, 21% at 250-150 µm, 23% at 150-75 µm and <75 µm 30%. Organic matter fractions differed according to the particle size distribution and the applicable soil management system. Stable organic matter content was significantly related to clay content and greatly influenced by the type of soil management used.

Keywords: Soil organic carbon, Soil inorganic carbon, Carbon storage, Particle size, Harran plain

1. Introduction

Soil carbon (C) is the largest terrestrial carbon reserve and contains about 1.5 Eg (ie 1.5×10^{18} g) of carbon, of which 0.68 Eg is organic carbon (Zhang et al. 2020). Soil organic matter (SOM) positively affects the physical, chemical and biological properties of the soil (Sakin & Yanardağ 2019). It is also one of the most important components in the soil due to its capacity to affect plant growth and yield (Bongiovanni & Labartini 2006). In C stabilization processes, the structure of organic compounds in SOM, their true resistance to weathering and their interactions with the soil mineral fraction are closely related (Marinari et al. 2010). The new origin of SOM is closely related to biological activity in the soil, while new and middle-aged organic matter can contribute to the improvement of the physical structure of the soil (Wander 2004). However, different soil types may also react differently to the stabilization and sequestration of C (Yanardağ et al. 2015).

Measuring the potential of agricultural soils to soil organic carbon (SOC) dynamics will help evaluate the contribution of cultivated soils to the global C balance as a carbon source or sink. However, there are many uncertainties about the impact of SOC dynamics on the soil system (Mermut et al. 2000; Li 2002), and the ultimate potential for C stabilization in soils is unknown (Smith 2004). The quality of SOM depends on its distribution between unstable and stable organic components. Stable organic compounds in the soil include humus materials and other macromolecules or are physically preserved by their adsorption on mineral surfaces or bound in aggregates (Tobiasova et al. 2012). One of the key elements to reliably evaluate SOM dynamics is the experimental identification of SOM pools associated with stabilization mechanisms (Abdul Kader 2006).

Soil organic matter can be analyzed based on different fractions and basic information about the processes and products of soil formation can be provided by soil particle size distributions (Gunal et al. 2011). Interactions of physical, chemical and biological processes in the soil affect aggregate formation and stabilization (Kocyyigit & Demirci 2010). These materials with a

particle size of $<2 \mu\text{m}$, mostly silt and clay, have slow cycle times and stabilize in the primary organo-mineral structure by interacting mainly with minerals (Chenu & Plante 2006). Here, the clay-sized OM usually accounts for more than 50% of the SOM, and the sum of clay and silt ($<20 \mu\text{m}$) can be over 90% (Christensen 1996). In addition, changes in organic matter levels caused by land use can be better understood by determining the distribution of fractions (Figueiredo et al. 2010). Dalal & Mayer (1986) reported that the change of some soil properties depends on which fractions of SOM are accumulated rather than the total amount of SOM.

The objectives of this study are (1) to determine the soil organic carbon, inorganic carbon, and total carbon storage potential of the Harran plain in 16 selected profiles, and (2) to determine the SOC and SIC distribution in five different particle size fractions (2000-425 μm , 425-150 μm , 150-106 μm , 106-75 μm , $<75 \mu\text{m}$).

2. Material and Methods

2.1. Description of the study area

Harran Plain is located in the south-eastern part of Şanlıurfa province, Turkey, which is in the center of Turkey's major irrigation and development project (Southeastern Anatolian Project, GAP). It lies between the longitudes of $38^{\circ}39'$ - $39^{\circ}30'$ E and the latitudes of $36^{\circ}43'$ - $37^{\circ}11'$ N and spans an area of 225 000 ha.

The elevation ranges between 350 and 450 m a.s.l. and it increases from the south to the north. The plain has a semi-arid climate with limited precipitation between June and September. The long-term mean annual temperature is about 18°C , the highest annual mean temperature is 31.4°C in July, and the lowest annual mean temperature is 5.8°C in January. The annual mean relative humidity and precipitation are 57% and 284.2 mm, relatively (Yesilnacar & Güllüoğlu 2007). The dominant crops in the area are cotton, corn, and wheat.

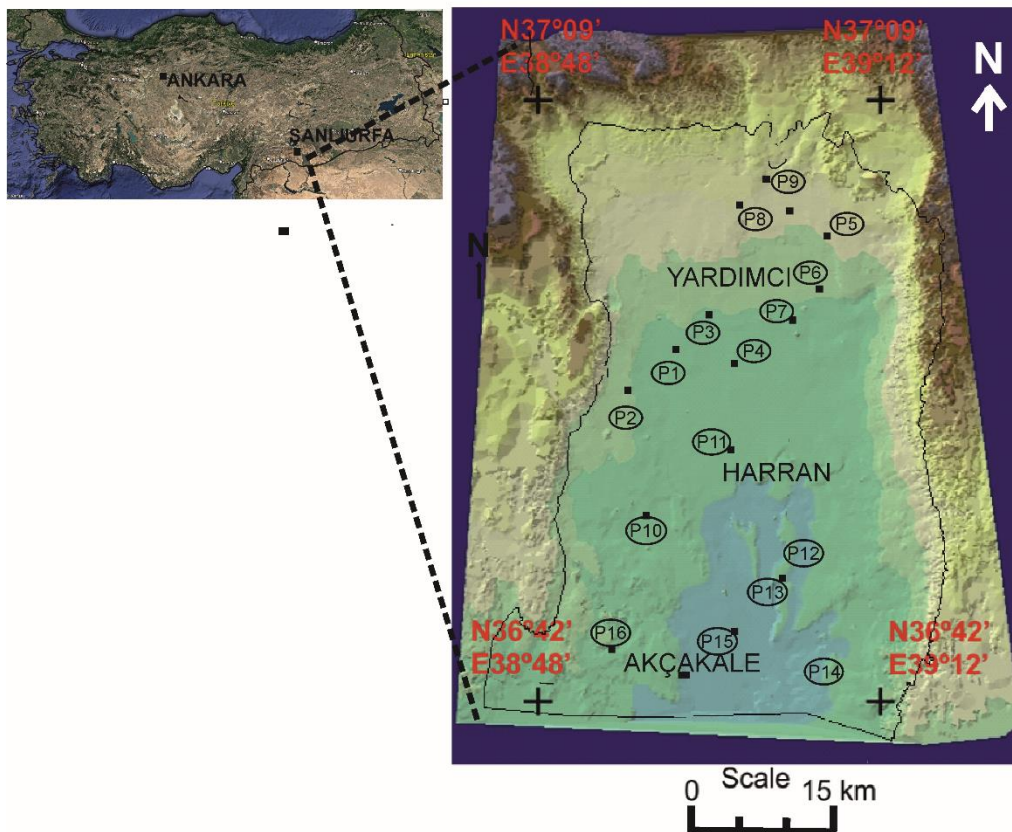


Figure 1- Distribution of 16 selected soil profiles in the studied area

Soil samples were taken from 16 series of genetic horizons in 3 replications in wheat fields in Harran Plain. In the study, soil profiles differ between 1.4 m and 3.6 m were dug up until reaching the main material. The distribution of 16 selected soil profiles (P) in the studied area is presented in Figure 1. The soil locations and taxonomies are Kısas 1 (P1) ($36^{\circ}58'00.3''\text{N}$, $38^{\circ}55'42.3''\text{E}$); Typic Torrert, Çekçek (P2) ($36^{\circ}56'49.9''\text{N}$, $38^{\circ}54'05.8''\text{E}$); Typic Torrifluent, Harran 1 (P3) ($37^{\circ}00'00.62''\text{N}$, $38^{\circ}58'57.3''\text{E}$); Vertic Camborthid, Kısas 2 (P4) ($36^{\circ}58'05.6''\text{N}$, $39^{\circ}01'09.5''\text{E}$); Typic Torrert, Bellitaş (P5) ($37^{\circ}01'09.6''\text{N}$, $39^{\circ}09'13.2''\text{E}$); Typic Torrifluent, Gürgelen 1 (P6) ($37^{\circ}00'0.504''\text{N}$, $39^{\circ}09'0.632''\text{E}$); Typic Calciorthid, İkizce (P7) ($37^{\circ}01'0.501''\text{N}$, $39^{\circ}07'0.299''\text{E}$); Vertic Torrifluent, Sırrın (P8) ($37^{\circ}05'0.461''\text{N}$, $39^{\circ}02'0.144''\text{E}$); Vertic Camborthid, İrice (P9) ($37^{\circ}06'0.062''\text{N}$,

39°03'0.766"E); Typic Calciorthid, Beğdeş (P10) (36°50'0.491"N, 38°54'0.169"E); Typic Torrert, Harran 2 (P11) (36°53'0.034"N, 38°57'0.567"E); Vertic Camborthid, Gürgelen 2 (P12) (36°47'0.136"N, 39°05'0.258"E); Typic Calciorthid, Akören (P13) (36°46'0.353"N, 39°04'0.529"E); Typic Calciorthid, Ekinyazı (P14) (36°43'0.374"N, 39°06'0.811"E); Typic Calciorthid, Akçakale (P15) (36°45'0.370"N, 39°58'0.538"E); Typic Torrert, Gürgelen 3 (P16) (36°44'0.370"N, 38°52'0.343"E); Typic Calciorthid. The soils of the plain are clayey with a slightly alkaline pH (pH_{H2O} 7.5–8.0). The minimum permeability values of the soils are between 0.22 and 3.51 m day⁻¹ (GDSHW 2003). The majority of soils in the plain are classified as Vertisol according to Soil Survey Staff (2006). The dominant silicate clay minerals are smectite, and palygorskite, however, illite and kaolinite are also found in the mixture. The soils are generally well developed with ABC horizons and although lime content is high, soil organic matter is usually around 1.0% (GDSHW 2003).

The selected physical-chemical soil characteristics were given in Table I. The soil textures were generally clayey and the amount of clay tended to increase towards the center of the study region. The southern sample sites had higher salinity (15.62 dS m⁻¹). Due to excessive and uncontrolled irrigation and fertilization, in addition to poor natural drainage, soil salinity was very high. The soils were alkaline and the pH was ranged between 7.37 and 8.40 (Table 1).

The studied area had high carbonate contents (mean 26.60%). The organic matter concentrations were between 0.87 and 2.12%. The studied area had high amount of clay, which were ranged between 30 and 60%. The dominant silicate clay minerals were smectite therefore, cation exchange capacities were high and ranged between 28.61 and 48.12 cmol⁺ kg⁻¹. The bulk density of 16 studied soil profiles was changed between 1.25 and 1.35 g cm⁻³ (Table I).

Table 1- Selected physical-chemical characteristics of the soil study

SP*	pH	EC dS m ⁻¹	OM %	CaCO ₃ %	CEC cmol ⁺ kg ⁻¹	BD g cm ⁻³
Mean	7.98	2.42	1.41	26.60	38.08	1.31
Std Dev	0.34	4.25	0.37	5.75	5.23	0.03
Min	7.37	0.48	0.87	14.81	28.61	1.25
Max	8.40	15.62	2.12	37.02	48.12	1.35
SP*	Sand %	Silt %	Clay %	Mg ⁺⁺ mg kg ⁻¹	K ⁺ mg kg ⁻¹	Na ⁺ mg kg ⁻¹
Mean	17.06	34.25	48.44	170.8	449.7	480.7
Std Dev	7.08	4.52	7.63	45.2	78.2	151.8
Min	5.00	24.00	30.00	100.1	328.5	303.6
Max	31.00	39.00	60.00	234.3	664.7	943.0

* **Statistical Properties of Level** EC: Electric conductivity, **CaCO₃**: Lime Content, **OM**: Organic Matter, **CEC**: Cation Exchange Capacity, **BD**: Bulk Density

2.2. Soil sampling and analysis

Soil samples were taken from 16 selected profiles to determine soil characteristics and especially carbon contents. The samples were air-dried, sieved to pass a 2-mm mesh, and stored in plastic bags for analysis of selected physical and chemical soil properties. Soil samples for particle size analysis were taken from each of the surface soils (0-20 cm).

The following soil analysis was carried out: pH measured in a 1:1 water soil ratio mixture according to Peech's method (1965); soluble salts according to Bower & Wilcox (1965) method; CaCO₃ by the Bernard calcimeter method (Vatan 1967); organic carbon according to Duchaufour (1970), cation exchange capacity (CEC) following the method of Chapman (1965). SOC, SIC, and TC in 16 profiles and each particle size fractions were measured by TOC analyzer (TOC – V-CSH Shimadzu (Kyoto-Japan)).

Particle size analysis was carried out by using the FAO-ISRIC system (1990) after the combination of the pipette Robinson and sieving. The fraction of bulk soils into five particle size fractions was conducted using sieves with the following sizes: 2000, 425, 150, 106, and 75 µm. These fractions were studied in the 20 cm surface soil from the studied area. For the quantification of soil organic carbon in each fraction, a subset of each particle size fraction was ground and determined according to Duchaufour (1970).

2.3. Statistical methods

For the statistical analysis, multiple linear tests were performed using analysis of variance (ANOVA) to determine whether there are any statistically significant differences between the means of the independent groups. Relationships among properties were studied using Pearson correlations. Soil chemical properties related to carbon content and pools were subjected to principal components analysis (PCA) to elucidate major variation patterns in terms of C pools. All statistical tests were performed with SPSS V26.0 and differences were considered significant when P<0.05.

3. Results and Discussion

3.1. Organic, Inorganic, and Total carbon storage of the soils

Storage of carbon (OC, IC, and TC) in the studied soil profiles were given in Figure 2. The total amount of SOC within soil profiles varied significantly among the selected areas ($P < 0.05$). The SOC concentration were 7.60 g kg^{-1} in P1, 7.96 g kg^{-1} in P2, 11.55 g kg^{-1} in P3, 10.84 g kg^{-1} in P4, 8.31 g kg^{-1} in P5, 13.94 g kg^{-1} in P6, 9.22 g kg^{-1} in P7, 12.81 g kg^{-1} in P8, 12.39 g kg^{-1} in P9, 9.65 g kg^{-1} in P10, 8.45 g kg^{-1} in P11, 6.76 g kg^{-1} in P12, 9.93 g kg^{-1} in P13, 14.93 g kg^{-1} in P14, 6.13 g kg^{-1} in P15, and 7.89 g kg^{-1} in P16, respectively. The SOC contents were low due to low precipitation and high temperature. Microbial activity in soil is highly affected by soil moisture and soil temperature, which has played an important role in CO_2 emissions and 65-85% of this emission is due to the soil temperature (Büyükkılıç Yanardağ et al. 2004). In addition, the CO_2 emission of the soils is very effective on the SOC and TN reserves. Furthermore, researchers indicated that the variability of soil C depends on soil texture, climate, vegetation, and land use and management, as well as differences in species and plant density (Yoo et al. 2006). Hontoria et al. (1999) stated that 45% of the variability in SOC in the Spanish peninsula can be explained by the annual precipitation, annual average temperature, and altitude parameters. In addition to the climate, the clay content and type of the soil in the region also affected the organic matter content. Also, the oxidation of organic matter was faster due to the calcareous soil character (Homann et al. 1995). It means that the presence of CaCO_3 in the soil might also contribute to the stabilization of poorly crystallized Fe forms; this will contribute to SOC retention, likely regarding triple Fe-Ca-SOC complexes (Sowers et al. 2018).

The highest SOC content was found in P14 while, lowest in P15. The elevation and climate conditions of these soils were approximately similar, whereas SOC ratios were varied due to different soil management practices. Soil conditions in turn were most influenced especially in our region by the temperature and soil moisture regimes, although the mineralogical and biological regimes were also important (Buringh 1984).

The inorganic C concentration of the soils ranged; 3.93 in P1, 3.51 in P2, 2.57 in P3, 4.44 in P4, 4.02 in P5, 3.04 in P6, 3.27 in P7, 3.41 in P8, 2.81 in P9, 2.99 in P10, 3.09 in P11, 2.76 in P12, 2.95 in P13, 2.43 in P14, 1.78 in P16, and 4.07% in P16, respectively. The plain soil had a high carbonate ratio, also pedogenic carbonate was predominant due to alkaline soils features. Khademi & Mermut (1998) stated that if there is sufficient calcium in the soil solution, that is when the pH range is between 7.3 and 8.5, secondary carbonate accumulations start, and calcite is formed in the soil. Therefore, the inorganic carbon concentration of the soils was high.

The vertical distribution of SOC, SIC, TC are given in Figure 2. The results showed that SOC concentrations were decreased with increasing soil depth. However, SOC levels were distributed along with the whole soil profile. Batjes (1996) observed that the highest SOC concentration was accumulated in upper soil layers, but a large amount was also stored between 1 and 2-m depth. Furthermore, the storage of OC in soil depended on the balance between the addition of organic material (freshly dead plants and animal waste) mixing into the soil and losses of C through decomposition (Sollins et al. 1996). The degradation or decomposition of the organic matter here depends on its chemical composition and physical relationship with other soil components (Rovira et al. 2008).

Inorganic C concentration of the selected soils was high and increased with soil depth. Primary carbonates dissolve under arid to semi-humid climatic conditions and combine with the CO_2 present in the soil solution and recrystallize and a significant amount of pedogenic (secondary) carbonates accumulate in the soil. In these soil horizons, carbonate accumulation is generally observed depending on the characteristics of the parent material and climatic conditions (Gocke et al. 2012).

3.2. Soil particle sizes distribution

The distribution of particle size fractions in the surface soil from study areas was given in Figure 3. The soil fraction distribution in the size of 2000-850 μm varied between 15.3% and 42.3%, in the size of 850-250 μm varied between 34.6% and 51.5%, in the size of 250-150 μm varied between 8.8 and 17.2%, in the size of 150-75 μm varied between 7.2 and 17.7%, and $<75 \mu\text{m}$ in size varied between 1.8 and 13.0%. The results showed that the dominant size fractions were the largest (850-250 and 850-2000 μm). Although the Harran Plain is Tethys Sea of sedimentary origin (Şengör et al. 1988), it can be easily observed that different land use has affected the soil particle size. Different soil management systems including cultivation and irrigation can modify soil particle distribution throughout the soil profile (Jaiyeoba 2003).

The high content of smectite in the soils and especially the transformation of palygorskite into this mineral enabled the plain soils to enrich with smectite. Soils dense as smectite are saturated with Ca^{++} ions (Seyrek et al. 2005). When we evaluated the clay results (between 30 and 60%), we thought that the reason for having the lowest percentage in $<75 \mu\text{m}$ would be that the high Ca^{++} ions in the soil bind the clay particles tightly together.

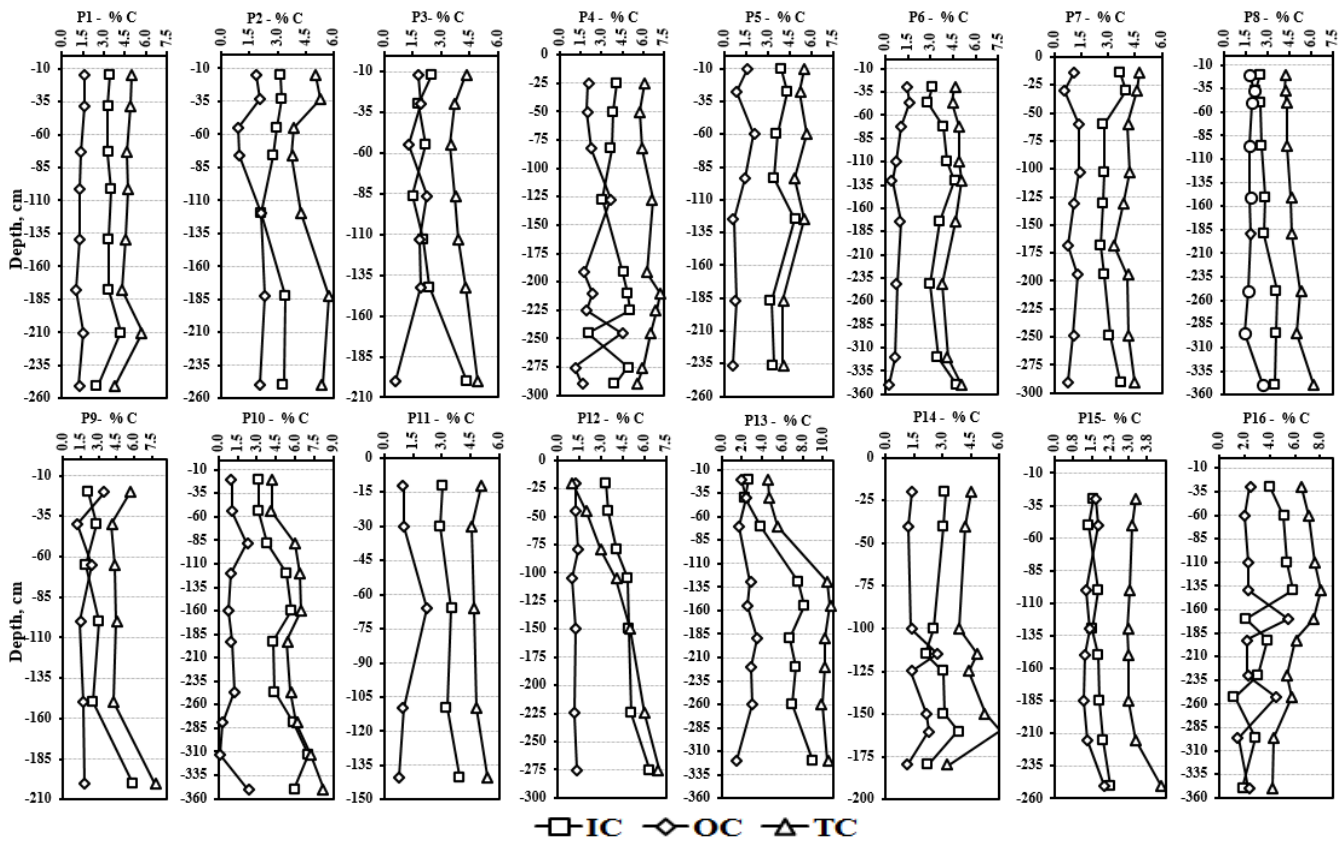


Figure 2- Carbon percentage concentration in 16 profiles (IC: Inorganic Carbon; OC: Organic Carbon; TC: Total Carbon, n=3)

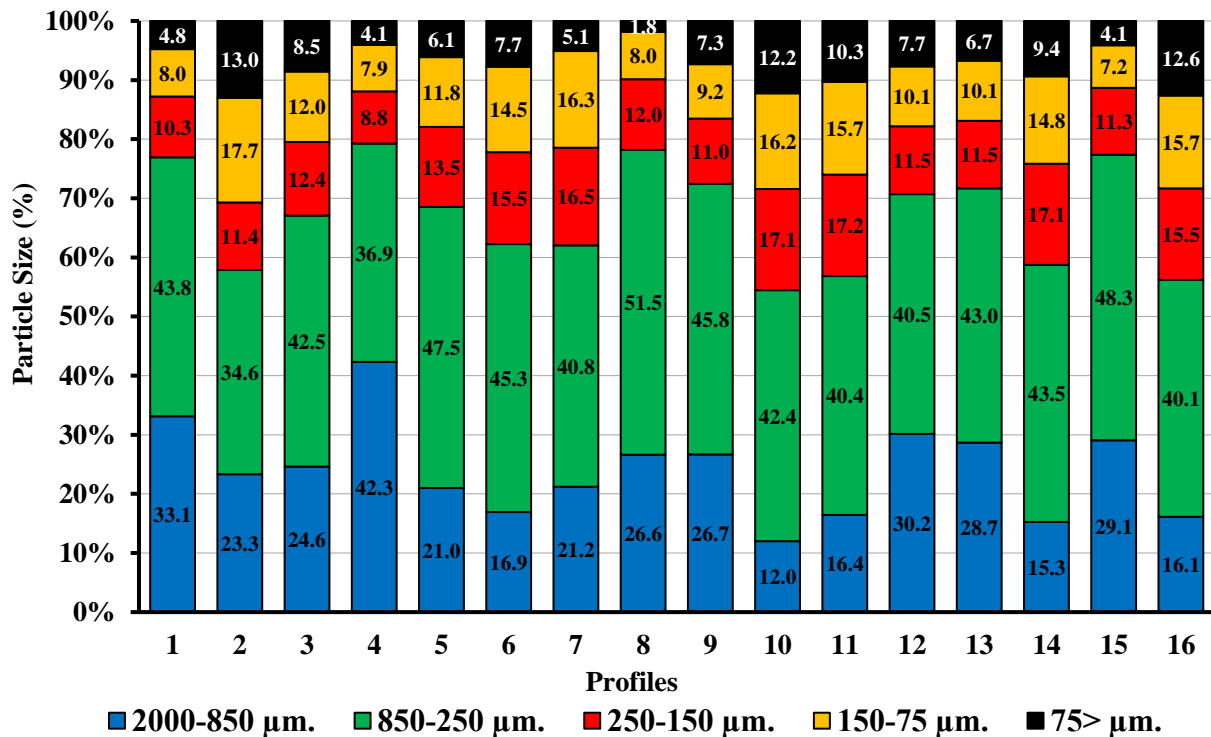


Figure 3- Distribution of particle size fractions in surface soil horizon

3.3. Soil organic and inorganic carbon distribution in the different particle sizes

Stable organic matter content at a particle size of <50 μm was significantly related to clay content, while coarse organic matter with a size of >100 μm was greatly affected by soil management systems (Quiroga et al. 1996). Distributions of SOC content in

five particle size fractions in the surface horizon were given in Figure 4. Soil organic C content was increased with small size fractions. The highest SOC accumulation was observed between 250-150 μm fractions.

Accoe et al. (2002) reported that SOC concentration was largest in small size fraction in a sandy loam textured soil. Carter et al. (2003) found that clay plus silt content (lower than 40%) consisted of 60% of total organic carbon in 15 different sandy loam to heavy clay textured soil. Zhang et al. (2006) reported that the highest organic carbon accumulated in the clay size fraction in silty textured soil in Loess Plateau, Gansu- China. Chenu et al. (2000) found a significant relationship between organic matter and particle size fractions in varied humic loamy soils. Chen & Chiu (2003), found a similar relationship in subalpine areas in central Taiwan. Contrarily, some researchers examined that the SOM level could reflect the intensity of soil use (Puget et al. 1995; Schulten et al. 1993).

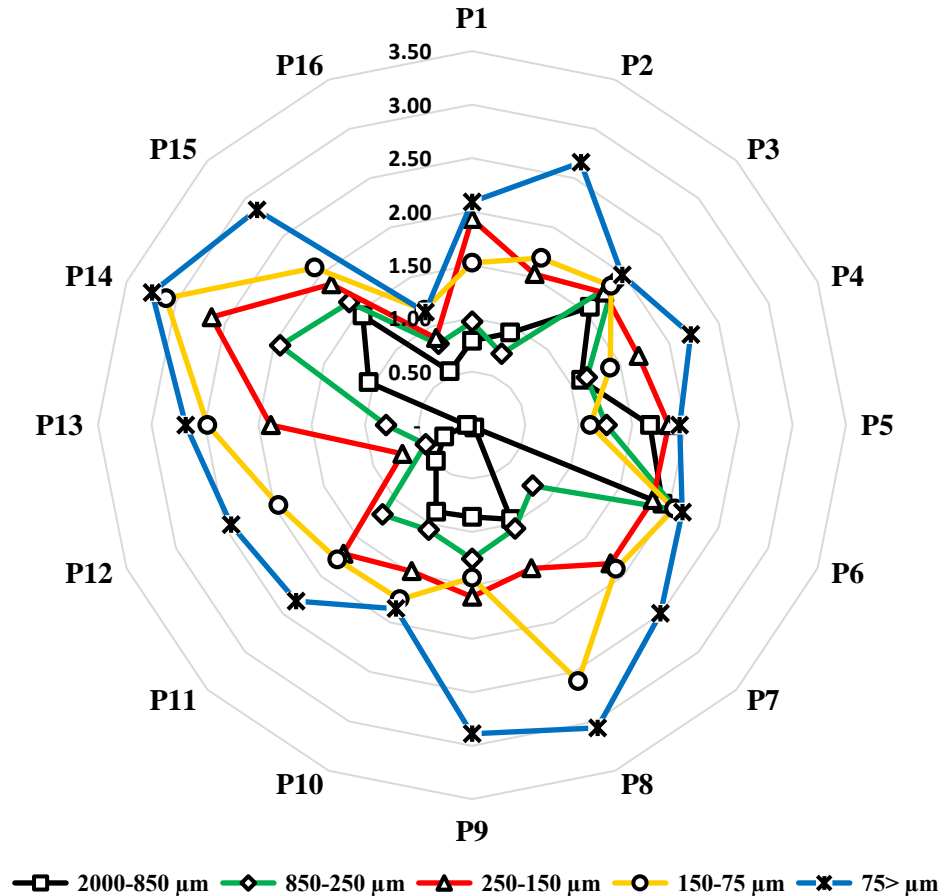


Figure 4- Distribution of soil organic carbon (% SOC) in the five particle size fractions analyzed in the surface soil samples

In general, the quantity and nature of the clay affected the amount of C stabilized in the soil. Clay size fraction contributed most of the organic matter both for organic carbon and for nitrogen, with considerably smaller contributions from a silt- and sand-sized fraction (Schmidt & Kögel-Knabber 2002). The clay content of the soil is one of the most important factors affecting SOC accumulation. If the clay content is high, it may have higher SOC under similar climatic conditions and land use compared to soils with low clay content. Also, here the climate factor is the main determinant of the decomposition rate and time of C in the soil, thus directly influencing the amount of SOC (Milne 2008).

The SIC ranged between 1.29% (in P11) and 6.49% (in P16) in the particle sizes of 850-2000 μm , ranged between 0.48% (in P6) and 5.12% (in P16) in the particle sizes of 250-850 μm , ranged between 0.71% (in P12) and 4.90% (in P4) in the particle sizes of 150-250 μm , ranged between 0.31% (in P10) and 5.39% (in P4) in the particle sizes of 75-150 μm , and ranged between 0.07% (in P10) and 4.62% (P1) in the particle sizes of <75 μm , respectively (Figure 5). Contrary to the SOC, the SIC results were more recent and there were no major differences between the results. It can be said here that SIC is more stable than SOC and is more resistant to weathering. Also, Dong et al. (2017) reported that carbonates have different stabilities in different particle fractions, and this stability is more intense in clay than in sand and silt (Loeppert & Suarez 1996).

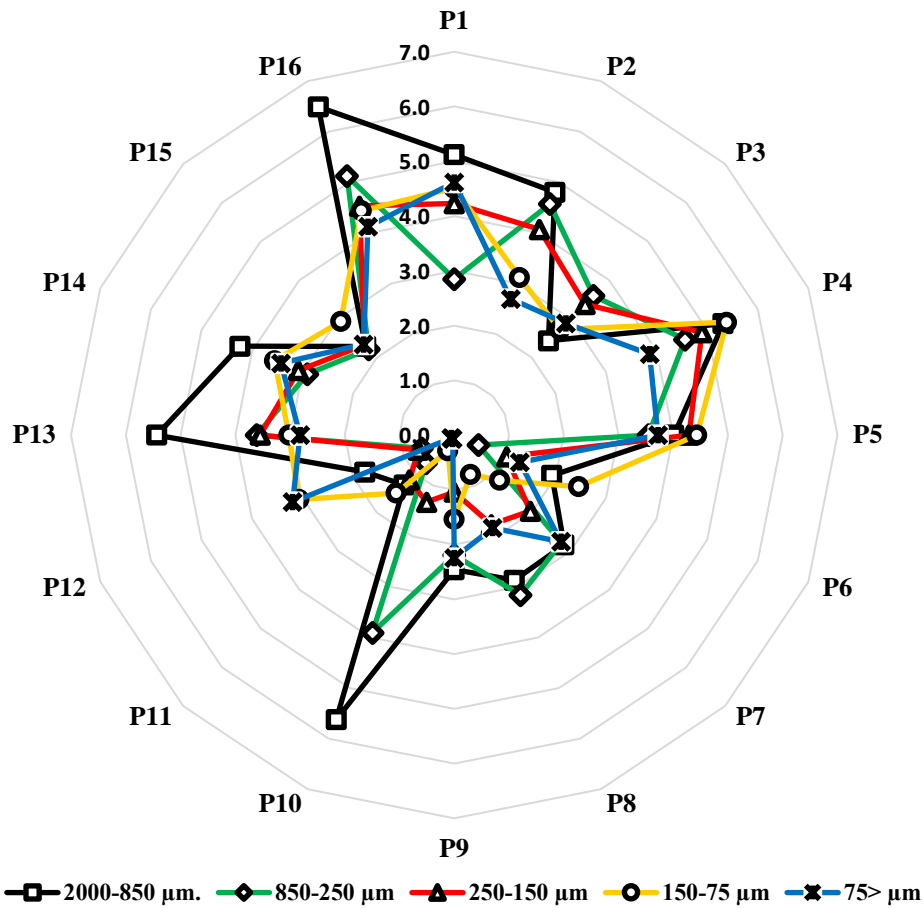


Figure 5- Distribution of soil inorganic carbon (% SIC) in five particle size fractions of the surface soils

As a result of the correlation analysis between SOC and SIC in the 5 different particles fractions analysed on the 16 soil profiles, it was observed that these two parameters did not have a statistically significant relationship with each other ($p > 0.05$) (Table 2). Dong et al. (2017) found a strong positive correlation between the SOC stock and SIC stock in selected 25 sites (3 in desert land, 9 in shrubland, and 13 in cropland) in soil from the semi-arid region in Yanqi Basin, China. With the breakdown of organic matter, there is an increase in the amount of CO_2 in the environment, where CO_2 combines with H_2O to form HCO_3^- and in the next phase, HCO_3^- combines with Ca^{++} ions found in large calcareous soils to form CaCO_3 (Wang et al. 2015). Therefore, a positive relationship is expected between SOC and SIC. However, if the organic matter of these soils is very limited, this relationship is likely not to be significant.

Table 2- The correlation analysis between SOC and SIC in the 5 different soil particles fractions in 16 soil profiles

		SIC				SOC				
Particle size		850-250 μm	250-150 μm	150-75 μm	<75 μm	2000-850 μm	850-250 μm	250-150 μm	150-75 μm	<75 μm
SIC	2000-850 μm	0.836**	0.718**	0.441	0.429	-0.179	-0.319	-0.013	-0.215	-0.385
	850-250 μm		0.778**	0.341	0.419	-0.039	-0.238	-0.031	-0.260	-0.298
	250-150 μm			0.796**	0.734**	0.109	-0.087	0.175	-0.314	-0.323
	150-75 μm				0.822**	0.197	0.006	0.062	-0.330	-0.303
	<75 μm					-0.038	-0.175	0.020	-0.217	-0.142
SOC	2000-850 μm						0.771**	0.304	-0.101	-0.082
	850-250 μm							0.632**	0.301	0.143
	250-150 μm								0.450	0.456
	150-75 μm									0.714**

** , Significant at $P < 0.01$.

In addition, a similarity was observed in the relationship between SIC and SOC fraction distributions. Accordingly, when the fractions were close to each other, the significance increased, and no relationship was observed between the largest and smallest fractions. It can be said that this result is expected. Because it is quite common for particle sizes to show similar distribution between fractions.

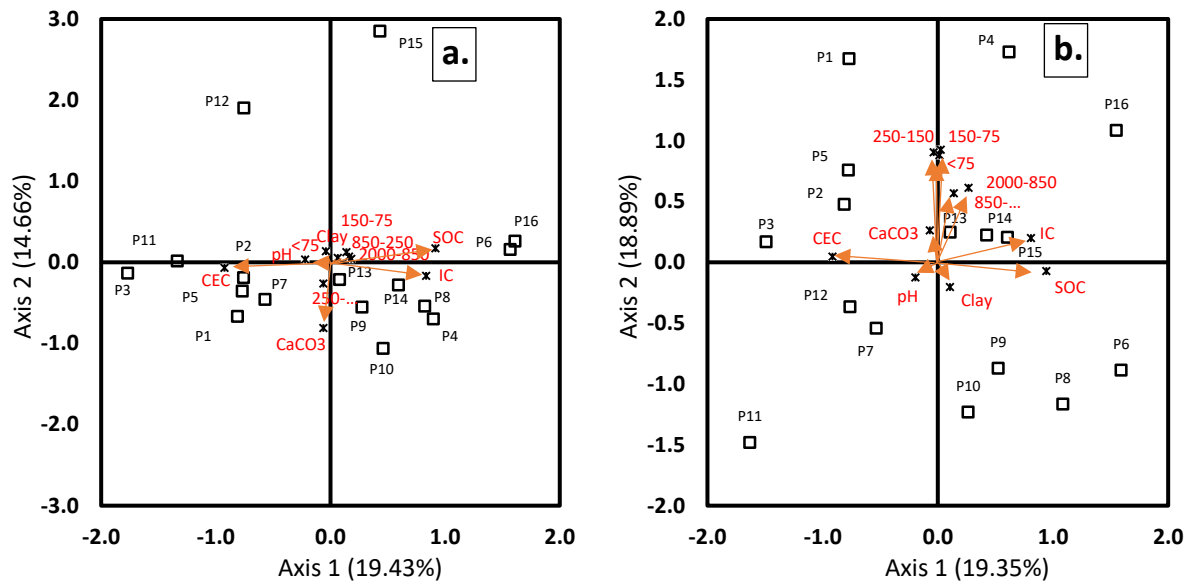


Figure 6- Biplot of principal component analysis (PCA) performed with SOC fractions (a) SIC fractions (b) and soil properties in 16 surface soil layers

The results of PCA analysis showed a distribution of 19.43% on axis 1 and 14.66% on axis 2 between SOC fractions and some soil properties in 16 profiles (Figure 6). In Axis 1, SOC, IC, fraction 2000-850 μm and fraction 850-250 μm showed a positive distribution, whereas pH and CEC showed a negative distribution. In Axis 2, the 250-150 μm fraction and CaCO_3 showed a negative distribution, no remarkable distribution was observed in other parameters. According to the PCA analysis results, it showed a distribution of 19.35% on axis 1 and 18.89% on axis 2 between inorganic C fractions and some soil properties in 16 profiles. Similar to the SOC fraction in Axis 1, SOC, IC, fraction 2000-850 μm and fraction 850-250 μm showed a positive distribution, whereas pH and CEC showed a negative distribution. In Axis 2, all IC fractions, IC, and CaCO_3 showed a positive distribution, a slightly negative distribution was observed for pH, SOC, and Clay.

4. Conclusions

Semi-arid climate conditions affected organic matter with the high temperature and deficiency of organic material affected the accumulation of organic carbon in the soil. Despite the high clay content of the soil, usually low organic matter and high lime contents depended on the structure was not developed well. Particle-size distribution of soils was very important to understand their properties especially in terms of soil classification. Also, the features of clay minerals were another important factor for the distribution of particle sizes. In addition to soil, cultivation was of other importance for the accumulation of organic matter. The particle size distribution of surface soil samples was founded 850-250 > 2000-850 > 250-150 > 150-75 > 75 μm , respectively. Distribution of SOC in particle size fractions were respectively 11% in 2000-850 μm , 15% in 850-250 μm , 21% in 250-150 μm , 23% in 150-75 μm and 30% in <75 μm . The particle size distribution influenced the quantity as well as the quality of soil organic matter. The high quantity of SOC accumulated in the below of 75 μm fraction and it was concluded that the most important fraction in storing SOC was clay, followed by silt. When the vertical distribution of SOC accumulation was evaluated, it was found that SOC did not differ significantly between soil depths in any of the 16 evaluated soils, but increased strongly in the surface soil layer due to root density. However, IC distribution among soil layers varied, possibly due to different land uses. This study demonstrated that there was an inverse relation between SOC and particle size in Vertisol soils. Organic matter fractions differed according to particle size distribution and the prevailing soil management system. Stable organic matter content was significantly related to clay content and was strongly influenced by the type of soil management utilized.

References

- Accoe F, Boeckx P, Van Cleemput O, Hofman, G X, Hui H Bin & Guanxiong C (2002). Characterization of soil Organic Matter Fraction from Grassland and Cultivated Soils via C Content and $\delta^{13}\text{C}$ Signature. *Rapid Commun Mass Spectrom* 16: 2157-2164. <https://doi.org/10.1002/rcm.827>
- Batjes N H (1996). Total carbon and nitrogen in the soils of the world. *European Journal of Soil Science* 47: 151-163. <https://doi.org/10.1111/j.1365-2389.1996.tb01386.x>

- Bongiovanni M D & Labartini J C (2006). Particulate organic matter, carbohydrate, humic acid contents in soil macro- and microaggregates as affected by cultivation. *Geoderma* 133: 660-665. <https://doi.org/10.1016/j.geoderma.2006.05.002>
- Bower C A & Wilcox L V (1965). Soluble salts In C. A Black (Ed) *Methods of Soils Analysis*. Madison, Wisconsin, USA, American Society of Agronomy 2: 933-940
- Büyükkılıç Yanardağ A, Faz Cano A, Mermut A, Yanardağ I H & Gomez Garrido M (2020) Organic carbon fluxes using column leaching experiments in soil treated with pig slurry in SE Spain, *Arid Land Research and Management*, 34:2, 136-151. <https://doi.org/10.1080/15324982.2019.1634158>
- Carter M R, Angers D A, Gregorich E G & Bolinder M A (2003). Characterizing organic matter retention for surface soils in eastern Canada using density and particle size fractions. *Canadian Journal of Soil Science* 83: 11–23. <https://doi.org/10.4141/s01-087>
- Chapman H D (1965). Cation Exchange Capacity. In: Black C A (ed) *Methods of Soil Analysis* American Society of Agronomy. Madison, Wisconsin, USA 2: 891-900. <https://doi.org/10.2134/agronmonogr9.1>
- Chen J S & Chiu C Y (2003). Characterization of soil organic matter in different particle-size fractions in humid subalpine soils by CP/MAS ¹³C NMR. *Geoderma* 117: 129–141. [https://doi.org/10.1016/s0016-7061\(03\)00160-5](https://doi.org/10.1016/s0016-7061(03)00160-5)
- Chenu C, Le Bissonnais Y & Arrouays D (2000). Organic matter influence on clay wettability and soil aggregate stability. *Soil Science Society of America Journal* 64: 1479-1486. <https://doi.org/10.2136/sssaj2000.6441479x>
- Dalal R C & Mayer R J (1986). Long-term trends in fertility of soils under continuous cultivation and cereal cropping in southern Queensland: IV Loss of organic carbon from different density fractions. *Aust J Soil Res* 24: 293–300. <https://doi.org/10.1071/sr9860301>
- Duchaufour P H (1970) *Precis de Pedologie*. Masson Paris 481
- FAO–ISRIC (1990). *Guidelines for soil description* 3rd edit FAO Roma, 70
- Figueiredo C C, Resck D V S & Carneiro M A C (2010). Labile and stable fractions of soil organic matter under management systems and native cerrado. *Revista Brasileira de Ciência do Solo* 34(3): 907-916. <https://doi.org/10.1590/s0100-06832010000300032>
- GDSHW - General Directorate of State Hydraulic Works (2003). *Problems of drainage and salinity in the Harran plain Summary Report, the 15th District Directorate of the State Hydraulic Works, Şanlıurfa, Turkey, 10* (in Turkish)
- Gocke M, Pustovoytov K & Kuzyakov Y (2012). Pedogenic carbonate formation: Recrystallization versus migration-Process rates and periods assessed by ¹⁴C labeling. *Global Biogeochemical Cycle*, Volume 26(1): 1-12. <https://doi.org/10.1029/2010GB003871>
- Homann P S, Sollins P, Chappell H N & Stangenberger A G (1995). Soil organic carbon in a mountainous, forested region: relation to site characteristics. *Soil Science Society of America Journal* 59: 1468–1475. <https://doi.org/10.2136/sssaj1995.03615995005900050037x>
- Hontoria C, Rodriguez-Murillo J C & Saa A (1999). Relationships between soil organic carbon and site characteristics in peninsular Spain. *Soil Science Society of America Journal* 63: 614-621. <https://doi.org/10.2136/sssaj1999.03615995006300030026x>
- Khademi H & Mermut A R (1998). Source of palygorskite in gypsiferous Aridisols and associated sediments from Central Iran. *Clay Minerals* 33: 561–578. <https://doi.org/10.1180/claymin.1998.033.4.04>
- Li C, Qiu J, Frolking S, Xia X, Salas W, Moore III B, Boles S, Huang Y & Sass R (2002). Reduced methane emissions from large scale changes in water management of China's rice paddies during 1980–2000. *Geophys Res Lett* 29 (20). <https://doi.org/10.1029/2002GL015370>
- Marinari S, Dell'Abate M T, Brunetti G & Dais C (2010). Differences of stabilized organic carbon fraction and microbiological activity along Mediterranean Vertisols and Alfisols profiles. *Geoderma* 156: 379-388. <https://doi.org/10.1016/j.geoderma.2010.03.007>
- Mermut A R, Amundson R & Cerling T E (2000). The use of stable isotopes in studying carbonates dynamics in soils. In: Lal R, Kimble JM, Eswaran H & Stewart BA, Editors, *Global Climate Change and Pedogenic Carbonates*, CRC Press, USA, pp. 65–85. <https://doi.org/10.1201/9780203753187>
- Milne E (2008). Soils, Land-use and land-cover change, Natural resource management and policy and Climate change. www.eoearth.org/article/Soil_organic_carbon
- Peech M (1965). Hydrogen-ion activity. In Black C A (Ed). *Methods of Soil Analysis*. American Society of Agronomy Madison, Wisconsin, USA 2: 914-916. <https://doi.org/10.2134/agronmonogr9.2.c9>
- Puget P, Chenu C & Balesdent J (1995). Total and young organic matter distributions in aggregates of silty cultivated soils. *Eur J Soil Sci* 46: 449–459. <https://doi.org/10.1111/j.1365-2389.1995.tb01341.x>
- Quiroga A R, Buschiazzo D E & Peinemann N (1996). Soil Organic Matter Particle Size Fractions in Soils of the Semiarid Argentinean Pampas. *Soil Science* 161 (2): 104-108. <http://dx.doi.org/10.1097/00010694-199602000-00004>
- Rovira P, Kurz-Besson C, Coûteaux M M & Vallejo V R (2008). Changes in litter properties during decomposition: a study by differential thermogravimetry and scanning calorimetry. *Soil Biol Biochem* 40: 172–185. <https://doi.org/10.1016/j.soilbio.2007.07.021>
- Schmidt M W I & Kögel-Knabber I (2002). Organic Matter in Particle Size Fraction from A and B Horizons of a Haplic Alfisol. *European Journal of Soil Science* 53: 383-391. <https://doi.org/10.1046/j.1365-2389.2002.00460.x>
- Schulten H R, Leinweber P & Sorge C (1993). Composition of organic matter in particle-size fractions of an agricultural soil. *Journal of Soil Science* 44: 611-691. <https://doi.org/10.1111/j.1365-2389.1993.tb02332.x>
- Smith P (2004). Carbon sequestration in croplands: the potential in Europe and the global context. 20(3): 229-236. <https://doi.org/10.1016/j.eja.2003.08.002>
- Soil Survey Staff (2006). *Keys to Soil Taxonomy*. 10th ed. US Department of Agriculture-Natural Resources. Conservation Service. Washington, DC, USA
- Sollins P, Homann P & Caldwell B A (1996). Stabilization and destabilization of soil organic matter: mechanisms and controls. *Geoderma* 74: 65-105. [https://doi.org/10.1016/s0016-7061\(96\)00036-5](https://doi.org/10.1016/s0016-7061(96)00036-5)
- Sowers T D, Stuckey, J W & Sparks D L (2018). The synergistic effect of calcium on organic carbon sequestration to ferrihydrite *Geochim. Trans.*, 19(2018), p. 4. <https://doi.org/10.1186/s12932-018-0049-4>
- Tobiasova E, Debska B & Banach-Szott M (2012). Influence of particle size distribution on soil on quantity and quality of soil organic matter. *Acta Fytotechnica et Zootechnica* 1, Nitra, Slovaca Universitas Agriculturae Nitriaepp. 13-18. <https://doi.org/10.2478/agri-2013-0001>
- Vatan M (1967). *Manuel de Sédimentologie*: Paris (Technip). ISBN 10: 271080073X
- Yanardağ I H, Zornoza R, Cano A F, Yanardağ A B & Mermut A R (2015). Evaluation of carbon and nitrogen dynamics in different soil types amended with pig slurry, pig manure and its biochar by chemical and thermogravimetric analysis. *Biology and Fertility of Soils* 51(2): 183–96. <https://doi.org/10.1007/s00374-014-0962-3>
- Yesilnacar M I & Güllüoğlu S M (2007). The effects of the largest irrigation of GAP project on groundwater quality, Şanlıurfa-Harran Plain, Turkey. *FEB* 16(2): 206-211. https://www.prt-parlar.de/download_feb_2016/

- Yoo K, Amundson R, Heimsath A M & Dietrich W E (2006). Spatial patterns of soil organic carbon on hillslopes: integrating geomorphic processes and the biological C cycle. *Geoderma* 130: 47–65. <https://doi.org/10.1016/j.geoderma.2005.01.008>
- Zhang J H, Quine T A, Ni S J & Ge F L (2006). Stocks and dynamics of SOC in relation to soil redistribution by water and tillage erosion. *Change Biol.* 12: 1834–1841. <https://doi.org/10.1111/j.1365-2486.2006.01206.x>



© 2022 by the author(s). Published by Ankara University, Faculty of Agriculture, Ankara, Turkey. This is an Open Access article distributed under the terms and conditions of the Creative Commons Attribution (CC BY) license (<http://creativecommons.org/licenses/by/4.0/>), which permits unrestricted use, distribution, and reproduction in any medium, provided the original work is properly cited.



The Effects of Gas Changes in the Shelter in the Summer Period on the Milk yield and Dry Material Consumption of Anatolian Water Buffalo (*Bubalus bubalis*)

Taşkın DEĞİRMENCİOĞLU^a

^aDepartment of Milk and Fattening, Karacabey Vocational School, Bursa Uludag University, Bursa, TURKIYE

ARTICLE INFO

Research Article

Corresponding Author: Taşkın DEĞİRMENCİOĞLU, E-mail: taskin@uludag.edu.tr

Received: 30 June 2021 / Revised: 08 October 2021 / Accepted: 09 October 2021 / Online: 01 September 2022

Cite this article

DEĞİRMENCİOĞLU T (2022). The Effects of Gas Changes in the Shelter in the Summer Period on the Milk yield and Dry Material Consumption of Anatolian Water Buffalo (*Bubalus bubalis*). Journal of Agricultural Sciences (Tarım Bilimleri Dergisi), 28(3):511-517. DOI: 10.15832/ankutbd.960280

ABSTRACT

In this study, the effects of in-shelter gas concentration on milk yield and total dry matter intake (TDMI) of buffaloes during the spring and summer periods were investigated. The research was carried out in a shelter with 20 main Anatolian buffaloes between March and July. Values for temperature, relative humidity, air velocity, and CH₄, NH₃, and CO₂ gases were recorded in the shelter. Data records were collected continuously for 24 hours for 4 days. Milk yield and DMI of buffaloes were also determined. As it was observed, higher air velocity in the house reduces the methane gas levels (P<0.01). The regression equation between milk yield and relative humidity was $Y = 6.011 - 0.03RH$ and showed a negative and low degree correlation. It was illustrated that TDMI varied between $11.00 \pm 0.12 - 13.20 \pm 0.06$ kg during the summer. The difference observed

between months in terms of feed intake was found to be statistically significant (P<0.05). Although the milk yield of water buffalo was low in March, it increased in April and May. However, there was a decrease in DMI (0.50 kg/day) and milk yield (264 mL/day) for an increase of +1 °C in air temperature. The recorded values for CO₂ concentration in the buffalo shelter during the summer period varied between 620-1120 ppm. Considering the obtained results, NH₃ and CO₂ gas levels in the shelter were below the higher limits and can be considered as not dangerous for animal and human health. It was determined that regression equation between feed intake and temperature was $Y = 9.901 + 0.089T^{**}$, regression coefficient was $R^2 = 0.19$ and correlation coefficient was $r = 0.44$ (P<0.001).

Keywords: Buffalo, *Bubalus bubalis*; Gas changes, Summer period; Milk yield; Feed intake

1. Introduction

Gas changes occurring in the shelter and indoor environmental conditions, in general, are important parameters that affect animal health and performance. In recent years, many studies have been conducted on examining the effects of indoor gas density and environmental conditions on feed intake and milk yield (Johnson 1985; Du Preez et al. 1990; Brose et al. 1998; Jungbluth et al. 2001; Bouraoui et al. 2002; Snell et al. 2003; Zhang et al. 2005; Zhao et al. 2007; Zhang et al. 2007 and Bjorneberg et al. 2009). It has been reported that in-house temperature and gas changes affect milk yield in cows. As a matter of fact, at high temperatures, the milk yield was decreased by 10-50% (McDowell et al. 1976; West et al. 2003 and Fournel et al. 2017). Fertility is also negatively affected and the conception rate could be decreased by 20-30% (De Rensis and Scaramuzzi 2003).

According to Steevens & Ricketts (1993), feed intake and milk yield of dairy cattle were significantly decreased at temperatures above 27 °C. Appropriate temperatures for buffaloes are within 10-27 °C (Schein & Hafez 1969). At the same time, the relative humidity in the shelter should be between 55-75% (Bickert 2001). Although buffaloes live in tropical areas, they are very sensitive to changing climatic conditions. They can be easily affected by increased temperature and humidity values (Degirmencioglu et al. 2020).

While conducting studies on in-house gas levels, their effects on human and animal health have been taken into account (Maghirang and Manbeck 1993). As previously indicated, when the ammonia concentration in animal shelters exceeds 50-60 ppm, feed intake and production are decreased (Alagoz et al. 1996). Moreover, when the shelter air is dry and relative humidity falls below 40%, the dust from litter and manure mixtures with the air and causes infections in the respiratory tract of animals (Okuroglu & Delibas 1986). In terms of occupational health and safety, in the country legislation, ammonia exposure limit values are 20 ppm for 8 hours (TWA) exposure, 50 ppm for 15 minutes (STEL) exposure, and carbon dioxide is 5000 ppm (Sainsbury 1981). Bayhan (1996) stated that the carbon dioxide concentration in the barn should not exceed 3300 ppm and the ammonia concentration should not exceed 20 ppm.

The present study aiming at the observation of the effects of changes in the environmental conditions inside the shelter on milk yield and dry matter intake in buffaloes. For this purpose, 24-hour continuous measurements were recorded for 4 days in the summer season at the buffalo shelter. Indoor environmental conditions such as NH_3 , CH_4 , and CO_2 gas concentrations and temperature, wind, and relative humidity were determined in the buffalo barn.

2. Material and Methods

2.1. Study site

Building materials such as sand, briquettes, and cement are used for the construction of shelter walls and bedding. Eternite roof is widely used for the cover of the roofs. There are 20 cm air inlets between the sidewalls and under the eaves.

The chimney height on the roof is 4 m. The length of the stall is 200 cm, the width of the stall is 116 cm, the height of the bar is 100 cm. Feeder path, width, and depth are also determined as 90 cm, 60 cm, and 40 cm respectively. When the barn size of the enterprise was examined; length, width, and height values were obtained as 20 m, 8 m, and 3 m respectively. Two windows are facing each other on the sidewalls of the shelter. The windows are rectangular and 60 cm high. Fertilizers accumulated in the shelter are transferred to the manure pit with a shovel.

The barn ventilation in the enterprise is provided by natural ventilation. The trial is planned in a semi-open barn system with a capacity of 20 milking buffalo cows. The barn stall design is a two-row structure. The buffaloes are taken to the birth chambers between January and February, and the calves (malaks) are kept in a two-month feeding program after birth. AWB (Anatolian Water Buffalo) (5 and 6 years old) at stage 50-60 days of lactation are randomly selected.

According to the 40-year average values in Bursa City, it is stated that the dominant wind direction is southwest and north direction in the first degree and be the south direction in the second degree. In the same report, average wind speeds were obtained as 2.1 and 1.5 m/sec, respectively (Anonymous 2016).

This study was carried out on a buffalo farm in Karaoglan village of Mustafakemalpaşa district (40° 05' 17'' N, 28° 30' 53'' E) as shown in Figure 1.

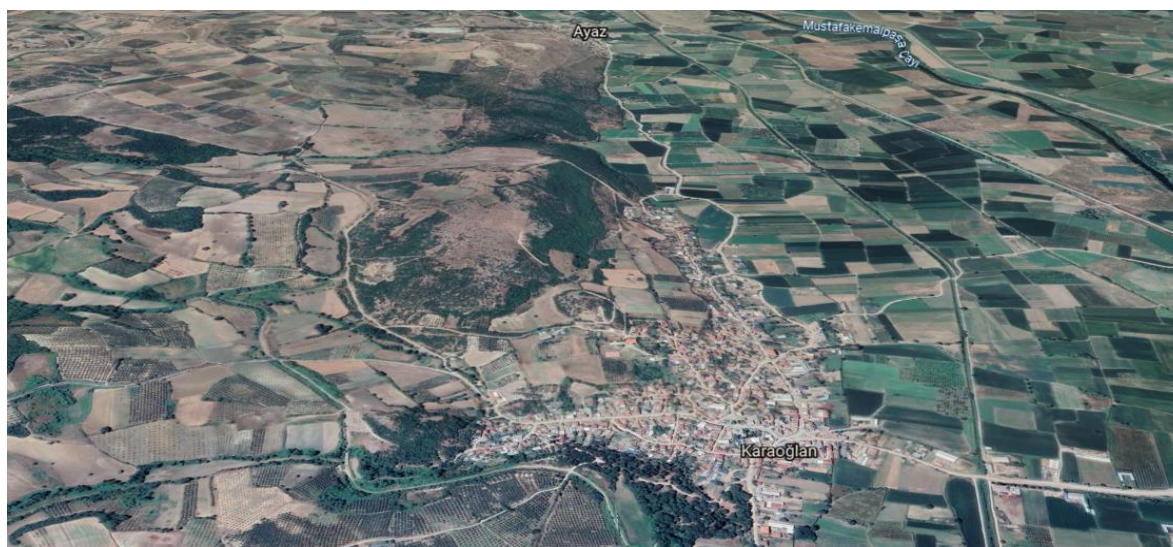


Figure 1- Location of Karaoglan District (Google Earth 2021)

2.2. Nutrition regime and milking of buffaloes

Alfalfa was provided at 6:00 a.m., and silage was offered once a day at 7:00 p.m. The buffaloes in the trial had free access to water and pasture. At the end of the study, the individual feed intake of buffalo cows was determined daily, taking into account the reports of Maynet and Gordon (1984). DMI was determined at the end of the sample collection period by weighing the offered diet and remnants from the previous day. Pasture intake cannot be measured since animals had free access to it. The animals were milked twice a day at 6:00 a.m. and 7:00 p.m. The concentrate feed mixture (CFM) consisted of 33% barley, 34% wheat, 31% sunflower meal, 1% marble powder, 0.75% salt and 0.25% vitamin+mineral mix. During the trial, all buffaloes were provided with corn silage (15 kg day⁻¹), alfalfa hay (6 kg day⁻¹), and 0.70 kg of the CFM (per 1.0 kg of milk per day) (193.9 g CP and 2830 kcal ME kg DM⁻¹) as shown in Table 1. Determination of CP was implemented according to the Association of Official Analytical Chemists (AOAC 1990) and that of fiber fractions (NDF and ADF) according to Van Soest et al. (1991). The

metabolizable energy value of the diet was calculated based on chemical analyses using computer software from the National Research Council (NRC 2001).

Table 1- Composition of feed mixture and roughages fed by experimental buffaloes

Ingredient Composition	Roughages for buffaloes		
	Concentrate Feed Mixture	Alfalfa hay	Corn silage
Barley, g kg ⁻¹	330		
Wheat, g kg ⁻¹	340		
Sunflower meal, g kg ⁻¹	310		
Marble powder, g kg ⁻¹	10		
Salt, g kg ⁻¹	7.5		
Vitamin+minerals ¹ , g kg ⁻¹	2.5		
Total	1000		
Nutrient composition			
DM ² , g kg ⁻¹	887.0	894.4	310.3
OM, g kg ⁻¹	850.7	803.8	261.1
CP, g kg ⁻¹	193.9	146.5	66.2
EE, g kg ⁻¹	19.4	15.2	23.2
CELL, g kg ⁻¹	114.2	330.4	190.0
CA, g kg ⁻¹	36.3	90.6	49.2
NFE, g kg ⁻¹	523.2	311.7	18.2
Starch, g kg ⁻¹	332.0	20.0	218.1
NDF, g kg ⁻¹	220.0	409.9	428.6
ADF, g kg ⁻¹	174.0	370.4	307.2
ADL, g kg ⁻¹	43.0	90.6	63.2
ME (kcal/kg DM) ³	2830	1780	696

¹Trace minerals and vitamins (per kg): 50.000 mg Niacin; 150 mg Co; 800 mg Iyot; 150 mg Se; 50.000 mg Mn; 50.000 mg Fe; Zn 50.000 mg; Cu 10.000 mg; 15.000.000 IU Vitamin A; 3.000.000 IU Vitamin D3;20.000 mg Vitamin E; ²DM: Dry Matter; OM: Organic Matter; CP: Crude Protein; EE: Ether Extract; CELL: Cellulose; CA: Crude Ash; NFE: Nitrogen Free Extract; NDF: Neutral Detergent Fibre; ADF: Acid Detergent Fibre;³ ADL: Acid Detergent Lignin; ³ME: Metabolizable Energy.

2.3. Shelters

Gas measurements were carried out with 3 gas measuring devices in 6 months and a total of 24 days of data were recorded. Temperature, relative humidity, and air velocity were measured with Testo 435 (Testo, Germany), and CH₄, NH₃, and CO₂ gases were measured with MultiRAE Lite multi-gas meter (Wireless Portable Multi-Gas Monitor- RAE Systems by Honeywell, USA) to show indoor conditions and air quality indicators. In this period, to be able to determine the gas condensation in the shelters, 24-hour data records were collected with instruments hung on measurement points in the shelter (Figure 2).



Figure 2- The general condition of measuring devices in the shelter

2.4. Statistical analysis

Variance analysis was used in determining the differences between the averages of in-shelter gas measurements, and the F test, test in determining the significance level of the differences observed between the averages (Turan 1995). Models were developed for the changes in gas concentration and indoor temperature and humidity in the buffalo shelter and multivariate regression analysis was applied. The linear regression method, which is the SPSS (2006) automatic regression determination system was used.

3. Results and Discussion

The daily average and maximum indoor CH₄, NH₃, and CO₂ gas concentrations are shown in Table 2.

As indicated in Table 2, methane concentrations increased from May to August as a result of temperature enhancement in the buffalo shelters. In March and April, no measurement was recorded because CH₄ concentrations were below the measurement limit value of the device. When the gas production results of methane are examined, the highest value was obtained in August with 7.12±0.15%. The other values were 4.88±0.13% for July, 3.72±0.09% for June, and 1.32±0.30% for May. Differences between all means were found to be statistically significant (P<0.05). As observed in Table 2, the average ammonia production value in the shelter of buffaloes during the experimental period varied between 11.12±0.42 and 2.40±0.18 (ppm). The highest average ammonia value in the shelter was obtained in August, followed by July, June, May, April, and March. Differences were found to be statistically significant (P<0.05). As reported in Table 2, the average CO₂ levels inside the shelter of buffaloes during the experimental period varied between 620±14.14 and 1196±40.61 ppm; CO₂ values were the highest in August and the lowest in March. It was observed that the differences among months in terms of CO₂ concentrations were statistically significant (P<0.05). The temperature inside the shelter has increased continuously throughout the experimental period from 15.60±0.08 to 28.15±0.28 (°C), with the highest temperature detected in August and the lowest in March. It was observed that the differences observed among months were statistically significant (P<0.05). As presented in Table 2, the humidity values in buffalo shelters varied between 49.08±3.023 and 75.57±0.74 (%). Humidity was the highest in March and the lowest in August (P<0.05). Finally, air velocity recorded in the buffalo barn varied between 0.157±0.08 and 0.025±0.03.

Table 2- Gas concentrations measured in the buffalo shelter during the summer period (mean±SE)

Buffalo shelter	March $\bar{X} \pm S_{\bar{x}}$	April $\bar{X} \pm S_{\bar{x}}$	May $\bar{X} \pm S_{\bar{x}}$	June $\bar{X} \pm S_{\bar{x}}$	July $\bar{X} \pm S_{\bar{x}}$	August $\bar{X} \pm S_{\bar{x}}$
CH ₄ (%)	0.00	0.00	1.32±0.30 ^d	3.72±0.09 ^c	4.88±0.13 ^b	7.12±0.15 ^a
NH ₃ (ppm)	2.40±0.18 ^e	5.84±0.41 ^d	6.32±0.20 ^c	7.28±0.60 ^c	9.04±0.40 ^b	11.12±0.42 ^a
CO ₂ (ppm)	620±14.14 ^e	632±18.90 ^c	644±13.01 ^c	676±10.45 ^c	920±42.81 ^b	1196±40.61 ^a
T (°C)	15.60±0.08 ^d	20.92±0.49 ^c	24.44±0.35 ^b	25.84±0.28 ^b	27.63±0.18 ^a	28.15±0.28 ^a
V (m/s)	0.157±0.08 ^a	0.133±0.01 ^b	0.137±0.09 ^b	0.047±0.04 ^c	0.060±0.05 ^c	0.025±0.03 ^d
RH (%)	75.92±0.74 ^a	67.74±2.13 ^b	67.87±2.15 ^b	64.80±2.15 ^{bc}	59.96±2.78 ^c	49.07±3.02 ^d
TDMC (kg d ⁻¹)	11.00±0.12 ^d	11.60±0.10 ^c	12.50±0.09 ^b	13.20±0.06 ^a	12.30±0.14 ^b	11.50±0.15 ^c
The milk yield (kg d ⁻¹)	4.90±0.07 ^c	5.50±0.97 ^b	6.67±0.027 ^a	6.30±0.06 ^a	6.00±0.07 ^b	5.45±0.09 ^{bc}

CH₄; average Methane, NH₃; average ammonia, CO₂; average Carbon dioxide, T; average temperature, V; air velocity, RH; average humidity, TDMC; average total dry matter consumption, a-b, c-d: (P<0.05) Different letters in the same line are significantly different.

It was determined that the gas concentration data obtained in the present study remained at normal values when compared with the literature. As indicated, the highest values for methane concentration were found during the summer period. Bjorneberg et al. (2009) confirm these findings since the CH₄ concentration in the compartments increased in June and September compared to January and March in their experiment. Controversial findings have emerged in studies conducted with ammonia during the summer period, and it has been reported that these discrepancies could be possibly attributed to the environmental conditions inside the shelter. Indeed, the researchers reported ammonia values within the shelter from 5.3 ppm (Jungbluth et al. 2001), 1.4-7 ppm (Zhao et al. 2007 & Zhang et al. 2007) to 8.2 ppm (Snell et al. 2003).

The CO₂ and NH₃ concentrations in the buffalo shelter recorded during the experimental period varied between 620-1200 and 2.40-11.10 ppm, respectively. According to the previous literature, values for CO₂ and NH₃ were within the normal limits (3300-5000 and 20-50 ppm, respectively) (Brose et al. 1998; Jungbluth et al. 2001) and can be considered as not dangerous for animal and human health.

The wide range of gas concentrations could be possibly attributed to the different manure removal systems applied in the shelters, the duration of the manure in the shelter, the different ventilation systems of the shelters, the different rationed proteins

given to the animals, and the structural differences of the shelters (Snell et al. 2003; Ndegwa et al. 2008; Zhang et al. 2008; Merino et al. 2008; Angel et al. 2008).

As can be observed in Table 2 and Figure 3, the total dry matter intake (TDMI) of buffaloes increased continuously until mid-summer. It was determined that TDMI varied between 11.00 ± 0.12 and 13.20 ± 0.06 kg during the experimental period. Water buffaloes had the highest feed intake (13.20 kg) in June due to their lactation stage. However, the feed intake of buffaloes decreased as an effect of the increase in air temperature. It was observed that the differences observed among months in terms of feed intake were statistically significant ($P < 0.05$). Although the milk yield of buffalo was low in March (4.90 ± 0.07), increased in April (5.50 ± 0.97). The milk yield of buffalo showed a linear increase and reached the highest level of 6.67 ± 0.027 in May. Afterward, the milk yield of buffaloes was decreased. The temperature increase in July and August further accelerated the decline in milk yield. It was observed that the difference observed among months in terms of milk yield was also statistically significant ($P < 0.05$). It can be concluded that this decrease is the result of the increase in ambient temperature, the increase in temperature caused by the breakdown of nutrients in the body, triggering heat stress in the buffaloes and the resulting reduction in feed intake, leading to insufficient ingestion of nutrients for milk synthesis (Degirmencioglu 2020). In addition to this, sudden temperature changes are thought to cause the aforementioned implications, as well as a decrease in the endocrine system function (endocrine glands) (Gantner et al. 2011). The findings obtained from the present research regarding the dry matter intake and milk yield as a result of the in-house gas densities in buffaloes are consistent with the findings of previous researchers (West et al. 2003; Fournel et al. 2017).

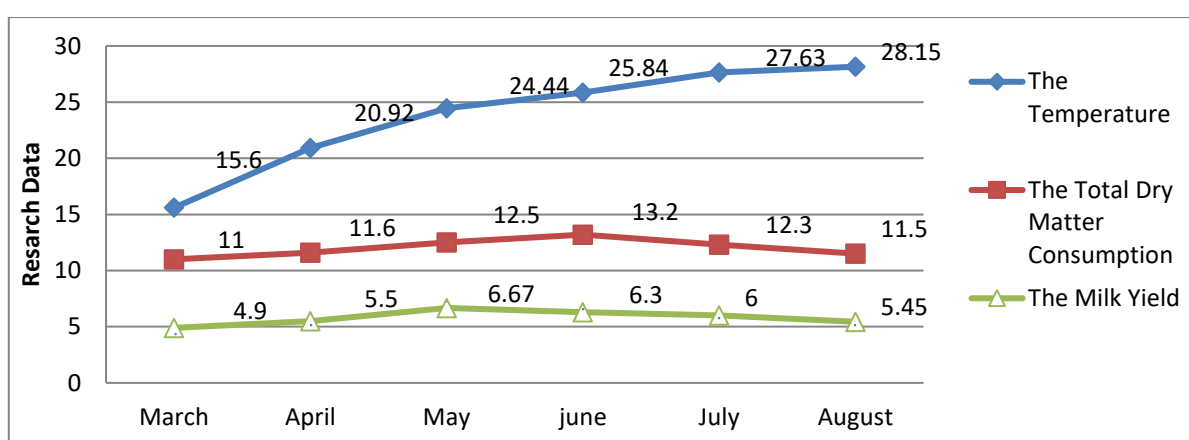


Figure 3- The Effects of Temperature Changes in Shelter on Dry Matter Consumption and Milk Yield

Monitoring the environmental conditions and gas concentration changes in the shelter is important in terms of controlling the health and productivity of the animals. The gas exchange model in the buffalo shelter is shown in Table 3. As indicated, while there is a negative interaction between humidity and indoor temperature in a buffalo shelter, there is a positive interaction between CO_2 , CH_4 , and NH_3 concentrations and indoor temperature.

Table 3- Gas exchange model in the buffalo shelter

Parameter	Polluting	Regression equation	R	R ²	P
	RH	$92.470 - 1.188T^*$	-0.40	0.16	0.00
	NH_3	$1.388 + 0.399T^{**} - 0.49RH^* - 7.483V$	0.76	0.57	0.00
	CH_4	$-2.940 + 0.351T^{**} - 0.021RH - 12.659V^{**}$	0.86	0.73	0.00
	CO_2	$77.744 + 29.602T^{**}$	0.55	0.29	0.00
The milk yield (kg d^{-1})	T ($^{\circ}\text{C}$)	$4.257 + 0.065T^{**}$	0.44	0.19	0.00
	RH	$6.011 - 0.03RH$	0.06	0.04	0.44
	T RH	$3.60 + 0.074T^{**} + 0.07RH$	0.46	0.21	0.00
<25 ($^{\circ}\text{C}$)		$2.074 + 0.658TDMC^{**}$	0.77	0.59	0.00
25> ($^{\circ}\text{C}$)		$1.724 + 0.347TDMC^{**}$	-0.54	0.29	0.00
TDMC(kg d^{-1})	T ($^{\circ}\text{C}$)	$9.901 + 0.089T^{**}$	0.44	0.19	0.00

T: Temperature; RH: humidity (%); NH_3 : ammonia, CH_4 : methane, V: air velocity (m/s) TDMC; total dry matter consumption * $P < 0.05$, ** $P < 0.01$

This interaction was statistically significant ($P < 0.01$). The fact rise in the temperature increases the NH_3 release supports the findings of Zhang et al. (2005). On the other hand, Kılıc (2011) stated that there is a negative interaction between other gas concentrations other than CO_2 and indoor temperature in dairy cattle barns. In our study, it was determined that there is a negative interaction between CH_4 and NH_3 concentrations and humidity and air velocity in buffalo shelters, with the inverse relationship between NH_3 concentration and humidity being statistically significant ($P < 0.05$). The results obtained by Zhang et al. (2008) support that CH_4 and NH_3 emissions can be reduced by properly designed ventilation systems in animal shelters. The regression equation between humidity and temperature was determined as $Y = 92.470 - 1.188T$, regression coefficient (R^2) 0.16 and

correlation coefficient (r) -0.40 ($P<0.001$). There is an inverse and moderate relationship between them. The coefficients calculated in this study are below the values obtained by Turkmen (2018) ($R^2= 95.36$ and $r= -0.98$). The multiple regression equation between ammonia and temperature, humidity and air velocity in the studied buffalo shelter was $Y = 1.388 + 0.399T^{**} - 0.49RH - 7.483V$, $R^2= 0.57$ and $r= 0.57$ ($P<0.001$).

Regression equation between methane and temperature, humidity, and air velocity was $Y= -2.940 + 0.351T^{**} - 0.021RH - 12.659V^{**}$, $R^2= 0.73$ and $r= 0.86$ ($P<0.001$).

Regression equation between milk yield and temperature in buffaloes was $Y= 4.257 + 0.065T^{**}$, $R^2= 0.19$ and $r= 0.44$ ($P<0.001$). The coefficients calculated in this relationship are lower than the values calculated by Turkmen (2018) ($R^2= 66.2\%$ and $r= 0.74$). On the other hand, although the temperature rise increased the milk yield, a decrease of 370 mL was detected in milk yield after May. The regression equation between milk yield and relative humidity was $Y= 6.011 - 0.03RH$ and showed a low degree of interaction.

Even at the highest humidity of 75.92% in March, the continuation of milk and feed intake of buffaloes was due to its harmony with nature and ability to endure hardships.

The multiple regression equation between milk yield and temperature, humidity and air velocity in the studied buffalo shelter is $Y= 3.60 + 0.074T^{**} + 0.07RH$, $R^2= 0.21$ and $r= 0.46$ ($P<0.001$). As variables, it had a positive effect with 0.074 coefficient in temperature and 0.07 coefficient in humidity.

As regression equality between milk yield and total dry matter intake at temperatures below 25 °C in buffaloes is $Y= 2.074 + 0.658TDMI$, $R^2= 0.59$ and $r= 0.77$. They showed a moderate interaction ($P<0.001$). Regression equation between milk yield in buffaloes and total dry matter consumption at temperatures above 25 °C is $Y= 1.724 - 0.347TDMI^{**}$, $R^2= 0.29$ and $r= -0.54$, so they showed a moderate inverse interaction ($P<0.001$). In the studied buffalo shelter, it was determined that regression equation between feed intake and temperature was $Y= 9.901 + 0.089T^{**}$, $R^2= 0.19$ and $r= 0.44$ ($P<0.001$). Basically, for an increase of +1 °C in air temperature, a 0.50 kg decrease in dry matter intake and a decrease of 264 ml in milk yield occurred. West et al. (2003) partially support the previous findings stating that the DM intake of cows decreased by 0.85 kg in case of an increase of 1 °C in air temperature. It can be concluded that the water buffaloes are less exposed to heat stress because they enter the pond to cool off and the gas density decreases with the manure cleaning and natural ventilation provided in the shelter, compared to dairy cows. Fournel et al. (2017) support the hypothesis that the decrease in feed intake and milk yield can be confined by reducing the temperature and humidity index of dairy cattle in open animal shelters where airflow is provided by the panel and basket-type fans.

4. Conclusions

Generally, it has been determined that in-barn temperature values reduce the feed intake and milk yield of buffaloes. For this purpose, positive contributions can be made to feed intake and milk yield in buffalo farms by installing fans especially throughout the feeder. It has been observed that in the in-house gas exchanges, the airflow is partially effective in reducing the level of methane, humidity, and ammonia. In hot weather, due to fact that long walks increase thermal stress for buffaloes, freeride areas and shower systems should be included outside the shelter.

References

- AOAC (1990). Official methods of analysis. 15th ed. Assoc. Off. Anal Chem. Arlington, VA, USA. (73)1: 189-191. <https://doi.org/10.1093/jaoac/73.1.189>
- Angel R., Powers W & Applegate T (2008). Diet impacts for mitigating air emissions from poultry. Livestock Environment VIII. 31 August - 4 September 2008, Iguassu Falls, Brazil. <https://doi.org/10.13031/2013.25514>
- Anonymous 2016. Report of the General Directorate of Meteorology of the Republic of Turkey (In Turkish), <http://www1.mgm.gov.tr/FILES/resmi-istatistikler/Turkiye-Ortalama-Ruzgar.pdf> (Accessed: 12.11.2020).
- Alagoz T, Kumova Y, Atilgan A & Akyuz A (1996). A Study on the wastes generated in Livestock Facilities and the negative effects of these wastes on the Environment
- Agricultural-Environmental Relations Symposium, 13-15 May 1996, M.Ü. Faculty of Engineering, Mersin (In Turkish)
- Bayhan A K (1996). A Research on Mechanization Status, Problems, and Solutions of Livestock Cattle in Erzurum Region. Ph.D. Thesis, Atatürk University, Institute of Science and Technology, Department of Agricultural Mechanization, Erzurum (Published in Turkish)
- Bouraoui R, Lahmar M, Majdoub A, Djemali M & Belyea R (2002). The relationship of the temperature-humidity index with milk production of dairy cows in a Mediterranean climate. *Animal Research* 51(6): 479-491. <https://doi.org/10.1051/animres:2002036>
- Brose G, Hartung E & Jungbluth T (1998). Influences on and measurement of ammonia and greenhouse gas emissions from dairy houses. *AgEng Oslo* 98, E-054.
- Bjorneberg D L, Leytem A B, Westermann D T, Griffiths P R, Shao L & Pollard M J (2009). Measurement of atmospheric ammonia, methane and nitrous oxide at the concentrated dairy production facility in southern Idaho using open-path FTIR spectrometry. *Transaction of ASABE*, 52(5): 1749-1756. <https://doi.org/10.13031/2013.29137>
- Bickert W G (2001). Ventilation and animal health. *Agricultural Engineering Newsletter*. Michigan State University
- De Rensis F & Scaramuzzi R J (2003). Heat Stress and Seasonal Effects on Reproduction in the Dairy Cow-A Review. *Theriogenology*, (60)6:1139-1151. [https://doi.org/10.1016/s0093-691x\(03\)00126-2](https://doi.org/10.1016/s0093-691x(03)00126-2)

- Degirmencioglu T (2020). Possibilities to Reduce Thermal Stress in Water Buffalo [*Bubalus bubalis* (Linnaeus, 1758)] *Anadolu. J. of AARI*, 30(1): 117-123. <https://doi.org/10.18615/anadolu.727123>
- Du Preez J H, Hatting P I, Giesecke W H & Eisenberg B E (1990). Heat stress in dairy cattle and other livestock under Southern African conditions. III. Monthly temperature-humidity index mean values and their significance in the performance of dairy cattle. *Onderstepoort J. Vet. Res* 57: 243-248
- Fournel S, Ouellet V & Charbonneau E (2017). Practices for alleviating heat stress of dairy cows in humid continental climates: A literature review *Animals*. 7(12):37. <https://doi.org/10.3390/ani7050037>
- Gantner V, Mijić P, Kuterovac K, Solić D & Gantner R (2011). Temperature-humidity index values and their significance on the daily production. *Daily production of dairy cattle*, *Mljekarstvo*. 61(1): 56-63
- Johnson H D (1985). Physiological responses and productivity of cattle. *Stress physiology in livestock. Basic principles*, Vol. 1, CRC Press, Boca Raton, Florida pp. 4-19
- Jungbluth T, Hartung E & Brose G (2001). Greenhouse gas emissions from animal houses and manure stores. *Nutrient Cycling in Agroecosystems*. 60: 133-145. <https://doi.org/10.1023/a:1012621627268>
- Kılıç I (2011). Characterization of air pollutants in animal barns. Ph.D. Thesis. Uludag University Graduate School of Natural and Applied Sciences Department of Biosystem Engineering. 202 pages. (Published in Turkish)
- Maghirang R G & Manbeck H B (1993). Dust, Ammonia, and carbon dioxide emission from a poultry house. ASAE. St Joseph. Michigan. Paper No. 93-4056
- Maynet C S & Gordon F J (1984). The Effect of Type of Concentrate and Level of Concentrate Feeding on Milk Production. *Anim. Sci.* 39(1): 65- 76. <https://doi.org/10.1017/s0003356100027628>
- Merino P, Arriaga, Salcedo G, Pinto M & Calsamiglia S (2008). Dietary modification in dairy cattle: field measurement to assess the effect on ammonia emissions in the Basque Country. *Agriculture, Ecosystems and Environment*. 123: 88-94. <https://doi.org/10.1016/j.agee.2007.05.003>
- McDowell R E, Hooven N W & Camoens J K (1976). Effects of climate on performance of Holsteins in the first lactation. *J. Dairy Sci.* 59(5): 965-971. [https://doi.org/10.3168/jds.s0022-0302\(76\)84305-6](https://doi.org/10.3168/jds.s0022-0302(76)84305-6)
- NRC (2001). Nutrient requirements of dairy cattle. National academy press. Washington.D.C341-353. <https://doi.org/10.17226/9825>
- Ndegwa P M, Hristov A N, Arogo J & Sheffield R E (2008). A review of ammonia emission mitigation techniques for concentrated animal feeding operations. *Biosystems Engineering*. 100(4): 453-469. <https://doi.org/10.1016/j.biosystemseng.2008.05.010>
- Okuroglu M & Delibas L (1986). Appropriate Environmental Conditions in Animal Shelters. *Livestock Seminar. TOKB. Tokat 61 Directorate*, 5-8 May (In Turkish)
- Van Soest P J, Robertson J B & Lewis B A (1991). Methods for Dietary Fiber, Neutral Detergent Fiber, and Nonstarch Polysaccharides in Relation to Animal Nutrition, *Journal of Dairy Science* 74(10): 3583 -3597 [https://doi.org/10.3168/jds.s0022-0302\(91\)78551-2](https://doi.org/10.3168/jds.s0022-0302(91)78551-2)
- Sainsbury D W B (1981). Health Problems in Intensive Animal Production. *Environmental Aspects of Housing for Animal Production, England* pp. 439-454. <https://doi.org/10.1016/b978-0-408-10688-7.50030-8>
- Schein M V & Hafez E S E (1969). The physical environment and behavior. In: *The behavior of domestic animals*. Balliere Tindelland Cassel London. pp. 63-94
- SPSS (2006). Statistical package for social sciences, Pc Version 15, SPSS Inc. 444 N. Michigan Avenue Chicago, USA
- Steevens B, & Ricketts R (1993). Feeding and housing dairy goats. Agricultural publication G3990. The University of Missouri.
- Snell H G J, Speilt F & Van dan Weghe H F A (2003). Ventilation rates and gaseous emissions from naturally ventilated dairy houses. *Biosystems Eng.* 86(1): 67-73. [https://doi.org/10.1016/s1537-5110\(03\)00113-2](https://doi.org/10.1016/s1537-5110(03)00113-2)
- Turan Z M (1995). Research and Experimental Methods. U. Univ. Zir. fac. Lecture Notes, Bursa, No: 62. 121p. (In Turkish).
- Turkmen E (1998). A research on the investigation of dairy farms supported with European union instrument for pre-accession assistance-rural development (ipard) in terms of animal welfare. Ph.D. Thesis. Uludag University Graduate School of Natural and Applied Sciences Department of Biosystems Engineering, 148 pages. (Published in Turkish)
- West J W, Mullinix B G & Bernard J K (2003). Effects of hot, humid weather on milk temperature, dry matter intake, and milk yield of lactating dairy cows. *Journal of Dairy Science* 86: 232-242
- Zhang G, Strøm JS, Li B Rom H B, Morsing S, Dahl P & Wang C (2005). Emission of ammonia and other contaminant gases from naturally ventilated dairy cattle Buildings. *Biosystems Engineering*, 92(3): 355-364. <https://doi.org/10.1016/j.biosystemseng.2005.08.002>
- Zhang Q, Zhou X J, Cicek N & Tenuta M (2007). Measurement of odor and greenhouse gas emissions in two swine farrowing operations. *Canadian Biosys.Eng.* 49: 13-20
- Zhang G, Bjerg B, Strøm J S, Morsing S, Kai P, Tong G & Ravn P (2008). Emission effects of three different ventilation control strategies A scale model study. *Biosystems Engineering* 100(1): 96-104. <https://doi.org/10.1016/j.biosystemseng.2008.01.012>
- Zhao L Y, Brugger M F, Manuzan R B, Arnold G & Imerman E (2007). Variations in the air quality of new Ohio dairy facilities with natural ventilation systems. *Appl. Engineering in Agriculture* 23(3): 339-346. <https://doi.org/10.13031/2013.22684>



© 2022 by the author(s). Published by Ankara University, Faculty of Agriculture, Ankara, Turkey. This is an Open Access article distributed under the terms and conditions of the Creative Commons Attribution (CC BY) license (<http://creativecommons.org/licenses/by/4.0/>), which permits unrestricted use, distribution, and reproduction in any medium, provided the original work is properly cited.



Genetic Characterization of Some Species of Vetch (*VICIA* L.) Grown in Turkey with SSR Markers

Cebrail YILDIRIM^a , Onur OKUMUŞ^b , Satı UZUN^b , Şeyda Nur TURKAY^a , Ahmet SAY^a ,
Melike BAKIR^{a*}

^aDepartment of Agricultural Biotechnology, Faculty of Agriculture, Erciyes University, Kayseri, 38039, TURKEY

^bDepartment of Field Crops, Faculty of Agriculture, Erciyes University, Kayseri, 38039, TURKEY

ARTICLE INFO

Research Article

Corresponding Author: Melike BAKIR, E-mail: melikecu@gmail.com

Received: 08 May2021 / Revised: 12 October 2021 / Accepted: 13 October 2021 / Online: 01 September 2022

Cite this article

YILDIRIM C, OKUMUŞ O, UZUN S, TURKAY Ş N, SAY A, BAKIR M (2022). Genetic Characterization of Some Species of Vetch (*VICIA* L.) Grown in Turkey with SSR Markers. *Journal of Agricultural Sciences (Tarim Bilimleri Dergisi)*, 28(3):518-524. DOI: 10.15832/ankutbd.934655

ABSTRACT

The genus vetch (*Vicia* L.) is grown worldwide for fodder, hay, grain and silage, and rich in protein, mineral substances, vitamins and an essential source of roughage in animal husbandry. However, genetic characterization studies in vetch are minimal. In this study, the genetic characterization of a total 37 accessions of five vetches (*Vicia* L.) species was investigated using SSR markers. A total of 18 SSR markers were used, and eight of them were showed polymorphism and used for genetic analysis of vetch accessions. The total number of alleles was 35, and the average number of alleles for each locus was determined as 4.38. The

average heterozygote rate was found to be 0.49. The polymorphism information content (PIC) value varied between 0.23 and 0.77, and the average value was 0.44. Although almost a clear distinction was observed among the species, very high similarities were found between some cultivars within the same species. This similarity may be due to the narrow structure of the vetch genome or the inability of the SSR markers used in this study to distinguish the narrow structure of the vetch genome. The results reported here will be contributed to future germplasm management efforts and for comparative studies in vetch.

Keywords: Cross-amplification, Genetic variation, Microsatellites, Vetch, *Vicia* L.

1. Introduction

The genus *Vicia* L. belongs to the Fabaceae family (Van de Wouw et al. 2001; Renzi et al. 2020), and it is divided into two subgenera as *Vicia* and *Vicilla* (Kupicha 1976; Bozkurt 2009). The genus *Vicia* has 190 species worldwide (Davis 1970; Agar et al. 2006; Avcioğlu et al. 2009) and, mainly distributed in Europe, Asia and North America, extending to temperate South America and tropical East Africa (Van de Wouw et al. 2001; Renna et al. 2014). The genus *Vicia* is represented by 59 species, 22 subspecies and, 18 varieties in Turkey (Davis 1970; Kıran et al. 2012) and five species and three subspecies of these are endemic in Turkey (Davis & Plitmann 1970). Common vetch, Hungarian vetch, narbon vetch, bitter vetch and, hairy vetch are economically important *Vicia* species grown in Turkey (Gençkan 1992). *Vicia* species are generally produced for fodder, hay, grain, silage, pasture, green manure and cover crop either in pure stands or in mixture with cereals as forage crops (Renzi et al. 2017; Kartal et al. 2020). Vetches have a very high feed value with their rich protein, mineral substances and vitamin content (Cheeke & Shull 1985; Avcioğlu et al. 2009; Larbi et al. 2010; Renna et al. 2014). Vetches are also important crops for sustainable agriculture as they can fix atmospheric nitrogen and improve soil properties (Ibanez et al. 2020).

Determination of the diversity among genotypes is of great importance for breeding studies (Nunome et al. 2009). In recent years, molecular markers have increased in genetic diversity and characterization studies (O'Neill et al. 2003; Nunome et al. 2009; Ozsensoy & Kurar 2012; Ertus et al. 2016; Zulkadir & İdikut 2021). Among the molecular markers, SSR markers are the most widely used markers (Tautz 1989; Mengoni et al. 2000) because of the high abundance in the genome, high polymorphism information content, random distribution within the genome, and its co-dominant inheritance (Dutta et al. 2011). SSR markers developed in *V. sativa* subsp. *sativa* was used to determine the genetic diversity and relationships of different *Vicia* species and analyzed their transferability to *Vicia* genomes (Raveendar et al. 2015). Additionally, cDNA-SSR markers developed in *Vicia sativa* subsp. *sativa* was used genetic diversity of *Vicia sativa* subsp. *sativa* accessions (Chung et al. 2013). Besides, genetic characterization studies in *Vicia ervilia* (L.) Willd. (El Fatehi et al. 2016), *Vicia narbonensis* L. (Bouabid et al. 2018) and *Vicia sativa* L. (De la Rosa et al. 2021) were carried out using SSR markers. Also, RAPD (Potokina et al. 2000; Agar et al. 2006), AFLP (Potokina et al. 2002; Maul et al. 2011) and ISSR markers (Unverdi 2007; Bozkurt 2009) were used in characterization studies in the genus *Vicia* L.

The present study aimed to reveal genetic diversity for registered Turkish vetch genotypes and some vetch lines using SSR markers. It is aimed that provided information about the genetic relationship among the vetch genotypes will help selection and more efficient utilization of the vetch genotypes in breeding programs and conservation of gene resources.

2. Material and Methods

2.1. Plant Material and DNA Extraction

The present study's *Vicia* species consist of 37 vetch genotypes (30 cultivars and 7 lines) obtained from different research centers in Turkey. A list of these genotypes and species and origin information were presented in Table 1.

Table 1- List of accessions used in this study

No	Accessions	Species	Origin
1	Yucel	<i>Vicia sativa</i> L.	Eastern Mediterranean Agricultural Research Institute
2	Ozveren	<i>Vicia sativa</i> L.	Eastern Mediterranean Agricultural Research Institute
3	Cumhuriyet-99	<i>Vicia sativa</i> L.	Aegean Agricultural Research Institute
4	Selcuk-99	<i>Vicia sativa</i> L.	Aegean Agricultural Research Institute
5	Alper	<i>Vicia sativa</i> L.	Aegean Agricultural Research Institute
6	Doruk	<i>Vicia sativa</i> L.	Aegean Agricultural Research Institute
7	Urkmez	<i>Vicia sativa</i> L.	Aegean Agricultural Research Institute
8	Ankara Moru-08	<i>Vicia sativa</i> L.	Field Crops Central Research Institute
9	Ayaz-09	<i>Vicia sativa</i> L.	Field Crops Central Research Institute
10	Zemheri-08	<i>Vicia sativa</i> L.	Field Crops Central Research Institute
11	Alimoglu-2001	<i>Vicia sativa</i> L.	Field Crops Central Research Institute
12	Bakir-2001	<i>Vicia sativa</i> L.	Field Crops Central Research Institute
13	Farukbey-2001	<i>Vicia sativa</i> L.	Field Crops Central Research Institute
14	Sari Elci	<i>Vicia sativa</i> L.	Ankara University, Faculty of Agriculture, Department of Field Crops
15	Tarman-2002	<i>Vicia narbonensis</i> L.	Field Crops Central Research Institute
16	Bozdog	<i>Vicia narbonensis</i> L.	Aegean Agricultural Research Institute
17	Balkan	<i>Vicia narbonensis</i> L.	Transitional Zone Agricultural Research Institute
18	Kansur	<i>Vicia pannonica</i> Crantz	Field Crops Central Research Institute
19	Anadolu Pembesi 2002	<i>Vicia pannonica</i> Crantz	Field Crops Central Research Institute
20	Oguz-2002	<i>Vicia pannonica</i> Crantz	Field Crops Central Research Institute
21	Tarım Beyazi -98	<i>Vicia pannonica</i> Crantz	Field Crops Central Research Institute
22	Dogu Beyazi	<i>Vicia pannonica</i> Crantz	East Anatolia Agricultural Research Institute
23	Aygun	<i>Vicia pannonica</i> Crantz	East Anatolia Agricultural Research Institute
24	Budak	<i>Vicia pannonica</i> Crantz	Transitional Zone Agricultural Research Institute
25	Ege Beyazi-79	<i>Vicia pannonica</i> Crantz	Aegean Agricultural Research Institute
26	Beta	<i>Vicia pannonica</i> Crantz	Unknown
27	Selcuklu-2002	<i>Vicia villosa</i> Roth	Field Crops Central Research Institute
28	Menemen-79	<i>Vicia villosa</i> Roth	Aegean Agricultural Research Institute
29	Efes-79	<i>Vicia villosa</i> Roth	Aegean Agricultural Research Institute
30	Segmen-2002	<i>Vicia villosa</i>	Field Crops Central Research Institute
31	Erac-2002	<i>Vicia villosa</i>	Field Crops Central Research Institute
32	Line – 1	<i>Vicia ervilia</i>	Ankara University, Faculty of Agriculture, Department of Field Crops
33	Line – 2	<i>Vicia ervilia</i>	Ankara University, Faculty of Agriculture, Department of Field Crops
34	Line – 9	<i>Vicia ervilia</i>	Ankara University, Faculty of Agriculture, Department of Field Crops
35	Line – 10	<i>Vicia ervilia</i>	Ankara University, Faculty of Agriculture, Department of Field Crops
36	Usak-Esme-1 (cream seed coated line)	<i>Vicia ervilia</i>	Usak province, Turkey
37	Usak-Esme-2 (blackish seed coated line)	<i>Vicia ervilia</i>	Usak province, Turkey

*lines: 14, 32, 33, 34, 35, 36, 37

2.2. SSR analysis

Genomic DNA was isolated from fresh, young seedlings according to the protocol described by Lefort et al. (1998) with minor modifications. The quality and quantity of the extracted DNA were determined in NanoDrop® ND-1000 Spectrophotometer (NanoDrop Technologies, Wilmington, DE, USA) and agarose gel electrophoresis (1%). A total of 18 SSR loci were used in this study. Thirteen of these (Lc_MCu 11, Lc_MCu 17, Lc_MCu41a, Lc_MCu 43, Lc_MCu47a, Lc_MCu71, Lc_MCu73, Lc_MCu75, Lc_MCu78, Lc_MCu83, Lc_MCu85, Lc_MCu95, Lc_MCu97) were developed in lentil (Bakır & Kahraman 2019) and five (KF008505, KF008507, KF008512, KF008526, KF008536) were developed for common vetch genetic studies (Chung et al. 2013) (Table 2).

Table 2- List of SSR markers used in the study

<i>Locus</i>	<i>Primer sequences (5'→3')</i>	<i>T_m (°C)</i>
Lc_MCu11F	GAGTGGGAAGGAGACCACAA	54
Lc_MCu11R	CGTGGTCAGGAGAGGAAATA	
Lc_MCu17F	GAAAGACAAAGAACGTGATAGAAGG	58
Lc_MCu17R	TGACCGTTGTTCCCAAATTC	
Lc_MCu41aF	TGTGTGAGGAAGATGATGAA	48
Lc_MCu41aR	AAGGAGTTCACACACACACA	
Lc_MCu43F	TCATAAAGCATTTGGCTAAAACA	50
Lc_MCu43R	CGCAAGCCTCAAGCCTATAA	
Lc_MCu47aF	TTAGTTCGGAGAGCGTTTAG	48
Lc_MCu47aR	TGAAGAAGTGGAGGAGAAGA	
Lc_MCu71F	CTCTCTAACACTATCACGCTCA	60
Lc_MCu71R	GAAGGAGTAGACAGGGAGAAG	
Lc_MCu73F	TGGGACTTGAGAGAAGATTG	58
Lc_MCu73R	GTCTCTCTCCCTCCTCATTT	
Lc_MCu75F	TCACGTCTTCTAGGAAGTCTCT	55
Lc_MCu75R	ATTGAGGATCCTGAGGTTG	
Lc_MCu78F	GGTTGGGTGACAGTGAGA	50
Lc_MCu78R	AACGAAGGAGTCCCAAAC	
Lc_MCu83F	ATCCTAAGCAAAGAATGACG	55
Lc_MCu83R	AAGGAGTCCACATACAAAACC	
Lc_MCu85F	CAGTCGTTTCATTCTCTTCC	55
Lc_MCu85R	GAGTACGGAACCGGAGAT	
Lc_MCu95F	CCTTCACTTACTCTCTCGTTC	55
Lc_MCu95R	CTTTCATTCACTCGTTCCTC	
Lc_MCu97F	CTACTCTCTCGTTCAGATCCTC	55
Lc_MCu97R	ATCCATAAGAGCCCGTATTT	
KF008505F	ATCCATGCCTCTTTTGCC	55
KF008505R	AGCCTCATTTTCAGCAGCA	
KF008507F	TGGTTTCTTTCTAAAGGGGTG	55
KF008507R	CGGCTCGATGGACAGTAG	
KF008512F	GGCCGGTATTCGTCAACT	55
KF008512R	CCCCGTATTTTCTCGGTC	
KF008526F	CACTGTGACTCAGTTTCGTTG	55
KF008526R	CGATTTTGAACCCTAACCG	
KF008536F	TGGTGGACGTCACTATGGA	55
KF008536R	CATGGTGCTTCCGACAAT	

PCR amplifications were performed using an M13-tailed primer according to method developed by Schuelke (2000). A tail M13 (-21), (TGAAAACGACGGCCAGT) universal sequence was added to the 5' end of each forward primers. PCR amplifications were performed in 20 µL reaction mixture containing 15 ng genomic DNA, 0.1 µM of each SSR primer, 0.1 µM labelled M13 (-21) universal primer, 0.2 mM dNTP, 1X DreamTaq Green Buffer (contains 2 mM MgCl₂ at a concentration of 2 mM) (Thermo Scientific, Waltham, MA, USA) and 0.5 U DreamTaq DNA Polymerase (Thermo Scientific, Waltham, MA, USA). Reaction mixtures without DNA were included as negative controls. PCR amplification was performed using the Bio-Rad T100 thermocycler device. The amplification program conditions involved an initial step of 3 min at 94 °C, followed by 35 cycles of 1 min at 94 °C, 1 min at 48-60°C, 2 min at 72 °C, followed by 8 cycles of 1 min at 94 °C, 1 min at 53 °C, 2 min at 72 °C, and a final step of 10 min at 72 °C. PCR products were controlled by %2 agarose gel electrophoresis.

The M13 (-21) was 5'-fluorescently tagged with HEX, FAM or ROX to facilitate multiplexing. A set of three PCR products (0.5 µL each) was mixed with 0.5 µL GeneScan-600 LIZ size standards (Applied Biosystems, USA) and 9.5 µL Hi-DiTM formamide (Applied Biosystems) and denatured at 95 °C for 5 min, chilled on ice and electrophoresed on the Applied Biosystems Prism 3500 Genetic Analyzer System (Applied Biosystems, USA). GENEMAPPER software v5.0 (Applied Biosystems, USA) was used to determine fragment size.

2.3. Statistical analysis

For each locus, the expected heterozygosity (He), observed heterozygosity (Ho) and the polymorphism information content (PIC) (Nei 1973) were calculated with PowerMarker V3.025 software (Liu & Muse 2005). The neighbour-joining (NJ) and UPGMA (unweighted pair-group method using arithmetic average) were used to construct and draw a dendrogram from the genetic similarity matrix by using the MEGA6 (Tamura et al. 2007) and PowerMarker software programs.

3. Result and Discussion

A total of 37 vetch accessions were analyzed using 18 SSR loci. Although the polymorphism rates of 18 loci were very high in the developed plants, only 8 showed polymorphism and used for analysis. Eight among the 13 markers developed by Bakır & Kahraman (2019) for lentil genetic analysis, namely Lc_MCu41a, Lc_MCu47, Lc_MCu71, Lc_MCu73, Lc_MCu75, Lc_MCu78, Lc_MCu83 and Lc_MCu85 could not be amplified, and Lc_MCu43 marker created multiple bands and discarded from the study. The polymorphism ratio of Lc_MCu11, Lc_MCu17, Lc_MCu95 and Lc_MCu97 markers developed in the same study was found similarly high. These results also showed that lentil SSR markers used in this study are transferable for vetch species and can use for genetic analysis in vetch. The rest of 5 SSR markers were chosen among the common vetch transferable 36 SSR markers developed for common vetch (Chung et al. 2013; Raveendar et al. 2015). Among these markers, while KF008505, KF008507, KF008512, and KF008526 loci were showed similar polymorphism; however, the KF008536 locus was not amplified.

A total of 35 alleles were generated from 37 vetch accessions using 8 SSR loci. The number of alleles per locus varied between 2 and 8, and the average locus value was found 4,38. The lentil SSR locus Lc_MCu17 had the highest number of alleles with 8 alleles (Table 3). The number of alleles per locus that we obtained was found to be low compared to the results obtained by Chung et al. (2013) in common vetch and Raveendar et al. (2015) in vetch species and but similar to the results obtained by Renzi et al. (2020) in hairy vetch and. However, the average locus value was similar to the results obtained by Renzi et al. (2020) in hairy vetch, but was lower than the results obtained by Chung et al. (2013) in common vetch and Raveendar et al. (2015) in vetch species. It is thought that the difference in the results obtained was due to the number of markers and the size of the population.

The expected heterozygosity value (H_e) obtained from this study ranged between 0.27 (Lc_MCu97 and Lc_MCu11) and 0.79 (Lc_MCu17) with an average of 0.49. The observed heterozygosity value (H_o) varied between 0.00 (Lc_MCu97 and Lc_MCu11) and 0.27 (KF008507) with the average 0.10 (Table 3). The value results of this study were similar to Chung et al. (2013), Raveendar et al. (2015), but were higher than Renzi et al. (2020). H_o values obtained from this study were found lower than Chung et al. (2013) and Raveendar et al. (2015).

The polymorphic information content (PIC) values varied between 0.23 (Lc_MCu11 and Lc_MCu97) and 0.77 (Lc_MCu17), and the average value was 0.44 (Table 3). The PIC values we obtained were found similar to the results obtained by Chung et al. (2013) and Raveendar et al. (2015).

Table 3- Genetic parameters for SSR markers

<i>Locus</i>	<i>n</i>	<i>He</i>	<i>Ho</i>	<i>PIC</i>
Lc_MCu11	2	0.27	0.00	0.23
Lc_MCu17	8	0.79	0.17	0.77
Lc_MCu95	4	0.34	0.08	0.30
Lc_MCu97	2	0.27	0.00	0.23
KF008505	6	0.61	0.17	0.53
KF008507	5	0.68	0.27	0.63
KF008512	5	0.48	0.03	0.41
KF008526	3	0.48	0.11	0.40
Total	35	3.92	0.83	3.52
Mean	4.38	0.49	0.10	0.44

n: number of alleles, *He*: expected heterozygosity, *Ho*: observed heterozygosity, *PIC*: polymorphism information content

In the dendrogram, it was seen that 37 vetch accessions were divided into two main groups. While the first group comprised lines (*V. ervilia*) collected from Turkey, the second group included cultivars registered in Turkey. The genetic similarities of the first group were also found far from other vetch species (Figure 1).

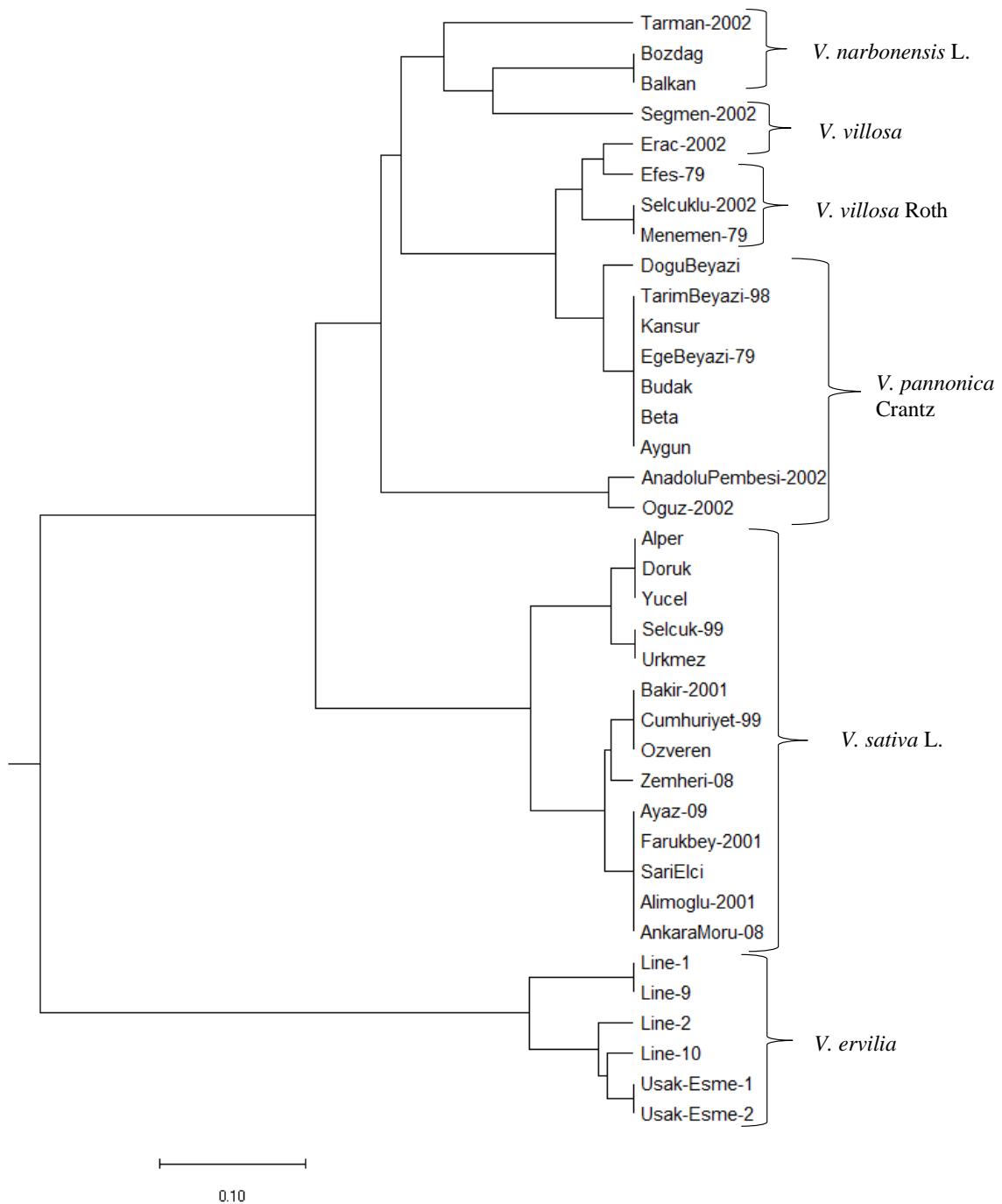


Figure 1- Genetic relationship dendrogram created using 8 polymorphic SSR markers in 37 vetch accessions

The majority of the cultivars, namely Beta, Aygun, Budak, Ege Beyazi-79, Kansur, Tarim Beyazi-98; Menemen-79, Selcuk-2002; Balkan, Bozdag; Alper, Doruk, Yucel; Selcuk-99, Urkmez; Bakir-2001, Cumhuriyet-99, Ozveren; Ayaz-09, Farukbey-2001, Sari Elci, Alimoglu-2001, Ankara Moru-08 were found to be genetically closer each other than the remaining accessions in the present study. This similarity may be due to the narrow structure of the vetch genome, and SSR markers used in this study might not be able to differentiate the narrow structure of the vetch genome, even if the markers provided an excellent distinction in the level of species. Furthermore, according to researchers in the research centers, the origin of registered cultivars might have arrived from the same resources to different research centers. The lowest genetic similarity rate among registered cultivars was observed between Dogu Beyazi and Alinoglu-2001, Alper, Ankara Moru-08, Ayaz-09, Doruk, Farukbey-2001, Yucel, Sari Elci (46%). Among the lines which were collected in Turkey, Line 1 and Line 9, as well as Usak-Esme 1 line, Usak-Esme 2 line was found genetically closer. The only morphological differences between Usak-Esme 1 and Usak-Esme 2 is seed coat colour. While the Usak-Esme 1 has cream seed coat colour, Usak-Esme 2 has blackish seed colour. This result also supports that SSR loci used in this study do not distinguish the narrow genetic structure of the vetch genome. The genetic similarity between registered

cultivars and collected lines varied between 0.32% (Balkan and Usak-Esme, Usak-Esme Black 2; Bozdag and Usak-Esme, Usak-Esme2; Zemheri-08 and Line 2) and 0.04% (Menemen-79 and Line 1, Line 9, Line 10) (Figure 1).

Potokina et al. (2000) used RAPD markers for genetic analysis of vetch genotypes. They reported that there are considerable differences between the genetic similarity value for inter- versus intra-specific genetic relationships as observed in the present study. However, Raveendar et al. (2015), on the other hand, stated that the dendrogram created using 36 SSR markers clustered in three groups but was not seen a clear division among *Vicia* accessions. Besides, a close genetic relationship was determined between *Vicia sativa* ssp. *nigra* and *V. sativa. cordata* (98%) using 8 RAPD markers (Agar et al. 2006). According to Potokina et al. (2002), the absence of a clear intra-species differentiation within *V. sativa* can be explained by three biological reasons; i) in the past, there has been a bottleneck of serious decrease in the number of individuals within the species, then the individuals spread rapidly to their existing areas without gaining distinct features, ii) the high probability of cross-pollination within the species (up to 10%; (Hanelt & Mettin 1989)) causes gene flow between populations and thus preventing the formation of different groups, iii) cross-pollination between seed materials brought to different regions by breeding studies and local materials can mask or eliminate area differences.

As a result, a genetic analysis of 37 vetch accessions was performed with 8 SSR markers showing polymorphism among a total of 18 SSR markers developed for common vetch and lentil. Besides, the rate of transferability of lentil markers grew for lentils to vetch species was also determined. According to the results, a high similarity rate was found between some cultivars. It has been determined that the markers used in the study make a relatively successful distinction among the species but were not shown difference within the high similarities species. It is thought that the results obtained from this study will contribute to molecular breeding studies and the conservation of genetic resources in vetch.

Acknowledgements

Thanks are extended to Betül-Ziya Eren Genome and Stem Cell Center of Erciyes University for their support throughout the experiments.

References

- Agar G, Adiguzel A, Baris O, Sengul M, Gulluce M, Sahin F & Bayrak O F (2006). FAME and RAPD Analysis of Selected *Vicia* Taxa from Eastern Anatolia, Turkey. In *Annales Botanici Fennici* (pp. 241-249). Finnish Zoological and Botanical Publishing Board
- Avcioglu R, Hatipoglu R & Karadag Y (2009). Vetches, Bitter Vetch and Black Lentils. In: TC. The Ministry of Agriculture and Forestry, General Directorate of Agricultural Production and Development. İzmir pp. 402-403
- Bakır M & Kahraman A (2019). Development of New SSR (Simple Sequence Repeat) Markers for Lentils (*Lens culinaris* Medik.) from Genomic Library Enriched with AG and AC Microsatellites. *Biochemical genetics* 57(2): 338-353. DOI: 10.1007/s10528-018-9893-2
- Bouabid S, Kourda H C, Boussaha A, Naceur M B & Khélil A Z (2018). Assessment of Genetic Diversity in Narbon vetch (*Vicia narbonensis* L.) Germplasm Using Morphological and Molecular Markers. *Crop and Pasture Science* 69(9): 904-914. DOI: 10.1071/CP18086
- Bozkurt M (2009). The Determination of Relationships of Some *Vicia* L. Species Growing in the Mediterranean and Central Anatolia by the Using Molecular Methods. Master thesis, University of Selcuk, Konya, Turkey. Thesis no:237523 in Council of Higher Education Thesis Center.
- Cheeke P R & Shull L R (1985). *Natural Toxicants in Feeds and Poisonous Plants*. AVI Publishing, Westport, CN.
- Chung J W, Kim T S, Sundan S, Lee S Y & Cho G T (2013). Development of 65 Novel Polymorphic cDNA-SSR Markers in Common Vetch (*Vicia sativa* subsp. *sativa*) Using Next-Generation Sequencing. *Molecules* 18: 8376-8392. DOI: 10.3390/molecules18078376
- Chung J W, Kim T S, Sundan S, Lee G A, Park J H, Cho G T, Lee H S, Lee J Y, Lee M C, Baek H J & Lee S Y (2014). New cDNA-SSR Markers in the Narrow-Leaved Vetch (*Vicia sativa* subsp. *nigra*) Using 454 Pyrosequencing. *Molecular Breeding* 33(3): 749-754. DOI: 10.1007/s11032-013-9980-3
- Davis P H (1970). *Flora of Turkey and the East Aegean Islands*. Edinburgh University Press, Edinburgh, pp. 328-369
- Davis P H & Plitmann U (1970). *Vicia* L. *Flora of Turkey and East Aegean Islands*. Edinburgh University Press, Edinburgh, Vol. 3
- De la Rosa L, López-Román M I, González J M, Zambrana E, Marcos-Prado T & Ramírez-Parra E (2021). Common Vetch, Valuable Germplasm for Resilient Agriculture: Genetic Characterization and Spanish Core Collection Development. *Frontiers in Plant Science* 12: 282. DOI: 10.3389/fpls.2021.617873
- Dutta S, Kumawat G, Singh B P, Gupta D K, Singh S, Dogra V, Gaikwad K, Sharma T R, Raje R S, Bandhopadhy T K, Datta S, Singh M N, Bashasab F, Kulwal P, Wanjari K B, Varshney R K, Cook D R & Singh N K (2011). Development of Genic-SSR Markers by Deep Transcriptome Sequencing in Pigeonpea [*Cajanus cajan* (L.) Millspaugh]. *BMC Plant Biology* 11(1): 17. DOI: 10.1186/1471-2229-11-17
- El Fatehi S, Béna G, Filali-Maltouf A & Ater M (2016). Genetic Diversity of Moroccan Bitter Vetch '*Vicia ervilia*'(L.) Willd. Landraces Revealed by Morphological and SSR Markers. *Australian Journal of Crop Science* 10(5): 717-725
- Ertus M M, Sabancı C O & Sensoy S (2016). Determination of Molecular Diversity with ISSR Markers in Some Cultivated Alfalfa (*Medicago sativa* L.) Ecotypes. *Journal of Field Crops Central Research Institute* 25(Special Issue-1): 249-254. DOI: 10.21566/tarbitderg.280503.
- Gençkan M S (1992). *Forage Crops Production*. Ege University Press, İzmir (in Turkish).
- Hanelt P & Mettin D (1989). Biosystematics of the Genus *Vicia* L. (Leguminosae). *Annual Review of Ecology Systematics* 20: 199-223. DOI: 10.1146/annurev.es.20.110189.001215
- Ibanez S, Medina M I & Agostini E (2020). *Vicia*: A Green Bridge to Clean up Polluted Environments. *Applied Microbiology and Biotechnology* 104(1): 13-21. DOI: 10.1007/s00253-019-10222-5
- Kartal G K, Senbek G, Karaca M & Acikgoz E (2020). Hybridization Studies in *Vicia sativa* Complex. *Euphytica* 216(2): 29. DOI: 10.1007/s10681-020-2566-3

- Kıran Y, Gedik O & Sahin A (2012). Karyological Investigate on Nine Species of *Vicia* Section from *Vicia* Genus Growing in Elazığ and Surrounding. *BEU. Journal of Science* 1(1): 11-18, 2012 (1)1: 11-18
- Kupicha F K (1976). The Infrageneric Structure of *Vicia* L. *R. Bot. Gard.* 32: 247-250
- Larbi A, Hassan S, Kattash G, Abd El-Moneim A M, Jammal B, Nabila H & Nakkoul H (2010). Annual Feed Legume Yield and Quality in Dryland Environments in North-West Syria: 2. Grain and Straw Yield and Straw Quality. *Animal Feed Science and Technology* 160: 90-97. DOI: 10.1016/j.anifeedsci.2010.07.004
- Lefort F, Lally M, Thompson D & Douglas G C (1998). Morphological Traits, Microsatellite Fingerprinting and Genetic Relatedness of A Stand of Elite Oaks (*Q. robur* L.) at Tullyally, Ireland. *Silvae Genetica* 47:5-6
- Liu K & Muse S V (2005). PowerMarker: An Integrated Analysis Environment for Genetic Marker Analysis. *Bioinformatics* 21: 2128-2129. DOI: 10.1093/bioinformatics/bti282
- Maul J, Mirsky S, Emche S & Devine T (2011). Evaluating a Germplasm Collection of the Cover Crop Hairy Vetch for Use in Sustainable Farming Systems. *Crop Science* 51(6): 2615-2625. DOI: 10.2135/cropsci2010.09.0561
- Mengoni A, Gori A & Bazzicalupo M (2000). Use of RAPD and Microsatellite (SSR) Variation to Assess Genetic Relationships Among Populations of Tetraploid Alfalfa, *Medicago sativa*. *Plant breeding* 119(4): 311-317. DOI: 10.1046/j.1439-0523.2000.00501.x.
- Nei M (1973). Analysis of Gene Diversity in Subdivided Populations. *The Proceedings of the National Academy of Science* 70: 3321-3323. DOI: 10.1073/pnas.70.12.3321
- Nunome T, Negoro S, Kono I, Kanamori H, Miyatake K, Yamaguchi H, Ohyama A & Fukuoka H (2009). Development of SSR Markers Derived from SSR-Enriched Genomic Library of Eggplant (*Solanum melongena* L.). *Theoretical and Applied Genetics* 119(6): 1143-1153. DOI 10.1007/s00122-009-1116-0
- O'Neill R, Snowdon R J & Kohler W (2003). Population Genetics Aspects of Biodiversity. *Progress in Botany* 64: 115-137. DOI: 10.1007/978-3-642-55819-1_7
- Ozsensoy Y & Kurar E (2012). Marker Systems and Applications in Genetic Characterization Studies. *Journal of Cell and Molecular Biology* 10(2): 11
- Potokina E, Vaughan D A, Eggi E E & Tomooka N (2000). Population Diversity of the *Vicia sativa* agg. (Fabaceae) in the Flora of the Former USSR Deduced from RAPD and Seed Protein Analyses. *Genetic Resources and Crop Evolution* 47(2): 171-183. DOI: 10.1023/A:1008756420011
- Potokina E, Blattner F, Alexandrova T & Bachmann K (2002). AFLP Diversity in the Common Vetch (*Vicia sativa* L.) on the World Scale. *Theoretical and Applied Genetics* 105(1): 58-67. DOI: 10.1007/s00122-002-0866-8
- Raveendar S, Lee G A, Jeon Y A, Lee Y J, Lee J R, Cho G T, Cho J H, Park J H, Ma K H & Chung J W (2015). Cross-Amplification of *Vicia sativa* subsp. *sativa* Microsatellites Across 22 Other *Vicia* Species. *Molecules*, 20: 1543-1550. DOI: 10.3390/molecules20011543
- Renna M, Gasmı-Boubaker A, Lussiana C, Battaglini L M, Belfayez K & Fortina R (2014). Fatty Acid Composition of the Seed Oils of Selected *Vicia* L. Taxa from Tunisia. *Italian Journal of Animal Science* 13:2: 3193. DOI: 10.4081/ijas.2014.3193
- Renzi J P, Chantre G R & Cantamutto M A (2017). Self-Regeneration of Hairy Vetch (*Vicia villosa* Roth) as Affected by Seedling Density and Soil Tillage Method in a Semi-Arid Agroecosystem. *Grass and Forage Science* 72(3): 524-533. DOI: 10.1111/gfs.12255
- Renzi J P, Chantre G R, Smýkal P, Presotto A D, Zubiaga L, Garayalde A F & Cantamutto M A (2020). Diversity of Naturalized Hairy Vetch (*Vicia villosa* Roth) Populations in Central Argentina as a Source of Potential Adaptive Traits for Breeding. *Frontiers in Plant Science* 11: 189. DOI: 10.3389/fpls.2020.00189
- Schuelke M (2000). An Economic Method for the Fluorescent Labelling of PCR Fragments. *Nature Biotechnology* 18: 233-234. DOI: 10.1038/72708
- Tamura K, Dudley J, Nei M & Kumar S (2007). MEGA4: Molecular Evolutionary Genetics Analysis (MEGA) Software Version 4.0. *Molecular Biology and Evolution* 24: 1596-1599. DOI: 10.1093/molbev/msm092
- Tautz D (1989). Hypervariability of Simple Sequence as a General Source for Polymorphic DNA Markers. *Nucl. Acids Res* 7: 6463-6470. DOI: 10.1093/nar/17.16.6463
- Unverdi M A (2007). Research on the Determination of Morphological and Molecular Diversity Among Some Vetch Cultivars Registered in Turkey. Master thesis, University of Cukurova, Adana, Turkey. Thesis no:178605 in Council of Higher Education Thesis Center.
- Van de Wouw M, Enneking D, Robertson L D & Maxted N (2001). Vetches (*Vicia* L.). In: Maxted N, Bennett S.J. (eds) *Plant Genetic Resources of Legumes in the Mediterranean*. *Current Plant Science and Biotechnology in Agriculture*, vol 39. Springer, Dordrecht. DOI: 10.1007/978-94-015-9823-1_8
- Zulkadir G & İdiküt L (2021). Genetic Diversity and Phylogenetic Relationships of Turkish Local Popcorn (*Zea mays everta*) Populations by Simple Sequence Repeats (SSRs). *Journal of Agricultural Sciences* 27(2): 170-178. DOI: 10.15832/ankutbd.626912



© 2022 by the author(s). Published by Ankara University, Faculty of Agriculture, Ankara, Turkey. This is an Open Access article distributed under the terms and conditions of the Creative Commons Attribution (CC BY) license (<http://creativecommons.org/licenses/by/4.0/>), which permits unrestricted use, distribution, and reproduction in any medium, provided the original work is properly cited.



Determining the Relationship of Evapotranspiration with Precipitation and Temperature Over Turkey

Mustafa KUZAY^{a*} , Mustafa TUNA^b , Mustafa TOMBUL^c 

^aEskişehir Osmangazi University, Department of Civil Engineering, 26040, Odunpazarı, ESKİŞEHİR

^bAnkara University, Faculty of Applied Sciences, Real Estate Development and Management Department, ANKARA

^cEskişehir Technical University, Department of Civil Engineering, 26555, Tepebaşı, ESKİŞEHİR

ARTICLE INFO

Research Article

Corresponding Author: Mustafa KUZAY, E-mail: kuzaymustafa@hotmail.com

Received: 15 June 2021 / Revised: 13 October 2021 / Accepted: 13 October 2021 / Online: 01 September 2022

Cite this article

KUZAY M, TUNA M, TOMBUL M (2022). Determining the Relationship of Evapotranspiration with Precipitation and Temperature Over Turkey. *Journal of Agricultural Sciences (Tarım Bilimleri Dergisi)*, 28(3):525-534. DOI: 10.15832/ankutbd.952845

ABSTRACT

Evapotranspiration (ET), which is a combination of the words evaporation and transpiration, is expressed as the sum of water due to water consumption and evaporation in plants. In this study, the NASA Drought Early Warning Systems Network Land Data Assimilation System model (FLDAS NOAH) was used to determine evapotranspiration data for the 2018-2019 water years (October 2017-September 2019) on Turkey. In addition, NASA Global Land Data Assimilation System (GLDAS NOAH) was used for temperature data. Total precipitation data with corrected error rates are taken from

MERRA-2 Model M2TMNXFLX. The relationship between the determined monthly total average evapotranspiration values and the monthly average precipitation and monthly average temperature values was determined by ArcGIS. It is important to examine the local evaporation and transpiration conditions in more detail in the regions where water resources planning will be made. The importance of water holding capacity in plants in determining agricultural and hydrological drought can be explained by evapotranspiration.

Keywords: *Drought, Hydrology, Climate Change, LDAS, FLDAS NOAH, GLDAS NOAH*

1. Introduction

One of the important hydrological processes in the planning of water resources is evaporation. Evaporation is defined as the transition of water from liquid to gas at temperatures below the boiling point of water, according to the World Meteorological Dictionary (WMO 2012). Evapotranspiration is one of the most important factors in understanding global hydrological budgets and is crucial to understanding accurate estimated water balance and developing efficient water resource management plans (Park & Choi 2015).

Water losses with the transformation into water vapor from the water surface are called evaporation, the loss of water from plants is called transpiration, and the loss of water from plants and the soil-water surface is called evapotranspiration. According to the studies conducted, approximately 90% of the water vapor in the atmosphere is due to evaporation and the remaining 10% is caused by the transpiration of plants (USGS 2019). Every water surface on earth is the source of water vapor in the atmosphere. Continuous evaporation occurs on almost all surfaces. Since the water cycle in the atmosphere is constant, the amount of water evaporating and the amount of water returning to the earth are approximately equal. However, this water cycle is not the same everywhere. On land surfaces, precipitation is more than evaporation, while on ocean surfaces, evaporation is more than precipitation (MGM 2019). However, in evaporation; meteorological factors (solar radiation, air vapor pressure, wind, temperature and pressure), geographical factors (latitude, altitude, aspect) and the quality and environment of the water are very important factors (MGM 2019).

Climate change is defined as "changes in the mean state and/or variability of the climate over a period of decades or more, regardless of the cause" (MGM 2019). The effects of climate change show not only with the increase in temperature, but also with consequences such as floods, drought, severe floods, increases in ocean and sea levels, increase in acidity in the oceans, which can develop suddenly and have great damage. For this reason, a detailed evaluation with a proactive method (long-term measurements, data analysis, trend analysis, spatial data analysis, etc.) is required. Evapotranspiration, precipitation, flow and temperature conditions are very important in the impact of climate change on the water cycle.

As an example of previous studies on this subject; remote sensing and spatial data has been performed for the evapotranspiration estimation and the result has been reached by correlating the experimental methods with the predicted values. Distributed hydrological model is used in the study. The process had a significant impact not only on the water table, but also on soil moisture and saturated water redistribution. This demonstrated the importance of modeling hydrological processes in mapping evapotranspiration. Drought indices based on thermal remote sensing of evapotranspiration have been evaluated. Drought indices based on remotely sensed evapotranspiration were determined by PALMER and SPI methods and a comparison was made between drought classifications reported in USDM from 2000 to 2009. As a result, it has been determined that potential evaporation can achieve clearer results in drought determination (Chen et al. 2005; Anderson et al. 2011).

Vegetation index and land surface temperature value were used to reflect these values measured at a measurement point where evapotranspiration and potential evapotranspiration are continuously measured at 10% error value to large areas. Between evapotranspiration and Vegetation Index, high accuracy has been determined in agricultural areas and natural ecosystems. In addition, modeling was supported by observations. It has been shown that this could be an achievable target if ground observations for measuring ET continue to improve. On the basis of the Priestley-Taylor equation combined with the time series and NDVI field, the surface temperature-Normalized Difference Vegetation Index feature area, MODIS (Medium Resolution Imaging Spectroradiometer) products and GLDAS (Global Land Data Assimilation System) were used to determine meteorological data. It was calculated using Tekesi River Basin as a pilot area. In addition, heat flow and Bowen Ratio were used for comparison between measurements. All these inputs were used to calculate ET and to identify anomalies. In addition, it has been determined that the effect of cloud formation during the day is very important for calculating ET (Glenn et al.2007). GLDAS data gave very successful results in areas where ET could not be determined by measurements (Du & Sun 2012).

Large-scale changes in continental water storage from satellite gravity data from the Gravity Recovery and Climate Experiment (GRACE) project were combined with river discharge data to obtain regionally average P-ET estimates. Additionally, the GRACE model has been compared and validated with the GLDAS. The GRACE model was compared seasonally and monthly to verify the model outputs (Swenson & Wahr 2006).

In this study, evapotranspiration losses due to precipitation and temperature were tried to be determined with spatial data and evaluations were made in certain periods in terms of hydrological and agricultural drought in Turkey.

2. Material and Methods

2.1. Study area

Turkey (36°-42° N, 26°-45° E) was chosen as the study area. More than half of the surface area of Turkey composed of a high area exceeding 1000 meters above sea level. Turkey elevation map was prepared using ArcGIS (Figure 1). Approximately thirty percent are covered with medium-high plains, plateaus and mountains, and ten percent with low areas. High and mountainous areas are mostly in the east of the country. The peak of Mount Ağrı, reaching 5137 meters, is the highest point in the country. The main wide plains are Konya Plain, Çukurova and Harran Plain. Kızılırmak, with a length of 1355 kilometers, is the longest river within the borders of the country. Covering an area of 3713 km², Lake Van is the largest natural lake in the country. Spreading over an area of 817 km², Atatürk Dam Lake is the largest artificial lake in the country. The total area of land masks is 770 760 km², and the total area of water areas is 9 820 km² (Cografya 2019).

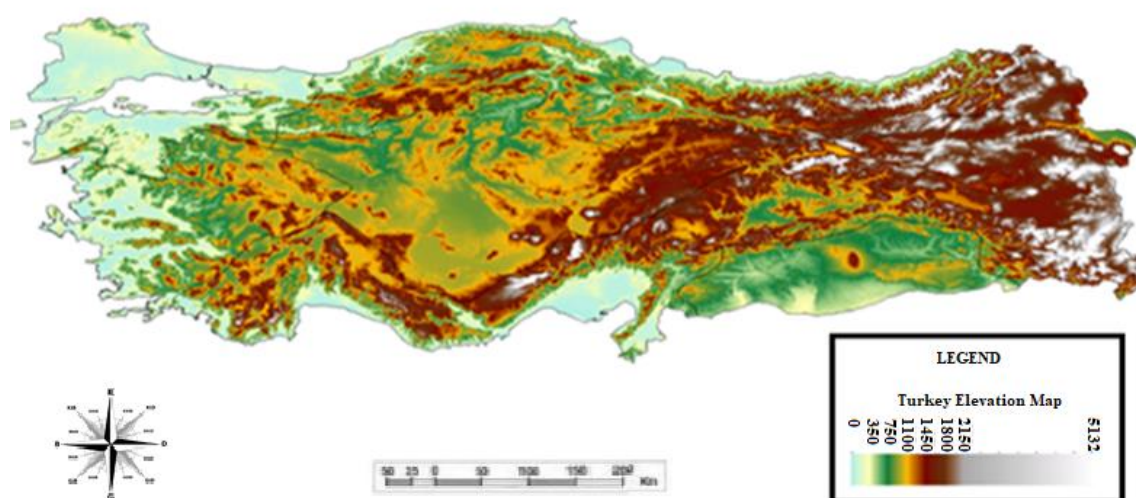


Figure 1- Elevation map of Turkey (SRTM DEM)

2.2. Spatial data

In this study, all data for the 2018-2019 water year period were obtained with Giovanni software (v 4.32), which is an environment in the NASA Earth Data system and where the resource (data line) is easily accessible. Giovanni provides an online environment for the display and analysis of geophysical parameters (GSFC 2019).

The NASA Geosciences Data and Information Services Center (GES DISC) provides access to LDAS datasets using multiple methods and the ability to sub-cluster spatial, temporal and variable. These datasets can also be accessed via Giovanni v4.32. Giovanni is an online application developed by GES DISC that allows researchers to quickly explore data so that spatial-temporal variability, anomalous conditions and patterns of interest can be analyzed online, optionally before downloading the data. Supported download formats include NetCDF, GeoTIFF and KMZ (Rodell et al. 2004).

Monthly Average Evapotranspiration was determined by FLDAS NOAH Model, monthly average surface temperature was determined by GLDAS NOAH Model and total precipitation with error rates corrected was determined by MERRA-2 M2TMNXFLX Model. Time-averaged maps of these three models were drawn every month in the 2018-2019 water years and compared. The FLDAS Model for ET (0.1 degree \times 0.1 degree spatial resolution) was also compared with the GLDAS Model (0.25 degree \times 0.25 degree spatial resolution) at specified times.

Evapotranspiration data, temperature data and precipitation data were determined with Giovanni software (v 4.32). Monthly Average Evapotranspiration was determined by FLDAS NOAH Model, monthly average surface temperature was determined by GLDAS NOAH Model and total precipitation with error rates corrected was determined by MERRA-2 M2TMNXFLX Model.

FLDAS is the Drought Early Warning Systems Network (FEWS NET) Land Data Assimilation System. FLDAS is a specific example of the NASA Land Information System (LIS) adapted to work with domains, data streams and monitoring. The aim of the FLDAS project is designed to enable more efficient use of limited available hydro-climatic observations and adopt them for routine use in FEWS NET decision support. The evapotranspiration unit in FLDAS is kg/m²s. However, with the operations in the GIS software, the evapotranspiration unit was converted to mm. The FLDAS model used in the study was taken as monthly data and it has a spatial scale of 0.1 degrees. FLDAS model has a data set for each latitude and longitude in global spatial scope from January 1981 until today. Data sets obtained from satellite measurements and atmospheric analyses are created in the model, and height description information is provided via SRTM. The definition of the ground is explained by the model defined by Reynolds, Jackson and Rawls in 1999. In addition, the land mask was defined with MODIS and land surface models were defined according to NOAH 3.6.1. (Loeser et al. 2020).

The purpose of the GLDAS is to obtain satellite and ground-based observational data products using advanced terrain surface modeling and data assimilation techniques to produce optimal areas of land surface states and fluxes. GLDAS processes terrain surface models, combines large amounts of observation-based data, operates globally at high resolutions and is capable of generating results in near real time. Simulations of NOAH, CLM, VIC, MOSAIC (spatial data models) and basin surface models have been supported by surface meteorological data and parameter maps that have been modelled and observed since 1948. In the GLDAS model, the evapotranspiration unit is kg/m²s. However, with the operations in the GIS software, the evapotranspiration unit was converted to mm. In addition, for the monthly average surface temperature used in the study, the GLDAS Model was used and Celsius was determined as the unit. The GLDAS model used in the study was taken as monthly data and has a spatial scale of 0.25 degrees. In the model, multiple data sets obtained from satellite measurements and atmospheric analyzes are provided since January 1948 at each latitude and longitude in all areas up to 60 degrees north. The height definition is explained by the GTOPO30 model, for the ground definition the model defined by Reynolds, Jackson and Rawls in 2000 is used. Land surface models are provided by Mosaic, CLM2, NOAH, VIC and Catchment LIS, and GRIB, NetCDF, ASCII and GDS are used as output format (Fang et al. 2009). GLDAS and FLDAS offer spatial data all over the world (Fang et al. 2009; Loeser et al. 2020).

Modern-Era Retrospective analysis for Research and Applications Version 2 (MERRA-2) is an atmospheric re-analysis using GEOS-5 as a result of combining Atmospheric Data Assimilation System (ADAS) and Goddard Earth Observation System Model. The MERRA project focuses on historical analysis for time scales of a wide variety of weather and climate events. It gives effective results all over the world with data assimilation. With this model (0.625 degree \times 0.5 degree), monthly average precipitation was obtained in mm (Reichle et al. 2017).

The average value for whole of Turkey is calculated as follows:

$$\overline{ET} = \frac{\sum ET_A \times A_{SR}}{A_T} \quad (1)$$

$$\overline{P} = \frac{\sum P_A \times A_{SR}}{A_T} \quad (2)$$

$$\bar{T} = \frac{\sum T_A \times A_{SR}}{A_T} \quad (3)$$

Where; \overline{ET} : average monthly evapotranspiration, ET_A : monthly evapotranspiration value, A_{SR} : spatial resolution area, A_T : total area, \bar{P} : average monthly precipitation, P_A : monthly precipitation value, \bar{T} : average monthly temperature, T_A : monthly temperature value.

3. Results and Discussion

Monthly average surface temperatures determined according to the GLDAS NOAH Model (spatial resolution of 0.25 degree×0.25 degree) between the water years 2018-2019 are given in Figure 2. The temperature scale is between -20 °C and 40 °C. The lowest temperature was seen in January and February, while the highest temperature was seen in August. The lowest temperature values were seen in January and February. The highest temperatures were seen in July and August (spatially).

Monthly average precipitation data were taken from the MERRA-2 (spatial resolution of 0.625 degree×0.5 degree) Model between the water years 2018-2019 and these data are given in Figure 3. The precipitation scale is between 0 and 455 mm. 455 mm/month value was seen in January 2019.

Monthly average evapotranspiration values determined according to the FLDAS NOAH Model (spatial resolution of 0.1 degree×0.1 degree) between the water years 2018-2019 are given in Figure 4. Evapotranspiration scale is between 0 and 225 mm. Evapotranspiration values started to increase in May and reached its highest value in July.

In addition to all these, a comparison was made between the two models in order to determine the evapotranspiration correctly with GIS software (FLDAS 0.1 degree and GLDAS 0.25 degree). A comparison was made according to average values from May to October in 2018. No significant difference was observed in the outcome, but it is clear that FLDAS NOAH with the higher spatial resolution gives accurate results at the areal scale.

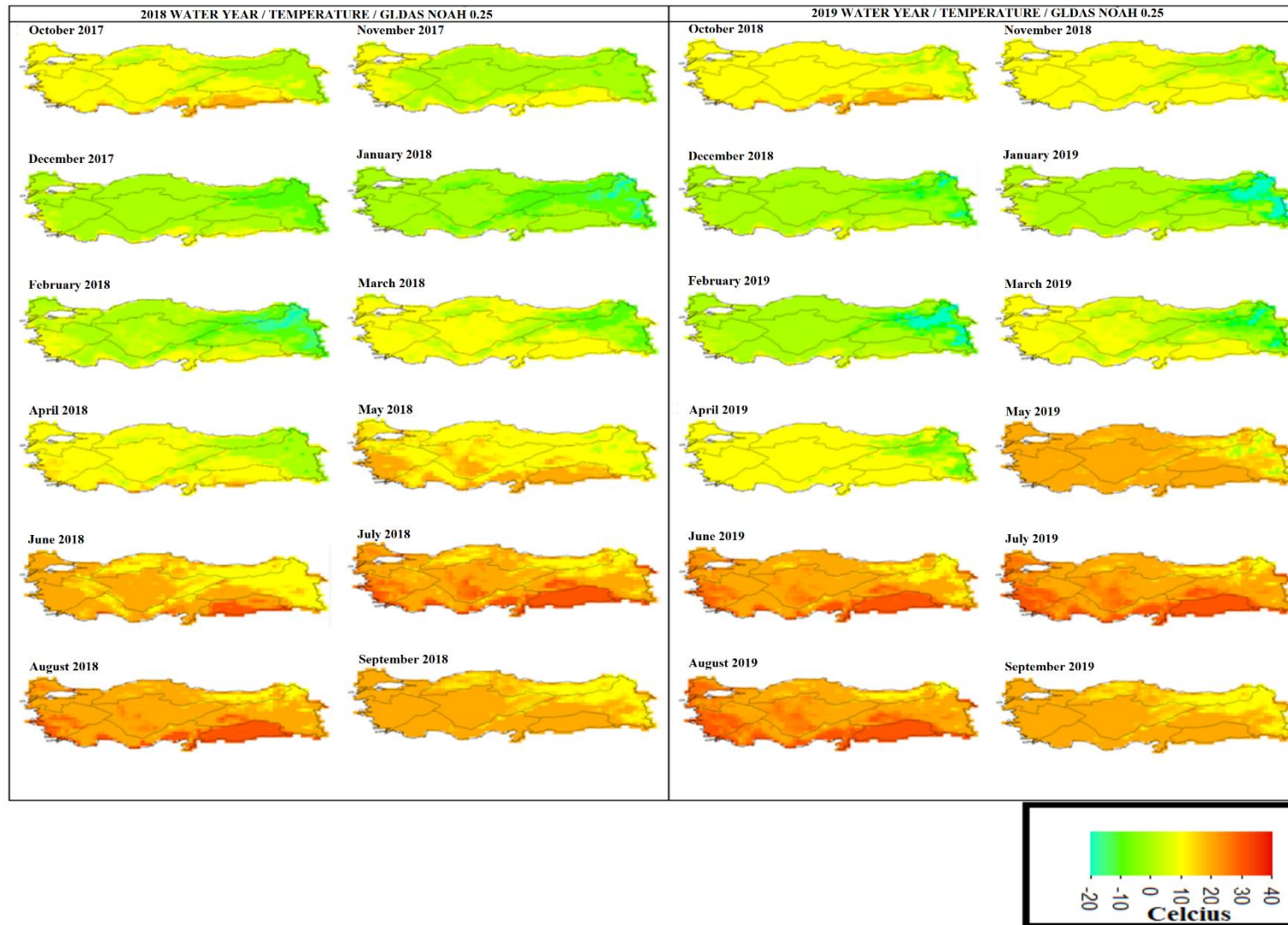


Figure 2- GLDAS NOAH Model monthly average surface temperature (°C)

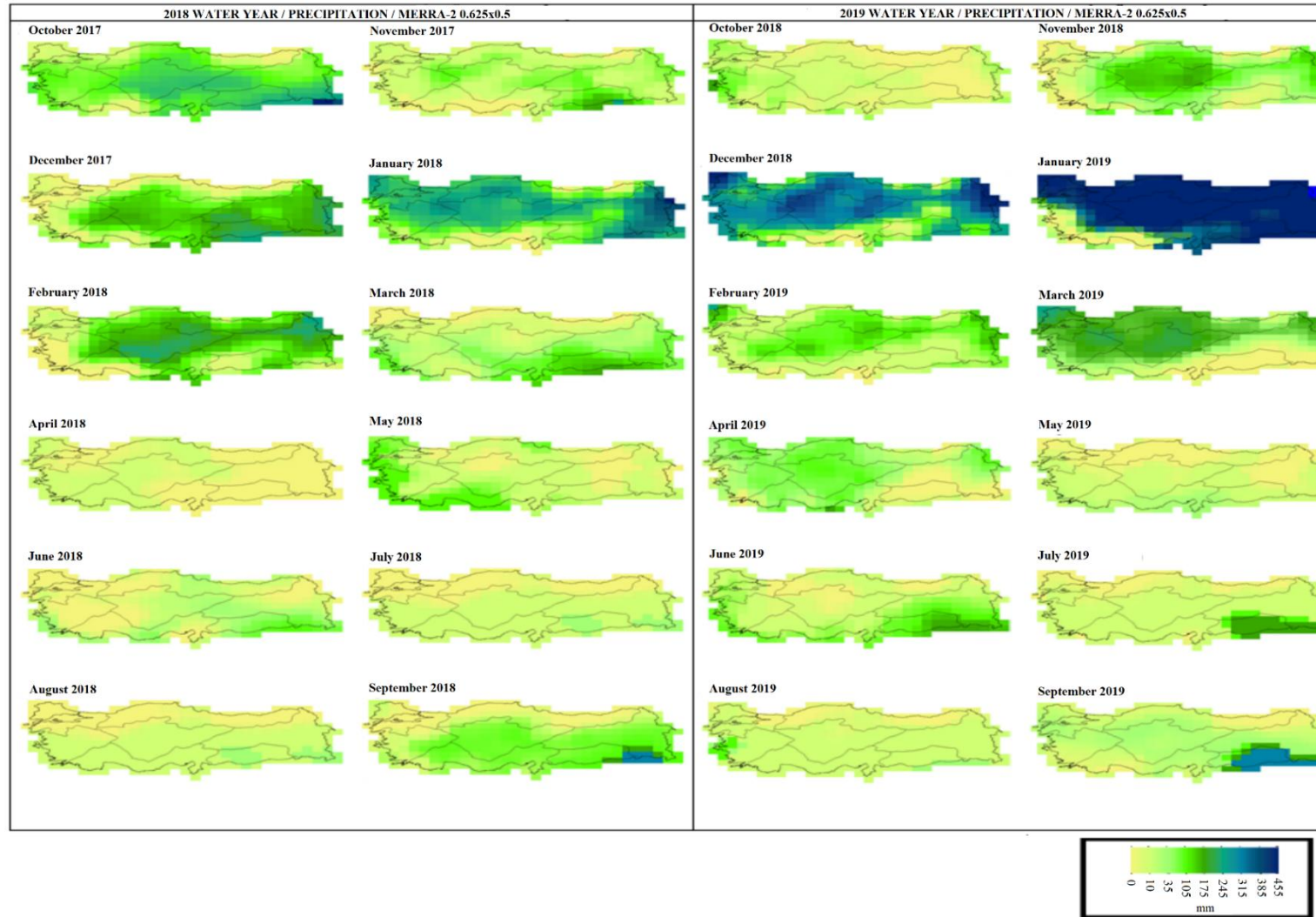


Figure 3- MERRA-2 Model monthly average precipitation (mm)

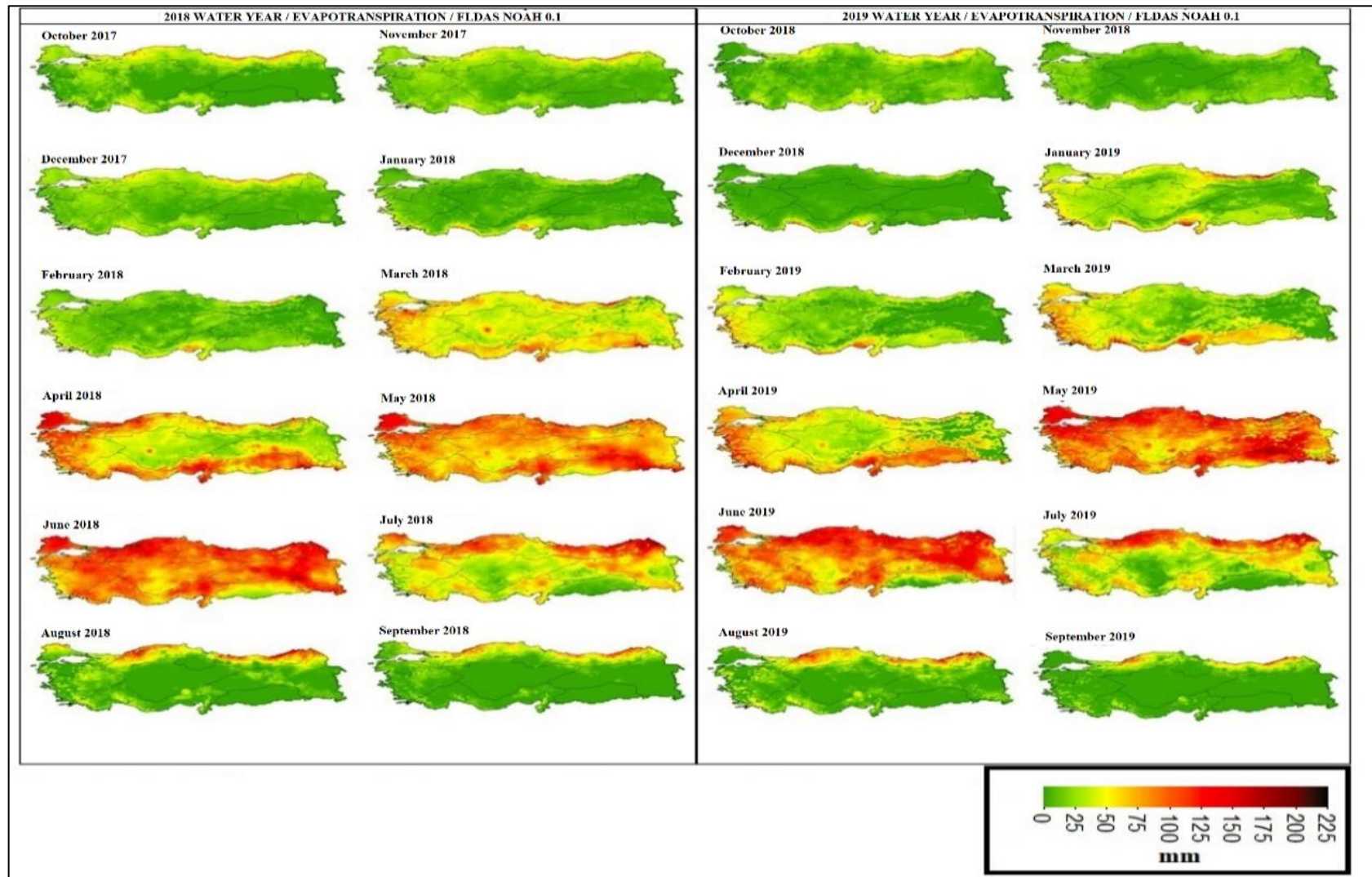


Figure 4- FLDAS NOAH Model monthly average evapotranspiration (mm)

The average value for whole of Turkey is calculated as follows:

$$\overline{ET} = \frac{\sum ET_A \times A_{SR}}{A_T} \quad (1)$$

$$\overline{P} = \frac{\sum P_A \times A_{SR}}{A_T} \quad (2)$$

$$\overline{T} = \frac{\sum T_A \times A_{SR}}{A_T} \quad (3)$$

Where; \overline{ET} : average monthly evapotranspiration, ET_A : monthly evapotranspiration value, A_{SR} : spatial resolution area, A_T : total area, \overline{P} : average monthly precipitation, P_A : monthly precipitation value, \overline{T} : average monthly temperature, T_A : monthly temperature value.

The findings obtained in the study, unit transformations and coloring of the maps were made with ArcGIS. Evapotranspiration values, temperature values and precipitation values calculated with spatial data from October 2017 to September 2019 are given in Table 1.

Table 1- Calculation of monthly averages using satellite images in Turkey

<i>Water Year</i>	<i>Month</i>	<i>Temperature (°C)</i>	<i>Precipitation (mm)</i>	<i>Evapotranspiration (mm)</i>
2018	October	16.37	72	35
	November	11.09	70	47
	December	6.88	65	45
	January	4.71	55	43
	February	6.53	60	61
	March	8.87	62	79
	April	14.67	33	108
	May	20.03	48	126
	June	23.99	39	160
	July	25.84	27	134
	August	27.21	28	113
	September	21.73	58	88
2019	October	16.98	60	71
	November	12.35	59	44
	December	6.63	82	53
	January	4.74	113	67
	February	6.32	62	71
	March	7.71	63	94
	April	13.12	46	112
	May	18.62	36	149
	June	23.85	35	163
	July	25.09	33	152
	August	26.22	41	91
	September	22.1	62	77

It is seen that there is a positive correlation between temperature and evapotranspiration in 2018-2019 water years (Figure 5). In addition, Figure 6 shows the inverse relationship between precipitation and evapotranspiration.

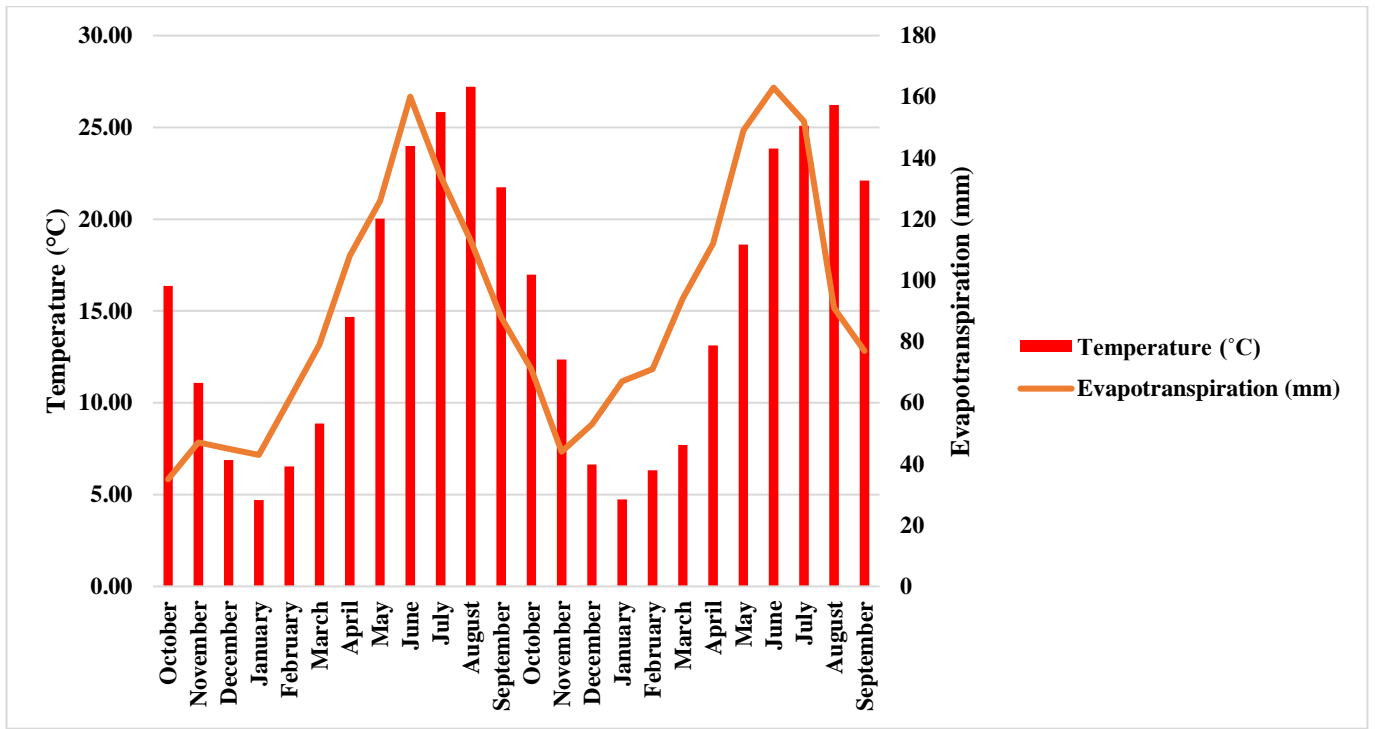


Figure 5- Relationship between evapotranspiration (FLDAS NOAH 0.1 degree) and temperature (GLDAS NOAH 0.25 degree) in 2018-2019 water years

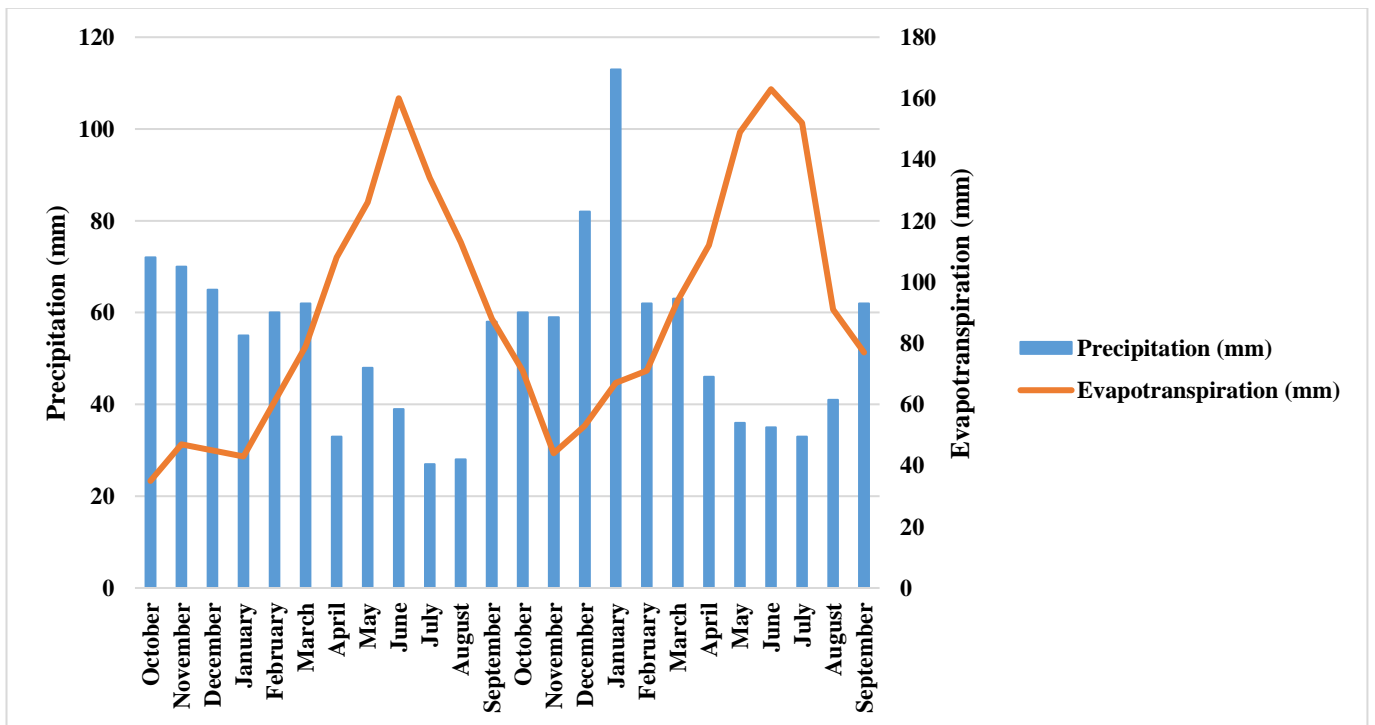


Figure 6- Relationship between evapotranspiration (FLDAS NOAH 0.1 degree) and precipitation (MERRA-2) in 2018-2019 water years

Values related to evapotranspiration on the land mask increase when the amount of precipitation on the surface flows and the temperature rises. In the 2018 water year, monthly average evapotranspiration reached a maximum level of 191 mm/month in July. Also, in the 2019 water year, the monthly average maximum value in July was determined as 175 mm/month. These maximum values are seen in northern Turkey. The reason for this is that the amount of flow increases, and the temperature rises significantly. However, when looking at the overall situation in Turkey in June, the average maximum evapotranspiration (163 mm/month) is reached. For this reason, the months of June and July can be considered critical according to the regions. In

addition, it is clearly evident that the temperature increased by 7-8 °C during these periods compared to the previous months. From May flow caused by rainfall and snowmelt is increasing in Turkey, and it is inevitable that the high value of evapotranspiration in June.

4. Conclusions

The change in the amount of evapotranspiration determined between 2018-2019 water years in the study is directly dependent on temperature, precipitation, and flow. For this reason, in addition to long or short-term heavy rains and temperature increases, which are seen as a result of climate change, the sudden change of evapotranspiration can be mentioned.

Considering all these results it can be said that temperature and evapotranspiration are directly proportional, and that evapotranspiration increases during the beginning of flow. In addition, evapotranspiration is as important as precipitation, flow, and temperature in determining the effects of climate change and water resources management.

Evapotranspiration (evaporation and transpiration) is very important in the hydrological cycle. It is inevitable to see the effects of climate change with evapotranspiration analysis based on long-term data. It is possible to reach clearer results by using regional analysis and quality spatial resolution satellite images when necessary. In addition, the reservoir evaporation conditions in dams, ponds, lakes or other structures to be supplied with water should be carefully examined. However, since this reservoir evaporation is open surface evaporation, it should never be confused with evapotranspiration. In addition, long-term satellite images, measurements and spatial data should be used for forecasting. In addition, this is a preliminary study. Datasets of 30-40 years (long term) are required to develop the scope of the study.

References

- Anderson M C, Kustas W P, Norman J M, Hain C R, Mecikalski J R, Schultz L, Gonzalez-Dugo M P, Cammalleri C, d'Urso G, Pimstein A. & Gao F (2011). Mapping daily evapotranspiration at field to continental scales using geostationary and polar orbiting satellite imagery. *Hydrology and Earth System Sciences* 15: 223-239. DOI: 10.5194/hess-15-223-2011
- Chen Y, Li X, Jing L, Shei P & Wen, D. (2005). Estimation of daily evapotranspiration using a two-layer remote sensing model. *International Journal of Remote Sensing* 26 (8): 1755-1762. DOI: 10.1080/01431160512331314074
- Coğrafya (2019). <http://www.cografya.gen.tr/siyasi/devletler/turkiye.htm>. Access date: 01.12.2019 (In Turkish)
- Du J P & Sun R (2012). Estimation of evapotranspiration for ungauged areas using MODIS measurements and GLDAS data. *Procedia Environmental Sciences* 13: 1718-1727. DOI: 10.1016/j.proenv.2012.01.165
- Fang H, Beaudoin H K, Rodell M, Teng W L, Vollmer B E (2009). Global land data assimilation system (GLDAS) products, services and application from NASA hydrology data and information services center (HDISC), In: ASPRS 2009 Annual Conference, Baltimore, Maryland, 8-13 March
- Glenn E P, Huete A R, Nagler P L, Hirschboeck K K & Brown P (2007). Integrating remote sensing and ground methods to estimate evapotranspiration. *Critical Reviews in Plant Sciences* 26(3): 139-168. DOI: 10.1080/07352680701402503
- GSFC (2019). Giovanni. Retrieved in November, 11, 2019 from <https://giovanni.gsfc.nasa.gov/giovanni>
- Loeser C, Rui H, Teng W, Ostrenga D, Wei J, McNally A, Jacob J P & Meyer D (2020). Famine early warning systems network (FEWS NET) land data assimilation system (LDAS) and other assimilated hydrological data at NASA GES DISC. In: American Meteorological Society Annual Meeting, 12 January, Boston.
- MGM (2019). Evaporation (Buharlaşma). Retrieved in November, 19, 2019 from <https://www.mgm.gov.tr/arastirma/buharlasma.aspx> (In Turkish)
- Park J & Choi M (2015). Estimation of evapotranspiration from ground-based meteorological data and global land data assimilation system (GLDAS). *Stochastic Environmental Research and Risk Assessment* 29: 1963-1992. DOI: 10.1007/s00477-014-1004-2
- Rodell M, Houser P R, Jambor U, Gottschalk J, Mitchell K, Meng C J, Arsenault K., Cosgrove B, Radakovich J, Bosilovich M, Entin J K, Walker J P, Lohmann D & Toll D (2004). The global land data assimilation system. *Bulletion of American Meteorological Society*, 85(3): 381-394
- Reichle R H, Draper C S, Liu Q, Giroto M, Mahanama S P, Koster R D & De Lannoy G J (2017). Assessment of MERRA-2 land surface hydrology estimates. *Journal of Climate* 30(8), 2937-2960. DOI: 10.1175/JCLI-D-16-0720.1
- Swenson S & Wahr J, (2006). Estimating large-scale precipitation minus evapotranspiration from GRACE satellite gravity measurements. *Journal of Hydrometeorology* 7(2): 252-270. DOI: 10.1175/JHM478.1
- USGS (2019). Evaporation and the Water Cycle. Retrieved in November, 20, 2019 from <https://water.usgs.gov/edu/watercycleevaporation.html>



© 2022 by the author(s). Published by Ankara University, Faculty of Agriculture, Ankara, Turkey. This is an Open Access article distributed under the terms and conditions of the Creative Commons Attribution (CC BY) license (<http://creativecommons.org/licenses/by/4.0/>), which permits unrestricted use, distribution, and reproduction in any medium, provided the original work is properly cited.



The Role of Different Planting Types in Mitigating Urban Heat Island Effects: A Case Study of Gaziantep, Turkey

Murat YÜCEKAYA^{a*} , Ahmet Salih GÜNAYDIN^b 

^aFaculty of Engineering and Architecture, Department of Landscape Architecture, Nevsehir Haci Bektas Veli University, Nevsehir, TURKEY

^bFaculty of Fine Arts and Design, Department of Landscape Architecture, Inonu University, Malatya, TURKEY

ARTICLE INFO

Research Article

Corresponding Author: Murat YÜCEKAYA, E-mail: muratyucekaya@nevsehir.edu.tr

Received: 16 March 2020 / Revised: 01 October 2021 / Accepted: 14 October 2021 / Online: 01 September 2022

[Cite this article](#)

YÜCEKAYA M, GÜNAYDIN A S (2022). The Role of Different Planting Types in Mitigating Urban Heat Island Effects: A Case Study of Gaziantep, Turkey. *Journal of Agricultural Sciences (Tarim Bilimleri Dergisi)*, 28(3):535-544. DOI: 10.15832/ankutbd.898103

ABSTRACT

The growth of cities and increase in their structural density lead to several problems. The most important of these is the formation of urban heat islands and the decrease in the bioclimatic comfort levels. This study focuses on the effect of different planting alternatives on bioclimatic comfort. In this context, different planting options with only leafy, only coniferous, leafy and coniferous at half at 4 m, 6 m, and 8 m intervals along with the current planting state of the study area in Gaziantep, Turkey were prepared. These plans were simulated with ENVI-met software. As a result of the study, coniferous plants were observed to have a cooling effect of approximately 2 °C – 2.5 °C compared to the leafy

ones. In the simulation results of the map obtained with coniferous mixed plants, it was determined that the cooling effect values of only coniferous and only leafy plants were at almost average. Relative humidity was 15% higher in the plan conducted with coniferous plants compared to leafy plants. It was about 8% higher than leafy ones in mixed planning. There was no significant change in wind speed maps. In the plans with 4 m intervals on average radiation temperature maps, the refreshing effect of the coniferous was more than the leafy. As a result of the study, it was found out that the highest cooling effect was achieved in the planting plan created at 4 m intervals using coniferous plants.

Keywords: ENVI-met, Outdoor thermal comfort, Urban heat island, Planting distance

1. Introduction

It is known that the development of cities has significantly changed the climate. The increase of impermeable surfaces such as roads and structures significantly reduces surface evaporation and increases heat storage. Thus, the temperature increased on the ground surface will be higher than the previous vegetative surface (Ca et al. 1998). Annual average temperature values are 2 - 3°C higher in urban areas than in rural areas (Miraboglu, 1977). The biggest difference in urban temperatures occurs on clear and still nights. During these times the temperature usually rises around 3-5 °C. Yet, it is still possible to observe an 8-10 °C increase. These temperature increases create the urban heat island (UHI)(Givoni 1998; Karatasou et al. 2006; Bowler et al. 2010).

Daily temperature averages are higher in urban areas with dense constructions compared to regions surrounded by rural areas (Oke 1987; Givoni 1998; Yu & Hien 2006). UHI effect is also increased due to the high heat capacity of impermeable surface materials. These materials absorb heat during the day and release it slowly at night. UHIs' methods of reducing negative energy and environmental impacts have become important research topics in sustainability programs (Wang & Akbari 2014).

Urban islands will affect more urban residents with the increase of urbanization. Therefore, it is reasonable to develop ecological approaches to reduce this effect in areas with thermal stress (Ca et al. 1998). The potential heating and cooling effect of urban green spaces is especially important in hot climates where the urban heat island creates undesirable effects (Potchter et al. 2006). Loss of vegetation cover increases UHI in cities. Increasing vegetation in urban areas will greatly reduce this effect. More comprehensive research is needed to determine the cooling effect levels of vegetation (Armson et al. 2012).

Vegetation has an impact on the climate of urban areas, and its deficiency can be significant cited as one of the main causes of urban heat island formation (Shashua-Bar et al. 2011; Wang & Akbari 2016). The vegetation lowers air temperature by remitting the heat from the sun through shading and evapotranspiration, and by converting the solar radiation into latent heat. Furthermore, the resulting low temperature leads to the reduction of long-wave radiation emitted from the ground and leaves, thus, expose people to a lower radiation load unlike artificial hard surfaces in the environment (Dimoudi and Nikolopoulou 2003).

Vegetation affects thermal energy balance both directly and indirectly in cities. It directly affects the microclimate by lowering the surface temperatures. Besides, it changes the urban climate by reducing the heat transfer in the occupied spaces and thus, the mechanical cooling loads and human-induced heat (Gunawardena et al. 2017). Replacing planted areas with low albedo materials is one of the causes of rising temperatures in urban environments. As a result, it can be considered as one of the main causes of urban heat island effects (Razzaghmanesh et al. 2016).

Plants can be used as an effective means to control sunrays. Various forms, textures, and colours of vegetative material offer endless benefits that add beauty to the landscape (Attia & Duchhart 2011). Control of solar radiation, increasing or decreasing temperature and humidity, creating or blocking the wind are the most important effects of plants on the climate (Altunkasa 1987). Areas covered with trees can protect the warm air by creating shade. Besides, grass areas that allow air flows can contribute to convection cooling (Bowler et al. 2010). Deciduous trees provide shade when they are leafy in summer, and allow sun rays to pass when they are leafless in winter, but have little effect on the winter wind. Coniferous trees provide shade in both summer and winter and reduce wind speed in winter (Brown 2010). In different studies, it has been determined that the use of trees and shrubs in urban areas can reduce the peak ambient temperature between 0.2 °C and 5 °C on average, with an average decrease of around 1 °C (Balany et al. 2020). For this reason, it is an important requirement to focus on green space planning at the planning stage (Yucekaya & Uslu 2020). In addition, planting designs in green areas are also considered extremely important in terms of bioclimatic comfort.

This study was conducted in Gaziantep province in Turkey. A public housing garden was identified as the study area. Along with the current planting status of the mass housing, plans were prepared in different combinations with only leafy plants, only coniferous plants, leafy and coniferous plants used in half, and the distance between the plants determined as 4 m, 6 m, and 8 m. This way, how the different plant compositions mentioned would affect the bioclimatic comfort was examined. In different studies, the contribution of plants to the climate has been investigated from different aspects. In this study, the effect of coniferous and leafy plants and the distance between these plants on bioclimatic comfort has been focused on, and in this respect, the study differs from the others.

The study objective is that the determination of planting options can provide optimum bioclimatic comfort conditions in regions with hot dry climate characteristics. Two specific questions were created in line with the main objective. These are i) Are bioclimatic comfort conditions achieved by using only coniferous plants, only leafy plants or both coniferous and leafy plants? ii) How is the bioclimatic comfort status affected when the distance between the plants is 4 m, 6 m, and 8 m? The answers to these questions constituted the analytical framework of the study

2. Material and Methods

Planting plans with only leafy, only coniferous, leafy and coniferous plants in half at 4 m, 6 m and 8 m intervals were created for the purpose. These alternative plans were simulated with ENVI-met software. Climatic findings obtained as a result of simulations were interpreted. The data focused on the determination of the change in the bioclimatic comfort state. It is considered that the study will provide important clues for vegetative designs to be created in hot dry climates.

2.1. Research case

The study was carried out in Gaziantep, Turkey. Gaziantep, located at the junction of the Mediterranean Region and the Southeastern Anatolia Region, lies between 36° 28' and 38° 01' E and 36° 38' and 37° 32' N (Provincial Directorate of Environment & Urbanism 2020). Located at an average altitude of 850 m, the city has a mixture of Mediterranean and continental climate (Sönmez 2012).

The study was conducted in Karatas neighbourhood in Şahinbey district of Gaziantep, the eighth-largest city in Turkey and a cosmopolitan city considering the population movement from Syria in recent years. While choosing the study area, it was considered that it should contain more than one building in the area, and green area size should allow for plant compositions that are intended to be created in the study. Therefore, a mass housing district with approximately 13000 m² area in Karatas was identified as the study area (Figure 1).

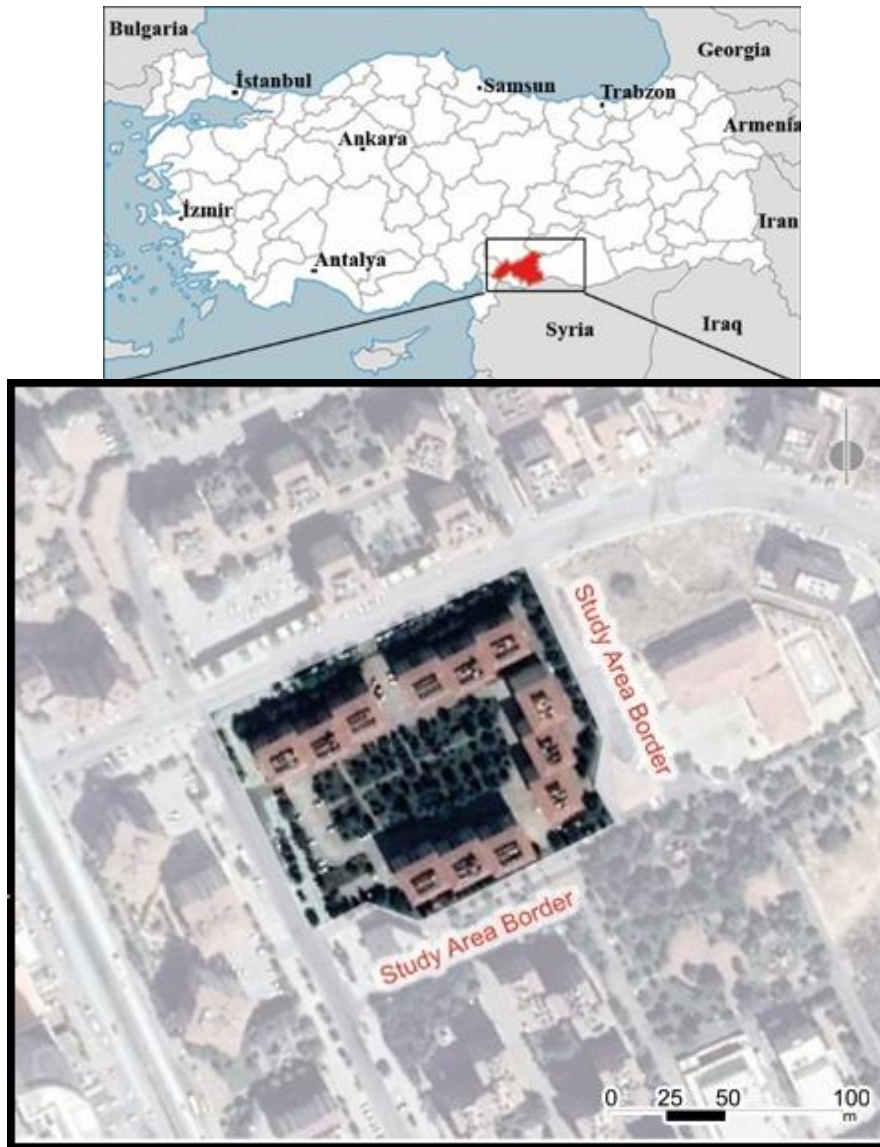


Figure 1- Study Area Location

The existing vegetation of the study area mainly consists of evergreen plants. Coniferous species *Cupressus sempervirens*, *Cupressus arizonica* and *Pinus brutia* are found in the green areas within the study area. Among these plants, there are *Malus floribunda*, *Morus alba*, *Pavlonia tomentosa* and *Acer negundo* as deciduous species.

2.2. ENVI-met

ENVI-met software solves partial differential equations and other steps in the model using the finite difference method. Indirectly, this reduces computational costs and allows the software to be used on normal computers (www.envimet.com).

ENVI-met software allows analysis of the effects of minor changes in urban design (plants, new residential areas, etc.) on microclimate under different medium-sized conditions (Bruse & Fleer 1998). ENVI-met is a holistic, three-dimensional, non-hydrostatic model for the simulation of surface-plant-air interactions. It is designed for microscale with a time frame of 24 to 48 hours with 0.5 to 10 m and 1 to 5 second time stages. This resolution allows us to analyse small-scale interactions between individual buildings, surfaces and plants (www.envi-met.com). The software can simulate air temperature, humidity, wind speed and direction, turbulence, radiation flow, gas and particle distribution and generate maps within this framework. Besides these structural configurations, ENVI-met includes some basic design characteristics. They are as follows; *i*) It simulates an entire climate system, including fluid mechanics, thermodynamics and pollutant distribution. *ii*) It provides the opportunity to create a high resolution model for analysing single buildings. *iii*) Simulates surface-plant-atmosphere processes such as the rate of photosynthesis (Ozkeresteci et al. 2003).

Different studies compared meteorological measurements performed in the field with the ENVI-met simulation software. The simulation results and actual measurement results were compared with the ones from those studies. As a result, it was

determined that the ENVI-met software gave results close to the real measurements, and the reliability of the software was proven (Bennet & Ewenz 2013; Elnabawi et al. 2013; Hedquist et al. 2009; Jeon et al. 2010; Lahme & Bruse 2013; Song & Park 2015).

2.3. Simulations

The place of vegetation cover was mapped in the study. In the next stage, alternative plans with 4 m, 6 m, and 8 m intervals were prepared (Figure 2).



Figure 2- Study area current status (top left), planting plans with 4 m (top right), 6 m (bottom left), and 8 m (bottom right) intervals

Long-term climate data (temperature (20 years), relative humidity (10 years), soil temperature (10 years), and cloudiness (10 years)) of Gaziantep province obtained from the General Directorate of Meteorology was used in the simulations. These data were used because 20 years of data were obtained for temperature and 10 years for relative humidity, wind speed and soil temperature. The simulations were made for 24 hours on June 21 when the solar radiation is at its highest, and the start time was determined as 06:00 in the morning. In addition, coniferous and leafy plants used in the simulation were similar in terms of their depth of roots (2 m), leaf density (medium intensity), and crown width (5 m). The data fed to the software are given in Table 1.

Table 1- Simulation Conditions

<i>Simulation area</i>	<i>Gaziantep / Turkey</i>
Modelling area dimensions	25x30x50
Grid Dimensions	2x2x2
Coordinates	37 ° 04' North Latitude / 37 ° 23' East Longitude
Simulation Date	21 June
Simulation Start Time	06:00
Simulation Duration	24 Hours
Temperature	Long Term Mean Temperature Min: 04:00 / 19.25 °C Max: 14:00 / 30.95 °C
Relative Humidity	Long Term Mean Relative Humidity Min: 11:00 / 20% Max: 02:00 / 52%
Wind Speed	Long Term Mean Wind Speed Direction: 245° Wind Speed: 1.1m/s
Soil Temperature	Long Term Soil Temperature Mean Initial Temperature: 24.65 °C
Road/Parking lot	Asphalt
Pedestrian Roads	Gray Concrete Coating
Green Area	10 cm Tall Medium Density Grass
Plants	Cylindric, Small Trunk, Sparse, Small (Plant Height: 5 m) Conic, Small Trunk, Sparse, Small (Plant Height:5 m)

Simulations were performed by defining 4 different interfaces in ENVI-met software. First, the drawings prepared were defined as grids in the Spaces section. Next, the simulation file was created by defining the climatic data of the region in the configwizard section. Then, the simulation process was initiated. Last, the simulated files were visualized in the Leonardo section and thus, climate maps were created.

ENVI-met software is capable of creating climate maps of many different meteorological parameters. The most important climatic variables related to bioclimatic conditions and temperature stress are air temperature, wind speed, relative humidity and average radiation temperature (Gaitani et al. 2007; Türkeş 2010; Walikewitz et al. 2015). Therefore, these 4 meteorological parameters were examined to bring the bioclimatic comfort to the desired levels.

The maps created as a result of simulations were interpreted. Then, how much area the temperature values occupy in the map in all of the air temperature maps was calculated as a percentage. A graph was created with the calculated values, and they were interpreted. Thus, the results of the study were simplified by showing all the air temperature values obtained on a single graphic.

2.4. Analytical framework

In the study, 10 different planting plans were created including;

1. Current status of the study area,
2. Three different combinations where only leafy plants were used at 4 m, 6 m and 8 m intervals,
3. Three different combinations where only coniferous plants were used at 4 m, 6 m and 8 m intervals,
4. Three different combinations where leafy and coniferous plants were used in half at 4 m, 6 m and 8 m intervals

While creating planting plans, main roads, structures, walkways, and other hard surfaces and green area sizes were considered fixed data sets. Variable datasets were distances between plants.

In the next stage of the study, 10 different planting plans were created firstly defined as grids with ENVI-met software.

3. Results and Discussion

At this stage of the study, planting plans that were previously described were created and their climatic simulations were made. A total of 40 maps obtained are given in figure 3. The legends of the maps are given in standard ranges to easily interpret the maps given in figure. Value ranges automatically given by ENVI-met software on air temperature, relative humidity, wind speed and mean radiant temperature maps. These values are the minimum and maximum values on the maps. They do not give any information about what values are on the map and in what proportions. However, it provides a rough framework on how vegetation alternatives affect the climate. Therefore, the values in this table are considered to be important in that they show the minimum and maximum limits.

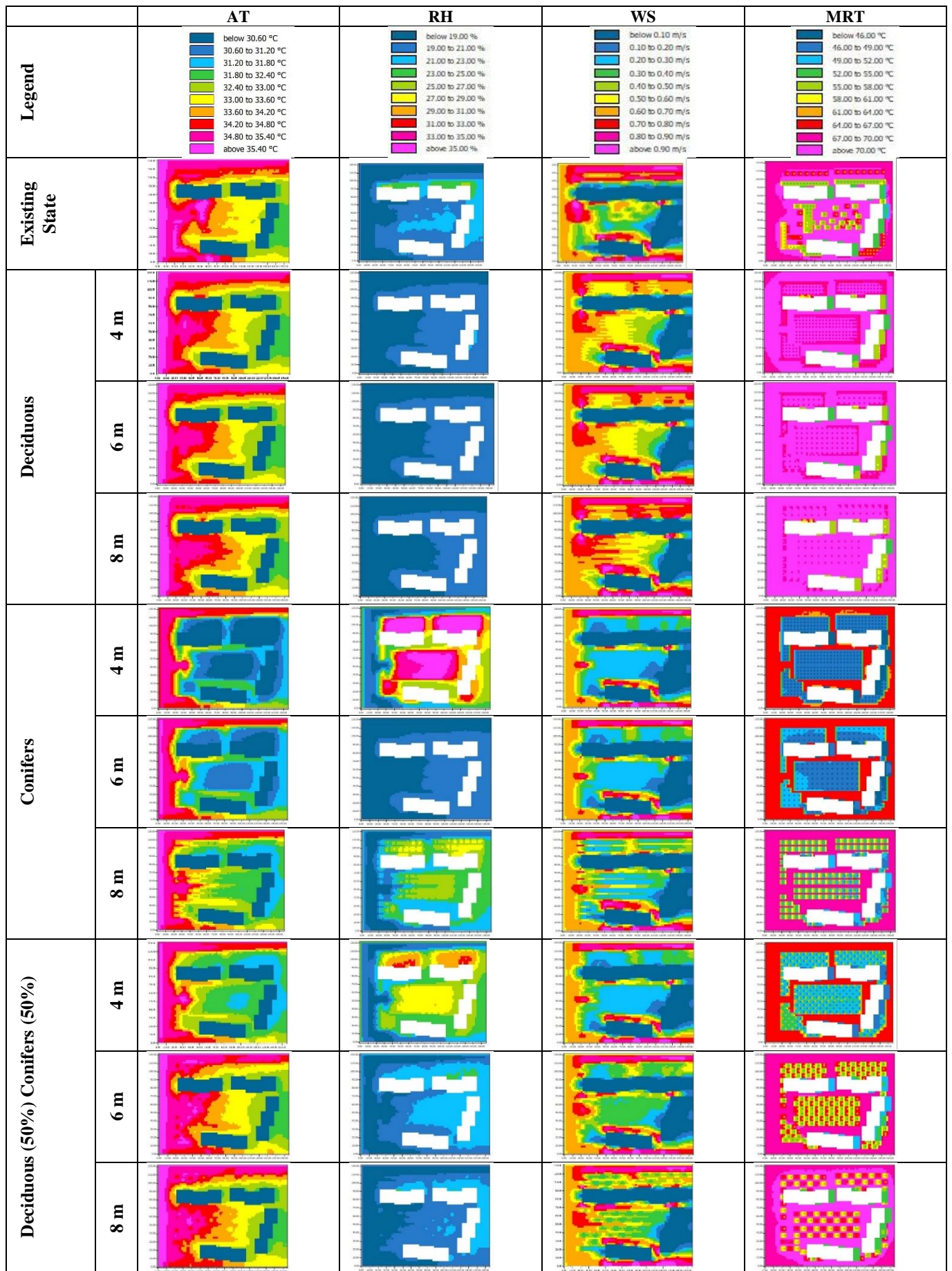


Figure 3- Analysis results (AT: Air Temperature, RH: Relative Humidity, WS: Wind Speed, MRT: Mean Radiant Temperature)

3.1. Air temperature

Coniferous plants showed approximately 2 °C – 2.5 °C more cooling effect than leafy ones. In the simulation results of the map obtained with coniferous mixed plants, it was found out that the cooling effect values of only coniferous and only leafy plants were almost average. There are no major differences between the current situation and the simulation results of only leafy ones. When the minimum and maximum values mentioned in the maps are examined, it is observed that while there is no big change in the minimum-maximum air temperature values in the maps with 4-6-8 m intervals, there is also a decrease in the temperature values as the intervals of coniferous plants decrease. A partial decrease was observed in the simulations of coniferous and leafy.

3.2. Relative humidity

The relative humidity is 15% higher in the plan made with coniferous plants compared to leafy ones. It was about 8% higher than leafy ones in mixed planning.

The minimum and maximum values were almost the same in 4-6-8 m simulations of leafy plants. While the minimum values did not change in coniferous simulations, there was a 5% difference between the moisture rates as the intervals decrease. While the simulations with 6-8 m intervals did not change much in mixed plans, a 7% increase in relative humidity was observed when the intervals were reduced to 4 m.

3.3. Wind Speed

Wind speed in coniferous and mixed plans was almost the same. It was approximately 0.2 m/s higher in leafy plans. Since there was no regular vegetation in the current situation, the wind speed also showed an uneven distribution.

There was no remarkable decrease or increase between minimum and maximum values in wind speed maps in any simulations.

3.4. Mean Radiant Temperature

The refreshing effect of the coniferous was about 18 °C higher than the leafy with plans at 4 m intervals. The high cooling effect of coniferous plants is clearly seen on the current situation map. In this map, the regions with coniferous plants have an 8 °C – 10 °C more cooling effect than leafy ones. The cooling effect is about 6 °C less than the coniferous in the mixed planting plan.

While there was no remarkable change in 4-6-8 m simulations of leafy plants, there were approximately 4 differences in the minimum and maximum values of simulations with 4 m intervals in the coniferous plants. The same situation with coniferous simulations applies to mixed plant simulations.

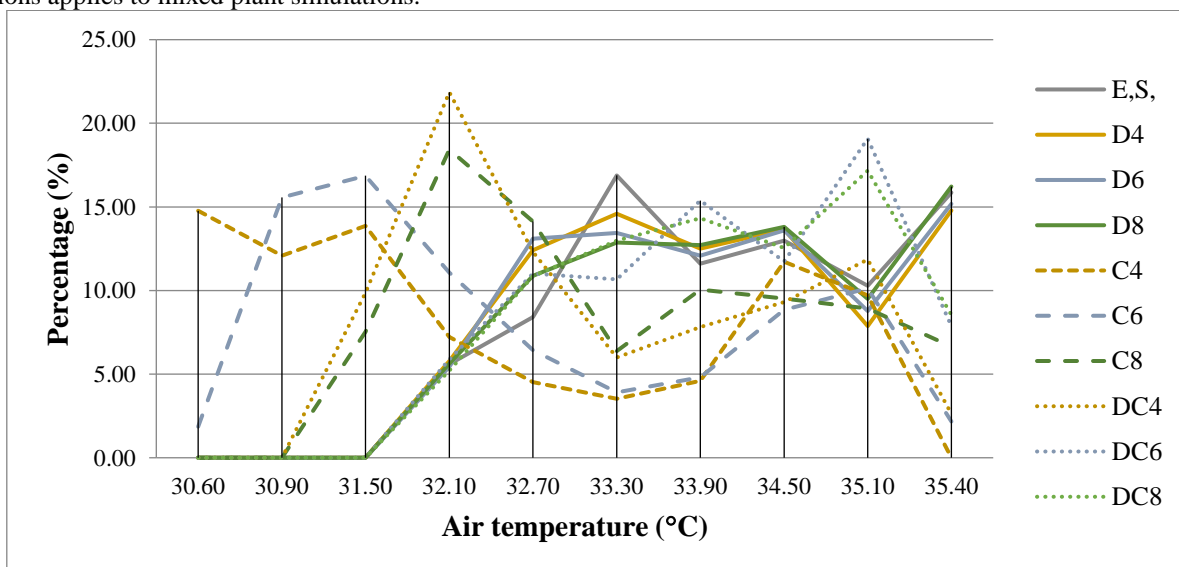


Figure 4- Air Temperature percentage distribution graph

(E.S: Existing State, D4: Deciduous 4 m interval, D6: Deciduous 6 m interval, D8: Deciduous 8 m interval C4: Conifer 4 m interval, C6: Conifer 6 m interval, C8: Conifer 8 m interval, DC4: Deciduous/Conifer 4 m interval, DC6: Deciduous/Conifer 6 m interval, DC8: Deciduous/Conifer 8 m interval)

The area covered by each temperature value in the map was calculated by measuring the percentage in the air temperature maps obtained as a result of the study. The obtained values were turned into a graph (Figure 4). It is seen in the graph that coniferous planting with 4 m intervals has high rates at low temperatures and low rates at high temperatures. Thus, it can be said that it creates the best cooling effect among all alternatives.

It is seen that the current situation and leafy planting alternatives create values close to each other. It can also be said that leafy vegetation creates the least cooling effect in the graph. As a result, it can be easily stated that the plants used are more important than the plant ranges.

It is observed that the cooling effect is more powerful especially in the close surroundings of the plants. In other words, there is a specific Cooling Effect Radius (CER) for each plant. There is approximately 1 °C difference in the asphalt areas with only coniferous plants compared to the areas with only leafy plants. Thus, it is necessary to build central refuges and correct planting options on the roads and pedestrian crossings to create a cooling effect, especially on asphalt surfaces. Thus, the plant CER is kept at an optimum level, and a cooling effect can be created in all areas possible.

When the plant intervals with coniferous plants are considered, it is observed that as plant intervals decrease, the temperature drops at 0.6 °C. Interval differences in leafy plants do not lead to a big change in temperature. There was about 0.6 °C differences at 4 - 6 m intervals in mixed planting. However, there was no significant change between 6 - 8 m intervals. Within the maps produced, the optimum cooling effect was provided by the planning with the coniferous plants at 4 m intervals. The cooling effect of this alternative planning was found to be approximately 2.5 °C higher than the current state of the area.

In their study, Wang and Akbari found out that significant decreases in temperature values can be seen with increasing tree size because larger shading areas in summer can reduce solar energy absorption (Wang & Akbari, 2016). This finding coincides with the finding that the cooling effect increases as the plant density increases.

Almost the same maps were obtained from the simulations of the leafy at 4 m interval and mixed plants at 8 m interval. Although the number of plants in the first case was twice that of the second case, the fact that the maps show similar characteristics in both cases can be seen as a clear indication that the refreshing effect of coniferous plants is much more than that of leafy plants.

With the intensification of the vegetation, the wind could not be canalized into the area and there was a decrease in wind speed. Coniferous plants appear to play a greater role than leafy plants in this decline. However, these decreases in wind speed were not at significant intervals.

It is seen that the humidity rate was high especially in the regions with plants but it was not much high in the other regions. It is seen that there was not a big change in relative humidity values in the simulation of only leafy plants, but in simulations with coniferous plants, the relative humidity rate increased as the plant intervals narrowed.

In the study, it was found out that the presence and density of green areas and keeping plant intervals low is an important factor in improving the climate. This finding is compatible with the findings by Chatzidimitriou & Yannas (2004), Yu & Hien (2006), Petralli et al. (2009), Latini et al. (2010), Yang et al. (2011), Ng et al. (2012), Papangelis et al. (2012), Srivanit & Hokao (2013), Yahia & Johansson (2014) which state that bioclimatic comfort will rise to higher levels as the density of vegetation is increased.

4. Conclusions

This study was designed to determine the effects of bioclimatic comfort by differentiating vegetation design in the mass housing area where different dwellings are located. As a result of the study, it was found out that the highest cooling effect was achieved in the planting plan made at 4 m intervals using coniferous plants.

While preparing planting plans in landscape architecture studies, plant intervals are determined according to the maximum crown width that each plant can reach. The findings here suggest that it may be appropriate to reduce the plant intervals when necessary to improve climatic comfort conditions. It will be a correct approach to use coniferous plants especially in median barrier plantings and to place them close to each other as much as possible.

This study concludes that residential gardens can partially minimize the negative effects of intensive housing on urban areas. This way, the bioclimatic comfort level can be increased to maximum levels only if house gardens are larger than certain standards. Thus, all actors including decision-makers and practitioners who play a role in urban design stages have a great responsibility.

Urban planning is a complex and multidisciplinary process that requires more and more actors to be in contact with each other. Higher data requirements, different methods, accepted assumptions and limitations in planning processes should be

carefully considered by the planners. Indicators evaluating bioclimatic comfort status represent very useful tools for planners and can provide sound foundations for local to develop policies that can create more liveable and healthy urban environments.

References

- Altunkasa, F (1987). A research on the determination of the principles in open and green spaces systems by using the bioclimatic data in Çukurova region (Unpublished Doctoral Thesis) (In Turkish). Cukurova University, Adana
- Armson D, Stringer P & Ennos A R (2012). The effect of tree shade and grass on surface and globe temperatures in an urban area. *Urban For. Urban Green* 11: 245–255. <https://doi.org/10.1016/j.ufug.2012.05.002>
- Attia, S., & Duchhart, I., (2011). Bioclimatic landscape design in extremely hot and arid climates. Presented at the Proceedings of 27th Conference of Passive and Low Energy Architecture (PLEA) 2011, PLEA, Belgium.
- Balany, F, Ng AW, Muttil N, Muthukumaran S& Wong M.S (2020). Green Infrastructure as an Urban Heat Island Mitigation Strategy—A Review. *Water* 12: 3577. <https://doi.org/10.3390/w12123577>
- Bennet MG& Ewenz & CM (2013). Increased Urban Heat Island Effect Due To Building Height Increase. Presented at the 20th International Congress on Modeling and Simulation, Adelaide, Australia pp. 2242–2246
- Bowler D E, Buyung-Ali L, Knight TM& Pullin AS (2010). Urban greening to cool towns and cities: A systematic review of the empirical evidence. *Landsc. Urban Plan* 97: 147–155. <https://doi.org/10.1016/j.landurbplan.2010.05.006>
- Brown R D (2010). *Design with microclimate: the secret to comfortable outdoor spaces*. Island Press, Washington.
- Bruse M& Fleer H (1998). Simulating surface–plant–air interactions inside urban environments with a three dimensional numerical model. *Environ. Model. Softw* 13: 373–384. [https://doi.org/10.1016/S1364-8152\(98\)00042-5](https://doi.org/10.1016/S1364-8152(98)00042-5)
- Ca V T, Asaeda T& Abu EM (1998). Reductions in air conditioning energy caused by a nearby park. *Energy Build* 29: 83–92. [https://doi.org/10.1016/S0378-7788\(98\)00032-2](https://doi.org/10.1016/S0378-7788(98)00032-2)
- Chatzidimitriou A& Yannas S (2004). Microclimatic Studies of Urban Open Spaces in Northern Greece. Presented at the Plea2004 - The 21st Conference on Passive and Low Energy Architecture, Eindhoven, The Netherlands pp. 1–6
- Dimoudi A& Nikolopoulou M (2003). Vegetation in the urban environment: microclimatic analysis and benefits. *Energy Build* 35: 69–76. [https://doi.org/10.1016/S0378-7788\(02\)00081-6](https://doi.org/10.1016/S0378-7788(02)00081-6)
- El nabawi M, Hamza N& Dudek S (2013). Use and Evaluation of the ENVI-met Model for Two Different Urban Forms in Cairo, Egypt: Measurements and Model Simulations. Presented at the 13th Conference of International Building Performance Simulation Association, France pp. 2800–2806
- Gaitani N, Mihalakakou G& Santamouris M (2007). On the use of bioclimatic architecture principles in order to improve thermal comfort conditions in outdoor spaces. *Build. Environ* 42: 317–324. <https://doi.org/10.1016/j.buildenv.2005.08.018>
- Givoni B (1998). *Climate considerations in building and urban design*. Van Nostrand Reinhold, New York.
- Gunawardena KR, Wells M J& Kershaw T (2017). Utilising green and bluespace to mitigate urban heat island intensity. *Sci. Total Environ.* (584–585): 1040–1055. <https://doi.org/10.1016/j.scitotenv.2017.01.158>
- Hedquist B C, Brazel A J, Sabatino S D, Carter W& Fernando H J S (2009). Phoenix Urban Heat Island Experiment: Micrometeorological Aspects. Presented at the Proceedings of the Eighth Conference on the Urban Environment, AMS 89th Annual Meeting, Phoenix, Arizona pp. 1–6
- Jeon M Y, Kim J O, Bae S H, Leigh SB& Kim T Y (2010). A Study on outdoor thermal comfort of apartment complex. Seoul, Korea pp. 151–154
- Karatasou S, Santamouris M& Geros V (2006). Urban Building Climatology, in: *Environmental Design of Urban Buildings: An Integrated Approach*. Earthscan, London ; Sterling, VA p. 322
- Lahme E& Bruse M (2013). Microclimatic Effects of a Small Urban Park in a Densely Build up Area: Measurements and Model Simulations. Presented at the ICUC5, Lodz.
- Latini G, Cocci Grifoni R& Tascini S (2010). Thermal Comfort and Microclimates in Open Spaces. Presented at the Buildings XI: Thermal Performance of Exterior Envelopes of Whole Buildings, ASHRAE.
- Miraboglu M (1977). Air Pollution Preventing Effect of Forest (In Turkish). İstanbul University Faculty of Forestry, İstanbul; Çelikkilt Matbaası.
- Ng E, Chen L, Wang Y& Yuan C (2012). A study on the cooling effects of greening in a high-density city: An experience from Hong Kong. *Build. Environ* 47: 256–271. <https://doi.org/10.1016/j.buildenv.2011.07.014>
- Oke T R (1987). *Boundary layer climates*, 2nd ed. ed. Methuen, London ; New York.
- Ozkeresteci I, Crewe K, Brazel A J& Bruse M (2003). Use and Evaluation of the ENVI-met Model for Environmental Design and Planning: An Experiment on Linear Parks. Presented at the Proceedings of the 21st International Cartographic Conference (ICC), Document Transformation Technologies, Durban, South Africa pp. 402–409
- Papangelis G, Tombrou M, Dandou A& Kontos T (2012). An urban “green planning” approach utilizing the Weather Research and Forecasting (WRF) modeling system. A case study of Athens, Greece. *Landsc. Urban Plan* 105: 174–183. <https://doi.org/10.1016/j.landurbplan.2011.12.014>
- Petralli M, Massetti L& Orlandini S (2009). Air Temperature Distribution in an Urban Park: Differences Between Open-Field and Below a Canopy. Presented at the e Urban on Conference International seventh T, Yokohama, Japan.
- Potchter O, Cohen P& Bitan A (2006). Climatic behavior of various urban parks during hot and humid summer in the mediterranean city of Tel Aviv, Israel. *Int. J. Climatol* 26: 1695–1711. <https://doi.org/10.1002/joc.1330>
- Provincial Directorate of Environment & Urbanism (2020). Gaziantep Province 2019 Environmental Status Report (In Turkish). Republic of Turkey Gaziantep Governorship Provincial Directorate of Environment and Urbanization, Gaziantep.
- Razzaghmanesh M, Beecham S& Salemi T (2016). The role of green roofs in mitigating Urban Heat Island effects in the metropolitan area of Adelaide, South Australia. *Urban For. Urban Green* 15: 89–102. <https://doi.org/10.1016/j.ufug.2015.11.013>
- Shashua-Bar L, Pearlmutter D& Erell E (2011). The influence of trees and grass on outdoor thermal comfort in a hot-arid environment. *Int. J. Climatol* 31: 1498–1506. <https://doi.org/10.1002/joc.2177>
- Song B& Park K (2015). Contribution of Greening and High-Albedo Coatings to Improvements in the Thermal Environment in Complex Urban Areas. *Adv. Meteorol* 2015: 1–14. <https://doi.org/10.1155/2015/792172>
- Sönmez E (2012). *Gaziantep in Terms of Settlement Site Selection and Spatial Development* (In Turkish). Özserhat Publishing, Malatya.

- Srivanit M& Hokao K (2013). Evaluating the cooling effects of greening for improving the outdoor thermal environment at an institutional campus in the summer. *Build. Environ* 66: 158–172. <https://doi.org/10.1016/j.buildenv.2013.04.012>
- Türkeş M (2010). *Climatology and Meteorology* (In Turkish). Kriter Publishing, İstanbul.
- Walikewitz N, Jänicke B, Langner M, Meier F& Endlicher W (2015). The difference between the mean radiant temperature and the air temperature within indoor environments: A case study during summer conditions. *Build. Environ* 84: 151–161. <https://doi.org/10.1016/j.buildenv.2014.11.004>
- Wang Y& Akbari H (2014). 3D Simulation Analysis of Urban Micro-Climates to Inform Heat Island Mitigation Policies in Cold Climates. Presented at the Summer Study on Energy Efficiency in Buildings, ACEEE, Washington, D.C. pp. 353–364
- Wang Y& Akbari H (2016). The effects of street tree planting on Urban Heat Island mitigation in Montreal. *Sustain. Cities Soc.* 27: 122–128. <https://doi.org/10.1016/j.scs.2016.04.013>
- Yahia M W& Johansson E (2014). Landscape interventions in improving thermal comfort in the hot dry city of Damascus, Syria—The example of residential spaces with detached buildings. *Landsc. Urban Plan* 125: 1–16. <https://doi.org/10.1016/j.landurbplan.2014.01.014>
- Yang F, Lau S S Y& Qian F (2011). Thermal comfort effects of urban design strategies in high-rise urban environments in a sub-tropical climate. *Archit. Sci. Rev* 54: 285–304. <https://doi.org/10.1080/00038628.2011.613646>
- Yu C& Hien W N (2006). Thermal benefits of city parks. *Energy Build* 38: 105–120. <https://doi.org/10.1016/j.enbuild.2005.04.003>
- Yucekaya M& Uslu C (2020). An analytical model proposal to design urban open spaces in balance with climate: A case study of Gaziantep. *Land Use Policy* 95: 104564. <https://doi.org/10.1016/j.landusepol.2020.104564>
- www.envimet.com , date of access: 17.06.2021



© 2022 by the author(s). Published by Ankara University, Faculty of Agriculture, Ankara, Turkey. This is an Open Access article distributed under the terms and conditions of the Creative Commons Attribution (CC BY) license (<http://creativecommons.org/licenses/by/4.0/>), which permits unrestricted use, distribution, and reproduction in any medium, provided the original work is properly cited.



Effects of Tillage Method, Drainage Management and Temporal Variability on Some Soil Physical Properties and Organic Matter

Mahmoud SHABANPOUR^a , Salman FEKRI^a , Iraj BAGHERI^b , Sayed Hossein PAYMAN^b ,
Fatemeh RAHIMI-AJDADI^{b*}

^aDepartment of Soil Sciences, Faculty of Agricultural Sciences, University of Guilan, P.O. box: 41996-13776, Rasht, IRAN

^bDepartment of Biosystems Engineering, Faculty of Agricultural Sciences, University of Guilan, P.O. box: 41996-13776, Rasht, IRAN

ARTICLE INFO

Research Article

Corresponding Author: Fatemeh RAHIMI-AJDADI, E-mail: rahimi_a@guilan.ac.ir

Received: 08 January 2021 / Revised: 07 July 2021 / Accepted: 14 July 2021 / Online: 01 September 2022

Cite this article

SHABANPOUR M, FEKRI S, BAGHERI I, PAYMAN S H, RAHIMI-AJDADI F (2022). Effects of Tillage Method, Drainage Management and Temporal Variability on Some Soil Physical Properties and Organic Matter. *Journal of Agricultural Sciences (Tarim Bilimleri Dergisi)*, 28(3):545-554. DOI: 10.15832/ankutbd.856328

ABSTRACT

Tillage is one of the most important practices affecting soil physical and hydraulic properties. Its effects may vary intensely according to the tillage method. This study aims to evaluate the effects of tillage methods (B1: moldboard plow+disk harrow, B2: moldboard plow+rotary tiller and B3: chisel plow+disk harrow), drainage (A1: subsurface drainage and A2: non-drainage) methods and temporal variability (T1: after planting and T2: after harvesting) on physical properties and organic matter of a clay loam soil under winter-wheat crop. The experiment was conducted in split-plot in time statistical design. Soil bulk density, soil particle density, aeration porosity, aggregate mean weight diameter (MWD), saturated moisture content and water infiltration rate were determined at two different times of T1 and T2. Results revealed that the tillage method had significant effect on organic matter content, such that the highest (1.35%) values were observed in chisel treatment. Tillage effect was significant on saturated moisture content, MWD, aeration porosity and infiltration

rate. The effect of time was significant on all investigated factors. The effect of drainage was significant on MWD and infiltration rate. Evaluating the effects of tillage and drainage indicated that the contribution of drainage on changing MWD is higher than the tillage methods. Further, in non-drainage condition, the tillage method had a significant effect on aeration porosity ($P < 0.05$), so that moldboard plow makes much more aeration porosity (25.48%) compared to chisel (17.17%). Conversely, the MWD of moldboard plow (2.4 mm) was significantly lower than that of chisel (2.8 mm), in non-drainage conditions ($P < 0.05$). According to the result, the lowest and highest values of MWD were obtained in the treatments of A1B1 and A2B3, respectively. The application of chisel is not recommended in no-drained areas having high level groundwater, because of the highest saturated moisture content and MWD along with the lowest aeration porosity compared to moldboard plow.

Keywords: Aeration porosity, Infiltration rate, Mean weight diameter, Moldboard plow

1. Introduction

Soil is one of the slowly renewable natural resources that its conservation or degradation depends on agricultural management (Mirzaee & Mahmoodabadai 2014). The main duty of soil is to provide optimum conditions for plant development and growth that is defined as soil fertility or soil quality (Demir & Isik 2020), which greatly relates to the soil structure (Abbaspour-Gilandeh & Rahimi-Ajdadi 2016). Fundamentally, granular soil structure is the most desirable (Rahimi-Ajdadi et al. 2016) and it is achieved by tillage practices that is considered as the key step in agricultural productions. Tillage is performed through soil physical disturbance in order to provide a proper seedbed, eliminate soil compaction and weed control with the aim of increasing crop production (Al-Suhaibani & Ghaly 2013). It is also affecting soil hydraulic and physical properties (Jabro et al. 2009) including bulk density, total porosity, pore size distribution, soil resistance against infiltration, water storage, infiltration rate, hydraulic conductivity, and aggregate stability (Gill 2012). While, the quality of soil structure, in turn depends on tillage methods (Alletto & Coquet 2009). Many farmers carry out the tillage practices without knowledge of its effects on soil physical properties and crop yield (Aikins & Afuakwa 2012). Inappropriate soil tillage operations can cause hardpan in subsoil, which in turn causes poor soil aeration, reduction of microorganism activity, limitation of root development, formation of runoff and eventually soil erosion (Asghari Meidani et al. 2012; Abbaspour-Gilandeh & Rahimi-Ajdadi 2016). Further, knowing that the tillage operation consumes more than half of the energy consumption of agricultural productions (Rahimi-Ajdadi et al. 2016), inappropriate soil tillage operations can cause great energy losses. Different tillage systems have different effects on the soil physical properties and consequently the quantity and quality of the final agricultural products (Gozubuyuk et al. 2014). Preparing seedbed or tillage operation are often carried out using moldboard plow in a conventional system. This makes some disadvantages as soil destruction, soil compaction, soil wind erosion and water erosion, which eventually cause crop yield losses (Seyed Olama et al. 2016). Another tillage method is minimum tillage with reduced soil manipulation. For instance, tillage operation with a chisel

plow only loosens surface layers of the soil (Sadeghnezhad & Eslami 2006) and does not turn the soil over. Despite, mechanical manipulation due to conventional tillage improves soil porosity and buries crop residues, manures, and weeds; it leads to increased soil erosion and loss of soil organic carbon, aggregate stability, and moisture (West & Marland 2002; Tadesse et al. 2020). Due to importance of tillage effects on soil properties, many studies were conducted to investigate the effect of tillage type, including conservation tillage (no till and reduced tillage) and conventional tillage on soil properties. Some researchers investigated the effect of tillage system on some soil properties, especially soil organic carbon (Hati et al. 2015; Jiang et al. 2015; Liu et al. 2015; Wang et al. 2019; Naseri et al. 2020; Wang et al. 2020).

Drainage management is one of the key factors affecting soil physical properties. At the global level, 146 million hectares of cultivable lands have drainage problem and require management to improve soil physical properties (e.g. soil aeration, water retention and aggregate formation) and the reduction of soil erosion. (Randall & Iragavarapu 1995). Low water infiltration rates, high groundwater levels, melting of snow and heavy rain in the spring will intensify the need for drainage management to increase and maintain stable high level of agricultural production (Nakajima & Lal 2014). If the land that requires drainage are not drained, the growth of plants is undesirably affected by lack of aeration, decrease in O₂ concentration and increase in CO₂ and CH₄ concentration (Lal & Taylor 1969).

Briefly, the selection of a proper tillage system that preserve the physical properties of the soil is essential for the successful growth of agricultural products (Jabro et al. 2009). The key point is that applied tillage system in a farm intensely affect drainage and this case has been ignored in most previous researches. Hence, these two issues were examined together in the present study. On the other hand, in addition to tillage methods and drainage condition, the effect of temporal variability was investigated in this research. Because, it has been reported as important factor for the medium- and fine-textured soils (Van Es et al. 1999; Alletto & Coquet 2009). Van Es et al. (1999) showed that temporal processes are a large source of variability, even more effective than spatial sources.

Based on above, the purpose of this study was to investigate the effect of different soil tillage methods, drainage managements and temporal variability on organic matter and some soil physical properties including bulk density, particle density, total porosity, aeration porosity, mean weight diameter of aggregates, soil infiltration rate, and saturated moisture content.

2. Material and Methods

The study was carried out in Moghan region, the north of Ardebil province, Iran (near the border of Azerbaijan Republic and Aras River) with area of about 900 km² and the geographical location of 39° 23' to 42° 39' N latitude and 47° 25' to 48° 23' E longitude. This wide and fertile plain has been created by alluvial deposits of the Aras River and its distributaries and is considered as one of the most important agricultural and livestock areas of the country. The average annual precipitation and temperature are 275 mm and 14.6 °C, respectively. The average altitude of the region is 45 m above sea level and the climate of region is semi-arid having cold winters and warm summers (Pars Abad synoptic weather station). The studied soil had a clay loam texture with Entisol classification. Some properties of the studied soil are represented in Table 1. The measurements were separately reported for each plot (drainage and no drainage).

Table 1- Initial soil properties at the depth of 0-20 cm

<i>Treatment</i>	<i>Clay (%)</i>	<i>Silt (%)</i>	<i>Sand (%)</i>	<i>Texture</i>	<i>O. M (%)</i>	<i>pH</i>	<i>EC (dS/m)</i>	<i>pb (g/cm³)</i>	<i>ps (g/cm³)</i>	<i>ρ (%)</i>	<i>Ks (cm/h)</i>	<i>MWD (mm)</i>
A1	34.0	44.0	22.0	Clay loam	1.8	7.8	0.7	1.50	2.74	45.25	1.03	2.23
A2	34.0	46.0	20.0	Clay loam	1.8	7.8	2.80	1.36	2.79	51.25	1.54	1.81

A1: Drainage, A2: No drainage, Ks: Saturated soil hydraulic conductivity, pb: Bulk density, ps: Particle density, MWD: Mean weight diameter, OM: Organic matter, EC: Electrical conductivity and ρ: Total porosity

Experimental design was set as a split plot design in time in order to investigate the effect of tillage and drainage methods on some soil physical properties. First, two main plots were considered: one plot had underground drainage at a depth of 1.5 m (A1) and the other land plot had no underground drainage (A2). The average depth of groundwater was measured about 160 and 100 cm for the plot of A1 and A2, respectively. The plots had the same dimensions (90 × 90 m²), organic matter and pH and they were 500 m apart. In each plot, nine subplots of 30 × 20 m² were prepared so that the total number of plots was 18 (Figure 1). Tillage operation was done in three treatments by three replications. Tillage levels are given below:

B1: Moldboard plow + disk harrow (as a conventional method in the region)

B2: Moldboard plow + rotary tiller

B3: Chisel plow+ disk harrow

The moldboard plow and chisel plow were set at a depth of 25 cm.

A1			A2		
A1T1R1	A1T2R1	A1T3R1	A2T3R1	A2T2R1	A2T1R1
A1T1R2	A1T3R2	A1T2R2	A2T2R2	A2T1R1	A2T3R1
A1T3R2	A1T2R2	A1T1R2	A2T1R3	A2T3R3	A2T2R3

Figure 1- Schematic diagram showing experimental design

Soil samples were taken from 0-20 cm depth and 10 days after wheat planting in early November (T1) and 10 days after harvest in late June (T2). The samples were passed through a sieve with the mesh of 2 mm after air-drying. The soil texture, organic carbon and pH were measured respectively by the hydrometer method (Gee & Or 2002), Walkley-Black method (Nelson & Sommers 1996) and pH meter in saturated paste (Thomas 1996). In addition, soil bulk density using the cylinder method, the mean particle density of samples using Pycnometer, soil infiltration rate (v_w) by double ring method, mean weight of aggregate diameter (MWD) by wet sieving method (Kemper & Rosenau 1996) and total porosity (P) by calculation method were measured. To calculate the aerial porosity, first, the soil was reached to field capacity (FC) moisture and then the moisture content of FC was measured. The aeration porosity (P_a) was obtained from Equation 1:

$$P_a = M_s - M_{FC} \quad (1)$$

Where: M_s , is saturated moisture content of soil and M_{FC} , is the soil moisture content at field capacity condition.

The data were analyzed using analysis of variance (ANOVA) and means comparison were done using Tukey test in MSTAT-C software to determine the effects of tillage method, drainage management and their interactions on the soil physical properties.

3. Results and Discussion

The results of analysis of variance relating to the effect of tillage methods and drainage management on some soil properties showed that the effect of time was significant on the soil bulk density and mean particle density ($P < 0.01$). The simple effect of time on soil porosity was significant, too ($P < 0.05$). The tillage effect (B) on the bulk density, mean particle density and porosity was not significant. Drainage effect was significant on all of water infiltration rate, soil organic matter and MWD ($P < 0.01$). The effects of studied factors on some soil physical properties are explained in the following.

3.1. Time

Results of mean comparison of time on some soil properties are given in Table 2. The results showed that the soil mean particle density after planting time was less than after harvesting. The reason can be attributed to decreased soil organic carbon at harvesting time, because, tillage operation causes the air to enter the soil which accelerate the oxidation of soil organic matter, reduce the soil organic matter and consequently the mean particle density increases. Another reason relates to a shorter time between tillage operation (seed preparation) and T1 (after planting) than T2 (after harvesting). Since, tillage operation initially pulverize the soil aggregates, causes to reduce the soil bulk density. However, over time the soil bulk density increases due to irrigation and displacement of soil fine particles. The obtained result is in accordance with Roldan et al. (2007).

The results also showed that the simple effect of time on soil porosity and soil aeration porosity was significant ($P < 0.05$). The soil porosity after planting time (T1) were much more than after harvesting time (T2) and also, the soil aeration porosity in T1 was more than T2 (Table 2). The reason is that, as time passes, the pores created by the tillage operation decreases caused by soil compaction, and hence the porosity of the soil decreases. This result is in consistent with Osunbitan et al. (2005). They stated that over time, the gradual compaction of soil happens due to rain and consequently, porosity decreases and bulk density increases.

Table 2- Mean comparison relating to the effect of sampling time on some soil properties

<i>Time</i>	ρ_b (g/cm ³)	ρ_s (g/cm ³)	<i>P</i> (%)	<i>Pa</i> (%)	<i>Ms</i> (%)	<i>O. M</i> (%)	<i>MWD</i> (mm)	v_w (cm/h)
T1	1.20b	2.66b	54.96a	25.92a	53.04b	1.29a	1.4b	2.23a
T2	1.35a	2.70a	45.29b	18.66b	62.97a	1.21b	2.7a	2.09b

Columns marked with the same letter do not differ significantly ($P \leq 0.05$).

According to the ANOVA results, the effect of time on the organic matter was significant ($P < 0.05$). Soil organic matter content measured after planting stage was more than after harvesting stage (T2) (Table 2). The reason can be explained that as time passed, soil organic matter decreased. Over time, degradation of soil organic matter occurs and tillage operation causes it to speed up.

The effect of time on soil saturated moisture content was significant ($P < 0.01$). The percentage of soil saturated water content in T1 was less than T2 (Table 2). Soil disturbance due to tillage operation just before planting increases total soil porosity and aeration porosity in T1 compared to T2. In addition, most of the porosity in T1 relates to the soil coarse porosity. However, over time (after harvesting) the pore size of the soil is finer and more capable of water storage. This result is in compliance with Kribaa et al. (2001).

The effect of time on MWD was significant ($P < 0.01$). The results showed that MWD at postharvest stage was greater than post-planting stage (Table 2). Therefore, MWD increased with passing time after tillage operation.

Surveying the effect of time on soil infiltration rate revealed that the water infiltration rate in the post-planting stage was greater than the post-harvest treatment (Table 2). The reason is that soil porosity reduces by tillage operations over time, which in turn decrease the water infiltration rate. This result complies with Osunbitan et al. (2005).

3.2. Tillage method

The tillage effect on bulk density and mean particle density was not significant. This result is consistent with the results obtained by Hill & Cruse (1985) and Bayat et al. (2008) who did not observe any significant effect between different tillage systems (no till, minimum and conventional tillage) and bulk density. However, they reported that the bulk density increased with increasing depth. Many researchers measured a higher bulk density in no till system than the conventional tillage system (Celik 2011; Rashidi & Keshavarzpour 2011; Aikins & Afuakwa 2012). The effect of tillage methods (moldboard plow, subsoiler and subsoiler with de-compactor) on some physical properties of a silty clay soil were studied by Ghasemi Abdoalmalaki et al. (2015). Their results showed that the lowest and highest values of bulk density belonged to the subsoiler and moldboard plow, respectively.

The effect of tillage methods in a sandy loam soil relating to a potato field were evaluated by Rasooli-Sharabiani & Abbaspour-Gilaneh (2008). They reported that soil bulk density after tillage operation was decreased in all treatments and the most reduction was obtained in the moldboard plow with disk harrow treatment. They explained that the reason of the further reduction of bulk density in this treatment was due to more soil loosening and increased soil porosity. Gozubuyuk et al. (2014) studied the effect of four different tillage practices including T1: Conventional tillage (moldboard plow + disk harrow + combined harrows + precision seeder); T2: Reduced tillage-I (cultivator + combined harrows + precision seeder); T3: Reduced tillage-II (rotary power harrow + precision seeder) and T4: No till. They observed a significant difference between soil bulk density (and porosity) and tillage treatments at depth 0-10 cm, so that the no-till treatment had the highest bulk density and the traditional tillage had the lowest bulk density. Similarly, Sekwakwa & Dikinya (2012) also measured the least amount of bulk density in no-till treatments. In general, it can be concluded that soil bulk density in tillage systems was lower than no-till systems (Osunbitan et al. 2005) and these differences can be ranked as follows: no-tillage > chisel plow > moldboard plow.

Although the effect of different tillage methods on soil porosity was not significant, however, soil porosity rank in different tillage treatments was B1 > B2 > B3, respectively. It should be mentioned that all of tillage treatments studied in this research were categorized as conventional or minimum tillage and no till was not applied. The insignificant effect of tillage treatments on bulk density and porosity can be attributed to the closeness of degree of pulverization of soil aggregates in the applied tillage treatments. Roseberg & McCoy (1992) and Safadoust et al. (2007) obtained the same result. They explained that although conventional tillage (moldboard plow) increases the total porosity of the soil, but it reduces the number, stability, and coherence of large pores (effective pores in water transfer).

The effect of different tillage methods on soil aeration porosity was significant ($P < 0.05$). Results of mean comparison showed that B3 and B1 treatments had the least and highest amount of aeration porosity, respectively (Table 3). The reason is that a moldboard plow creates large air-filled pores in soil because of increased soil disturbance compared to a chisel plow. Elder & Lal (2008) in a research farm in Ohio studied the effect of different tillage methods, and measured less bulk density and more aeration porosity for moldboard plow treatment.

Table 3- Mean comparison relating the effect of tillage practice on some soil properties

<i>Tillage</i>	<i>Pa (%)</i>	<i>P (%)</i>	<i>Ms (%)</i>	<i>O.M (%)</i>	<i>v_w (cm/h)</i>	<i>pb (g/cm³)</i>	<i>ps (g/cm³)</i>	<i>MWD</i>
B1	24.37 a	48.00	54.03 b	1.18 b	2.30 b	1.43 a	2.76 a	2.25
B2	22.12 ab	49.00	58.02 ab	1.24 ab	2.38 b	1.42 a	2.76 a	2.12
B3	20.08 b	48.00	61.36 a	1.35 a	3.26 a	1.44 a	2.76 a	2.78

Columns marked with the same letter do not differ significantly ($P \leq 0.05$)

The effect of tillage method on soil organic matter was significant ($P < 0.05$). Results of mean comparison showed that the lowest and highest amounts of organic matter were obtained for moldboard plow (B1) and chisel plow treatments, respectively (Table 3). Abasi et al. (2014) also measured the lowest amount of organic matter in the moldboard plow treatment.

The effect of tillage method on saturated moisture content was significant at 5% of probability level. In B3 and B1, the highest (61.36%) and lowest (54.03%) amounts of saturated moisture content were obtained, respectively (Table 3). The reason for this case is the low intensity of tillage and the higher percentage of small pores in the chisel plow compared to the moldboard plow. Many researchers have obtained less saturated moisture content in moldboard plow (traditional tillage) than minimum tillage method. The reason for this is that in the moldboard plow, there is a less amount of micro-pores, which play a major role in water storage in the soil (Fernandez-Ugalde et al. 2009; Gozubuyuk et al. 2014).

Effect of tillage method was insignificant on soil aggregate MWD. In this case, there are different results obtained in other studies, depending on treatments and their conditions.

For instance, Hajabbasi & Hemmat (2000) reported that different tillage systems consisted of conventional and conservation tillage system has no significant effect on the stability of aggregates in the first year. However, after four years, conservation tillage system has a positive and significant effect on the stability of the soil structure. Hajabbasi et al. (1999) also reported that tillage increased the percentage of fine aggregates (smaller than 0.25 mm) during a two-year study. However, Ghasemi Abdoalmalaki et al. (2015) in a study on soil aggregate stability obtained a significant difference between different tillage treatments. They measured the highest stable aggregate when the moldboard plow was used. Safadoust et al. (2007) stated that the stability of the aggregate is significantly affected by different tillage methods and soil aggregate stability increased with this order, no till > chisel plow > moldboard plow. Baker et al. (2004) reported similar results. They stated that by increasing the intensity of tillage, the amount of organic carbon decreased and MWD was reduced.

The effect of tillage methods on infiltration rate showed that B3 had the highest infiltration rate and B1 had the lowest value (Table 3). The reason can be explained by the fact that the conservation of the continuity of pores in the chisel plow is more than moldboard plow treatment. This result is consistent with the findings of Freebarin et al. (1986). Ghasemi Abdoalmalaki et al. (2015) stated that although tillage at the early times increases water infiltration rate of soil, it decreases over time. They measured the minimum of infiltration rate in the moldboard plow treatment. Gozubuyuk et al. (2014) reported that water infiltration rate in the soil may be increased by appropriate methods of tillage operations, resulting in cracks in the soil. They measured higher infiltration rate in minimum tillage and no till compared to conventional tillage (moldboard plow with disk harrow). They also explained that it might be due to the extra stable aggregates and pores continuity in the minimum tillage and no tillage treatments.

3.3. Drainage

The effect of drainage on MWD was significant ($P < 0.01$). In this study, MWD in drainage treatment was less than no drainage treatment (Table 4). The results showed that drainage reduces MWD in the surface layer. The reason can be explained by reducing the organic matter in the drainage treatment (Table 4). In other words, drainage provides the necessary conditions for organic matter decomposition; it reduces organic carbon and thus reduces MWD. Baker et al. (2004) examined the effect of drainage and subsurface irrigation on MWD. Their results showed that MWD in the surface layers of 0-20 and 20-30 cm in drainage treatment was lower than subsurface irrigation treatment. However, in lower layers, MWD was larger in drainage treatment. They stated that soils in lower layers that are under irrigated condition couldn't be dried. Therefore, small aggregates or primary micro particles cannot form a larger aggregate.

Table 4- The effect of drainage on MWD, water infiltration rate and organic matter

<i>Drainage management</i>	<i>Pa (%)</i>	<i>P (%)</i>	<i>Ms (%)</i>	<i>O.M (%)</i>	<i>v_w (cm/h)</i>	<i>pb (g/cm³)</i>	<i>ps (g/cm³)</i>	<i>MWD(mm)</i>
Drainage	24.00	45.00	49.00	1.17 b	2.34 b	1.50	2.74	1.57 b
Non-drainage	26.00	51.00	58.00	1.32 a	2.97 a	1.36	2.79	2.5 a

Columns marked with the same letter do not differ significantly ($P < 0.05$).

The water infiltration rate in drained treatment was less than that of no drainage treatment (Table 4). The reason is that leaching of salts in the drained treatment layer decreases the EC, resulting in the dispersion of soil particles and finally reduction of water infiltration rate in the soil. Similarly, Chaudhry & Sidhu (2001) reported a decrease in EC and water infiltration rate in the drained layer.

3.4. Interaction effect of drainage and tillage method

The interaction effect between drainage and tillage methods was classified into three groups (Table 5). The results showed that A2B1 treatment and A2B3 had the highest (25.48%) and lowest (17.17%) aeration porosity, respectively. The means comparison indicated that there was no significant difference among A1B3, A1B2 and A1B1 treatments regarding aeration porosity (Table 5). Consequently, application of moldboard plow in drained condition cannot significantly affect increasing the aeration porosity. However, the significant difference between A2B1 and A2B3 treatments indicated that selecting tillage method has an important and effective role on aeration porosity in no drainage condition. In other words, when the drainage is not applied, moldboard plow makes more aeration porosity in the soil compared to chisel plow.

Table 5- The interaction of drainage and tillage methods on aeration porosity, saturation moisture and MWD

Property	A1B1	A2B1	A1B2	A2B2	A1B3	A2B3
Pa (%)	23.32 ab	25.48 a	22.34 ab	22.41 ab	23.02 ab	17.17 b
Ms (%)	54.65 b	53.70 b	58.41 ab	58.43 ab	54.41 b	66.5 a
MWD (mm)	1.72 c	2.40 b	1.58 c	2.59 ab	1.55 c	2.8 a

Columns marked with the same letter do not differ significantly ($P \leq 0.05$).

The interaction effects of drainage and tillage methods on saturation moisture content are represented in Table 6. The results showed that A2B1 and A2B3 treatments had the lowest (53.70%) and highest (66.50%) saturated moisture content, respectively (Table 5). A higher saturated moisture content measured in the chisel plow treatment and no drainage condition, indicates that the inefficiency of the chisel in developing aeration porosity in such condition. There was significant difference between A2B3 and A1B3 treatments, in terms of saturated moisture content; however, there was no significant difference between A1 and A2 in other tillage methods. Therefore, the application of chisel plow is not recommended in no-drained areas.

The interaction effects between drainage and tillage methods were investigated on MWD (Table 5). The results showed that A1B3 treatment with 1.55 mm had the least MWD and A2B3 treatment with 2.80 mm had the highest MWD. There was a significant difference between A2B3 and A1B1, A1B2 and A1B3 treatments, but there were no significant differences between A1B1, A1B2 and A1B3 treatments. Therefore, it can be concluded that the effect of drainage on changes of MWD was higher than the tillage methods. The results also showed that the tillage treatments were significantly effective in no drainage lands, conversely drainage conditions.

3.5. Interaction effect of time and drainage

The interaction effect between time and drainage was investigated on water infiltration rate (Figure 2).

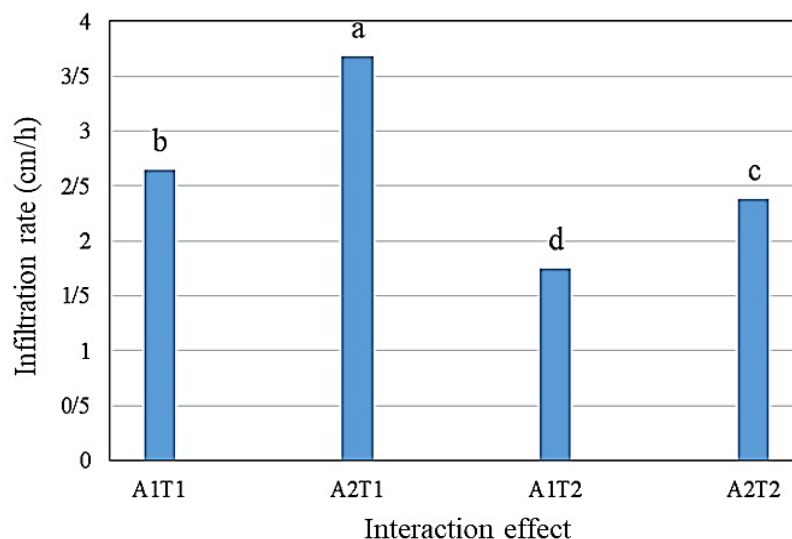


Figure 2- The interaction effect of drainage and time on water infiltration rate

The results showed that A2T1 treatment had the highest infiltration rate and A1T2 treatment had the lowest rate. All treatments had the significant difference, together. As observed, the infiltration rate decreased in T2 compared to T1, and this decrease were 37% and 32% in no drainage and drainage treatments, respectively. Therefore, it can be concluded that the drainage contributes to the continuity of infiltration.

3.6. Interaction effect of time and tillage method

The combination of time and tillage methods was represented in Figure 3. The results showed that the highest infiltration rate was observed for T1B3 treatment, and the lowest one was obtained for the T2B1 followed by T2B2. The difference among T1B1, T1B2 and T2B3 were insignificant. According to the results, infiltration rate after harvesting decreased compared to after planting in all tillage treatments (Figure 3). According to Van Es et al. (1999), tillage and time is a significant factor for infiltrability in the medium and fine-textured soils. The reason for the higher infiltration rate at T1 is that a little time has passed between tillage operation and sampling, and as a result the soil porosity is high. But at T2, the consecutive irrigations and traffic of agricultural machinery (between planting and harvesting) cause more soil compaction and thus reduce porosity. Alletto and Coquet (2009) reported similar results for inter-row position and attributed it to the low stability of porosity created by tillage (Osunbitan et al., 2005).

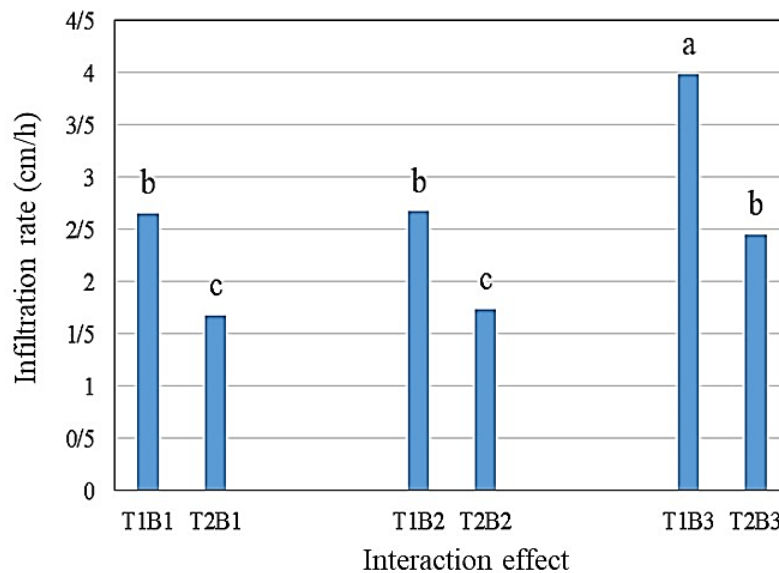


Figure 3- The interaction effect of interaction of time and tillage on water infiltration rate

3.7. Triple effect of the factors

The triple combination among the levels of time, drainage and tillage methods on MWD were investigated (Figure 4).

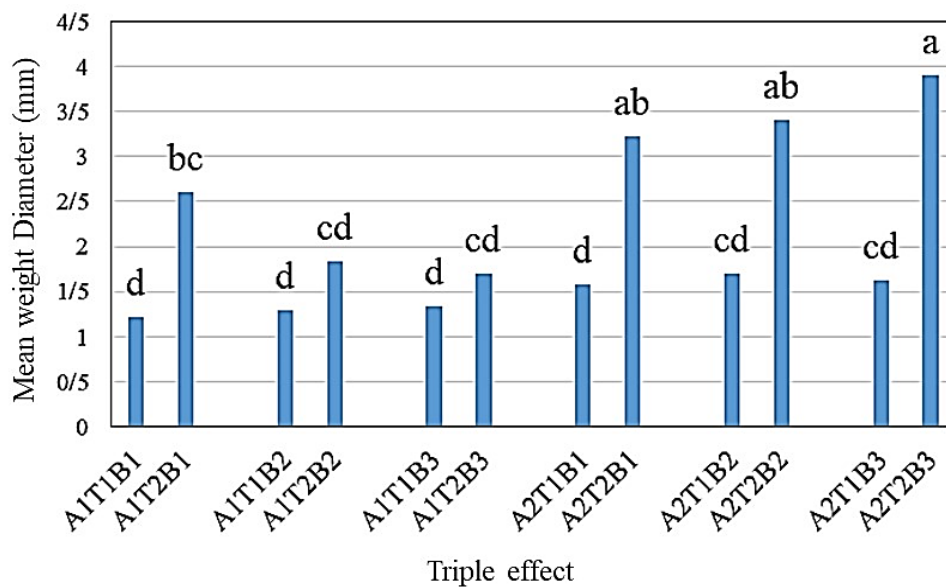


Figure 4- The interactions among, time, drainage, and tillage methods on MWD

The results showed that A1T1B1 treatment (drainage, after planting and moldboard plow) had the lowest MWD and A2T2B3 treatment (no drainage, after harvest and chisel plow) had the highest MWD.

The difference between A2T2B3 treatment and A2T2B1 and A2T2B2 treatments was not significant. This indicates that in no drainage condition, the tillage methods do not have significant effect on MWD at postharvest time. However, there was a significant difference between A2T2B3 and 11 other treatments. According to Figure 4, in all treatments, MWD increased over time, in both no drainage and drainage conditions. Overall, this increase was higher in no drainage treatment compared to the drainage treatment. The reason relates to the high amount of organic carbon in no drainage treatment compared to the drainage treatment.

4. Conclusions

The effect of tillage methods on soil aeration porosity is completely related to drainage conditions. It was insignificant under drained conditions, however, in non-drainage condition, when moldboard plow is used, the soil aeration porosity will be 48.41% higher than that of chisel. In addition, the soil prepared by chisel has 23.84% more saturated moisture content than moldboard plow. As a result, it is recommended to use a moldboard plow (B1) instead of a chisel in non-drained conditions. Similarly, the choice of tillage method is very critical on MWD in non-drainage condition so that the size of aggregates created by the chisel is about 16.7% larger than moldboard plow (B1) in non-drainage condition. The contribution of drainage on changing MWD is higher than the tillage methods. Infiltration rate after harvesting decreases compared to after planting due to irrigation and traffic of machinery. According to the results of MWD, it increased over time, in all treatments. This was higher in non-drainage treatments compared to the drainage. Overall, the treatments of A1T1B1 (drainage/ after planting/moldboard plow+disk harrow) and A2T2B3 (non-drainage/ after harvesting/ chisel plow+disk harrow) have the lowest and highest MWD, respectively.

Abbreviations and Symbols

MWD	Mean weight diameter
A1	Subsurface drainage
A2	Non-drainage
B1	Moldboard plow + harrow
B2	Moldboard plow + rotary tiller
B3	Chisel plow + disk harrow
T1	After planting
T2	After harvesting
FC	Field Capacity
P_a	Aeration porosity
P	Porosity
v_w	Infiltration rate
Ms	Saturated moisture content condition
M_{FC}	Soil moisture content at Field capacity
pb	Bulk density
Ps	Mean particle density
Ks	Saturated hydraulic conductivity
O.M	Organic matter

References

- Abasi H, Khodaverdiloo H, Ghorbani Dashtaki S & Ahmadi Moghadam P (2014). The effect of some tillage methods on soil physical quality index in arid and semi-arid region. *Journal of Agricultural Mechanization* 1(2): 37-45 (In Persian)
- Abbaspour-Gilandeha Y & Rahimi-Ajdadi F (2016). Design, construction and field evaluation of a multiple blade soil mechanical resistance sensor. *Soil & Tillage Research* 157: 93-100. <https://doi.org/10.1016/j.still.2015.11.013>
- Aikins S H M & Afuakwa J J (2012). Effect of four different tillage practices on soil physical properties under cowpea. *Agriculture and Biology Journal of North America* 3: 17-24. DOI: 10.5251/abjna.2012.3.1.17.24
- Alletto L & Coquet Y (2009). Temporal and spatial variability of soil bulk density and near saturated hydraulic conductivity under two contrasted tillage management systems. *Geoderma* 152: 85-94. <https://doi.org/10.1016/j.geoderma.2009.05.023>
- Al-Suhaibani S A & Ghaly A E (2013). Comparative study of the kinetic parameters of three chisel plows operating at different depths and forward speed in a sandy soil. *The International Journal of Engineering and Science (IJES)* 2: 42-59
- Asghari Meidani J, Karimi E & Mousavi S B (2012). Tillage Effects on Wheat Yield and Soil Water Content and Bulk Density in Dryland Wheat-Fallow Rotation in Maragheh. *Journal of Science and Technology of Agriculture and Natural Resources* 16: 119-129
- Baker B J, Fausey N R & Islam K R (2004). Comparison of soil physical properties under two different water table management regimes. *Soil Science Society of America Journal* 68(6): 1973-1981. DOI: 10.2136/sssaj2004.1973
- Bayat H, Mahbobi A A, Hajabbasi M A & Mosaddeghi M R (2008). Tillage and Tractor Effects on Bulk Density, Cone Index and Structural Stability of a Sandy Loam Soil. *Journal of Science and Technology of Agriculture and Natural Resources* 11(42): 451-461
- Celik I (2011). Effects of tillage methods on penetration resistance, bulk density and saturated hydraulic conductivity in a clayey soil conditions. *Journal of Agricultural Science* 17: 143-156. DOI: 10.1501/Tarimbil_0000001166
- Chaudhry M & Sidhu M (2001). Impact of sub surface drainage on soil salinity and crops yield under farmers management practices. *Journal of Drainage and Water Management* 5(2): 35-45. <https://doi.org/10.1023/B:IRRI.0000019475.42469.33>
- Demir Z & Isik D (2020). The impact of different cover crops, mechanical cultivation and herbicide treatment on the soil quality variables and yield in apple (*Malus domestica* Borkh.) orchard with a coarse-textured soil. *Journal of Agricultural Sciences (Tarim Bilimleri Dergisi)* 26: 452-470. DOI: 10.15832/ankutbd.527445

- Elder J W & Lal L (2008). Tillage effects on physical properties of agricultural organic soils of north central Ohio. *Soil & Tillage Research* 98(2): 208-210. <https://doi.org/10.1016/j.still.2007.12.002>
- Fernandez-Ugalde O, Virto I, Bescansa P, Imaz M J, Enrique A & Karlen D L (2009). No tillage improvement of soil physical quality in calcareous degradation-prone semiarid soils. *Soil Tillage Research* 106: 29-35. <https://doi.org/10.1016/j.still.2009.09.012>
- Freebarin D M, Wockner G H & Silburn D M (1986). Effects of catchment management on runoff, water quality and yield potential from Vertisols. *Agricultural Water Management* 12: 1-19. [https://doi.org/10.1016/0378-3774\(86\)90002-8](https://doi.org/10.1016/0378-3774(86)90002-8)
- Gee G W & Or D (2002). Particle-size analysis. In: J H Dane & C Topp G C (Eds.), *Methods of Soil Analysis, Part 4- Physical methods*. Agronomy Monograph, Madison pp. 255-293
- Ghasemi Abdoalmalaki Y, Ghajar Sepanlou M & Bahmanyar M A (2015). Effects of Different Methods of Tillage on Some Physical Characteristics of Soil. *Journal of Soil Research* 29(3): 309-320 (In Persian)
- Gill S M (2012). Temporal variability of soil hydraulic properties under different soil management practices. PhD Thesis, University of Guelph. Ontario, Canada. DOI: 10.13140/RG.2.2.12625.94566
- Gozubuyuk K, Sahin U, Ozturk I, Celik A & Cemal Adiguzel M (2014). Tillage effects on certain physical and hydraulic properties of a loamy soil under a crop rotation in a semi-arid region with a cool climate. *Catena* 118: 195-205. <https://doi.org/10.1016/j.catena.2014.01.006>
- Hajabbasi M A & Hemmat A (2000). Tillage impacts on aggregate stability and crop productivity in a clay-loam soil in central Iran. *Soil Tillage Research* 56: 205-212. [https://doi.org/10.1016/S0167-1987\(00\)00140-9](https://doi.org/10.1016/S0167-1987(00)00140-9)
- Hajabbasi M A, Mirlahi A F & Sadrarhami M (1999). Impact of converting Rangelands to cultivated Land on physical and chemical properties of soils in West and Sounwest of Isfahan. *Journal of Science and Technology of Agriculture and Natural Resources* 3(3): 18-24
- Hati K M, Chaudhary R S, Mandal K G, Bandyopadhyay K K, Singh R K, Sinha N K, Mohanty M, Somasundaram J & Saha R (2015). Effects of tillage, residue and fertilizer nitrogen on crop yields, and soil physical properties under soybean-wheat rotation in vertisols of central India. *Agricultural Research* 4 (1): 48-56. <https://doi.org/10.1007/s40003-014-0141-7>
- Hill R L & Cruse R M (1985). Tillage effect on bulk density and soil strength of two Mollisols. *Soil Science Society of America Journal* 74: 1270-1273. <https://doi.org/10.2136/sssaj1985.03615995004900050040x>
- Jabro J D, Stevens W B, Evans R G & Iversen W M (2009). Tillage effects on physical properties in two soils of the Northern Great Plains, Applied Engineering in Agriculture 25(3): 37-382. DOI: 10.13031/2013.26889
- Jiang X, Hu Y, Bedell J H, Xie D & Wright A L (2015). Soil organic carbon and nutrient content in aggregate-size fractions of a subtropical rice soil under variable tillage. *Soil Use Manage.* 27(1): 28-35. doi: 10.1111/j.1475-2743.2010.00308.x
- Kemper W D & Rosenau R C (1996). Aggregate Stability and size distribution. In: A Klute (Ed.), *Methods of soil Analysis, Part 1: physical and Mineralogical Methods, 2nd Ed.*) American Society of Agronomy. Madison, W.I. pp. 425-442. <https://doi.org/10.2136/sssabookser5.1.2ed.c17>
- Kribaa M, Hallaire V, Curmi P & Lahmar R (2001). Effect of various cultivation methods on the structure and hydraulic properties of a soil in a semi-arid climate. *Soil and Tillage Research* 60: 43-53. DOI: 10.1016/S0167-1987(01)00171-4
- Lal R & Taylor G S (1969). Drainage and nutrient effects in a field lysimeter study. Corn yield and soil conditions. *Science Society of America Journal* 33(6): 937-941. <https://doi.org/10.2136/sssaj1969.03615995003300060039x>
- Liu E, Chen B, Yan C, Zhang Y, Mei X & Wang J (2015). Seasonal changes and vertical distributions of soil organic carbon pools under conventional and No-till practices on Loess Plateau in China. *Soil Science Society of America Journal* 79: 517-526
- Mirzaee M & Mahmoodabadi M (2014). The effect of kind and different crop residues management on some of physical properties and infiltration. *Iranian journal of Soil and Water Research* 28(4): 659-671 (In Persian)
- Nakajima T & Lal R (2014). Tillage and drainage management effect on soil gas diffusivity. *Soil & Tillage Research* 135: 71-78. <https://doi.org/10.1016/j.still.2013.09.003>
- Naseri H, Gholami Parashkoochi M, Ranjbar I & Mohammad Zamani D (2020). Sustainability of quantitative and qualitative indicators of sugarcane production under different tillage systems (case study: Khuzestan province of Iran). *Environmental and Sustainability Indicators* 8, 100046. <https://doi.org/10.1016/j.indic.2020.100046>
- Nelson D W & Sommers L E (1996). Total carbone organic carbone and organic matter. In: D L Sparks (Ed.), *Methods of soil analysis, Part 3- chemical methods*. Agronomy Monograph, ASA and SSSA, Madison, WI. Pp. 961-1010. <https://doi.org/10.2136/sssabookser5.3.c34>
- Osunbitan J A, Oyedele D J & Adekalu K O (2005). Tillage effects on bulk density, hydraulic conductivity and strength of a loamy sand soil in southwestern Nigeria. *Soil & Tillage Research* 82: 57-64. <https://doi.org/10.1016/j.still.2004.05.007>
- Rahimi Ajdadi F, Abbaspour Gilandeh Y, Mollazade K & Hasanzadeh R P R (2016). Application of machine vision for classification of soil aggregate size. *Soil & Tillage Research* 162: 8-17. <https://doi.org/10.1016/j.still.2016.04.012>
- Randall G W & Iragavarapu T K (1995). Impact of long-term tillage systems for continuous corn on nitrate leaching to tile drainage. *Journal of Environmental Quality* 24: 360-366. <https://doi.org/10.2134/jeq1995.00472425002400020020x>
- Rashidi M & Keshavarzpour F (2011). Effect of different tillage methods on some physical and mechanical properties of soil in the arid lands of Iran. *World Applied Science Journal* 14: 1555-1558
- Rasooli-Sharabiani V & Abbaspour-Gilandeh Y (2008). Effects of tillage methods on soil physical properties. In: Proceeding of the 5th National Congress on Agricultural Machinery Engineering and Mechanization of Iran, 27-28 August, Mashhad, pp. 1-7
- Roldan A, Salinas-Garsia J R, Alguacil M M & Caravaca F (2007). Soil sustainability indicators following conservation tillage practices under subtropical maize and bean crops. *Soil & Tillage Research* 93: 273-282. <https://doi.org/10.1016/j.still.2006.05.001>
- Roseberg R J & McCoy E L (1992). Tillage- and traffic-induced changes in macroporosity and macropore continuity: air permeability assessment. *Soil Science Society of America Journal* 56: 1261-1267. <https://doi.org/10.2136/sssaj1992.03615995005600040042x>
- Sadeghnezhad H R & Eslami K (2006). The comparison of wheat yield under different tillage methods. *Journal of Agricultural Sciences* 12 (1): 103-112
- Safadoust A, Mosaddeghi M R, Mahboubi A A, Nouroozi A & Asadian G (2007). Short-Term Tillage and Manure Influences on Soil Structural Properties. *Journal of Science and Technology of Agriculture and Natural Resources* 11(41): 91-101 (In Persian)
- Sekwakwa O & Dikinya O (2012). Tillage-induced compaction: effects on physical properties of agricultural loamy soils. *Scientific Research and Essays* 7: 1584-1591. DOI: 10.5897/SRE11.2203
- Seyed Olama S N, Asadi H & Zavareh M (2016). Effect of Tillage Erosion on Soil Displacement and productivity (Case Study: Tutkabon, Guilan). *Journal of Soil and water Research* 46(4): 769-780 (In Persian)

- Tadesse H K, Moriasi D N, Gowda P H , Wagle P, Starks P J, Steiner J L, Talebizadeh M, Neel J P S & Nelson A M (2020). Comparison of Evapotranspiration and Biomass Simulation in Winter Wheat under Conventional and Conservation Tillage Systems using APEX Model. *Ecohydrology & Hydrobiology* 21(1) 55-66. <https://doi.org/10.1016/j.ecohyd.2020.08.003>
- Thomas G W (1996). Soil pH and soil activity. In: D L Sparks (Ed), *Methods of soil analysis, Part 3- Chemical Methods*. Agronomy Monograph, ASA and SSSA, Madison. WI, pp. 475-490. DOI: 10.4236/gep.2016.45008
- Van Es H M, Ogden C B, Hill R L, Schindelbeck R R, Tsegaye T (1999). Integrated assessment of space, time, and management-related variability of soil hydraulic properties. *Soil Science Society of America Journal* 63: 1599-1608. DOI: 10.2136/sssaj1999.6361599x
- Wang X, Qi J Y, Zhang X Z, Li S S, Virk A L, Zhao X, Xiao X P & Zhang H L (2019). Effects of tillage and residue management on soil aggregates and associated carbon storage in a double paddy cropping system. *Soil & Tillage Research* 194: 104339. <https://doi.org/10.1016/j.still.2019.104339>
- Wang H, Wang S, Yu Q, Zhang Y, Wang R, Li J & Wang X (2020). No tillage increases soil organic carbon storage and decreases carbon dioxide emission in the crop residue-returned farming system. *Journal of Environmental Management* 261: 110261. <https://doi.org/10.1016/j.jenvman.2020.110261>
- West T O & Marland G (2002). A synthesis of carbon sequestration, carbon emissions, and net carbon flux in agriculture: comparing tillage practices in the United States. *Agriculture, Ecosystems & Environment* 91(1-3): 217-232 doi:10.1016/S0167-8809(01)00233-X



© 2022 by the author(s). Published by Ankara University, Faculty of Agriculture, Ankara, Turkey. This is an Open Access article distributed under the terms and conditions of the Creative Commons Attribution (CC BY) license (<http://creativecommons.org/licenses/by/4.0/>), which permits unrestricted use, distribution, and reproduction in any medium, provided the original work is properly cited.

